

University of Nebraska - Lincoln

DigitalCommons@University of Nebraska - Lincoln

Civil Engineering Theses, Dissertations, and
Student Research

Civil Engineering

Fall 12-4-2009

WIM Based Live Load Model for Bridge Reliability

Marek Kozikowski

University of Nebraska at Lincoln, mkozikowski2@unl.edu

Follow this and additional works at: <https://digitalcommons.unl.edu/civilengdiss>



Part of the [Civil Engineering Commons](#), and the [Structural Engineering Commons](#)

Kozikowski, Marek, "WIM Based Live Load Model for Bridge Reliability" (2009). *Civil Engineering Theses, Dissertations, and Student Research*. 2.

<https://digitalcommons.unl.edu/civilengdiss/2>

This Article is brought to you for free and open access by the Civil Engineering at DigitalCommons@University of Nebraska - Lincoln. It has been accepted for inclusion in Civil Engineering Theses, Dissertations, and Student Research by an authorized administrator of DigitalCommons@University of Nebraska - Lincoln.

WIM BASED LIVE LOAD MODEL FOR BRIDGE RELIABILITY

by

Marek Kozikowski

A DISSERTATION

Presented to the Faculty of

The Graduate Collage at the University of Nebraska

In Partial Fulfillment of Requirements

For The Degree of Doctor of Philosophy

Major: Engineering

(Civil Engineering)

Under the Supervision of Professor Andrzej S. Nowak

Lincoln, Nebraska

December, 2009

WIM BASED LIVE LOAD MODEL FOR BRIDGE RELIABILITY

Marek Kozikowski, Ph.D.

University of Nebraska, 2009

Adviser: Andrzej S. Nowak

Development of a valid live load model is essential for assessment of serviceability and safety of highway bridges. The current HL-93 load model is based on the Ontario truck measurements performed in 1975. Since that time truck loads have changed significantly. Therefore, the goal of this study is to analyze 2005-2007 Weigh-In-Motion (WIM) data and develop a new statistical live load model.

The analyzed WIM data includes 47,000,000 records obtained from different states. A special program was developed to calculate the maximum live load effect. Comparison of the old and new truck data showed that on average Ontario trucks are heavier than the vehicles obtained from the available WIM and extrapolation of the data will yield the same maximum value. Exceptions are the extremely loaded sites from New York Sites and California.

Three types of live load models were developed; heavy, medium and light. Assuming 75 year return period the cumulative distribution functions of the load effects were extrapolated.

Development of the HL93 load was based on the analysis of several loading cases and it was found that two fully correlated trucks produce the maximum load effect. To verify simultaneous occurrence of two fully correlated trucks on the bridge a coefficient of correlation for available WIM data was determined and multiple presence analysis was performed. Analysis showed that this assumption is conservative. Based on the available data simultaneous occurrence of two fully correlated trucks is negligible.

Six steel girder bridges were selected and designed according to AASHTO LRFD code. FEM analysis of the selected bridges showed that the code girder distribution factors are conservative. Probabilistic analysis was performed and resulted with reliability indices higher than the target reliability 3.5. Based on this study it can be stated that HL93 load model is still valid for the highway bridges across US. An exception can be state of New York. Although the minimum calculated reliability index is equal to 3.8 a closer analysis of sites in New York is necessary.

ACKNOWLEDGEMENT

I wish to express my deepest gratitude to my advisor Professor Andrzej S. Nowak for his kind instructions, continuous guidance, and encouragement throughout this study. I would also like to express my sincere thanks to Professor Maria M. Szerszen, Professor George Morcous, Professor Christopher Y. Tuan and Professor Atorod Azizinamini.

Many thanks to my colleagues and friends Dr Piotr Paczkowski , Dr Tomasz Lutomirski, Marta Lutomirska, Remigiusz Wojtal, Przemyslaw Rakoczy, Ania Rakoczy and Jędrzej Kowalczyk, for their support and valuable advice.

Special thanks are due to Professor Henryk Zobel who introduced the author to the field of bridge engineering and provided the motivation for further study.

Especially, I would like to give my special thanks to my wife Ashley whose patient love enabled me to complete this work. I wish to express my love to my family, my mom, dad and my sister for their belief in me.

CONTENTS

LIST OF FIGURES	iv
LIST OF TABLES	viii
Chapter 1. INTRODUCTION	1
1.1. Problem Statement	1
1.2. Objective and Scope of the Research	2
1.3. Proir Investigations	3
1.4. Organization of the Thesis	4
Chapter 2. STRUCTURAL RELIABILITY MODELS	6
2.1. Introduction	6
2.2. Probability distributions	6
2.2.1 The Extreme Value Distribution	7
2.2.2 The Generalized Extreme Value Distribution	10
2.2.3 The Generalized Pareto Distribution	11
2.2.4 Nonparametric Method	12
2.3. Probability of Failure and Limit State Function	15
2.4. Reliability Index	18
Chapter 3. RECENT WEIGH-IN-MOTION	21
3.1. Introduction	21
3.2. Ontario Truck Survey	22
3.2.1 Interpolations and Extrapolations of Live Load Effects	30
3.3. Recent Weigh-In-Motion Data	36
3.4. Truck Data Analysis	47
3.5. Sensitivity Analysis	58
Chapter 4. LIVE LOAD ANALYSIS	71
4.1. Florida – Live Load Effect	71
4.2. California – Live Load Effect	82
4.3. New York – Live Load Effect	93

Chapter 5. Multiple Presence.....	105
5.1. Coefficient of Correlation	105
5.2. Load Model for Multiple Lane.....	117
5.3. Load Distribution Model.....	117
5.3.1 Code Specified GDF	118
5.3.2 Finite Element Model.....	119
Chapter 6. LOAD Combinations	127
6.1. Introduction	127
6.2. Dead Load	127
6.3. Live Load and Truck Dynamic	128
Chapter 7. Resistance Model.....	134
7.1. Moment Capacity of Composite Steel Girders	135
7.2. Shear Capacity of Steel Girders	137
Chapter 8. RELIABILITY ANALYSIS.....	141
8.1. Design of Girders	141
8.2. Reliability Index Calculations.....	145
8.3. Target Reliability and Summary of the Results	152
Chapter 9. CONCLUSIONS AND RECOMMENDATIONS	154
9.1. Summary	154
9.2. Conclusions.....	157
REFERENCES	160
APPENDIX A.....	163
Oregon – Live Load Effect	163
Florida – Live Load Effect.....	188
Indiana – Live Load Effect	220
Mississippi – Live Load Effect.....	251
California – Live Load Effect.....	284
New York – Live Load Effect	322

LIST OF FIGURES

Figure 2-1 Cumulative distribution function	9
Figure 2-2 Probability density function	9
Figure 2-3 Probability density function for three basic forms of GEV	11
Figure 2-4 Probability density function for three basic forms of GPD.....	12
Figure 2-5 Example of kernel density estimation for different bandwidths	14
Figure 2-6 The joint probability density function of the random variables.....	17
Figure 2-7 Probability density function for load and resistance (Nowak and Collins 2000)	18
Figure 3-1 AASHTO LRFD HL93 Design Load	22
Figure 3-2 Cumulative Distribution Functions of Positive HS20 Moments due to Surveyed Trucks	24
Figure 3-3 Cumulative Distribution Functions of Positive HL93 Moments due to Surveyed Trucks	25
Figure 3-4 Cumulative Distribution Functions of Negative HS20 Moments due to Surveyed Trucks	26
Figure 3-5 Cumulative Distribution Functions of Negative HL93 Moments due to Surveyed Trucks	27
Figure 3-6 Cumulative Distribution Functions of HS20 Shear due to Surveyed Trucks .	28
Figure 3-7 Cumulative Distribution Functions of HL93 Shear due to Surveyed Trucks .	29
Figure 3-8 Example of Extrapolation for Positive HS20 Moments due to Surveyed Trucks	31
Figure 3-9 Cumulative Distribution Functions of GVW- Oregon and Ontario.....	41
Figure 3-10 Cumulative Distribution Functions of GVW - Florida and Ontario	42
Figure 3-11 Cumulative Distribution Functions of GVW - Indiana and Ontario.....	43
Figure 3-12 Cumulative Distribution Functions of GWV - Mississippi and Ontario.....	44
Figure 3-13 Cumulative Distribution Functions of GVW - California and Ontario.....	45
Figure 3-14 Cumulative Distribution Functions of GVW– New York and Ontario	46
Figure 3-15 Bias – Span 30ft - different return periods for different locations.....	53
Figure 3-16 Bias – Span 60ft - different return periods for different locations.....	54
Figure 3-17 Bias – Span 90ft - different return periods for different locations.....	55
Figure 3-18 Bias – Span 120ft - different return periods for different locations.....	56
Figure 3-19 Bias – Span 200ft - different return periods for different locations.....	57
Figure 3-20 Data removal New York 0580	64
Figure 3-21 Data removal New York 2680	65
Figure 3-22 Data removal New York 8280	66
Figure 3-23 Data removal New York 8382	67
Figure 3-24 Data removal New York 9121	68
Figure 4-1 Cumulative Distribution Functions of Simple Span Moment– Florida – I-10	72
Figure 4-2 Cumulative Distribution Functions of Shear – Florida I-10	73
Figure 4-3 Low loaded bridge, moment, span 30ft – nonparametric fit to data	75
Figure 4-4 Low loaded bridge, moment, span 30ft – extrapolation to 75 year return period	76
Figure 4-5 Low loaded bridge, moment, span 60ft – nonparametric fit to data	76

Figure 4-6 Low loaded bridge, moment, span 60ft – extrapolation to 75 year return period	77
Figure 4-7 Low loaded bridge, moment, span 90ft – nonparametric fit to data	78
Figure 4-8 Low loaded bridge, moment, span 90ft – extrapolation to 75 year return period	78
Figure 4-9 Low loaded bridge, moment, span 120ft – nonparametric fit to data	79
Figure 4-10 Low loaded bridge, moment, span 120ft – extrapolation to 75 year return period	79
Figure 4-11 Low loaded bridge, moment, span 200ft – nonparametric fit to data	80
Figure 4-12 Low loaded bridge, moment, span 200ft – extrapolation to 75 year return period	81
Figure 4-13 Cumulative Distribution Functions of Moment – California – Lodi	83
Figure 4-14 Cumulative Distribution Functions of Shear – California – Lodi	84
Figure 4-15 Medium loaded bridge, moment, span 30ft – nonparametric fit to data	86
Figure 4-16 Medium loaded bridge, moment, span 30ft – extrapolation to 75 year return period	86
Figure 4-17 Medium loaded bridge, moment, span 60ft – nonparametric fit to data	87
Figure 4-18 Medium loaded bridge, moment, span 60ft – extrapolation to 75 year return period	88
Figure 4-19 Medium loaded bridge, moment, span 90ft – nonparametric fit to data	88
Figure 4-20 Medium loaded bridge, moment, span 90ft – extrapolation to 75 year return period	89
Figure 4-21 Medium loaded bridge, moment, span 120ft – nonparametric fit to data	90
Figure 4-22 Medium loaded bridge, moment, span 120ft – extrapolation to 75 year return period	90
Figure 4-23 Medium loaded bridge, moment, span 200ft – nonparametric fit to data	91
Figure 4-24 Medium loaded bridge, moment, span 200ft – extrapolation to 75 year return period	92
Figure 4-25 Cumulative Distribution Functions of Simple Span Moment– New York - Site 8382	94
Figure 4-26 Cumulative Distribution Functions of Shear – New York Site 8382	95
Figure 4-27 High loaded bridge, moment, span 30ft – nonparametric fit to data	97
Figure 4-28 Heavy loaded bridge, moment, span 30ft – extrapolation to 75 year return period	97
Figure 4-29 High loaded bridge, moment, span 60ft – nonparametric fit to data	98
Figure 4-30 High loaded bridge, moment, span 60ft – extrapolation to 75 year return period	99
Figure 4-31 High loaded bridge, moment, span 90ft – nonparametric fit to data	99
Figure 4-32 High loaded bridge, moment, span 90ft – extrapolation to 75 year return period	100
Figure 4-33 High loaded bridge, moment, span 120ft – nonparametric fit to data	101
Figure 4-34 High loaded bridge, moment, span 120ft – extrapolation to 75 year return period	101
Figure 4-35 High loaded bridge, moment, span 200ft – nonparametric fit to data	102
Figure 4-36 High loaded bridge, moment, span 200ft – extrapolation to 75 year return period	103

Figure 5-1 Two cases of the simultaneous occurrence	106
Figure 5-2 Scatter plot – Trucks Side by Side – Florida I-10	108
Figure 5-3 Scatter plot – Trucks Side by Side – New York	109
Figure 5-4 Comparison of the mean GVW to the GVW of the whole population - Florida	110
Figure 5-5 Comparison of the mean GVW to the GVW of the whole population – New York	111
Figure 5-6 Scatter plot – Trucks One after another – Florida I-10	113
Figure 5-7 Scatter plot – Trucks one after another – New York	114
Figure 5-8 Comparison of the mean GVW to the GVW of the whole population - Florida	115
Figure 5-9 Comparison of the mean GVW to the GVW of the whole population –New York	116
Figure 5-10 Transverse position of two HS20 trucks to cause the maximum load effect in a girder	119
Figure 5-11 Finite Element Bridge Model.....	120
Figure 5-12 Surface-based tie algorithm (ABAQUS v.6.6 Documentation).....	121
Figure 5-13 Transverse trucks position causing the maximum bending moment in girder G2 – Bridge B1	122
Figure 6-1 Dynamic and Static Strain under a Truck at Highway Speed (Eom 2001)...	131
Figure 7-1 Moment – Curvature curves for a composite W24x76 steel section (Nowak 1999).....	138
Figure 7-2 Moment – Curvature curves for a composite W33x130 steel section (Nowak 1999).....	139
Figure 7-3 Moment – Curvature curves for a composite W36x210 steel section (Nowak 1999).....	139
Figure 7-4 Moment – Curvature curves for a composite W36x300 steel section (Nowak 1999).....	140
Figure 8-1 Cross-sections of Considered Bridges	144
Figure 8-2 Reliability Index for Span 60ft and Live Load Model for High Loaded Bridge	147
Figure 8-3 Reliability Index for Span 60ft and Live Load Model for Medium Loaded Bridge.....	148
Figure 8-4 Reliability Index for Span 60ft and Live Load Model for Low Loaded Bridge	148
Figure 8-5 Reliability Index for Span 120ft and Live Load Model for High Loaded Bridge.....	149
Figure 8-6 Reliability Index for Span 120ft and Live Load Model for Medium Loaded Bridge.....	149
Figure 8-7 Reliability Index for Span 120ft and Live Load Model for Low Loaded Bridge	150
Figure 8-8 Comparison of Reliability Indices for Different Span Lengths – Heavy Loaded Bridge.....	150
Figure 8-9 Comparison of Reliability Indices for Different Span Lengths – Medium Loaded Bridge.....	151

Figure 8-10 Comparison of Reliability Indices for Different Span Lengths – Light Loaded Bridge.....	151
---	-----

LIST OF TABLES

Table 1 Number of Trucks with Corresponding Probability and Time Period.....	30
Table 2 Simple Span Moment , $M(HS20)$, $M(HL93)$, and Mean Maximum 75 Year Moment, $M(75)$	32
Table 3 Mean Maximum Moments for Simple Span Due to a Single Truck (Divided by Corresponding HS20 Moment).....	32
Table 4 Mean Maximum Moments for Simple Span Due to a Single Truck (Divided by Corresponding HL-93 Moment)	32
Table 5 Simple Span Shear, $S(HS20)$, $S(HL93)$, and Mean Maximum 75 Year Moment, $S(75)$	33
Table 6 Mean Maximum Shears for Simple Span Due to a Single Truck (Divided by Corresponding HS20 Shear)	33
Table 7 Mean Maximum Shears for Simple Span Due to a Single Truck (Divided by Corresponding HL-93 Shear).....	34
Table 8 Negative Moment for Continuous Span, $Mn(HS20)$, $Mn(HL93)$, and Mean Maximum 75 Year Negative Moment, $Mn(75)$	34
Table 9 Mean Max. Negative Moments for Continuous Span Due to a Single Truck (Divided by Corresponding HS20 Negative Moment)	35
Table 10 Mean Max. Negative Moments for Continuous Span Due to a Single Truck (Divided by Corresponding HL-93 Negative Moment).....	35
Table 11 Summary of collected WIM data.....	40
Table 12 Mean Maximum Moments for Simple Span 30ft Due to a Single Truck (Divided by Corresponding HL93 Moment).....	48
Table 13 Mean Maximum Moments for Simple Span 60ft Due to a Single Truck (Divided by Corresponding HL93 Moment).....	49
Table 14 Mean Maximum Moments for Simple Span 90ft Due to a Single Truck (Divided by Corresponding HL93 Moment).....	50
Table 15 Mean Maximum Moments for Simple Span 120ft Due to a Single Truck (Divided by Corresponding HL93 Moment)	51
Table 16 Mean Maximum Moments for Simple Span 200ft Due to a Single Truck (Divided by Corresponding HL93 Moment)	52
Table 17 Removal of the heaviest vehicles New York.....	59
Table 18 Removal of the heaviest vehicles California	61
Table 19 Removal of the heaviest vehicles Mississippi	63
Table 20 Number of Trucks with Corresponding Probability and Time Period.....	74
Table 21 Mean Maximum Moments for Simple Span for 1 year and 75 years.....	81
Table 22 Mean Maximum Shear for Simple Span for 1 year and 75 years.....	82
Table 23 Number of Trucks with Corresponding Probability and Time Period.....	85
Table 24 Mean Maximum Moments for Simple Span for 1 year and 75 years.....	92
Table 25 Mean Maximum Shear for Simple Span for 1 year and 75 years.....	93
Table 26 Number of Trucks with Corresponding Probability and Time Period.....	96

Table 27 Mean Maximum Moments for Simple Span for 1 year and 75 years.....	103
Table 28 Mean Maximum Shear for Simple Span for 1 year and 75 years.....	104
Table 29 Composite Steel Girders Used In FEM Analysis	122
Table 30 Bending moments for different transverse position of two trucks Bridge B1 .	122
Table 31 Bending moments for different transverse position of two trucks Bridge B2 .	123
Table 32 Bending moments for different transverse position of two trucks Bridge B3 .	123
Table 33 Bending moments for different transverse position of two trucks Bridge B4 .	123
Table 34 Bending moments for different transverse position of two trucks Bridge B5 .	123
Table 35 Bending moments for different transverse position of two trucks Bridge B6 .	124
Table 36 Girder Distribution Factor – Maximum Bending Moment - Bridge B1	124
Table 37 Girder Distribution Factor – Maximum Bending Moment - Bridge B2	125
Table 38 Girder Distribution Factor – Maximum Bending Moment - Bridge B3	125
Table 39 Girder Distribution Factor – Maximum Bending Moment - Bridge B4	125
Table 40 Girder Distribution Factor – Maximum Bending Moment - Bridge B5	126
Table 41 Girder Distribution Factor – Maximum Bending Moment - Bridge B6	126
Table 42 The Statistical Parameters of Dead Load.....	128
Table 43 Low Loaded Bridge - Mean Ratio M_T/M_{HL93}	129
Table 44 Medium Loaded Bridge - Mean Ratio M_T/M_{HL93}	129
Table 45 High Loaded Bridge - Mean Ratio M_T/M_{HL93}	129
Table 46 Low Loaded Bridge - Coefficient of Variation of LL	130
Table 47 Medium Loaded Bridge - Coefficient of Variation of LL	130
Table 48 High Loaded Bridge - Coefficient of Variation of LL.....	130
Table 49 Low Loaded Bridge - Coefficient of Variation of LL with Dynamic Load	133
Table 50 Medium Loaded Bridge - Coefficient of Variation of LL with Dynamic Load	133
Table 51 High Loaded Bridge - Coefficient of Variation of LL with Dynamic Load....	133
Table 52 Statistical Parameters of Resistance	135
Table 53 Composite Steel Girders	143
Table 54 Example of Reliability Index Calculations	146
Table 55 Reliability Index for Span 60ft	147
Table 56 Reliability Index for Span 120ft	147
Table 57 Recommended target reliability indices	153

CHAPTER 1. INTRODUCTION

1.1. PROBLEM STATEMENT

The public and government agencies are concerned about the safety and serviceability of aging bridge infrastructure. In the United States according to Federal Highway Administration there are 601,411 bridges in which 151,391 are functional obsolete or structurally deficient. The major factors that have contributed to the present situation are: the age of the structures, inadequate maintenance, increasing load spectra, and environmental contamination. Potential replacement or rehabilitation requires substantial amounts of capital expenditure. Federal funds are limited and there is a need to quantify the safety margin of existing infrastructure subjected to new conditions.

Current bridge specifications are based on Load and Resistance Factor design. The boundaries of acceptable performance are specified by limit state functions. Implementation of load and resistance factors guaranties the satisfactory margin of safety. Finding the balance between both sides of the equation became important to the engineering community.

The reliability of new structural systems had increased because of the increase in the performance of materials, quality of execution and improvement in analytical and numerical methods. Oppositely, the increase in truck traffic and unpredictable gross vehicle weight brought uncertainty in determination of satisfactory margin of safety.

While the capacity of a bridge can be determined with a high accuracy by diagnostics, field inspections and adequate analysis methods, the correct prediction of live load is complicated. The increase in truck traffic raised a concern that the HL93 AASHTO load may not be representative for US traffic loads. Therefore there is a need to verify the accuracy of the current code load by analyzing available Weigh-In-Motion measurements and develop a new statistical live load model.

1.2. OBJECTIVE AND SCOPE OF THE RESEARCH

The main objective of this study is to develop a statistical model for live load for highway bridges based on new weigh-in-motion (WIM) data. The extensive WIM data were collected under normal truck traffic in several states. These weigh-in-motion measurements provide an unbiased truck traffic data and serve as a remarkable basis for the reliability-based code calibration. Expected extreme loads effects were determined for various time periods. Multiple presence of vehicles in a lane and in adjacent lanes was considered. Unique approach was developed to model the degree of correlation for multiple occurrence of trucks.

The specific plan includes the following tasks:

- Review of the reliability analysis procedures and various statistical methods
- Processing of the available Weigh-In-Motion data.
- Development of statistical models for moments and shears

- Development of the proposed design live load model
- Assessment of correlation for multiple presence
- Simulation of multiple presence using the Finite Element Method models for selected bridges
- The reliability analysis of selected bridges to verify the developed live load model

Short and medium span simply supported girder bridges are considered for the evaluation of structural safety. The design of the bridges is performed according to AASHTO LRFD Code provisions for Strength I limit state. Girder spacing of 6, 8 and 10 ft and spans of 60 ft and 120ft are studied. The statistics for resistance of bridge girders are obtained from the available literature.

1.3. PROIR INVESTIGATIONS

The use of Weigh-In-Motion data for analysis of bridge live load was investigated by many researchers. The available analysis is presented in many reports, dissertations and articles. WIM was a basis to develop new live load models or to verify the existing ones. Nowak and Hong (1991), (Hong 1990), presented a statistical procedure for development of live load model based on the Ontario truck survey data which was used in NCHRP Report 368 (Nowak 1999). Ghosn and Moses (1998) defined the bridge resistance as the maximum gross vehicle load that is causing the formation of a collapse mechanism.

Hwang (1990) added dynamic load induced by the vehicular load to the statistical model of live load. (Hwang 1990). NCHRP Project 12-76 (Sivakumar et al. 2008) presented protocol for collecting of Weigh-In-Motion records. WIM data from NCHRP Project 12-76 was used in this study.

First implementation of reliability analysis in code calibration was proposed by (Galambos and Ravindra 1978) for buildings and by (Nowak and Lind 1979) for bridges. Nowak and Tharmabala (1988) used reliability models in bridge evaluation. Application of extreme value theory for extrapolation to a given return period was performed by (Castillo 1988), (Coles 2001).

Multiple presence was analyzed by many researchers (Bakht and Jaeger L. G. 1990), (Eom 2001; Eom and Nowak 2001), (Zokai et al. 1991), (Tabsh and Nowak 1991).

1.4. ORGANIZATION OF THE THESIS

The dissertation is organized in 9 Chapters and Appendix A.

Chapter 1 presents the introduction, problem statement, objective and scope of the presented dissertation.

Chapter 2 summarizes basic concepts of structural reliability. Extreme value theory is presented and the methods to calculate reliability index.

Chapter 3 presents available Weigh-In-Motion data. Analysis of the load spectra for different states is shown.

Chapter 4 presents in depth analysis of three selected sites. Static part of the live load model is developed.

Chapter 5 presents multiple presence analysis. Degree of correlation is determined. Girder distribution factors for multiple lane loading is analyzed using Finite Element Method

Chapter 6 summarizes load combinations.

Chapter 7 summarizes resistance model.

Chapter 8 studies the reliability of steel composite girders.

Chapter 9 summarizes the findings of the research and concludes the study.

Appendix A presents extensive analysis of available Weigh-In-Motion data.

CHAPTER 2. STRUCTURAL RELIABILITY MODELS

2.1. INTRODUCTION

Structural engineering nowadays is based on the structural reliability which can be defined as the capacity of the structure to carry out its performance under specified conditions within its span live. It can also be defined as the probability of exceeding the limit states at every stage of live of the construction. The modern structural design requires implementing a precise estimation of uncertainties which could include numerical models, geometry, material properties, fabrication processes and parameters of loads. This study shows the structural reliability in terms of reliability index which will be defined later in this chapter.

2.2. PROBABILITY DISTRIBUTIONS

The probability density function and cumulative distribution function describes the performance of a random variable. The random variable can be categorized as discrete or continuous. The most common discrete distributions are: Bernoulli, Binomial, Continuous, Geometric, Hypergeometric, Negative Binomial, Poisson, Uniform. The cumulative distribution function for the discrete variables is the sum of probability functions for all values and can be represented graphically as steps. The cumulative distribution function for the continuous distribution is an integral of probability functions and the graphical representation is the smooth line. In this chapter only continuous distributions are presented and more specifically extreme ones. The more information

about different distribution can be found in (Nowak and Collins 2000) and other reliability publications (Ang and Tang 1975), (Ang and Tang 1984), (Ayyub and McCuen 1997) .

2.2.1 The Extreme Value Distribution

Extreme value distributions are often used to model the smallest or largest value among a large set of independent, identically distributed random values representing measurements or observations. Extreme values by definition are rare. They are needed for return periods much higher than the observed sample. Extrapolation from the observed sample to the assumed future level like 75 year maximum moment requires implementation of the extreme value theory. Extreme value analysis includes probability of occurrence of events that are beyond observed sample (Castillo 1988), (Gumbel 1958), (Gumbel 1941), (Gumbel 1949).

Looking at extreme, the smallest and the largest values from the sample with a given size n independent observations have to be considered. In this study only maximum values were taken into consideration.

$$M_n = \max(X_1, \dots, X_n) \quad \text{Eq - 1}$$

Where X_1, \dots, X_n is a sequence of independent random variables having the same distribution function $F(x)$. Assuming that n is the number of observations and $X_1, X_2, X_3, \dots, X_n$ are independent, and identically distributed, then:

$$F_{X_1}(x) = F_{X_2}(x) = \dots = F_{X_n}(x) = F_X(x) \quad \text{Eq - 2}$$

Observing that M_n is less than the particular maximum value m then all the variables (X_1, \dots, X_n) are less than m . The cumulative distribution function of X_n can be represented as:

$$F_{M_n}(m) = F_X(m)^n \quad \text{Eq - 3}$$

and the probability density function $f_{M_n}(m)$:

$$f_n(m) = nF(m)^{n-1} f(m) \quad \text{Eq - 4}$$

Graphical representation of CDF and PDF for initial variable X with the exponential probability density function is shown in Figure 2-1 and Figure 2-2.

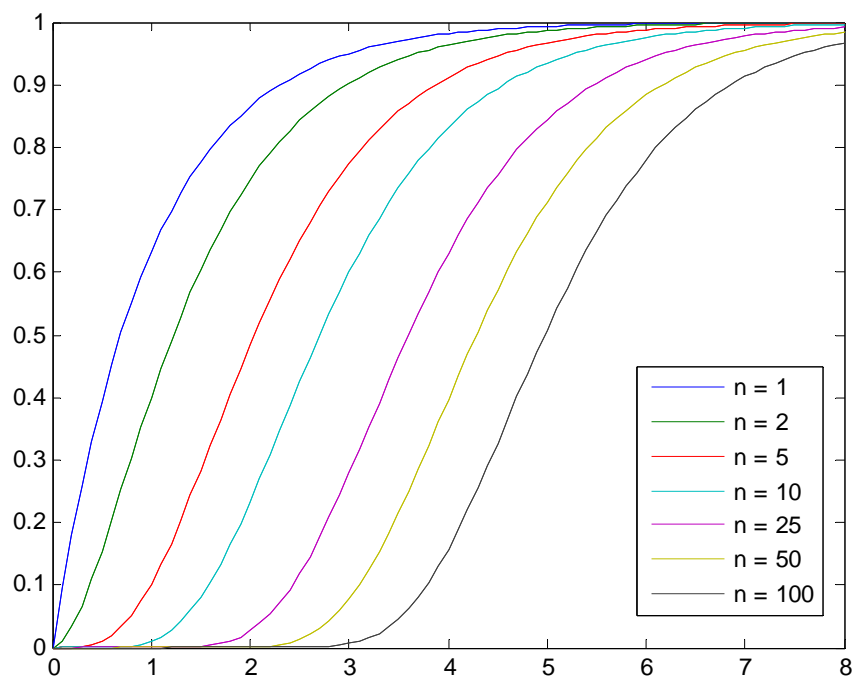


Figure 2-1 Cumulative distribution function

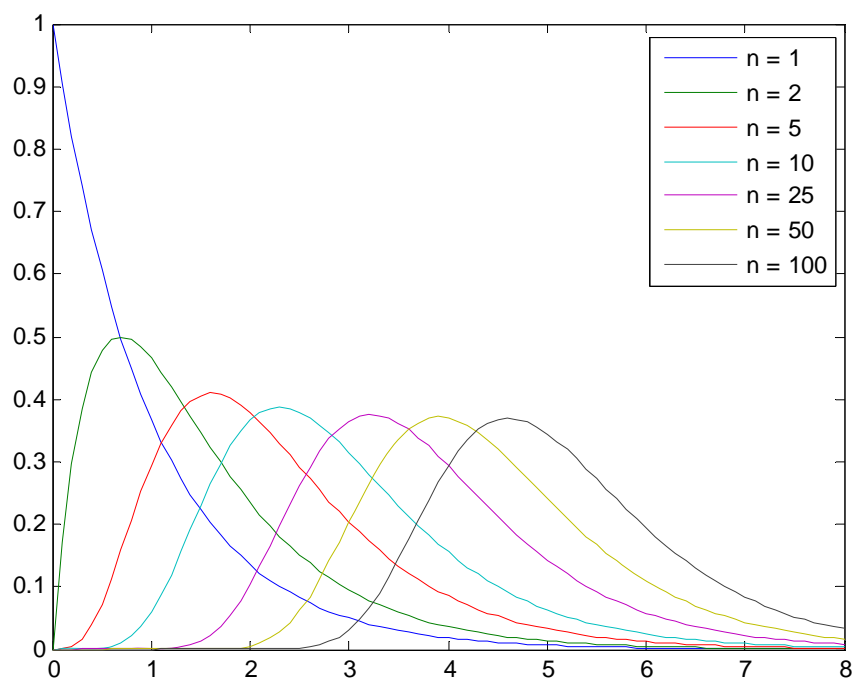


Figure 2-2 Probability density function

2.2.2 The Generalized Extreme Value Distribution

The generalized extreme value (GEV) distribution contains a family of three types of distributions I, II and III which are named Gumbel, Frechet, Weibull respectively (Gumbel 1958), (Coles 2001), (Fisher and Tippett 1928). These types of the asymptotic distributions depend on the behavior of the tails of the probability density functions. If the initial distribution tail is:

- Exponentially decreasing - than it is a Type I
- Decreasing with a polynomial function - than it is a Type II
- Decreasing with a polynomial function but the extreme value is limited - than it is a Type III

Implementation of these three types into one helps to decide the best fit for the distribution tail without using engineering judgment. The cumulative distribution function for generalized extreme value (GEV) is as follows:

$$F(x; \mu, \sigma, \xi) = \begin{cases} \exp\left[-\left(1 + \xi\left(\frac{x-\mu}{\sigma}\right)\right)^{-\frac{1}{\xi}}\right] & \xi \neq 0 \\ \exp\left[-\exp\left[-\left(\frac{x-\mu}{\sigma}\right)\right]\right] & \xi = 0 \end{cases} \quad \text{for } 1 + \frac{\xi(x-\mu)}{\sigma} > 0 \quad \text{Eq - 5}$$

Where $\mu \in [-\infty, \infty]$ is the location parameter, $\sigma \in (0, \infty)$ is the scale parameter, $\xi \in [-\infty, \infty]$ is the shape parameter. An example of the probability density function for three basic types of GEV is shown in Figure 2-3.

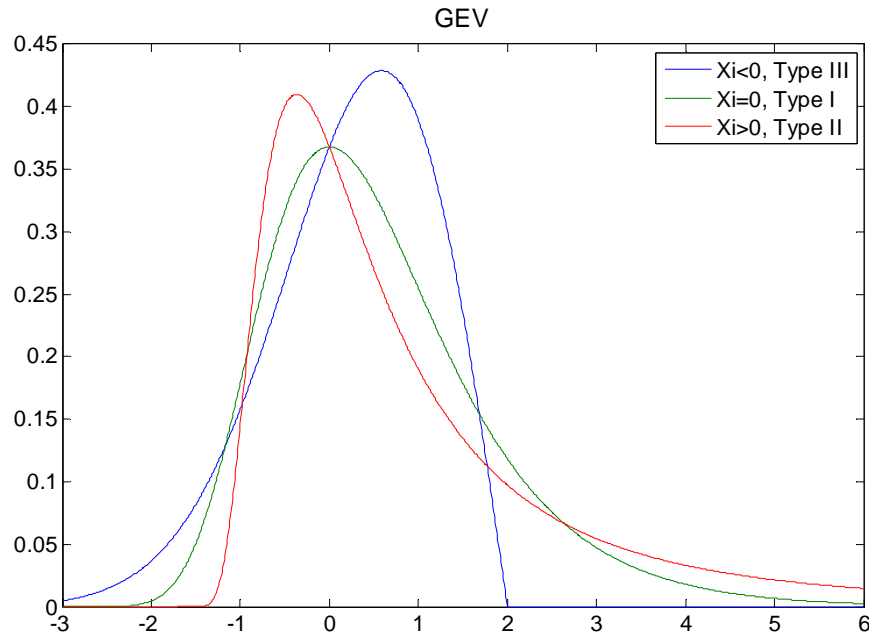


Figure 2-3 Probability density function for three basic forms of GEV

2.2.3 The Generalized Pareto Distribution

The Generalized Pareto Distribution (GPD) can be used in approximating of the upper tail of the distribution (Coles 2001). It is also a family of certain distributions and can be described using three parameters: $\sigma \in (0, \infty)$ the scale parameter, $\xi \in [-\infty, \infty]$ the shape parameter, θ is the threshold parameter. Data points above the given threshold are taken into consideration and the fit to these observations is modeled (Castillo and Hadi 1997).

The tree basic forms of GPD are:

- $\xi = 0$ for distributions with tails decreasing exponentially
- $\xi > 0$ for distributions with tails decreasing polynomially
- $\xi < 0$ for distributions with tails that are finite

The cumulative distribution function for Generalized Pareto Distribution is as follows:

$$F(x; \sigma, \xi, \theta) = \begin{cases} \left(\frac{1}{\sigma}\right) \left(1 + \xi \frac{(x-\theta)}{\sigma}\right)^{-1-\frac{1}{\xi}} & \text{for } \theta < x \text{ when } \xi > 0 \\ \left(\frac{1}{\sigma}\right) e^{-\frac{(x-\theta)}{\sigma}} & \text{for } \theta < x < -\frac{\sigma}{\xi} \text{ when } \xi < 0 \\ \left(\frac{1}{\sigma}\right) e^{-\frac{(x-\theta)}{\sigma}} & \text{for } \theta < x \text{ when } \xi = 0 \end{cases} \quad \text{Eq - 6}$$

In the Figure 2-4 PDF for three basic forms of GPD is shown.

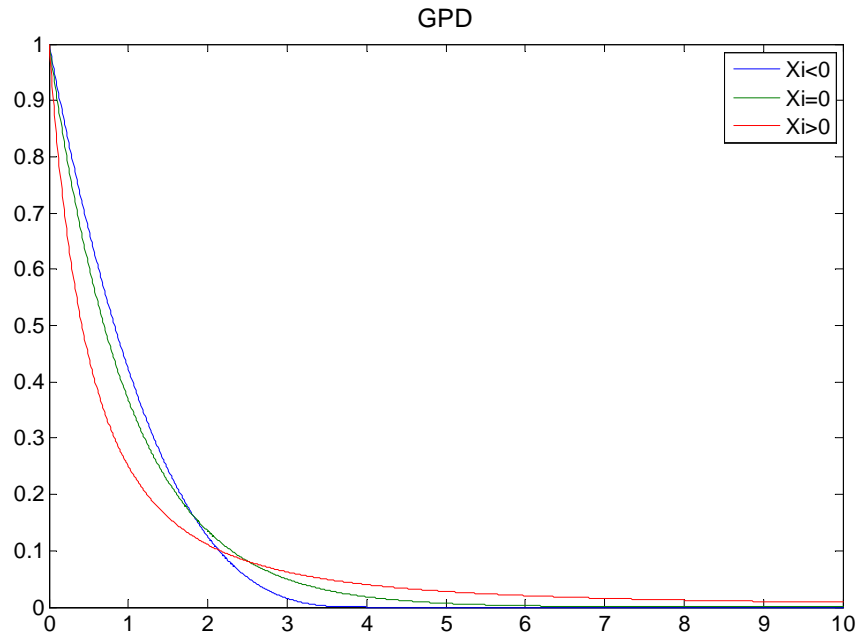


Figure 2-4 Probability density function for three basic forms of GPD

2.2.4 Nonparametric Method

During the research it became obvious that the live load data cannot be approximated with any of known type of distribution. The parametric statistics used to describe the behavior of the sample incorporated extensive engineering judgment. It was needed to include the elements of distribution-free methods.

The difference between the nonparametric and parametric models is that the nonparametric ones are developed on the basis of the given data without any parameters like mean, skew and variance. The parametric distributions can only follow the defined shapes where the nonparametric can adjust the probability density function to any given distribution of the data (Faucher et al. 2001), (Faucher et al. 2001). Using kernel density estimation it is possible to estimate the PDF for the whole data set (Wand and Jones 1995), (Adamowski 1989).

The probability density function $f(x)$ developed from nonparametric approach is as follows (Wand and Jones 1995):

$$f(x) = \frac{1}{nh} \sum_{i=1}^n K\left(\frac{x - X_i}{h}\right) \quad \text{Eq - 7}$$

where X_1, \dots, X_n are the observations, K is the kernel function and h is the bandwidth.

Kernel function is a weight function that cannot be negative and has to follow these conditions:

- $\int K(z)dz = 1$
- $\int zK(z)dz = 0$
- $\int z^2 K(z)dz = C \neq 0$

where C is known as a kernel variance. Typically kernel functions are assumed to be symmetric about the zero. The frequently used kernel functions are: Rectangular, Gaussian, Triangle and Epanechnikov. Center of the weighing function is positioned over

each data point. The contribution from each point is smooth out over a local width (Faucher et al. 2001).

The choice of the kernel function is less important than the estimation of the bandwidth which can be called smoothing factor. The overestimating or underestimating the value of h leads to bad estimation of the probability density function. In this study it was assumed that the bandwidth has to be the most favorable for estimating normal densities (Bowman and Azzalini 1997). In the

Figure 2-5 an example of underestimating and overestimating of the bandwidth is shown. Fits number 2 and 3 represents the overestimating and underestimating of the bandwidth respectively and the fit number 1 shows the optimum one.

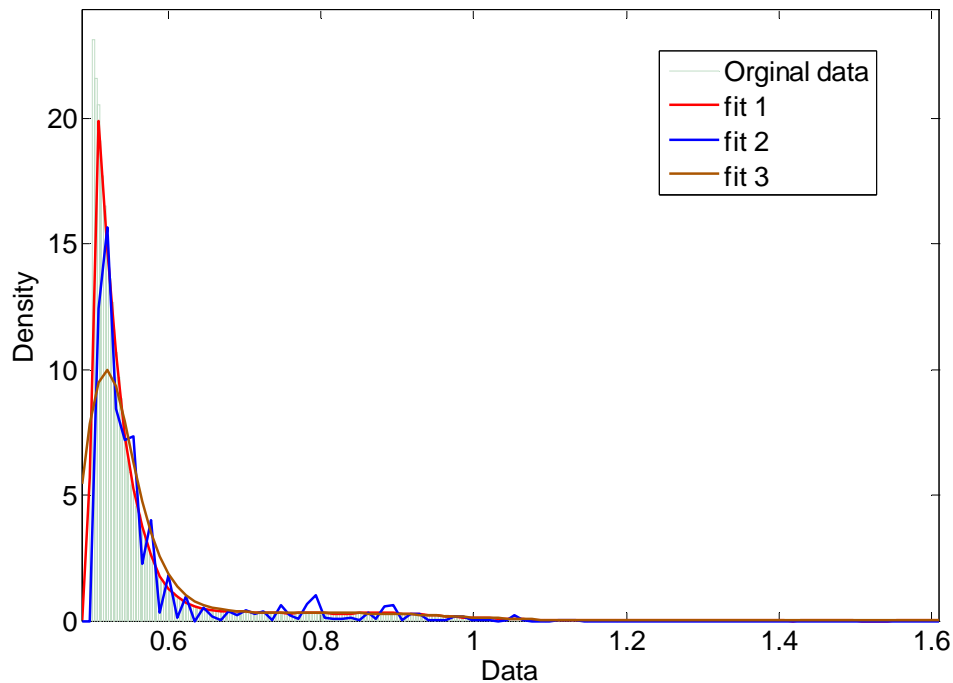


Figure 2-5 Example of kernel density estimation for different bandwidths

2.3. PROBABILITY OF FAILURE AND LIMIT STATE FUNCTION

Structures design is based on the limit states functions. The main concept behind the limit state function is to set the boundary between acceptable and unacceptable behavior of the structure. The typical limit states according to AASHTO are:

- Strength Limit States
- Serviceability Limit States
- Extreme Event Limit State
- Fatigue and Fracture

Each limit state can be described as a function:

$$g(R, Q) = R - Q \quad \text{Eq - 8}$$

where R is the resistance and Q is the load. Setting the border $g(R, Q) = 0$ between acceptable and unacceptable performance, the limit state function $g(R, Q) > 0$ represents the safe performance and $g(R, Q) < 0$ failure. Following the definition of the structural reliability it can be defined that:

$$P_f = P((R - Q) < 0) = P(g < 0) \quad \text{Eq - 9}$$

where P_f is the probability of failure. R, Q and in result g can be a function of n random variables:

$$g(X) = g(X_1, X_2, \dots, X_n) \quad \text{Eq - 10}$$

The two types of random variables discrete and continuous can be represented by the cumulative distribution function (CDF) $F_X(x)$. The first derivative of $F_X(x)$ is called probability density function $f_X(x)$.

The probability of failure can be obtained as follows (Thoft-Christensen and Baker 1982):

$$P_f = \int_{X_1} \dots \int_{X_n} f_X(x_1, x_2, \dots, x_n) dx_1 dx_2 \dots dx_n \quad \text{Eq - 11}$$

in which $f_X(x)$ is the joint probability density function of the random variables.

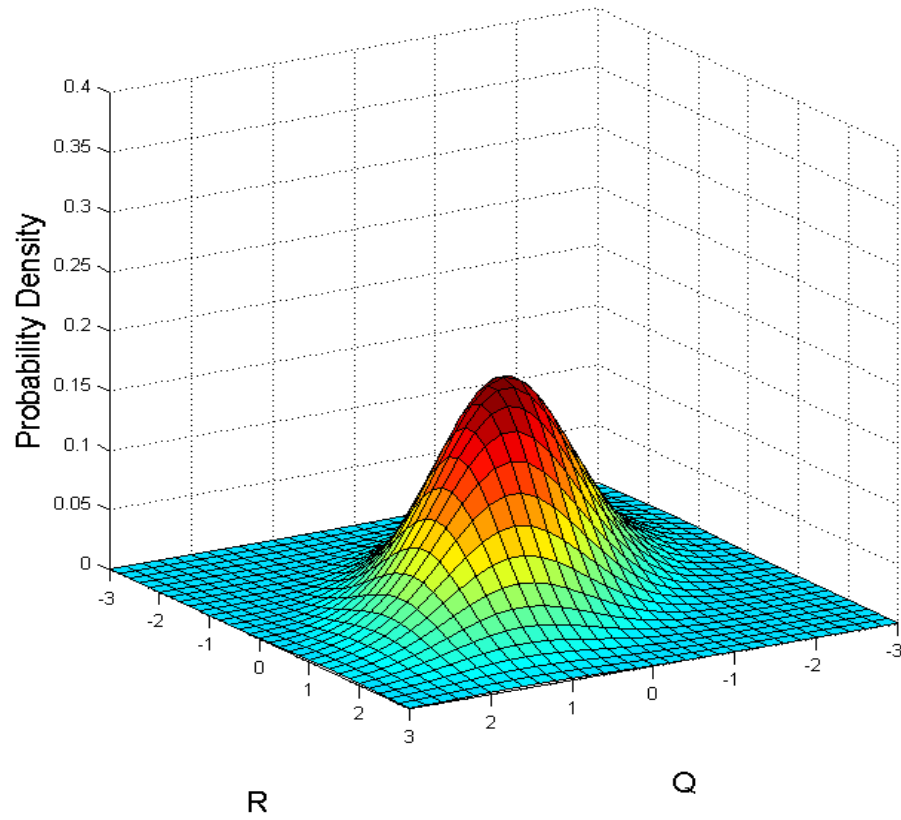


Figure 2-6 The joint probability density function of the random variables.

Having resistance and load as a continuous random variables the probability of failure can be represented as:

$$P_f = \int_{-\infty}^{\infty} F_R(x_i) f_Q(x_i) dx_i$$

Eq - 12

where F_R is the cumulative distribution function of R and f_Q is the probability density function of load.

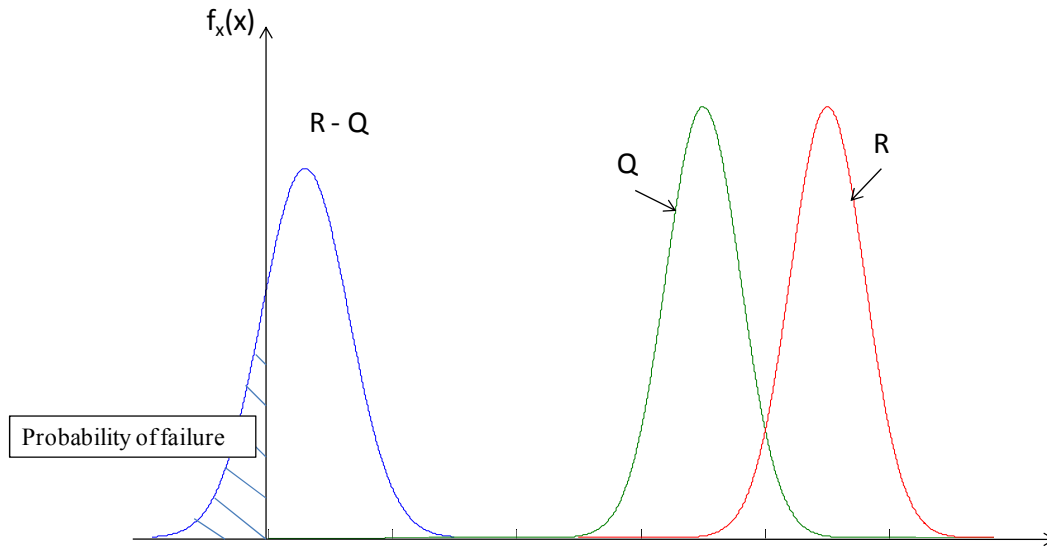


Figure 2-7 Probability density function for load and resistance (Nowak and Collins 2000)

Because of the complexity of the random variables equations 11 and 12 cannot be solved directly. Insufficient number of data to predict correct statistical distribution leads to the statement that the most suitable prediction of failure is based on the reliability index (Galambos and Ravindra 1978), (Thoft-Christensen and Murotsu 1986).

2.4. RELIABILITY INDEX

Probabilistic methods used in structural design are based on the reliability index. Assuming that the limit state is normally distributed the reliability index is related to probability of failure as:

$$\beta = -\Phi^{-1}(P_f) \quad \text{Eq - 13}$$

where $-\Phi^{-1}$ is the inverse standard normal distribution function (Cornell 1967).

First-Order Second-Moment Reliability Index

The simplest method to calculate the reliability index is the First-Order Second-Moment method (Nowak and Collins 2000). This method takes into consideration the linear limit state functions or their linear approximation using Taylor series. First order means that only the first Taylor derivative is used in calculations and Second-Moment refers to the second moment of the random variable (Der Kiureghian et al. 1987), (Ditlevsen and Madsen 1996). First moment is the expected value $E(X)$ and the second moment $E(X^2)$ is a measure of the dispersion in other words variance.

For the uncorrelated random variables X_i the limit state function:

$$g(X_1, \dots, X_n) = g(\mu_{X_1}, \dots, \mu_{X_n}) + \sum_{i=1}^n (X_i - \mu_{X_i}) \frac{\partial g}{\partial X_i} \quad \text{Eq - 14}$$

where $\frac{dg}{dX_i}$ is evaluated at μ_{X_i} .

Knowing that X_i are statistically independent random variables the reliability index is as follows:

$$\beta = \frac{\mu_g}{\sigma_g} = \frac{g(\mu_{X_1}, \dots, \mu_{X_n}) + \sum_{i=1}^n (X_i - \mu_{X_i}) \frac{\partial g}{\partial X_i}}{\sqrt{\sum_{i=1}^n \sigma_{X_i}^2 \left(\frac{\partial g}{\partial X_i} \right)^2}} \quad \text{Eq - 15}$$

If the load and resistance are normally distributed then for the limit state function $g(R, Q)$, the mean value of g is as follows:

$$\mu_g = \mu_R + \mu_Q \quad \text{Eq - 16}$$

Standard deviation:

$$\sigma_g = \sqrt{\sigma_R^2 + \sigma_Q^2} \quad \text{Eq - 17}$$

The reliability index (Cornell 1969),(Cornell 1967):

$$\beta = \frac{\mu_R - \mu_Q}{\sqrt{\sigma_R^2 + \sigma_Q^2}} \quad \text{Eq - 18}$$

If the load and resistance follow the lognormal distribution then for the limit state function $g(R,Q)$, the reliability index is as follows:

$$\beta = \frac{\ln \left(\frac{\mu_R}{\mu_Q} \sqrt{\frac{V_Q^2 + 1}{V_R^2 + 1}} \right)}{\ln((V_Q^2 + 1)(V_R^2 + 1))} \quad \text{Eq - 19}$$

The implementation of the First-Order Second-Moment (FOSM) method is simple. Calculations can be performed only for the normal distributions. The reliability index for distributions other than normal includes considerable level of error (Nowak and Collins 2000; Thoft-Christensen and Murotsu 1986).

CHAPTER 3. RECENT WEIGH-IN-MOTION

3.1. INTRODUCTION

Accurate and economical methods are desired to determine the actual load spectra experienced by the bridge. Serviceability issues must be addressed as deficient bridges are posted, repaired, or replaced. To maximize the use of resources and minimize the cost of repair or avoid the cost of replacement, the evaluation must assess both the present and future capacity of the bridge as well as predict the loads to be experienced for the evaluation period.

Bridge live load is a dynamic load which may be considered as a sum of static and dynamic forces. This study is concerned with the static portion of the load. Actual truck axle weights, axle spacing, gross vehicle weights, average daily truck traffic, (ADTT), and the load effects of the trucks such as moments, shears, and stresses are important parameters used in the effective evaluation of a bridge. Truck data is available from highway weigh station logs as well as through the use of weigh-in-motion (WIM) measurements. The stationary weigh scales at weigh stations are biased and will not reflect accurately the distribution of truck axle weights, axle spacing, and gross vehicle weights due to avoidance of scales by illegally loaded trucks. WIM measurements of trucks can be taken discretely, resulting in unbiased data for a statistically accurate sample of truck traffic traveling a particular highway. In this section the live load spectra at different locations are analyzed based on the WIM data obtained from FHWA and NCHRP Project 12-76. For the comparison reasons it was needed to present the Ontario Truck Survey and the results of the calibration of the AASHTO LRFD Code.

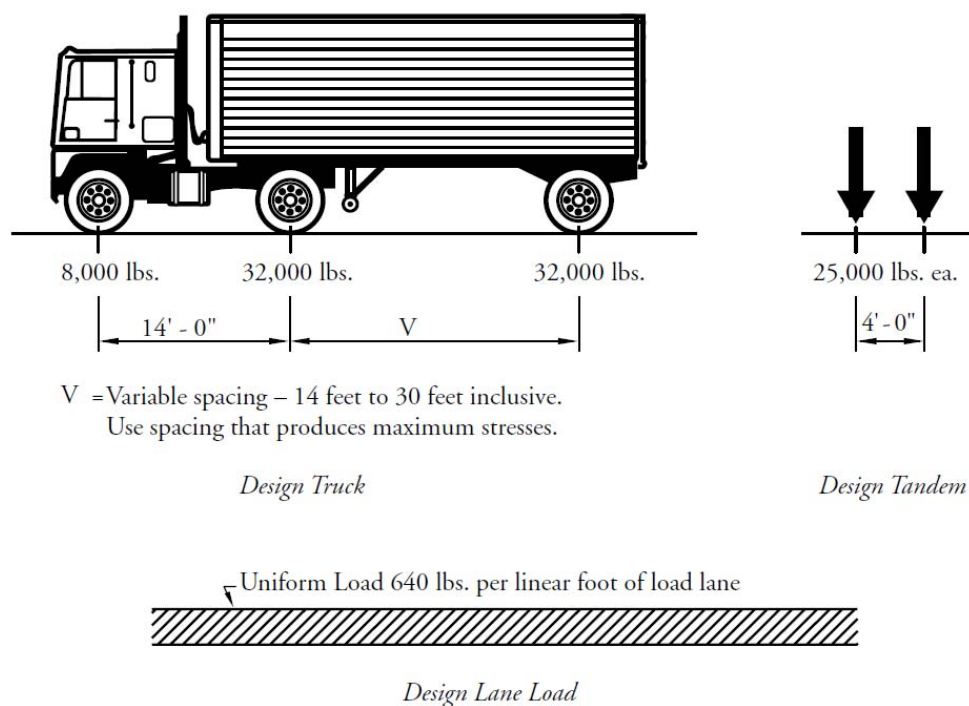


Figure 3-1 AASHTO LRFD HL93 Design Load

3.2. ONTARIO TRUCK SURVEY

At the time of calibration of the AASHTO LRFD Code, there was no reliable truck data available for the USA. Therefore, the live load model was based on the truck survey results provided by the Ontario Ministry of Transportation. The survey was carried out in conjunction with calibration of the Ontario Highway Bridge Design Code (OHBD 1979). However, multiple presence and extrapolations for longer time periods were considered using analytical simulations.

The survey was carried out in mid 1970's and included 9,250 vehicles, measured at various locations in the Province of Ontario, Canada. For each measured vehicle, the record include: number of axles, axle spacing, axle loads and gross vehicle weight. Only the vehicles that appeared to be heavily loaded were stopped and weighed. It was assumed that the surveyed trucks represent two weeks of heavy traffic on a two lane bridge with ADTT = 1000 (in one direction).

For each vehicle from the survey the maximum bending moment, shear force and negative moment for two span bridges was determined. The calculations were carried out for span lengths from 30 ft through 200 ft. The resulting cumulative distribution functions (CDF) for positive moment, negative moment and shear, were plotted on the normal probability paper for an easier interpretation and extrapolation. The CDF's were presented for the surveyed truck moments divided by the HS20 and HL93 moment and are shown in Figure 3-2 to Figure 3-7. The results indicate that the moments are not normally distributed and vary for different span lengths.

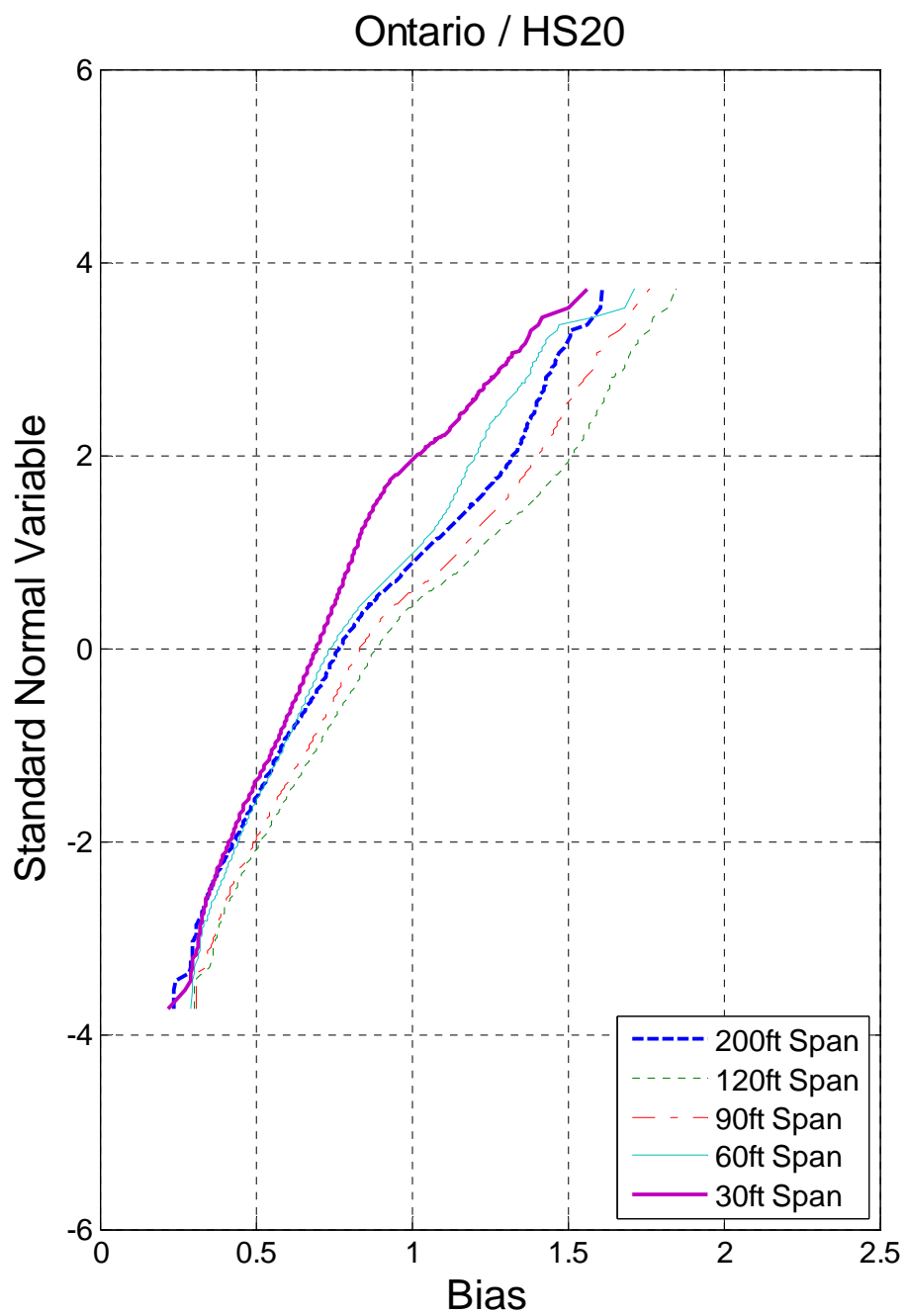


Figure 3-2 Cumulative Distribution Functions of Positive HS20 Moments due to Surveyed Trucks

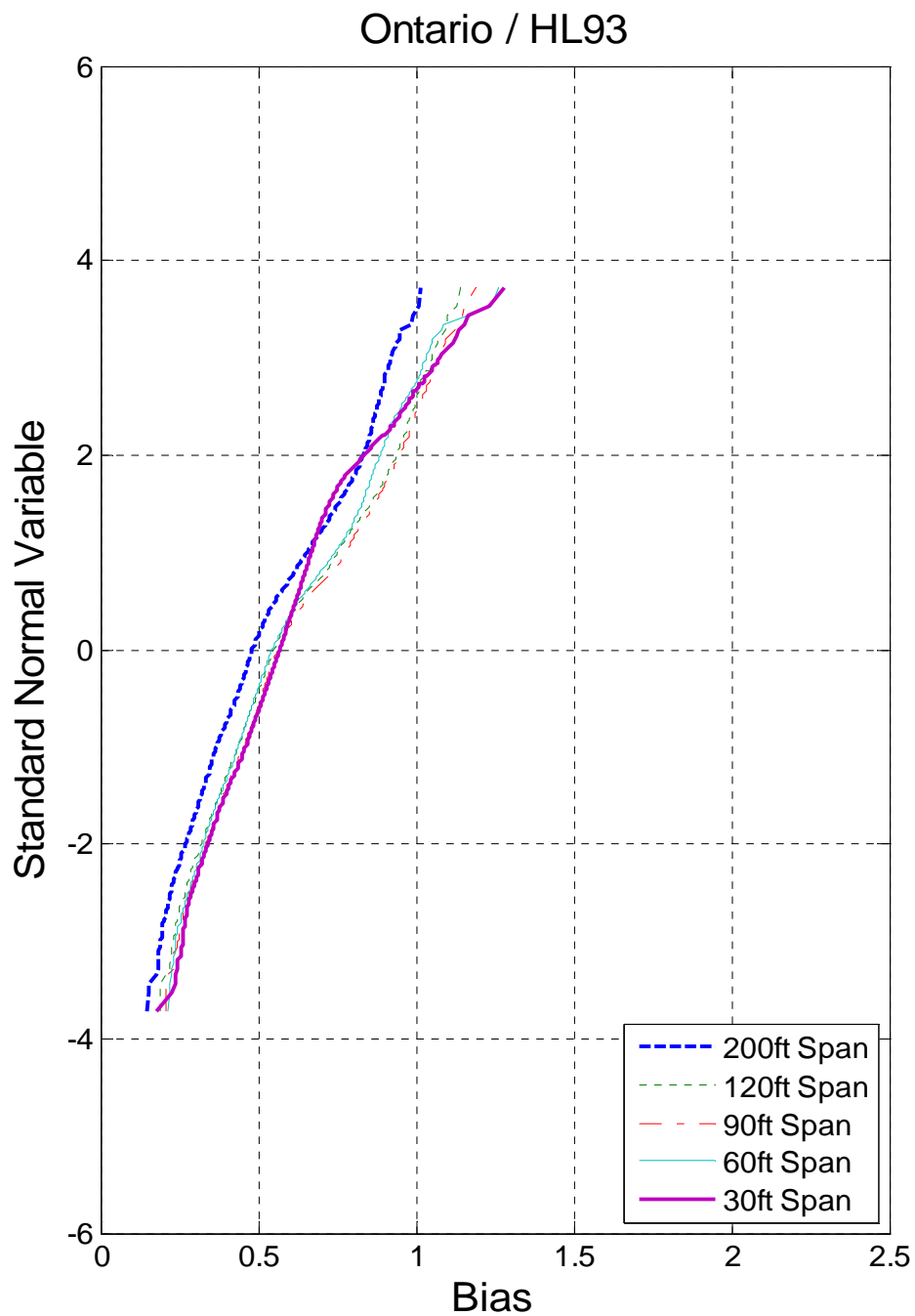


Figure 3-3 Cumulative Distribution Functions of Positive HL93 Moments due to Surveyed Trucks

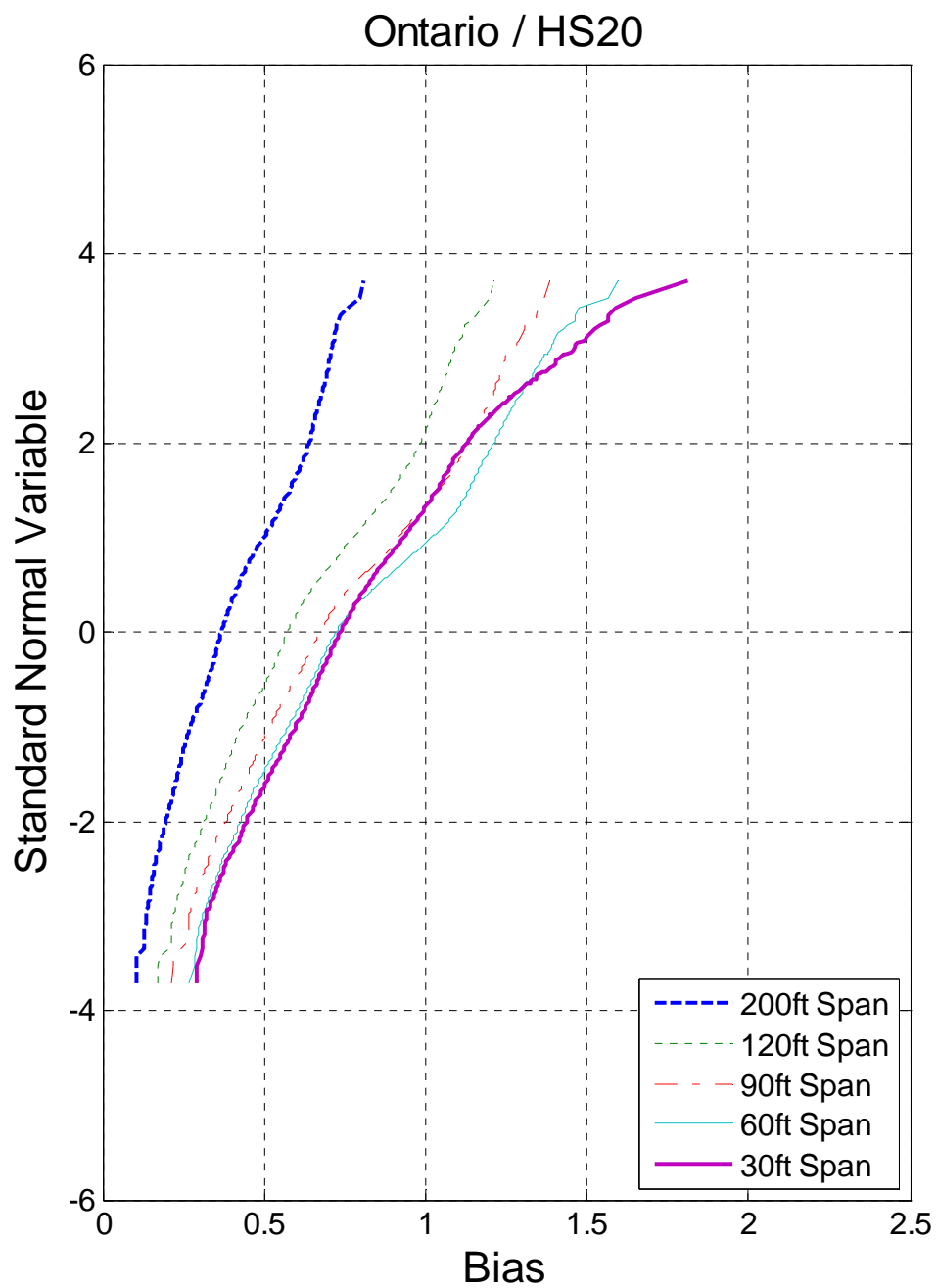


Figure 3-4 Cumulative Distribution Functions of Negative HS20 Moments due to Surveyed Trucks

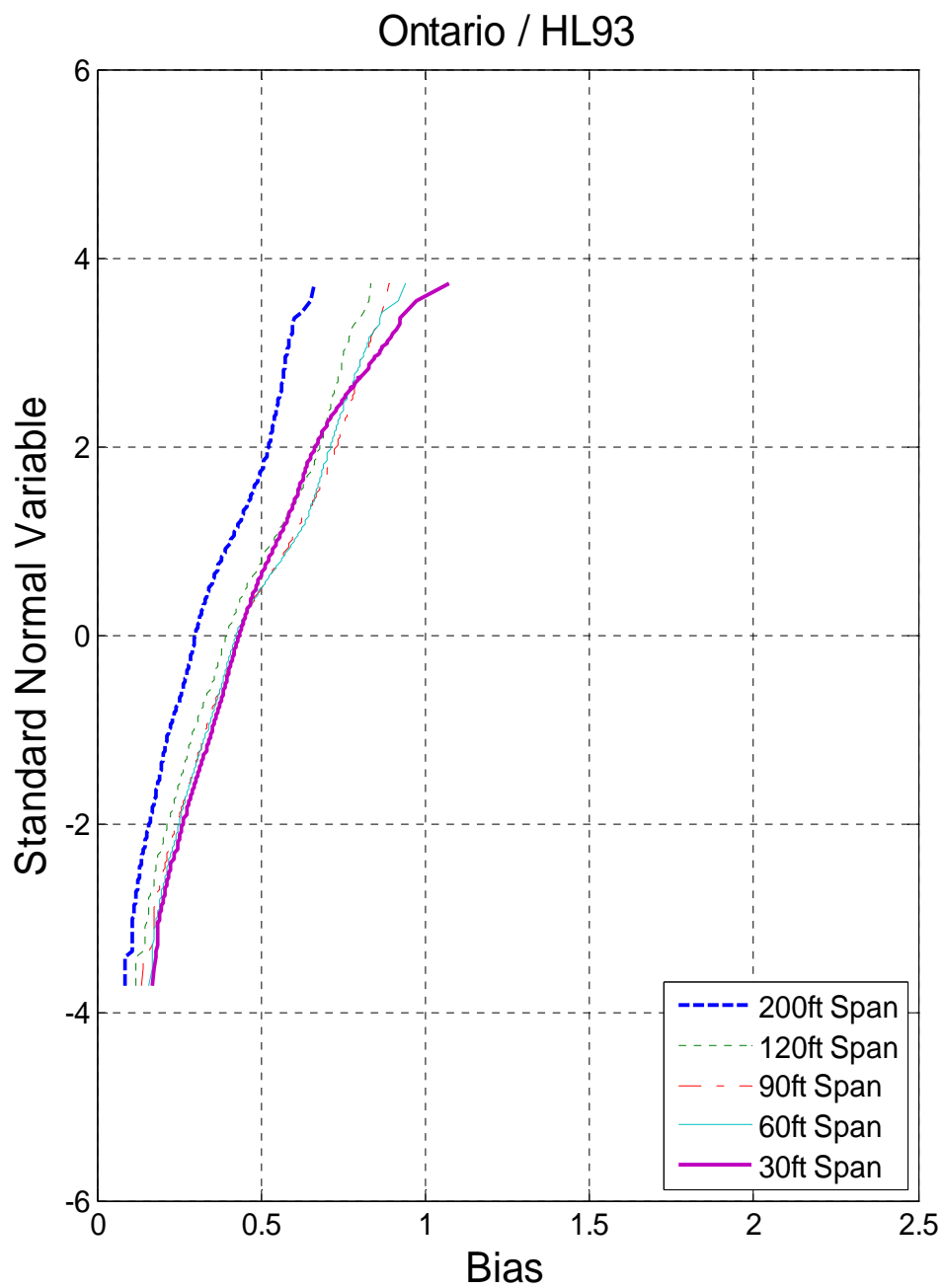


Figure 3-5 Cumulative Distribution Functions of Negative HL93 Moments due to Surveyed Trucks

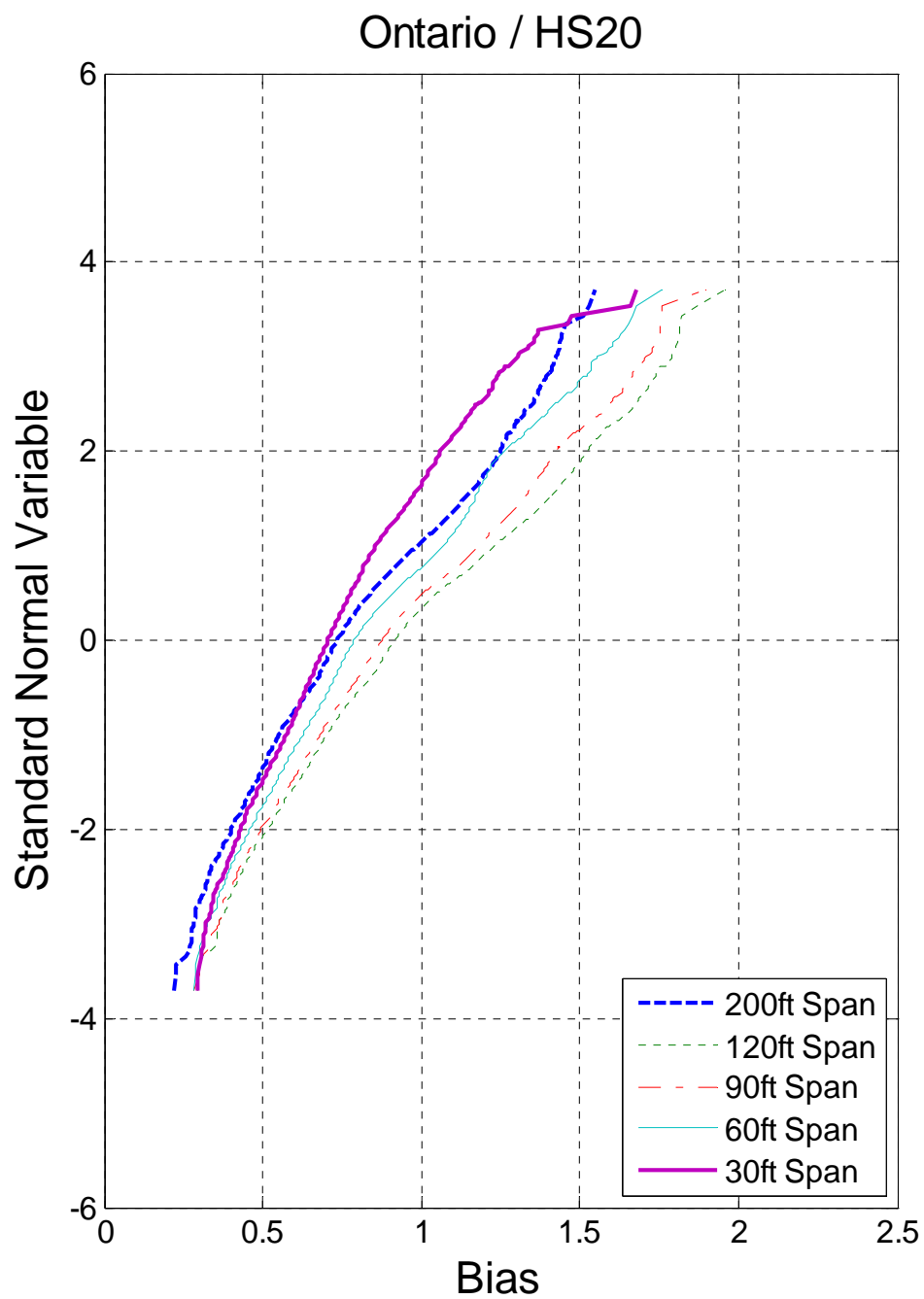


Figure 3-6 Cumulative Distribution Functions of HS20 Shear due to Surveyed Trucks

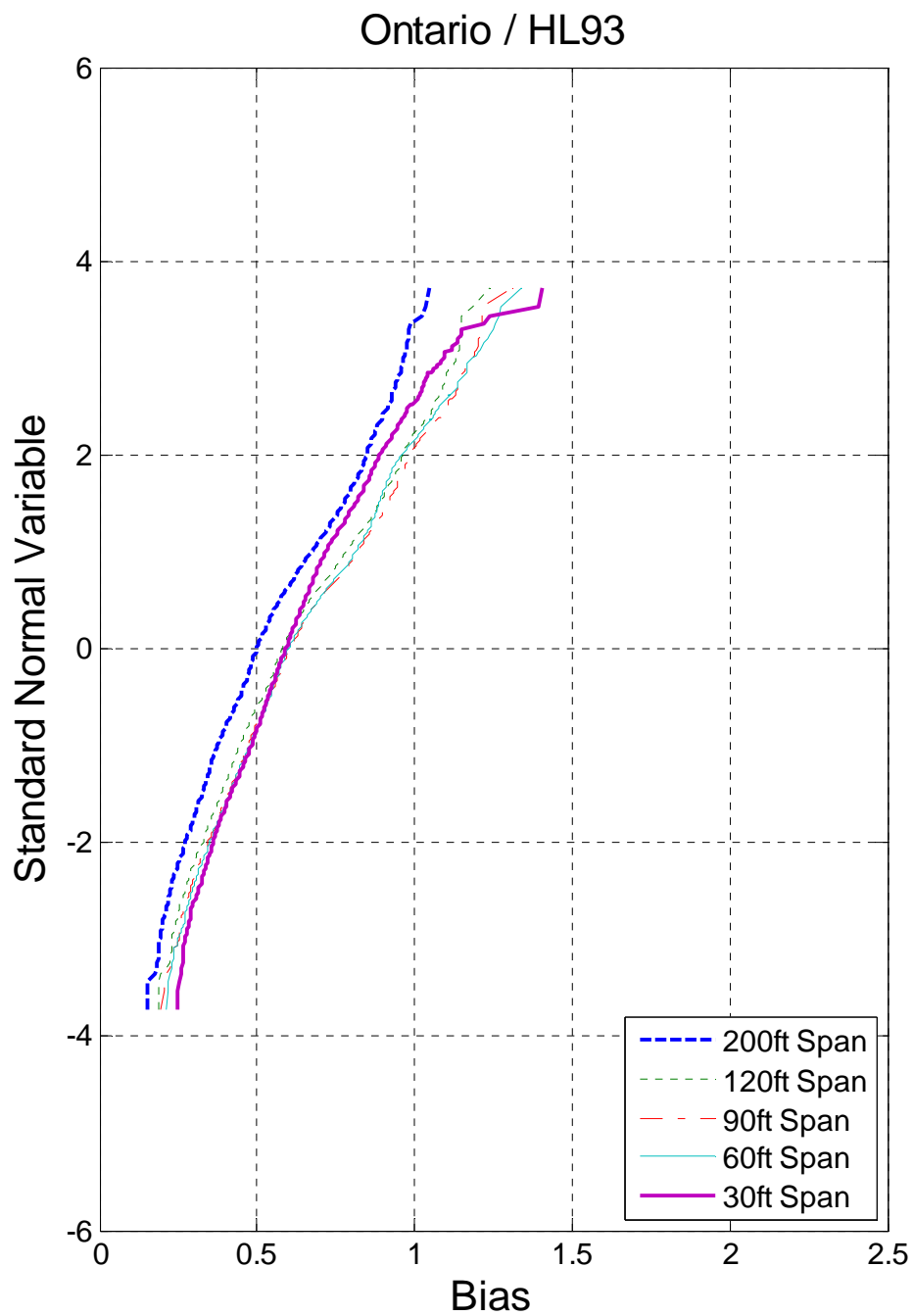


Figure 3-7 Cumulative Distribution Functions of HL93 Shear due to Surveyed Trucks

3.2.1 Interpolations and Extrapolations of Live Load Effects

The most important step in developing the live load model is the prediction of maximum 75 year load effect. It was assumed that the survey data represents two weeks of heavy traffic on a bridge with ADTT = 1000.

Different time periods correspond to different values on the vertical axis. The total number of trucks in the survey is 9250. This corresponds to the probability of $1/9250 = 0.00011$, the inverse normal standard distribution function corresponding to this probability is 3.71. For 75 years, the corresponding value on the vertical axis is 5.33 for probability equal to $5E10^{-8}$ and the number of trucks $N = 20,000,000$. The number of trucks with corresponding probabilities and time periods T is shown in Table 1.

Table 1 Number of Trucks with Corresponding Probability and Time Period

Time period	Number of trucks, N	Probability, 1/N	Inverse normal, z
1 day	1,000	1.00E-03	3.09
2 weeks	10,000	1.00E-04	3.72
1 month	30,000	3.33E-05	3.99
2 months	50,000	2.00E-05	4.11
6 months	150,000	6.67E-06	4.35
1 year	300,000	3.33E-06	4.50
5 years	1,500,000	6.67E-07	4.83
50 years	15,000,000	6.67E-08	5.27
75 years	20,000,000	5.00E-08	5.33

Following the engineering judgment the upper tail of the CDF was represented with the straight line and extrapolated to 75 year level. The example of this extrapolation is shown in Figure 3-8. For ADTT = 1000, the results were tabulated and shown in Table 2 to Table 10.

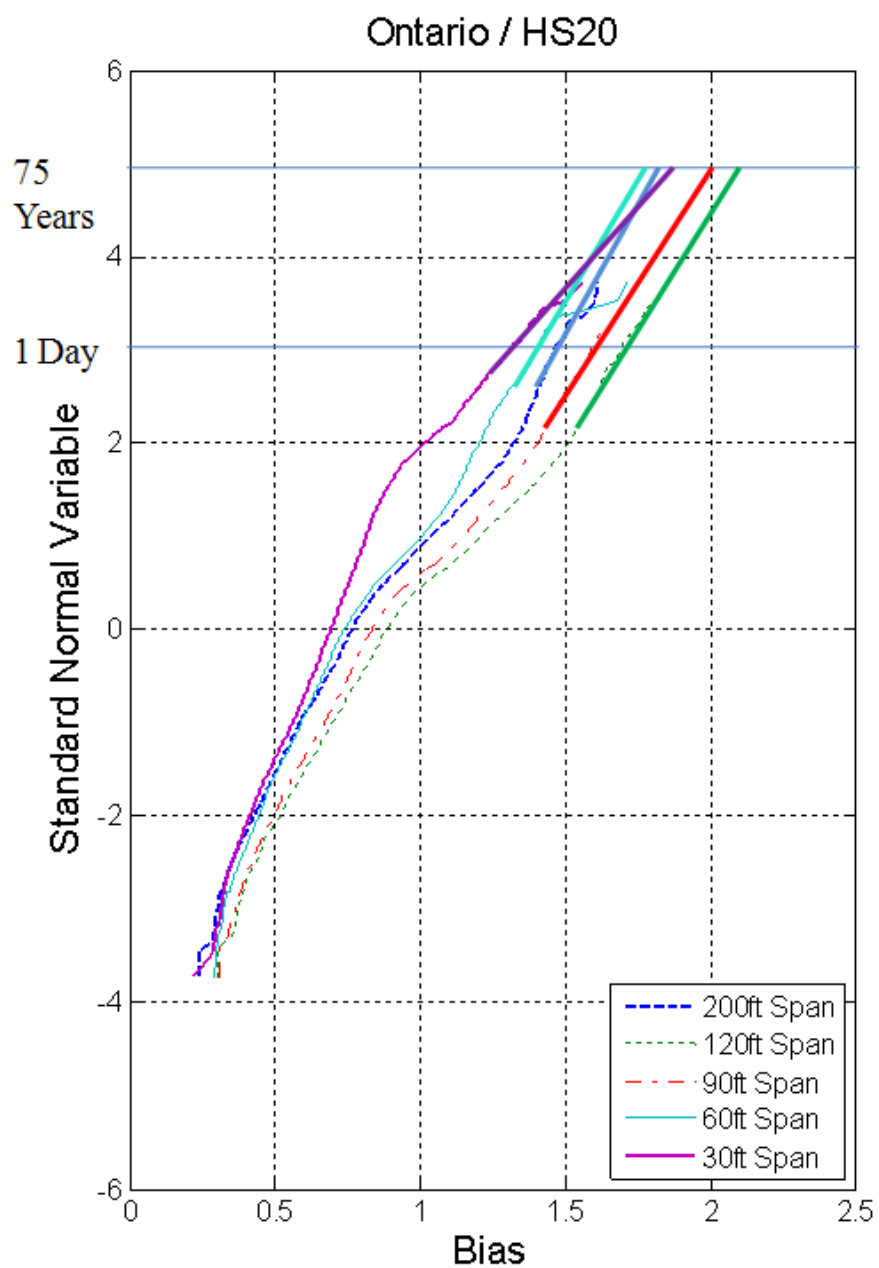


Figure 3-8 Example of Extrapolation for Positive HS20 Moments due to Surveyed Trucks

Table 2 Simple Span Moment , M(HS20), M (HL93), and Mean Maximum 75 Year Moment, M(75)

Span (ft)	M(HS20) (k-ft)	M(HL93) (k-ft)	M(75) (k-ft)
30	315	399	537
60	807	1093	1444
90	1344	1989	2608
120	1883	3034	3917
200	4100	6520	8036

Table 3 Mean Maximum Moments for Simple Span Due to a Single Truck (Divided by Corresponding HS20 Moment)

Span (ft)	average	1 day	2 weeks	1 month	2 months	6 months	1 year	5 years	50 years	75 years
30	0.74	1.20	1.32	1.37	1.42	1.47	1.52	1.61	1.70	1.72
60	0.72	1.37	1.47	1.52	1.56	1.60	1.64	1.69	1.77	1.79
90	0.79	1.51	1.60	1.64	1.68	1.72	1.78	1.84	1.92	1.94
120	0.85	1.63	1.72	1.76	1.80	1.85	1.90	1.97	2.06	2.08
200	0.70	1.38	1.48	1.54	1.57	1.60	1.64	1.71	1.80	1.82

Table 4 Mean Maximum Moments for Simple Span Due to a Single Truck (Divided by Corresponding HL-93 Moment)

Span (ft)	average	1 day	2 weeks	1 month	2 months	6 months	1 year	5 years	50 years	75 years
30	0.58	0.95	1.04	1.08	1.12	1.16	1.20	1.27	1.34	1.36
60	0.53	1.01	1.09	1.12	1.15	1.18	1.21	1.25	1.31	1.32
90	0.53	1.02	1.08	1.11	1.14	1.16	1.20	1.24	1.30	1.31
120	0.53	1.01	1.07	1.09	1.12	1.15	1.18	1.22	1.28	1.29
200	0.44	0.87	0.93	0.97	0.99	1.01	1.03	1.08	1.13	1.14

Table 5 Simple Span Shear, S(HS20), S(HL93), and Mean Maximum 75 Year Moment, S(75)

Span (ft)	S(HS20) (kips)	S(HL93) (kips)	S(75) (kips)
30	49.6	59.2	73.9
60	60.8	80.0	98.5
90	64.5	93.3	119.3
120	66.4	104.8	128.2
200	90.0	132.6	154.8

Table 6 Mean Maximum Shears for Simple Span Due to a Single Truck (Divided by Corresponding HS20 Shear)

Span (ft)	average	1 day	2 weeks	1 month	2 months	6 months	1 year	5 years	50 years	75 years
30	0.68	1.14	1.24	1.29	1.31	1.35	1.38	1.42	1.48	1.49
60	0.73	1.30	1.40	1.44	1.46	1.49	1.52	1.56	1.61	1.62
90	0.80	1.48	1.58	1.62	1.64	1.69	1.72	1.76	1.84	1.85
120	0.83	1.58	1.67	1.71	1.73	1.77	1.80	1.86	1.92	1.93
200	0.68	1.27	1.36	1.39	1.41	1.43	1.47	1.52	1.59	1.60

Table 7 Mean Maximum Shears for Simple Span Due to a Single Truck (Divided by Corresponding HL-93 Shear)

Span (ft)	average	1 day	2 weeks	1 month	2 months	6 months	1 year	5 years	50 years	75 years
30	0.57	0.96	1.04	1.08	1.10	1.13	1.16	1.19	1.24	1.25
60	0.55	0.99	1.06	1.09	1.11	1.13	1.16	1.19	1.22	1.23
90	0.55	1.02	1.09	1.12	1.13	1.17	1.19	1.22	1.27	1.28
120	0.53	1.00	1.06	1.08	1.10	1.12	1.14	1.18	1.22	1.22
200	0.46	0.86	0.92	0.94	0.96	0.97	1.00	1.03	1.08	1.09

Table 8 Negative Moment for Continuous Span, Mn(HS2O), Mn(HL93), and Mean Maximum 75 Year Negative Moment, Mn(75)

Span (ft)	Mn(HS2O) (k-ft)	Mn(HL93) (k-ft)	Mn(75) (k-ft)
30	192	264	338
60	496	806	1008
90	960	1652	1982
120	1568	2493	2992
200	3893	5350	6420

Table 9 Mean Max. Negative Moments for Continuous Span Due to a Single Truck
(Divided by Corresponding HS20 Negative Moment)

Span (ft)	average	1 day	2 weeks	1 month	2 months	6 months	1 year	5 years	50 years	75 years
30	0.89	1.50	1.59	1.62	1.64	1.66	1.68	1.72	1.76	1.77
60	0.73	1.34	1.44	1.49	1.51	1.54	1.56	1.61	1.66	1.67
90	0.55	1.11	1.18	1.21	1.22	1.25	1.26	1.29	1.32	1.33
120	0.48	1.00	1.06	1.08	1.09	1.11	1.12	1.15	1.17	1.18
200	0.33	0.78	0.83	0.84	0.85	0.87	0.88	0.89	0.91	0.92

Table 10 Mean Max. Negative Moments for Continuous Span Due to a Single Truck
(Divided by Corresponding HL-93 Negative Moment)

Span (ft)	average	1 day	2 weeks	1 month	2 months	6 months	1 year	5 years	50 years	75 years
30	0.65	1.09	1.16	1.18	1.19	1.21	1.22	1.25	1.28	1.29
60	0.45	0.82	0.89	0.92	0.93	0.95	0.96	0.99	1.02	1.03
90	0.32	0.65	0.69	0.70	0.71	0.73	0.73	0.75	0.77	0.77
120	0.30	0.63	0.67	0.68	0.69	0.70	0.70	0.72	0.74	0.74
200	0.24	0.57	0.60	0.61	0.62	0.63	0.64	0.65	0.66	0.67

3.3. RECENT WEIGH-IN-MOTION DATA

The truck weigh-in-motion (WIM) data was obtained from Federal Highway Administration and NCHRP Project 12-76. The raw data was filtered and preprocessed to ignore any errors in weight per axle and spacing between axles:

- weight per axle – 0.45kip – 45 kips
- spacing – 0.64ft – 49.2 ft
- total number of axles less or equal 12

An additional filter was also implemented to verify the class of the vehicle.

The Database includes truck records from different states and different sites. Total number of trucks exceeds 47,000,000. The truck data is summarized in Table 11. Each record provides information about the gross vehicle weight, the number of axles, the load per axle, the axle spacing. In this summary the information about the number of lanes on which the truck was recorded was neglected. The cumulative distribution functions of GVW were plotted on the probability paper and are shown in Figure 3-9 to Figure 3-14.

WIM data includes states of Oregon, Florida, Indiana, Mississippi, California and New York. To follow the NCHRP Report 368 (Nowak 1999), the data were plotted on the probability paper. Gross weight of the vehicle varies from 10 to 280 kips and it is strongly site specific. The upper tails of the distributions show large variations which indicate that the live load is strongly site-specific event. For the comparison reasons it was needed to include on the plots the truck measurements performed by the Ontario

Ministry of Transportation which were used in the calibration of the AASHTO LRFD Code.

Data obtained from NCHRP projects is summarized in Table 11 and includes trucks recorded from:

- California
 - Lodi – Site 003 – data recorded continuously from June 2006 till March 2007
 - Antelope East bound – Site 003 – data recorded almost continuously from April 2006 till March 2007 (107 days missing)
 - Antelope West bound – Site 003 – data recorded almost continuously from April 2006 till March 2007 (109 days missing)
 - LA 710 South Bound – Site 059 – data recorded continuously from April 2006 till March 2007
 - LA 710 North Bound – Site 060 – data recorded almost continuously from April 2006 till March 2007 (32 days missing)
 - Bowman – Site 072 - data recorded almost continuously from April 2006 till February 2007 (139 days missing)
- Florida
 - US29 – Site 9916 – data recorded continuously from January 2005 till December 2005 (11 days missing)
 - I-95 – Site 9919 – data recorded continuously from January 2005 till December 2005 (16 days missing)
 - I-75 – Site 9926 – data recorded almost continuously from January 2005 till December 2005 (100 days missing)
 - I-10 – Site 9936 – data recorded almost continuously from January 2005 till December 2005 (100 days missing)
 - State Route – Site 9927 – data recorded almost continuously from January 2004 till December 2004 (5 days missing)
- Indiana
 - Site 9511 – data recorded continuously from January 2006 till December 2006
 - Site 9512 – data recorded continuously from January 2006 till December 2006

- Site 9532 – data recorded continuously from January 2006 till December 2006
- Site 9534 – data recorded continuously from January 2006 till December 2006
- Site 9552 – data recorded continuously from January 2006 till December 2006
- Mississippi
 - I-10 – Site 3015 – data recorded continuously from January 2006 till December 2006 (28 days missing)
 - I-55 – Site 2606 – data recorded continuously from January 2006 till December 2006 (16 days missing)
 - I-55 – Site 4506 – data recorded almost continuously from March 2006 till December 2006 (39 days missing)
 - US49 – Site 6104 – data recorded continuously from January 2006 till December 2006 (5 days missing)
 - US61 – Site 7900 – data recorded almost continuously from January 2006 till December 2006 (49 days missing)
- New York
 - I-95 North Bound – Site 0199 – data recorded continuously from March 2006 till December 2006
 - I-95 South Bound – Site 0199 – data recorded continuously from July 2006 till November 2006
 - I-495 West Bound – Site 0580 – data recorded continuously from January 2006 till December 2006
 - I-495 East Bound – Site 0580 – data recorded continuously from January 2006 till December 2006
 - Highway 12 – Site 2680 – data recorded continuously from January 2005 till December 2005
 - I-84 (east bound and west bound) – Site 8280 – data recorded continuously from January 2006 till December 2006
 - I-84 (east bound and west bound) – Site 8382 – data recorded continuously from January 2005 till December 2005
 - I-81 (north sound and south bound) – Site 9121 – data recorded continuously from January 2005 till December 2005
 - Highway 17 (east bound and west bound) – Site 9631 – data recorded continuously from February 2006 till December 2006

- Oregon

- I-95 North Bound – Site 0199 – data recorded continuously from March 2006 till December 2006
- I-95 South Bound – Site 0199 – data recorded continuously from July 2006 till November 2006
- I-495 West Bound – Site 0580 – data recorded continuously from January 2006 till December 2006
- I-495 East Bound – Site 0580 – data recorded continuously from January 2006 till December 2006

Table 11 Summary of collected WIM data

NCHRP WIM Data		
State	Site Location or Site #	Number of trucks
Oregon	I-5 Woodburn NB	611,830
	I-84 Emigrant Hill WB	213,017
	OR 58 Lowell WB	91,696
	US 97 Bend NB	59,223
	Σ	975,766
Florida	I-10	1,654,006
	I-75	2,679,288
	I-95	2,226,480
	StateRoute	647,965
	US29	728,544
	Σ	7,936,283
Indiana	9511	4,511,842
	9512	2,092,181
	9532	783,352
	9534	5,351,423
	9552	252,315
	Σ	12,991,113
Mississippi	I-10RI	2,548,678
	I-55RI	1,453,909
	I-55UI	1,328,555
	US49PA	1,172,254
	US61PA	206,467
	Σ	6,709,863
California	Antelope EB 003	693,339
	Antelope WB 004	766,188
	Bowman 072	486,084
	LA710 NB 060	2,987,141
	LA710 SB 059	3,343,151
	Lodi 001	2,556,978
	Σ	10,832,881
New York	0199	2,531,866
	0580	2,874,124
	2680	100,488
	8280	1,828,020
	8382	1,594,674
	9121	1,289,295
	9631	105,035
	Σ	7,791,636

NCHRP Data - Oregon

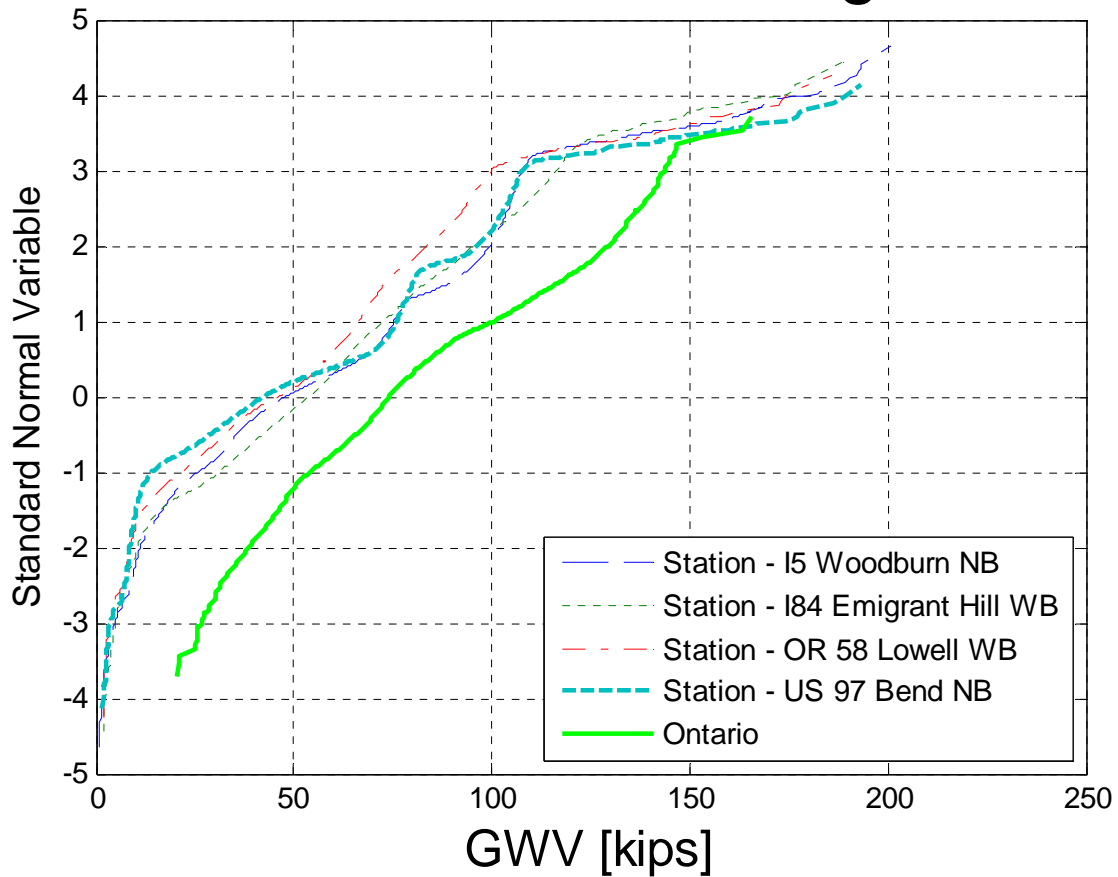


Figure 3-9 Cumulative Distribution Functions of GVW- Oregon and Ontario

Figure 3-9 represents cumulative distribution functions of the gross vehicle weight (GVW) for Oregon plotted on the probability paper. Data collected from four sites represents four months of traffic. The maximum truck GVW's in the data was 200 kips. Mean values varied from 40 to 50 kip and were much lower than the trucks from Ontario measurements. This indicates that majority of the Ontario trucks represents heavy trucks.

NCHRP Data - Florida

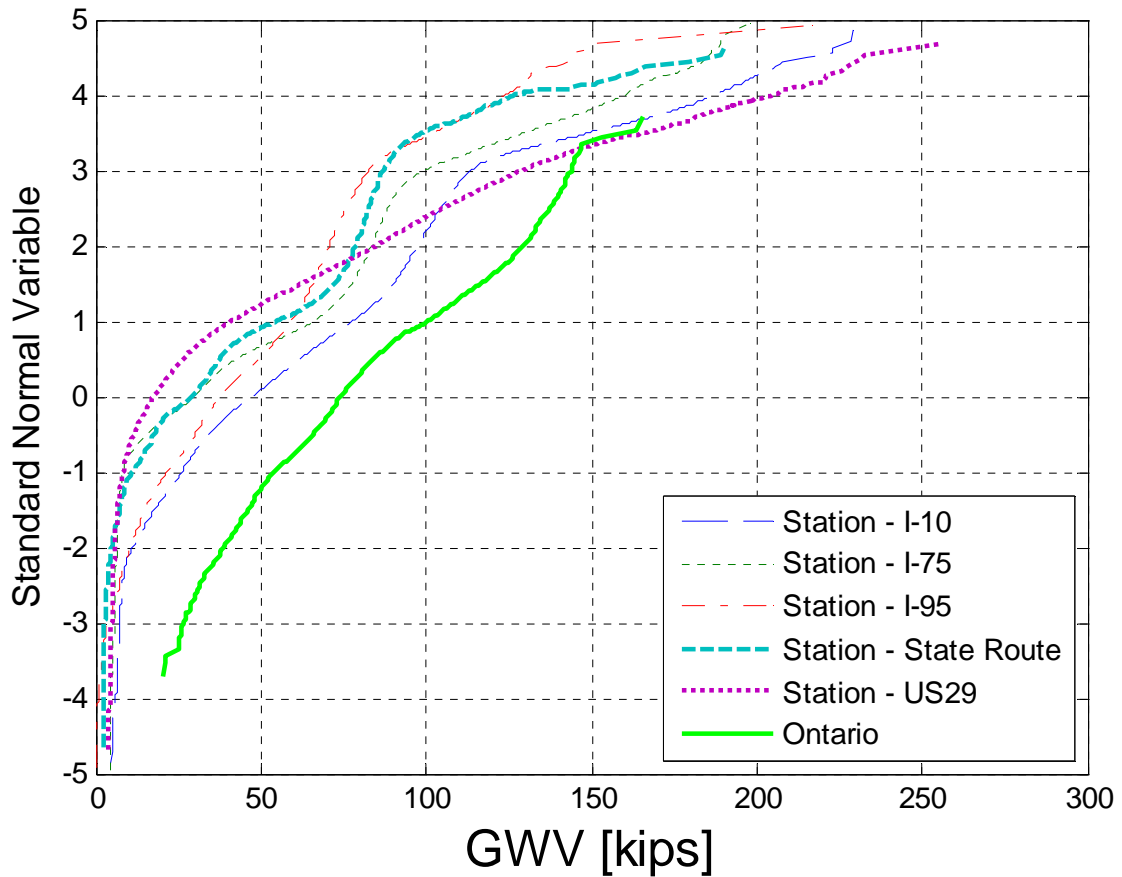


Figure 3-10 Cumulative Distribution Functions of GVW - Florida and Ontario

Figure 3-10 represents cumulative distribution functions of the gross vehicle weight (GVW) for Florida plotted on the probability paper. Data collected from five sites represents one year of traffic. The maximum truck GVW's in the data was above 250 kips. Mean values are also lower than Ontario but maximum values are much larger. Extrapolation of the Ontario data will result in the same values of maximum GVW.

NCHRP Data - Indiana

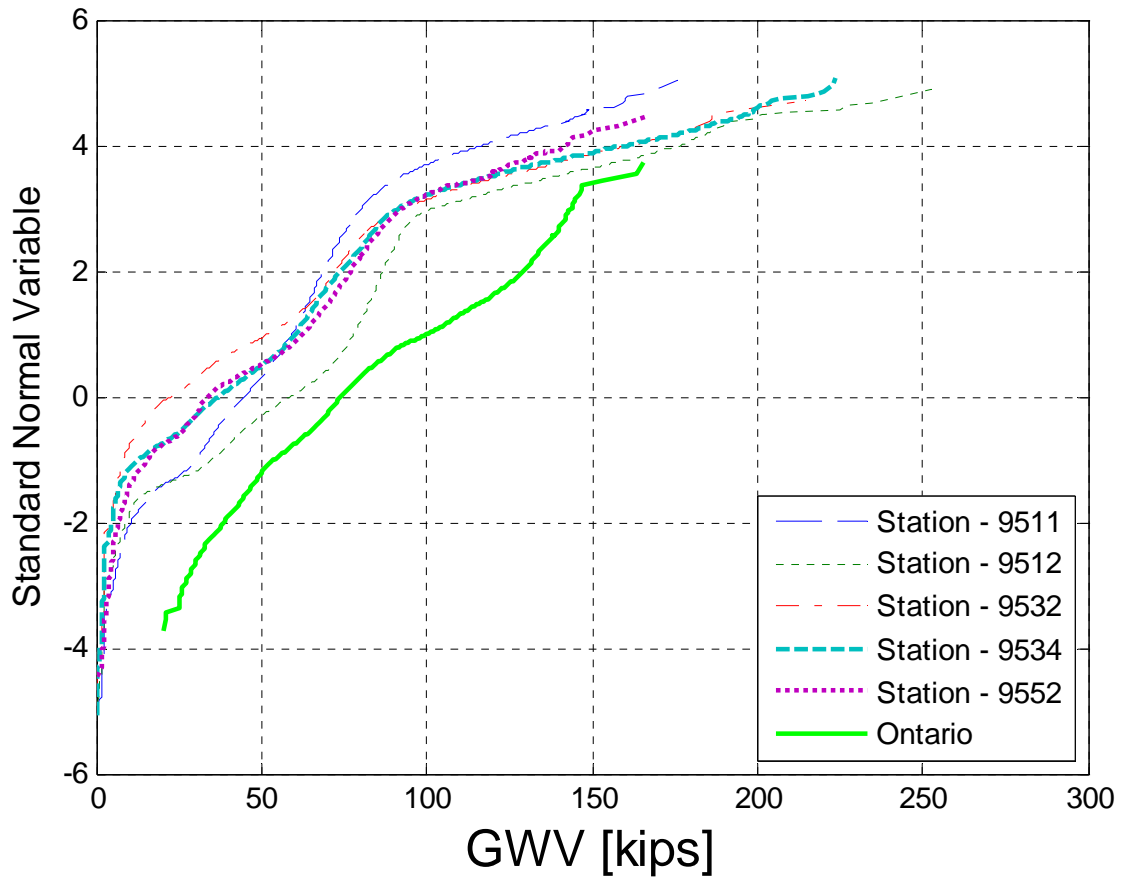


Figure 3-11 Cumulative Distribution Functions of GVW - Indiana and Ontario

Figure 3-11 represents cumulative distribution functions of the gross vehicle weight (GVW) for Indiana plotted on the probability paper. Data collected from five sites represents one year of traffic. The maximum truck GVW's in the data was above 250 kips. Mean values are lower than Ontario and extrapolation of the Ontario truck will result in the same maximum values of GVW.

NCHRP Data - Mississippi

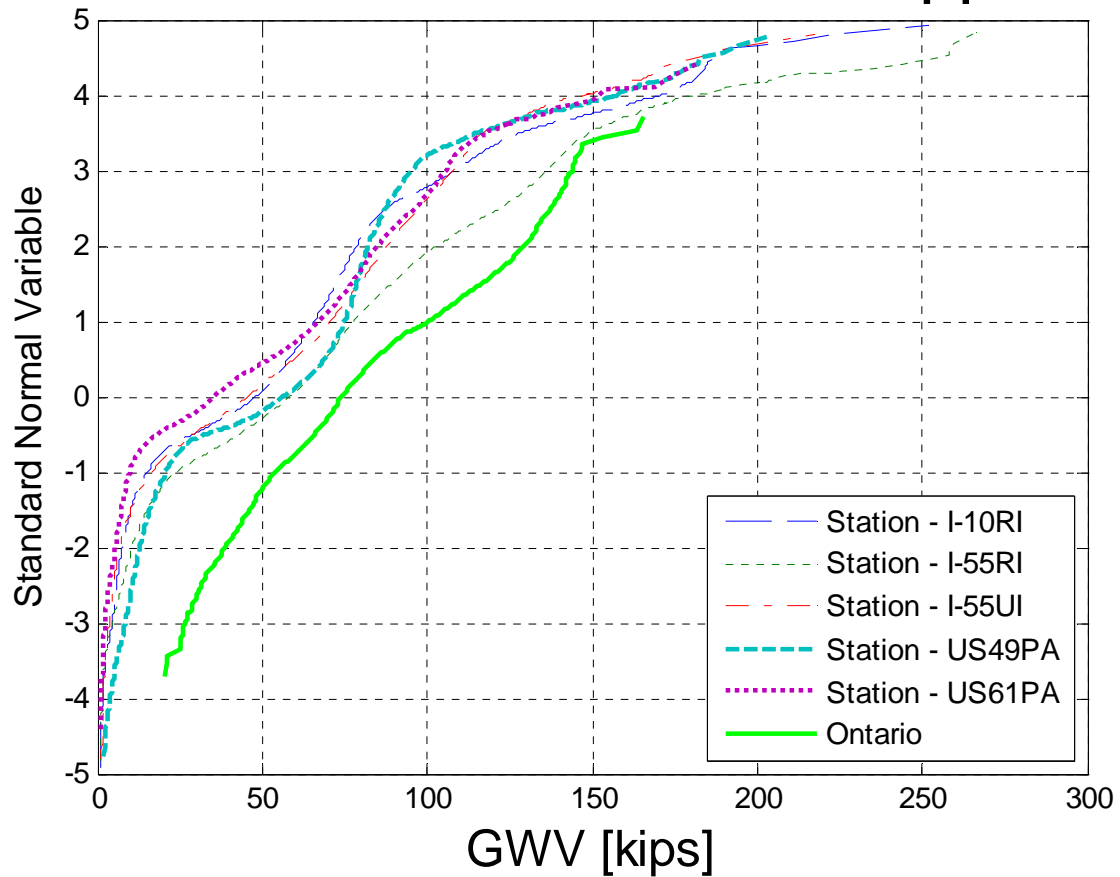


Figure 3-12 Cumulative Distribution Functions of GVW - Mississippi and Ontario

Figure 3-12 represents cumulative distribution functions of the gross vehicle weight (GVW) for Mississippi plotted on the probability paper. Data collected from five sites represents one year of traffic. The maximum truck GVW's in the data was above 260 kips. Mean values are lower than Ontario and extrapolation of the Ontario truck will result in the same maximum values of GVW.

NCHRP Data - California

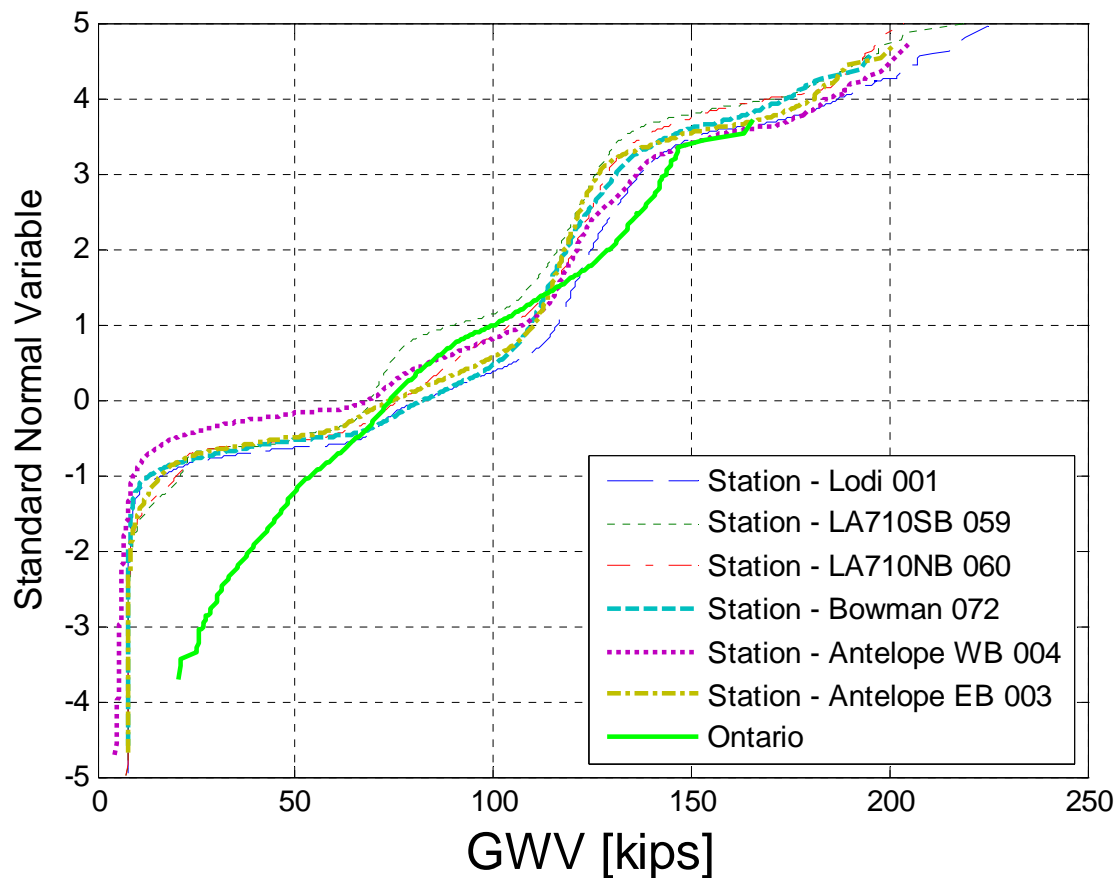


Figure 3-13 Cumulative Distribution Functions of GVW - California and Ontario

Figure 3-13 represents cumulative distribution functions of the gross vehicle weight (GVW) for California plotted on the probability paper. Data collected from six sites represents one year of traffic. The maximum truck GVW's in the data was above 225 kips. Mean values are about the same as mean value for Ontario. Extrapolation of the distribution of the Ontario truck will result in the same maximum values of GVW.

NCHRP Data - New York

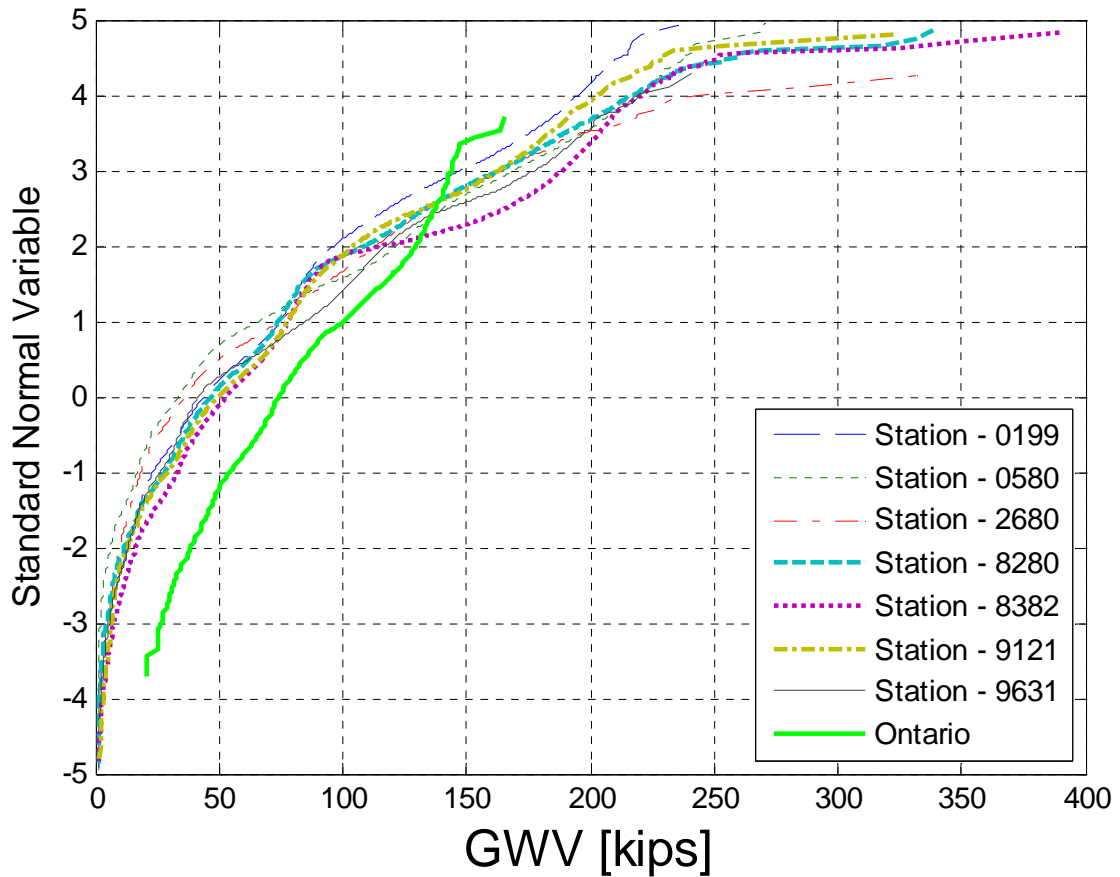


Figure 3-14 Cumulative Distribution Functions of GVW— New York and Ontario

Figure 3-14 represents cumulative distribution functions of the gross vehicle weight (GVW) for California plotted on the probability paper. Data collected from seven sites represents one year of traffic. The maximum truck GVW's in the data was above 380 kips. Mean values 35-50 kips are lower than for Ontario but the maxima are much larger. Even the extrapolation of the distribution of the Ontario truck will not result in the same maximum values of GVW. This indicates that New York sites are extremely heavy and requires special attention.

3.4. TRUCK DATA ANALYSIS

WIM data was analyzed to obtain the maximum live load effect. Live load effect was presented in terms of simple span moment and shear. Because of the amount of data it was necessary to develop a program using Matlab software to calculate the maximum truck load effect. The maximum moment and shear from each database truck was recorded and divided by the corresponding HL93 load. Spans of 30, 60, 90, 120 and 200 ft were considered. The cumulative distribution functions (CDF) of the ratio (bias) of truck moment to HL93 load moment and the ratio of truck shear to HL93 shear for all spans were plotted on the normal probability paper. It was needed to compare the results of the analysis with the data used in the calibration of AASHTO LRFD (Nowak 1999). All the probability plots are included in the Appendix A.

Due to the fact that the light loaded trucks (less than 0.15 HL93) have little or no effect on the performance of the bridge it was decided to include the additional filter. The function of this filter was to remove the biases that are less than 0.15 kip-ft for moment and 0.15 kip for shear. Implementation of this filter resulted in the slightly different distributions of the load effects. As an example Table 12 to Table 16 shows the mean maximum moment for different span lengths due to a single truck divided by the HL93 load for different return periods. Figure 3-15 to Figure 3-19 is the graphical representation of the data from the Table 12 to Table 16.

Table 12 Mean Maximum Moments for Simple Span 30ft Due to a Single Truck (Divided by Corresponding HL93 Moment)

Site	# of trucks, bias > 0.15 kip-ft	1 day	1 week	2 weeks	1 month	2 months	6 months
New York 9631	99,181	1.05	1.27	1.31	1.35	1.39	1.41
New York 9121	1,244,422	1.23	1.38	1.44	1.52	1.60	1.70
New York 8382	1,554,446	1.37	1.51	1.56	1.65	1.73	1.98
New York 8280	1,723,326	1.30	1.48	1.56	1.64	1.66	1.72
New York 2680	89,481	1.15	1.38	1.44	1.51	1.59	1.68
New York 0580	2,550,269	1.53	1.75	1.81	1.90	1.94	1.99
Mississippi I10	2,160,436	0.83	0.96	1.10	1.16	1.25	1.41
Mississippi I55R	1,236,606	1.02	1.41	1.55	1.65	1.69	1.73
Mississippi I55U	1,132,513	0.77	0.83	0.85	0.87	0.89	0.94
Mississippi US49	1,126,214	0.71	0.83	0.93	1.09	1.23	1.65
Indiana 9511	4,212,993	0.85	1.00	1.07	1.14	1.18	1.29
Indiana 9512	1,971,207	0.85	0.98	1.05	1.10	1.14	1.15
Indiana 9532	485,710	0.89	1.04	1.12	1.21	1.35	1.67
Indiana 9534	4,240,887	0.95	1.10	1.15	1.22	1.28	1.40
Florida I10	1,543,855	0.96	1.12	1.17	1.23	1.28	1.31
Florida I75	1,910,691	1.12	1.24	1.28	1.39	1.47	1.58
Florida I95	2,032,797	0.89	0.98	1.01	1.05	1.07	1.32
Florida State Route	482,020	0.89	1.01	1.05	1.13	1.26	1.32
Florida US29	481,201	1.15	1.40	1.48	1.57	1.62	1.69
California Antelope EB	605,367	1.03	1.10	1.13	1.14	1.16	1.34
California Antelope WB	595,144	1.04	1.12	1.16	1.22	1.28	1.36
California Bowman	413,753	0.99	1.05	1.08	1.10	1.14	1.33
California LA 710 NB	2,733,284	1.13	1.21	1.26	1.49	1.56	1.59
California LA 710 SB	3,082,446	1.10	1.16	1.18	1.21	1.24	1.43
California Lodi	2,227,010	1.10	1.16	1.18	1.25	1.33	1.47

Table 13 Mean Maximum Moments for Simple Span 60ft Due to a Single Truck (Divided by Corresponding HL93 Moment)

Site	# of trucks, bias > 0.15 kip-ft	1 day	1 week	2 weeks	1 month	2 months	6 months
New York 9631	99,835	1.02	1.22	1.27	1.36	1.48	1.60
New York 9121	1,247,796	1.18	1.38	1.44	1.51	1.59	1.70
New York 8382	1,558,643	1.32	1.42	1.49	1.55	1.73	1.86
New York 8280	1,731,755	1.41	1.75	1.80	1.84	1.95	2.01
New York 2680	91,122	1.14	1.35	1.43	1.50	1.57	1.69
New York 0580	2,552,508	1.82	2.00	2.04	2.09	2.12	2.16
Mississippi I10	2,159,371	0.80	0.99	1.09	1.16	1.19	1.32
Mississippi I55R	1,236,507	0.92	1.13	1.21	1.31	1.53	1.70
Mississippi I55U	1,138,740	0.75	0.85	0.88	0.93	0.95	1.00
Mississippi US49	1,122,310	0.74	0.85	0.91	0.98	1.06	1.20
Indiana 9511	4,240,585	0.81	0.98	1.08	1.16	1.26	1.45
Indiana 9512	1,963,348	0.82	1.03	1.13	1.19	1.23	1.25
Indiana 9532	495,868	0.85	1.05	1.16	1.31	1.45	1.80
Indiana 9534	4,273,584	0.93	1.12	1.21	1.27	1.30	1.50
Florida I10	1,566,402	0.92	1.09	1.16	1.28	1.34	1.40
Florida I75	1,894,012	1.03	1.15	1.22	1.30	1.40	1.65
Florida I95	2,050,928	0.77	0.84	0.87	0.92	0.99	1.32
Florida State Route	482,754	0.82	0.95	1.01	1.14	1.20	1.24
Florida US29	445,470	1.15	1.40	1.48	1.56	1.60	1.79
California Antelope EB	601,214	1.14	1.23	1.28	1.31	1.38	1.53
California Antelope WB	583,214	1.19	1.31	1.36	1.41	1.44	1.63
California Bowman	408,324	1.13	1.21	1.24	1.33	1.36	1.41
California LA 710 NB	2,719,045	1.16	1.30	1.35	1.41	1.51	1.63
California LA 710 SB	3,071,947	1.14	1.27	1.30	1.36	1.41	1.68
California Lodi	2,207,721	1.24	1.38	1.50	1.60	1.65	1.87

Table 14 Mean Maximum Moments for Simple Span 90ft Due to a Single Truck (Divided by Corresponding HL93 Moment)

Site	# of trucks, bias > 0.15 kip-ft	1 day	1 week	2 weeks	1 month	2 months	6 months
New York 9631	98,731	1.08	1.31	1.37	1.46	1.55	1.61
New York 9121	1,235,963	1.23	1.39	1.47	1.52	1.58	1.61
New York 8382	1,551,454	1.37	1.46	1.49	1.58	1.66	1.86
New York 8280	1,717,972	1.45	1.73	1.77	1.82	1.89	1.96
New York 2680	89,286	1.11	1.33	1.37	1.47	1.57	1.84
New York 0580	2,474,407	1.76	1.93	1.96	2.00	2.03	2.09
Mississippi I10	2,103,302	0.84	1.00	1.14	1.19	1.24	1.41
Mississippi I55R	1,218,632	0.97	1.08	1.17	1.23	1.33	1.40
Mississippi I55U	1,117,276	0.78	0.86	0.89	0.95	0.97	0.99
Mississippi US49	1,096,883	0.73	0.85	0.91	0.99	1.02	1.10
Indiana 9511	4,216,415	0.75	0.90	1.01	1.14	1.24	1.39
Indiana 9512	1,950,776	0.80	1.01	1.10	1.21	1.25	1.32
Indiana 9532	472,549	0.78	1.06	1.17	1.29	1.45	1.67
Indiana 9534	4,212,184	0.88	1.12	1.24	1.31	1.39	1.51
Florida I10	1,555,488	0.92	1.09	1.15	1.22	1.25	1.39
Florida I75	1,839,087	0.95	1.11	1.22	1.28	1.34	1.61
Florida I95	2,019,956	0.71	0.80	0.84	0.89	0.95	1.18
Florida State Route	468,100	0.73	0.89	0.97	1.08	1.11	1.26
Florida US29	406,346	1.08	1.32	1.40	1.45	1.49	1.66
California Antelope EB	587,160	1.08	1.25	1.33	1.36	1.41	1.47
California Antelope WB	565,799	1.13	1.35	1.39	1.42	1.46	1.63
California Bowman	401,560	1.07	1.18	1.29	1.34	1.38	1.41
California LA 710 NB	2,676,044	1.12	1.36	1.39	1.42	1.44	1.61
California LA 710 SB	3,022,329	1.09	1.34	1.37	1.39	1.42	1.66
California Lodi	2,174,378	1.19	1.42	1.50	1.57	1.59	1.82

Table 15 Mean Maximum Moments for Simple Span 120ft Due to a Single Truck
(Divided by Corresponding HL93 Moment)

Site	# of trucks, bias > 0.15 kip-ft	1 day	1 week	2 weeks	1 month	2 months	6 months
New York 9631	97,420	1.10	1.32	1.38	1.47	1.53	1.61
New York 9121	1,220,905	1.24	1.39	1.45	1.52	1.54	1.57
New York 8382	1,541,822	1.39	1.48	1.52	1.56	1.63	1.99
New York 8280	1,700,685	1.41	1.64	1.68	1.73	1.78	1.86
New York 2680	86,322	1.07	1.30	1.36	1.47	1.52	1.79
New York 0580	2,374,506	1.65	1.81	1.84	1.88	1.91	1.97
Mississippi I10	2,047,651	0.85	0.99	1.15	1.22	1.26	1.35
Mississippi I55R	1,198,325	0.98	1.09	1.16	1.22	1.31	1.41
Mississippi I55U	1,095,630	0.79	0.88	0.90	0.95	0.98	1.04
Mississippi US49	1,068,165	0.72	0.87	0.92	0.99	1.02	1.07
Indiana 9511	4,188,186	0.71	0.87	0.98	1.10	1.20	1.31
Indiana 9512	1,941,128	0.84	1.04	1.12	1.17	1.23	1.29
Indiana 9532	449,832	0.75	1.00	1.12	1.26	1.36	1.56
Indiana 9534	4,172,033	0.88	1.13	1.27	1.35	1.39	1.44
Florida I10	1,540,092	0.95	1.12	1.16	1.20	1.24	1.37
Florida I75	1,781,427	0.93	1.11	1.19	1.29	1.32	1.52
Florida I95	1,980,859	0.69	0.79	0.83	0.87	0.90	1.19
Florida State Route	447,635	0.69	0.82	0.95	1.01	1.11	1.27
Florida US29	372,389	1.05	1.27	1.31	1.37	1.40	1.53
California Antelope EB	574,301	1.02	1.22	1.29	1.34	1.37	1.42
California Antelope WB	551,705	1.07	1.32	1.35	1.40	1.41	1.56
California Bowman	396,849	1.01	1.15	1.25	1.31	1.34	1.36
California LA 710 NB	2,630,562	1.08	1.34	1.37	1.40	1.41	1.53
California LA 710 SB	2,981,677	1.05	1.31	1.34	1.39	1.44	1.57
California Lodi	2,147,370	1.17	1.38	1.44	1.49	1.52	1.73

Table 16 Mean Maximum Moments for Simple Span 200ft Due to a Single Truck
(Divided by Corresponding HL93 Moment)

Site	# of trucks, bias > 0.15 kip-ft	1 day	1 week	2 weeks	1 month	2 months	6 months
New York 9631	93,026	1.00	1.19	1.24	1.31	1.35	1.46
New York 9121	1,172,676	1.13	1.24	1.30	1.35	1.38	1.42
New York 8382	1,504,970	1.27	1.35	1.39	1.44	1.46	2.12
New York 8280	1,641,396	1.23	1.43	1.46	1.52	1.56	1.78
New York 2680	77,420	0.93	1.15	1.22	1.31	1.39	1.62
New York 0580	2,073,107	1.39	1.53	1.55	1.58	1.62	1.65
Mississippi I10	1,918,535	0.81	0.95	1.08	1.12	1.16	1.20
Mississippi I55R	1,145,596	0.90	1.00	1.06	1.17	1.27	1.42
Mississippi I55U	1,035,487	0.72	0.82	0.88	0.93	0.97	1.01
Mississippi US49	974,334	0.67	0.87	0.90	0.93	0.97	1.00
Indiana 9511	4,102,293	0.64	0.78	0.86	0.96	1.01	1.11
Indiana 9512	1,914,033	0.82	0.99	1.06	1.10	1.13	1.21
Indiana 9532	401,301	0.68	0.90	0.99	1.10	1.16	1.32
Indiana 9534	3,974,949	0.83	1.06	1.16	1.23	1.26	1.34
Florida I10	1,471,439	0.89	1.08	1.12	1.15	1.20	1.26
Florida I75	1,637,195	0.85	1.00	1.08	1.15	1.18	1.28
Florida I95	1,859,894	0.64	0.74	0.77	0.79	0.84	1.21
Florida State Route	387,731	0.59	0.73	0.79	0.90	1.02	1.16
Florida US29	297,562	0.92	1.13	1.19	1.23	1.24	1.27
California Antelope EB	547,462	0.87	1.10	1.15	1.18	1.20	1.25
California Antelope WB	526,050	0.93	1.16	1.18	1.22	1.25	1.33
California Bowman	387,479	0.86	1.03	1.09	1.15	1.18	1.22
California LA 710 NB	2,452,764	0.94	1.18	1.22	1.24	1.26	1.30
California LA 710 SB	2,791,995	0.91	1.16	1.19	1.23	1.28	1.34
California Lodi	2,083,388	1.04	1.23	1.26	1.30	1.33	1.47

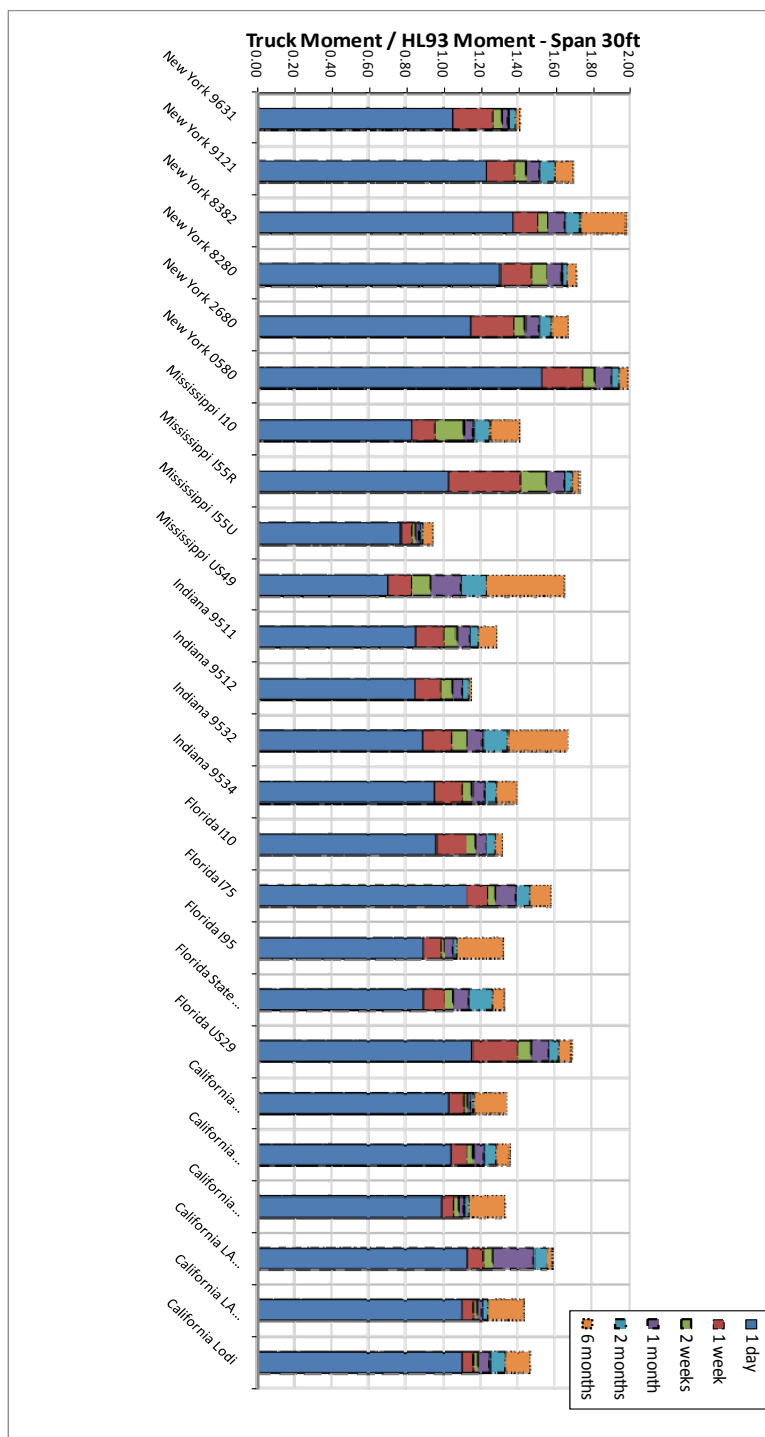


Figure 3-15 Bias – Span 30ft - different return periods for different locations.

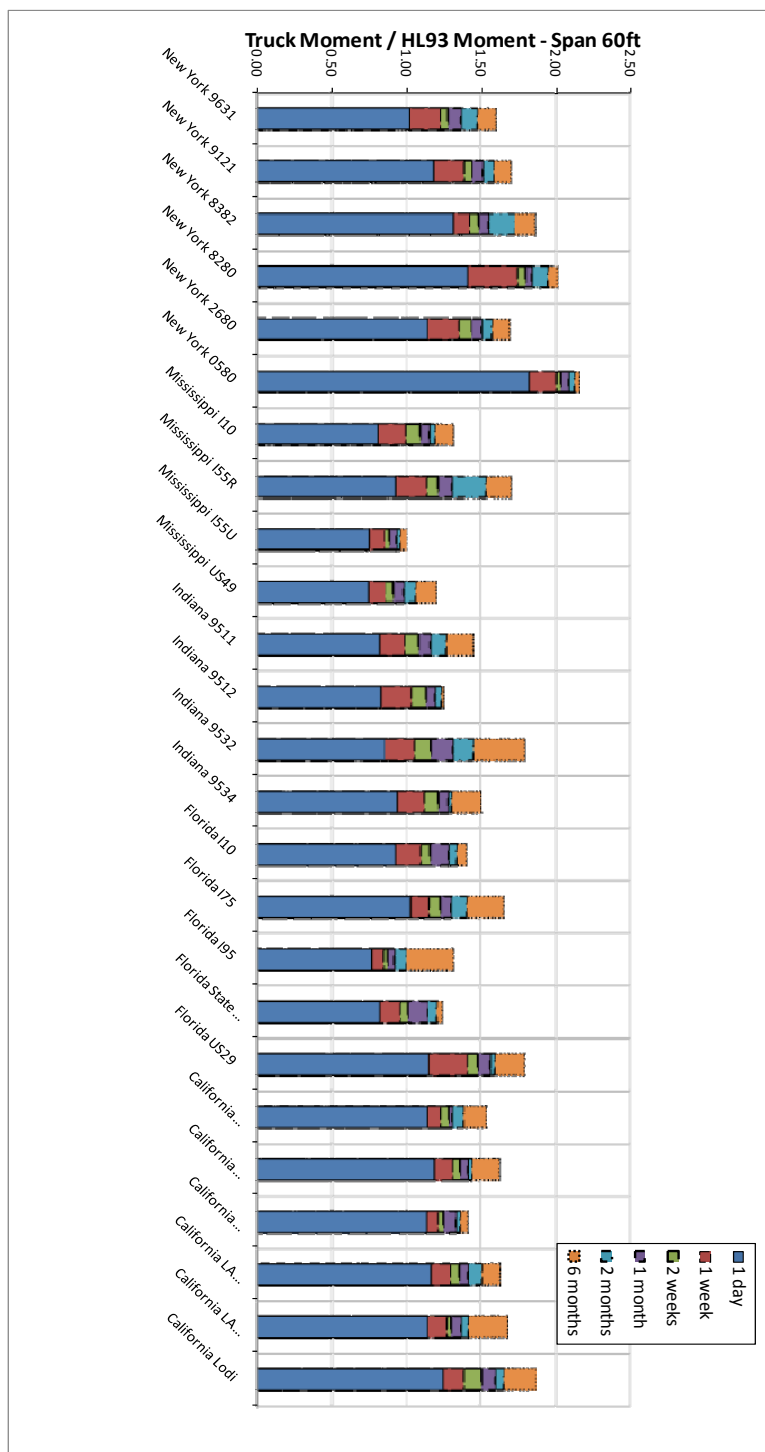


Figure 3-16 Bias – Span 60ft - different return periods for different locations.

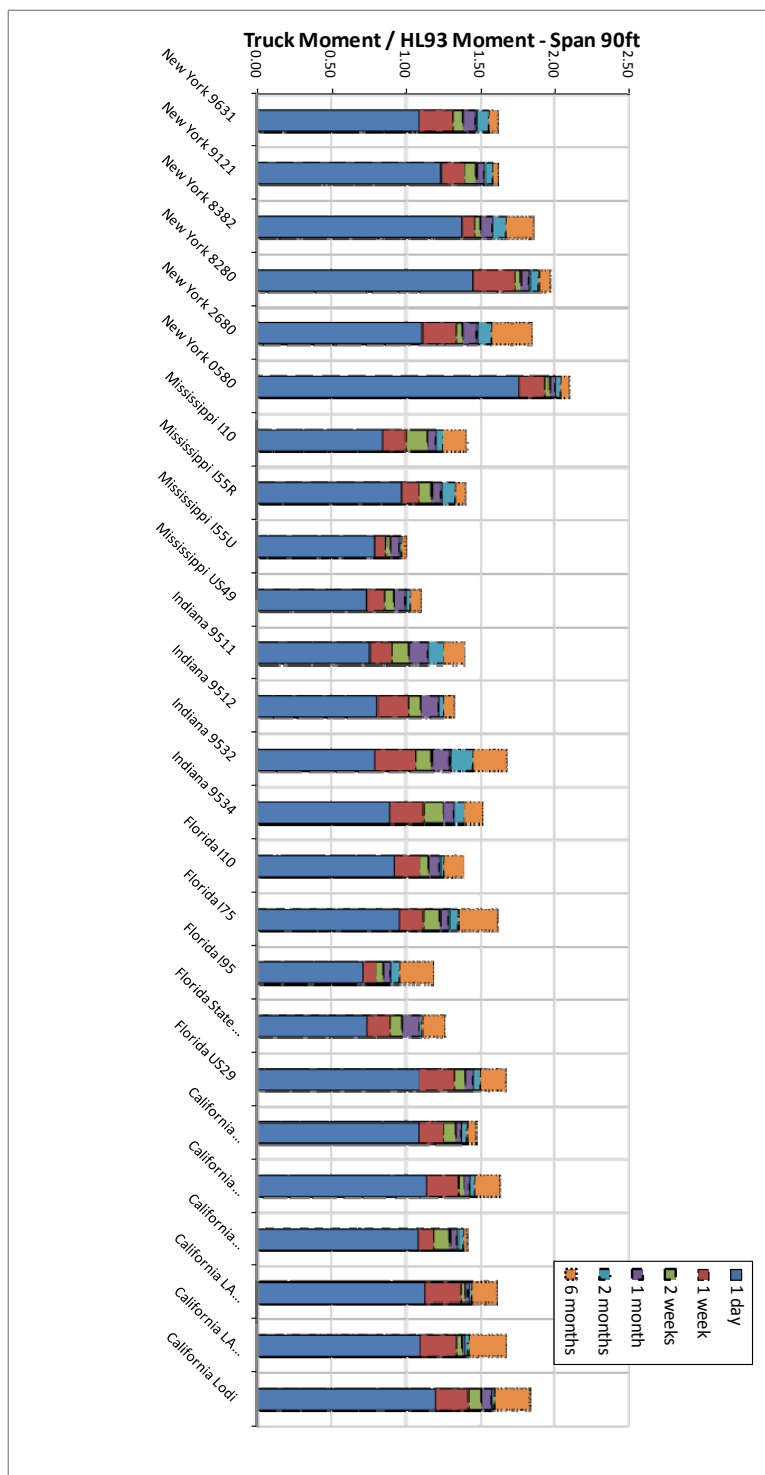


Figure 3-17 Bias – Span 90ft - different return periods for different locations.

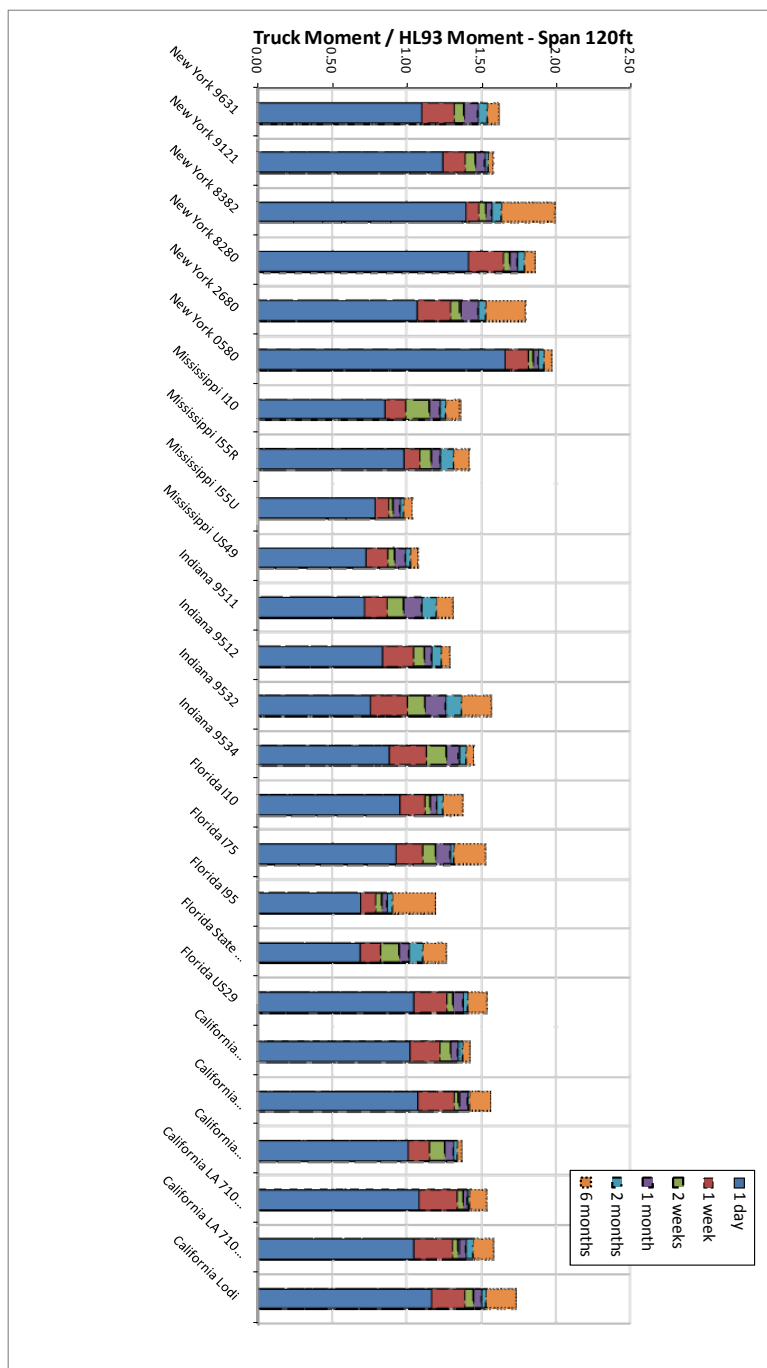


Figure 3-18 Bias – Span 120ft - different return periods for different locations.

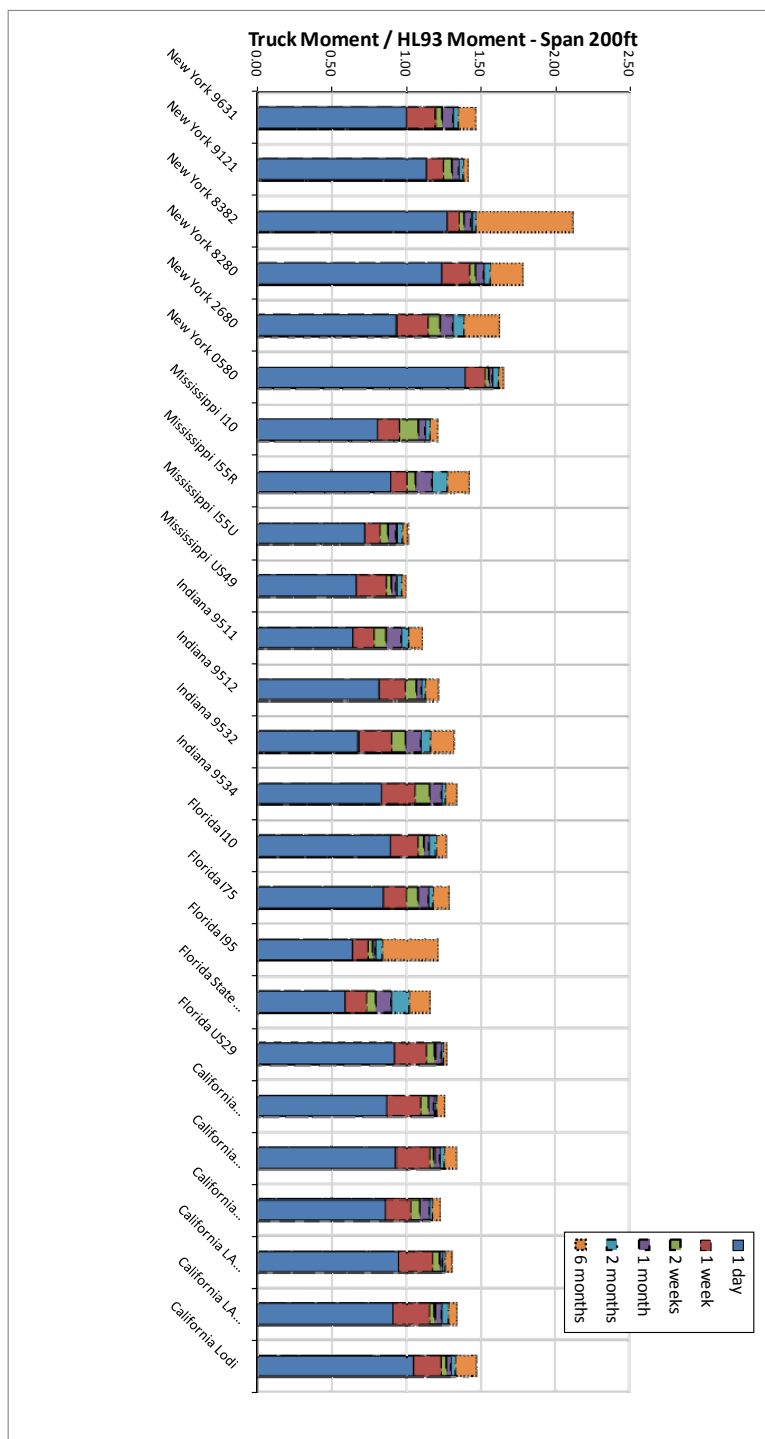


Figure 3-19 Bias – Span 200ft - different return periods for different locations.

Analysis of the WIM data showed that the live load is strongly site specific. Mean maximum live load effect varies for different sites as well as for different span lengths. The mean maximum ratio (MMR) of moments for all considered sites for one day varies from 0.53 for Florida site 9927 localized on the route SR-546 and span 200ft to 1.82 for New York site 0580 localized in Queens and span 60ft. One week MMR varies from 0.73 to 2.00 for the same sites and span lengths.

The extremely loaded sites are located in New York State. Localization of these sites is as follows:

- Site 9631 – located on Southern Tier Expy 17 by Liberty
- Site 9121 – located on I- 81 by Whitney Point
- Site 8382 – located on I-84 by Port Jervis
- Site 8280 – located on I-84 by Fishkill
- Site 2680 – located on Route 12 by Deerfield
- Site 0580 – located on I-495 – Queens New York City

3.5. SENSITIVITY ANALYSIS

The goal of this analysis was to observe the change in the top of the distribution by removing extremely heavy vehicles form the database. Two different cases of removing the heavy trucks were considered:

- Ratio of Truck Moment to HL93 Moment $M_T/M_{HL93} > 0.15$

- Ratio of Truck Moment to HL93 Moment $M_T/M_{HL93} > 0.15$ and Ratio of Truck Moment to HL93 Moment $M_T/M_{HL93} < 1.35$

Ratio 1.35 was the maximum ratio obtained from Ontario measurements. The results of the analysis for three states New York, California and Mississippi are plotted on the probability paper in Figure 3-20 to Figure 3-24 and tabularized in Table 17 to Table 19.

Table 17 Removal of the heaviest vehicles New York

New York 0580				
Fliter	Number of trucks after filtering	Nr of trucks above upper limit	Number of all removed trucks - additional filtering criteria	
original filter on spacing, axles and speed	2,874,124.00	N/A	0	
$M_{truck}/M_{HL93} > 0.15$ kips-ft	2,474,407.00	0	399717	16.15%
$M_{truck}/M_{HL93} > 0.15$ kips-ft and $M_{truck}/M_{HL93} < 1.35$	2,468,952.00	5455	5455	0.22%
New York 2680				
Fliter	Number of trucks after filtering	Nr of trucks above upper limit	Number of all removed trucks - additional filtering criteria	
original filter on spacing, axles and speed	100,488.00	N/A	0	
$M_{truck}/M_{HL93} > 0.15$ kips-ft	89,286.00	0	11202	0.45%
$M_{truck}/M_{HL93} > 0.15$ kips-ft and $M_{truck}/M_{HL93} < 1.35$	89,250.00	36	36	0.04%
New York 8280				
Fliter	Number of trucks after filtering	Nr of trucks above upper limit	Number of all removed trucks - additional filtering criteria	
original filter on spacing, axles and speed	1,828,020.00	N/A	0	
$M_{truck}/M_{HL93} > 0.15$ kips-ft	1,717,972.00	0	110048	4.45%
$M_{truck}/M_{HL93} > 0.15$ kips-ft and $M_{truck}/M_{HL93} < 1.35$	1,717,428.00	544	544	0.03%

New York 8382

Fliter	Number of trucks after filtering	Nr of trucks above upper limit	Number of all removed trucks - additional filtering criteria
original filter on spacing, axles and speed	1,594,674.00	N/A	0
$M_{truck}/M_{HL93} > 0.15$ kips-ft	1,551,454.00	0	43220 1.75%
$M_{truck}/M_{HL93} > 0.15$ kips-ft and $M_{truck}/M_{HL93} < 1.35$	1,550,914.00	540	540 0.03%

New York 9121

Fliter	Number of trucks after filtering	Nr of trucks above upper limit	Number of all removed trucks - additional filtering criteria
original filter on spacing, axles and speed	1,291,252.00	N/A	0
$M_{truck}/M_{HL93} > 0.15$ kips-ft	1,235,963.00	0	55289 2.23%
$M_{truck}/M_{HL93} > 0.15$ kips-ft and $M_{truck}/M_{HL93} < 1.35$	1,235,886.00	77	77 0.01%

After initial filtering of the site 8382 located in state of New York the total number of vehicles was 1,594,674. An additional filter was applied on the truck moments to observe possible change in the distribution. Truck causing moment larger than 1.35 HL93 moment was removed from the database. Number of removed trucks was 540. Figure 3-23 represents cumulative distribution function of ratio of moments for span 90 ft plotted on the normal probability paper. Diamond markers show a distribution of ratio of moments after initial filtering and the continuous line represents a new cumulative distribution after removal of the heaviest trucks.

Table 18 Removal of the heaviest vehicles California

California Antelope EB				
Fliter	Number of trucks after filtering	Nr of trucks above upper limit	Number of all removed trucks - additional filtering criteria	
original filter on spacing, axles and speed	693,339.00	N/A	0	
$M_{truck}/M_{HL93} > 0.15$ kips-ft	587,160.00	0	106179	4.29%
$M_{truck}/M_{HL93} > 0.15$ kips-ft and $M_{truck}/M_{HL93} < 1.35$	587,143.00	17	17	0.00%
California Antelope WB				
Fliter	Number of trucks after filtering	Nr of trucks above upper limit	Number of all removed trucks - additional filtering criteria	
original filter on spacing, axles and speed	766,188.00	N/A	0	
$M_{truck}/M_{HL93} > 0.15$ kips-ft	565,799.00	0	200389	8.10%
$M_{truck}/M_{HL93} > 0.15$ kips-ft and $M_{truck}/M_{HL93} < 1.35$	565,749.00	50	50	0.01%
California Bowman				
Fliter	Number of trucks after filtering	Nr of trucks above upper limit	Number of all removed trucks - additional filtering criteria	
original filter on spacing, axles and speed	486,084.00	N/A	0	
$M_{truck}/M_{HL93} > 0.15$ kips-ft	401,560.00	0	84524	3.42%
$M_{truck}/M_{HL93} > 0.15$ kips-ft and $M_{truck}/M_{HL93} < 1.35$	401,551.00	9	9	0.00%
California LA710 NB				
Fliter	Number of trucks after filtering	Nr of trucks above upper limit	Number of all removed trucks - additional filtering criteria	
original filter on spacing, axles and speed	2,987,141.00	N/A	0	
$M_{truck}/M_{HL93} > 0.15$ kips-ft	2,676,044.00	0	311097	12.57%
$M_{truck}/M_{HL93} > 0.15$ kips-ft and $M_{truck}/M_{HL93} < 1.35$	2,675,988.00	56	56	0.002%

California LA710 SB

Fliter	Number of trucks after filtering	Nr of trucks above upper limit	Number of all removed trucks - additional filtering criteria	
original filter on spacing, axles and speed	3,343,151.00	N/A	0	
$M_{truck}/M_{HL93} > 0.15$ kips-ft	3,022,329.00	0	320822	12.97%
$M_{truck}/M_{HL93} > 0.15$ kips-ft and $M_{truck}/M_{HL93} < 1.35$	3,022,290.00	39	39	0.001%

California Lodi

Fliter	Number of trucks after filtering	Nr of trucks above upper limit	Number of all removed trucks - additional filtering criteria	
original filter on spacing, axles and speed	2,556,978.00	N/A	0	
$M_{truck}/M_{HL93} > 0.15$ kips-ft	2,174,378.00	0	382600	15.46%
$M_{truck}/M_{HL93} > 0.15$ kips-ft and $M_{truck}/M_{HL93} < 1.35$	2,174,273.00	105	105	0.005%

After initial filtering of the site LA710 SB located in state of California the total number of vehicles was 3,022,329.00. An additional filter was applied on the truck moments to observe possible change in the distribution. Truck causing moment larger than 1.35 HL93 moment was removed from the database. Number of removed trucks was 39.

Table 19 Removal of the heaviest vehicles Mississippi

Mississippi I10				
Fliter	Number of trucks after filtering	Nr of trucks above upper limit	Number of all removed trucks - additional filtering criteria	
original filter on spacing, axles and speed	2,548,678.00	N/A	0	
$M_{truck}/M_{HL93} > 0.15$ kips-ft	2,103,302.00	0	445376	18.00%
$M_{truck}/M_{HL93} > 0.15$ kips-ft and $M_{truck}/M_{HL93} < 1.35$	2,103,300.00	2	2	0.00%
Mississippi I55R				
Fliter	Number of trucks after filtering	Nr of trucks above upper limit	Number of all removed trucks - additional filtering criteria	
original filter on spacing, axles and speed	1,325,011.00	N/A	0	
$M_{truck}/M_{HL93} > 0.15$ kips-ft	1,218,632.00	0	106379	4.30%
$M_{truck}/M_{HL93} > 0.15$ kips-ft and $M_{truck}/M_{HL93} < 1.35$	1,218,628.00	4	4	0.00%
Mississippi I55U				
Fliter	Number of trucks after filtering	Nr of trucks above upper limit	Number of all removed trucks - additional filtering criteria	
original filter on spacing, axles and speed	1,328,555.00	N/A	0	
$M_{truck}/M_{HL93} > 0.15$ kips-ft	1,117,276.00	0	211279	8.54%
$M_{truck}/M_{HL93} > 0.15$ kips-ft and $M_{truck}/M_{HL93} < 1.35$	1,117,276.00	0	0	0.00%

Data from New York, California and Mississippi was analyzed to determine types of distributions after removal of the heavy vehicles. In the first step, trucks without light ones (less than 0.15 HL93) were plotted on normal probability paper (see Figure 3-20 to Figure 3-24). The second step was to remove heavy trucks from the population. It was

observed that regardless of the site, removal of 0.001% of trucks can change the shape of the top of the distribution.

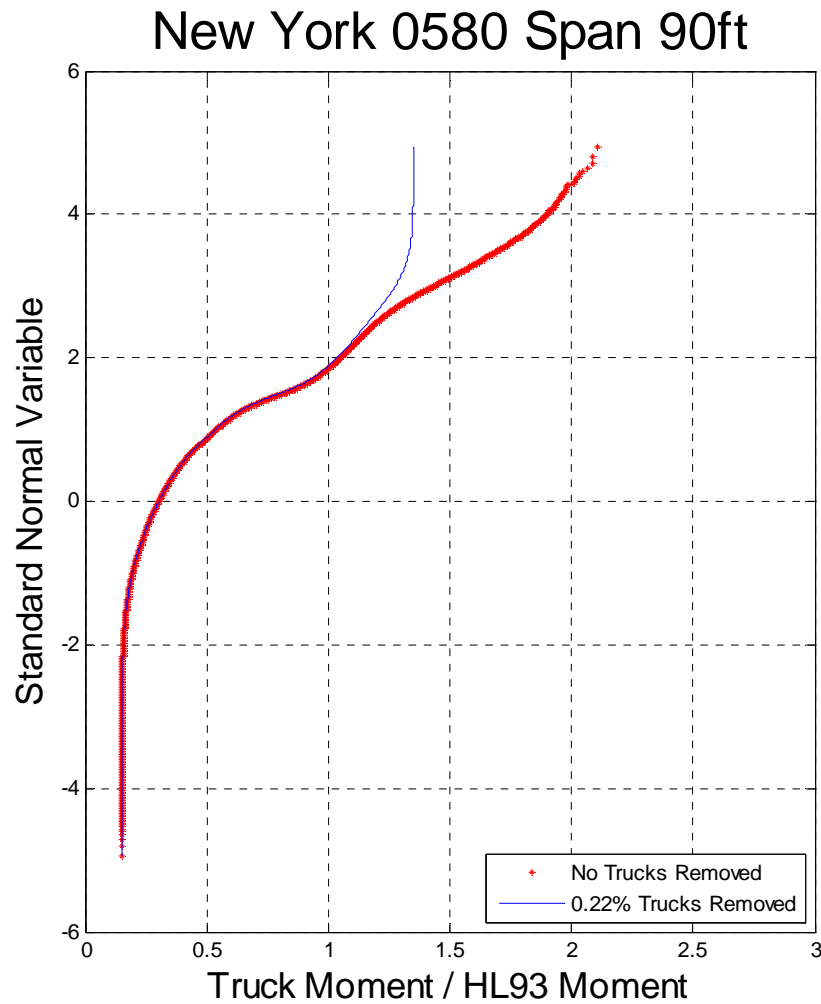


Figure 3-20 Data removal New York 0580

The number of trucks removed from New York site 0580 was 5455. The analysis of this site showed that removal of 0.22% of trucks can change the maximum ratio of truck

moment to HL93 moment from 2.2 to 1.35 but didn't change the main body of the distribution.

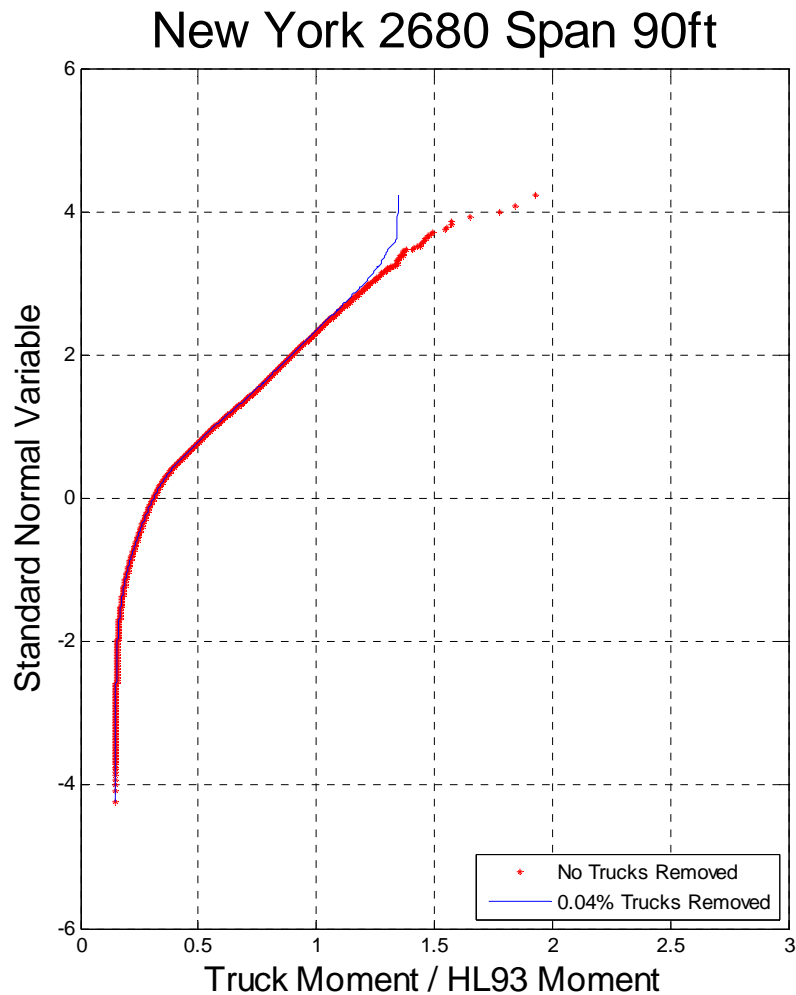


Figure 3-21 Data removal New York 2680

The number of trucks removed from New York site 2680 was 36. The analysis of this site showed that removal of 0.04% of trucks can change the maximum ratio of truck moment to HL93 moment from 1.95 to 1.35 but also didn't change the main body of the distribution.

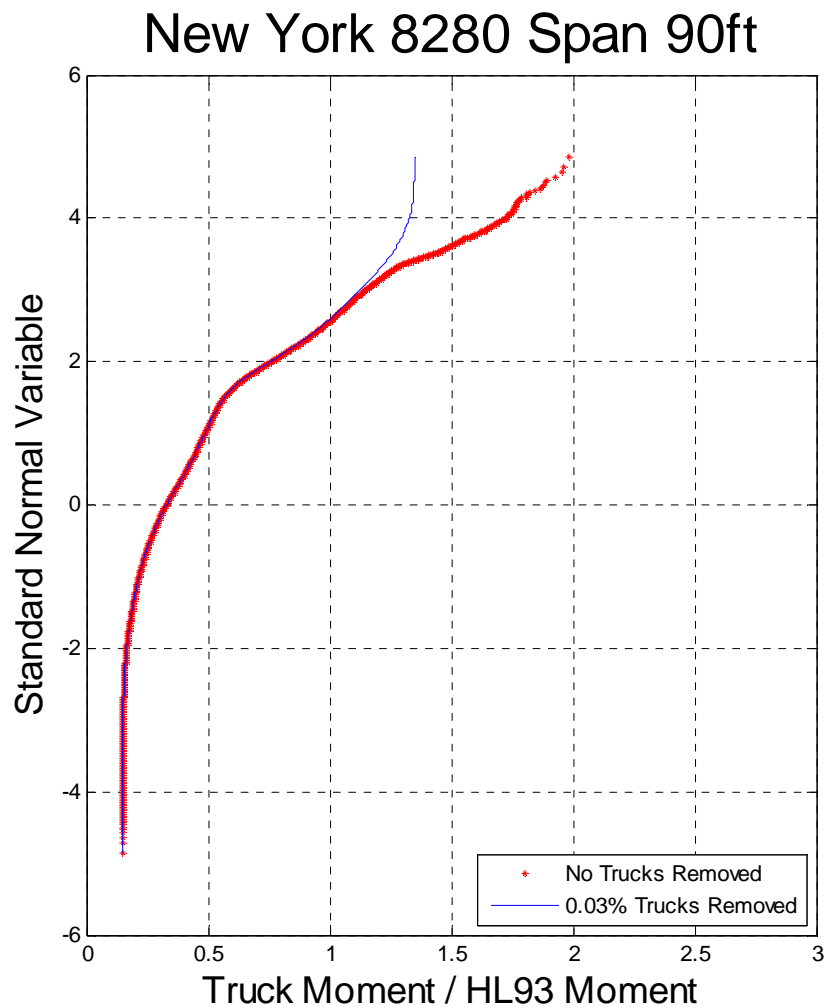


Figure 3-22 Data removal New York 8280

The number of trucks removed from New York site 8280 was 544. The analysis of this site showed that removal of 0.03% of trucks can change the maximum ratio of truck moment to HL93 moment from 2 to 1.35 but also didn't change the main body of the distribution.

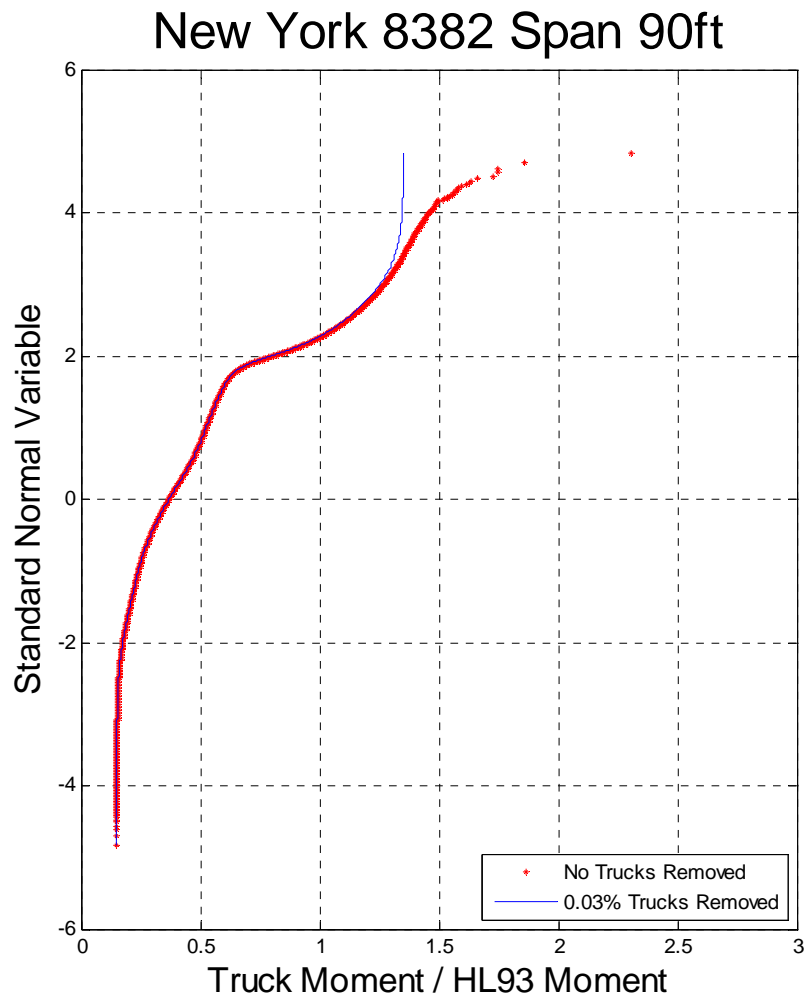


Figure 3-23 Data removal New York 8382

The number of trucks removed from New York site 8382 was 540. The analysis of this site showed that removal of 0.03% of trucks can change the maximum ratio of truck moment to HL93 moment from 2.5 to 1.35 but also didn't change the main body of the distribution. The maximum moment 2.5 HL93 for this site was produced by a single vehicle and can be assumed as an outlier.

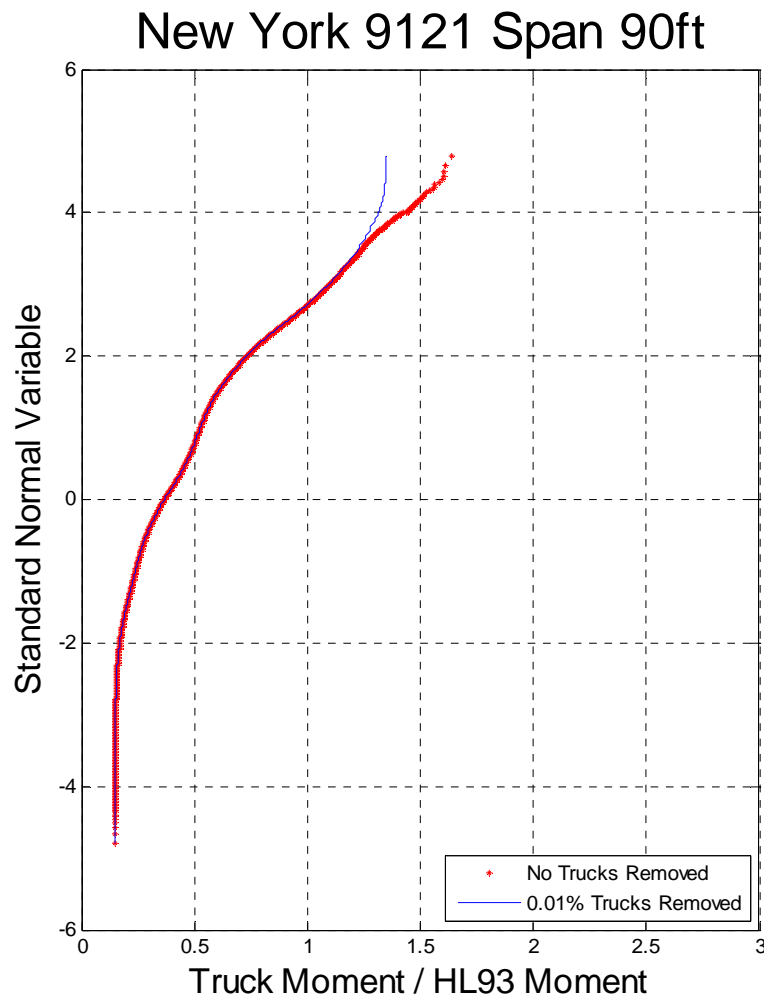


Figure 3-24 Data removal New York 9121

The number of trucks removed from New York site 9121 was 77. The analysis of this site showed that removal of 0.01% of trucks can change the maximum ratio of truck moment to HL93 moment from 1.65 to 1.35 but also didn't change the main body of the distribution.

Sensitivity analysis was performed on three states but only New York is represented on the probability paper. New York sites can be described as extremely loaded and it was necessary to check those heavy trucks. Two examples of the extremely heavy sites were

selected to include in the main body of this dissertation. For sites 0580 and 8280 three trucks were chosen. The example includes number of axles, spacing and the configuration of the trucks.

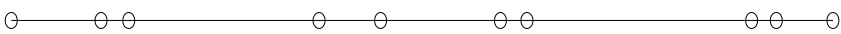
Examples of extremely heavy trucks:

1. Site 0580 – three extreme trucks from the database:

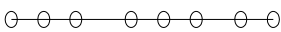
GVW(kips)	A1 (kips)	A2	A3	A4	A5	A6	A7	A8	A9	A10	A11	A12
270.6	19.6	28.7	27.9	26.3	23.6	20.1	29.9	30.7	29.8	34	0	0
268.7	16.8	28.3	28.2	13.9	33.8	31.8	15	25.7	30.4	25.3	19.5	0
254.1	32.7	32.1	37	37.2	29.8	28.8	28.2	28.3	0	0	0	0

Length	S1(ft)	S2	S3	S4	S5	S6	S7	S8	S9	S10	S11
136.4	14.9	4.6	31.6	10.2	19.9	4.4	37.3	4.1	9.4	0	0
107.6	13.9	4.4	27.7	4.2	4.5	13.5	4.3	26.6	4.2	4.3	0
43.5	5.4	5.3	9.2	5.4	5.4	7.4	5.4	0	0	0	0

Configuration of the trucks:

Truck 3 GVW = 270.6k 

Truck 4 GVW = 268.7k 

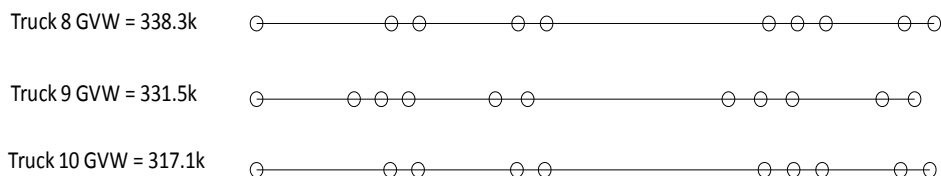
Truck 5 GVW = 254.1k 

2. Site 8280 – three extreme trucks from the database:

GVW(kips)	A1 (kips)	A2	A3	A4	A5	A6	A7	A8	A9	A10	A11	A12
338.3	27	44.2	35.9	30.5	41.5	32	33.9	25.6	37.1	30.6	0	0
331.5	20.6	21.5	33	30.3	37.6	35.3	37.7	33	30.4	26.1	26	0
317.1	22.9	40.3	40.6	24.4	40.2	29.1	30.5	21.7	36.1	31.3	0	0

Length	S1(ft)	S2	S3	S4	S5	S6	S7	S8	S9	S10	S11
107	21.3	4.4	15.6	4.5	35.1	4.5	4.5	12.4	4.7	0	0
103.9	15.4	4.3	4.3	13.7	5.1	31.7	5.1	5	14.2	5.1	0
106.3	21.1	4.4	15.6	4.4	34.7	4.6	4.5	12.4	4.6	0	0

Configuration of the trucks:



Configuration of the extremely heavy trucks shows that these vehicles are realistic. Last truck from the site 0580 with the GVW equal to 254.1 kips could be an eight axle crane. Configuration of these vehicles suggests that these trucks are probably permit trucks. Unfortunately there is no other way than an engineering judgment to determine if these trucks are suitable for the live load model.

Analysis of the extremely heavy trucks shows that their weight can be five times above the legal limit for regular truck. After verification of the extreme vehicles from various states it was assumed to include all the extreme cases for the live load model determination.

CHAPTER 4. LIVE LOAD ANALYSIS

Live load model is an important part of the code calibration. After the WIM data was processed and analyzed to find the mean maximum moments and shear it was necessary to build a new consistent live load model that could be implemented in the AASHTO LRFD code (Nowak and Szerszen 1998), . To follow the NCHRP Report 368 (Nowak 1999) it was needed to include the extrapolation to the future time period of 75 year and multiple presence statistics. In depth study of different sites resulted in the selection of three representative locations for further analysis. The first selected location was Florida I-10 with the maximum bias for moment less than 1.5. It was assumed that this site will be the representation of low loaded bridge. The next chosen locations to represent the medium and extreme heavy loaded bridges were California Lodi and New York 8382 respectively.

4.1. FLORIDA – LIVE LOAD EFFECT

WIM data for Florida

The WIM data includes 12 months of traffic recorded at the site 9936 in Florida located on the Interstate 10. The total number of records is 1,654,006 trucks. The data includes number of axles, gross vehicle weight (GVW), weight per axle and spacing between axles as well as a lane position.

Maximum Simple Span Moments

The maximum moment was calculated for each truck from the data. Analysis included simple spans with the span varying from 30 to 200 ft. The maximum moment was also calculated for the HL93 load and Tandem. Ratio between the data truck moment and the AASHTO LRFD load moment was plotted on the probability paper (Figure 4-1).

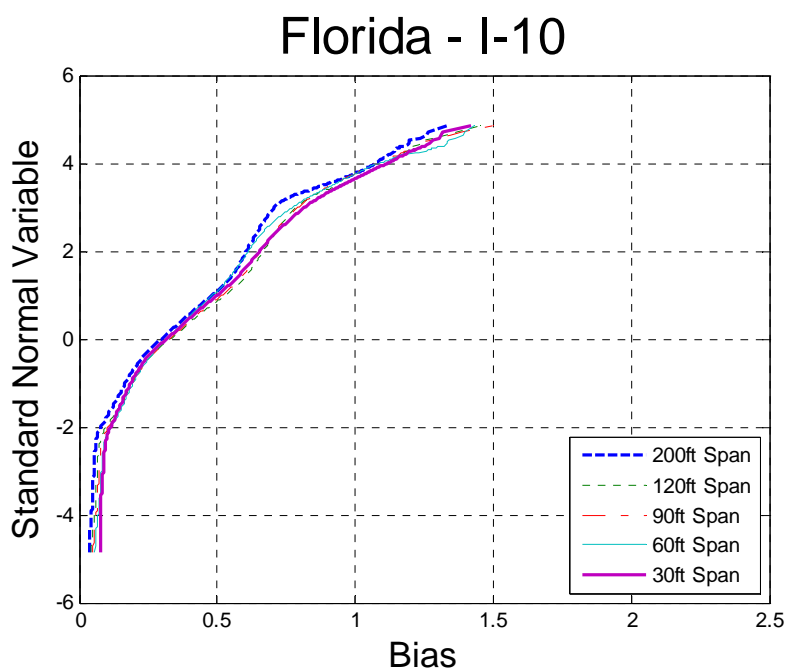


Figure 4-1 Cumulative Distribution Functions of Simple Span Moment– Florida – I-10

Maximum Shear

The maximum shear was calculated for each truck from the data. Analysis included simple spans with the span varying from 30 to 200 ft. The ratio of shear obtained from the data truck and the HL-93 load was plotted on the probability paper (Figure 4-2).

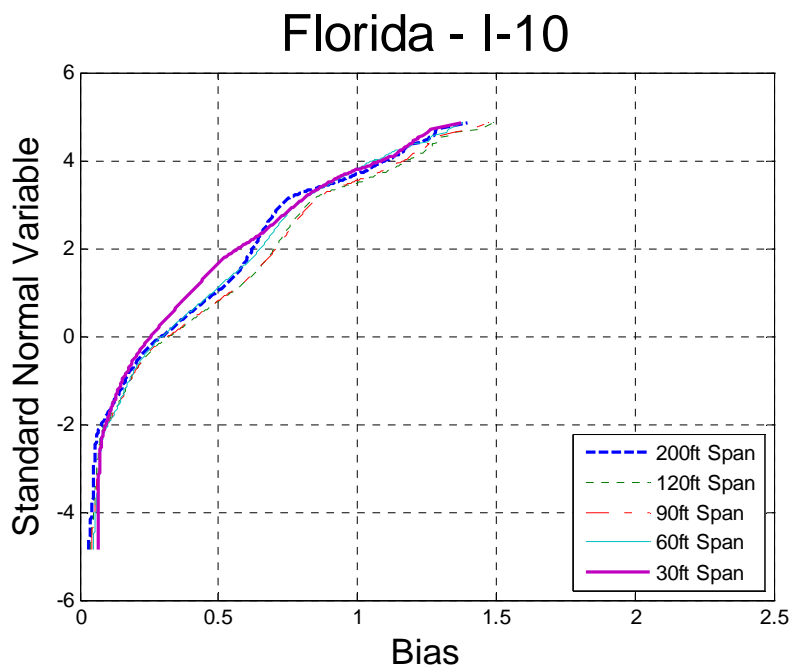


Figure 4-2 Cumulative Distribution Functions of Shear – Florida I-10

Maximum Load Effect for Different Return Period

The total number of trucks, equal to 1,654,006, represents one year of traffic on a bridge. To predict the maximum live load effect that will occur in 75 years one requires an extrapolation of a CDF plot to the 75 year return period. One year of traffic corresponds to the probability of 1 over 1,654,006 equal to 6.05×10^{-7} and this corresponds to the standard normal variable z equal to 4.85. To find the 75 year return period on the vertical axis and the corresponding probability, the number of trucks from one year was multiplied by 75. The 75 year volume of traffic would be 124,050,450 with the assumption that there will be no traffic increase in that period of time. The probability that heaviest truck will occur only once in 75 year is equal to 8.06×10^{-9} which

corresponds to 5.65 on the vertical axis. The total number of trucks for different time period is tabularized and shown in Table 20.

Table 20 Number of Trucks with Corresponding Probability and Time Period

Time period	Number of trucks, N	Probability, 1/N	Inverse normal, z
1 month	137,834	7.26E-06	4.34
2 months	275,668	3.63E-06	4.49
6 months	827,003	1.21E-06	4.71
1 year	1,654,006	6.05E-07	4.85
5 years	8,270,030	1.21E-07	5.16
50 years	82,700,300	1.21E-08	5.58
75 years	124,050,450	8.06E-09	5.65

Extrapolation to 75 year return period

The approach using parametric distributions was not applicable. The upper tail of the live load effect plotted on the probability paper does not follow any known type of the distribution. Therefore extension of the upper tail was performed using nonparametric approach described in Chapter 2 of this dissertation. The extrapolations were prepared for moment and shear. The simple span moment ratio extrapolations and nonparametric fit to data are shown on Figure 4-3 to Figure 4-12. Moments and shear for different return periods are tabulated and shown in Table 21 and Table 22.

The unique approach to extrapolate data up to a certain return period was based on the non parametric approach. Using kernel function as normal and the bandwidth 0.0314 for the distribution of live load for light loaded bridge span 30 ft resulted in the best fit to the whole data set. Trend of the end of the fit tail depends on the distance of the last point of the data set from the other points. Low loaded fit is shown in Figure 4-3.

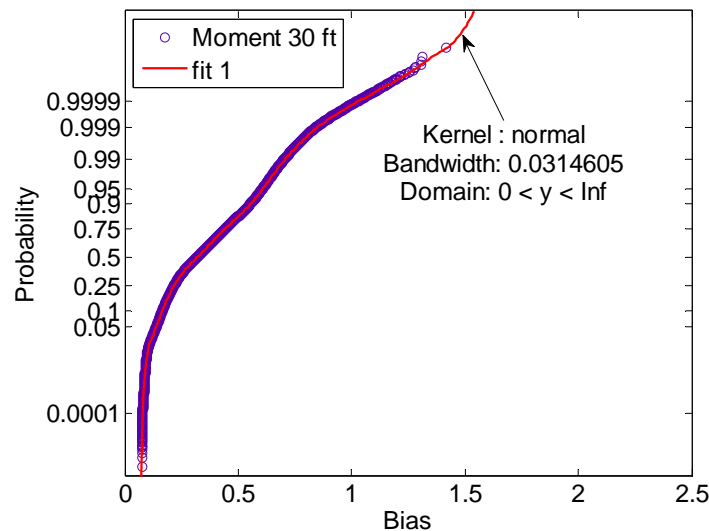


Figure 4-3 Low loaded bridge, moment, span 30ft – nonparametric fit to data

Extrapolation to 75 year for low loaded bridge span 30ft is presented is presented in Figure 4-4. Extreme value theory is used to determine distribution of 75 year live load. Mean value is equal to 1.52 and the coefficient of variation is calculated based on the green dashed line.

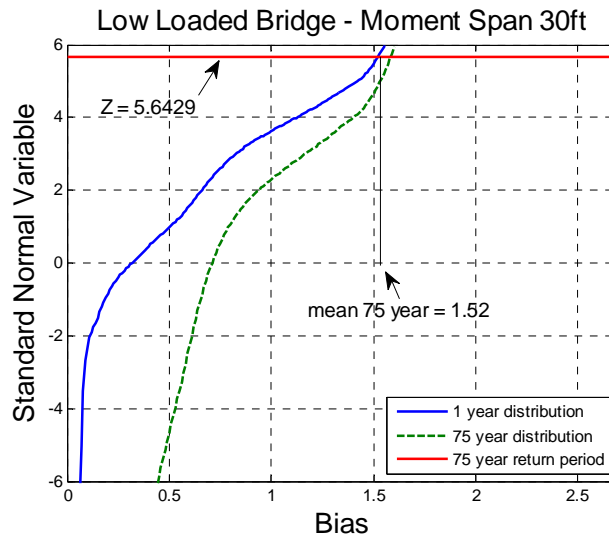


Figure 4-4 Low loaded bridge, moment, span 30ft – extrapolation to 75 year return period

Using kernel function as normal and the bandwidth 0.0284 for the distribution of live load for light loaded bridge span 60 ft resulted in the best fit to the whole data set. Domain was assumed as positive. Trend of the end of the fit tail depends on the distance of the last point of the data set from the other points. Low loaded fit is shown in Figure 4-5.

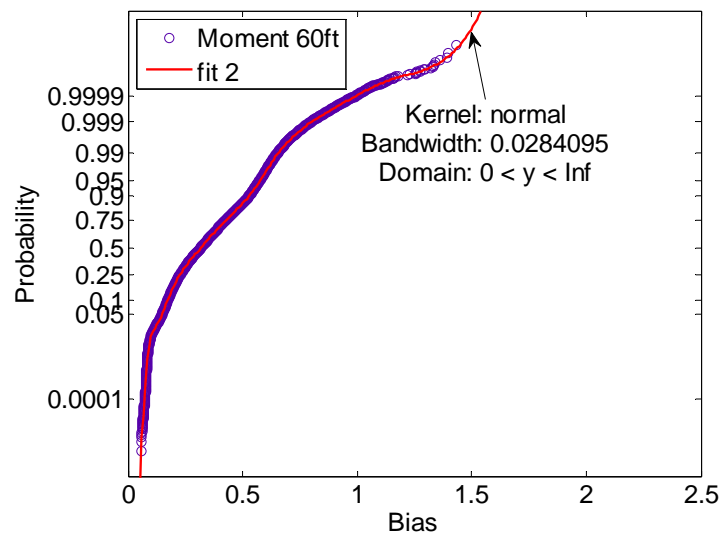


Figure 4-5 Low loaded bridge, moment, span 60ft – nonparametric fit to data

Extrapolation to 75 year for low loaded bridge span 60ft is presented is presented in Figure 4-6. Extreme value theory is used to determine distribution of 75 year live load. Mean value is equal to 1.53 and the coefficient of variation is calculated based on the green dashed line.

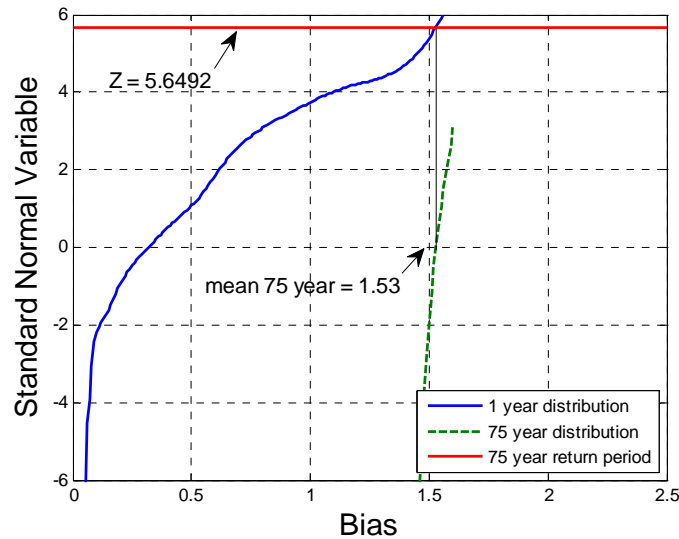


Figure 4-6 Low loaded bridge, moment, span 60ft – extrapolation to 75 year return period

Kernel normal function and the bandwidth 0.0313 were assumed for the distribution of live load for light loaded bridge span 90 ft. It resulted in the best fit to the whole data set. Domain was assumed as positive. Trend of the end of the fit tail depends on the distance of the last point of the data set from the other points. Low loaded fit is shown in Figure 4-7.

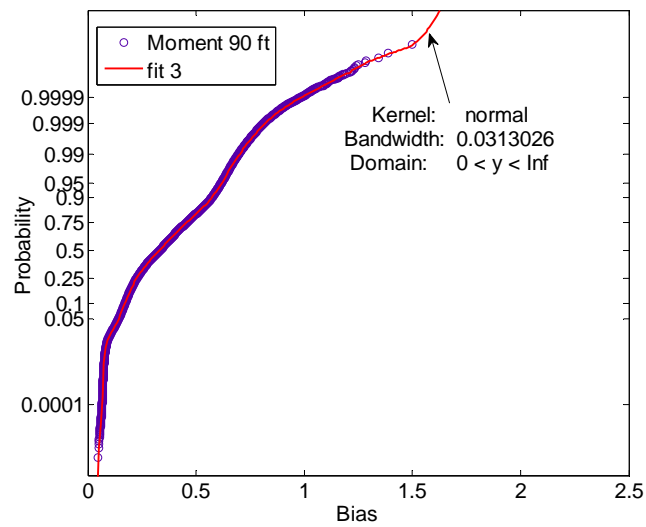


Figure 4-7 Low loaded bridge, moment, span 90ft – nonparametric fit to data

Extrapolation to 75 year for low loaded bridge span 90ft is presented is presented in Figure 4-8. Extreme value theory is used to determine distribution of 75 year live load. Mean value is equal to 1.61 and the coefficient of variation is calculated based on the green dashed line.

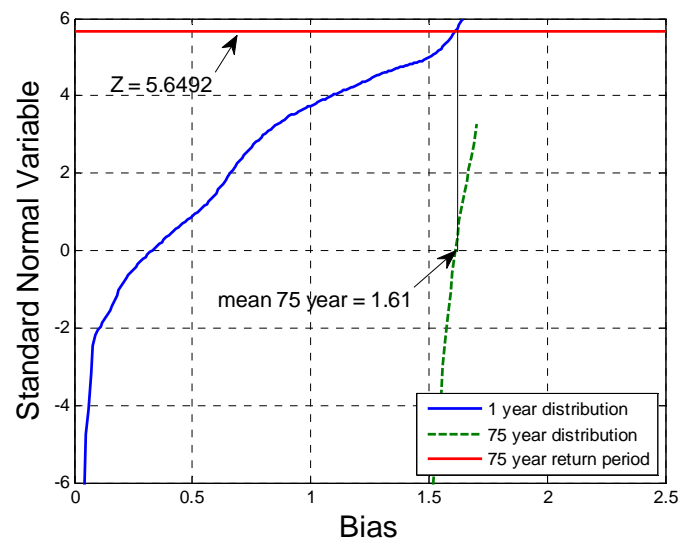


Figure 4-8 Low loaded bridge, moment, span 90ft – extrapolation to 75 year return period

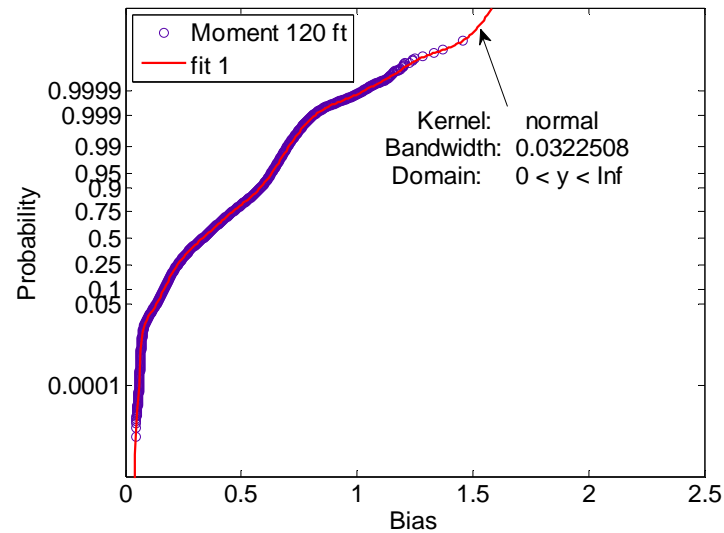


Figure 4-9 Low loaded bridge, moment, span 120ft – nonparametric fit to data

Kernel normal function and the bandwidth 0.0322 were assumed for the distribution of live load for light loaded bridge span 120 ft. It resulted in the best fit to the whole data set. Domain was assumed as positive. Trend of the end of the fit tail depends on the distance of the last point of the data set from the other points. Low loaded fit is shown in Figure 4-7.

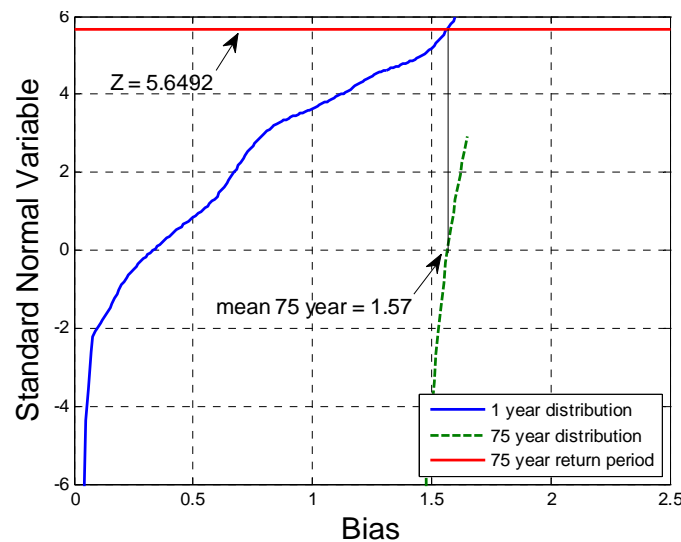


Figure 4-10 Low loaded bridge, moment, span 120ft – extrapolation to 75 year return period

Extrapolation to 75 year for low loaded bridge span 120ft is presented is presented in Figure 4-8. Extreme value theory is used to determine distribution of 75 year live load. Mean value is equal to 1.57 and the coefficient of variation is calculated based on the green dashed line.

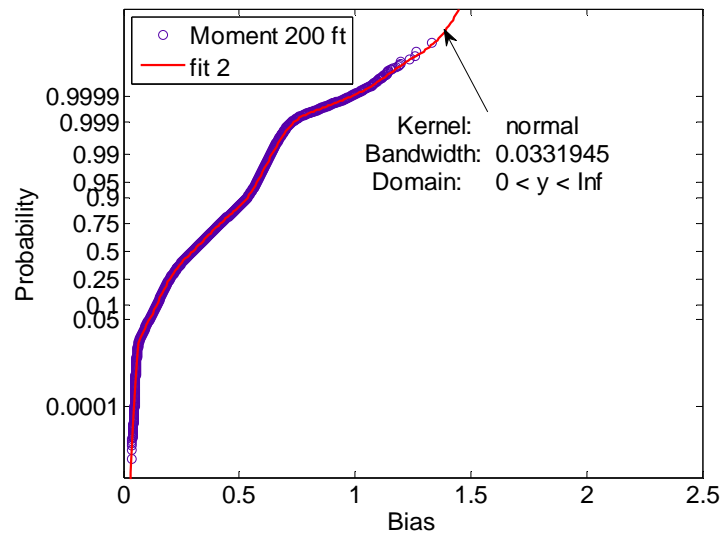


Figure 4-11 Low loaded bridge, moment, span 200ft – nonparametric fit to data

Kernel normal function and the bandwidth 0.0332 were assumed for the distribution of live load for light loaded bridge span 200 ft. It resulted in the best fit to the whole data set. Domain was assumed as positive. Trend of the end of the fit tail depends on the distance of the last point of the data set from the other points. Low loaded fit is shown in Figure 4-7.

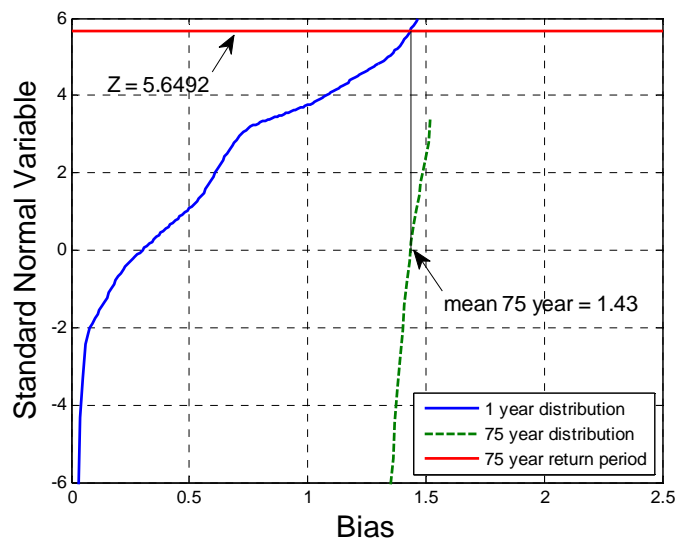


Figure 4-12 Low loaded bridge, moment, span 200ft – extrapolation to 75 year return period

Extrapolation to 75 year for low loaded bridge span 200ft is presented is presented in Figure 4-8. Extreme value theory is used to determine distribution of 75 year live load. Mean value is equal to 1.43 and the coefficient of variation is calculated based on the green dashed line.

All the mean values are consistent and the coefficients of variation are in the range of 0.14-0.17. Statistical parameters for moment and for shear are tabularized in Table 22 and Table 22 respectively.

Table 21 Mean Maximum Moments for Simple Span for 1 year and 75 years

Span (ft)	1 year	75 years	CoV for 75 year
30	1.42	1.52	0.12
60	1.43	1.53	0.11
90	1.50	1.61	0.12
120	1.46	1.57	0.12

200	1.33	1.43	0.13
-----	------	------	------

Table 22 Mean Maximum Shear for Simple Span for 1 year and 75 years

Span (ft)	1 year	75 years	CoV for 75 year
30	1.38	1.47	0.12
60	1.38	1.47	0.11
90	1.47	1.59	0.12
120	1.49	1.61	0.12
200	1.40	1.49	0.13

4.2. CALIFORNIA – LIVE LOAD EFFECT

WIM data for California

The WIM data includes 12 months of traffic recorded at the site 001 in California located close to Lodi on the Interstate 5. The total number of records is 2,556,978 trucks. The data includes number of axles, gross vehicle weight (GVW), weight per axle and spacing between axles as well as a lane position.

Maximum Simple Span Moments

The maximum moment was calculated for each truck from the data. Analysis included simple spans with the span varying from 30 to 200 ft. The maximum moment was also calculated for the HL93 load and Tandem. Ratio between data truck moment and code load moment was plotted on the probability paper (Figure 4-13).

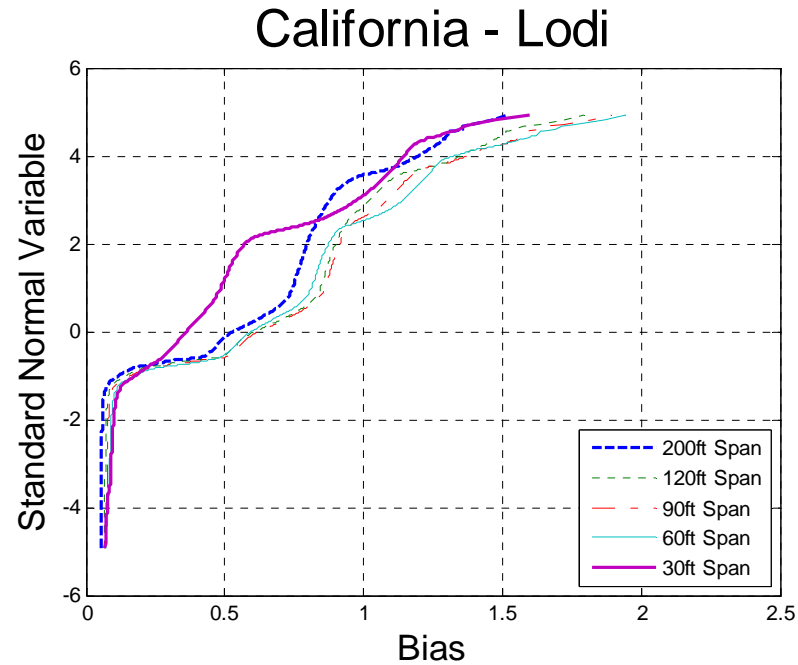


Figure 4-13 Cumulative Distribution Functions of Moment – California – Lodi

Maximum Shear

The maximum shear was calculated for each truck from the data. Analysis included simple spans with the span varying from 30 to 200 ft. The ratio of shear obtained from the data truck and the HL-93 load was plotted on the probability paper (Figure 4-14).

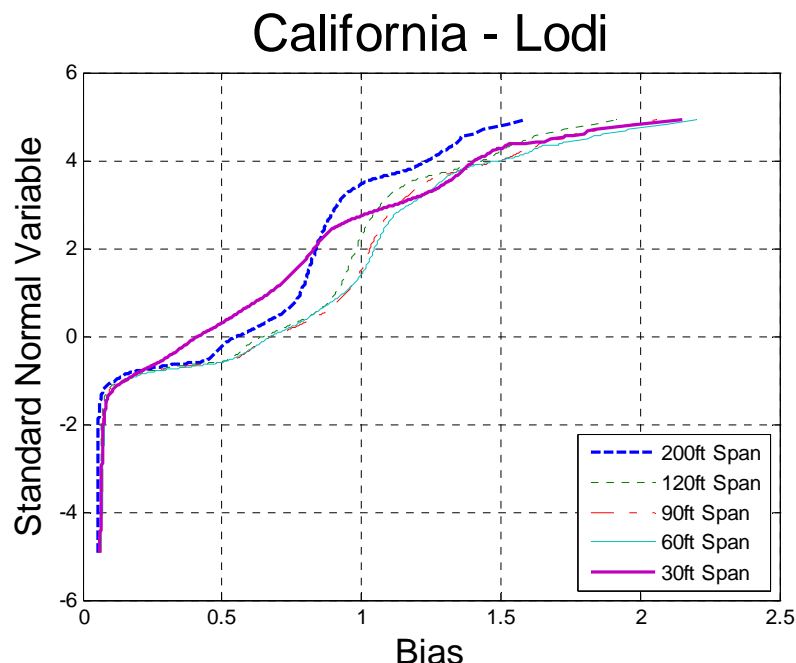


Figure 4-14 Cumulative Distribution Functions of Shear – California – Lodi

Maximum Load Effect for Different Return Period

The total number of trucks, equal to 2,556,978, represents one year of traffic on a bridge. To predict the maximum live load effect that will occur in 75 years only one requires an extrapolation of a CDF plot to the 75 year return period. One year of traffic corresponds to the probability of 1 over 2,556,978 equal to $3.91\text{E-}07$ and this corresponds to the standard normal variable z equal to 4.94. To find the 75 year return period on the vertical axis and the corresponding probability, the number of trucks from one year was multiplied by 75. The 75 year volume of traffic would be 191,773,350 with the assumption that there will be no traffic increase in that period of time. The probability that heaviest truck will occur only once in 75 year is equal to $5.21\text{E-}09$ which corresponds to 5.72 on the vertical axis. The total number of trucks for different time period is tabularized and shown in Table 23.

Table 23 Number of Trucks with Corresponding Probability and Time Period

Time period	Number of trucks, N	Probability, 1/N	Inverse normal, z
1 month	213,082	4.69E-06	4.43
2 months	426,163	2.35E-06	4.58
6 months	1,278,489	7.82E-07	4.80
1 year	2,556,978	3.91E-07	4.94
5 years	12,784,890	7.82E-08	5.24
50 years	127,848,900	7.82E-09	5.65
75 years	191,773,350	5.21E-09	5.72

Extrapolation to 75 year return period

The approach using parametric distributions was not applicable. The upper tail of the live load effect plotted on the probability paper does not follow any known type of the distribution. Therefore extension of the upper tail was performed using nonparametric approach described in Chapter 2 of this dissertation. The extrapolations were prepared for moment and shear. The simple span moment ratio extrapolations and nonparametric fit to data are shown on Figure 4-15 to Figure 4-24. Moments and shear for different return periods are tabulated and shown in Table 21 and Table 22.

Kernel normal function and the bandwidth 0.0209 were assumed for the distribution of live load for medium loaded bridge span 30 ft. It resulted in the best fit to the whole data set. Domain was assumed as positive. Trend of the end of the fit tail depends on the distance of the last point of the data set from the other points. Medium loaded fit is shown in Figure 4-7.

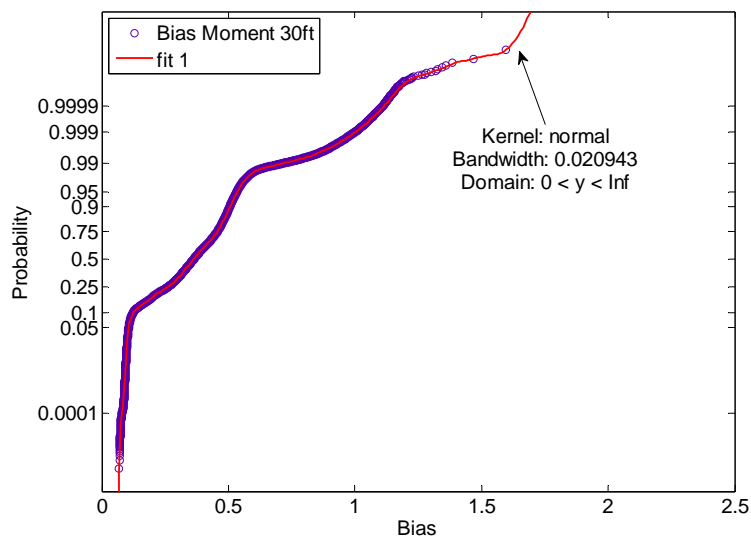


Figure 4-15 Medium loaded bridge, moment, span 30ft – nonparametric fit to data

Extrapolation to 75 year for medium loaded bridge span 30ft is presented in Figure 4-8. Extreme value theory is used to determine distribution of 75 year live load. Mean value is equal to 1.67 and the coefficient of variation is calculated based on the green dashed line.

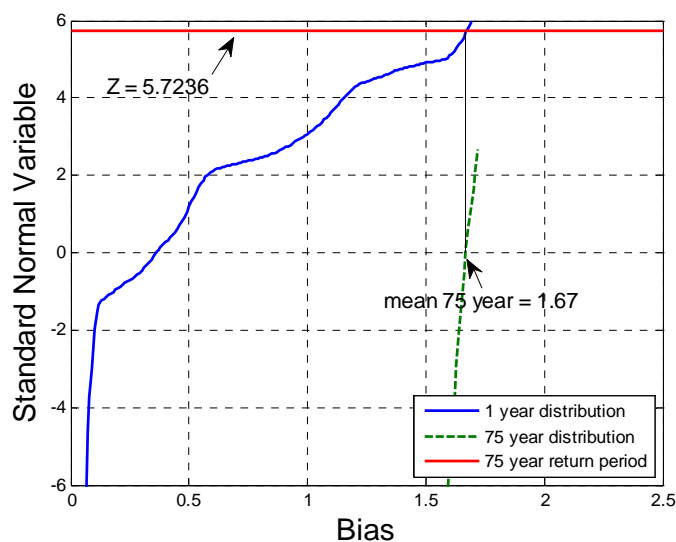


Figure 4-16 Medium loaded bridge, moment, span 30ft – extrapolation to 75 year return period

Kernel normal function and the bandwidth 0.0223 were assumed for the distribution of live load for medium loaded bridge span 60 ft. It resulted in the best fit to the whole data set. Domain was assumed as positive. Trend of the end of the fit tail depends on the distance of the last point of the data set from the other points. Medium loaded fit is shown in Figure 4-7.

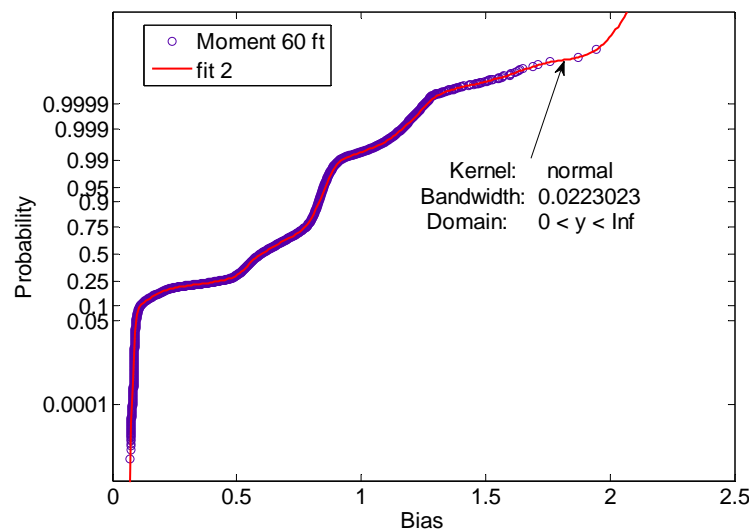


Figure 4-17 Medium loaded bridge, moment, span 60ft – nonparametric fit to data

Extrapolation to 75 year for medium loaded bridge span 60ft is presented is presented in Figure 4-8. Extreme value theory is used to determine distribution of 75 year live load. Mean value is equal to 2.05 and the coefficient of variation is calculated based on the green dashed line.

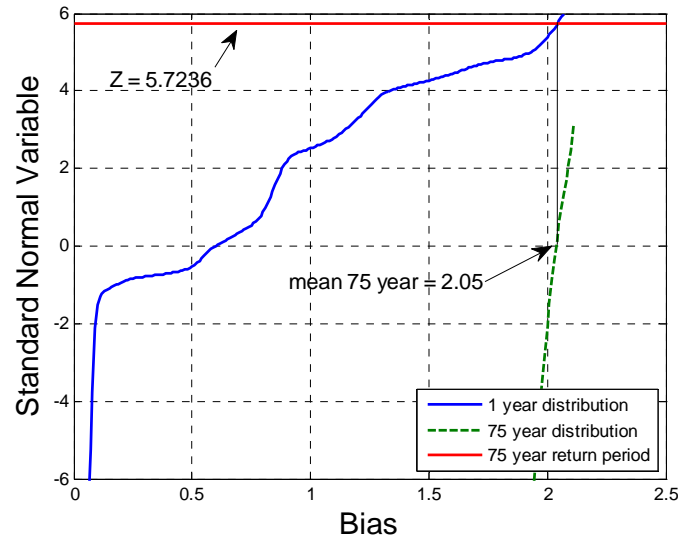


Figure 4-18 Medium loaded bridge, moment, span 60ft – extrapolation to 75 year return period

Kernel normal function and the bandwidth 0.0236 were assumed for the distribution of live load for medium loaded bridge span 90 ft. It resulted in the best fit to the whole data set. Domain was assumed as positive. Trend of the end of the fit tail depends on the distance of the last point of the data set from the other points. Medium loaded fit is shown in Figure 4-7.

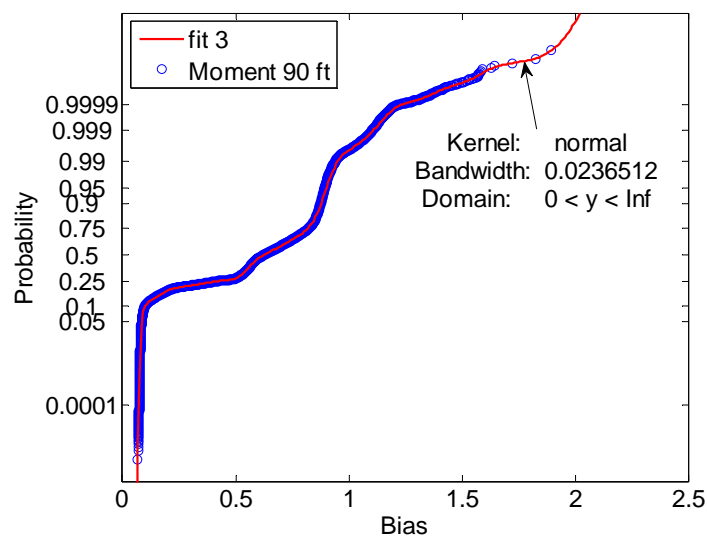


Figure 4-19 Medium loaded bridge, moment, span 90ft – nonparametric fit to data

Extrapolation to 75 year for medium loaded bridge span 90ft is presented is presented in Figure 4-8. Extreme value theory is used to determine distribution of 75 year live load. Mean value is equal to 1.99 and the coefficient of variation is calculated based on the green dashed line.

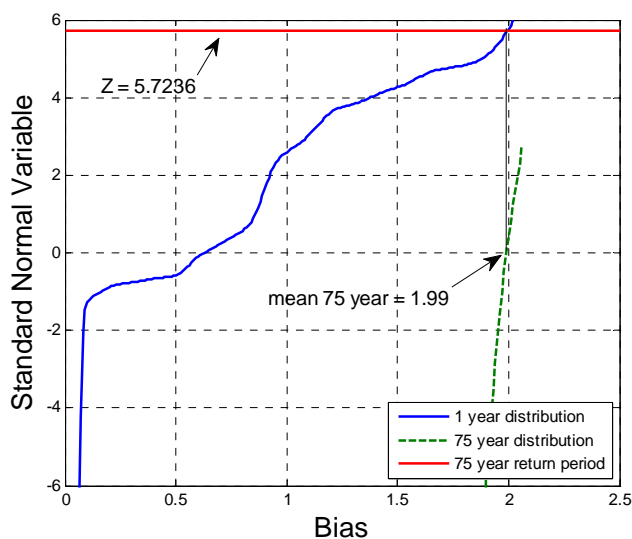


Figure 4-20 Medium loaded bridge, moment, span 90ft – extrapolation to 75 year return period

Kernel normal function and the bandwidth 0.0244 were assumed for the distribution of live load for medium loaded bridge span 120 ft. It resulted in the best fit to the whole data set. Domain was assumed as positive. Trend of the end of the fit tail depends on the distance of the last point of the data set from the other points. Medium loaded fit is shown in Figure 4-7.

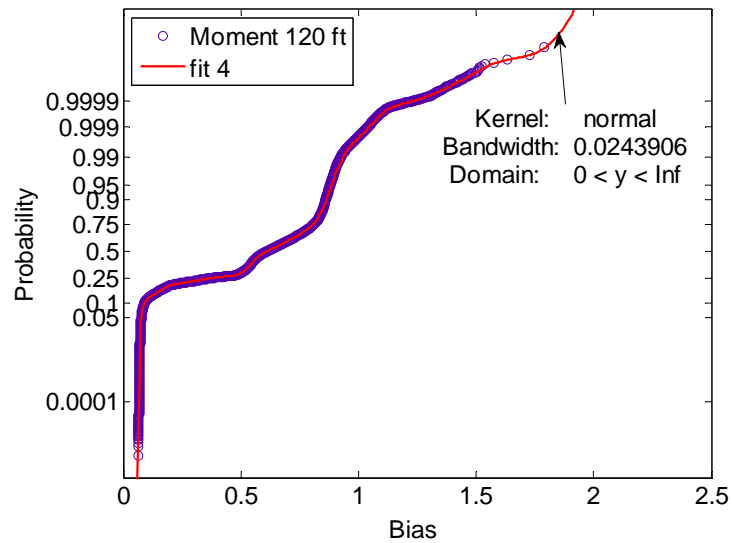


Figure 4-21 Medium loaded bridge, moment, span 120ft – nonparametric fit to data

Extrapolation to 75 year for medium loaded bridge span 120ft is presented in Figure 4-8. Extreme value theory is used to determine distribution of 75 year live load. Mean value is equal to 1.88 and the coefficient of variation is calculated based on the green dashed line.

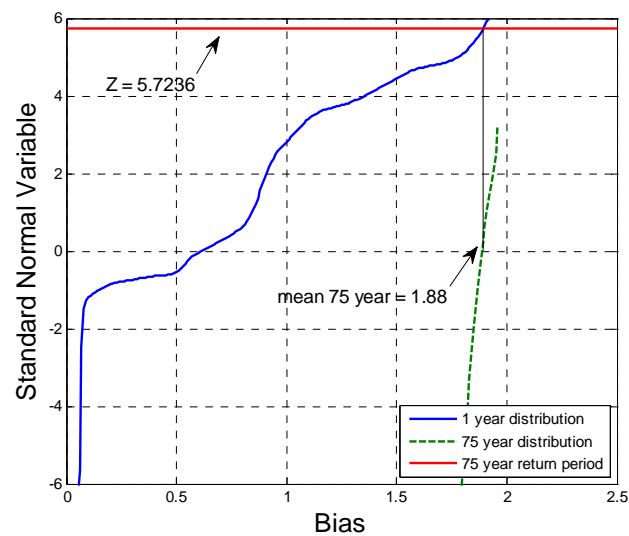


Figure 4-22 Medium loaded bridge, moment, span 120ft – extrapolation to 75 year return period

Kernel normal function and the bandwidth 0.0249 were assumed for the distribution of live load for medium loaded bridge span 200 ft. It resulted in the best fit to the whole data set. Domain was assumed as positive. Trend of the end of the fit tail depends on the distance of the last point of the data set from the other points. Medium loaded fit is shown in Figure 4-7.

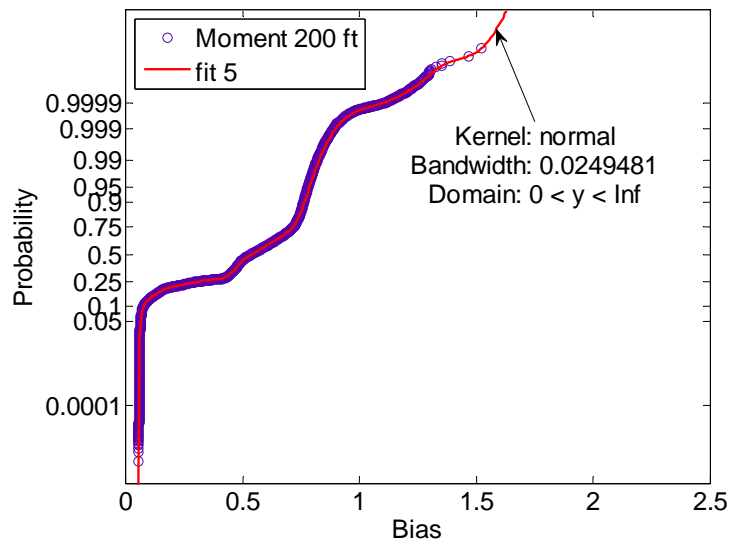


Figure 4-23 Medium loaded bridge, moment, span 200ft – nonparametric fit to data

Extrapolation to 75 year for medium loaded bridge span 200ft is presented is presented in Figure 4-8. Extreme value theory is used to determine distribution of 75 year live load. Mean value is equal to 1.60 and the coefficient of variation is calculated based on the green dashed line.

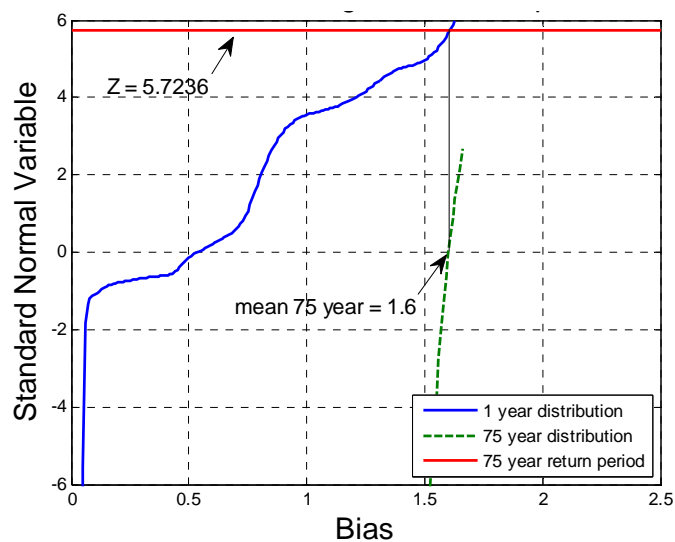


Figure 4-24 Medium loaded bridge, moment, span 200ft – extrapolation to 75 year return period

All the mean values and the coefficients of variation are in the range of 0.11-0.12. Statistical parameters for moment and for shear are tabularized in Table 22 and Table 22 respectively.

Table 24 Mean Maximum Moments for Simple Span for 1 year and 75 years

Span (ft)	1 year	75 years	CoV for 75 year
30	1.60	1.67	0.12
60	1.84	2.05	0.11
90	1.79	1.99	0.11
120	1.72	1.88	0.12
200	1.52	1.60	0.12

Table 25 Mean Maximum Shear for Simple Span for 1 year and 75 years

Span (ft)	1 year	75 years	CoV for 75 year
30	2.15	2.21	0.12
60	2.20	2.33	0.13
90	2.06	2.17	0.12
120	1.91	2.01	0.12
200	1.58	1.66	0.13

4.3. NEW YORK – LIVE LOAD EFFECT

WIM data for New York

The WIM data includes 12 months of traffic recorded at the site 8382 in New York located close to Port Jervis. The total number of records is 1,594,674 trucks. The data includes number of axles, gross vehicle weight (GVW), weight per axle and spacing between axles as well as a lane position.

Maximum Simple Span Moments

The maximum moment was calculated for each truck from the data. Analysis included simple spans with the span varying from 30 to 200 ft. The maximum moment was also calculated for the HL93 load and Tandem. The ratio between data truck moment and code load moment was plotted on the probability paper (Figure 4-25).

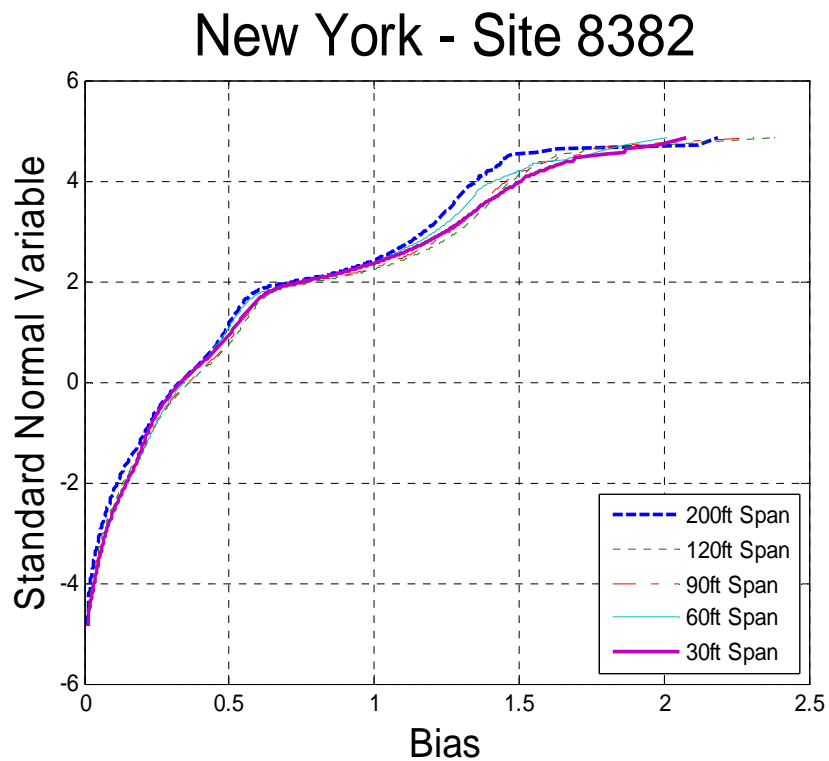


Figure 4-25 Cumulative Distribution Functions of Simple Span Moment– New York - Site 8382

Maximum Shear

The maximum shear was calculated for each truck from the data. Analysis included simple spans with the span varying from 30 to 200 ft. The ratio of shear obtained from the data truck and the HL-93 load was plotted on probability paper presented in Figure 4-26.

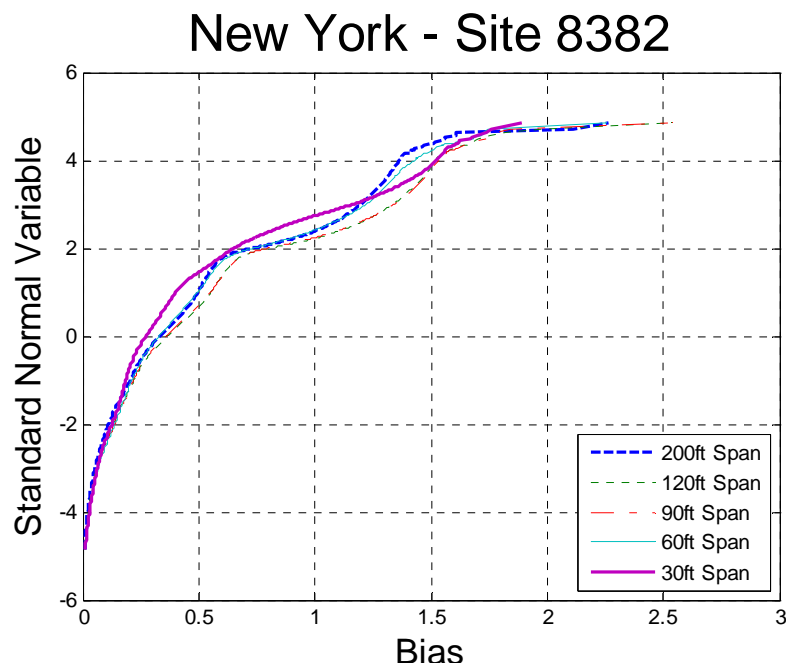


Figure 4-26 Cumulative Distribution Functions of Shear – New York Site 8382

Maximum Load Effect for Different Return Period

The total number of trucks, equal to 1,594,674, represents one year of traffic on a bridge. To predict the maximum live load effect that will occur in 75 years only ones requires an extrapolation of a CDF plot to the 75 year return period. One year of traffic corresponds to the probability of 1 over 1,594,674 equal to $6.27\text{E-}07$ and this corresponds to the standard normal variable z equal to 4.85. To find the 75 year return period on the vertical axis and the corresponding probability, the number of trucks from one year was multiplied by 75. The 75 year volume of traffic would be 119,600,550 with the assumption that there will be no traffic increase in that period of time. The probability that heaviest truck will occur only once in 75 year is equal to $8.36\text{E-}09$ which corresponds to 5.64 on the vertical axis. The total number of trucks for different time period is tabularized and shown in Table 26.

Table 26 Number of Trucks with Corresponding Probability and Time Period

Time period	Number of trucks, N	Probability, 1/N	Inverse normal, z
1 month	132,890	7.53E-06	4.33
2 months	265,779	3.76E-06	4.48
6 months	797,337	1.25E-06	4.71
1 year	1,594,674	6.27E-07	4.85
5 years	7,973,370	1.25E-07	5.16
50 years	79,733,700	1.25E-08	5.57
75 years	119,600,550	8.36E-09	5.64

Extrapolation to 75 year return period

The approach using parametric distributions was not applicable. The upper tail of the live load effect plotted on the probability paper does not follow any known type of the distribution. Therefore extension of the upper tail was performed using nonparametric approach described in Chapter 2 of this dissertation. The extrapolations were prepared for moment and shear. The simple span moment ratio extrapolations and nonparametric fit to data are shown on Figure 4-27 to Figure 4-36. Moments and shear for different return periods are tabulated and shown in Table 27 and Table 28.

Kernel normal function and the bandwidth 0.0284 were assumed for the distribution of live load for medium loaded bridge span 30 ft. It resulted in the best fit to the whole data set. Domain was assumed as positive. Trend of the end of the fit tail depends on the distance of the last point of the data set from the other points. Heavy loaded fit is shown in Figure 4-7.

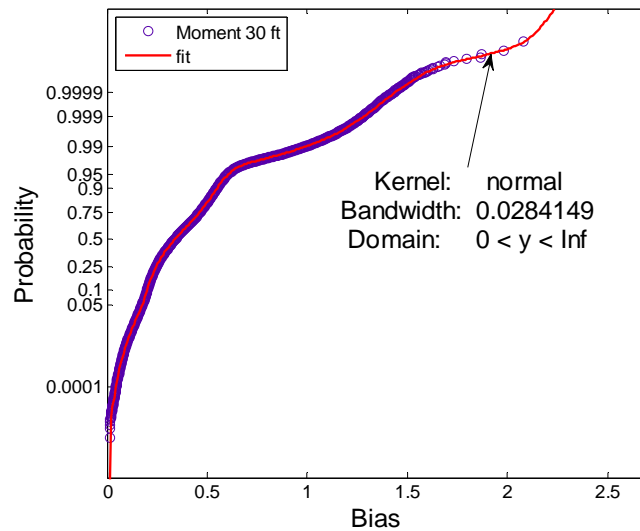


Figure 4-27 High loaded bridge, moment, span 30ft – nonparametric fit to data

Extrapolation to 75 year for low loaded bridge span 30ft is presented is presented in Figure 4-8. Extreme value theory is used to determine distribution of 75 year live load. Mean value is equal to 2.22 and the coefficient of variation is calculated based on the green dashed line.

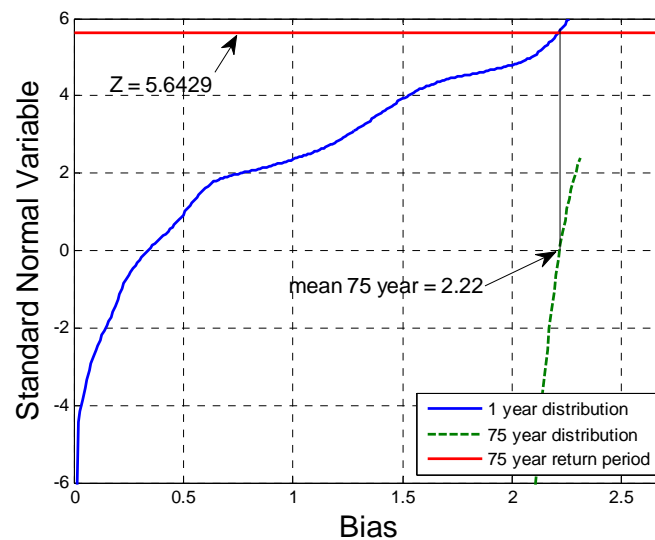


Figure 4-28 Heavy loaded bridge, moment, span 30ft – extrapolation to 75 year return period

Kernel normal function and the bandwidth 0.0245 were assumed for the distribution of live load for medium loaded bridge span 60 ft. It resulted in the best fit to the whole data set. Domain was assumed as positive. Trend of the end of the fit tail depends on the distance of the last point of the data set from the other points. Heavy loaded fit is shown in Figure 4-7.

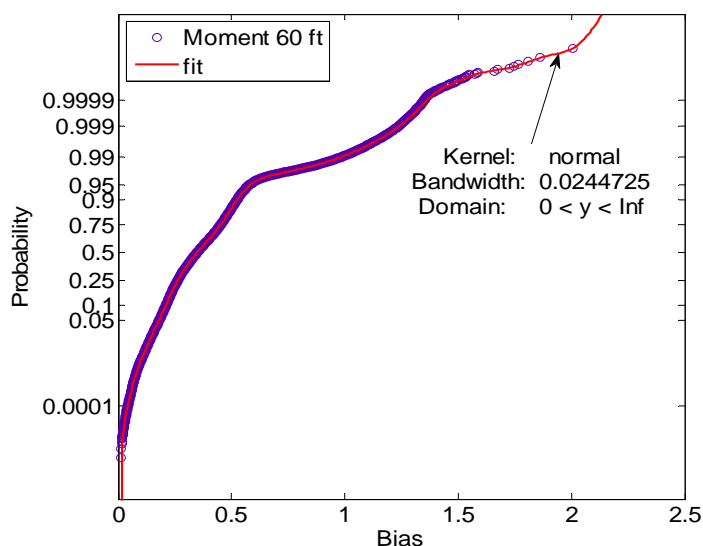


Figure 4-29 High loaded bridge, moment, span 60ft – nonparametric fit to data

Extrapolation to 75 year for heavy loaded bridge span 60ft is presented is presented in Figure 4-8. Extreme value theory is used to determine distribution of 75 year live load. Mean value is equal to 2.12 and the coefficient of variation is calculated based on the green dashed line.

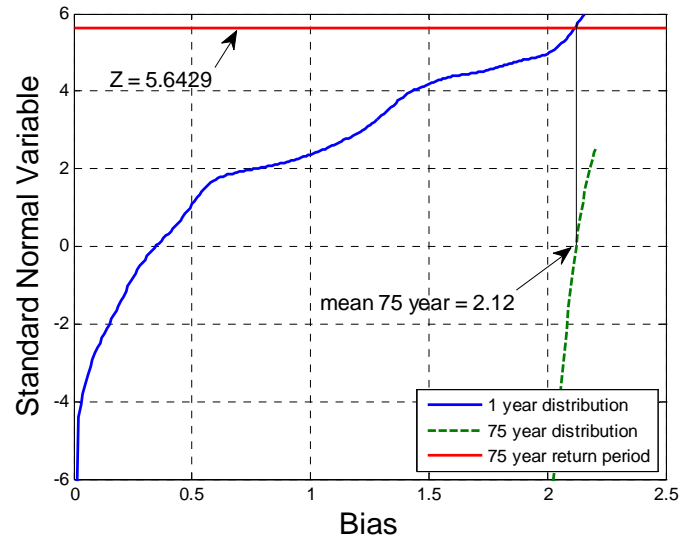


Figure 4-30 High loaded bridge, moment, span 60ft – extrapolation to 75 year return period

Kernel normal function and the bandwidth 0.0268 were assumed for the distribution of live load for medium loaded bridge span 90 ft. It resulted in the best fit to the whole data set. Domain was assumed as positive. Trend of the end of the fit tail depends on the distance of the last point of the data set from the other points. Heavy loaded fit is shown in Figure 4-7.

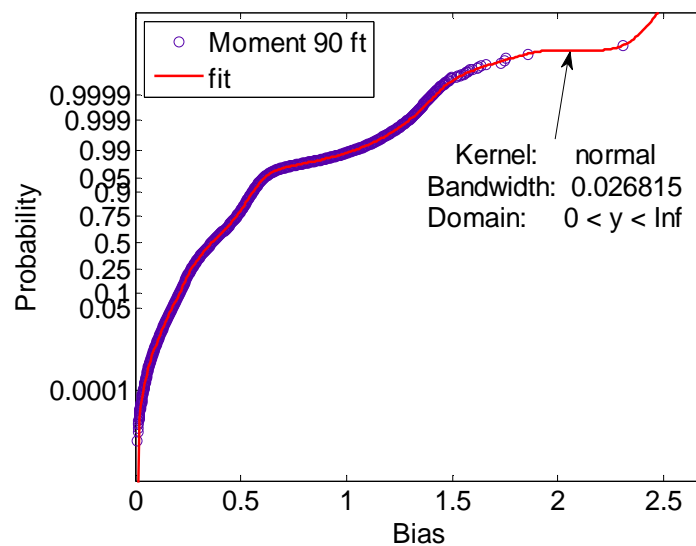


Figure 4-31 High loaded bridge, moment, span 90ft – nonparametric fit to data

Extrapolation to 75 year for heavy loaded bridge span 90ft is presented in Figure 4-8. Extreme value theory is used to determine distribution of 75 year live load. Mean value is equal to 2.45 and the coefficient of variation is calculated based on the green dashed line.

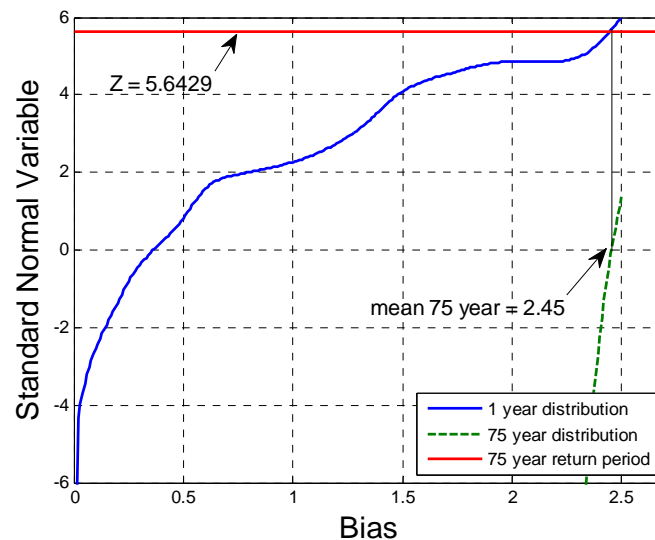


Figure 4-32 High loaded bridge, moment, span 90ft – extrapolation to 75 year return period

Kernel normal function and the bandwidth 0.0273 were assumed for the distribution of live load for medium loaded bridge span 120 ft. It resulted in the best fit to the whole data set. Domain was assumed as positive. Trend of the end of the fit tail depends on the distance of the last point of the data set from the other points. Heavy loaded fit is shown in Figure 4-7.

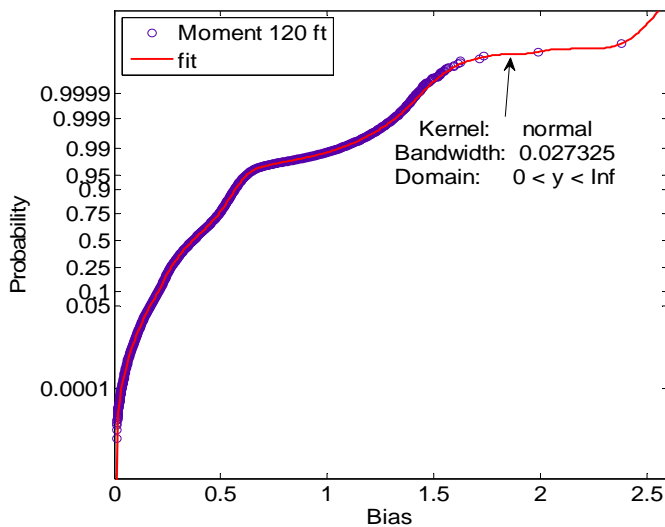


Figure 4-33 High loaded bridge, moment, span 120ft – nonparametric fit to data

Extrapolation to 75 year for heavy loaded bridge span 120ft is presented in Figure 4-8. Extreme value theory is used to determine distribution of 75 year live load. Mean value is equal to 2.55 and the coefficient of variation is calculated based on the green dashed line.

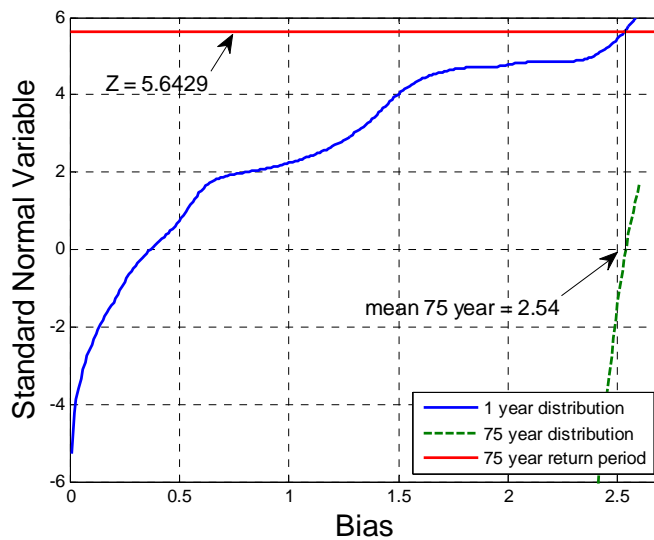


Figure 4-34 High loaded bridge, moment, span 120ft – extrapolation to 75 year return period

Kernel normal function and the bandwidth 0.0278 were assumed for the distribution of live load for medium loaded bridge span 200 ft. It resulted in the best fit to the whole data set. Domain was assumed as positive. Trend of the end of the fit tail depends on the distance of the last point of the data set from the other points. Heavy loaded fit is shown in Figure 4-7.

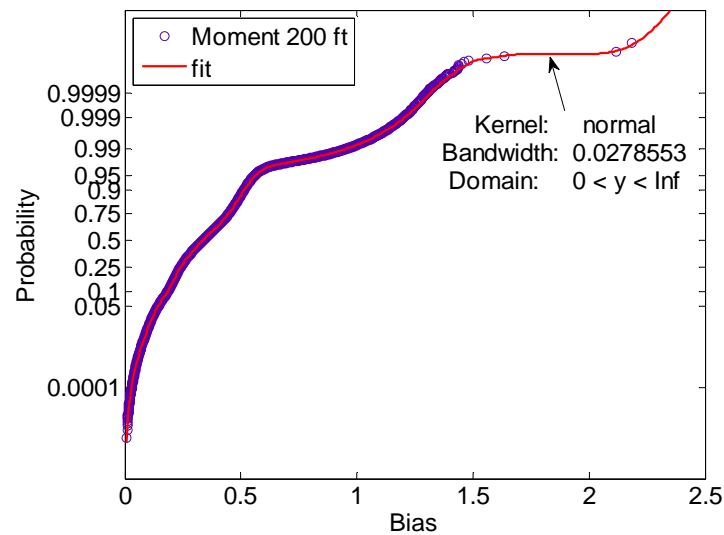


Figure 4-35 High loaded bridge, moment, span 200ft – nonparametric fit to data

Extrapolation to 75 year for heavy loaded bridge span 200ft is presented in Figure 4-8. Extreme value theory is used to determine distribution of 75 year live load. Mean value is equal to 2.33 and the coefficient of variation is calculated based on the green dashed line.

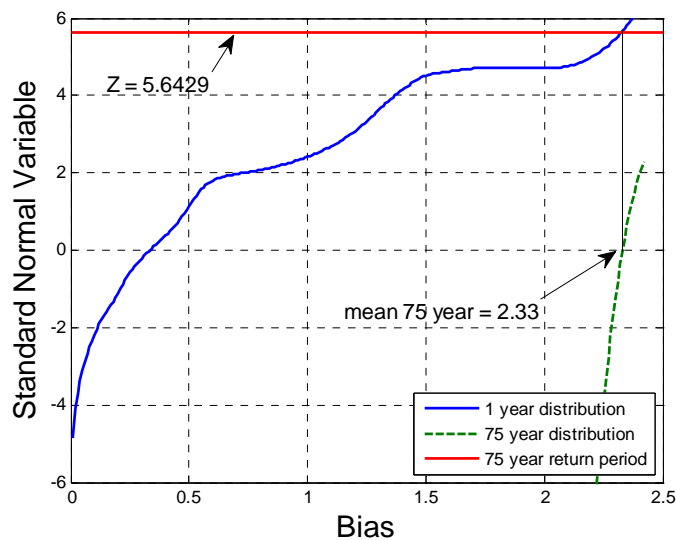


Figure 4-36 High loaded bridge, moment, span 200ft – extrapolation to 75 year return period

All the mean values and the coefficients of variation are in the range of 0.13-0.14. Statistical parameters for moment and for shear are tabularized in Table 22 and Table 22 respectively.

Table 27 Mean Maximum Moments for Simple Span for 1 year and 75 years

Span (ft)	1 year	75 years	CoV for 75 year
30	2.08	2.22	0.11
60	2.01	2.12	0.11
90	2.31	2.45	0.11
120	2.38	2.54	0.12
200	2.19	2.33	0.11

Table 28 Mean Maximum Shear for Simple Span for 1 year and 75 years

Span (ft)	1 year	75 years	CoV for 75 year
30	1.89	2.02	0.12
60	2.26	2.38	0.11
90	2.54	2.67	0.12
120	2.54	2.7	0.12
200	2.26	2.42	0.11

CHAPTER 5. MULTIPLE PRESENCE

5.1. COEFFICIENT OF CORRELATION

Simultaneous occurrence of two or more trucks on the bridge can generate the extreme load effect in the structure. The statistical parameters of these effects are influenced by the degree of correlation. AAHSTO LRFD Code calibration (Nowak 1999) was based on the Ontario data. Total number of records was almost ten thousand. Researchers assumed three coefficients of correlation: $\rho = 0$, $\rho = 0.5$ and $\rho = 1$ for single and multiple lanes loaded.

The correct development of the load model has to include the degree of correlation. The analysis of the simultaneous occurrence of two trucks in one lane or in adjacent lanes was needed. A special program was developed to filter the data using the time of a record and a speed of the truck. The filter resulted in selecting of two trucks with the headway distance less than 200 ft. Two analyzed cases of simultaneous occurrence are showed in Figure 5-1. These cases can cause the maximum load effect in the structure. Based on the research of Nowak, it was assumed that two correlated trucks in adjacent lane produce the maximum moment in the girder. WIM data from Florida, California and New York includes records from four lanes of traffic.

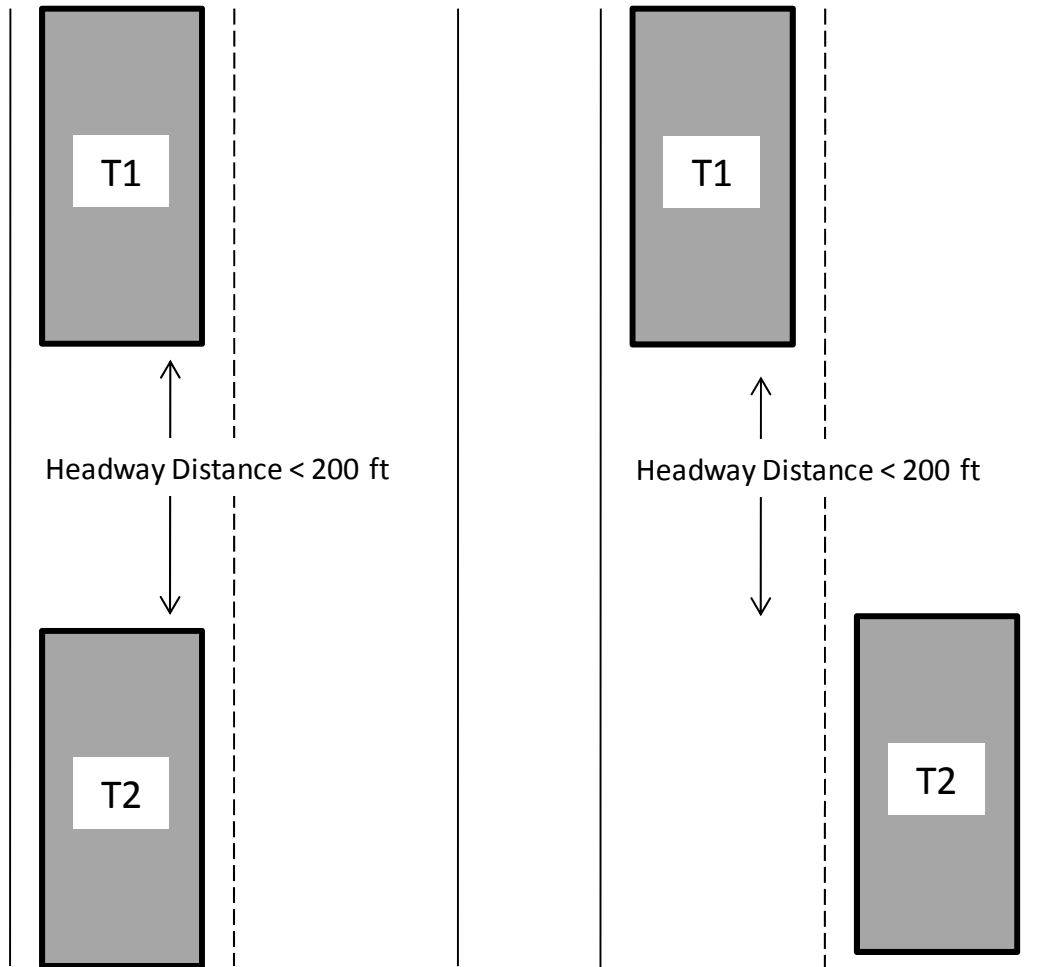


Figure 5-1 Two cases of the simultaneous occurrence

The objective of the correlation analysis was to select two trucks, within the group of vehicles that simultaneously occurred on the bridge, which geometry parameters and weight followed the assumptions:

- Two trucks have to have the same number of axles
- GVW of the trucks has to be within the $\pm 5\%$ limit
- Spacing between each axle has to be within the $\pm 10\%$ limit

Two Trucks – Side By Side

The analysis of the degree of correlation was performed on the site 9936 in Florida along I-10 and 8382 in New York with total number of records equal to 1,654,004 and 1,594,674 respectively. The filtering of the data resulted in selection of 2518 fully correlated trucks in adjacent lanes in Florida. A scatter plot is shown in Figure 5-2. The horizontal axis represents the gross vehicle weight of 1259 trucks in one lane and the vertical the gross vehicle weight of the corresponding 1259 trucks in adjacent lane. The filtering of the New York site data resulted in selection of 3748 fully correlated trucks in adjacent lanes. A scatter plot of these trucks is shown in Figure 5-2. The horizontal axis represents the gross vehicle weight of 1874 trucks in one lane and the vertical the gross vehicle weight of the corresponding 1874 trucks in adjacent lane.

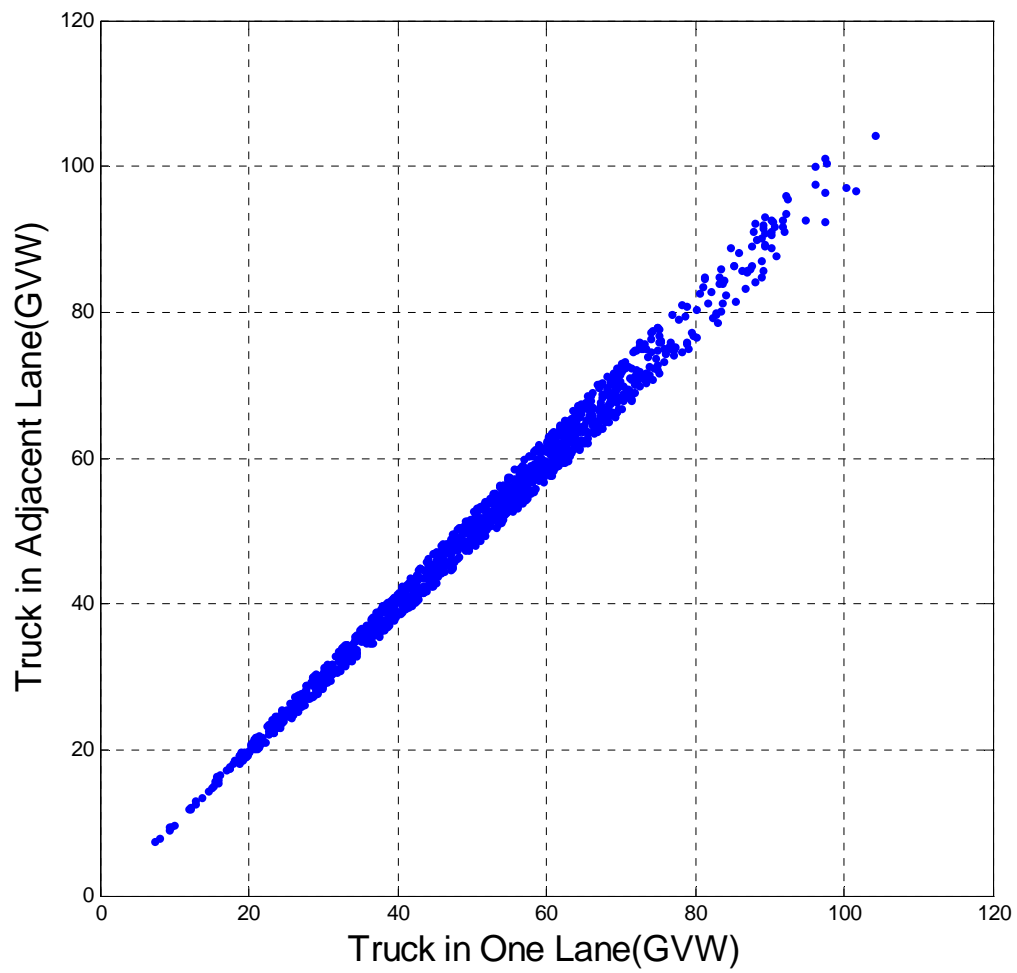


Figure 5-2 Scatter plot – Trucks Side by Side – Florida I-10

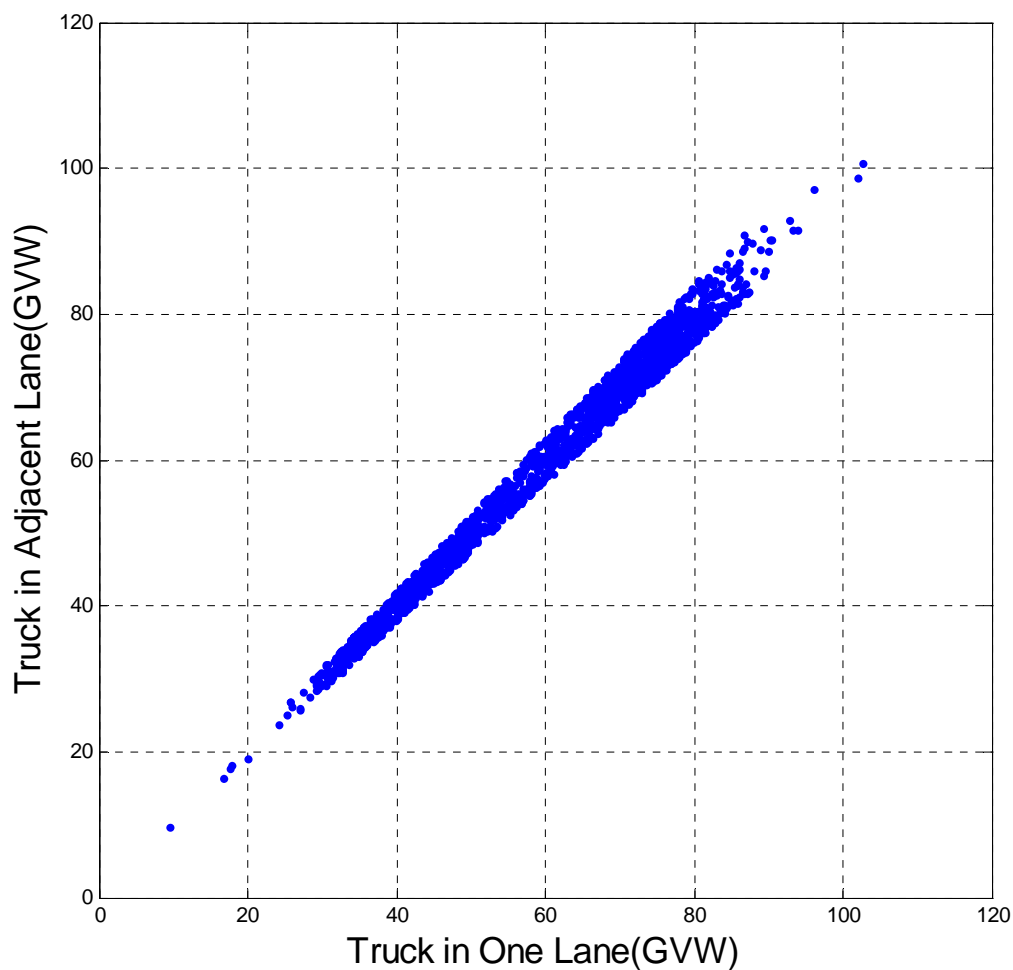


Figure 5-3 Scatter plot – Trucks Side by Side – New York

It was needed to include the selected trucks on the probability paper and compare them with the whole recorded population of vehicles. The gross vehicle weights of two corresponding trucks were added to each other and divided by two to obtain the mean GVW. The comparison of the mean correlated GVW of the trucks recorded in adjacent lanes with the GVW of the whole data from Florida and New York are shown in Figure 5-4 and Figure 5-5 respectively.

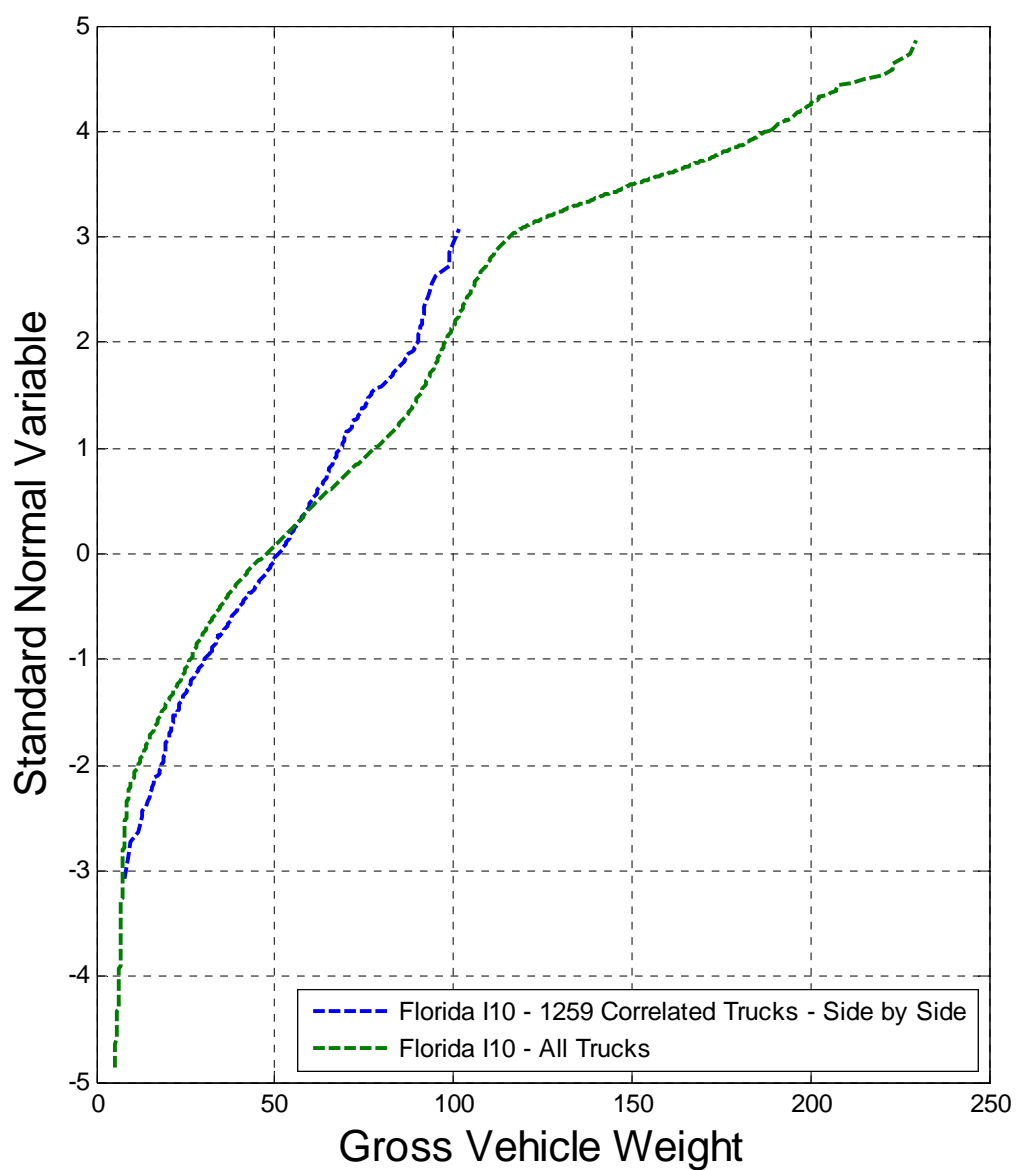


Figure 5-4 Comparison of the mean GVW to the GVW of the whole population - Florida

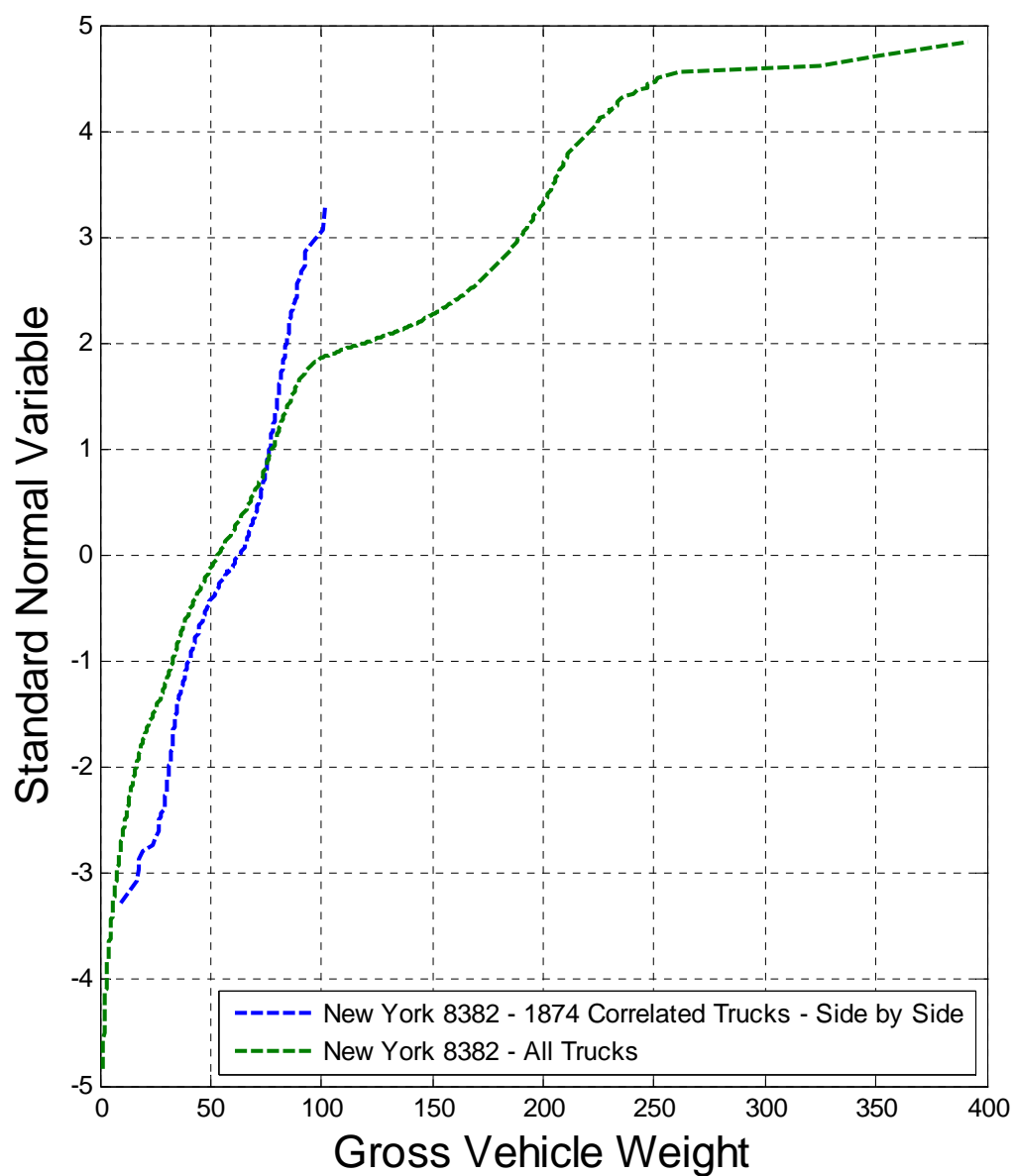


Figure 5-5 Comparison of the mean GVW to the GVW of the whole population – New York

Two Trucks – One after another

The filtering of the data resulted in selection of 8380 fully correlated trucks in one lane in Florida. A scatter plot is shown in Figure 5-6. The horizontal axis represents the gross vehicle weight of 4190 leading trucks in one lane and the vertical the gross vehicle weight of the corresponding 4190 following trucks. The filtering of the New York site data resulted in selection of 9868 fully correlated trucks in one lane. A scatter plot of these trucks is shown in Figure 5-7. The horizontal axis represents the gross vehicle weight of 4934 leading trucks and the vertical the gross vehicle weight of the corresponding 4934 following trucks.

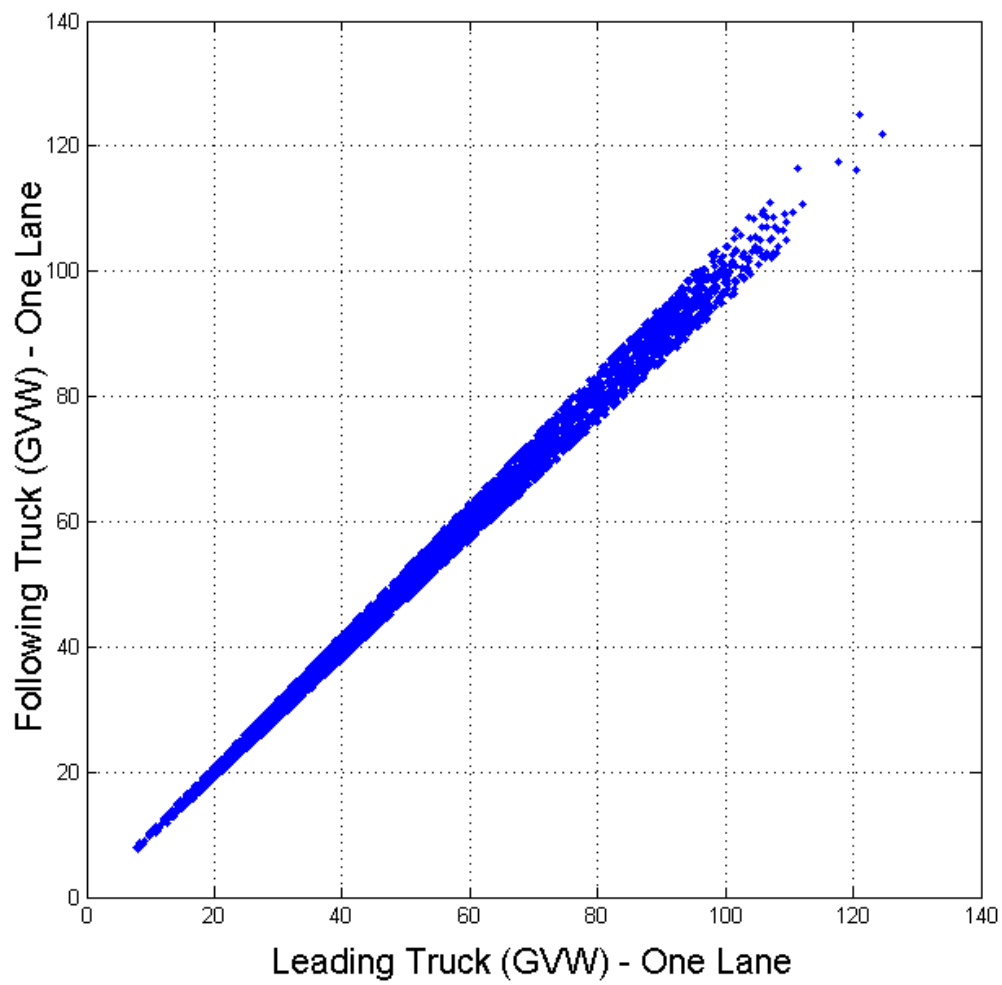


Figure 5-6 Scatter plot – Trucks One after another – Florida I-10

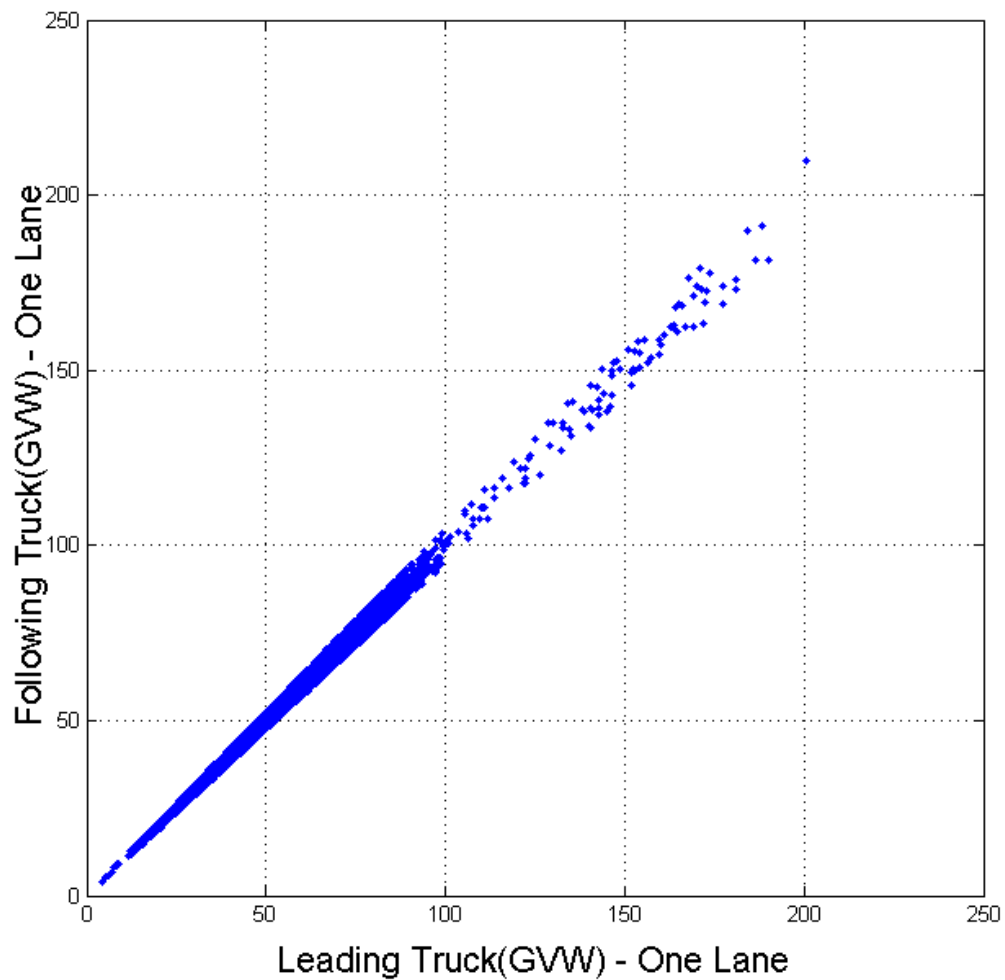


Figure 5-7 Scatter plot – Trucks one after another – New York

The comparison of the mean correlated GVW of the trucks recorded in one lane with the GVW of the whole data from Florida and New York are shown in Figure 5-8 and Figure 5-9 respectively.

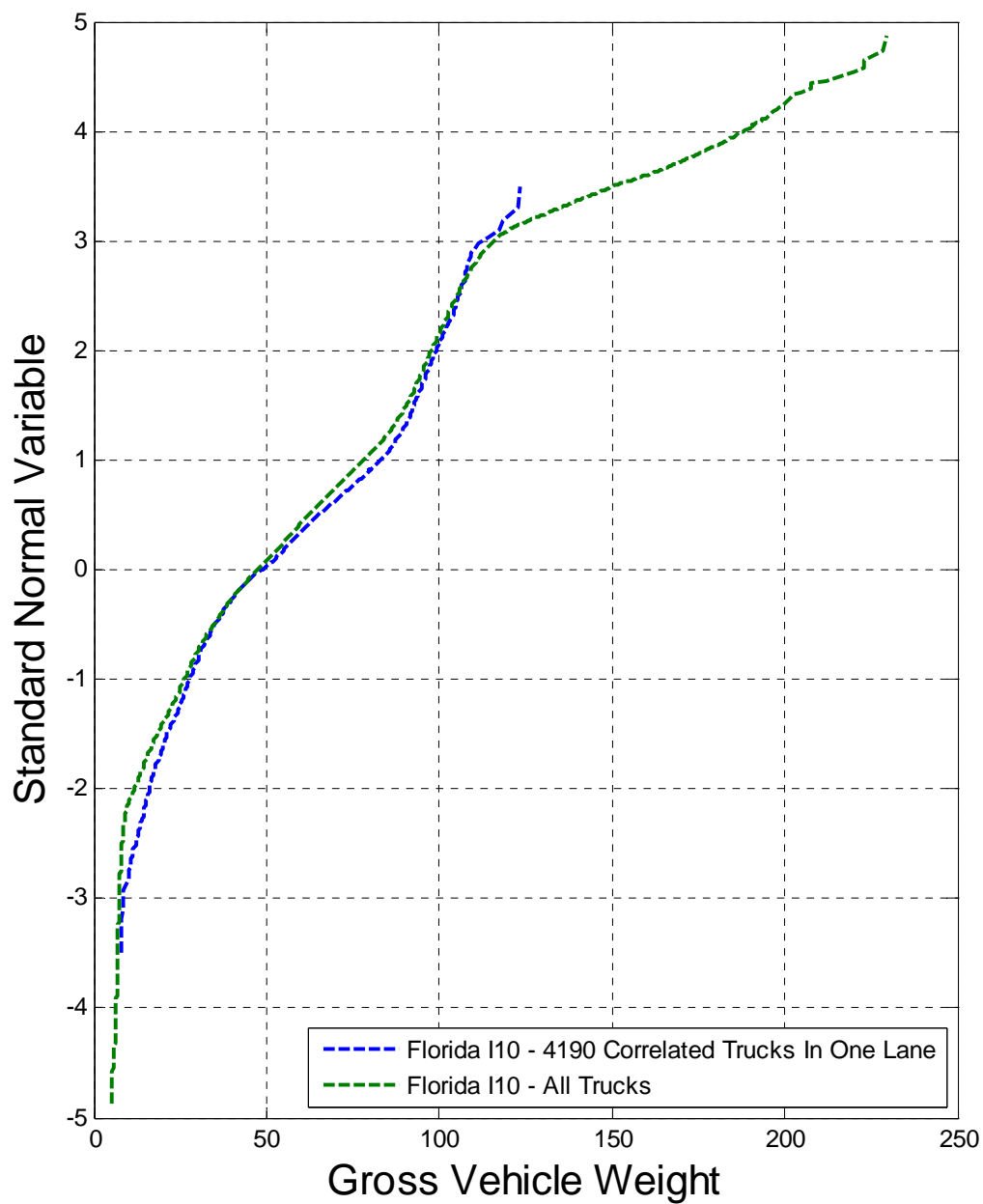


Figure 5-8 Comparison of the mean GVW to the GVW of the whole population - Florida

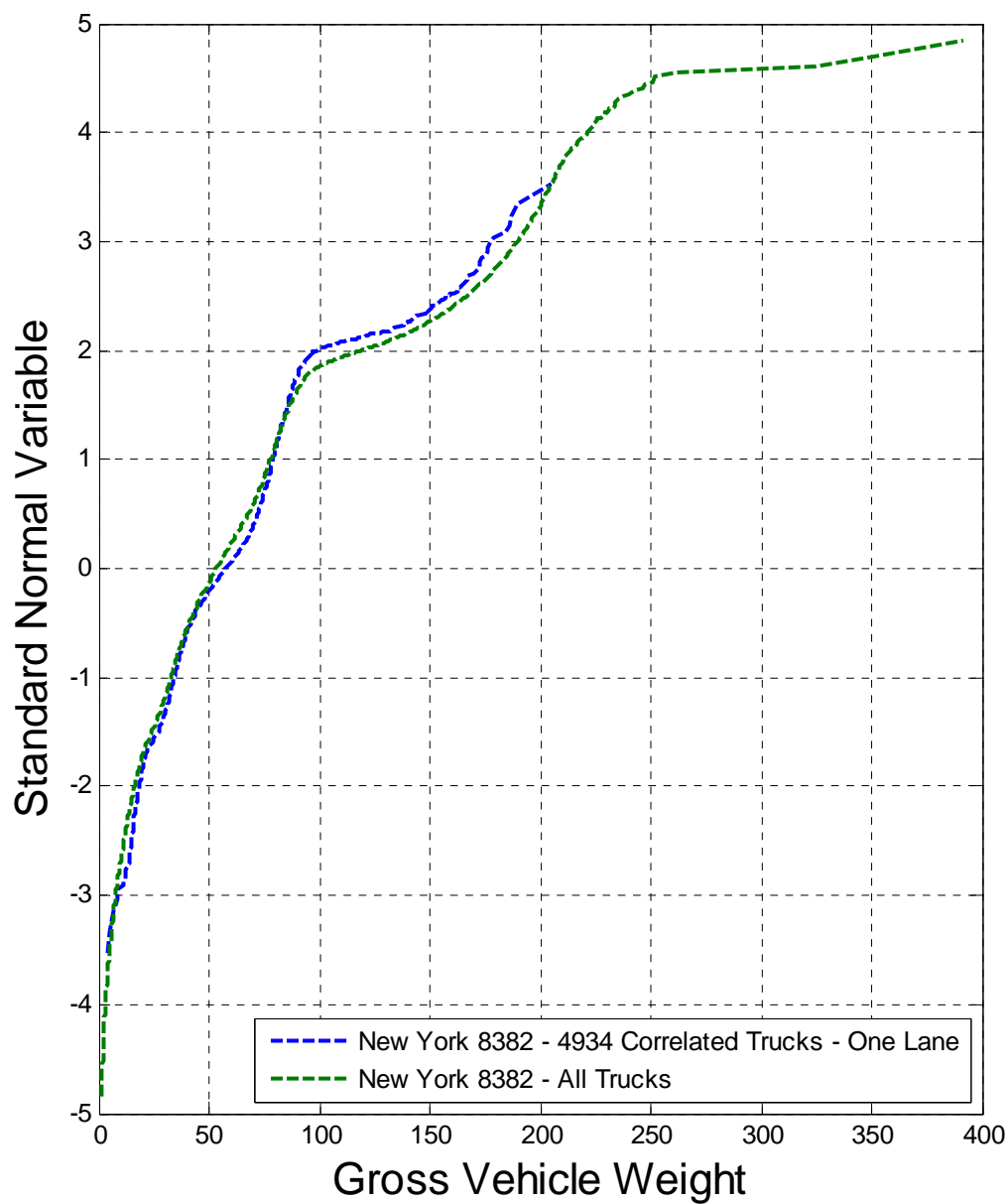


Figure 5-9 Comparison of the mean GVW to the GVW of the whole population –New York

5.2. LOAD MODEL FOR MULTIPLE LANE

Extreme moments and shear depends on the span length and different headway distances between the trucks. Two lanes loaded with two trucks side-by-side can produce the maximum load effect. It was assumed that the trucks are positioned on the bridge to cause a maximum load effect. In the analysis of two trucks in two lanes lane the following cases were considered:

- Only one lane loaded with the maximum 75 Year truck
- 1 year maximum truck in one lane, average truck in adjacent lane.

5.3. LOAD DISTRIBUTION MODEL

An individual response of a girder to live load is presented in this Section. Previous research (Eom 2001) indicated that the multiple-lane loading causes the maximum load effect in the girder. To determine the live load effect in a girder an accurate girder distribution factor is needed. A validation of code specified GDF was presented by many researchers (Kim and Nowak 1997b), (Eom and Nowak 2001), (Eom 2001). Based on the field testing researchers discovered, that the load carrying capacity of an existing bridge is much higher than the load carrying capacity of the design one due to involvement of nonstructural elements like railing in sharing the load. In this study a finite element method was used to build a load distribution model.

5.3.1 Code Specified GDF

The NCHRP Project 12-26 "Distribution of Wheel Loads on Highway Bridges," resulted in implementation of girder distribution factors as a function of girder spacing, span length, stiffness parameters, and bridge skewness into the AASHTO LRFD Code (Zokai et al. 1991). The girder distribution factor for moment in interior beam with multiple lane loaded can be presented as:

$$g = 0.075 + \left(\frac{S}{9.5}\right)^{0.6} \left(\frac{S}{L}\right)^{0.2} \left(\frac{n(I + Ae_g^2)}{12.0Lt_s^3}\right)^{0.1} \quad \text{Eq - 20}$$

Where the following assumptions must be fulfilled:

- Girder spacing: $3.5\text{ft} \leq S \leq 16.0\text{ft}$
- Depth of the concrete slab: $4.5\text{in} \leq t_s \leq 12.0\text{ in}$
- Span length: $20\text{ft} \leq L \leq 240\text{ft}$
- Number of girders $N_b \geq 4$

The longitudinal stiffness parameter K_g for the initial design can be assumed 1. Girder distribution factor with multiple lane loaded for shear can be described with the following equation:

$$g = 0.2 + \frac{S}{12} - \left(\frac{S}{35}\right)^2 \quad \text{Eq - 21}$$

Field testing performed by previously mentioned researchers showed that the code specified GDF are conservative and they cannot be used in development of live load model. Conservative prediction of the load transfer onto girders can lead to inaccurate reliability indices.

5.3.2 Finite Element Model

To analyze a multiple lane load it was necessary to build a FEM 3D model of a bridge. In this study the structural analysis of a bridge system was performed using a FEM software tool ABAQUS 6.6. Six simply supported bridges with steel composite girder, span 60ft, 120 ft and spacing 6, 8, 10ft were considered. The selection of these cases is summarized in Chapter 6 of this dissertation.

The main goal of the FEM simulation was to determine the most loaded girder and verify the load transfer from two HS20 trucks to girders (Mabsout et al. 1997a), (Bakht and Jaeger L. G. 1990), (Mabsout et al. 1997b), (Eamon and Nowak A.S. 2002). The trucks were positioned longitudinally on the bridge to cause the maximum moment and moved transversally to determine the maximum loaded girder (Eom 2001), (Eom and Nowak 2001), (Eamon and Nowak 2004), (Bishara et al. 1993), (Kim and Nowak 1997b), (Kim and Nowak 1997a). An example of a transverse position of two trucks is shown in Figure 5-10.

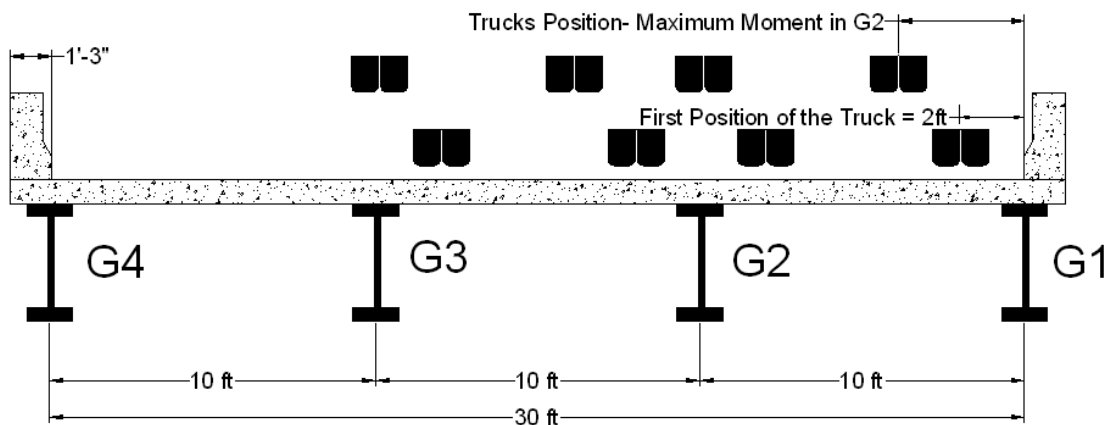


Figure 5-10 Transverse position of two HS20 trucks to cause the maximum load effect in a girder

It was assumed, that a 3D FEM model based on elastic linear approach is adequate. Girders and rails were simulated using B33 2-node cubic beam elements in three-dimensional space. Slab was simulated using S4R 4-node doubly curved general-purpose shell, reduced integration with hourglass control and finite membrane strains. An example of the modeled bridge is shown in Figure 5-11

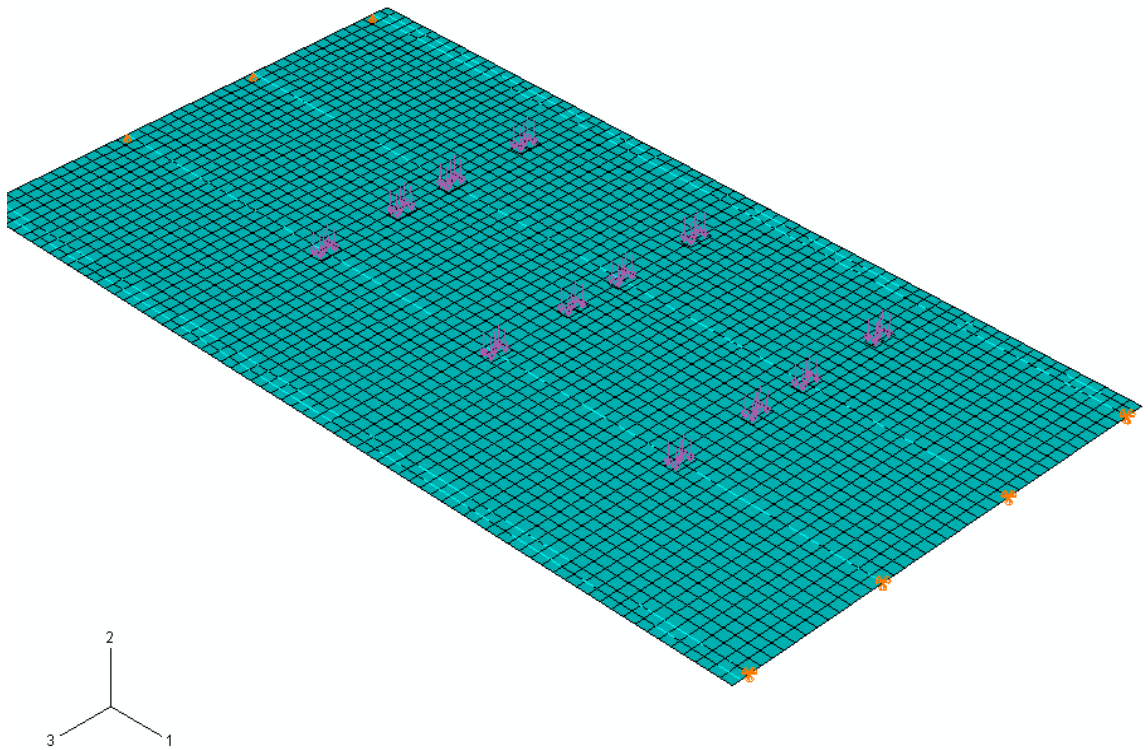


Figure 5-11 Finite Element Bridge Model

Load applied on the bridge was defined as two HS20 trucks. Supports were modeled to represent simply supported structure. Girders, rails and slab were connected using tie constraints.

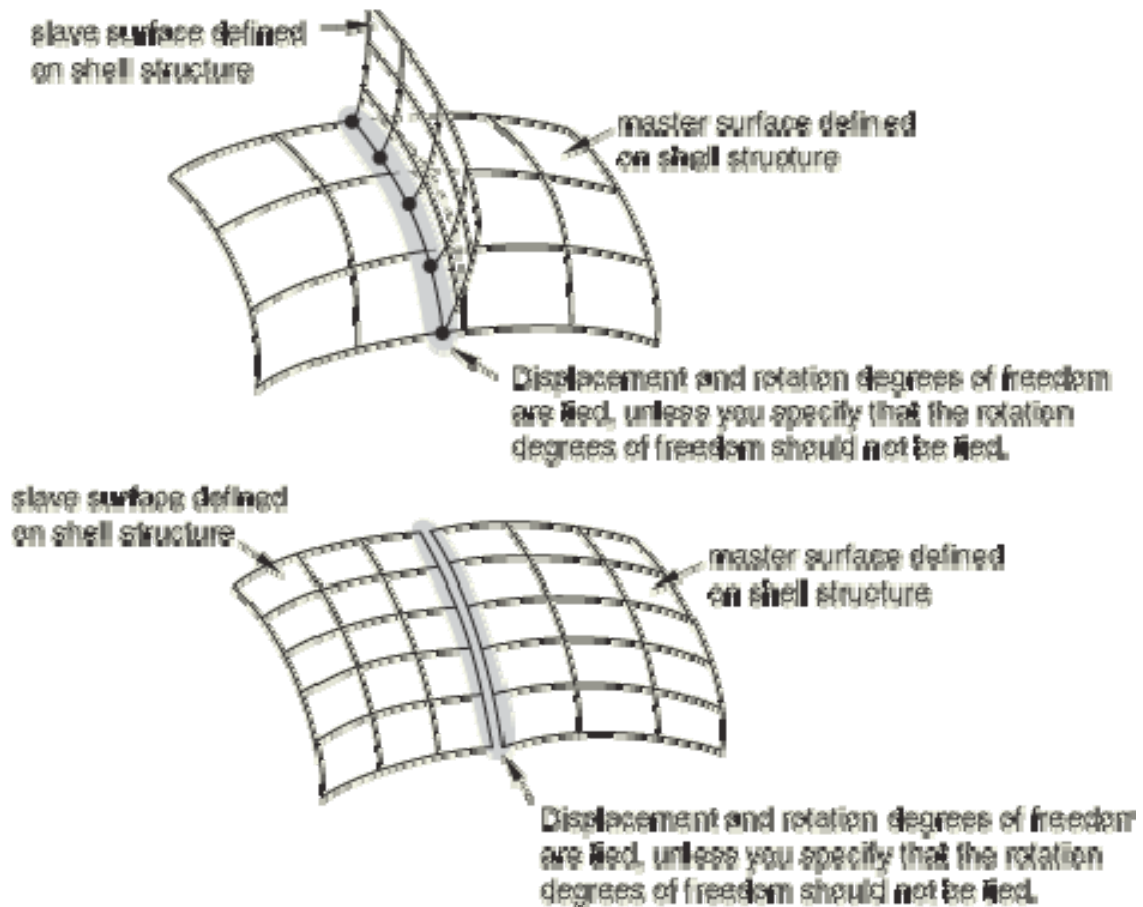


Figure 5-12 Surface-based tie algorithm (ABAQUS v.6.6 Documentation)

Types of steel girders used in the analysis are tabularized in Table 29. Spans 60ft and 120ft were considered in the calculations with different types of composite steel girders.

Maximum bending moment in bridge B1 was observed in girder G2 with truck position showed in Figure 5-13. The results for bridge B1 are shown in Table 30. The bending moment for bridges B2, B3, B4, B5, B6 are presented in Table 30 to Table 35.

Table 29 Composite Steel Girders Used In FEM Analysis

Bridge	B1	B2	B3	B4	B5	B6
Span	60ft	60ft	60ft	120ft	120ft	120ft
Steel Section	W30x108	W27x94	W24x84	W44x262	W44x224	W40x199
Spacing	10ft	8ft	6ft	10ft	8ft	6ft
Table	Table 30	Table 31	Table 32	Table 33	Table 34	Table 35

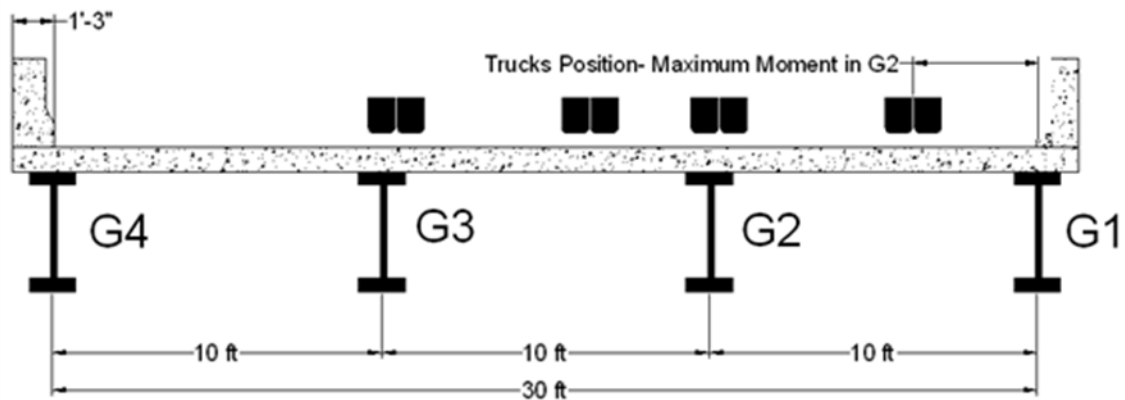


Figure 5-13 Transverse trucks position causing the maximum bending moment in girder

G2 – Bridge B1

Table 30 Bending moments for different transverse position of two trucks Bridge B1

Girder	Position 1	Position 2	Position 3	Position 4	Maximum Moment Position
G1	-853.6	-738.8	-632.3	-533.9	-716.8
G2	-1303.6	-1343.8	-1295.1	-1243.7	-1347.5
G3	-992.7	-1128.1	-1183.5	-1243.6	-1150.5
G4	-289.3	-362.0	-443.7	-534.0	-377.3

Table 31 Bending moments for different transverse position of two trucks Bridge B2

Girder	Position 1	Position 2	Position 3	Position 4	Position 5	Position 6	Maximum Moment Position
G1	-678.7	-589.3	-505.2	-428.0	-358.4	-295.78	-473.29
G2	-1018.9	-971.2	-935.9	-899.8	-851.1	-761.05	-921.59
G3	-956.7	-1018.0	-1084.6	-1095.4	-1090.2	-1102.1	-1107.3
G4	-582.6	-666.1	-746.4	-829.2	-897.9	-928.02	-778.58
G5	-180.4	-229.5	-284.15	-345.29	-413.46	-489.25	-307.86

Table 32 Bending moments for different transverse position of two trucks Bridge B3

Girder	Position 1	Position 2	Position 3	Position 4	Maximum Moment Position
G1	-513.0	-443.2	-378.5	-319.0	-354.2
G2	-684.8	-653.8	-628.4	-577.6	-620.0
G3	-769.6	-761.0	-775.5	-756.4	-785.2
G4	-655.1	-683.0	-720.6	-756.4	-732.9
G5	-398.4	-458.6	-517.16	-577.62	-539.24
G6	-172.6	-216.8	-265.34	-318.98	-286.2

Table 33 Bending moments for different transverse position of two trucks Bridge B4

Girder	Position 1	Position 2	Position 3	Maximum Moment Position
G1	-4353.2	-3844.8	-3361.6	-3844.8
G2	-4609.5	-4615.0	-4388.9	-4615.0
G3	-3399.8	-3776.7	-3966.1	-3776.7
G4	-1668.8	-2051.3	-2463.1	-2051.3

Table 34 Bending moments for different transverse position of two trucks Bridge B5

Girder	Position 1	Position 2	Position 3	Position 4	Maximum Moment Position
G1	-3525.9	-3119.9	-2728.4	-2359.4	-3525.9
G2	-3820.9	-3576.3	-3390.9	-3194.3	-3820.9
G3	-3195.9	-3318.5	-3463.1	-3468.4	-3195.9
G4	-2090.8	-2360.8	-2629.5	-2911.6	-2090.77

G5	-1066.3	-1342.2	-1635.6	-1949.7	-1066.3
----	---------	---------	---------	---------	---------

Table 35 Bending moments for different transverse position of two trucks Bridge B6

Girder	Position 1	Position 2	Maximum Moment Position
G1	-2892.48	-2544.33	-2892.48
G2	-2998.47	-2815.17	-2998.47
G3	-2940.55	-2842.38	-2940.55
G4	-2446.48	-2510.86	-2446.48
G5	-1688.07	-1926.34	-1688.07
G6	-1077.9	-1335.67	-1077.9

The FEM analysis resulted in establishing the most stressed girder in the system. The girder distribution factors were determined for the position of the trucks causing the maximum bending moment. It was necessary to verify the contribution of each truck into a girder bending moment. Results of the analysis are shown in Table 36 to Table 41.

Table 36 Girder Distribution Factor – Maximum Bending Moment - Bridge B1

Girder	Moment - One Truck	Moment - Adjacent Truck	GDF form Truck 1	GDF form Truck 2	Total GDF
G1	-302.209	-192.343	0.161	0.103	0.264
G2	-753.99	-623.752	0.403	0.333	0.736
G3	-624.265	-754.258	0.333	0.403	0.736
G4	-192.471	-302.28	0.103	0.161	0.264

Table 37 Girder Distribution Factor – Maximum Bending Moment - Bridge B2

Girder	Moment - One Truck	Moment - Adjacent Truck	GDF form Truck 1	GDF form Truck 2	Total GDF
G1	-351.333	-121.956	0.203	0.066	0.268
G2	-556.408	-365.183	0.321	0.197	0.518
G3	-498.453	-608.836	0.287	0.328	0.616
G4	-261.519	-517.065	0.151	0.279	0.430
G5	-66.3424	-241.516	0.038	0.130	0.168

Table 38 Girder Distribution Factor – Maximum Bending Moment - Bridge B3

Girder	Moment - One Truck	Moment - Adjacent Truck	GDF form Truck 1	GDF form Truck 2	Total GDF
G1	-265.021	-89.186	0.162	0.053	0.215
G2	-399.526	-220.447	0.245	0.131	0.375
G3	-421.996	-363.2	0.258	0.216	0.474
G4	-304.6	-428.298	0.187	0.254	0.441
G5	-176.678	-362.564	0.108	0.215	0.323
G6	-65.3307	-220.868	0.040	0.131	0.171

Table 39 Girder Distribution Factor – Maximum Bending Moment - Bridge B4

Girder	Moment - One Truck	Moment - Adjacent Truck	GDF form Truck 1	GDF form Truck 2	Total GDF
G1	-2679.52	-1165.31	0.381	0.161	0.542
G2	-2535.91	-2079.07	0.360	0.287	0.647
G3	-1372.37	-2404.34	0.195	0.332	0.527
G4	-448.375	-1602.95	0.064	0.221	0.285

Table 40 Girder Distribution Factor – Maximum Bending Moment - Bridge B5

Girder	Moment - One Truck	Moment - Adjacent Truck	GDF form Truck 1	GDF form Truck 2	Total GDF
G1	-2412.2	-1113.73	0.362	0.158	0.520
G2	-2165.1	-1655.82	0.324	0.236	0.560
G3	-1301.9	-1894.04	0.195	0.270	0.465
G4	-650.9	-1439.86	0.098	0.205	0.302
G5	-142.4	-923.931	0.021	0.131	0.153

Table 41 Girder Distribution Factor – Maximum Bending Moment - Bridge B6

Girder	Moment - One Truck	Moment - Adjacent Truck	GDF form Truck 1	GDF form Truck 2	Total GDF
G1	-1992.8	-899.703	0.292	0.125	0.416
G2	-1821.3	-1177.16	0.266	0.163	0.430
G3	-1421.1	-1519.43	0.208	0.211	0.419
G4	-922.7	-1523.76	0.135	0.211	0.346
G5	-502.2	-1185.85	0.073	0.164	0.238
G6	-174.9	-902.954	0.026	0.125	0.151

CHAPTER 6. LOAD COMBINATIONS

6.1. INTRODUCTION

Bridge structure can be subjected to many various types of loads which can be categorized according to AASHTO LRFD into two groups: Permanent Loads and Transient Loads. The major loads impacting the short and medium span bridges are dead load and live load with impact therefore in this study only these are considered. Each load component can be expressed in terms random variable. As presented in previous Chapters the variation of all load components is defined by their cumulative distribution function, and other statistical parameters.

6.2. DEAD LOAD

Dead load of structural components and nonstructural attachments, DC , as well as dead load of wearing surfaces and utilities, DW , is a gravity load. According to NCHRP Report 368 (Nowak 1999) the components of dead load can be represented as:

- DC_1 – weight of factory made elements
- DC_2 – weight of cast-in-place concrete members
- DW_1 – weight of the wearing surface
- DW_2 – miscellaneous weight (rails,

All the components are represented by the cumulative distribution function taken as normal. The statistical parameters of dead load are summarized in Table 42 and are based on research of Nowak and Zhou (Nowak and Zhou 1985), (Zhou 1987).

Table 42 The Statistical Parameters of Dead Load

Component	Bias Factor	Coefficient of Variation
DC ₁	1.03	0.08
DC ₂	1.05	0.10
DW ₁	3.5 in (mean)	0.25
DW ₂	1.03-1.05	0.08-0.10

6.3. LIVE LOAD AND TRUCK DYNAMIC

Based on the Weigh-In-Motion analysis of many sites it was necessary to choose the representative sites that will cover the whole spectrum of loads and would be a basis for eventual new live load model. The site selection was presented in Chapter 4 of this dissertation. Three types of vehicular live load acting on the bridge were defined as follows:

- Light
- Medium
- Heavy

The mean values of ratios M_T/M_{HL93} are summarized in Table 43, Table 44 and Table 45 for low, medium and high loaded bridge respectively. The coefficients of variation of LL are presented in Table 46, Table 47 and Table 48.

Table 43 Low Loaded Bridge - Mean Ratio M_T/M_{HL93}

Span, ft	Maximum 75 Year Ratio M_T/M_{HL93}	Maximum 1 Year Ratio M_T/M_{HL93}	Mean Ratio M_T/M_{HL93}
30	1.52	1.42	0.31
60	1.53	1.43	0.31
90	1.61	1.50	0.30
120	1.57	1.46	0.30

Table 44 Medium Loaded Bridge - Mean Ratio M_T/M_{HL93}

Span, ft	Maximum 75 Year Ratio M_T/M_{HL93}	Maximum 1 Year Ratio M_T/M_{HL93}	Mean Ratio M_T/M_{HL93}
30	1.67	1.60	0.40
60	2.05	1.84	0.55
90	1.99	1.79	0.56
120	1.88	1.72	0.55

Table 45 High Loaded Bridge - Mean Ratio M_T/M_{HL93}

Span, ft	Maximum 75 Year Ratio M_T/M_{HL93}	Maximum 1 Year Ratio M_T/M_{HL93}	Mean Ratio M_T/M_{HL93}
30	2.22	2.08	0.40
60	2.12	2.01	0.41
90	2.45	2.31	0.42
120	2.54	2.38	0.41

Table 46 Low Loaded Bridge - Coefficient of Variation of LL

Span, ft	Maximum 75 Year CoV	Maximum 1 Year CoV	Mean CoV
30	0.12	0.13	0.61
60	0.11	0.13	0.61
90	0.12	0.12	0.67
120	0.12	0.12	0.67

Table 47 Medium Loaded Bridge - Coefficient of Variation of LL

Span, ft	Maximum 75 Year CoV	Maximum 1 Year CoV	Mean CoV
30	0.12	0.13	0.20
60	0.11	0.11	0.42
90	0.12	0.12	0.39
120	0.11	0.12	0.42

Table 48 High Loaded Bridge - Coefficient of Variation of LL

Span, ft	Maximum 75 Year CoV	Maximum 1 Year CoV	Mean CoV
30	0.11	0.12	0.25

60	0.11	0.11	0.22
90	0.11	0.12	0.19
120	0.12	0.13	0.22

Based on research performed at the University of Michigan (Hwang 1990), (Hwang and Nowak 1991), (Eom 2001) the dynamic part of vehicular load can be obtained as the ratio of dynamic strain and static strain. Dynamic load is a function of road surface roughness

The researcher conducted

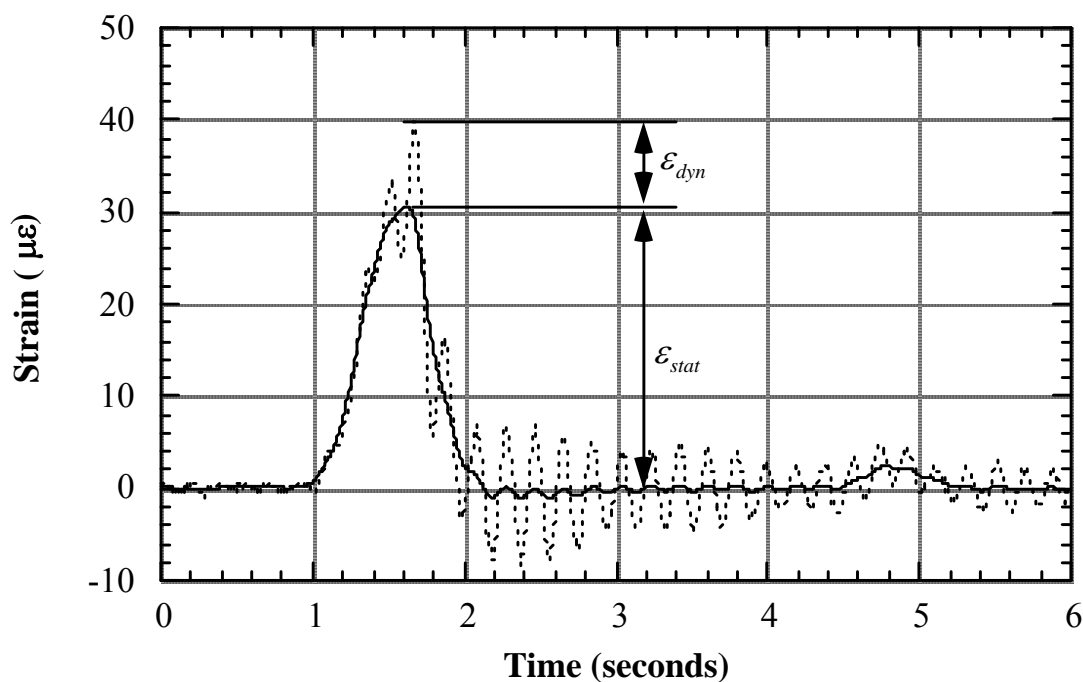


Figure 6-1 Dynamic and Static Strain under a Truck at Highway Speed (Eom 2001)

The mean dynamic load is assumed according to NCHRP Report 368 as 0.1 of the mean live load for two trucks. The corresponding coefficient of variation is equal to 0.80. The static and dynamic load combination is modeled based on statistical parameters of static portion of live load and dynamic. Following AASHTO LRFD calibration report the

coefficient of variation of static load can be assumed as a product of static live load SLL and the live load analysis factor P and can be formulated as follows:

$$V_{SLLP} = \sqrt{V_{SLL}^2 + V_P^2} \quad \text{Eq - 22}$$

The standard deviation of SLL and analysis factor is given as:

$$\sigma_{SLLP} = V_{SLLP} \mu_{SLL} \mu_P \quad \text{Eq - 23}$$

Where mean value and coefficient of variation of P is 1.0 and 0.12 respectively.

The mean maximum 75 year live load with impact is given as:

$$\mu_{SLLP+IM} = \mu_{SLL} \mu_P (1 + \mu_{IM}) \quad \text{Eq - 24}$$

Standard deviation and coefficient of variation is given as:

$$\sigma_{SLLP+IM} = \sqrt{\sigma_{SLLP}^2 + \sigma_{IM}^2} \quad \text{Eq - 25}$$

$$V_{SLLP+IM} = \frac{\sigma_{SLLP+IM}}{\mu_{SLLP+IM}} \quad \text{Eq - 26}$$

Following the above equations and assuming a loading case of two lanes loaded, the recalculated values for coefficient of variation including dynamic load are presented in Table 49, Table 50 and Table 51.

Table 49 Low Loaded Bridge - Coefficient of Variation of LL with Dynamic Load

Maximum 75 Year $V_{SLLP+IM}$	Maximum 1 Year $V_{SLLP+IM}$	Mean $V_{SLLP+IM}$	Combined CoV of Maximum 1 Year and Mean
0.16	0.17	0.61	0.18
0.16	0.17	0.61	0.18
0.16	0.16	0.66	0.17
0.16	0.16	0.66	0.18

Table 50 Medium Loaded Bridge - Coefficient of Variation of LL with Dynamic Load

Maximum 75 Year $V_{SLLP+IM}$	Maximum 1 Year $V_{SLLP+IM}$	Mean $V_{SLLP+IM}$	Combined CoV of Maximum 1 Year and Mean
0.16	0.17	0.28	0.14
0.15	0.15	0.42	0.15
0.16	0.16	0.40	0.15
0.15	0.16	0.42	0.16

Table 51 High Loaded Bridge - Coefficient of Variation of LL with Dynamic Load

Maximum 75 Year $V_{SLLP+IM}$	Maximum 1 Year $V_{SLLP+IM}$	Mean $V_{SLLP+IM}$	Combined CoV of Maximum 1 Year and Mean
0.15	0.16	0.31	0.14
0.15	0.15	0.29	0.14
0.15	0.16	0.27	0.14
0.15	0.16	0.29	0.15

CHAPTER 7. RESISTANCE MODEL

The resistance model of a bridge component takes into consideration uncertainties arising from the material properties, quality of fabrication and the accuracy of the theoretical model used in analysis. Resistance R as a product of the nominal resistance, specified by the code, material, fabrication and professional factor can be shown as:

$$R = R_n M F P \quad \text{Eq - 27}$$

and the statistical parameters of R as:

$$\mu_R = R_n \mu_M \mu_F \mu_P \quad \text{Eq - 28}$$

$$V_R = \sqrt{V_M^2 + V_F^2 + V_P^2} \quad \text{Eq - 29}$$

where μ_R and V_R are the mean and coefficient of variation of resistance respectively. The statistical parameters of the material, fabrication and professional factors can be found in the available literature (Tabsh and Nowak 1991), (Nowak et al. 1994), (Nowak and Zhou 1985), (Nowak and Zhou 1990), (Ellingwood et al. 1980). In this study statistical

parameters for resistance are based on AASHTO LRFD Calibration (Nowak 1999) and are summarized in the Table 52.

Table 52 Statistical Parameters of Resistance

Type of Structure	Material and Fabrication Factors, F M		Professional Factor, P		Resistance, R	
	λ	V	λ	V	λ	V
Composite girders						
Moment	1.07	0.08	1.05	0.06	1.12	0.10
Shear	1.12	0.08	1.02	0.07	1.14	0.105

The nominal load carrying capacity of steel composite girders was based on the AASHTO LRFD code provisions and will be presented in the next Chapter.

7.1. MOMENT CAPACITY OF COMPOSITE STEEL GIRDERS

The behavior of composite steel was presented by Tantawi (1986). The research included flexural, torsional and shear stresses. The ultimate torsional capacity of the cross section was also analyzed. Material properties (strength and dimensions) were modeled by taking into consideration data given by Kennedy (Kennedy 1982) and Ellingwood, Galambos, MacGregor and Cornell (1980). The dominant failure mode was crushing of concrete in

the positive moment region and the longitudinal reinforcement was minimal. Assumption of a complete composite action between steel and concrete was made. The effect of the slip was neglected.

The moment-curvature relationship was analyzed by Tabsh (1990). A composite beam action analysis was depending on the stress-strain relationship of the structural steel, concrete, reinforcing steel, and the effective flange width of the cross section. The monotonically increasing loading was considered for several different cross sections.

The following assumptions were made (Nowak 1999):

- A complete composite action between concrete and steel section. The effect of slip was neglected.
- The typical stress-strain curves for concrete, reinforcing steel and structural steel were used. In the analysis, the curves were generated by Monte Carlo simulations.
- The tensile strength of concrete was neglected.
- The effect of existing stress and strain in the cross section before composite action takes place, in case of unshored construction, was not considered.

Development of the nonlinear moment-curvature analysis was based on the iterative method and was done by Tantawi (Tantawi 1986). Some assumptions were made including idealization of the section by implementing a set of rectangular layers. Strain was increased regularly by increments. At each level of the increment of the strain corresponding moment was calculated by taking into consideration nonlinear stress-strain relationships of the materials. The other assumption was to take strain throughout the

section as constant during the analysis.

A closed form expression for the moment-curvature was developed by Zhou (1987) and Zhou and Nowak (1988) which can be applicable for many cross sections.

The equation can be shown as follows:

$$f = M/EI_e + C_1(M/M_y)^{C_2} \quad \text{Eq - 30}$$

where: f = curvature; EI_e = elastic bending rigidity; M_y = yield moment; and M = internal moment due to applied load; C_1 and C_2 are constants controlling the shape of the curve. Constants C_1 , C_2 are taken at yield and at ultimate stress or strain. For composite girders C_2 ranges between 16 and 24 whereas C_1 ranges between 0.00015/ft and 0.0003/ft.

The moment-curvature relationship is shown from Figure 7-1 to Figure 7-4 (Nowak 1999). The concrete slab width considered was 6 ft, whereas the thickness was 7 in. For the statistical data for material and fabrication factor and the professional factor, the resistance parameters were calculated and are equal for the ultimate moment to $\lambda = 1.12$ and $V = 0.10$.

7.2. SHEAR CAPACITY OF STEEL GIRDERS

The ultimate shear capacity of steel sections, V_u , can be calculated as follows:

$$V_u = 1/3 A_w F_y$$

Eq - 31

where A_w = area of the web.

This equation was used for determination of statistical parameters for shear for composite steel girders.

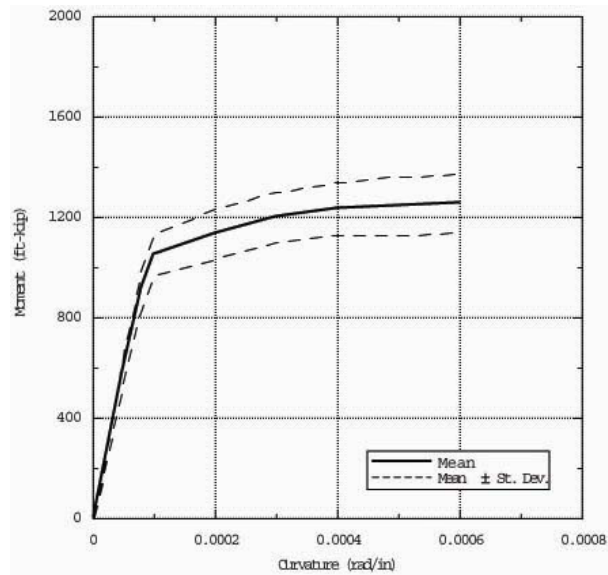


Figure 7-1 Moment – Curvature curves for a composite W24x76 steel section (Nowak 1999)

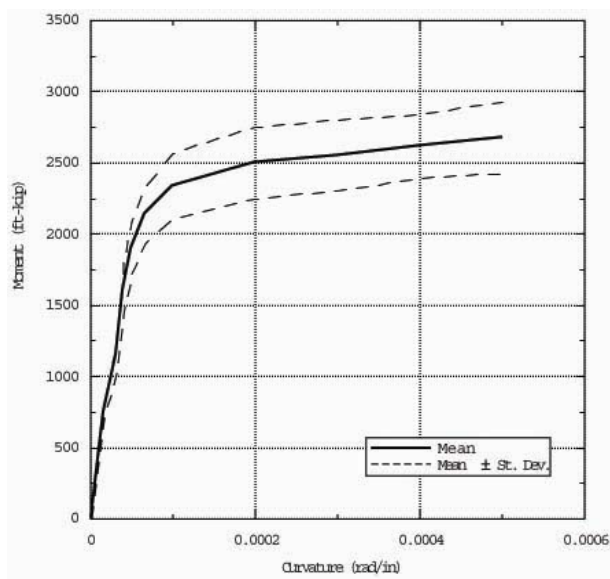


Figure 7-2 Moment – Curvature curves for a composite W33x130 steel section (Nowak 1999)

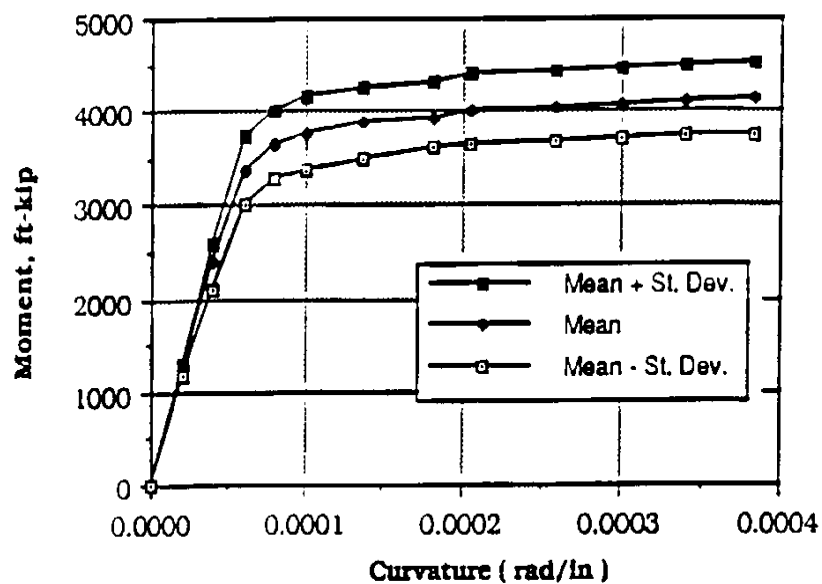


Figure 7-3 Moment – Curvature curves for a composite W36x210 steel section (Nowak 1999)

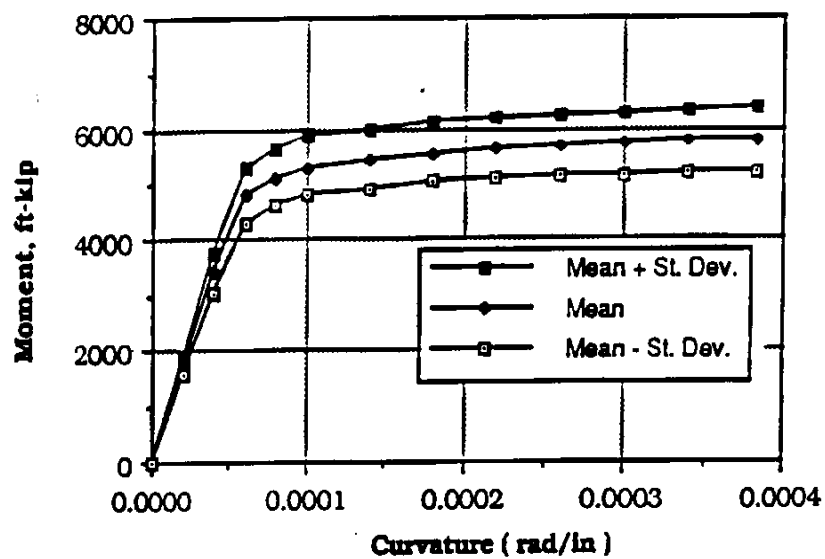


Figure 7-4 Moment – Curvature curves for a composite W36x300 steel section (Nowak 1999)

CHAPTER 8. RELIABILITY ANALYSIS

This Chapter will present a reliability analysis for steel composite girders. The main objective was to implement a new live load model derived from Weigh-In-Motion measurements. Six steel composite girder bridges were design according to AASHTO LRFD Strength I limit state. The design covered flexure and shear. Load applied on the bridge was HL93 code load. Design spans were 60 and 120ft. Three different girder spacings were considered 6, 8 and 10ft. The concrete slab was taken as 9in thick with three inches of asphalt surface. Rails were assumed as 32in New Jersey type. Statistical models of load and resistance are taken according to Chapter 5. The reliability index, described in Chapter 2 will be calculated for different bridges and load combinations. Following NCHRP Report 368 (Nowak 1999) the total load will be normally distributed and the resistance lognormally.

8.1. DESIGN OF GIRDERS

According to AASHTO LRFD the total factored force is as follows:

$$Q = \sum n_i \gamma_i Q_i \quad \text{Eq - 32}$$

where n_i is a load modifier, γ_i is the load factor and Q_i is the force effect. The total factored force has to be less or equal to ϕR_n , where ϕ is a resistance factor and R_n is the nominal resistance.

In this study only Strength I limit state is considered, therefore Eq - 31 can be rewritten as follows:

$$Q = 1.25(DC_1 + DC_2) + 1.5DW + 1.75(LL + IM) \quad \text{Eq - 33}$$

where IM is a dynamic load allowance. The nominal resistance for Strength I limit state can be calculated as:

$$R_n = \frac{1.25(DC_1 + DC_2) + 1.5DW + 1.75(LL + IM)}{\phi} \quad \text{Eq - 34}$$

Resistance factors for moment and shear according to AASHTO LRFD code is: $\phi_f = 1.0$ and $\phi_v = 1.0$.

All six bridges were designed according to the code so that the corresponding target reliability for girders was equal to 3.5. After calculations of the ultimate moment caused by the load, six different hot-rolled steel girders were chosen, which are summarized in Table 53. Next step was to determine if the plastic moment fulfils the AASHTO code requirements. To check the acceptance the following equation was verified:

$$\phi M_p \geq M_u \quad \text{Eq - 35}$$

Figure 8-1 shows the typical cross-section of the bridge that was considered in this study.

Table 53 Composite Steel Girders

Span (ft)	Spacing (ft)	Shape	A	d	tw	bf	tf
120	10	W44x262	77.2	43.3	0.79	15.8	1.42
120	8	W44X224	65.8	43.31	0.787	11.811	1.416
120	6	W40x199	58.5	38.7	0.65	15.8	1.07
60	10	W30x108	31.7	29.8	0.545	10.5	0.76
60	8	W27x94	27.7	26.9	0.49	9.99	0.745
60	6	W24x84	24.7	24.1	0.47	9.02	0.77

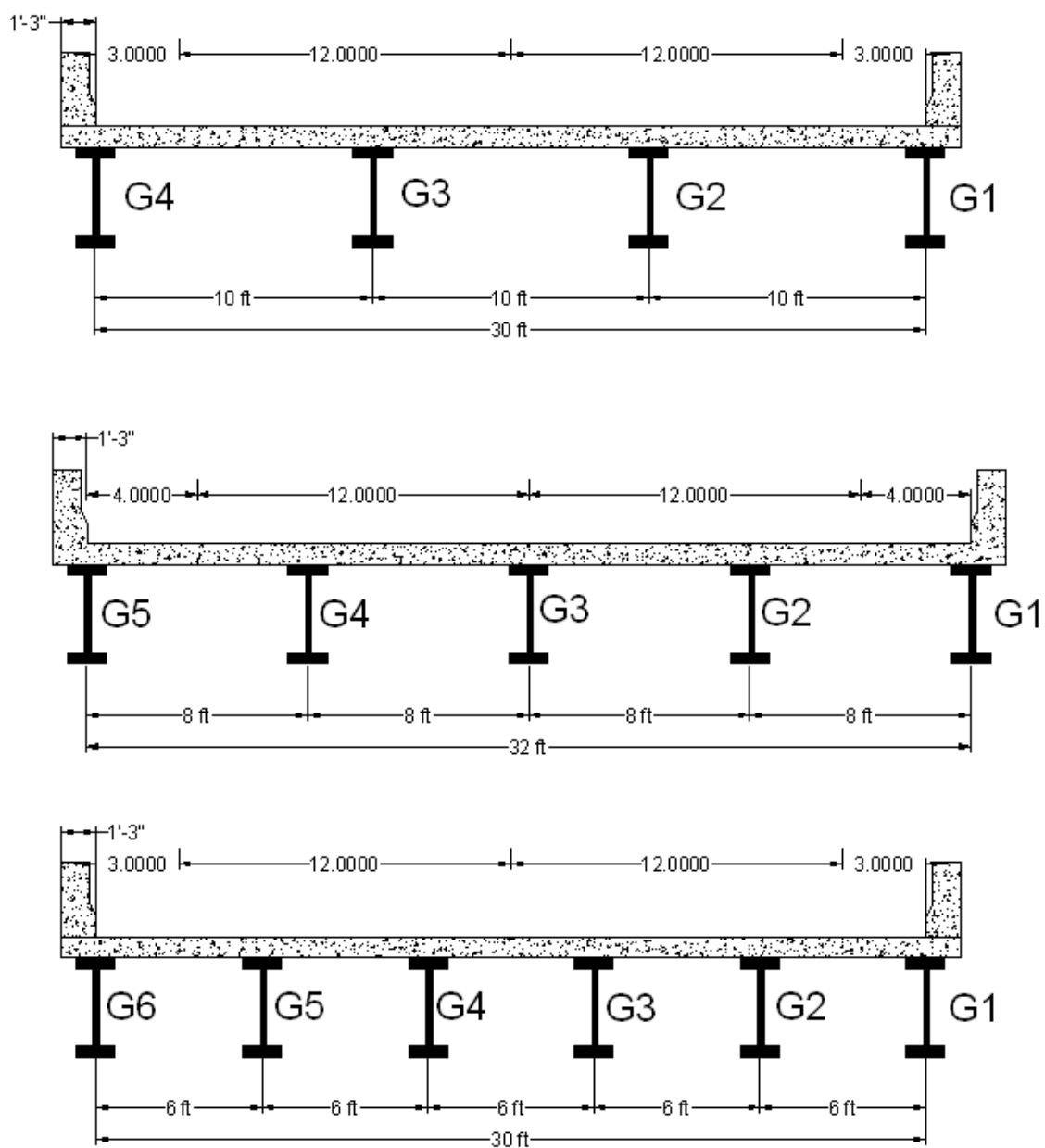


Figure 8-1 Cross-sections of Considered Bridges

8.2. RELIABILITY INDEX CALCULATIONS

In this study the reliability is based on the calculations of the reliability index, β , which can be defined as the function of probability of failure. The equation to calculate β can be defined as follows (Nowak and Collins 2000):

$$\beta = \frac{\lambda_R R_n [1 - k V_R] [1 - \ln(1 - k V_R)] - \mu_Q}{\sqrt{(\lambda_R R_n [1 - k V_R] V_R)^2 + (\sigma_Q)^2}} \quad \text{Eq - 36}$$

where:

- λ_R bias of resistance,
- V_R coefficient of variation of resistance,
- R_n nominal resistance,
- μ_Q mean of total load,
- σ_Q standard deviation of total load,
- k is the measure of the shift from the mean value in standard deviation units, assumed equal to 2.

An example of the reliability calculations is shown in Table 54. The calculations in this example were performed for span 60ft and the live load model for high loaded bridge.

The rest of the results for span 60ft and for different live load models are summarized in Table 55. The reliability indices for span 60 ft are also plotted in Figure 8 2, Figure 8 3 and Figure 8 4 Figure 8 4. The indices for span 120ft are presented in Table 56 and are plotted in Figure 8 5, Figure 8 6 and Figure 8 7 Figure 8 7. Figure 8 9 to Figure 8 10 shows the comparison of reliability indices for span 60ft and 120ft.

Table 54 Example of Reliability Index Calculations

Reliability Analysis - High Loaded Bridge						
Steel Section	W30x108					
Two Lanes Loaded						
Span (ft)	60					
Spacing (ft)	10					
Live Load per Lane						
Design Truck	1092.4					
Lane Load	288.0					
Total LL	1380.4					
Dynamic	360.5					
LL + IM	1740.9					
GDF	0.796					
Nominal Live Load per Girder	1098.3					
Nominal Live and Impact per Girder	1385.2					
HIGH Loaded Bridge	One Year Maximum	Adjacent Average				
Survey Ratio M_{Truck}/M_{HL93}	2.01	0.41				
GDF - ABAQUS	0.403	0.333				
Bias (M_T/M_{HL93})	1.189					
Mean Live Load per Girder	1305.5					
Mean Live and Impact	1436.0					
CoV for Live and Impact	0.15					
Standard Deviation of Live and Impact	215.4					
Dead Load	Nominal	Bias	COV	Mean	σ	
DC1 girder	48.6	1.03	0.08	50.1	4.00	
DC2 (slab)	506.3	1.05	0.10	531.6	53.16	
DW	140.6	1.00	0.25	140.6	35.15	
Total Load	Mean Total Load	σ_Q				
	2158.26	170.38				
Resistance (lognormal)	Nominal	LL factor	Bias	CoV	Mean	σ_R
	3328.5	1.75	1.12	0.1	3727.94	372.79
Reliability Index	β					
First Truck Maximum 1 Year; Adjacent Truck - Average	4.3					

Table 55 Reliability Index for Span 60ft

Live Load Model	W30x108 Spacing 10ft	W27x94 Spacing 8ft	W24x84 Spacing 6ft
High	4.3	4.5	4.8
Medium	4.4	4.6	4.8
Low	5.5	5.7	5.7

Table 56 Reliability Index for Span 120ft

Live Load Model	W44x262 Spacing 10ft	W44x224 Spacing 8ft	W40x199 Spacing 6ft
High	4.1	4.2	3.8
Medium	4.3	4.8	4.7
Low	5.6	5.6	5.5

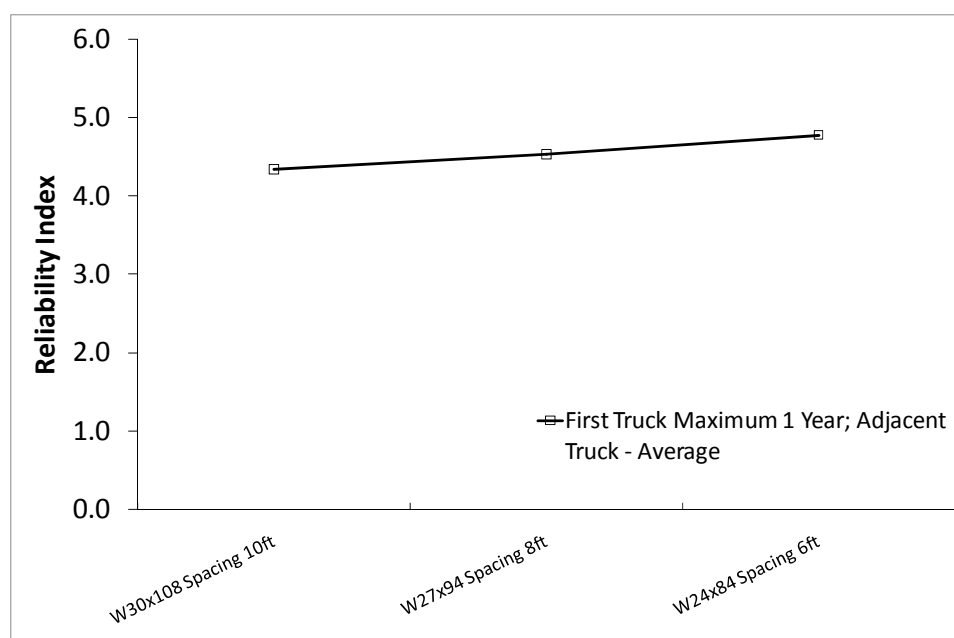


Figure 8-2 Reliability Index for Span 60ft and Live Load Model for High Loaded Bridge

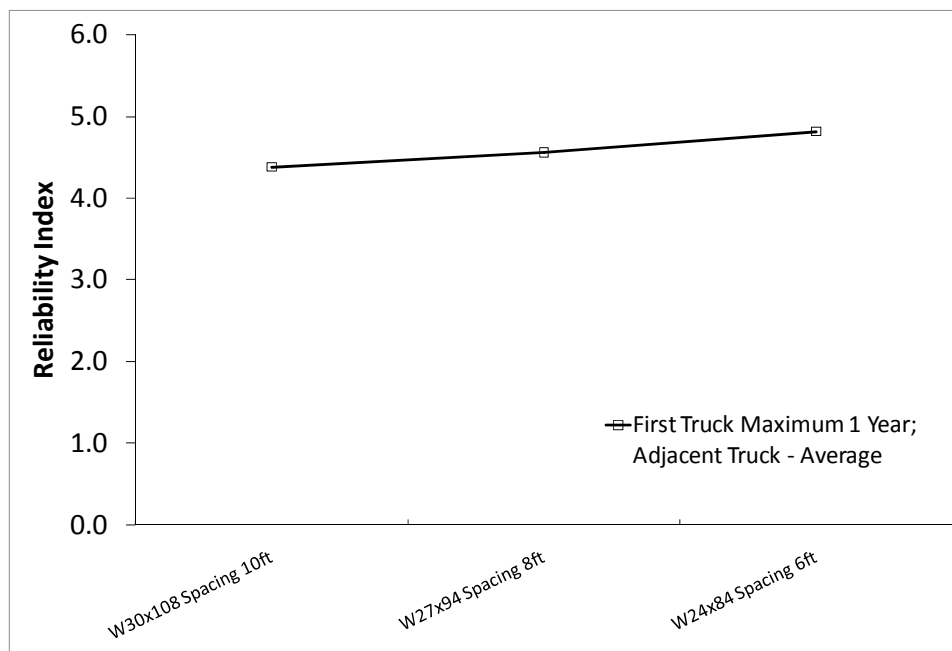


Figure 8-3 Reliability Index for Span 60ft and Live Load Model for Medium Loaded Bridge

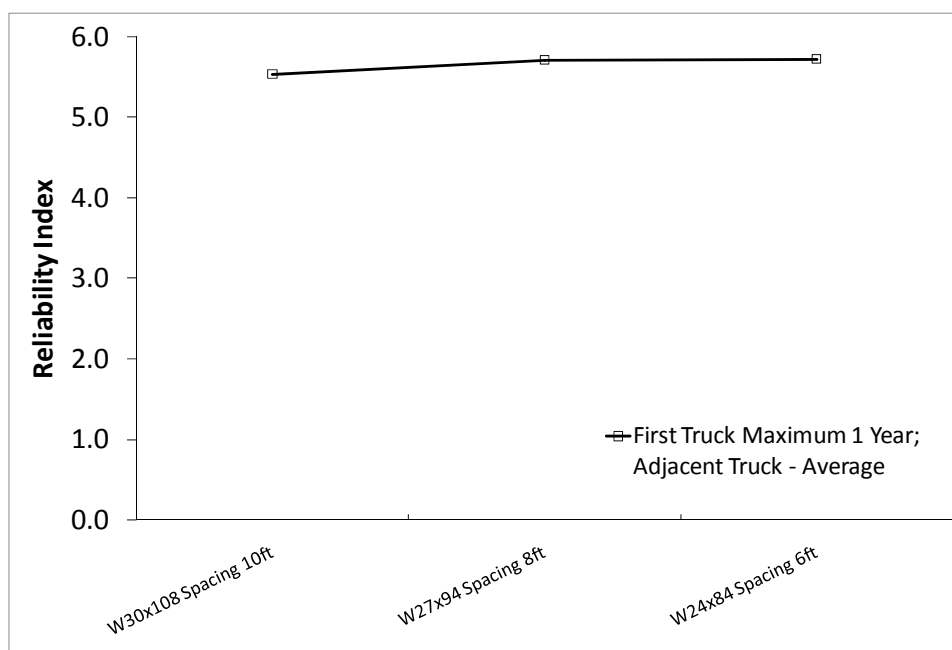


Figure 8-4 Reliability Index for Span 60ft and Live Load Model for Low Loaded Bridge

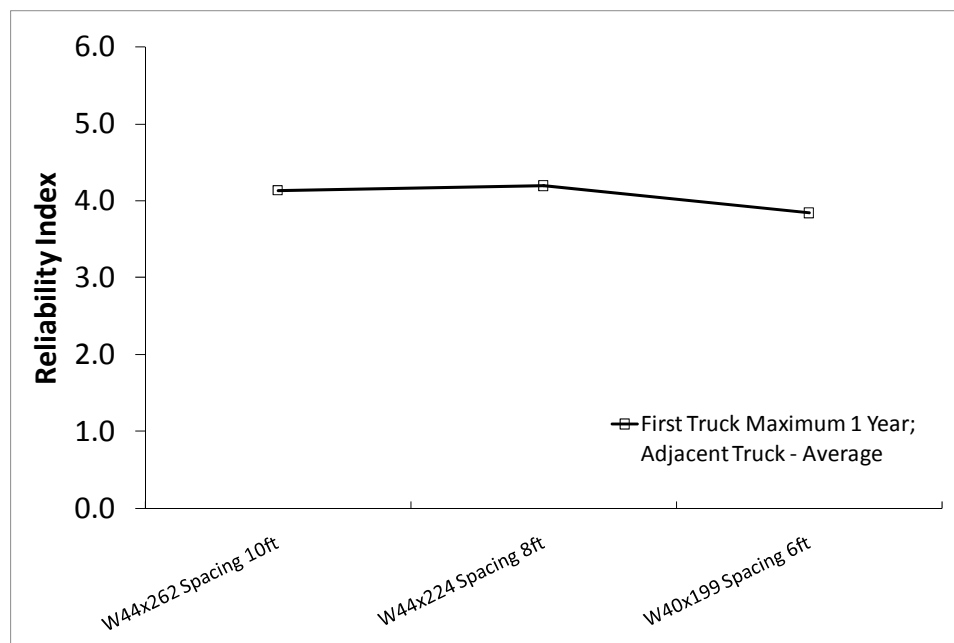


Figure 8-5 Reliability Index for Span 120ft and Live Load Model for High Loaded Bridge

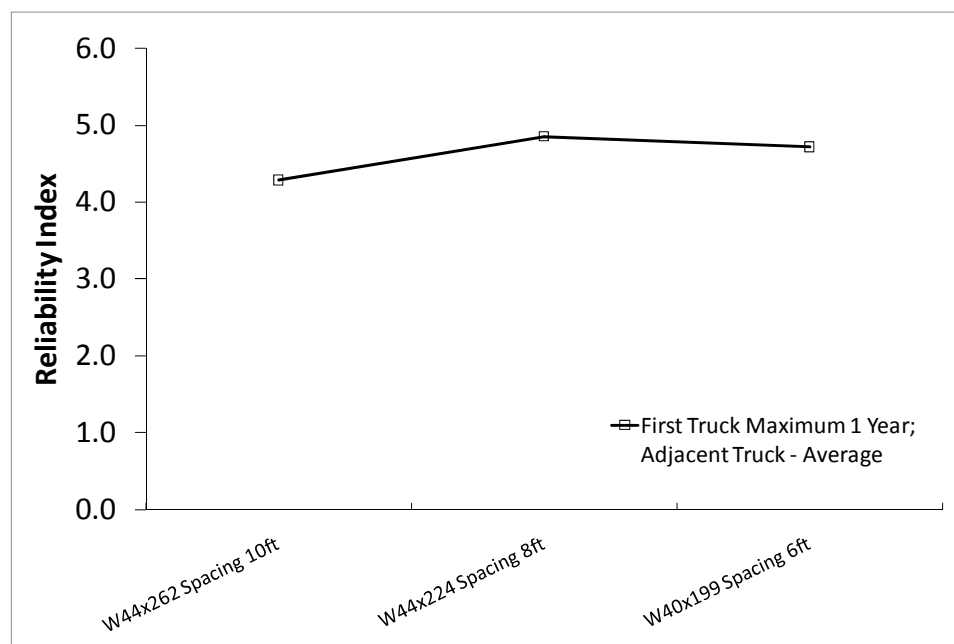


Figure 8-6 Reliability Index for Span 120ft and Live Load Model for Medium Loaded Bridge

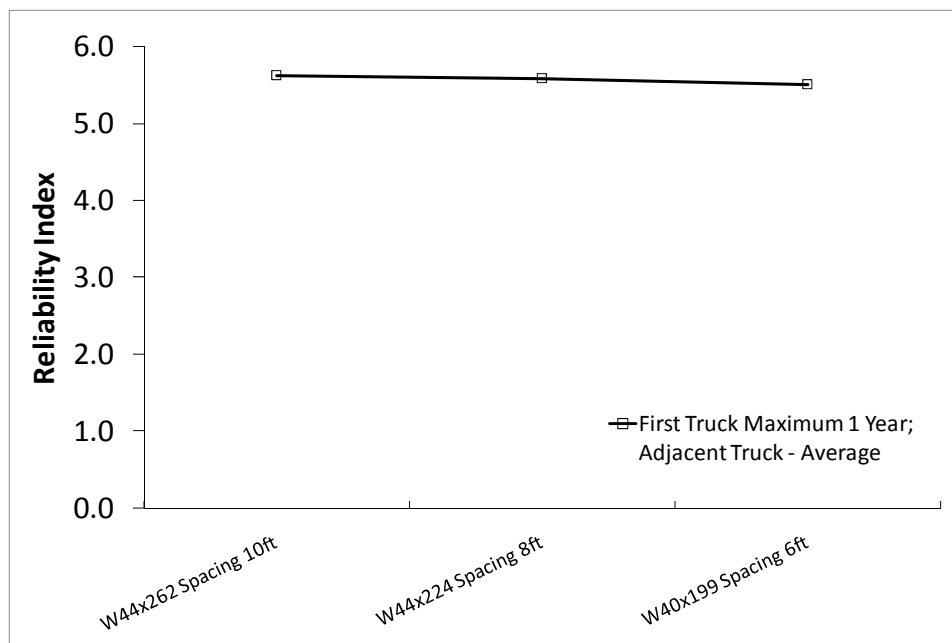


Figure 8-7 Reliability Index for Span 120ft and Live Load Model for Low Loaded Bridge

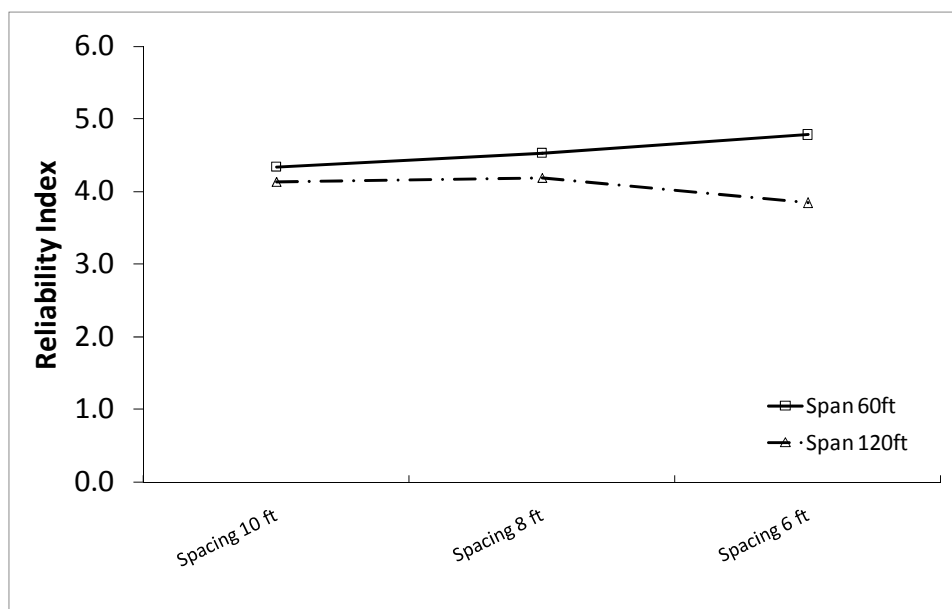


Figure 8-8 Comparison of Reliability Indices for Different Span Lengths – Heavy Loaded Bridge

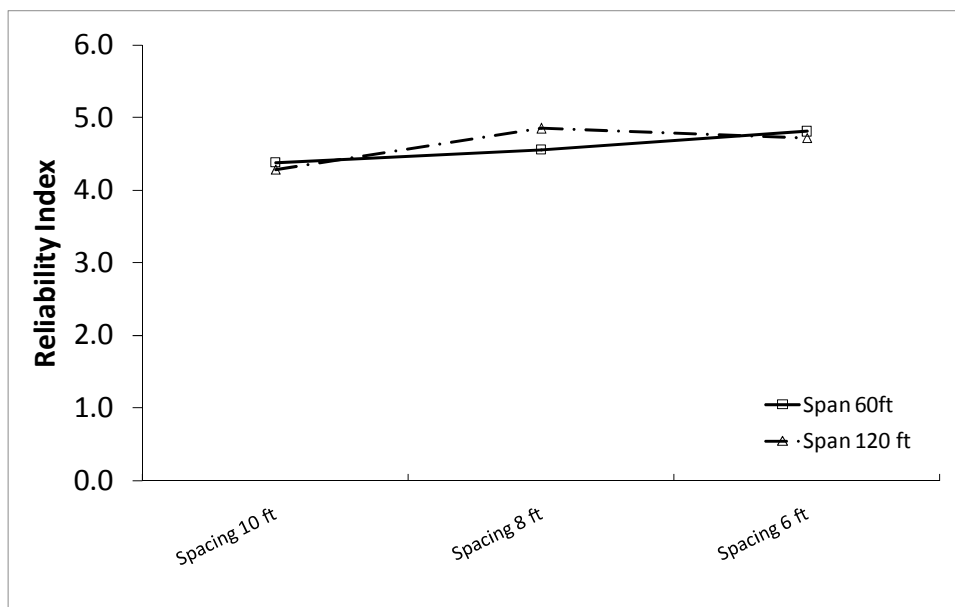


Figure 8-9 Comparison of Reliability Indices for Different Span Lengths – Medium Loaded Bridge

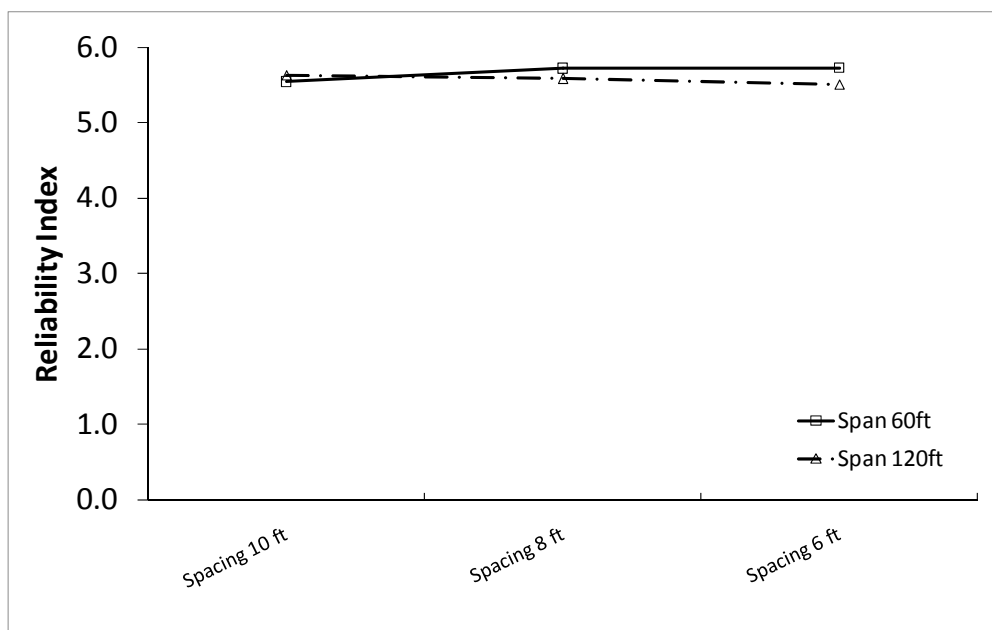


Figure 8-10 Comparison of Reliability Indices for Different Span Lengths – Light Loaded Bridge

8.3. TARGET RELIABILITY AND SUMMARY OF THE RESULTS

In this reliability analysis for steel composite girders is presented. Three bridges with girder spacing 6, 8, 10ft and span 60ft, and three bridges with the same spacing but span length 120ft were designed according to AASHTO Strength I limit state. Reliability index calculations were performed assuming the resistance as lognormal and load as normal.

Reliability index for primary and secondary components depends on the consequences of failure. For ultimate limit state, reliability index for moment and shear varies depending on the spacing between the girders. It is also higher for single load path components compared to multi-load path components.

Target reliability indices calculated for newly designed bridges and existing structures are different for many reasons. Reference time period is different for newly designed and existing bridges. New structures are designed for 50 year life time and existing bridges are checked for 5 or 10 year periods. Load model, used to calculate reliability index depends on the reference time period. Maximum moments and shears are smaller for 5 or 10 year periods than for 50 year life time. However, the coefficient of variation is larger for shorter periods. Single load path components require a different treatment than multiple load path components. In new designs, single load path components are avoided, but such components can be found in some existing bridges. Target reliability index is higher for single load path components.

Load and resistance models for highway bridges indicate a considerable degree of variation (large scatter). The main load combination includes dead load, live load and

dynamic load. Dead load model is not time-dependent. Live load varies as it was shown in this study. Dynamic load allowance, as a fraction of the live load, is changing with time too. Resistance also depends on the reference time period because of deterioration of the structure, particularly strength loss due to corrosion or fatigue.

The analysis was performed for the ultimate limit states (ULS). For the ultimate limit states, calculated reliability indices represent component reliability rather than system reliability. The reliability indices calculated for structural system are larger than for individual components by about 2. Therefore, selection of the target reliability level should be based on consideration of the system.

Recommended values of the target reliability indices for design and evaluation of bridges are listed in Table 57. The numbers are rounded off to the nearest 0.25.

Table 57 Recommended target reliability indices

Time Period	Primary Components		Secondary Components
	Single Path	Multiple Path	
5 years	3.50	3.00	2.25
10 years	3.75	3.25	2.50
50 years	4.00	3.50	2.75

Analysis showed that the results are above target reliability for girder bridges equal to 3.5. Probabilistic models of live load combined with the FEM models resulted in reliability index for girders for heavy loaded bridge equal to 3.8. Based on this study it can be concluded that HL93 load model is still valid for the majority of bridges across US.

CHAPTER 9. CONCLUSIONS AND RECOMMENDATIONS

9.1. SUMMARY

Safety and reliability of bridge infrastructure is a major concern for many state highway agencies. A considerable percentage of highway bridges that are structurally deficient must be posted, repaired or replaced. The foremost factors influencing structural deficiency are aging and observed increase in traffic volumes. High cost of any repair or replacement can be avoided by predicting accurately the load carrying capacity and loads. While, the capacity of a bridge can be determined with a high accuracy by diagnostics, field tests and adequate analysis methods, the correct prediction of live load is complicated. The Weigh-In-Motion measurements can provide the unbiased truck traffic data and it can be a remarkable basis to develop the statistical model of live load.

At the time of calibration of the AASHTO LRFD Code, there was no reliable truck data available for the USA. Therefore, the live load model was based on the truck survey results provided by the Ontario Ministry of Transportation. The survey was carried out in conjunction with calibration of the Ontario Highway Bridge Design Code in 1975. In recent years many projects sponsored by the National Cooperative Highway Research Program and state DOT's conducted that the HL93 AASHTO load cannot be representative to US traffic loads.

Therefore the goal of this study was to analyze recent Weigh-In-Motion data from six different states with different traffic patterns and load spectra, develop a new statistical live load model and check the level of acceptance of HL93 load.

Chapter 1 presents a literature review including: code calibration procedures, available research regarding Weigh-In-Motion measurements, as well as an objective and scope of the research.

Chapter 2 is a summary of structural reliability models; extreme value and nonparametric theory to approximate a given distribution.

In Chapter 3 most recent (2005-2008) Weigh-In-Motion data is presented. Ontario truck measurements used in AASHTO LRFD calibration is summarized. Five different spans of bridges were considered 30ft, 60ft, 90ft, 120ft and 200ft. Analysis of the Ontario data included determination of live load effect for positive, negative moment and shear. Results were plotted on the normal probability paper.

The analyzed Weigh-In-Motion data includes 47,000,000 records obtained from six different states. The data provides the gross vehicle weight, the number of axles, the load per axle, the axle spacing, as well as speed, number of lane and time of record. Although WIM measurement technique has been improved, still the raw data can contain records with an error. Therefore the whole database was filtered to neglect the errors. The filter including verification of weight per axle, spacing length, speed and classification was implemented. The gross vehicle weights of the preprocessed trucks were plotted on the normal probability paper and compared with Ontario data.

A special program was developed to calculate the maximum live load effect. Five simply supported bridges with different span lengths were considered. Maximum load effects in terms of bending moment and shear were calculated for each truck. The results of the analyses were plotted on the probability paper and compared with Ontario trucks. All the plots are included in Appendix A.

In Chapter 4 three types of live load model were developed; high, medium and low. In depth analysis of three representative sites was performed following procedures used in calibration of AASHTO LRFD (Nowak 1999). For each live load model equivalent return period was calculated with the assumption that the bridge design period is 75 years. The maximum load effect plotted on the probability paper was extrapolated to this return period using nonparametric approach. Statistical parameters of load effect in terms of ratio of moments (truck moment/ HL93 moment) were obtained for different return periods.

Chapter 5 shows multiple presence analysis. HL93 load model was based on two fully correlated trucks. To verify this assumption a coefficient of correlation for available WIM data was determined. In order to establish degree of correlation a simultaneous occurrence of two trucks on the bridge was considered. Two cases were analyzed: two trucks in one lane and two trucks in adjacent lanes. A filter was implemented to determine the simultaneous occurrence of two trucks with the assumption that the maximum headway distance was 200 ft for both cases. Another filter was implemented to obtain the coefficient of correlation of two trucks with the assumption that both trucks have to have the same number of axles; weight has to be in $\pm 5\%$ difference limit and the spacing in $\pm 10\%$ difference limit between them. The results of the analysis were plotted on the normal probability paper. Multiple presence analysis required determination of load distribution model. Six composite steel girder bridges were design according to AASHTO LRFD. FEM model was build to establish girder distribution factors for two HS20 trucks. Trucks were longitudinally positioned on the bridge to cause

the maximum bending moment and then moved transversally to obtain the maximum stressed girder.

Chapter 6 of this dissertation presents load combination which includes the development of the statistical models for total load and resistance. Parameters of live load were based on the three live load models developed in previous Chapter and were recalculated to incorporate the dynamic part of the truck load. Based on NCHRP Report 368 statistical parameters of dead load were summarized.

Chapter 7 shows resistance model.

Chapter 8 presents reliability analysis for steel composite girders. Three bridges with girder spacing 6, 8, 10ft and span 60ft, and three bridges with the same spacing but span length 120ft were designed according to AASHTO Strength I limit state. Reliability index calculations were performed assuming the resistance as lognormal and load as normal.

9.2. CONCLUSIONS

Reduced cost of a repair or potential replacement of a bridge is in special interest of all bridge owners. A valid live load model is one of the aspects of proper managing of a bridge infrastructure and improved Weigh-In-Motion measurements are an indispensable tool. Current HL-93 load model was based on the Ontario truck measurements performed in 1975. Since that time truck load has changed significantly. Therefore, the goal of this study was to analyze recent 2005-2007 Weigh-In-Motion data and develop a new statistical live load model.

WIM stations are usually hidden from the truck driver. Probable illegal overweight vehicles that can cause the maximum load effect are included in the records and can provide the unbiased load spectra. Although a WIM data measurement has improved, there is a need to filter the records. There is no widely acceptable guideline for data filtering and this procedure has a major impact on the live load distribution. Different projects resulted with different filtering criteria. It is understandable to remove the unrealistic trucks from the population but no heavy vehicles can be discarded. Based on the sensitivity analysis performed on various sites it was observed that removal of only 0.03% of all trucks from the top of the distribution can cut the maximum load effect by 32%. This can lead to the conclusion that all trucks in the filtered database have a great importance in live load prediction and correct filtering criteria are needed.

Comparison of old and new truck data showed that on average Ontario trucks are heavier than the vehicles obtained from the available WIM. Exceptions are the extremely loaded New York Sites and overloaded California sites. The heaviest trucks observed in New York exceed Ontario twice. It can be concluded that although Ontario data contains only 10 000 records and was gathered in mid 70's, cannot be disregarded. It can be stated that the quality of data is more important than the quantity.

Analysis of selected sites included extrapolation to the 75 year return period. Based on this study it can be concluded that WIM data collection from one year period is not adequate. Application of extreme value theory for the extrapolation yields highly variable results. A sufficiently large sample of annual maxima is necessary in prediction of mean maximum 75 year truck load.

Multiple presence and degree of correlation analysis showed that the time of record of the passing truck has to have 0.01 second accuracy otherwise it is difficult to determine the accurate headway distance. Development of the HL93 load was based on the assumption that two heavy side by side trucks producing the maximum load effect. Coefficient of correlation analysis showed that this assumption is conservative and based on the available data two fully correlated trucks are negligible.

As it was discovered by many researchers AASHTO LRFD girder distribution factors are conservative and for the purpose of the live load model determination more accurate methods like FEM analysis is needed to verify the load transfer into girders. A large representative data base of bridges is needed.

Probabilistic models of live load combined with the FEM models resulted in reliability index for girders that are above the target level 3.5. Based on this study it can be concluded that HL93 load model is still valid for the majority of bridges across US. An exception can be State of New York. Although the minimum reliability index calculated for the heaviest site 8283 is equal to 3.8 a closer analysis of all sites in New York is necessary. The WIM data recorded in this state showed an extremely heavy traffic that can have an influence on the serviceability of the bridges. A quality dataset from this state can be a basis for the determination of live load model for extremely loaded bridges. Extremely loaded sites can be verified by the owner using WIM data and the owner can decide to use a different live load factor than specified in AASHTO LRFD.

REFERENCES

- Adamowski, K. (1989). "A Monte Carlo Comparison of Parametric And Nonparametric Estimation of Flood Frequencies." *Journal of Hydrology*, Vol. 108, 295-308.
- Ang, A. H.-S., and Tang, W. H. (1975). *Probability Concepts in Engineering Planning and Design, Volume I: Basic Principles*, John Wiley & Sons, New York.
- Ang, A. H.-S., and Tang, W. H. (1984). *Probability Concepts in Engineering Planning and Design, Volume II: Decision, Risk, and Reliability*, John Wiley & Sons, New York.
- Ayyub, B. M., and McCuen, R. H. (1997). *Probability, Statistics, and Reliability for Engineers*, CRC Press, Boca Raton.
- Bakht, B., and Jaeger L. G. (1990). "Bridge Evaluation for Multipresence of Vehicles." *Journal of Structural Engineering*, Vol. 116.
- Bishara, A. G., Liu, M. C., and El-Ali, N. D. (1993). "Wheel Load Distribution on Simply Supported Skew I-Beam Composite Bridges." *Journal of Structural Engineering*, ASCE, Vol. 119, pp. 399-419.
- Bowman, A. W., and Azzalini, A. (1997). *Applied Smoothing Techniques for Data Analysis*, Oxford University Press, New York.
- Castillo, E. (1988). *Extreme Value Theory in Engineering*, Academic Press., San Diego.
- Castillo, E., and Hadi, A. (1997). "Fitting the generalized Pareto distribution to data." *Journal of American Statistical Association*, Vol. 92, 1609-1620.
- Coles, S. (2001). *An Introduction to Statistical Modeling of Extreme Values*, Springer-Verlag, London.
- Cornell, C. A. (1967). "Bounds on the Reliability of Structural Systems." *Journal of the Structural Division, ASCE*, Vol. 93, 171-200.
- Cornell, C. A. (1969). "A Probability Based Structural Code." *ACI Journal*, Vol. 66, 974-985.
- Der Kiureghian, A., Liz, H. Z., and Hwang, S. J. (1987). "Second Order Reliability Approximations." *Journal of Engineering Mechanics, ASCE*, Vol. 113, pp. 1208-1225.
- Ditlevsen, O., and Madsen, H. O. (1996). *Structural Reliability Methods*, John Wiley & Sons Inc., New York.
- Eamon, C., and Nowak A.S. (2002). "Effects of edge-stiffening elements and diaphragms on bridge resistance and load distribution." *Journal of Bridge Engineering*.
- Eamon, C., and Nowak, A. S. (2004). "Effect of secondary elements on bridge structural system reliability considering moment capacity." *Structural Safety*.
- Ellingwood, B., Galambos, T. V., MacGregor, J. G., and Cornell, C. A. (1980). "Development of a Probability Based Load Criterion for American National Standard A58." National Bureau of Standards, Washington, DC.
- Eom, J. (2001). "'Verification of the Bridge Reliability Based on Field Testing'," University of Michigan, Ann Arbor.

- Eom, J., and Nowak, A. S. (2001). "Live Load Distribution for Steel Girder Bridges." *Journal of Bridge Engineering*, ASCE, Vol. 6, pp. 489-497.
- Faucher, D., Rasmussen, P. F., and Bobee, B. (2001). "A Distribution Function Based Bandwidth Selection Method for Kernel Quantile Estimation." *Journal of Hydrology*, Vol. 250, 1-11.
- Fisher, R. A., and Tippett, L. H. (1928). "On the Estimation of the Frequency Distributions of the Largest or Smallest Member of a Sample." *Proceedings of the Cambridge Philosophical Society*, Vol. 24, 180-190.
- Galambos, T. V., and Ravindra, M. K. (1978). "Load and Resistance Factor Design." *Journal of Structural Division*, ASCE, Proc. Paper 14008.
- Gumbel, E. J. (1941). "The Return Period of Flood Flows." *The Annals of Mathematical Statistics*, Vol. 12, 163-190.
- Gumbel, E. J. (1949). "The Statistical Forecast of Floods." Bulletin No. 15, Ohio Water Resources Board, 1-21.
- Gumbel, E. J. (1958). *Statistics of Extremes*, Columbia University Press, New York.
- Hong, Y.-K. (1990). "Live Load Models for Girder Bridges," University of Michigan,, Ann Arbor.
- Hwang, E. S. (1990). "Dynamic Loads for Girder Bridges," University of Michigan, Ann Arbor.
- Hwang, E. S., and Nowak, A. S. (1991). "Simulation of Dynamic Load for Bridges." *Journal of Structural Engineering*, ASCE, Vol. 117, pp. 1413-1434.
- Kennedy, D. J. L. (1982). "Study of Performance Factors for Section 10 Ontario Highway Bridge Design Code." Morrison, Hershfield, Burgess & Huggins, Ltd., Ontario, Canada, , Toronto, .
- Kim, S.-J., and Nowak, A. S. (1997a). "Load Distribution and Impact Factors for I-Girder Bridges." *Journal of Bridge Engineering*, ASCE, Vol. 2.
- Kim, S.-J., and Nowak, A. S. (1997b). "Load distribution and impact factors for I-girder bridges." *Journal of Bridge Engineering*, ASCE, Vol. 2 pp. 97-104.
- Mabsout, M. E., Tarhini, K. M., Frederick, G. R., and Kobrosly, M. (1997a). "Influence of Sidewalks and Railings on Wheel Load Distribution in Steel Girder Bridges." *Journal of Bridge Engineering*, ASCE, Vol. 2, pp. 88-96.
- Mabsout, M. E., Tarhini, K. M., Frederick, G. R., and Tayar, C. (1997b). "Finite Element Analysis of Steel Girder Highway Bridges." *Journal of Bridge Engineering*, ASCE, Vol. 2, pp. 83-86.
- Nowak, A. S. (1999). "Calibration of LRFD Bridge Design Code." 368, NCHRP, Washington, D.C.
- Nowak, A. S., and Collins, K. R. (2000). *Reliability of Structures*, McGraw-Hill, New York.
- Nowak, A. S., and Lind, N. D. (1979). "Practical Bridge Code Calibration." *Journal of Structural Division*, ASCE,.
- Nowak, A. S., and Szerszen, M. M. (1998). "Bridge Load and Resistance Models." *Engineering Structures*, Vol. 20.
- Nowak, A. S., Yamani, A. S., and Tabsh, S. W. (1994). "Probabilistic Models for Resistance of Concrete Bridge Girders." *ACI Journal*, Vol. 91(3).
- Nowak, A. S., and Zhou, J. H. (1985). "Reliability Models for Bridge Analysis." University of Michigan, Ann Arbor.

- Nowak, A. S., and Zhou, J. H. (1990). "System Reliability Models for Bridges." *Journal of Structural Safety*.
- Sivakumar, B., Ghosn, M., Moses, F., and Lichtenstein Consulting Engineers, I. (2008). "Protocols for Collecting and Using Traffic Data in Bridge Design." National Cooperative Highway Research Program, TRB.
- Tabsh, S. W., and Nowak, A. S. (1991). "Reliability of Highway Girder Bridges." *Journal of Structural Engineering*, Vol. 117(8).
- Tantawi, H. M. (1986). "Ultimate Strength of Highway Girder Bridges," University of Michigan, Ann Arbor.
- Thoft-Christensen, P., and Baker, M. J. (1982). *Structural Reliability Theory and Its Applications*, Springer-Verlag, New York.
- Thoft-Christensen, P., and Murotsu, Y. (1986). *Application of Structural Systems Reliability Theory*, Springer-Verlag, New York.
- Wand, M. P., and Jones, M. C. (1995). *Kernel Smoothing*, Chapman & Hall.
- Zokai, T., Osterkamp, T. A., and Imbsen, R. A. (1991). "Distribution of wheel loads on highway bridges." Transportation Research Board, Washington, D.C.

APPENDIX A

OREGON – LIVE LOAD EFFECT

WIM data for Oregon

The truck survey includes weigh-in-motion (WIM) truck measurements obtained from Oregon DOT. The data includes 4 months of traffic recorded at different locations. The total number of records is shown in Table 58. The data includes number of axles, gross vehicle weight (GVW), weight per axle and spacing between axles.

Table 58

Site	Number of Trucks
I-5 Woodburn NB	611,830
I-84 Emigrant Hill WB	213,017
OR 58 Lowell WB	91,696
US 97 Bend NB	59,223
TOTAL	975,766

Maximum Simple Span Moments

The maximum moment was calculated for each truck from the data. Analysis included simple spans with the span varying from 30 to 200 ft. The maximum moment was also calculated for the HL93 load and Tandem. Ratio between the data truck moment and code load moment was plotted on the probability paper.

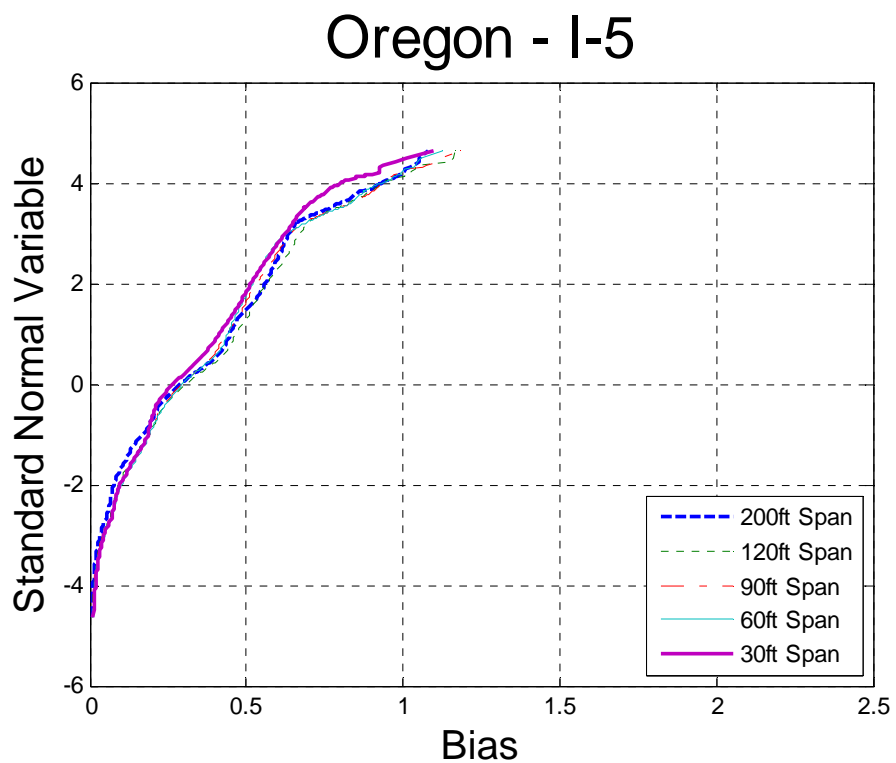
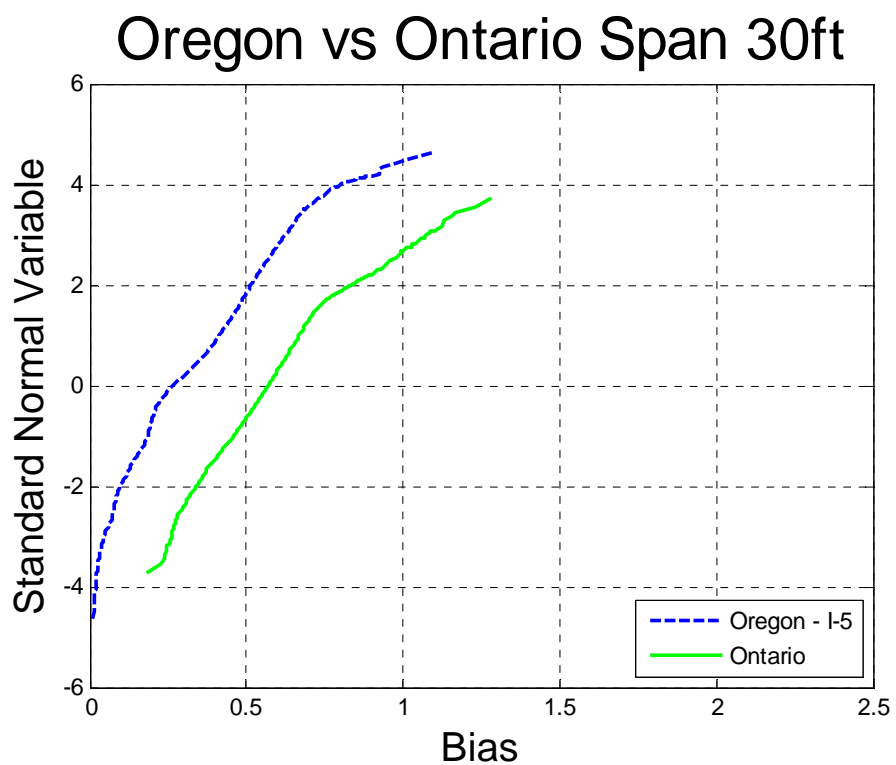
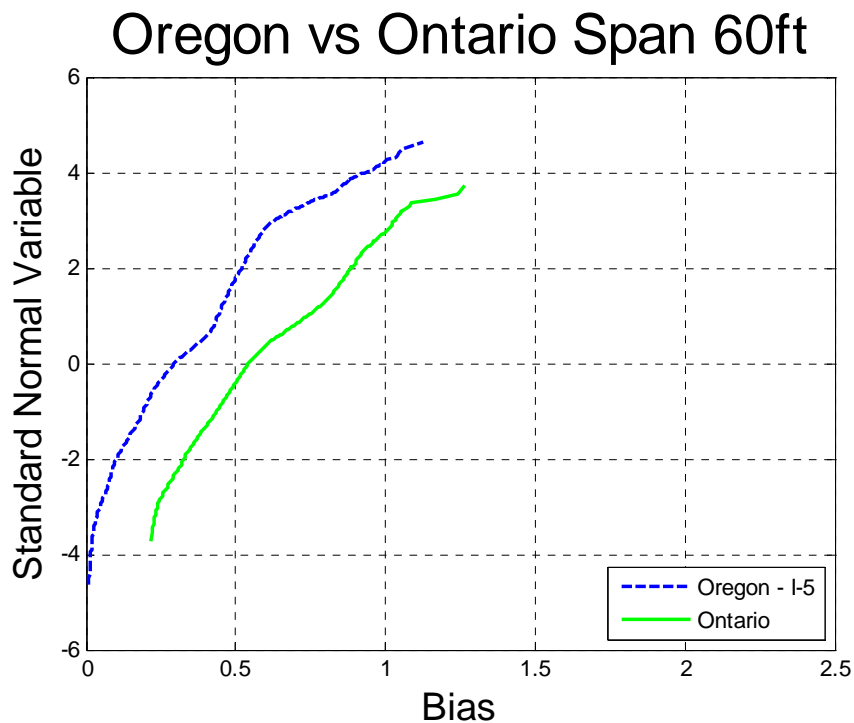


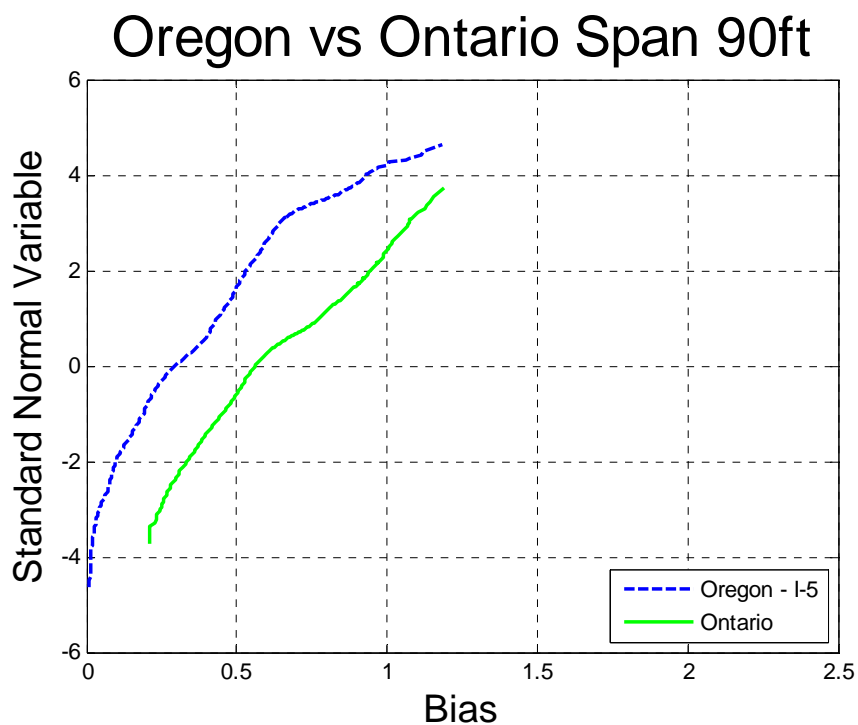
Figure 0-1 Cumulative Distribution Functions of Simple Span Moment– Oregon – I-5



0-2 Comparison of Simple Span Moment – Oregon – I-5 vs. Ontario – Span 30ft

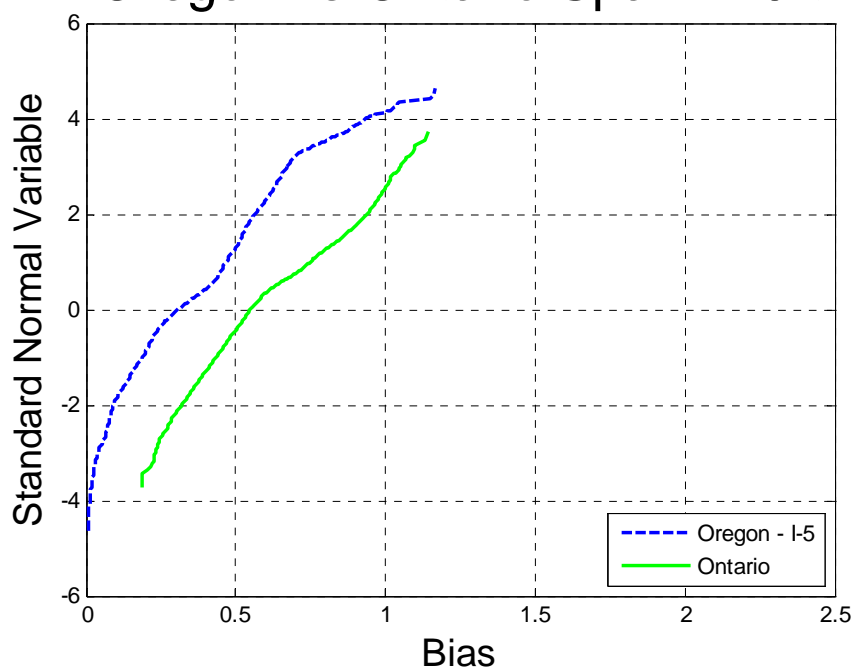


0-3 Comparison of Simple Span Moment – Oregon – I-5 vs. Ontario – Span 60ft



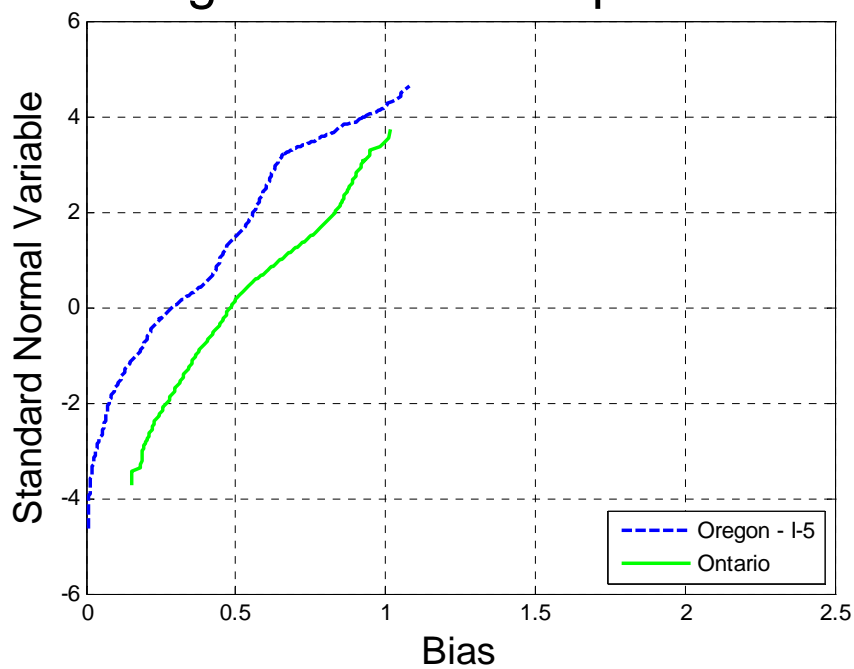
0-4 Comparison of Simple Span Moment – Oregon – I-5 vs. Ontario – Span 90ft

Oregon vs Ontario Span 120ft



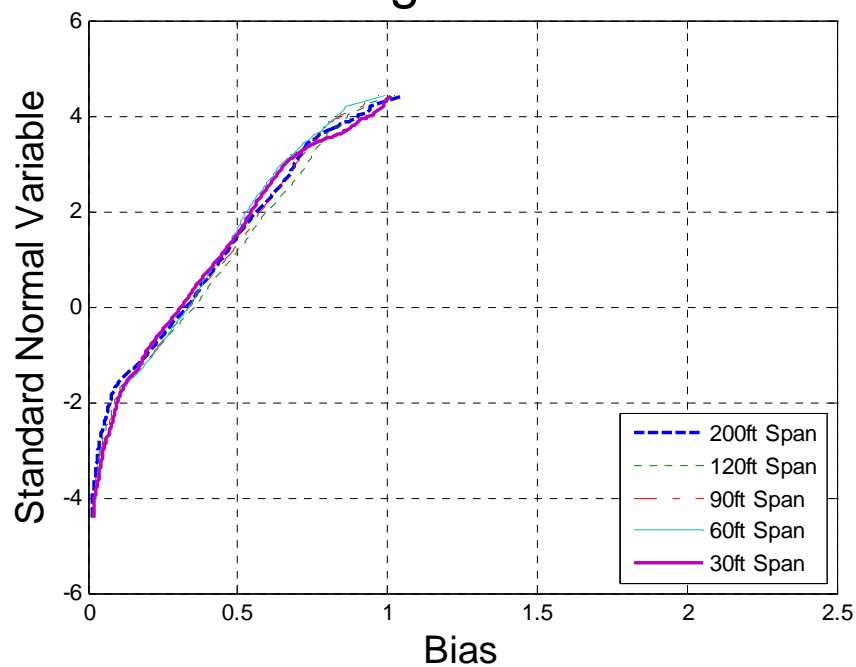
0-5 Comparison of Simple Span Moment – Oregon – I-5 vs. Ontario – Span 120ft

Oregon vs Ontario Span 200ft



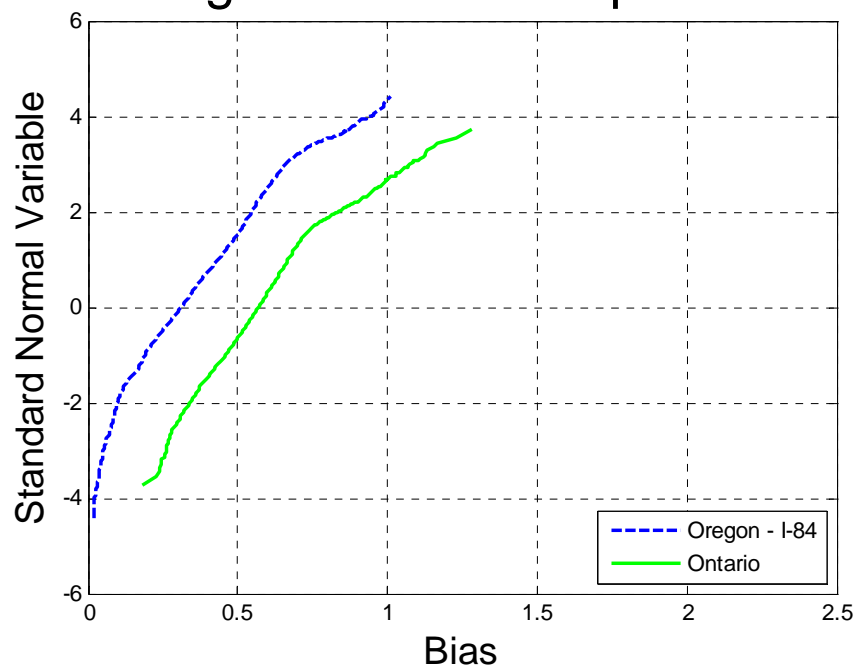
0-6 Comparison of Simple Span Moment – Oregon – I-5 vs. Ontario – Span 200ft

Oregon - I-84



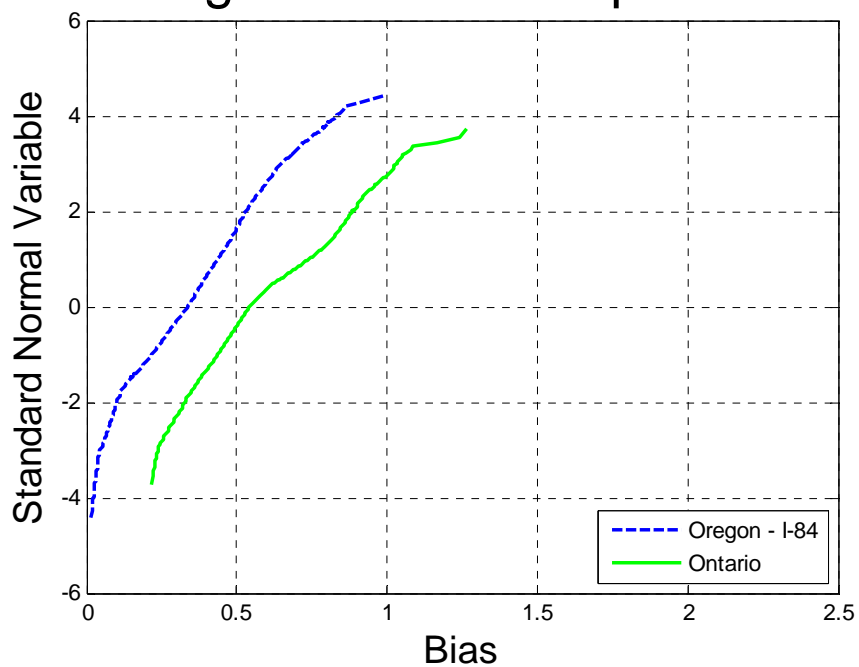
0-7 Cumulative Distribution Functions of Simple Span Moment– Oregon – I-84

Oregon vs Ontario Span 30ft



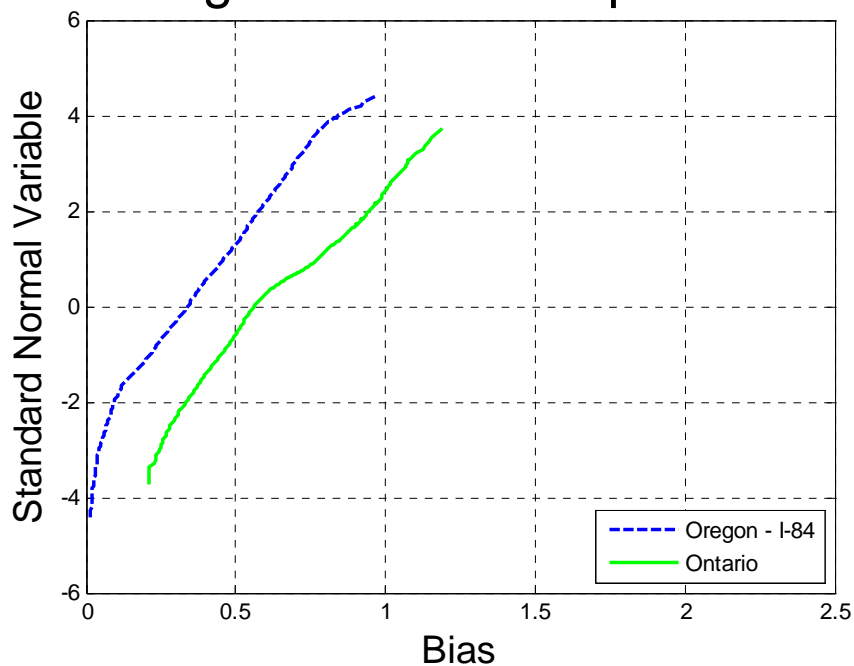
0-8 Comparison of Simple Span Moment – Oregon – I-84 vs. Ontario – Span 30ft

Oregon vs Ontario Span 60ft



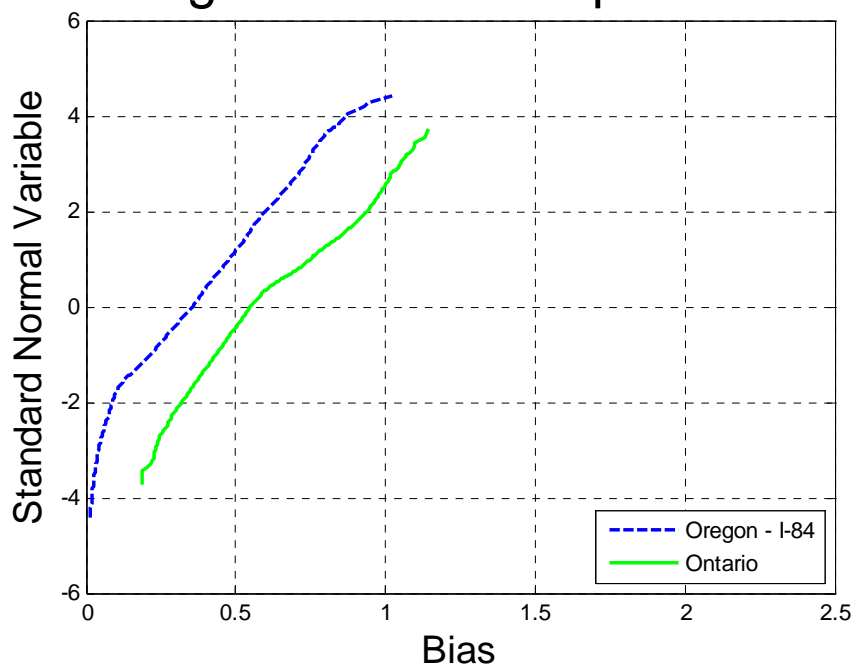
0-9 Comparison of Simple Span Moment – Oregon – I-84 vs. Ontario – Span 60ft

Oregon vs Ontario Span 90ft



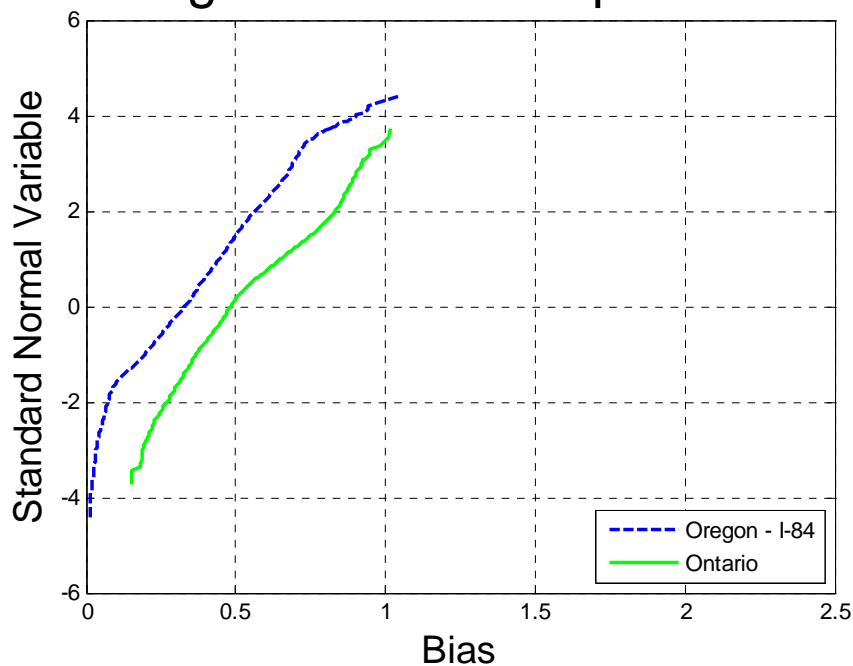
0-10 Comparison of Simple Span Moment – Oregon – I-84 vs. Ontario – Span 90ft

Oregon vs Ontario Span 120ft



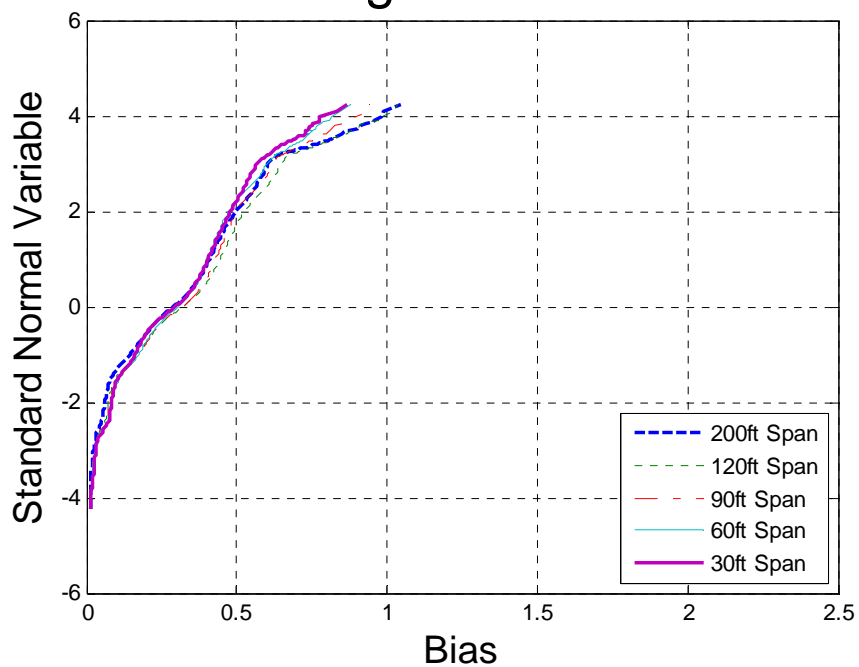
0-11 Comparison of Simple Span Moment – Oregon – I-84 vs. Ontario – Span 120ft

Oregon vs Ontario Span 200ft



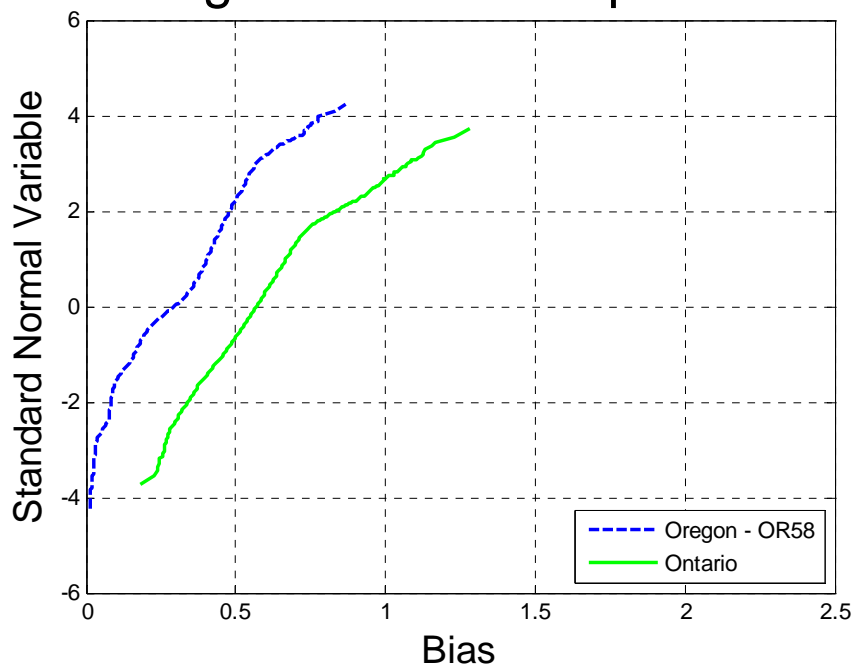
0-12 Comparison of Simple Span Moment – Oregon – I-84 vs. Ontario – Span 200ft

Oregon - OR58



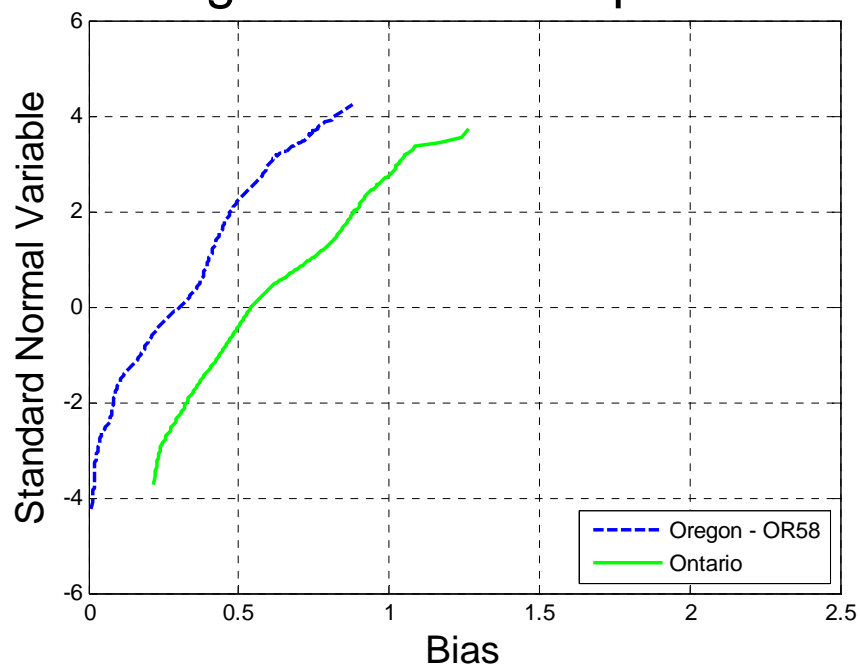
0-13 Cumulative Distribution Functions of Simple Span Moment– Oregon – OR58

Oregon vs Ontario Span 30ft



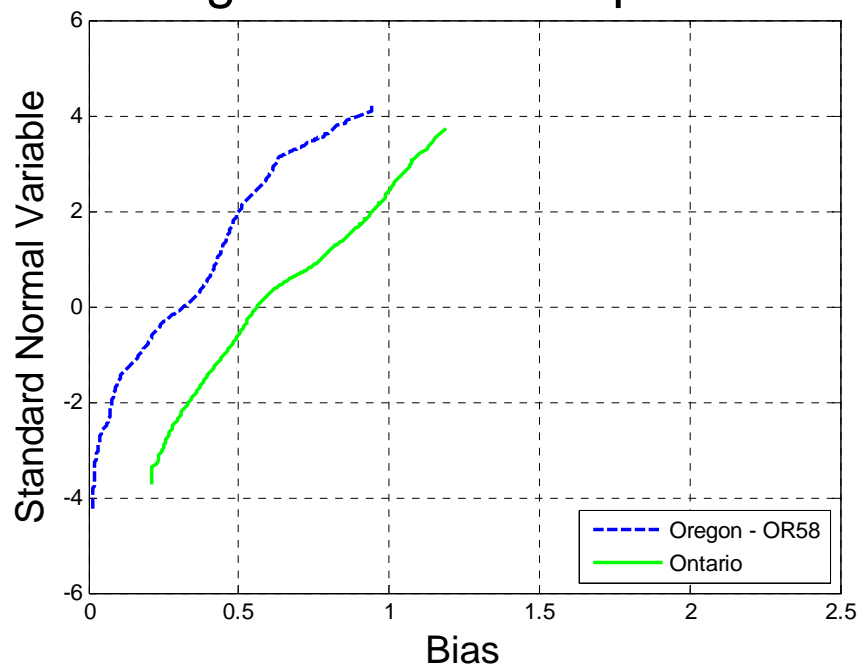
0-14 Comparison of Simple Span Moment – Oregon – OR58 vs. Ontario – Span 30ft

Oregon vs Ontario Span 60ft



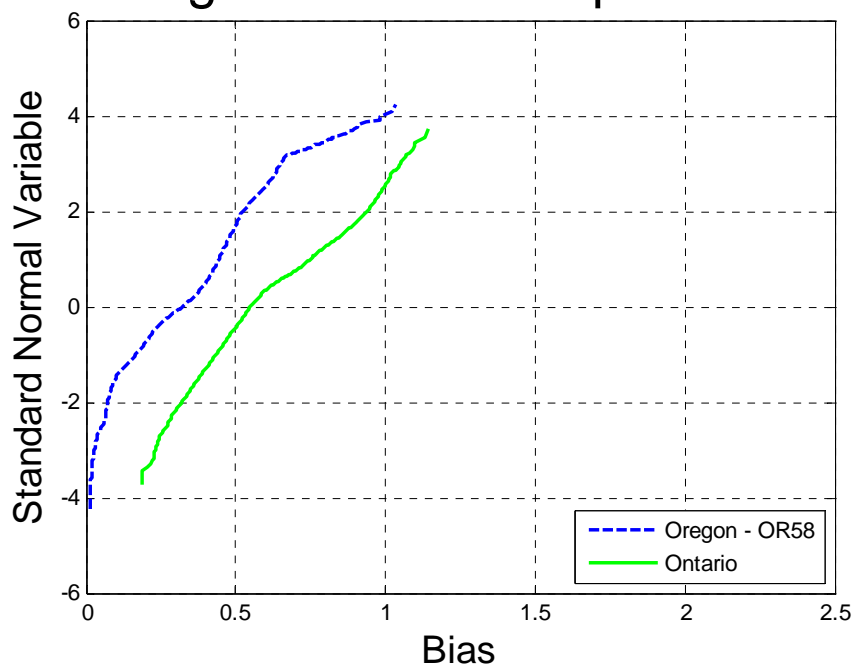
0-15 Comparison of Simple Span Moment – Oregon – OR58 vs. Ontario – Span 60ft

Oregon vs Ontario Span 90ft



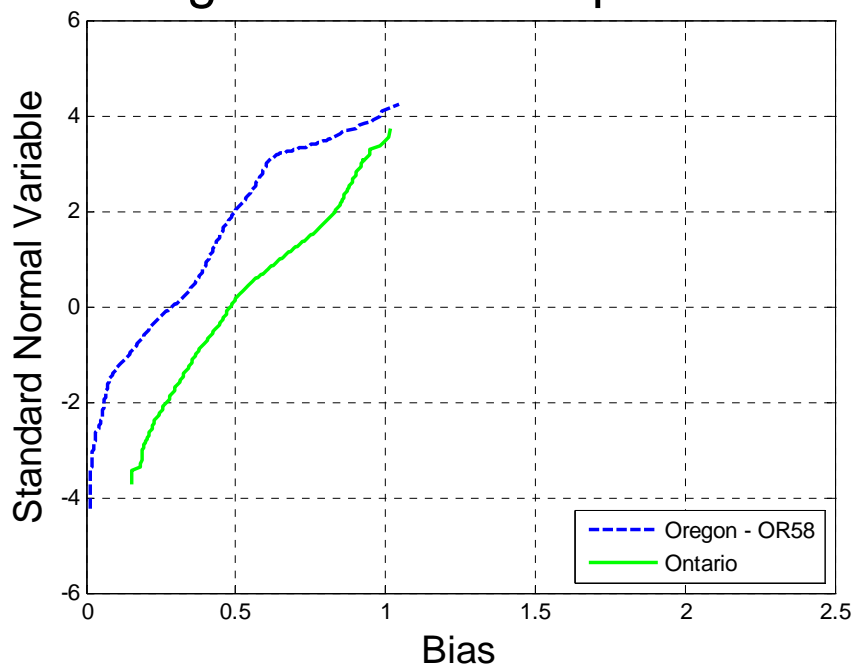
0-16 Comparison of Simple Span Moment – Oregon – OR58 vs. Ontario – Span 90ft

Oregon vs Ontario Span 120ft



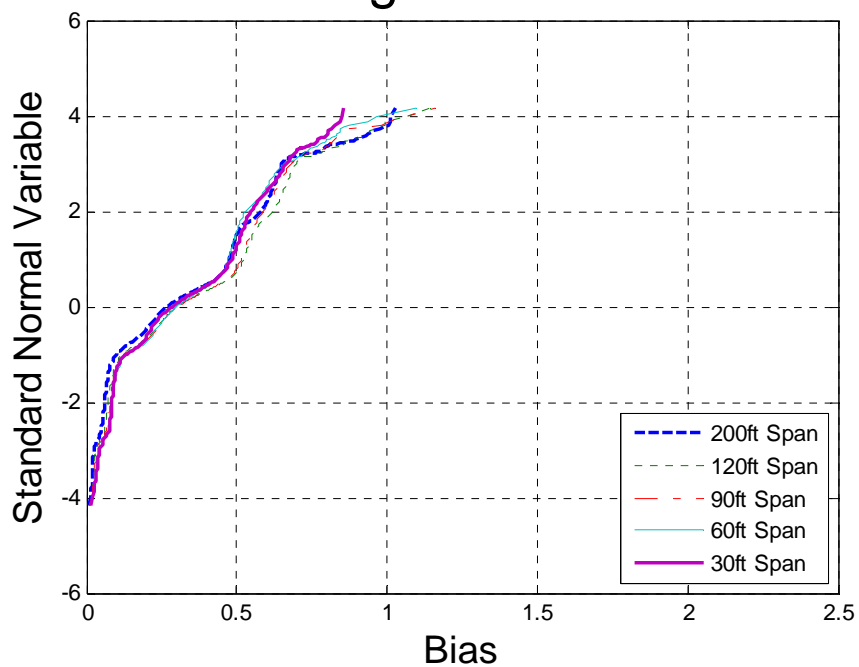
0-17 Comparison of Simple Span Moment – Oregon – OR58 vs. Ontario – Span 120ft

Oregon vs Ontario Span 200ft



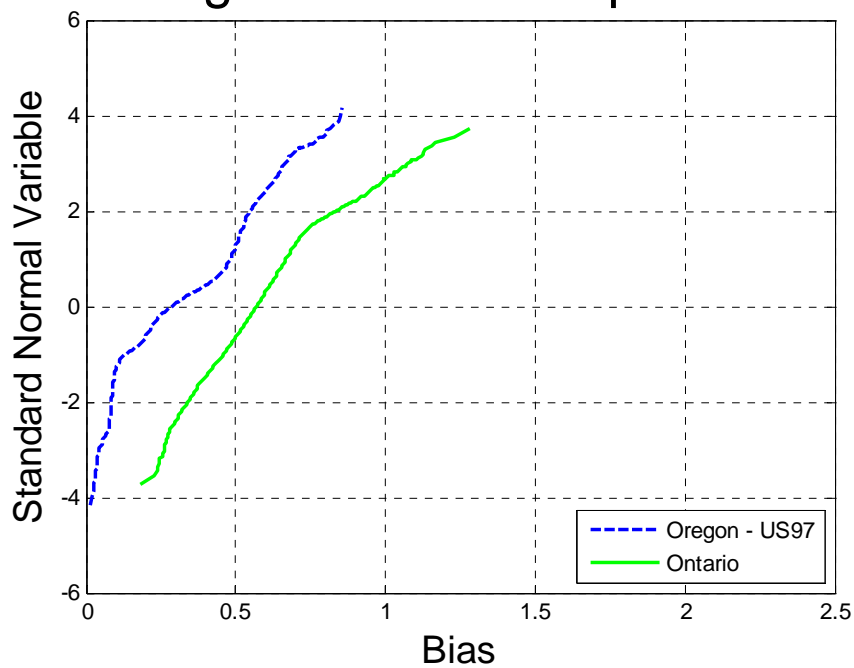
0-18 Comparison of Simple Span Moment – Oregon – OR58 vs. Ontario – Span 200ft

Oregon - US97



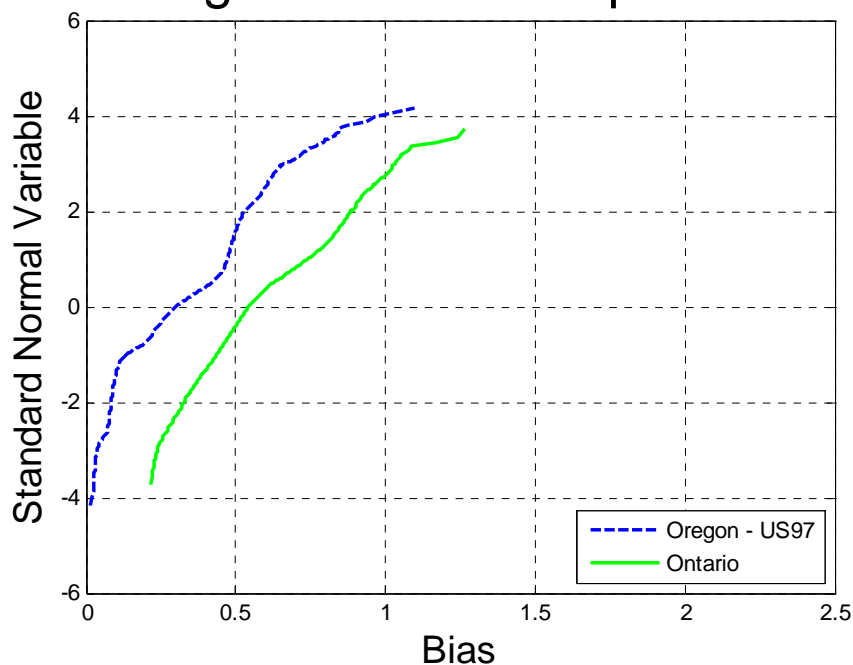
0-19 Cumulative Distribution Functions of Simple Span Moment– Oregon – US97

Oregon vs Ontario Span 30ft



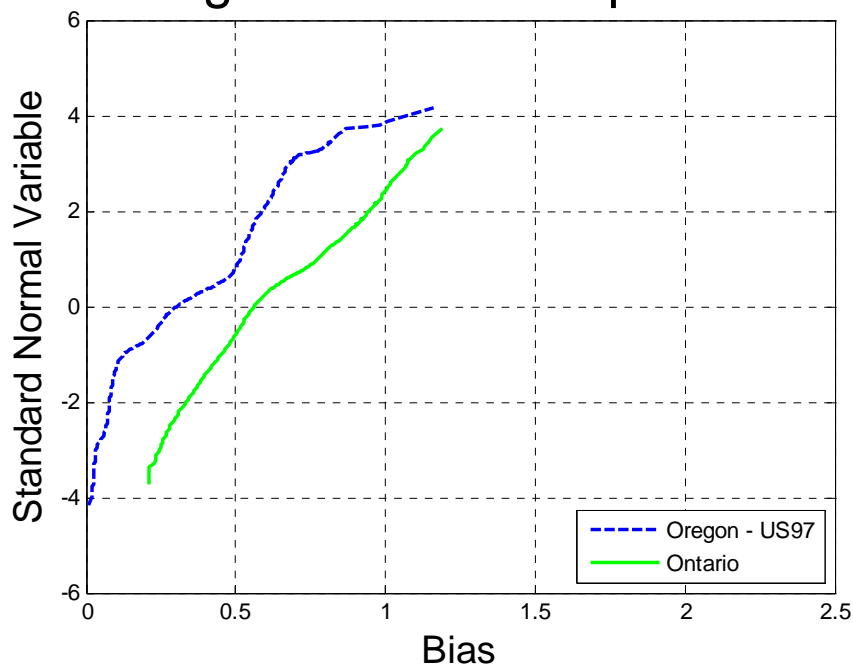
0-20 Comparison of Simple Span Moment – Oregon – US97 vs. Ontario – Span 30ft

Oregon vs Ontario Span 60ft



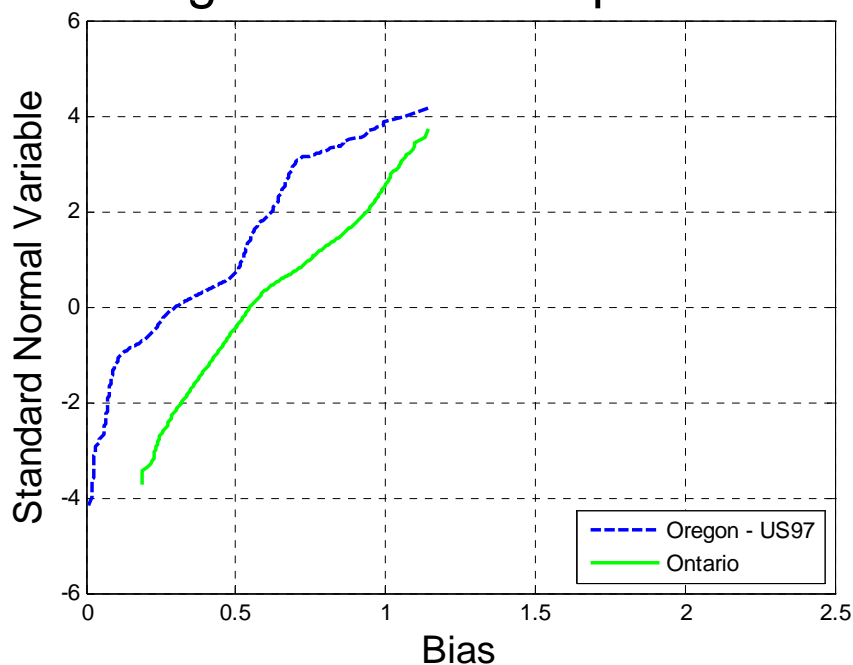
0-21 Comparison of Simple Span Moment – Oregon – US97 vs. Ontario – Span 60ft

Oregon vs Ontario Span 90ft



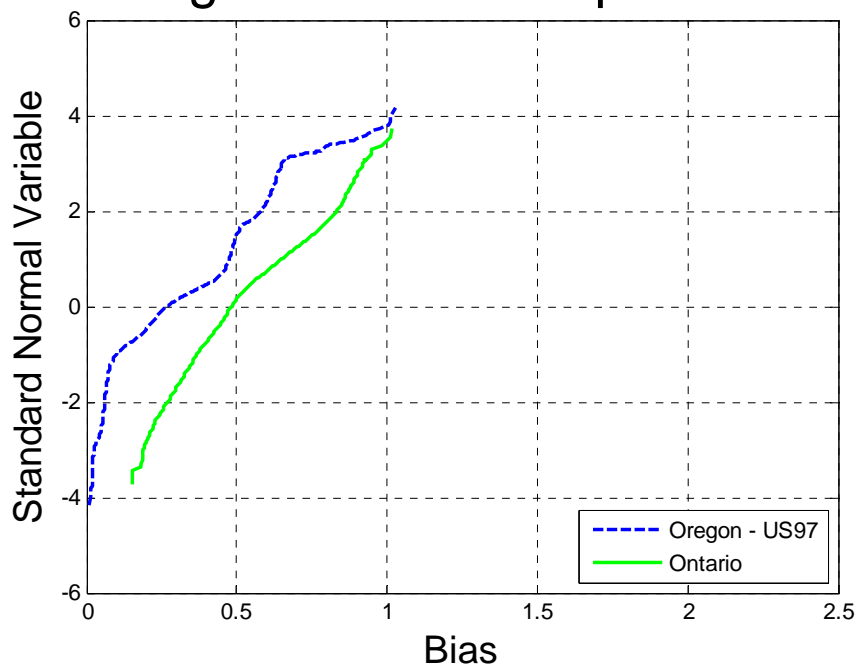
0-22 Comparison of Simple Span Moment – Oregon – US97 vs. Ontario – Span 90ft

Oregon vs Ontario Span 120ft



0-23 Comparison of Simple Span Moment – Oregon – US97 vs. Ontario – Span 120ft

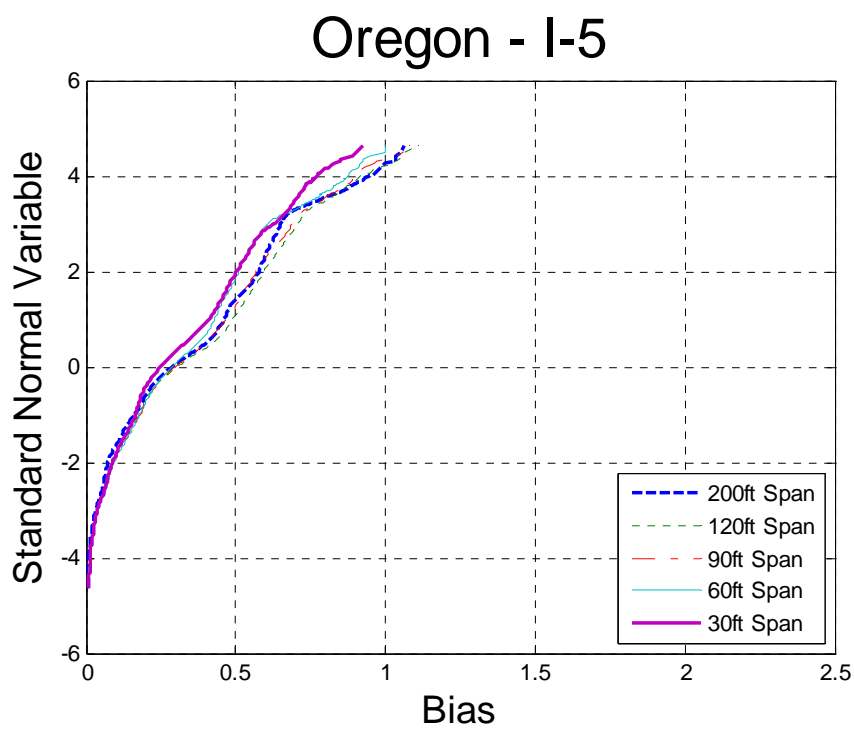
Oregon vs Ontario Span 200ft



0-24 Comparison of Simple Span Moment – Oregon – US97 vs. Ontario – Span 200ft

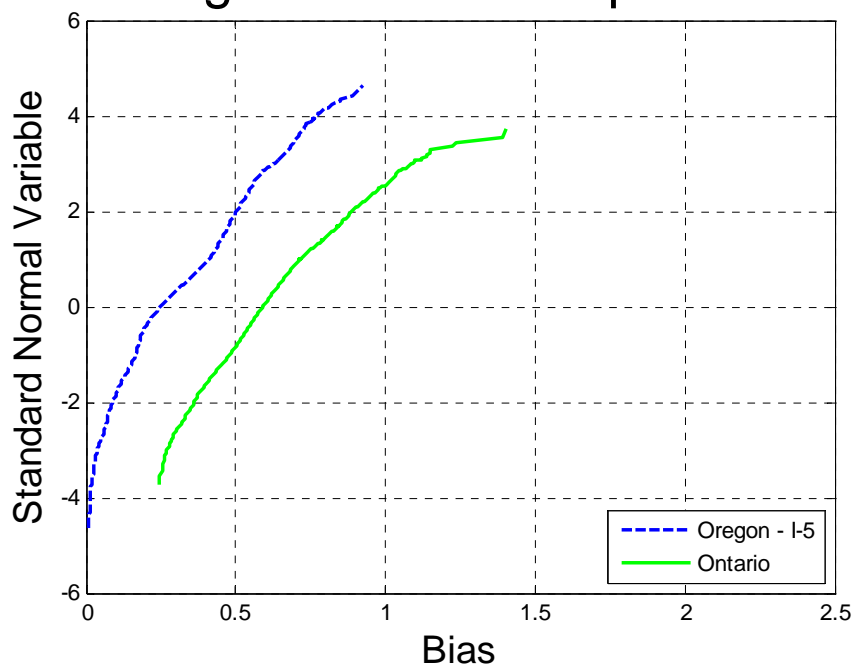
Maximum Shear

The maximum shear was calculated for each truck from the data. Analysis included simple spans with the span varying from 30 to 200 ft. The ratio of shear obtained from the data truck and the HL-93 load was plotted on the probability paper.



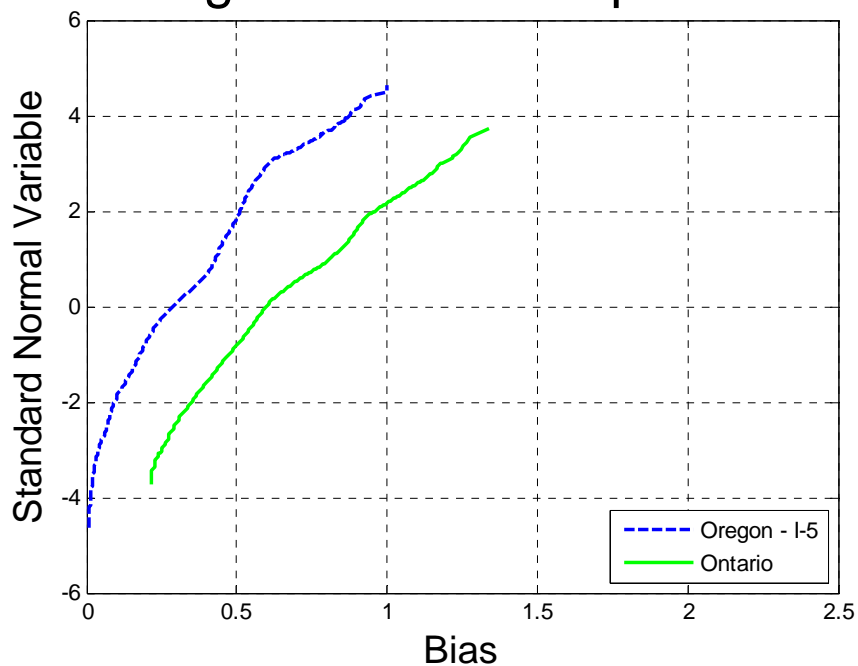
0-25 Cumulative Distribution Functions of Shear – Oregon I-5

Oregon vs Ontario Span 30ft

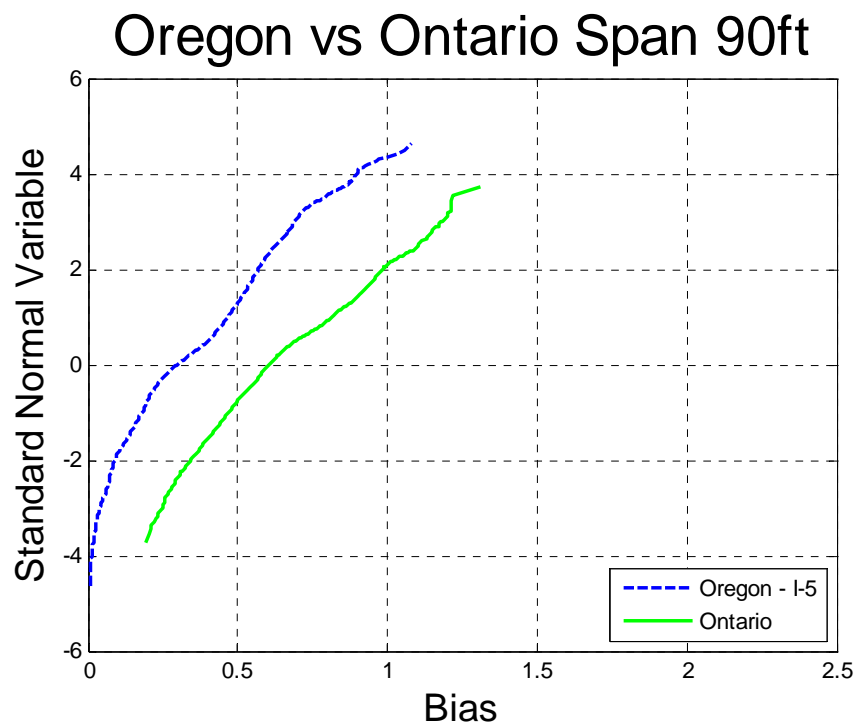


0-26 Comparison of Shear – Oregon I-5 vs. Ontario – Span 30ft

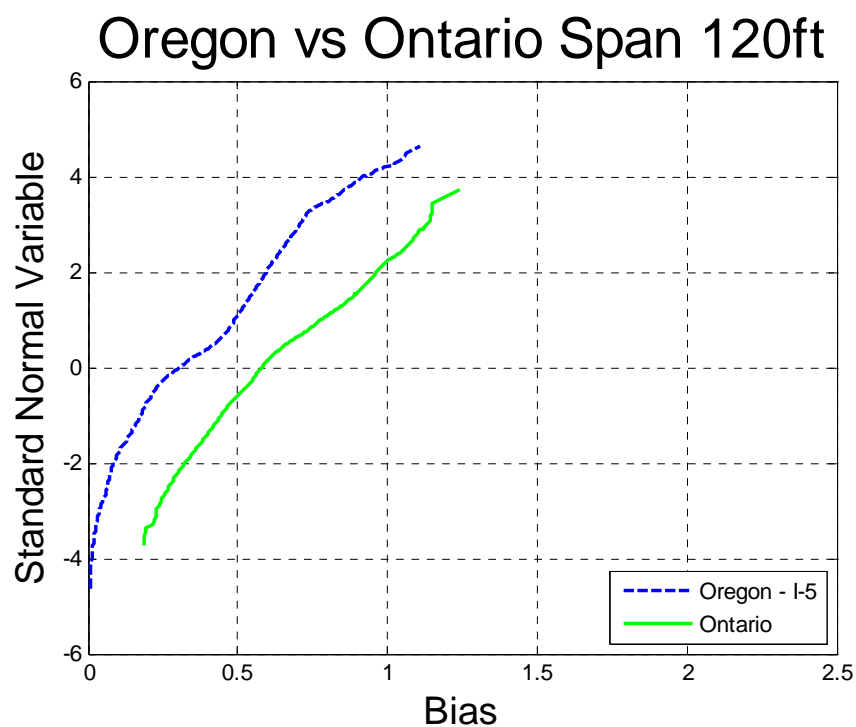
Oregon vs Ontario Span 60ft



0-27 Comparison of Shear – Oregon I-5 vs. Ontario – Span 60ft

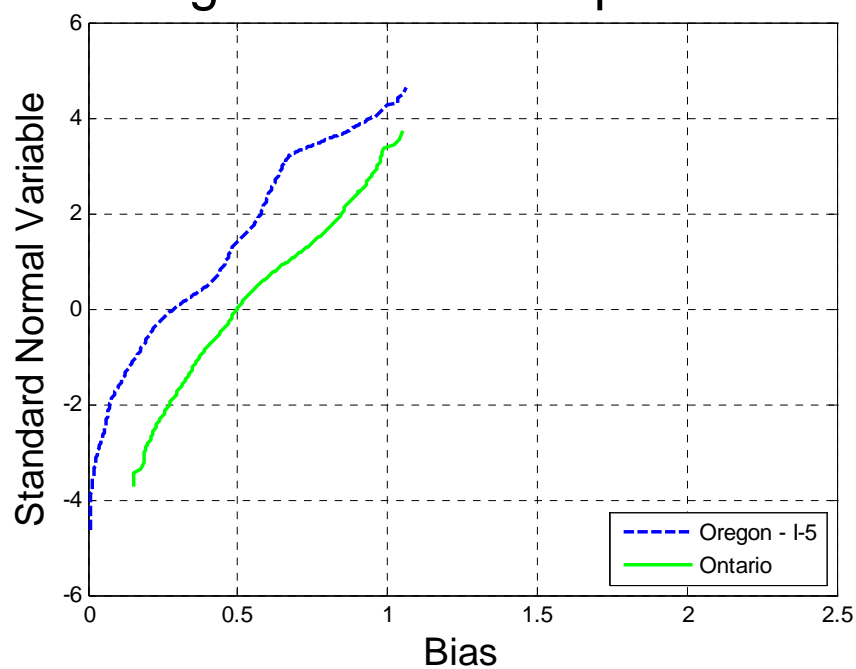


0-28 Comparison of Shear – Oregon I-5 vs. Ontario – Span 90ft



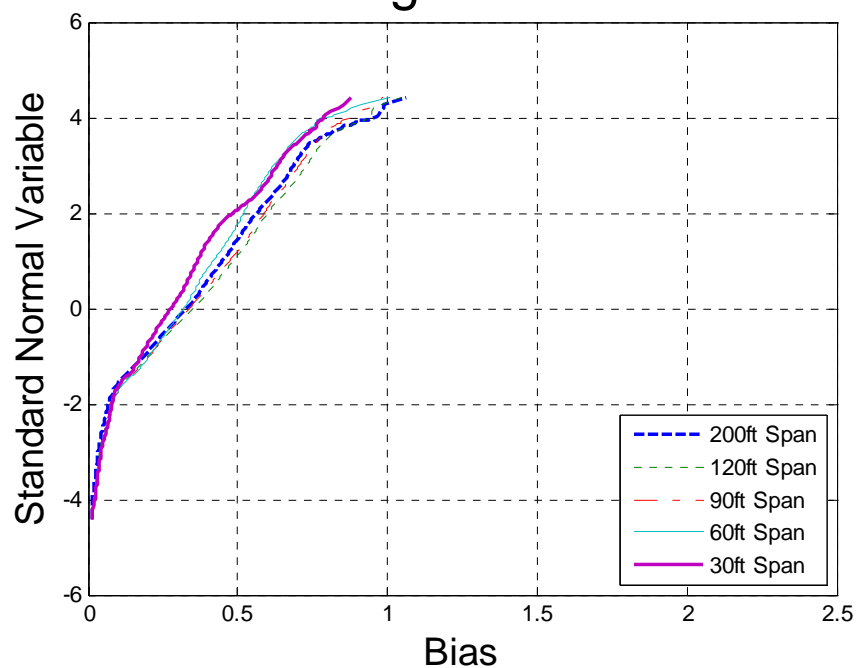
0-29 Comparison of Shear – Oregon I-5 vs. Ontario – Span 120ft

Oregon vs Ontario Span 200ft



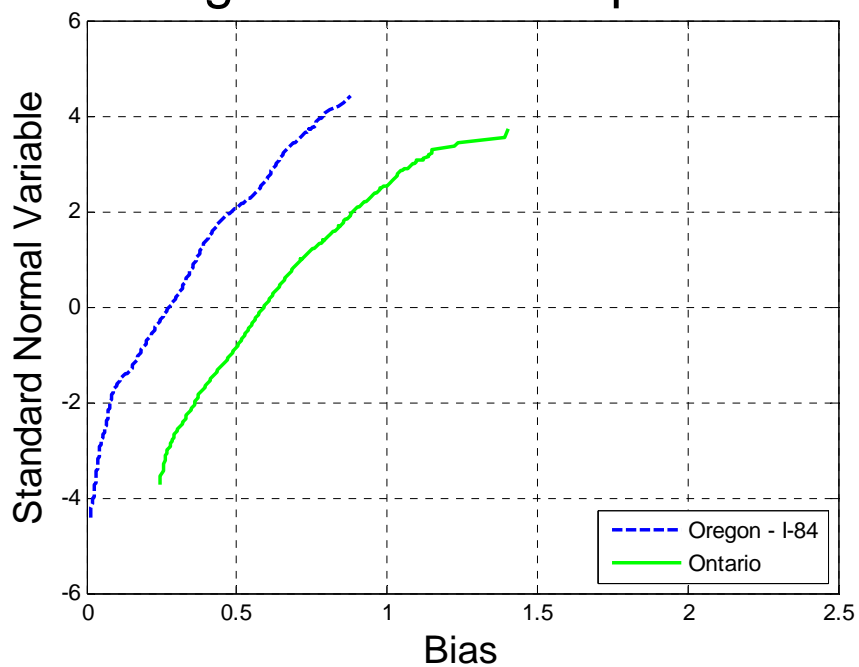
0-30 Comparison of Shear – Oregon I-5 vs. Ontario – Span 200ft

Oregon - I-84



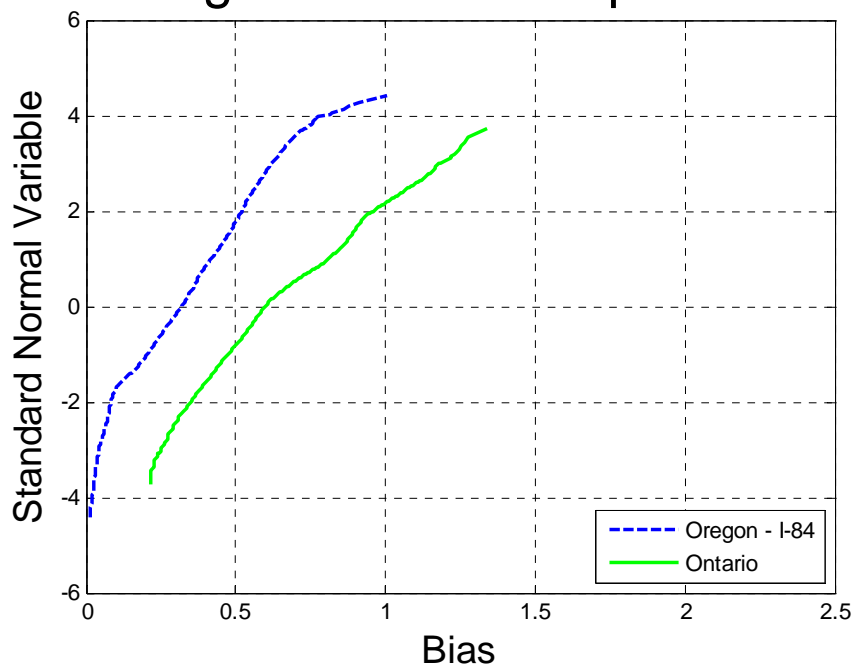
0-31 Cumulative Distribution Functions of Shear – Oregon I-84

Oregon vs Ontario Span 30ft



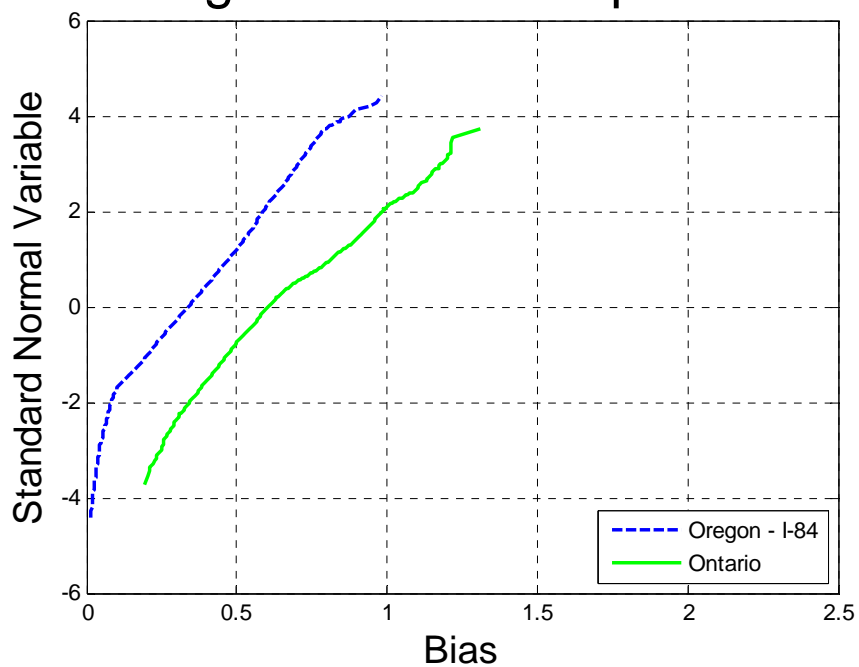
0-32 Comparison of Shear – Oregon I-84 vs. Ontario – Span 30ft

Oregon vs Ontario Span 60ft



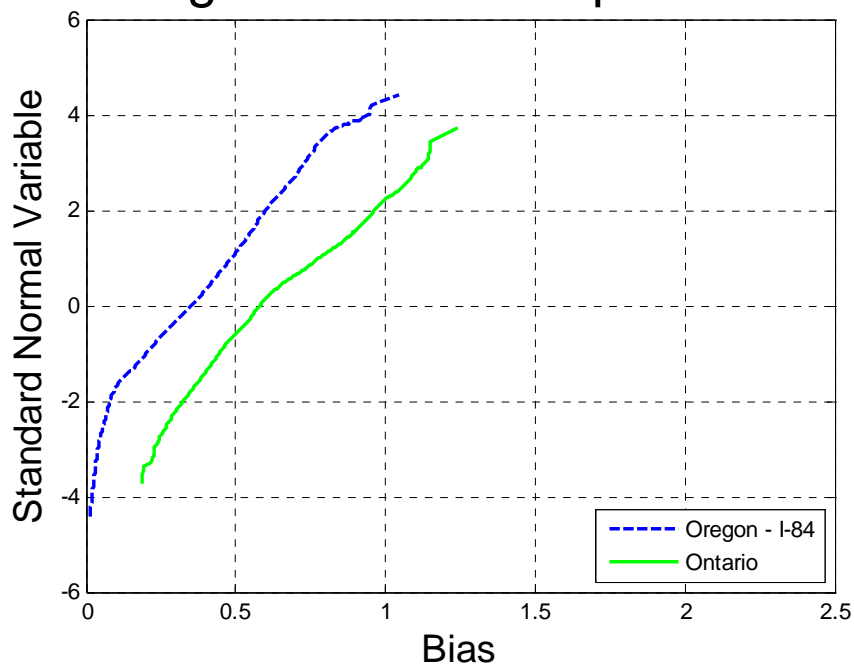
0-33 Comparison of Shear – Oregon I-84 vs. Ontario – Span 60ft

Oregon vs Ontario Span 90ft



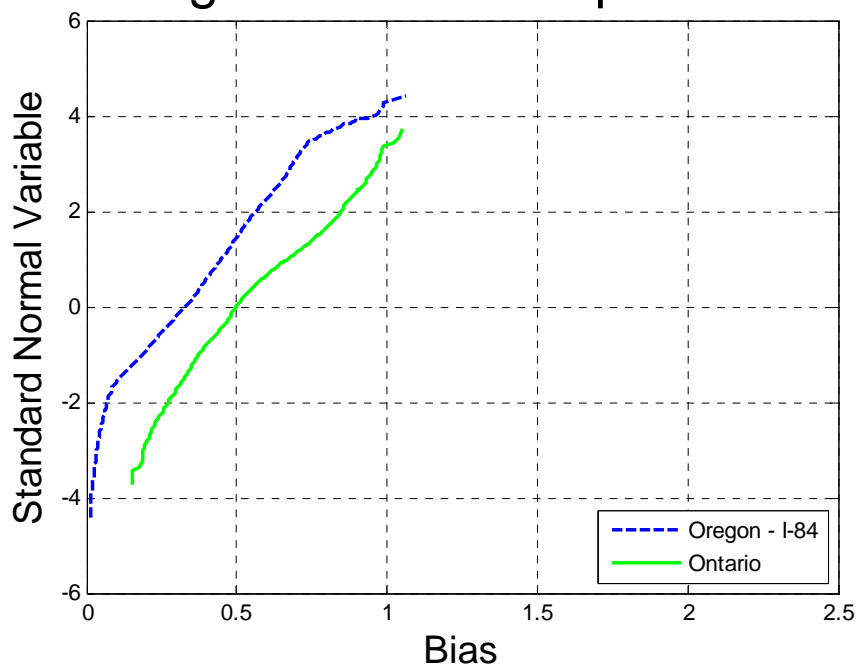
0-34 Comparison of Shear – Oregon I-84 vs. Ontario – Span 90ft

Oregon vs Ontario Span 120ft



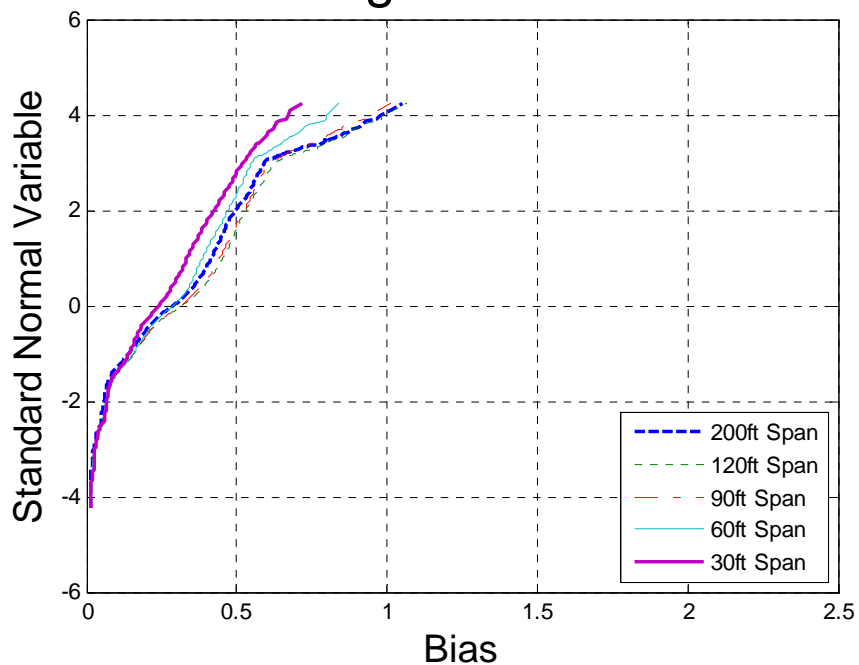
0-35 Comparison of Shear – Oregon I-84 vs. Ontario – Span 120ft

Oregon vs Ontario Span 200ft



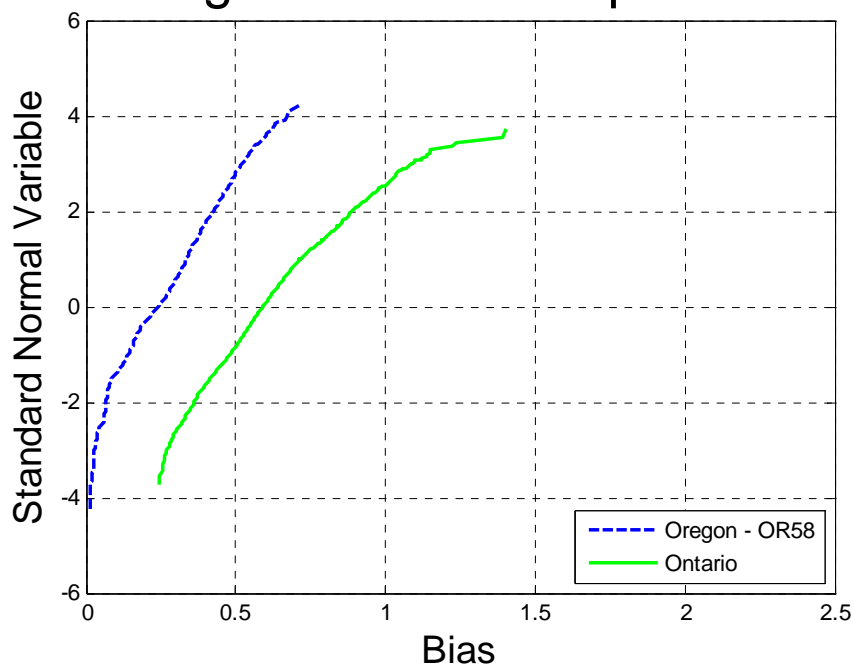
0-36 Comparison of Shear – Oregon I-84 vs. Ontario – Span 200ft

Oregon - OR58



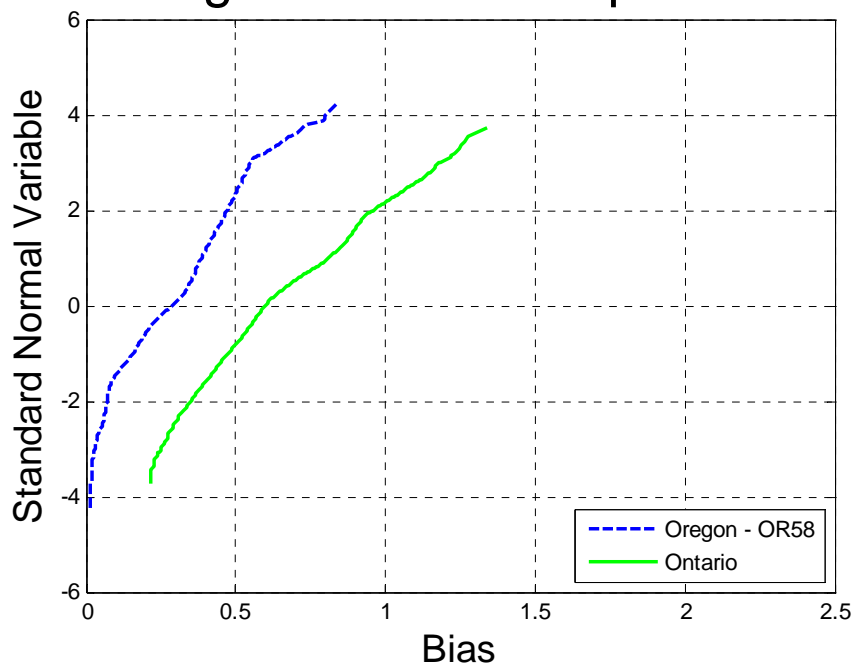
0-37 Cumulative Distribution Functions of Shear – Oregon OR58

Oregon vs Ontario Span 30ft



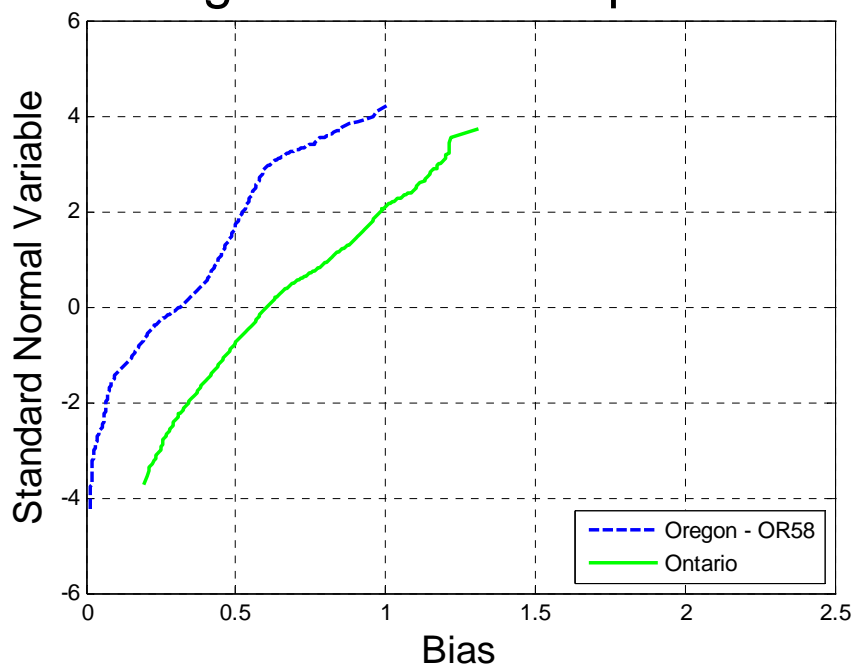
0-38 Comparison of Shear – Oregon OR58 vs. Ontario – Span 30ft

Oregon vs Ontario Span 60ft



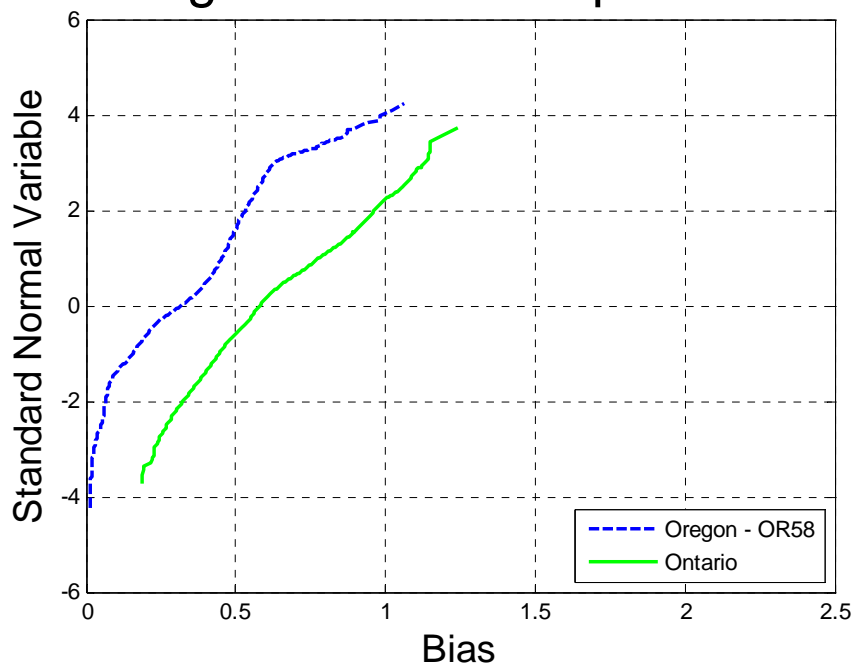
0-39 Comparison of Shear – Oregon OR58 vs. Ontario – Span 60ft

Oregon vs Ontario Span 90ft



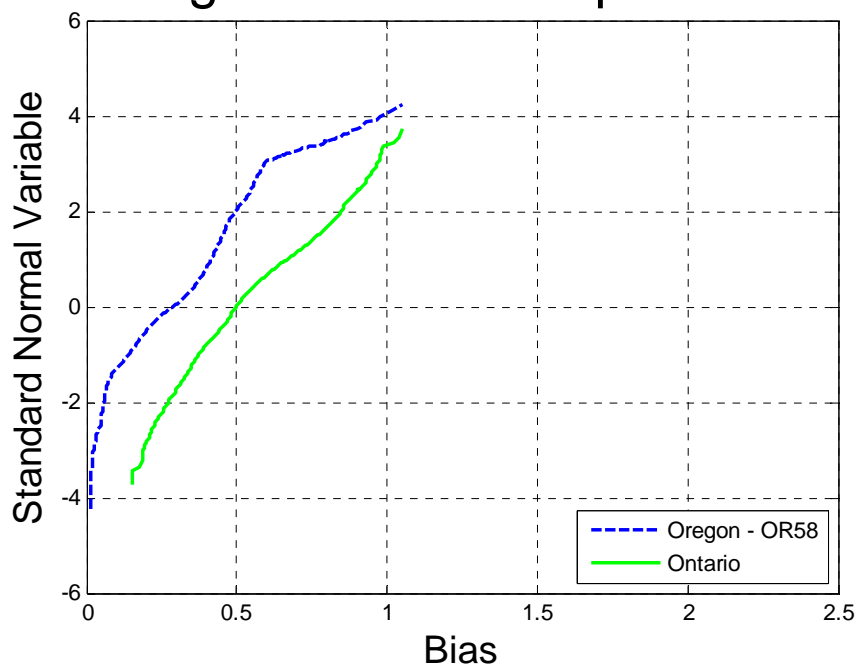
0-40 Comparison of Shear – Oregon OR58 vs. Ontario – Span 90ft

Oregon vs Ontario Span 120ft



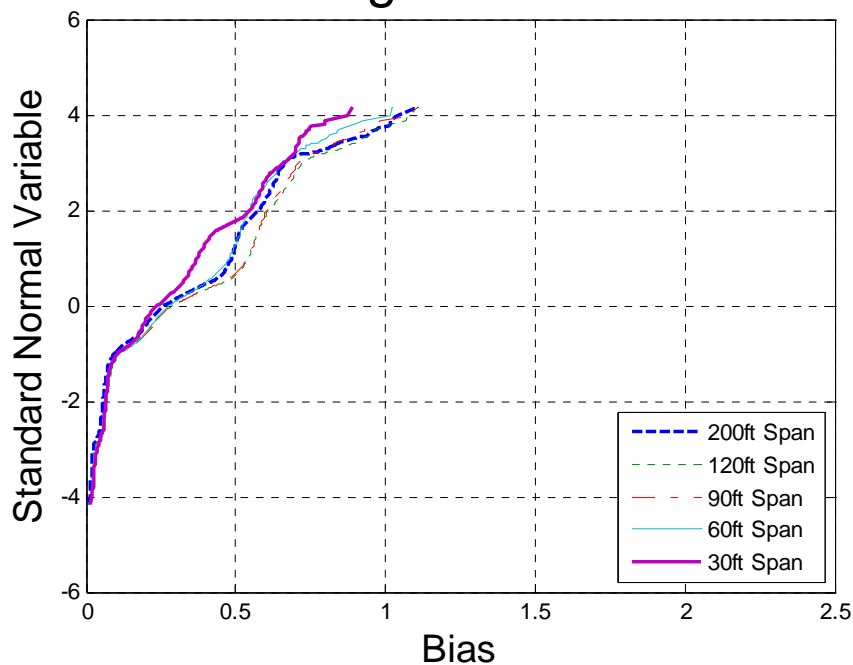
0-41 Comparison of Shear – Oregon OR58 vs. Ontario – Span 120ft

Oregon vs Ontario Span 200ft



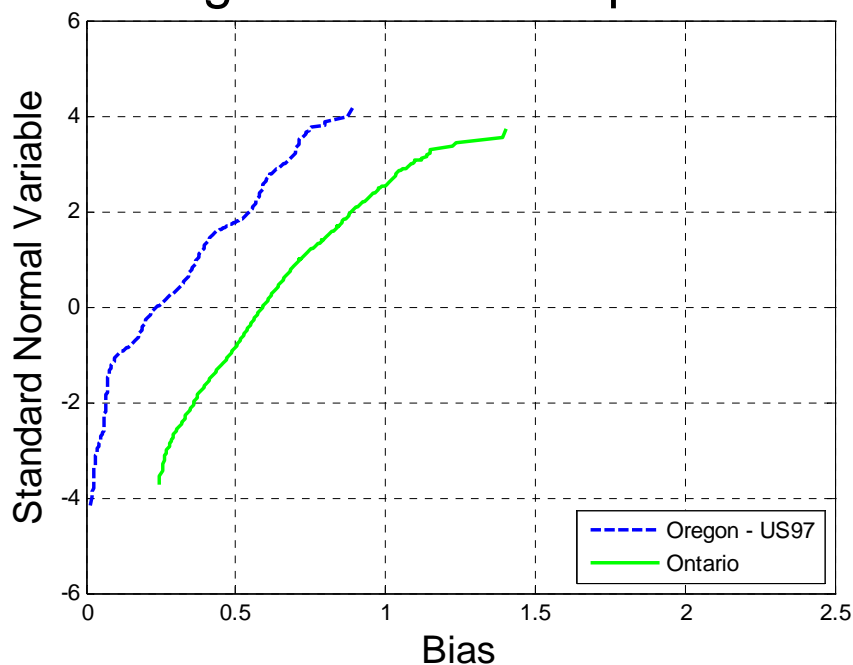
0-42 Comparison of Shear – Oregon OR58 vs. Ontario – Span 200ft

Oregon - US97



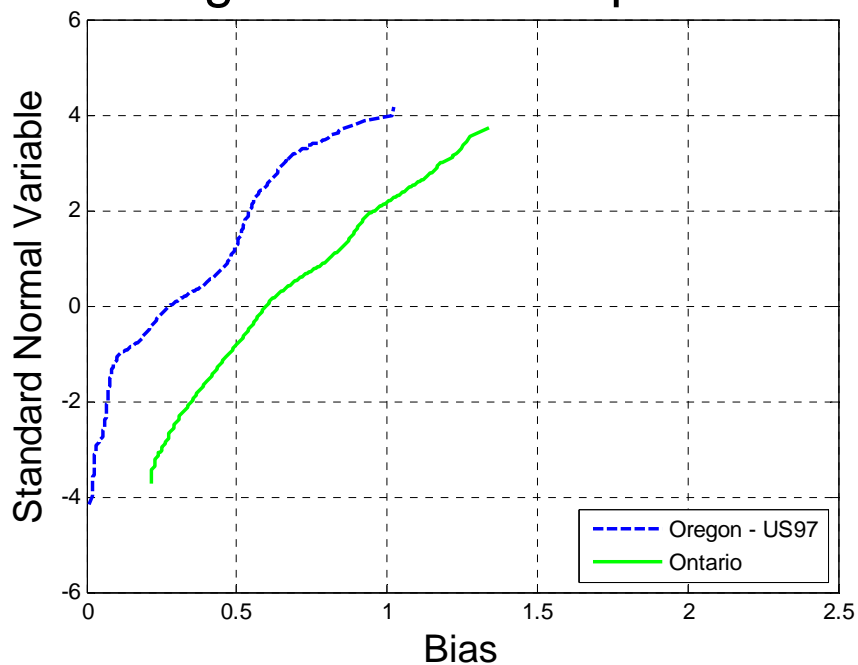
0-43 Cumulative Distribution Functions of Shear – Oregon US97

Oregon vs Ontario Span 30ft



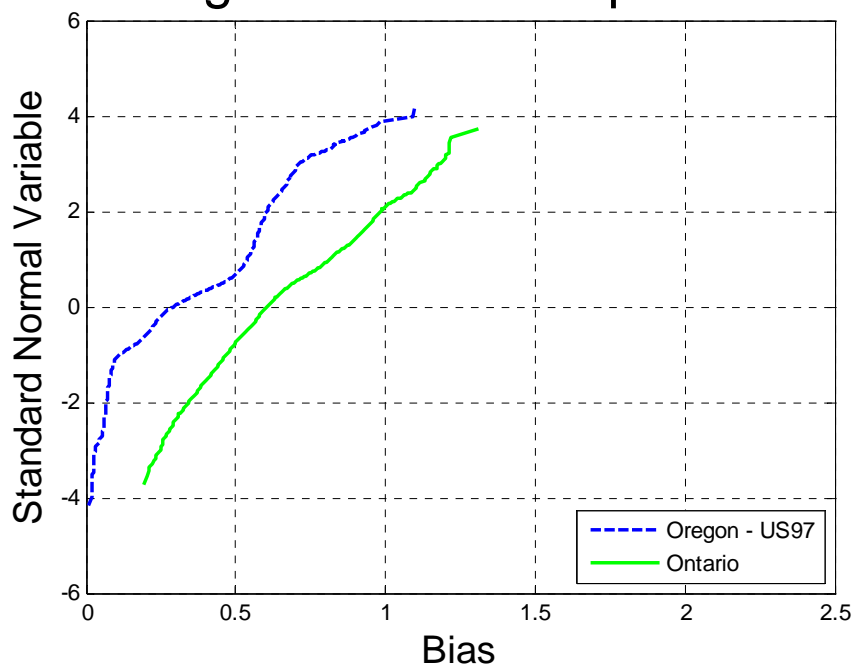
0-44 Comparison of Shear – Oregon US97 vs. Ontario – Span 30ft

Oregon vs Ontario Span 60ft



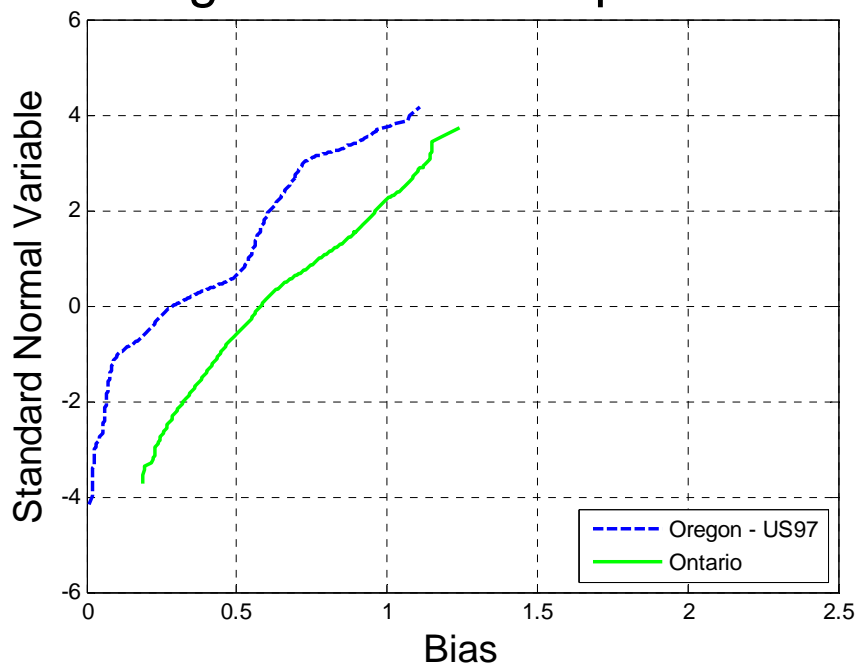
0-45 Comparison of Shear – Oregon US97 vs. Ontario – Span 60ft

Oregon vs Ontario Span 90ft

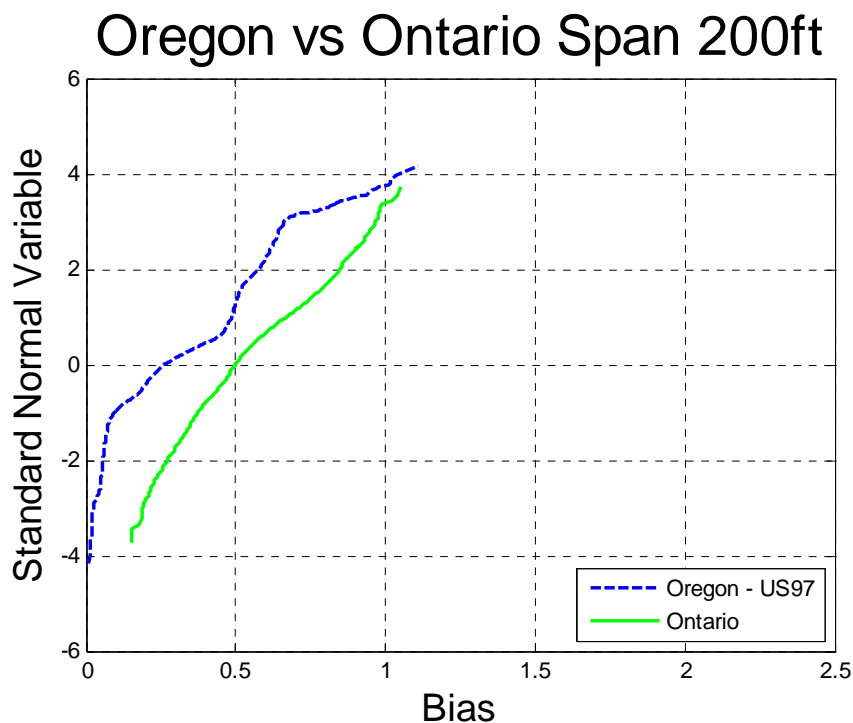


0-46 Comparison of Shear – Oregon US97 vs. Ontario – Span 90ft

Oregon vs Ontario Span 120ft



0-47 Comparison of Shear – Oregon US97 vs. Ontario – Span 120ft



0-48 Comparison of Shear – Oregon US97 vs. Ontario – Span 200ft

FLORIDA – LIVE LOAD EFFECT

WIM data for Florida

The truck survey includes weigh-in-motion (WIM) truck measurements obtained from NCHRP project. The data includes 12 months of traffic recorded at different locations. The total number of records is shown in Table 59. The data includes number of axles, gross vehicle weight (GVW), weight per axle and spacing between axles.

Table 59

Site	Number of Trucks
I-10	1,654,006
I-75	2,679,288
I-95	2,226,480
State Route	647,965
US29	728,544

TOTAL	7,936,283
-------	-----------

Maximum Simple Span Moments

The maximum moment was calculated for each truck from the data. Analysis included simple spans with the span varying from 30 to 200 ft. The maximum moment was also calculated for the HL93 load and Tandem. Ratio between the data truck moment and the AASHTO LRFD load moment was plotted on the probability paper.

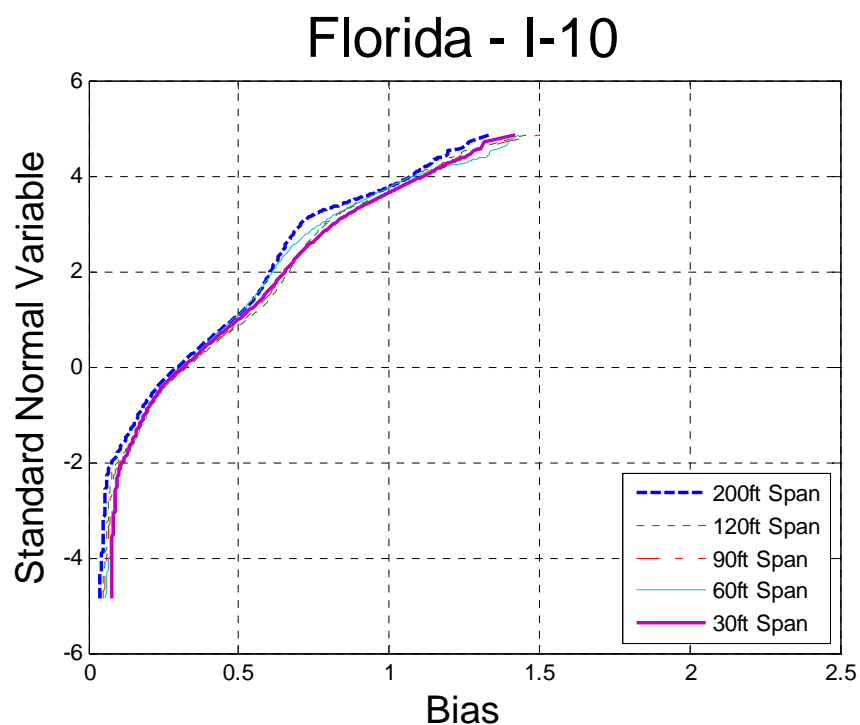


Figure 0-49 Cumulative Distribution Functions of Simple Span Moment– Florida – I-10

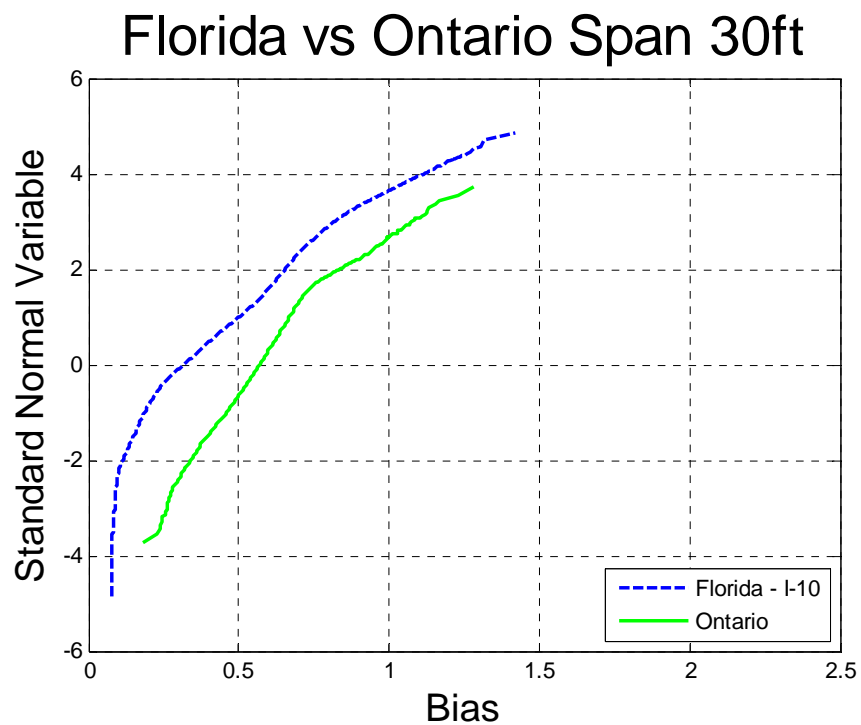


Figure 0-50 Comparison of Simple Span Moment – Florida – I-10 vs. Ontario – Span 30ft

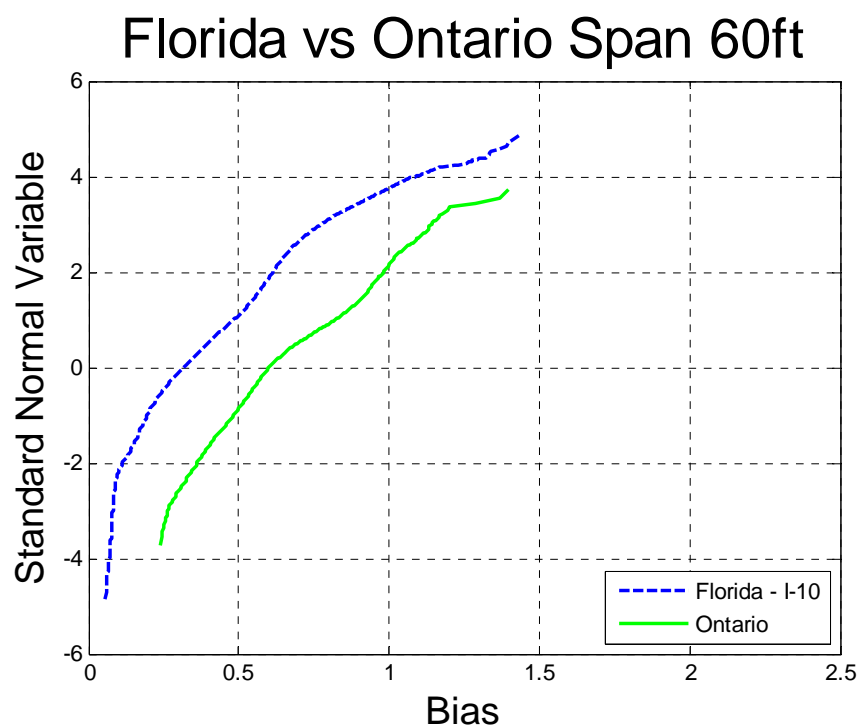


Figure 0-51 Comparison of Simple Span Moment – Florida – I-10 vs. Ontario – Span 60ft

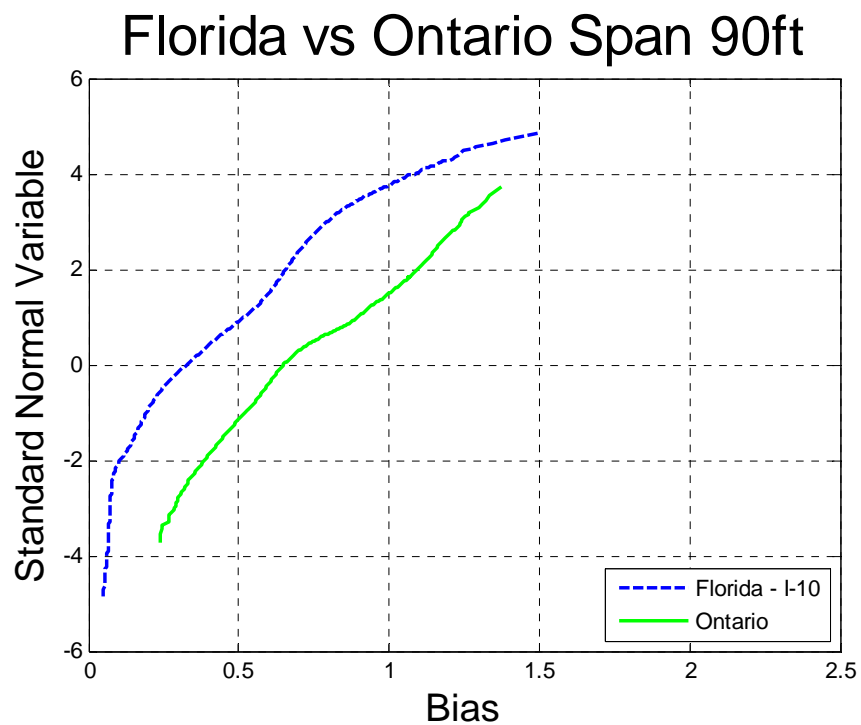


Figure 0-52 Comparison of Simple Span Moment – Florida – I-10 vs. Ontario – Span 90ft

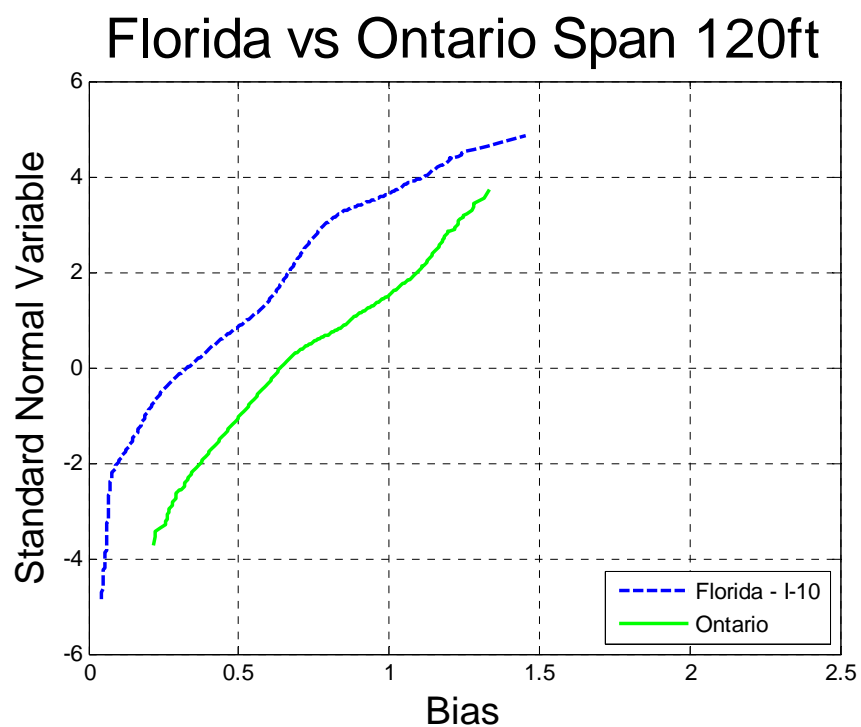


Figure 0-53 Comparison of Simple Span Moment – Florida – I-10 vs. Ontario – Span 120ft

Florida vs Ontario Span 200ft

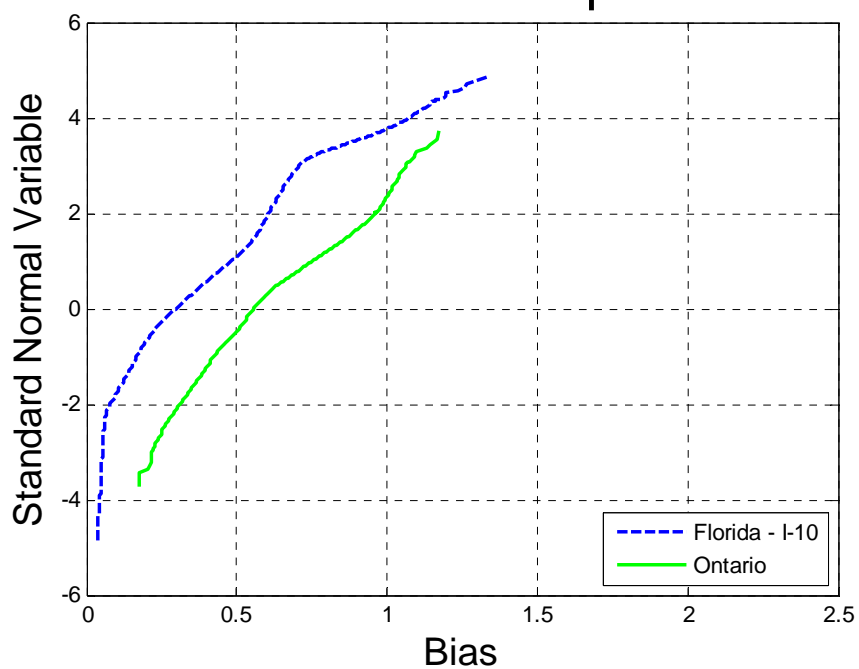


Figure 0-54 Comparison of Simple Span Moment – Florida – I-10 vs. Ontario – Span 200ft

Florida - I-75

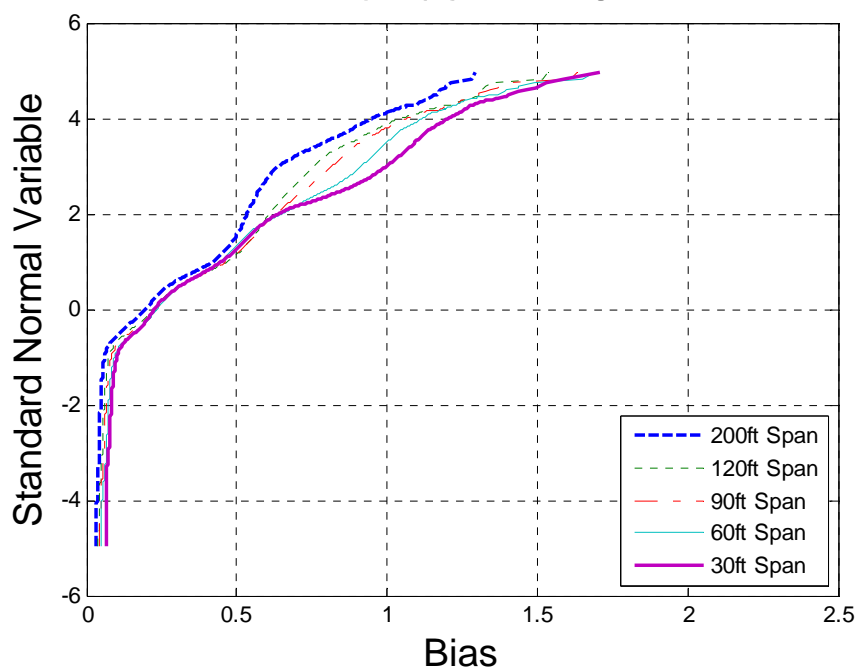


Figure 0-55 Cumulative Distribution Functions of Simple Span Moment– Florida – I-75

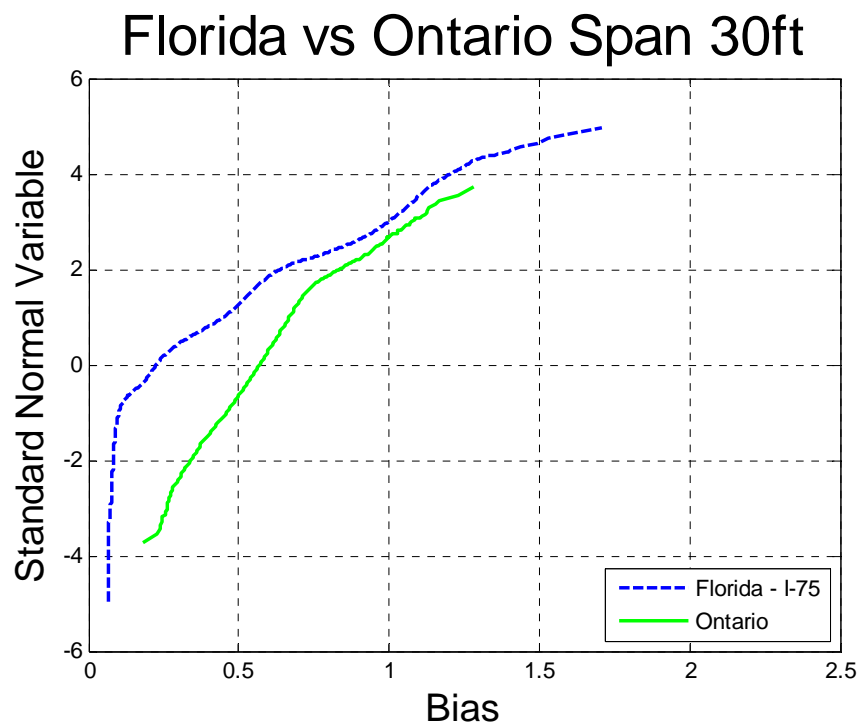


Figure 0-56 Comparison of Simple Span Moment – Florida – I-75 vs. Ontario – Span 30ft

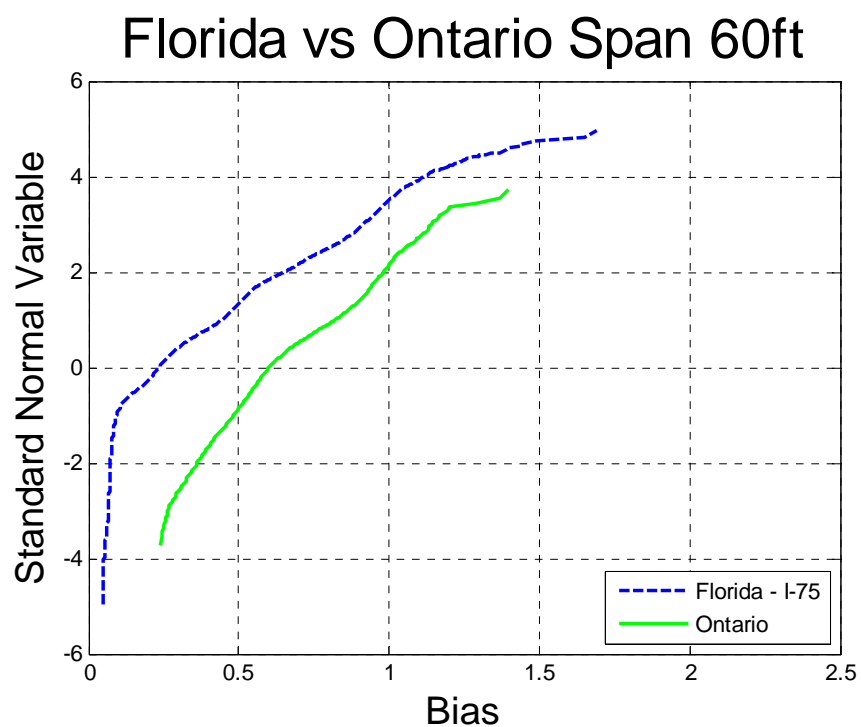


Figure 0-57 Comparison of Simple Span Moment – Florida – I-75 vs. Ontario – Span 60ft

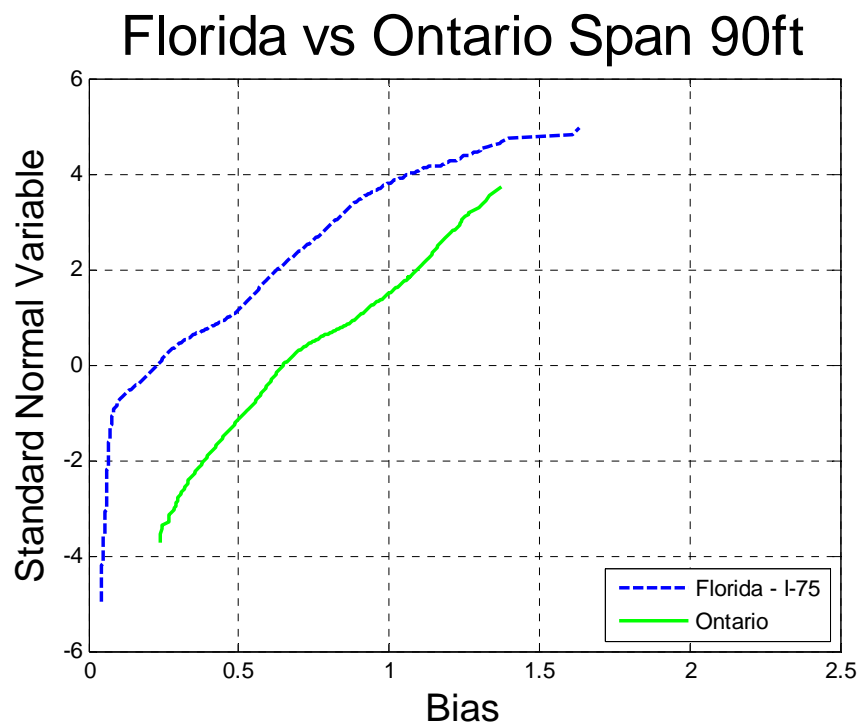


Figure 0-58 Comparison of Simple Span Moment – Florida – I-75 vs. Ontario – Span 90ft

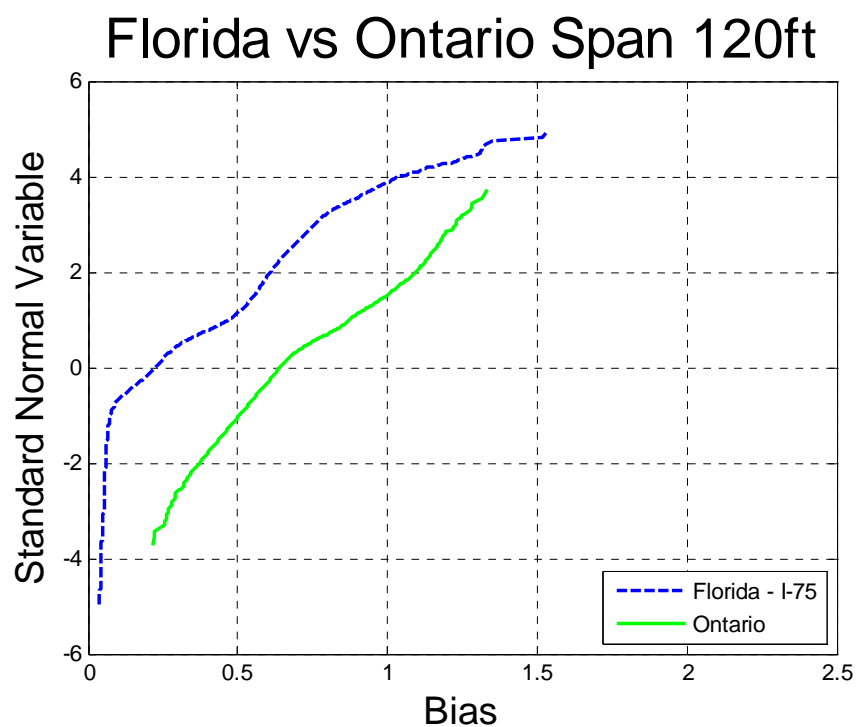


Figure 0-59 Comparison of Simple Span Moment – Florida – I-75 vs. Ontario – Span 120ft

Florida vs Ontario Span 200ft

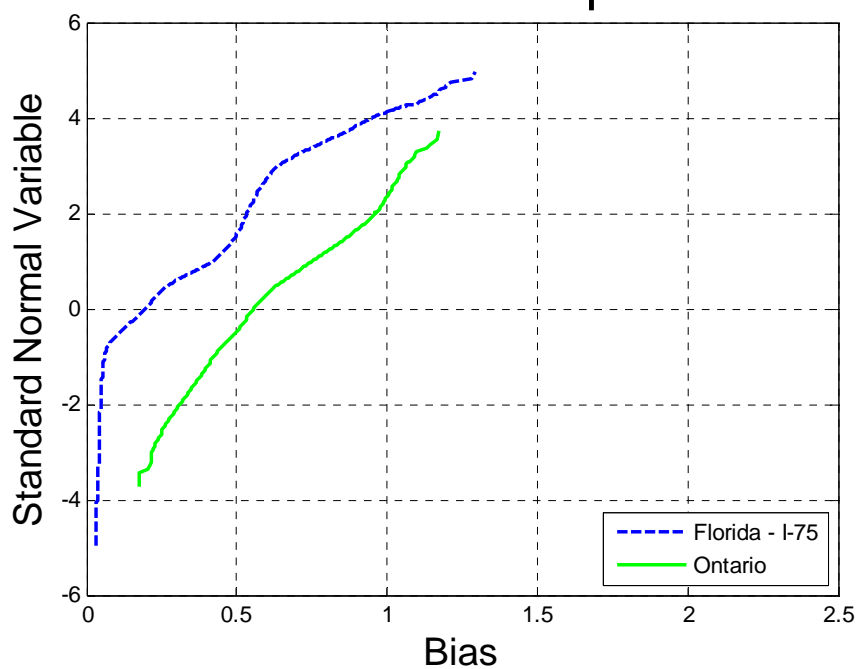


Figure 0-60 Comparison of Simple Span Moment – Florida – I-75 vs. Ontario – Span 200ft

Florida - I-95

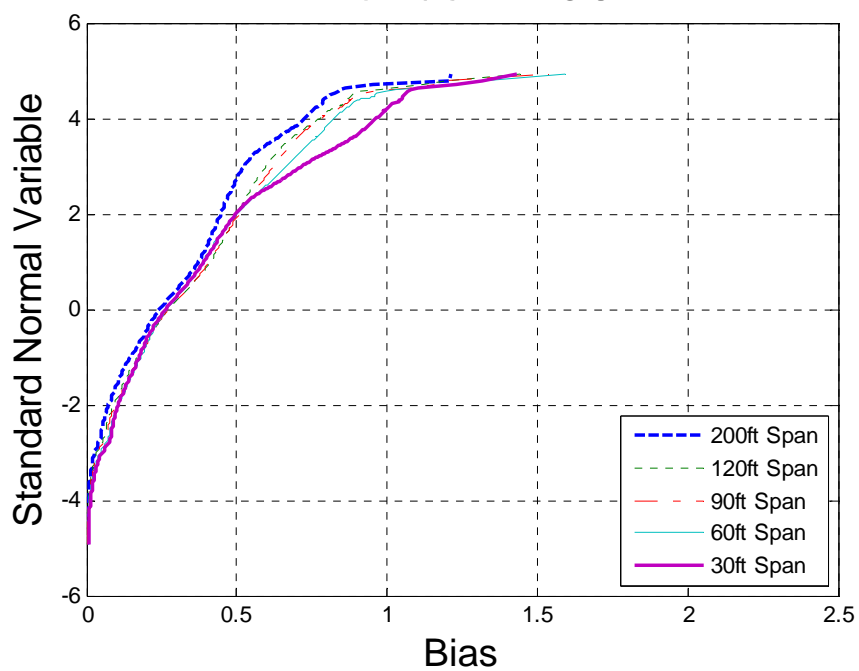


Figure 0-61 Cumulative Distribution Functions of Simple Span Moment– Florida – I-95

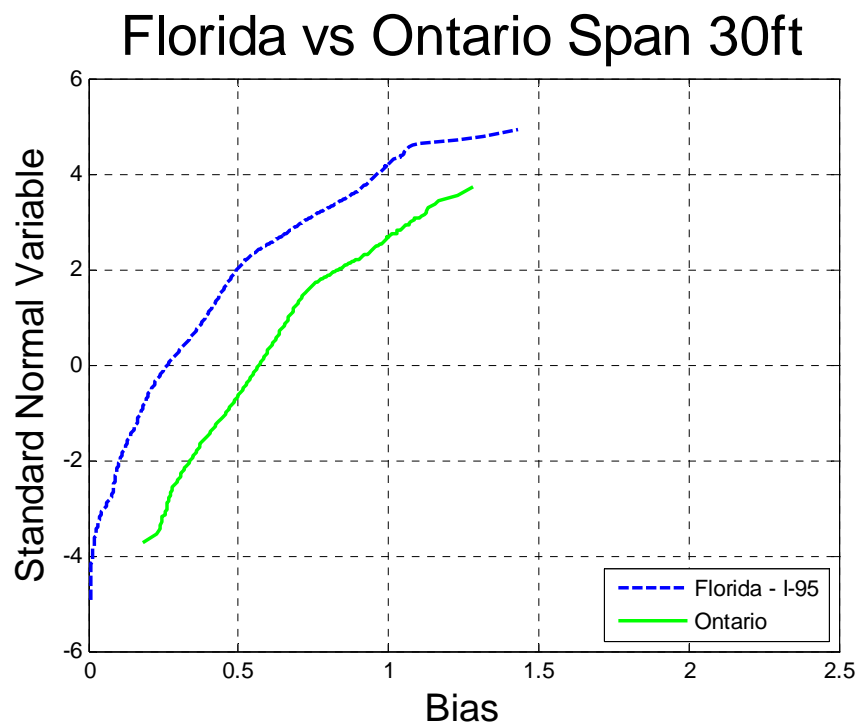


Figure 0-62 Comparison of Simple Span Moment – Florida – I-95 vs. Ontario – Span 30ft

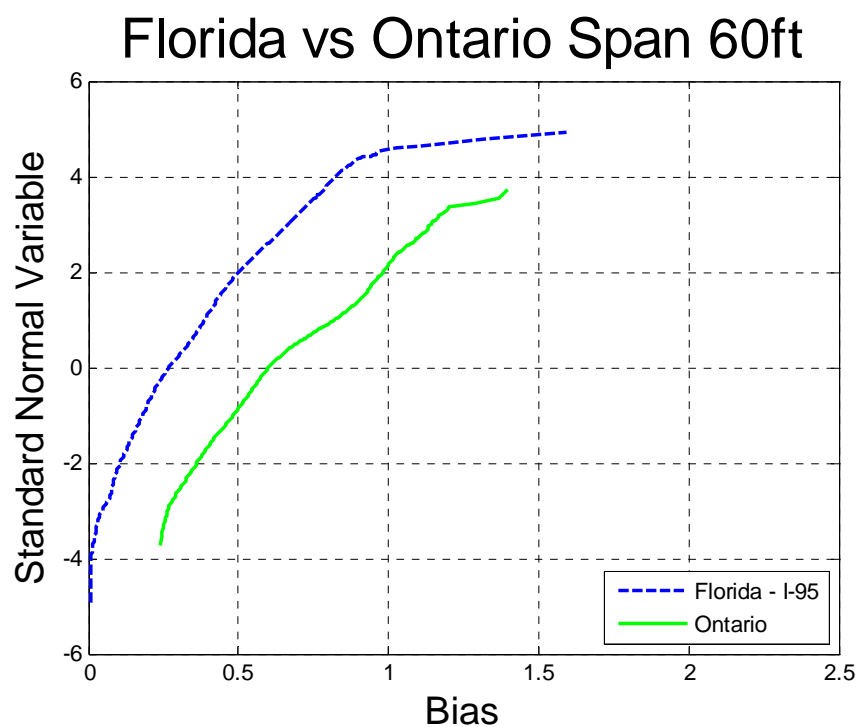


Figure 0-63 Comparison of Simple Span Moment – Florida – I-95 vs. Ontario – Span 60ft

Florida vs Ontario Span 90ft

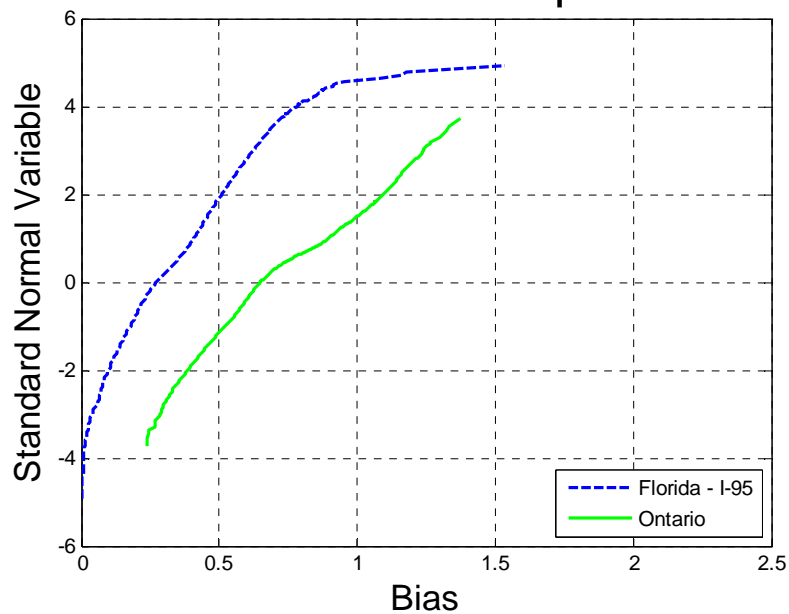


Figure 0-64 Comparison of Simple Span Moment – Florida – I-95 vs. Ontario – Span 90ft

Florida vs Ontario Span 120ft

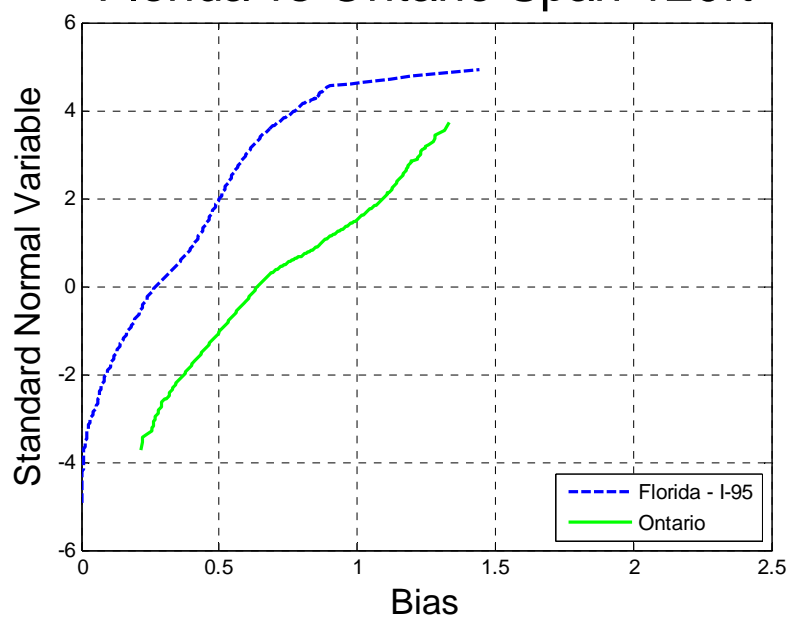


Figure 0-65 Comparison of Simple Span Moment – Florida – I-95 vs. Ontario – Span 120ft

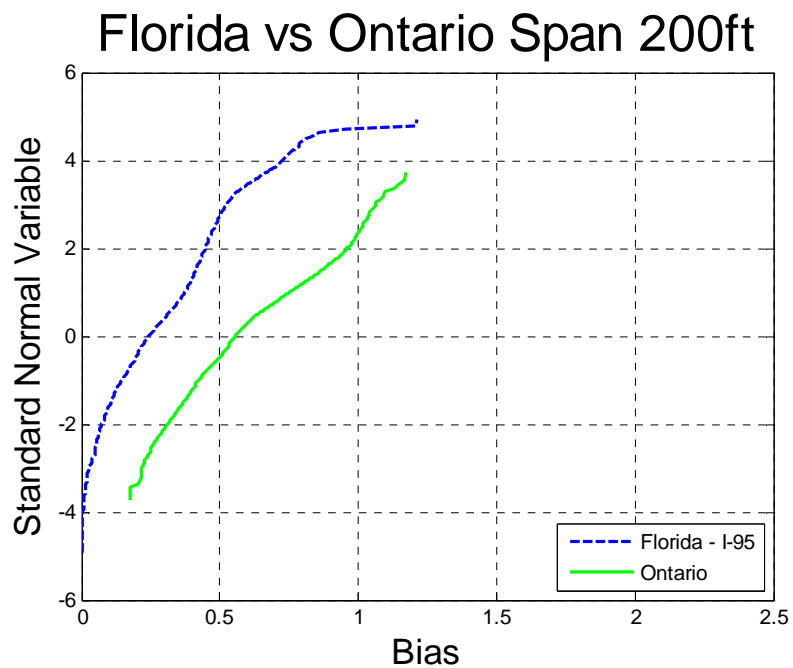


Figure 0-66 Comparison of Simple Span Moment – Florida – I-95 vs. Ontario – Span 200ft

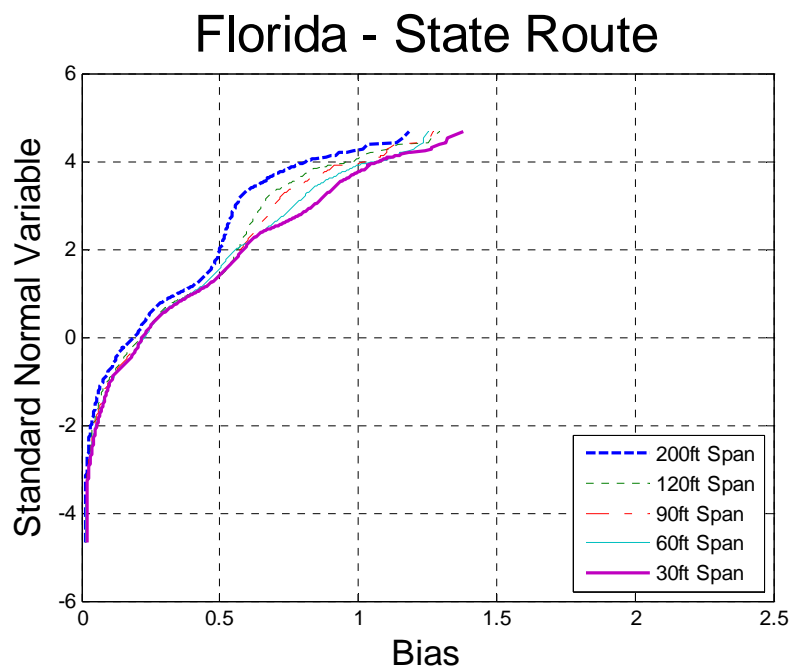


Figure 0-67 Cumulative Distribution Functions of Simple Span Moment– Florida – State Route

Florida vs Ontario Span 30ft

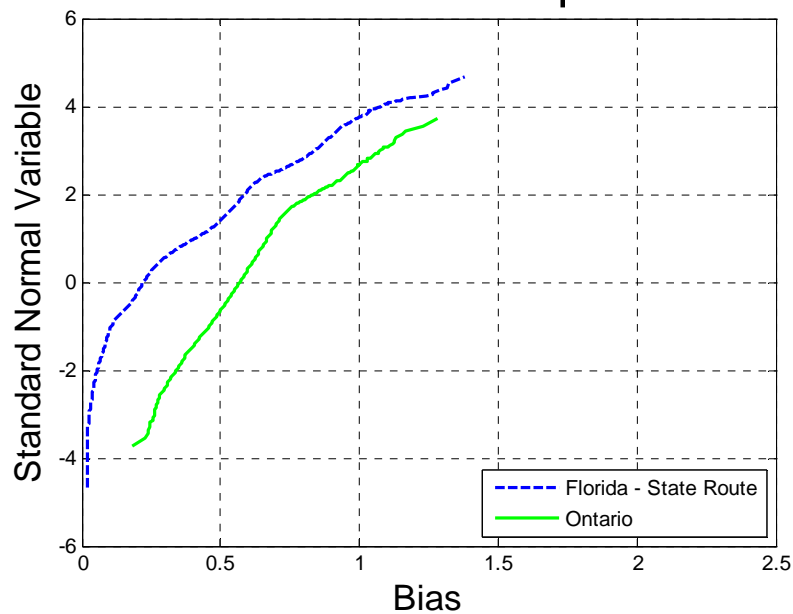


Figure 0-68 Comparison of Simple Span Moment – Florida – State Route vs. Ontario – Span 30ft

Florida vs Ontario Span 60ft

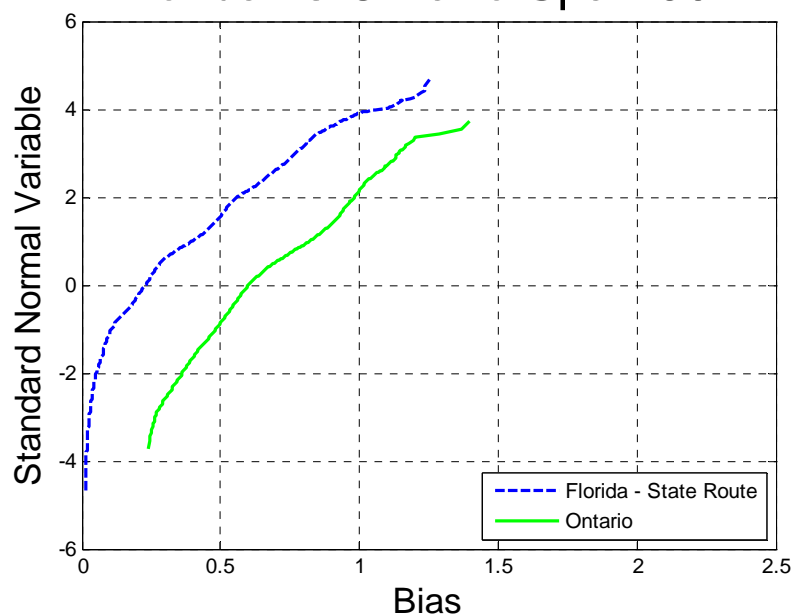


Figure 0-69 Comparison of Simple Span Moment – Florida – State Route vs. Ontario – Span 60ft

Florida vs Ontario Span 90ft

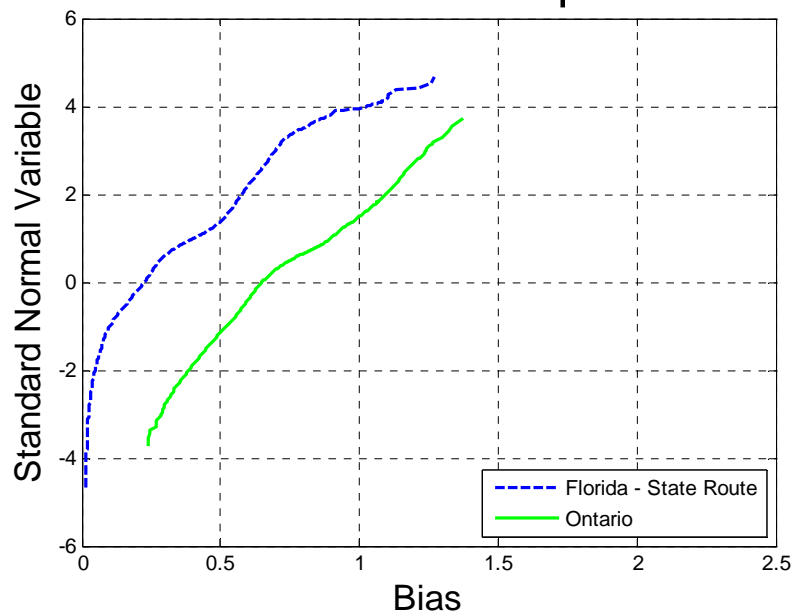


Figure 0-70 Comparison of Simple Span Moment – Florida – State Route vs. Ontario – Span 90ft

Florida vs Ontario Span 120ft

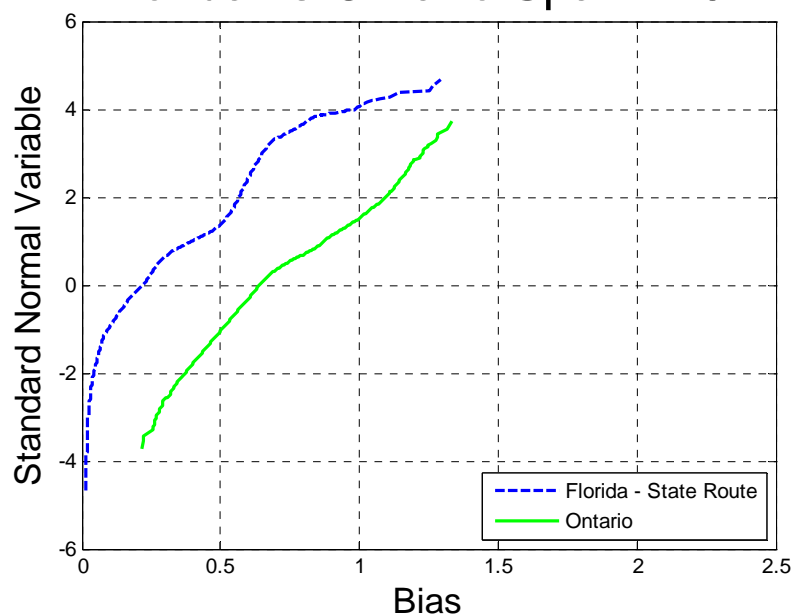


Figure 0-71 Comparison of Simple Span Moment – Florida – State Route vs. Ontario – Span 120ft

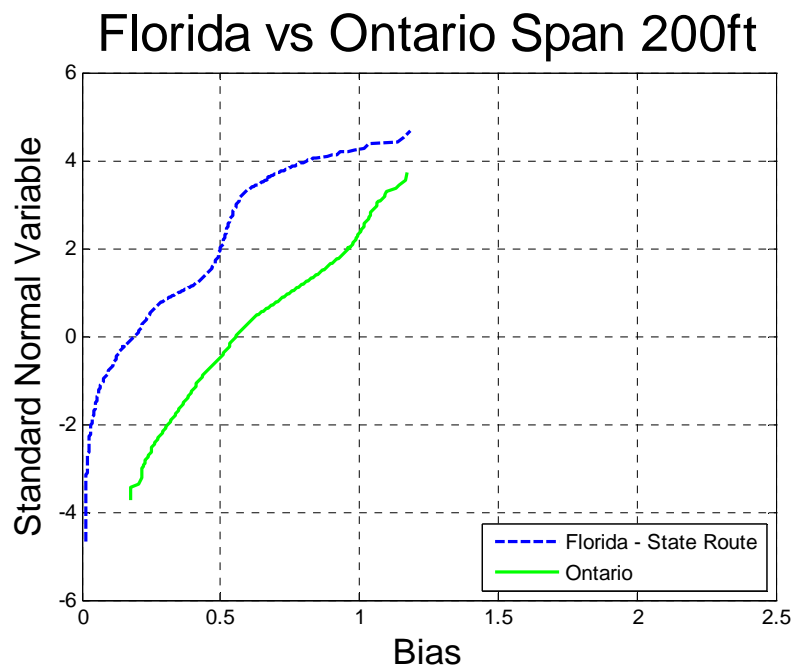


Figure 0-72 Comparison of Simple Span Moment – Florida – State Route vs. Ontario – Span 200ft

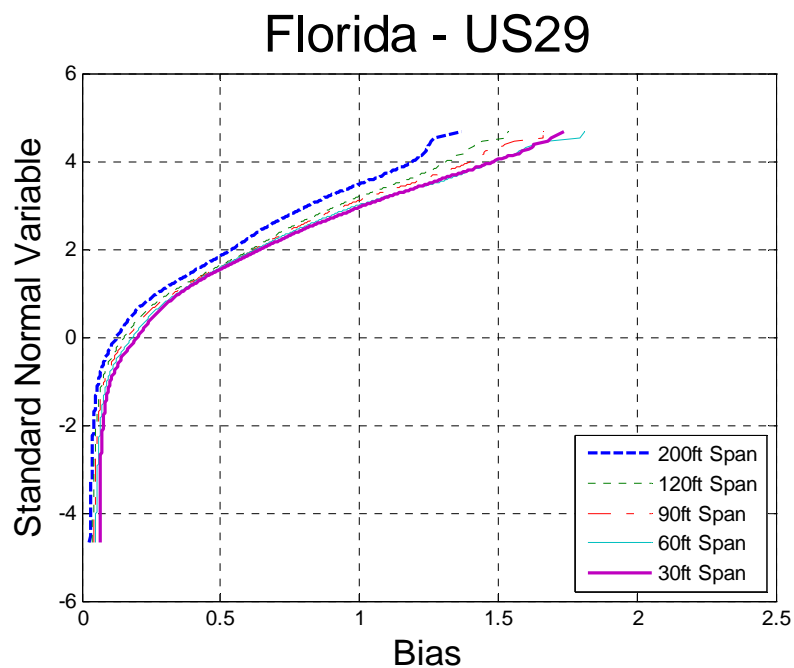


Figure 0-73 Cumulative Distribution Functions of Simple Span Moment– Florida – US29

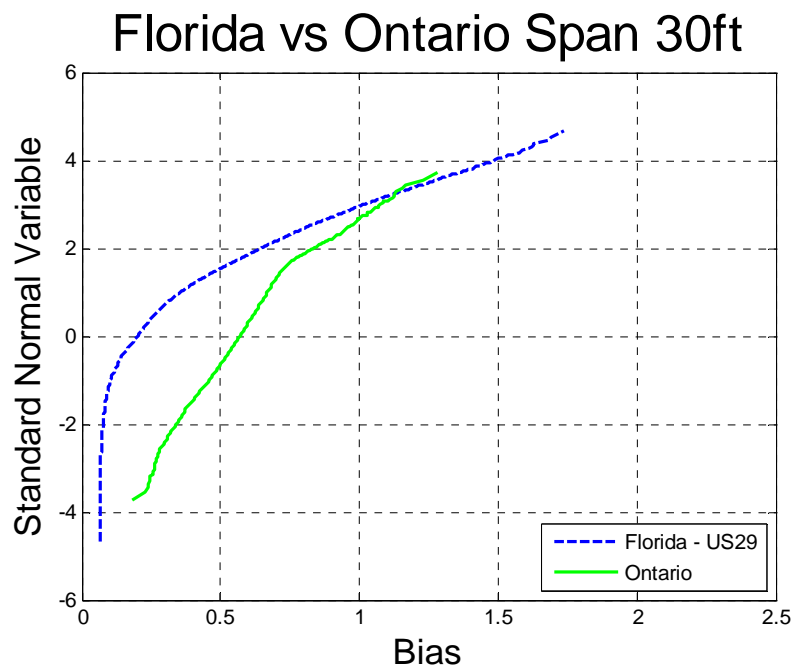


Figure 0-74 Comparison of Simple Span Moment – Florida – US29 vs. Ontario – Span 30ft

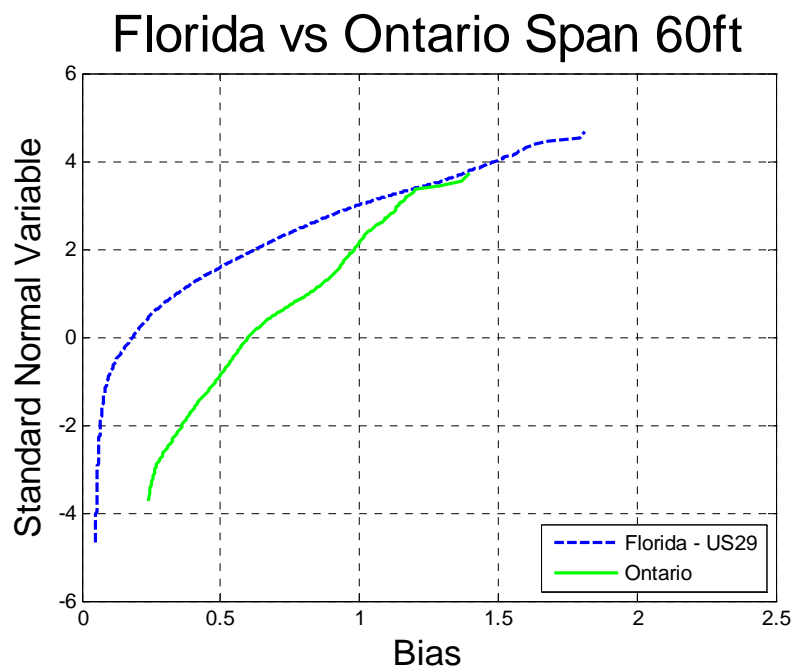


Figure 0-75 Comparison of Simple Span Moment – Florida – US29 vs. Ontario – Span 60ft

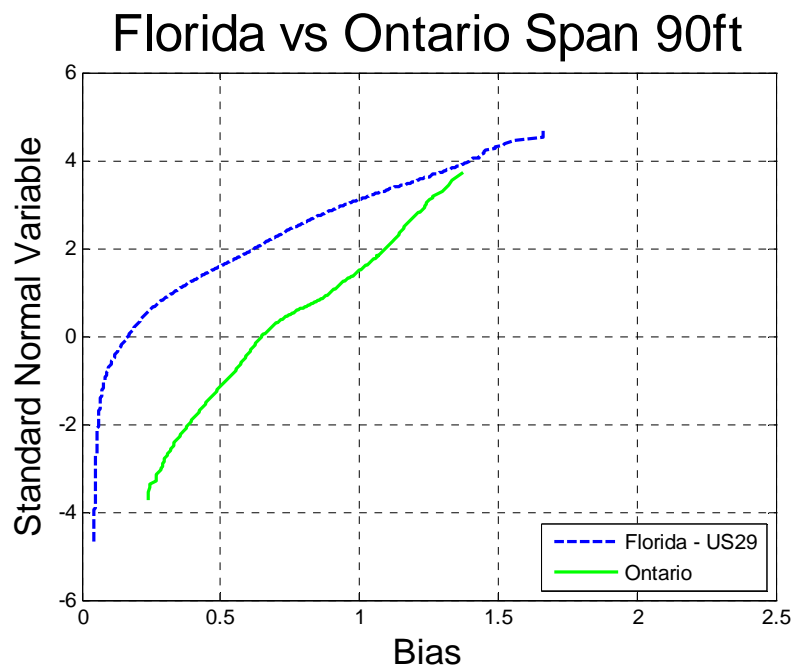


Figure 0-76 Comparison of Simple Span Moment – Florida – US29 vs. Ontario – Span 90ft

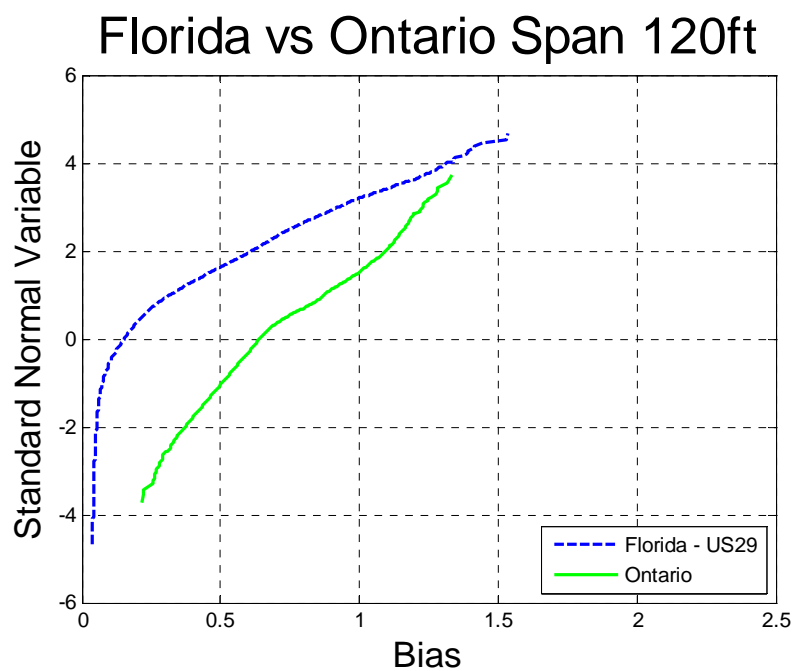


Figure 0-77 Comparison of Simple Span Moment – Florida – US29 vs. Ontario – Span 120ft

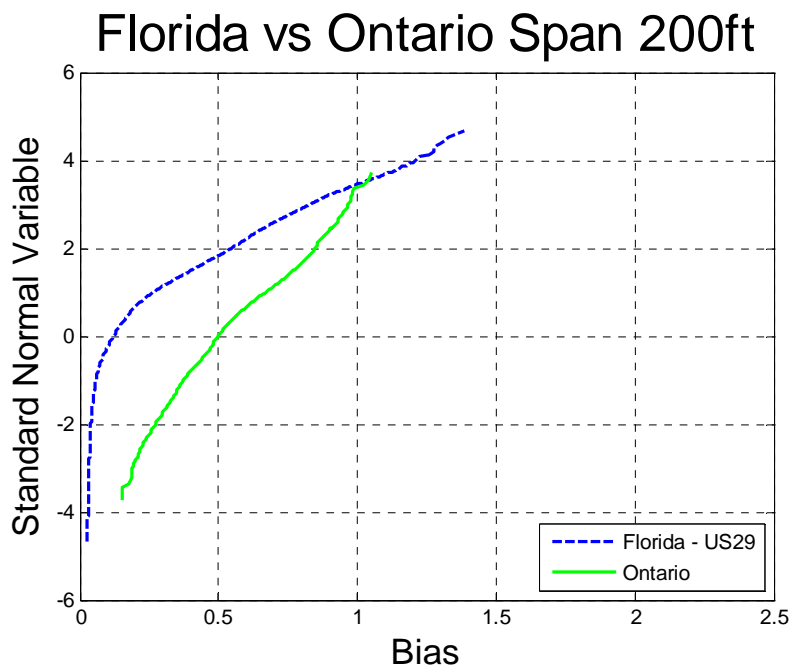


Figure 0-78 Comparison of Simple Span Moment – Florida – US29 vs. Ontario – Span 200ft

Maximum Shear

The maximum shear was calculated for each truck from the data. Analysis included simple spans with the span varying from 30 to 200 ft. The ratio of shear obtained from the data truck and the HL-93 load was plotted on the probability paper.

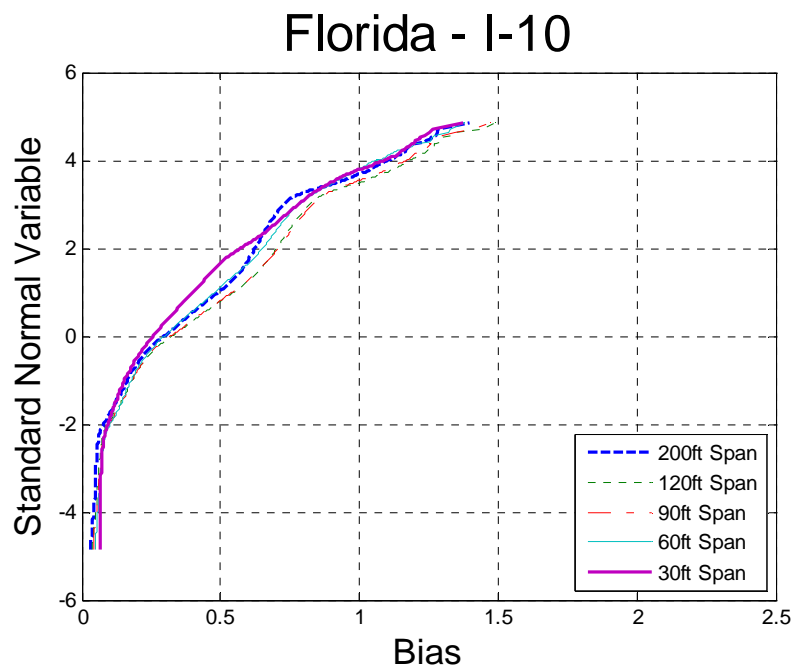


Figure 0-79 Cumulative Distribution Functions of Shear – Florida I-10

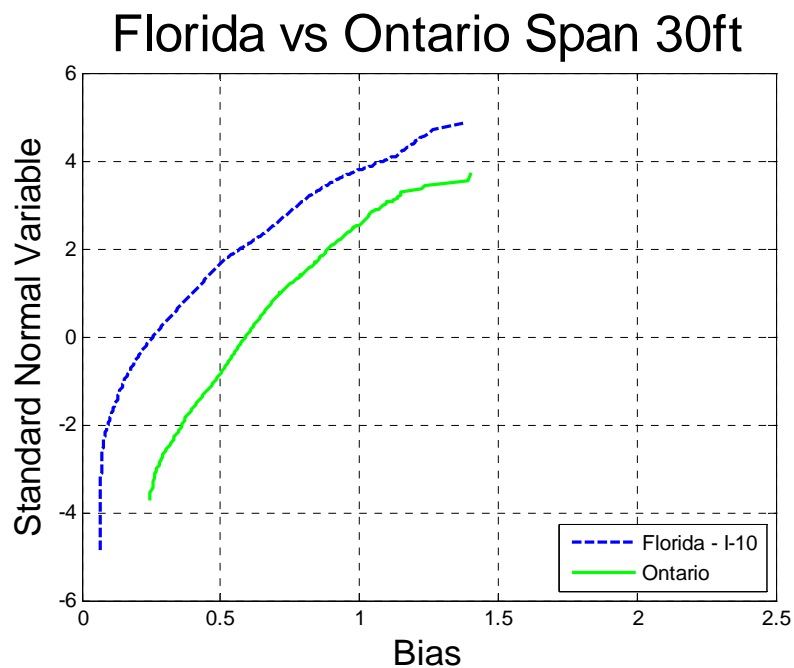


Figure 0-80 Comparison of Shear – Florida I-10 vs. Ontario – Span 30ft

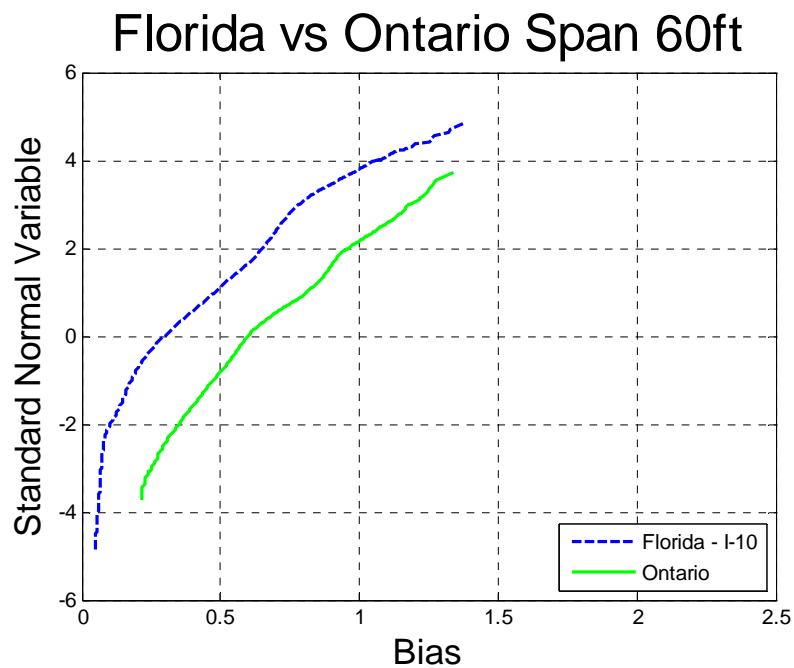


Figure 0-81 Comparison of Shear – Florida I-10 vs. Ontario – Span 60ft

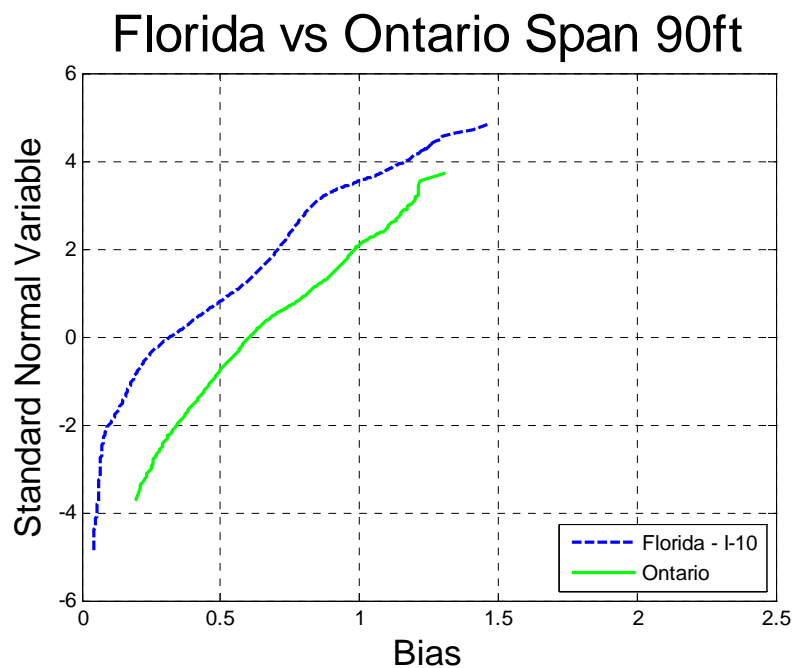


Figure 0-82 Comparison of Shear – Florida I-10 vs. Ontario – Span 90ft

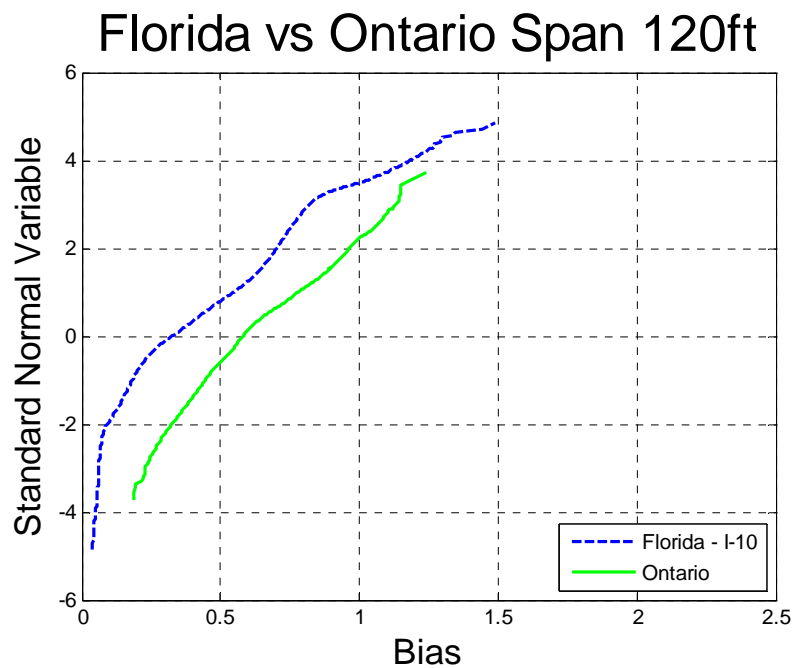


Figure 0-83 Comparison of Shear – Florida I-10 vs. Ontario – Span 120ft

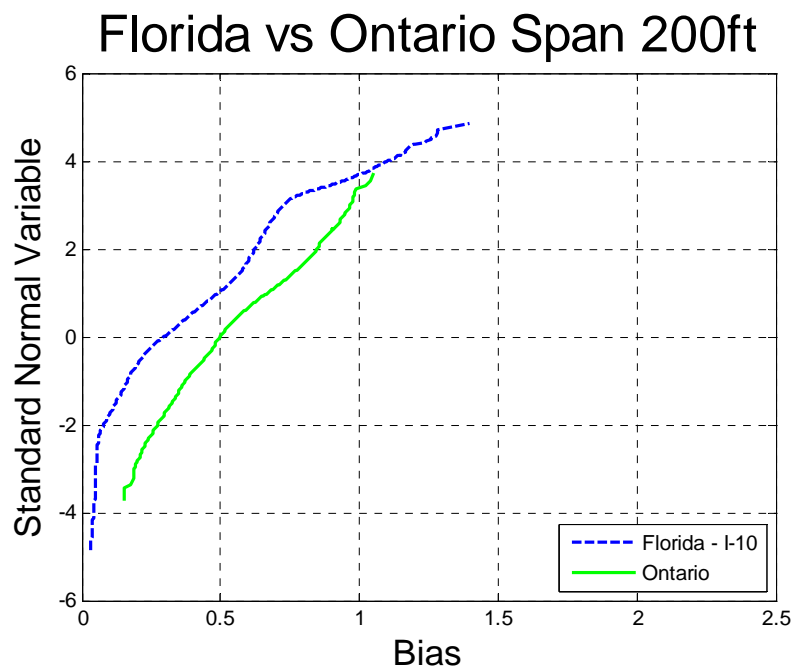


Figure 0-84 Comparison of Shear – Florida I-10 vs. Ontario – Span 200ft

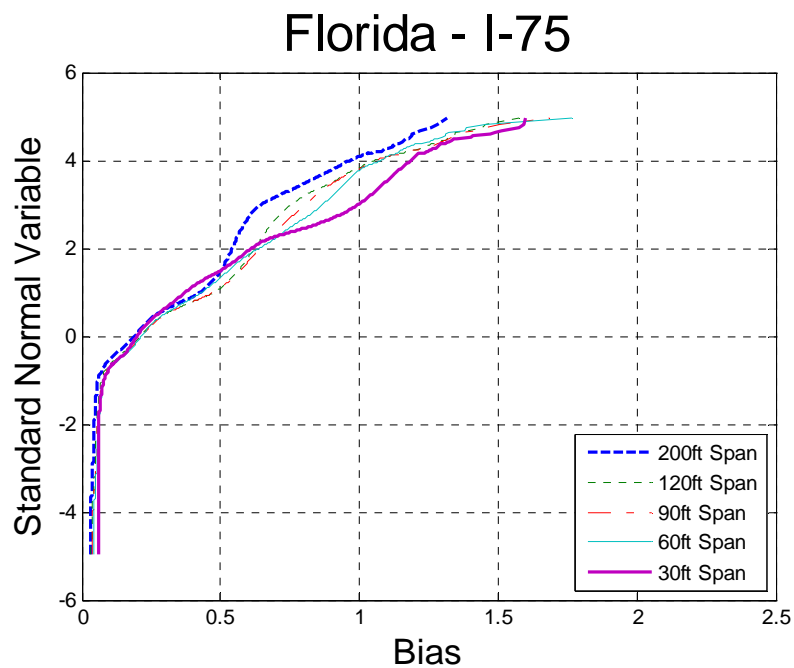


Figure 0-85 Cumulative Distribution Functions of Shear – Florida I-75

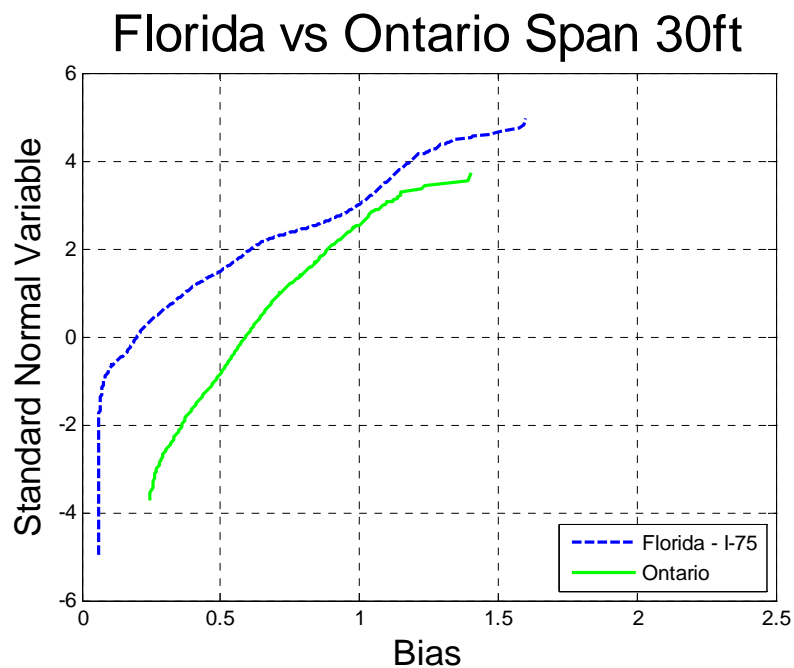


Figure 0-86 Comparison of Shear – Florida I-75 vs. Ontario – Span 30ft

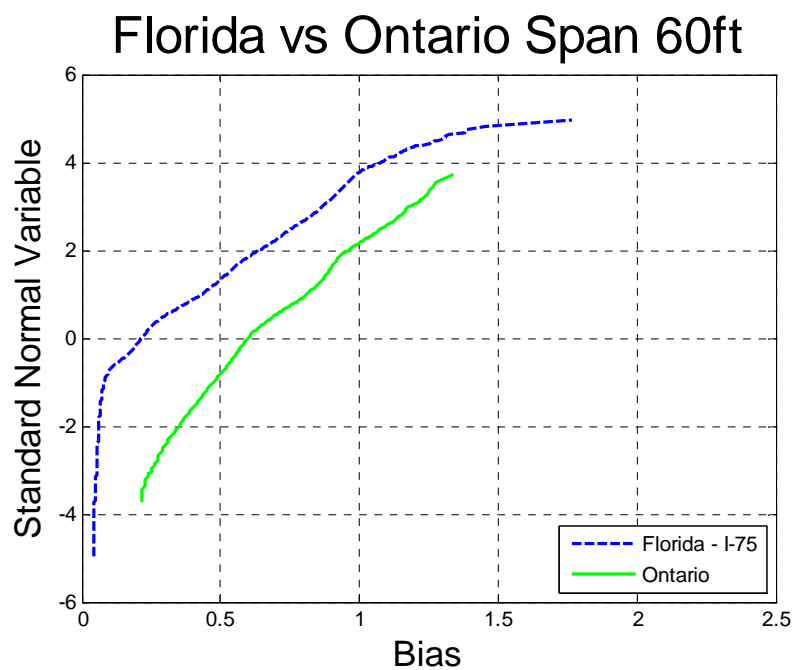


Figure 0-87 Comparison of Shear – Florida I-75 vs. Ontario – Span 60ft

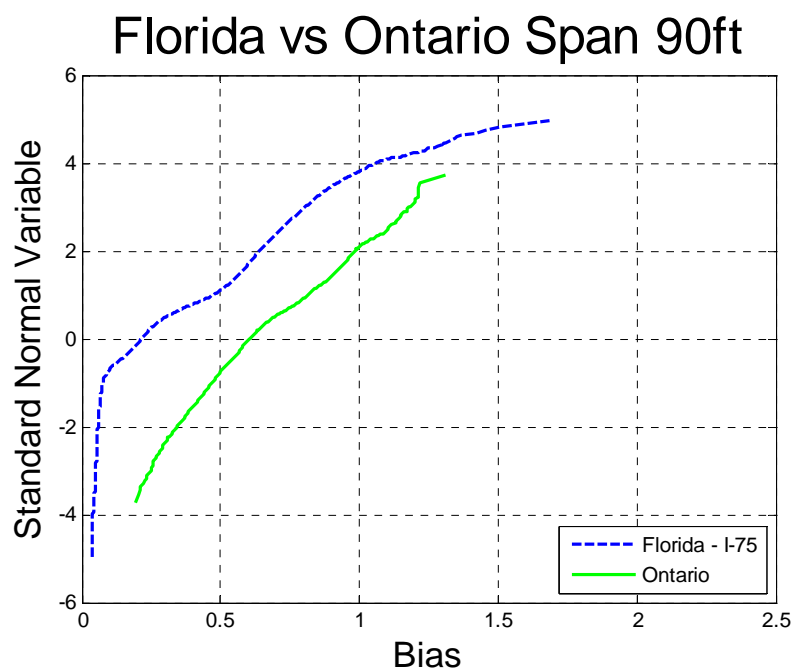


Figure 0-88 Comparison of Shear – Florida I-75 vs. Ontario – Span 90ft

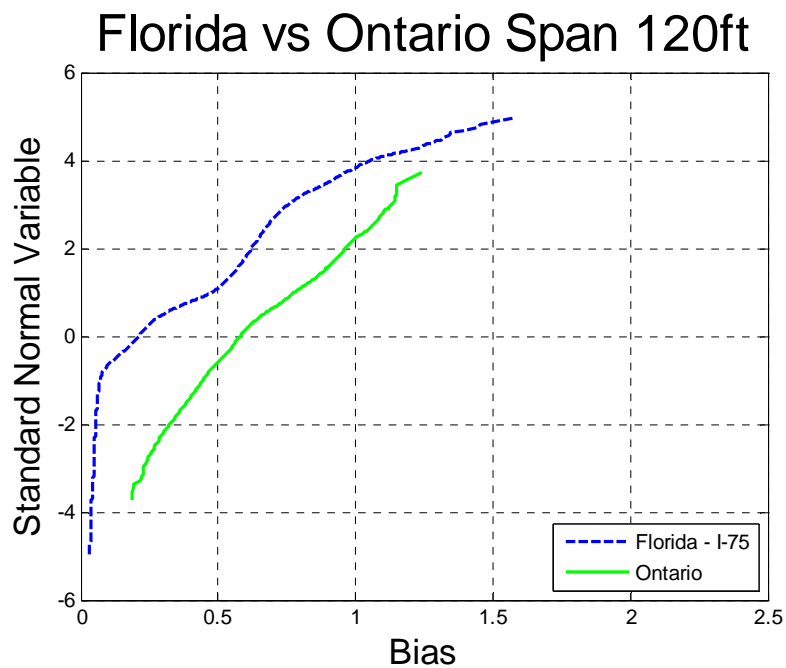


Figure 0-89 Comparison of Shear – Florida I-75 vs. Ontario – Span 120ft

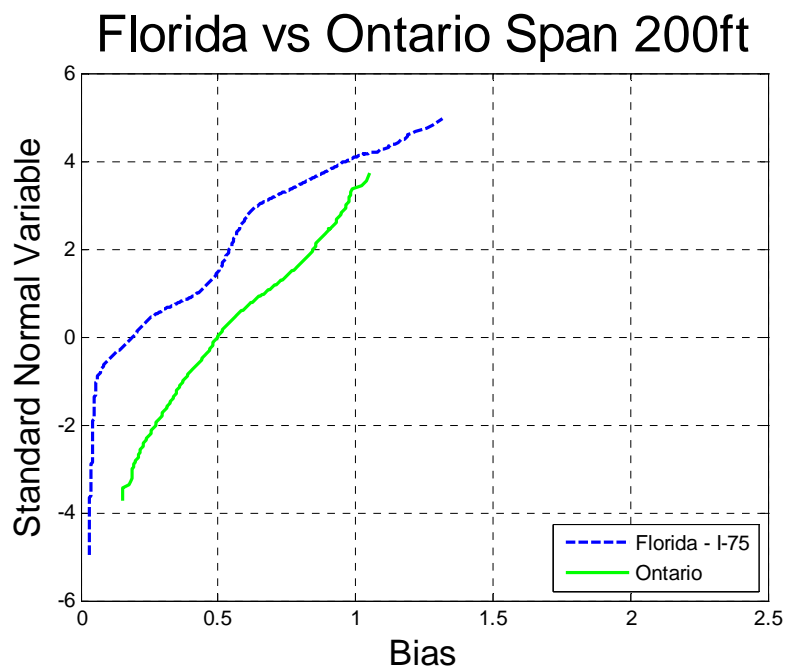


Figure 0-90 Comparison of Shear – Florida I-75 vs. Ontario – Span 200ft

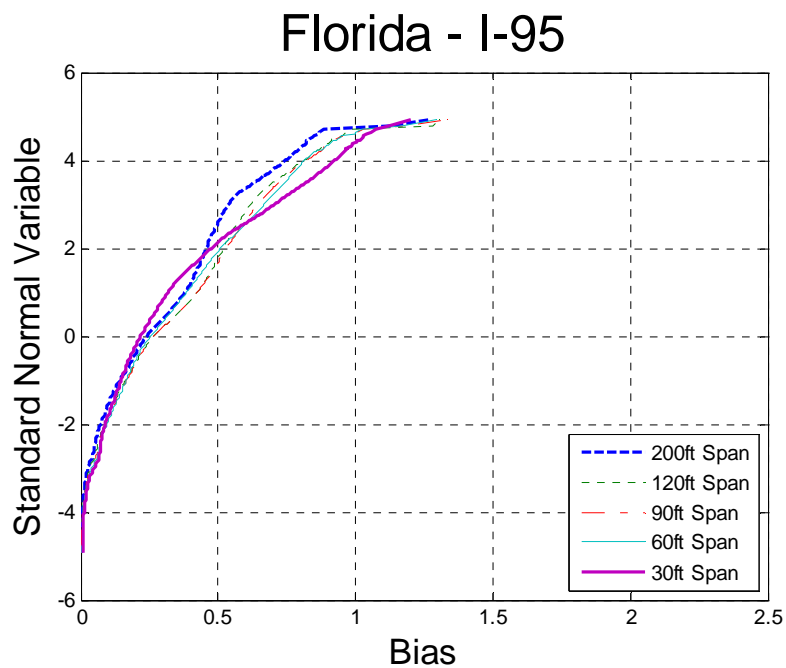


Figure 0-91 Cumulative Distribution Functions of Shear – Florida I-95

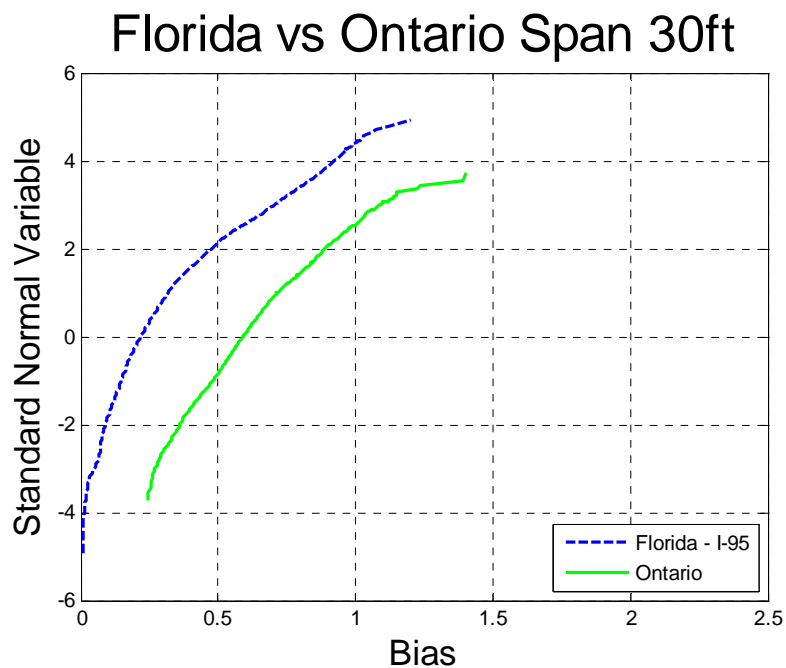


Figure 0-92 Comparison of Shear – Florida I-95 vs. Ontario – Span 30ft

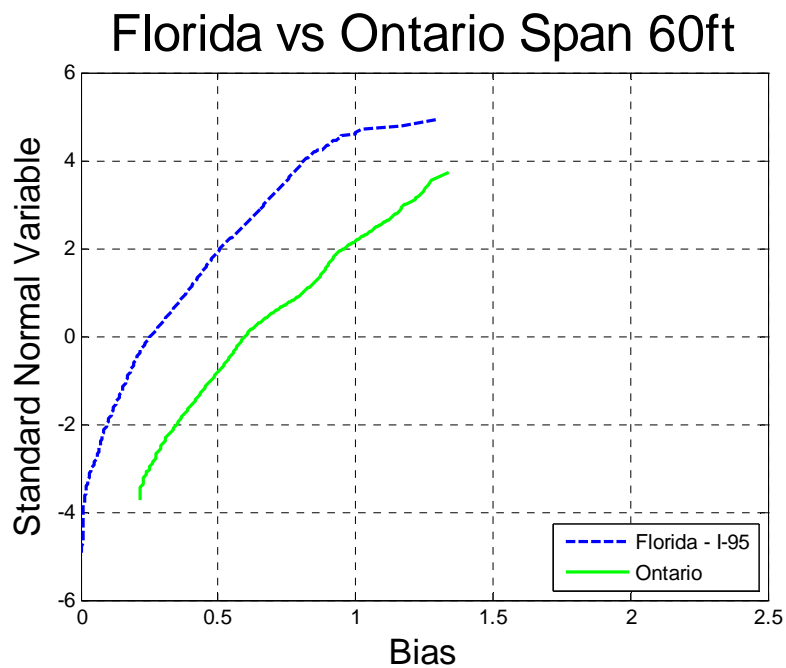


Figure 0-93 Comparison of Shear – Florida I-95 vs. Ontario – Span 60ft

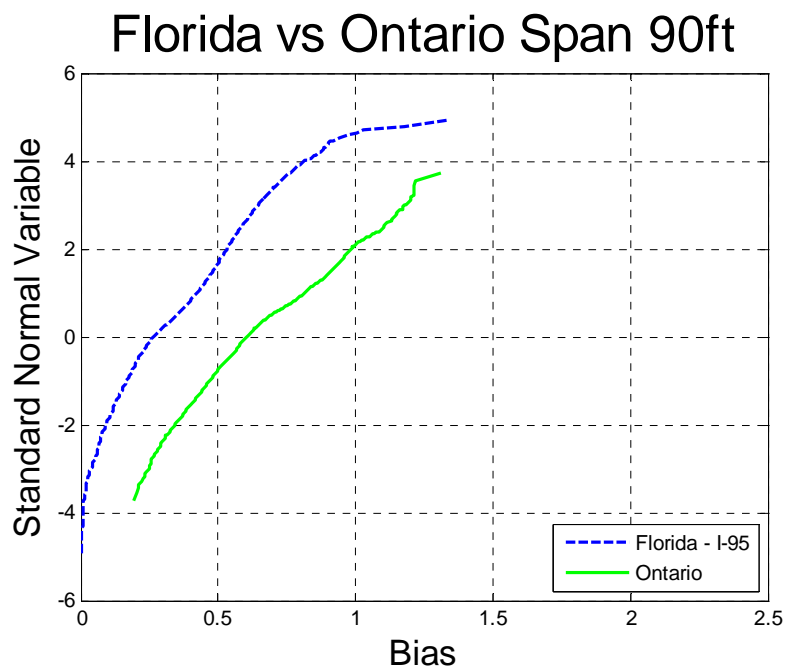


Figure 0-94 Comparison of Shear – Florida I-95 vs. Ontario – Span 90ft

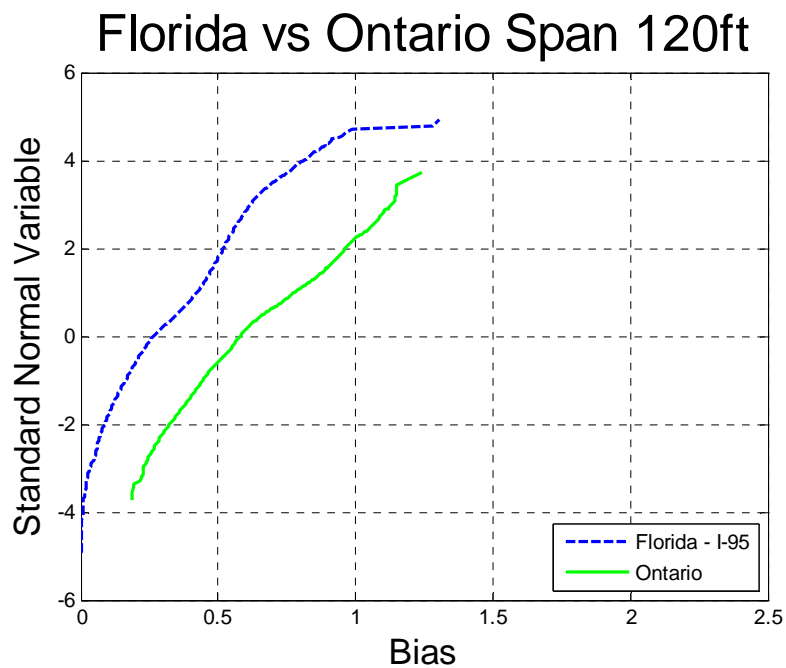


Figure 0-95 Comparison of Shear – Florida I-95 vs. Ontario – Span 120ft

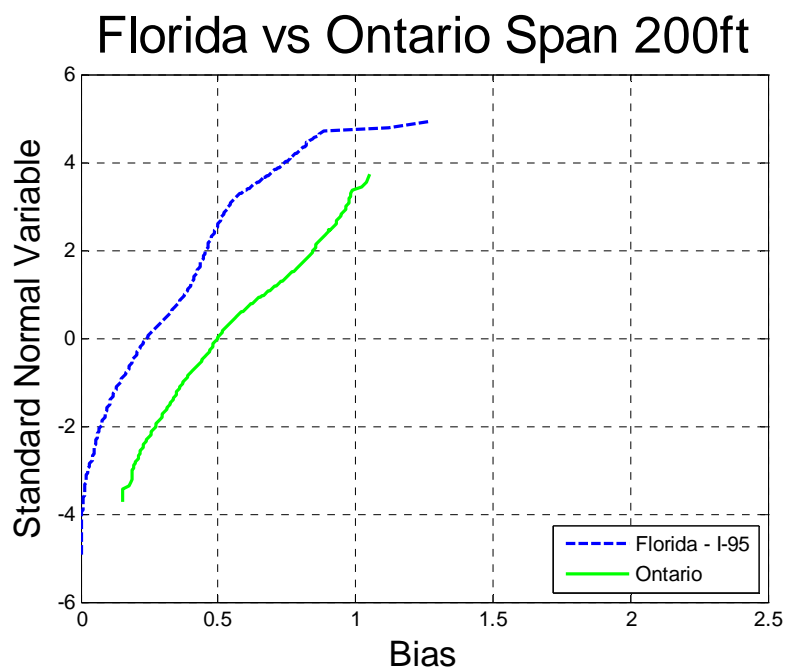


Figure 0-96 Comparison of Shear – Florida I-95 vs. Ontario – Span 200ft

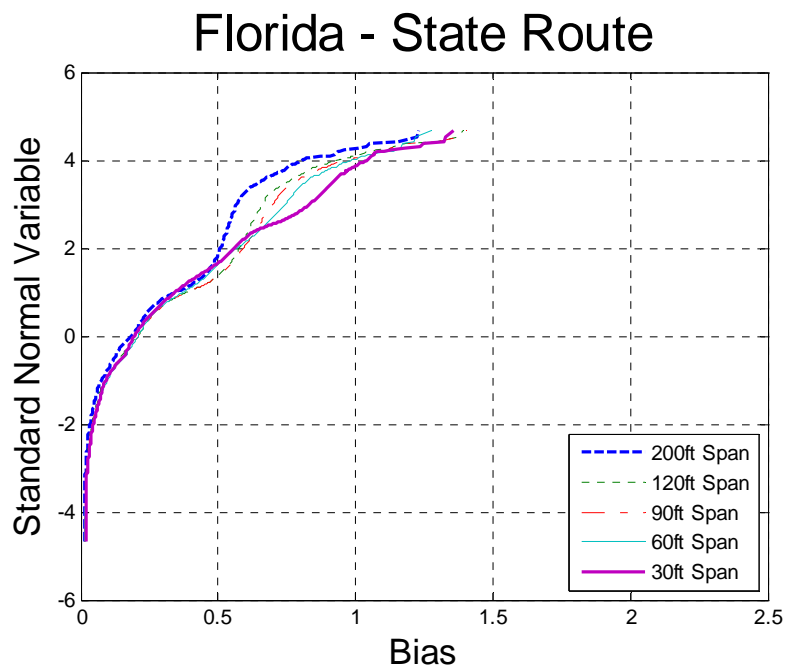


Figure 0-97 Cumulative Distribution Functions of Shear – Florida State Route

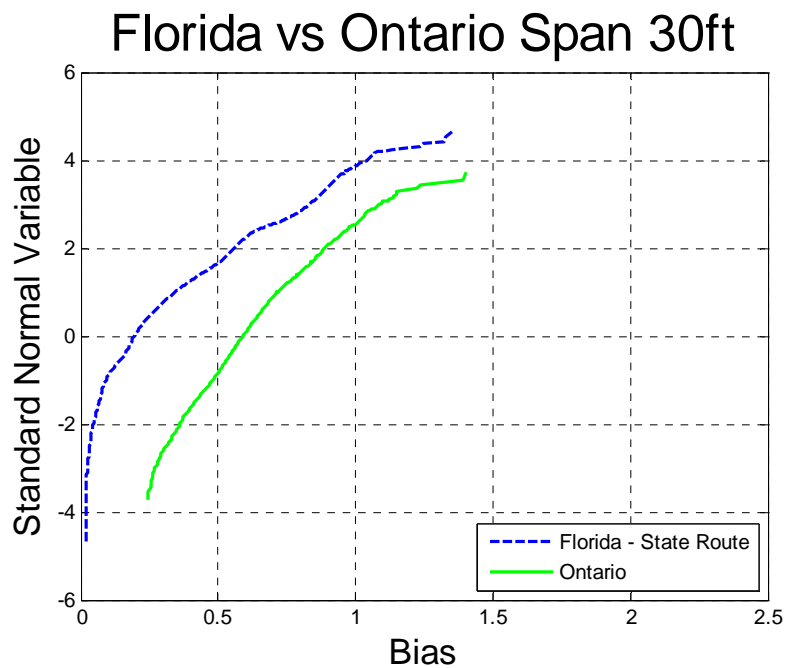


Figure 0-98 Comparison of Shear – Florida State Route vs. Ontario – Span 30ft

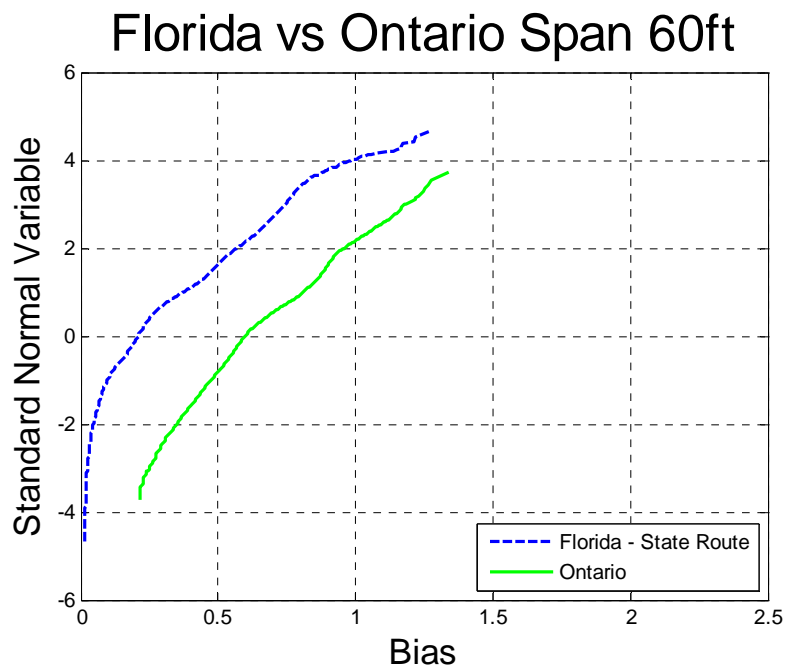


Figure 0-99 Comparison of Shear – Florida State Route vs. Ontario – Span 60ft

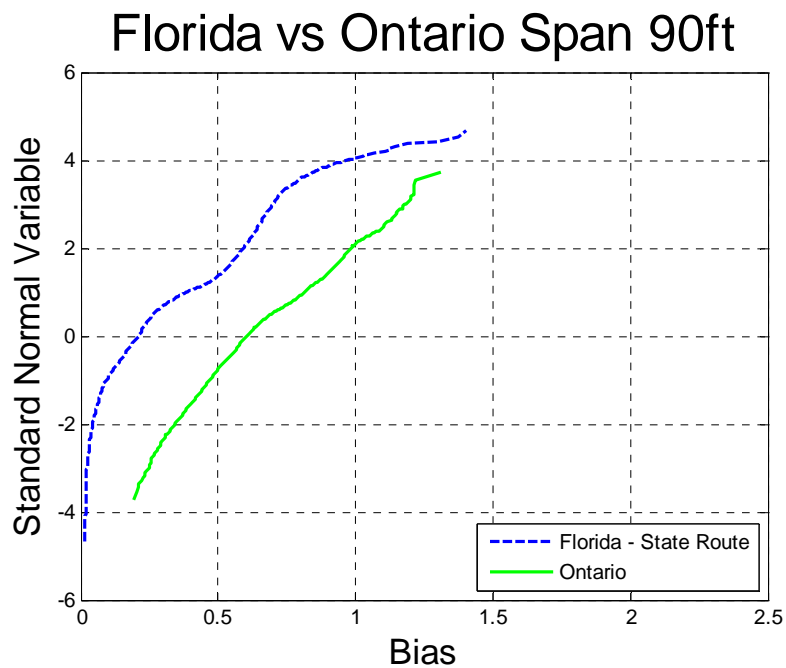


Figure 0-100 Comparison of Shear – Florida State Route vs. Ontario – Span 90ft

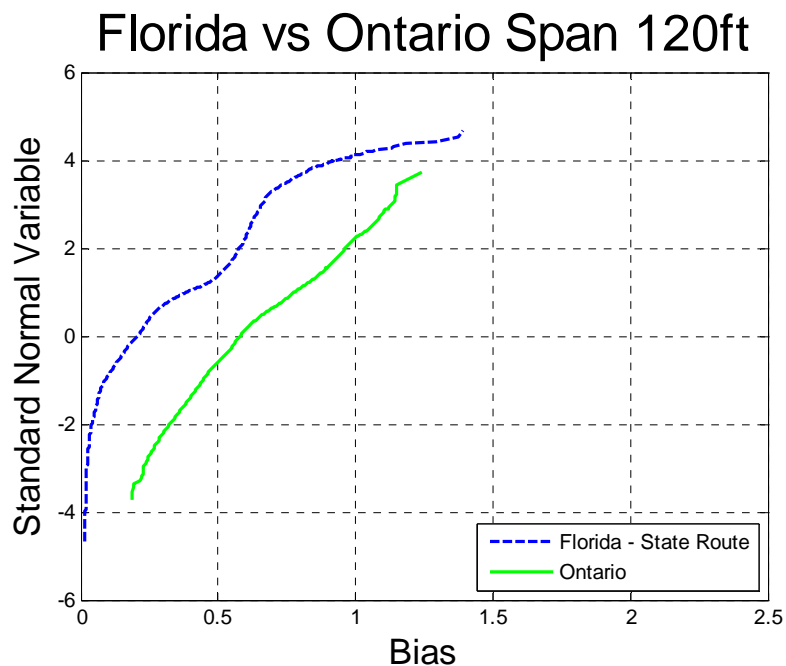


Figure 0-101 Comparison of Shear – Florida State Route vs. Ontario – Span 120ft

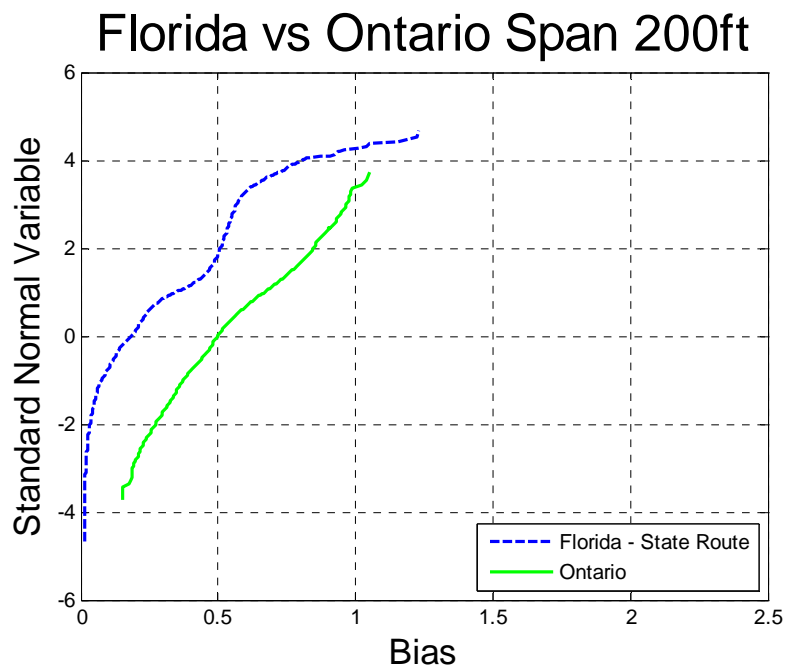


Figure 0-102 Comparison of Shear – Florida State Route vs. Ontario – Span 200ft

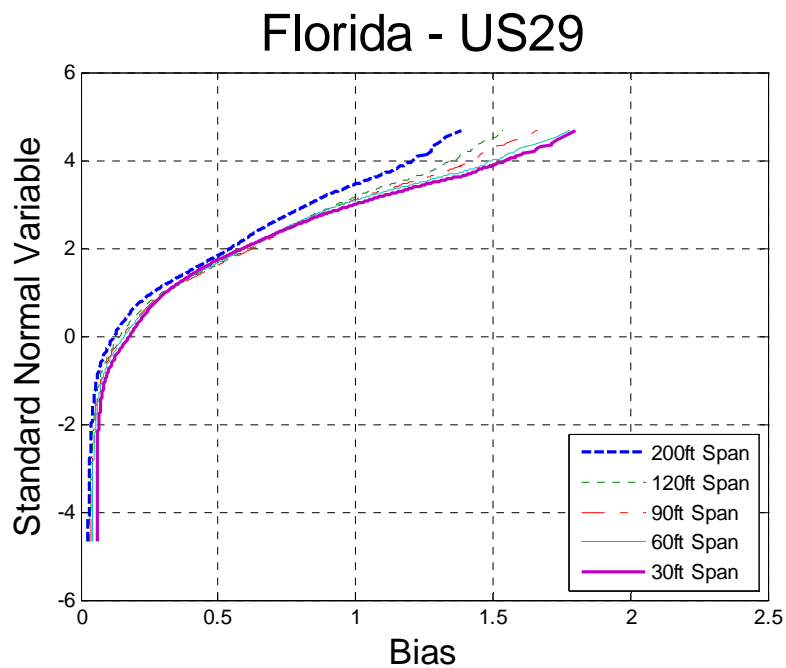


Figure 0-103 Cumulative Distribution Functions of Shear – Florida US29

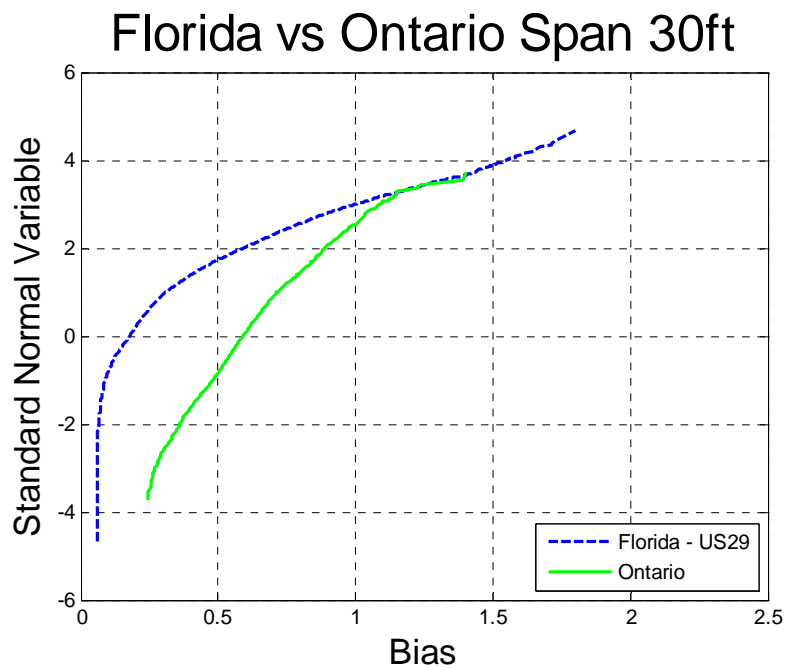


Figure 0-104 Comparison of Shear – Florida US29 vs. Ontario – Span 30ft

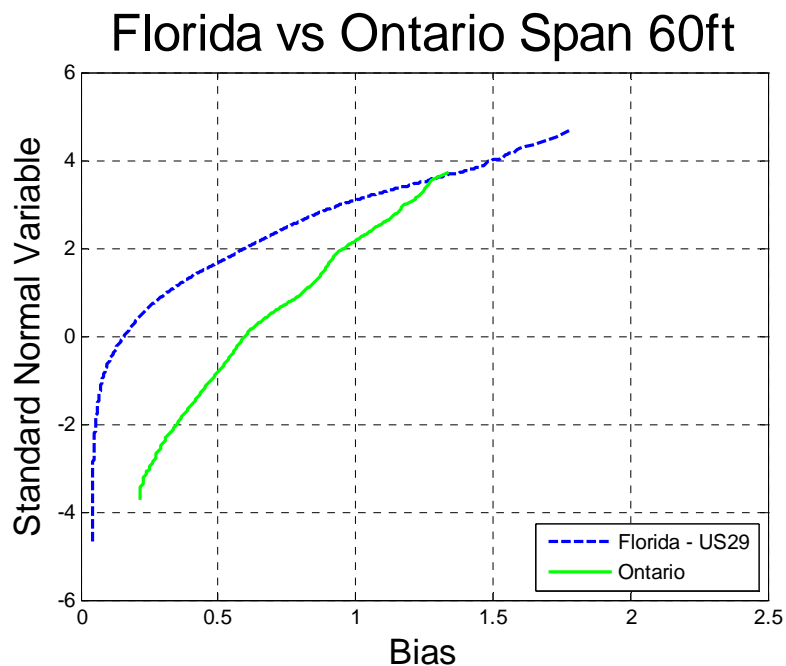


Figure 0-105 Comparison of Shear – Florida US29 vs. Ontario – Span 60ft

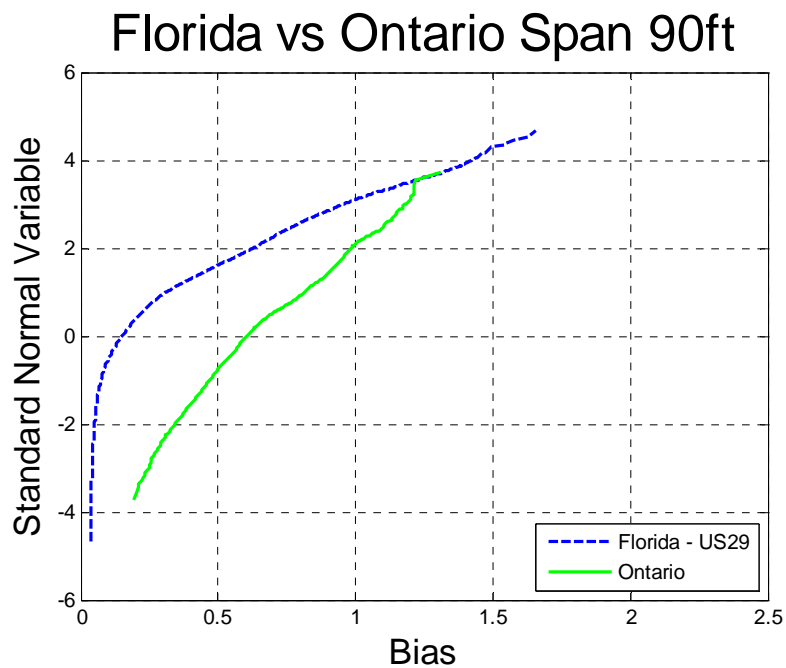


Figure 0-106 Comparison of Shear – Florida US29 vs. Ontario – Span 90ft

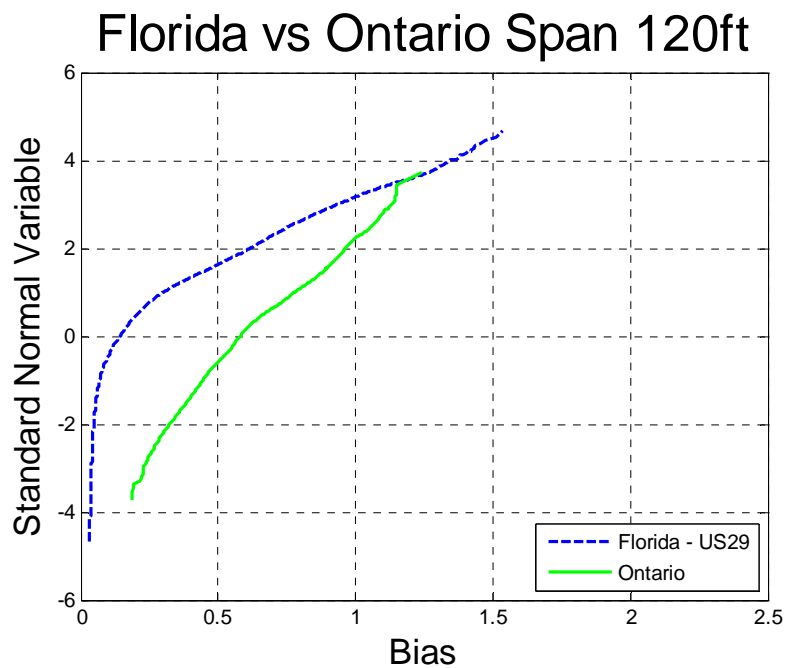


Figure 0-107 Comparison of Shear – Florida US29 vs. Ontario – Span 120ft

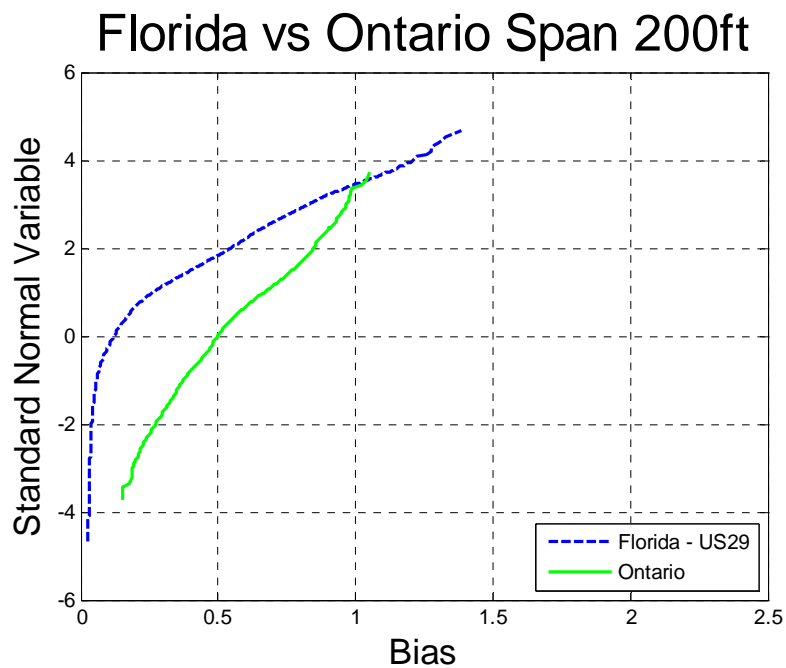


Figure 0-108 Comparison of Shear – Florida US29 vs. Ontario – Span 200ft

Indiana – Live Load Effect

WIM data for Indiana

The truck survey includes weigh-in-motion (WIM) truck measurements obtained from NCHRP project. The data includes 12 months of traffic recorded at different locations. The total number of records is shown in Table 60. The data includes number of axles, gross vehicle weight (GVW), weight per axle and spacing between axles.

Table 60

Site	Number of Trucks
Site 9511	4,511,842
Site 9512	2,092,181
Site 9532	783,352
Site 9534	5,351,423
Site 9552	252,315
TOTAL	12,991,113

Maximum Simple Span Moments

The maximum moment was calculated for each truck from the data. Analysis included simple spans with the span varying from 30 to 200 ft. The maximum moment was also calculated for the HL93 load and Tandem. Ratio between data truck moment and code load moment was plotted on the probability paper.

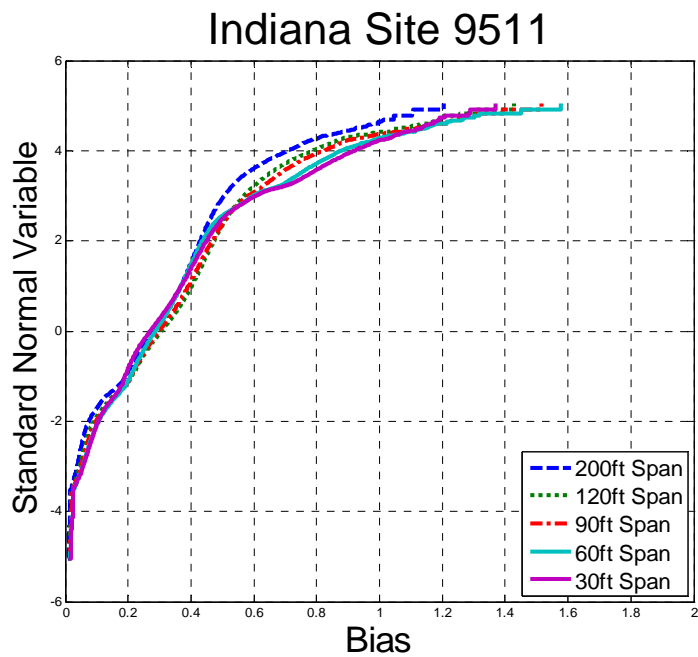


Figure 0-109 Cumulative Distribution Functions of Simple Span Moment– Indiana Site

9511

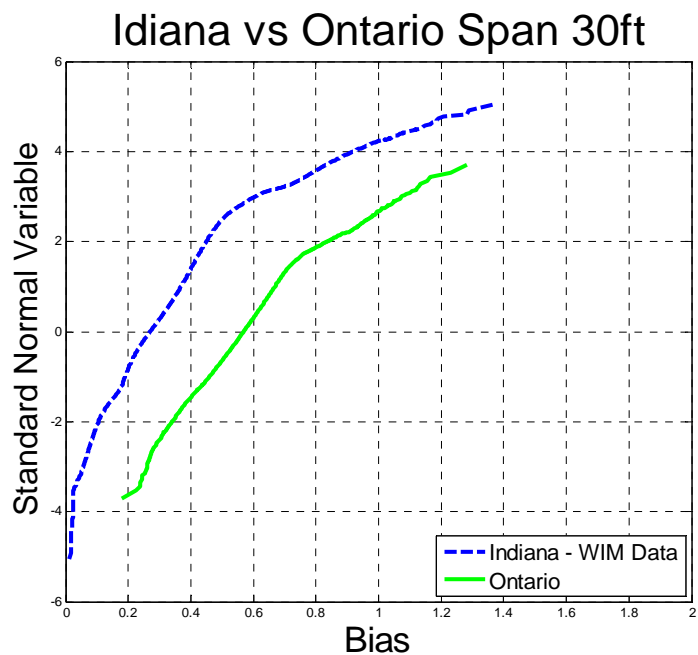


Figure 0-110 Comparison of Simple Span Moment – Indiana Site 9511 vs. Ontario –
Span 30ft

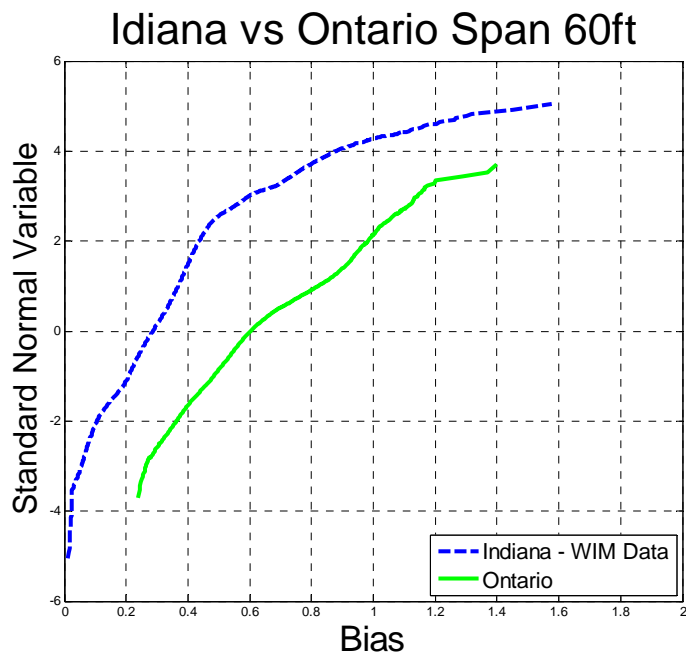


Figure 0-111 Comparison of Simple Span Moment – Indiana Site 9511 vs. Ontario –
Span 60ft

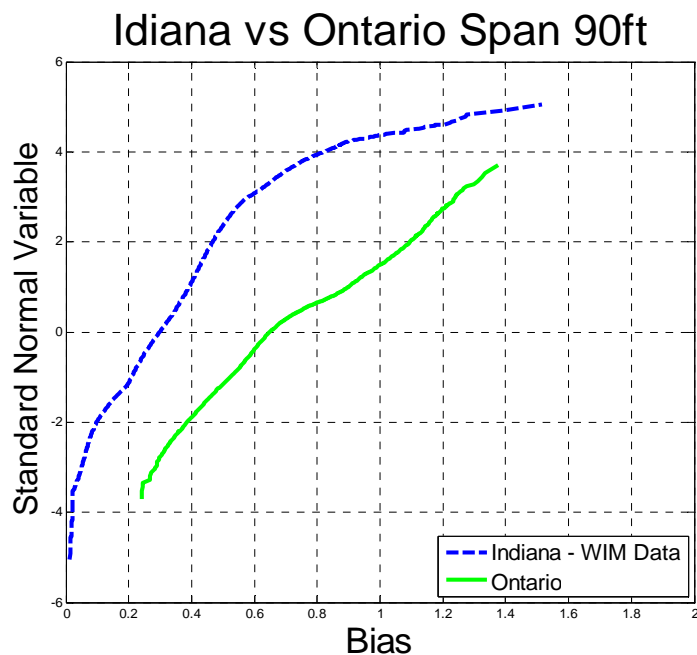


Figure 0-112 Comparison of Simple Span Moment – Indiana Site 9511 vs. Ontario –
Span 90ft

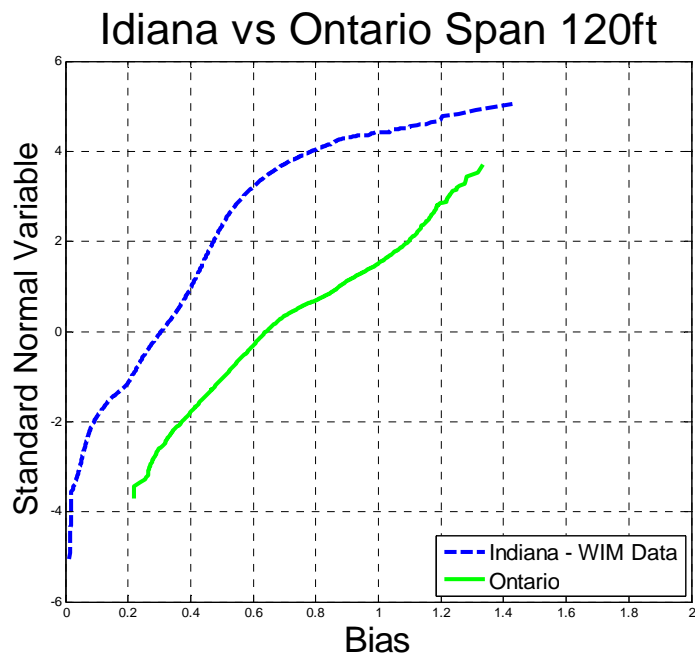


Figure 0-113 Comparison of Simple Span Moment – Indiana Site 9511 vs. Ontario –
Span 120ft

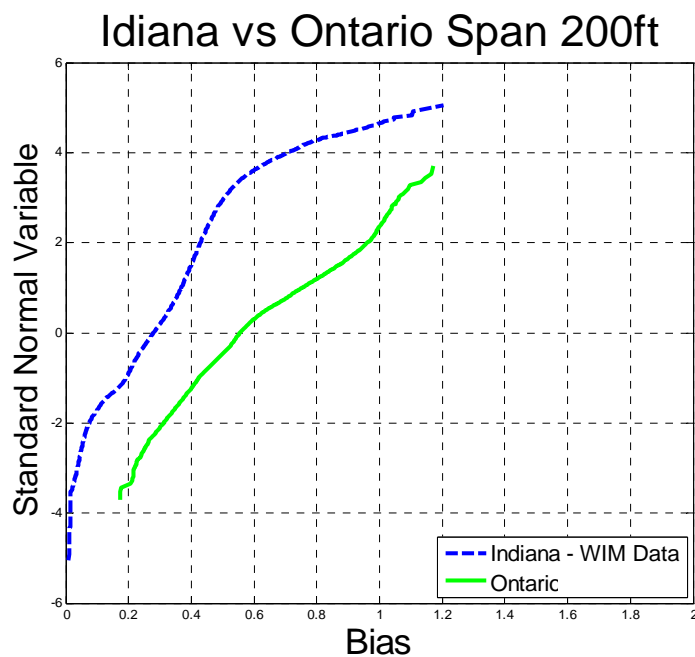


Figure 0-114 Comparison of Simple Span Moment – Indiana Site 9511 vs. Ontario –
Span 200ft

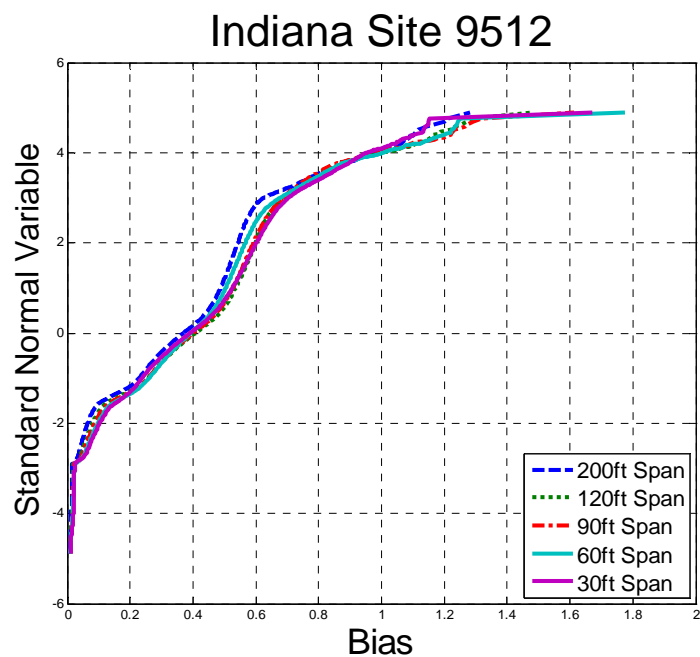


Figure 0-115 Cumulative Distribution Functions of Simple Span Moment– Indiana Site 9512

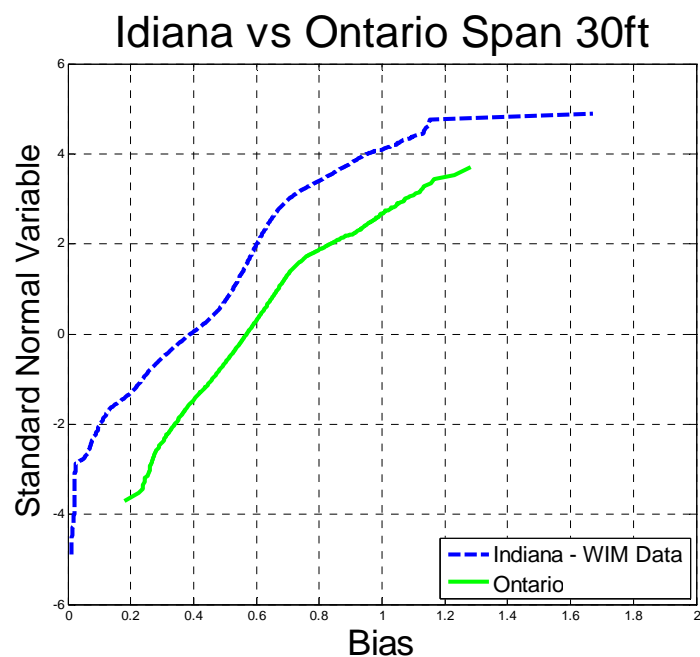


Figure 0-116 Comparison of Simple Span Moment – Indiana Site 9512 vs. Ontario – Span 30ft

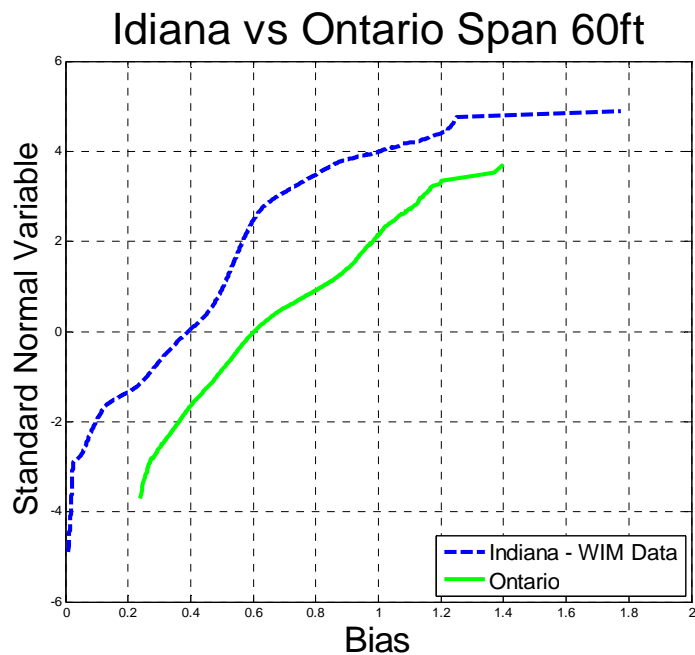


Figure 0-117 Comparison of Simple Span Moment – Indiana Site 9512 vs. Ontario –
Span 60ft

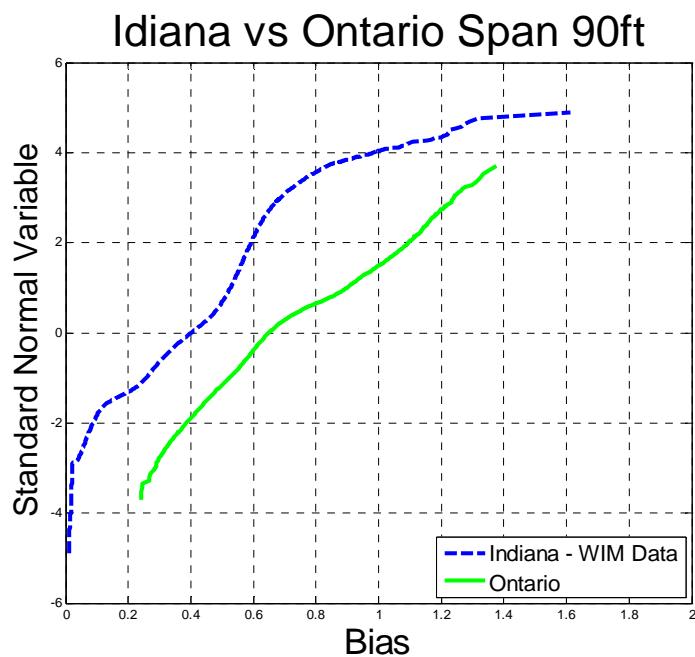


Figure 0-118 Comparison of Simple Span Moment – Indiana Site 9512 vs. Ontario –
Span 90ft

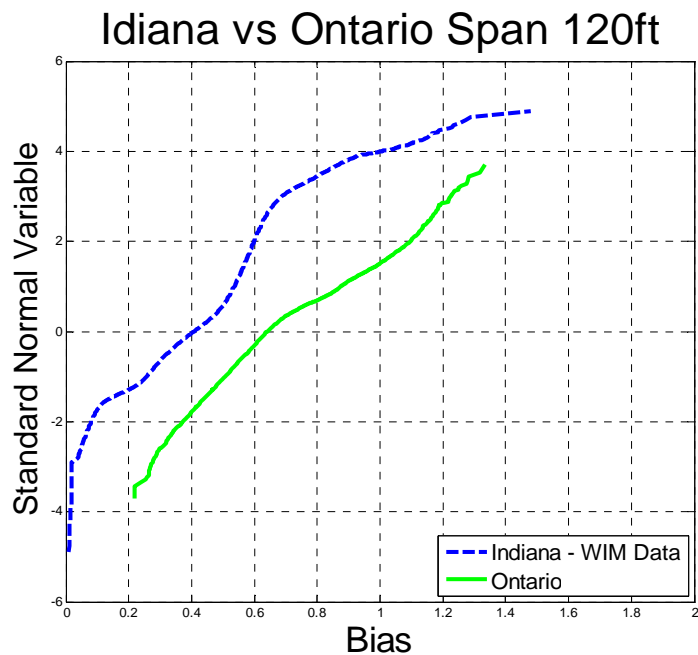


Figure 0-119 Comparison of Simple Span Moment – Indiana Site 9512 vs. Ontario –
Span 120ft

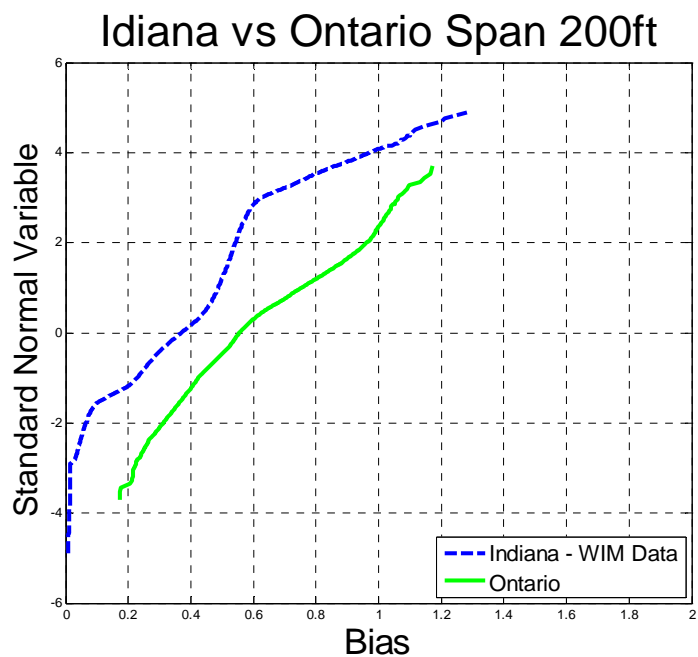


Figure 0-120 Comparison of Simple Span Moment – Indiana Site 9512 vs. Ontario –
Span 200ft

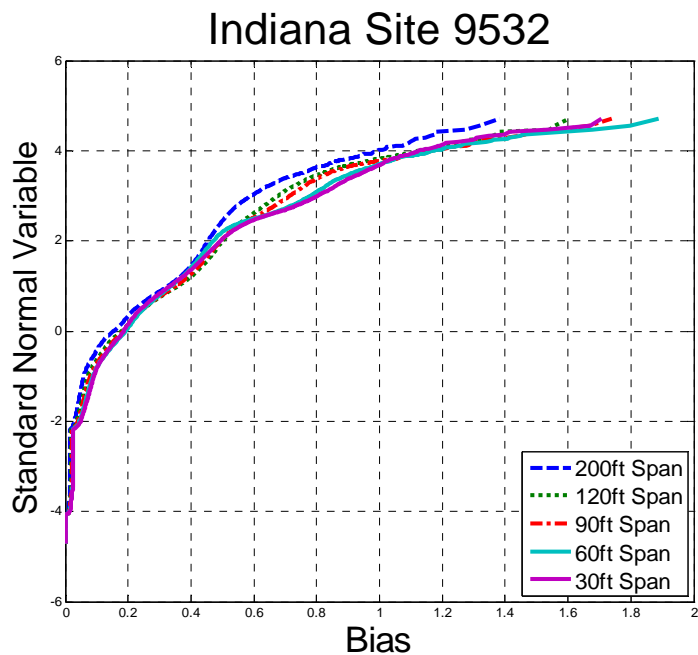


Figure 0-121 Cumulative Distribution Functions of Simple Span Moment– Indiana Site 9532

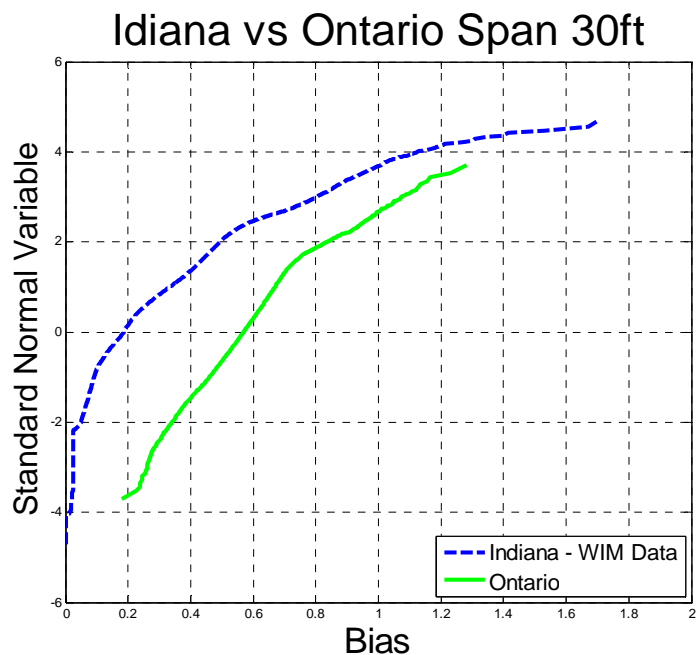


Figure 0-122 Comparison of Simple Span Moment – Indiana Site 9532 vs. Ontario – Span 30ft

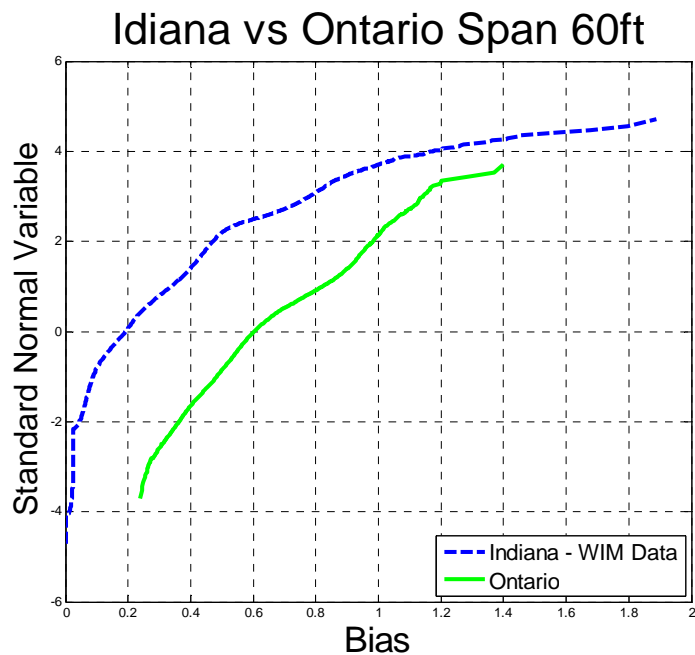


Figure 0-123 Comparison of Simple Span Moment – Indiana Site 9532 vs. Ontario – Span 60ft

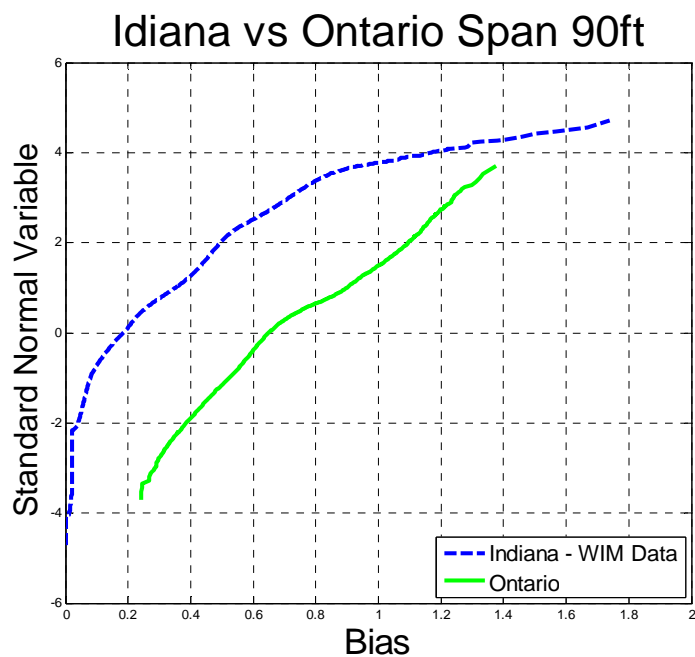


Figure 0-124 Comparison of Simple Span Moment – Indiana Site 9532 vs. Ontario – Span 90ft

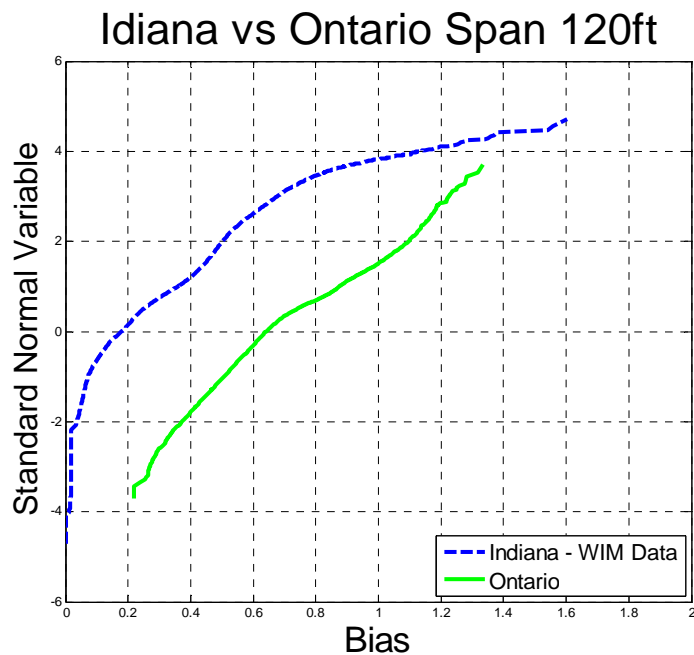


Figure 0-125 Comparison of Simple Span Moment – Indiana Site 9532 vs. Ontario –
Span 120ft

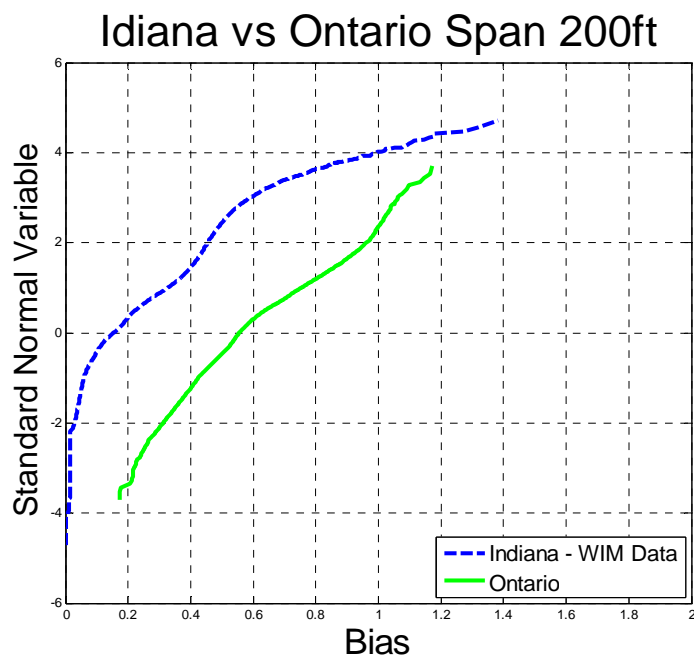


Figure 0-126 Comparison of Simple Span Moment – Indiana Site 9532 vs. Ontario –
Span 200ft

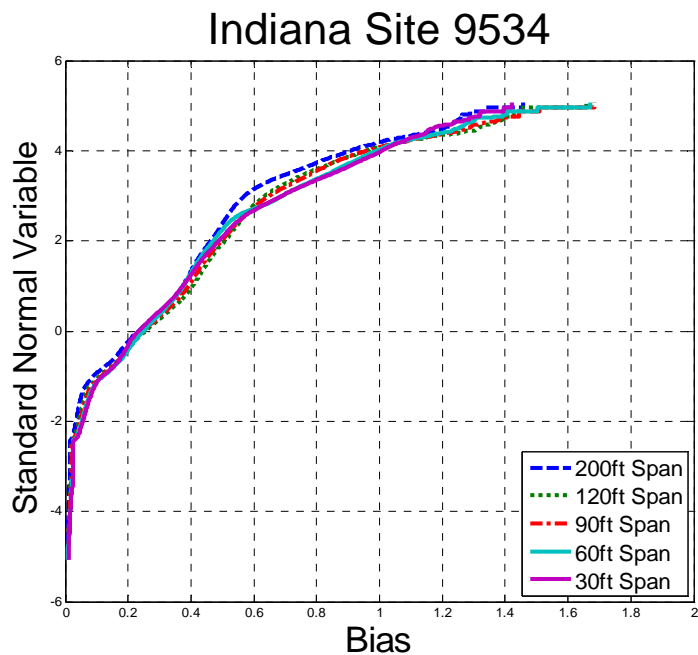


Figure 0-127 Cumulative Distribution Functions of Simple Span Moment– Indiana Site 9534

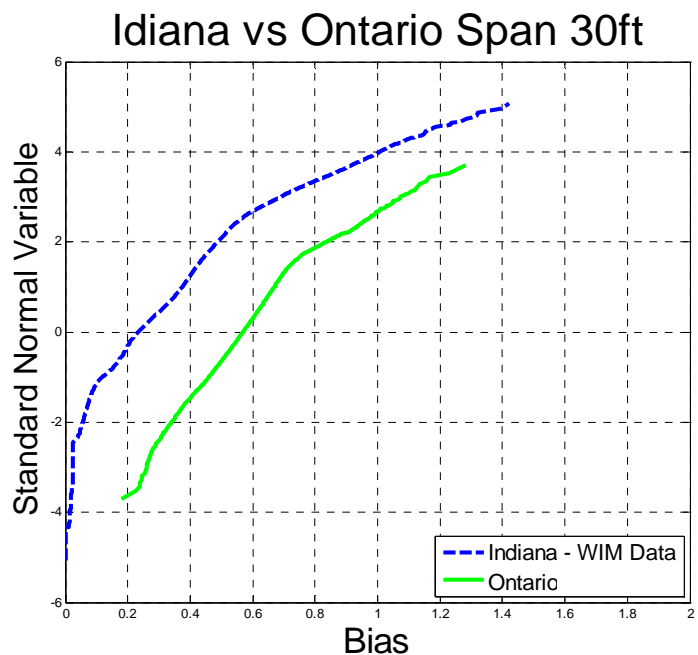


Figure 0-128 Comparison of Simple Span Moment – Indiana Site 9534 vs. Ontario – Span 30ft

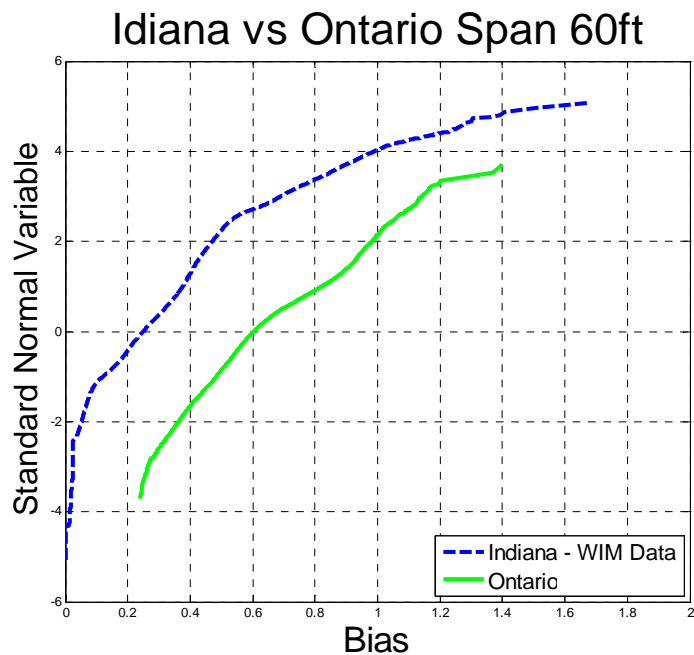


Figure 0-129 Comparison of Simple Span Moment – Indiana Site 9534 vs. Ontario –
Span 60ft

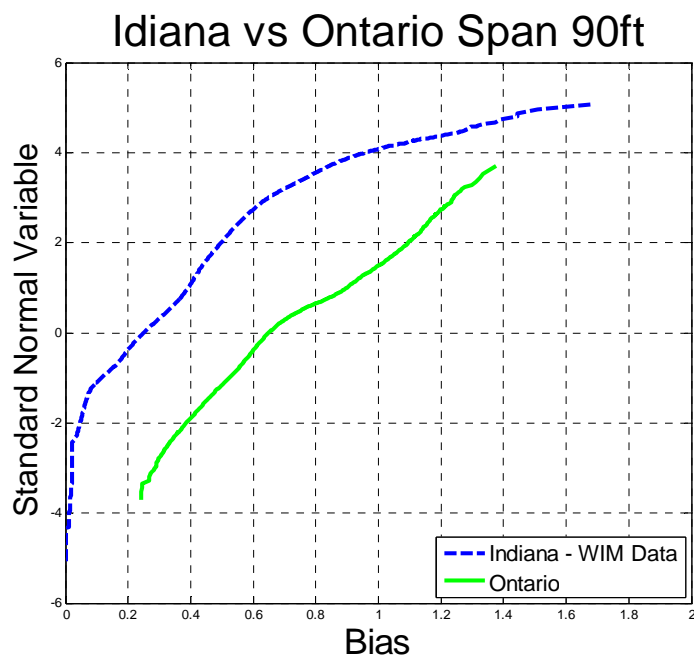


Figure 0-130 Comparison of Simple Span Moment – Indiana Site 9534 vs. Ontario –
Span 90ft

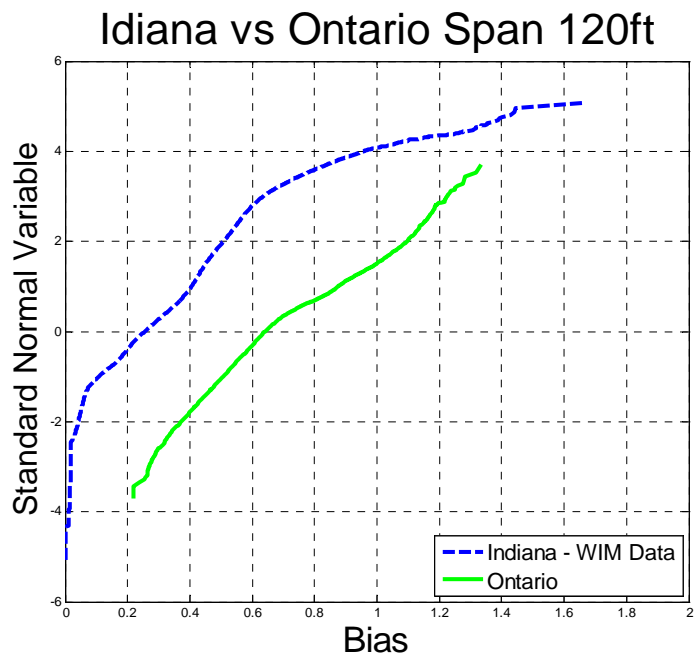


Figure 0-131 Comparison of Simple Span Moment – Indiana Site 9534 vs. Ontario –
Span 120ft

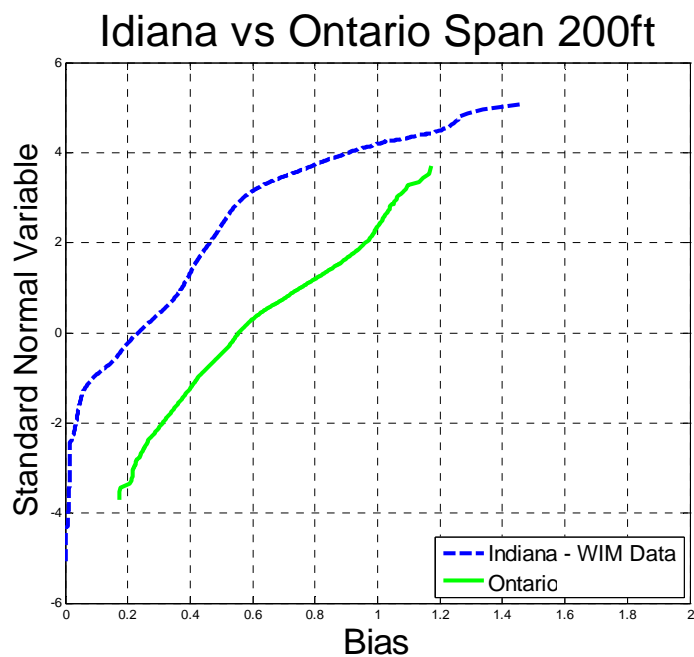


Figure 0-132 Comparison of Simple Span Moment – Indiana Site 9534 vs. Ontario –
Span 200ft

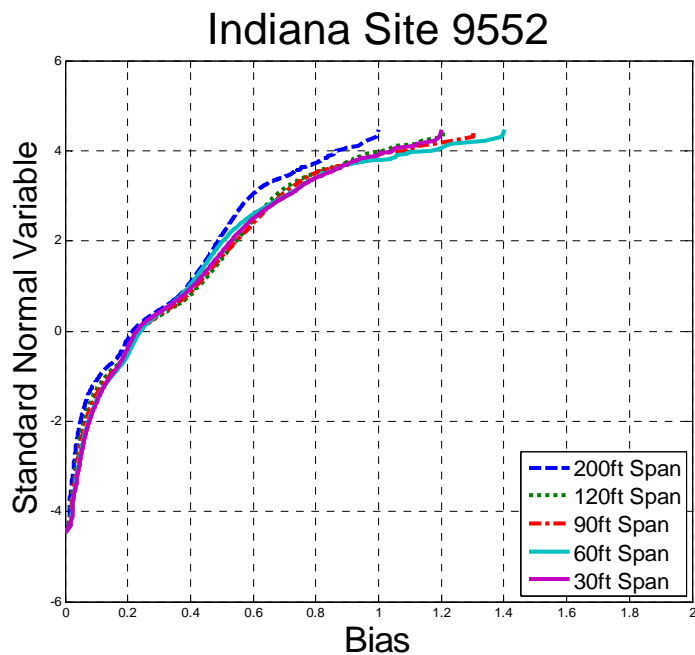


Figure 0-133 Cumulative Distribution Functions of Simple Span Moment– Indiana Site 9552

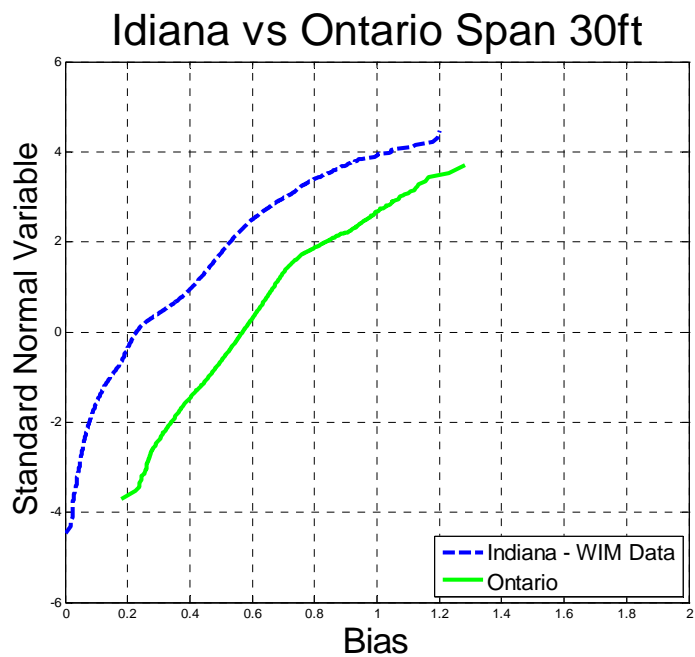


Figure 0-134 Comparison of Simple Span Moment – Indiana Site 9552 vs. Ontario – Span 30ft

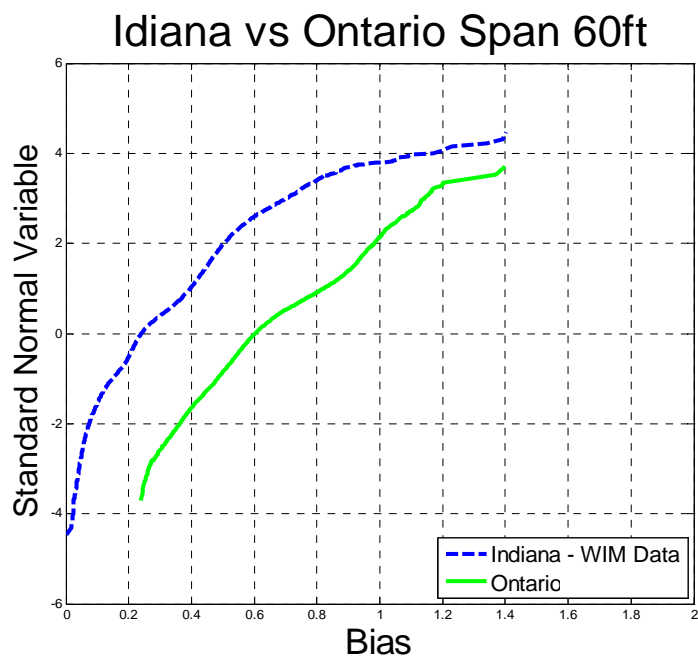


Figure 0-135 Comparison of Simple Span Moment – Indiana Site 9552 vs. Ontario –
Span 60ft

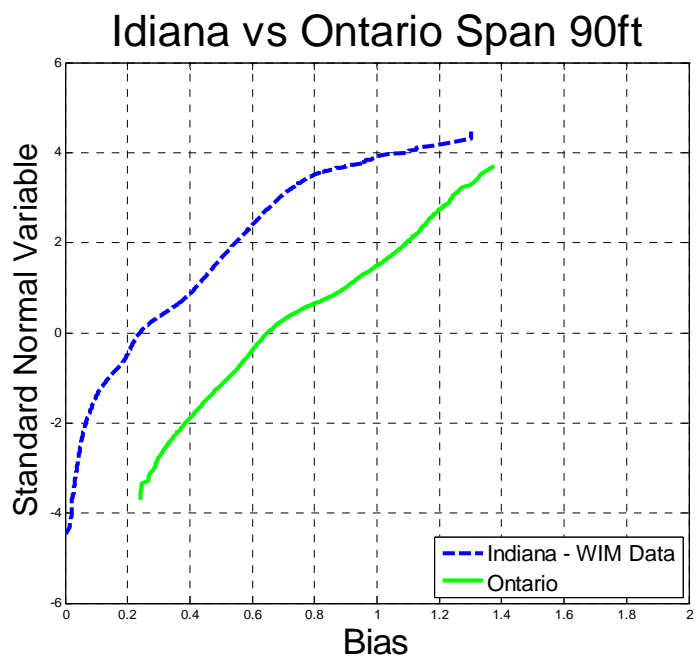


Figure 0-136 Comparison of Simple Span Moment – Indiana Site 9552 vs. Ontario –
Span 90ft

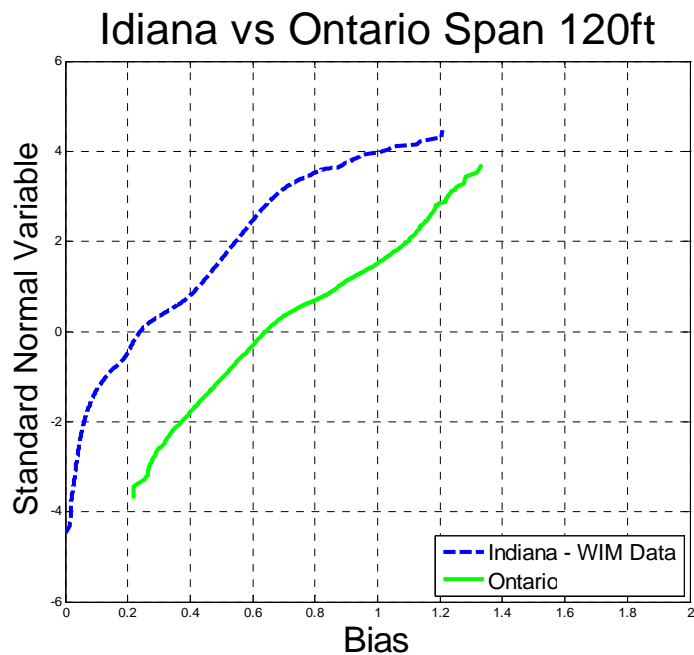


Figure 0-137 Comparison of Simple Span Moment – Indiana Site 9552 vs. Ontario –
Span 120ft

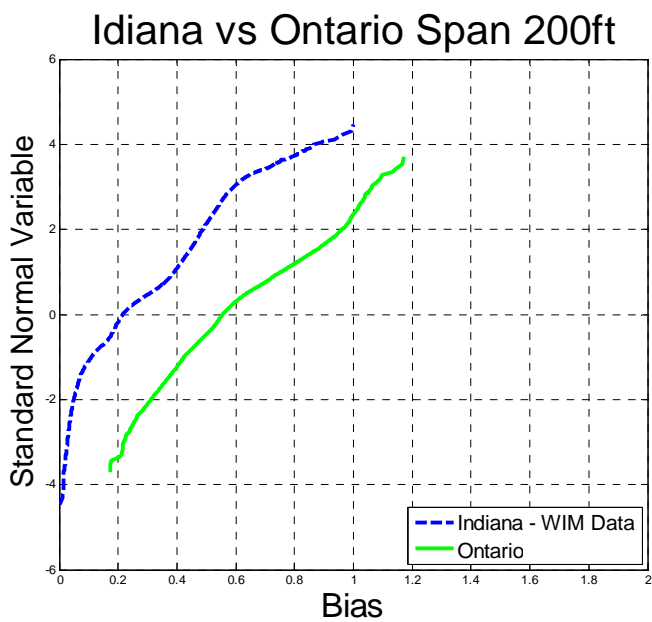


Figure 0-138 Comparison of Simple Span Moment – Indiana Site 9552 vs. Ontario –
Span 200ft

Maximum Shear

The maximum shear was calculated for each truck from the data. Analysis included simple spans with the span varying from 30 to 200 ft. The ratio of shear obtained from the data truck and the HL-93 load was plotted on the probability paper.

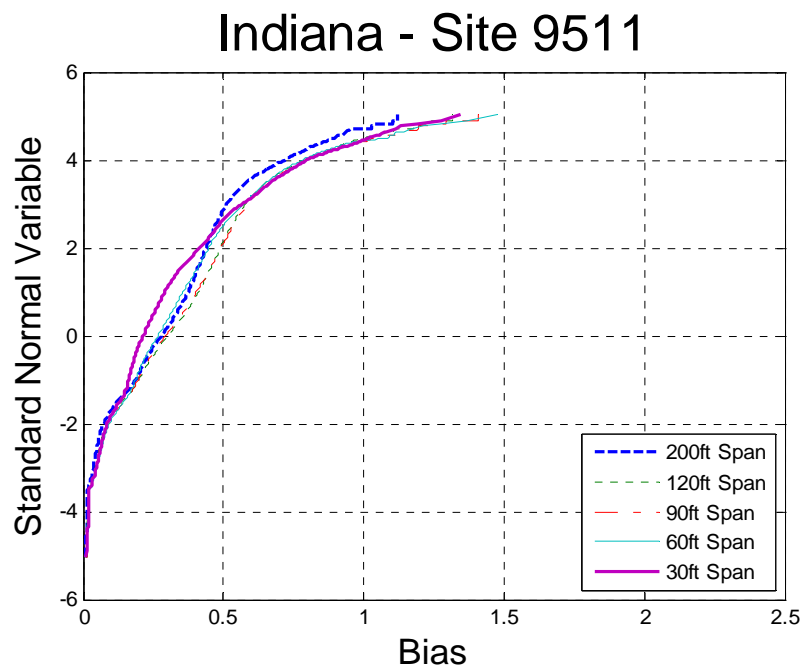


Figure 0-139 Cumulative Distribution Functions of Shear – Indiana Site 9511

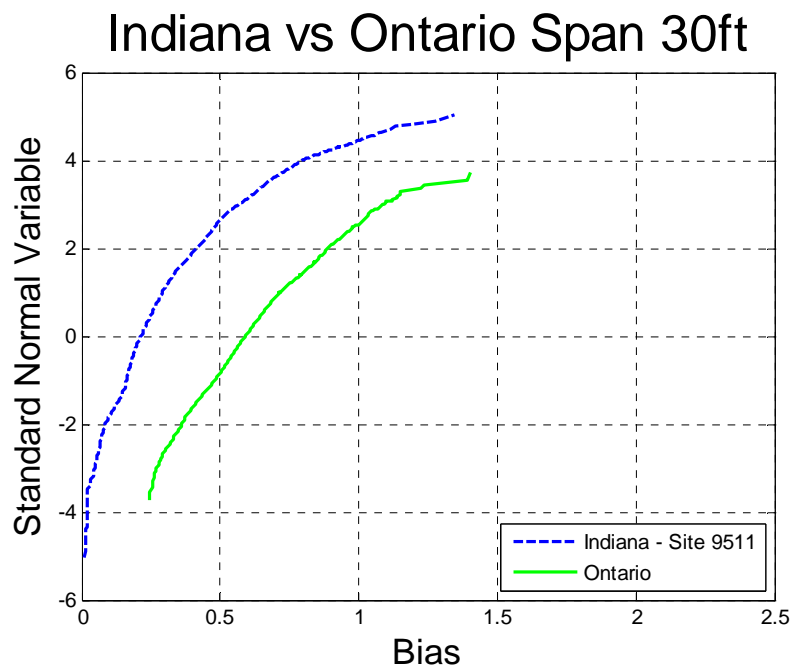


Figure 0-140 Comparison of Shear – Indiana Site 9511 vs. Ontario – Span 30ft

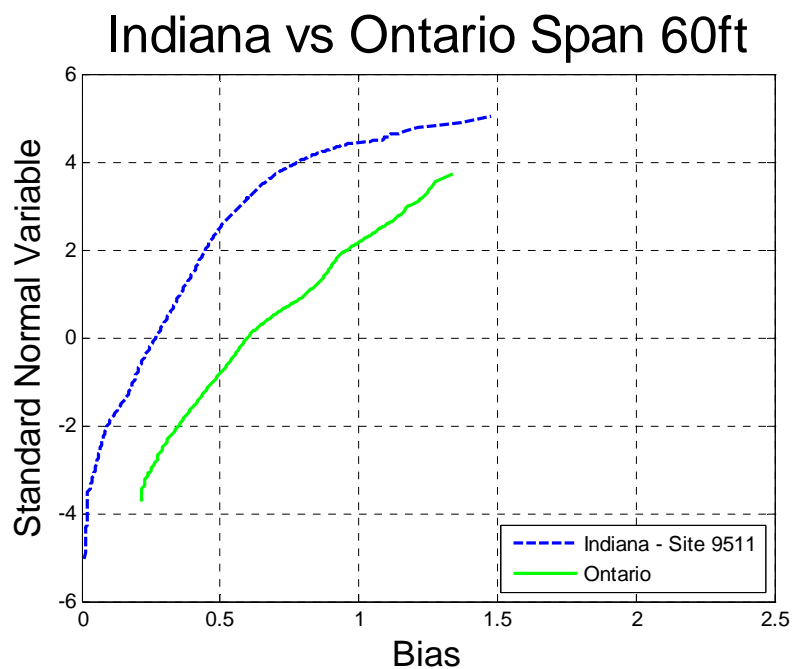


Figure 0-141 Comparison of Shear – Indiana Site 9511 vs. Ontario – Span 60ft

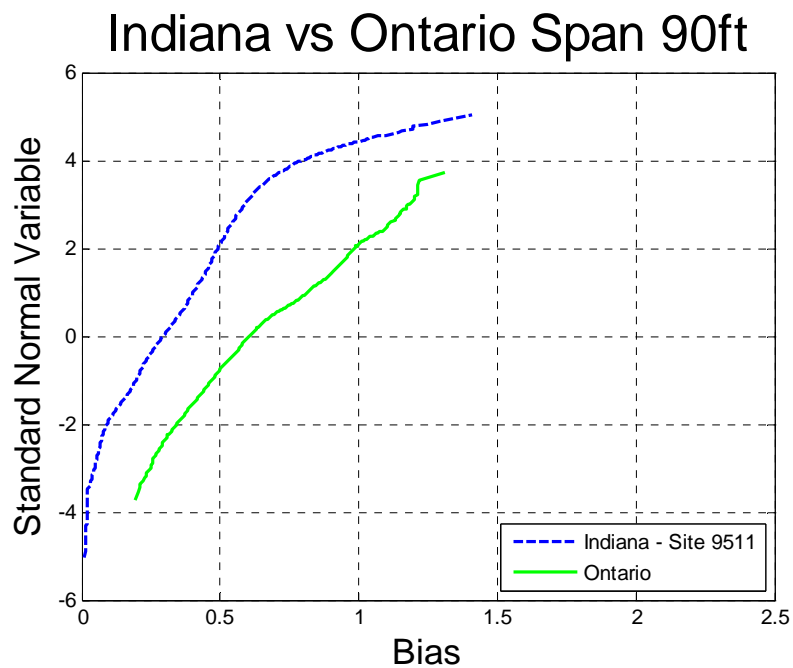


Figure 0-142 Comparison of Shear – Indiana Site 9511 vs. Ontario – Span 90ft

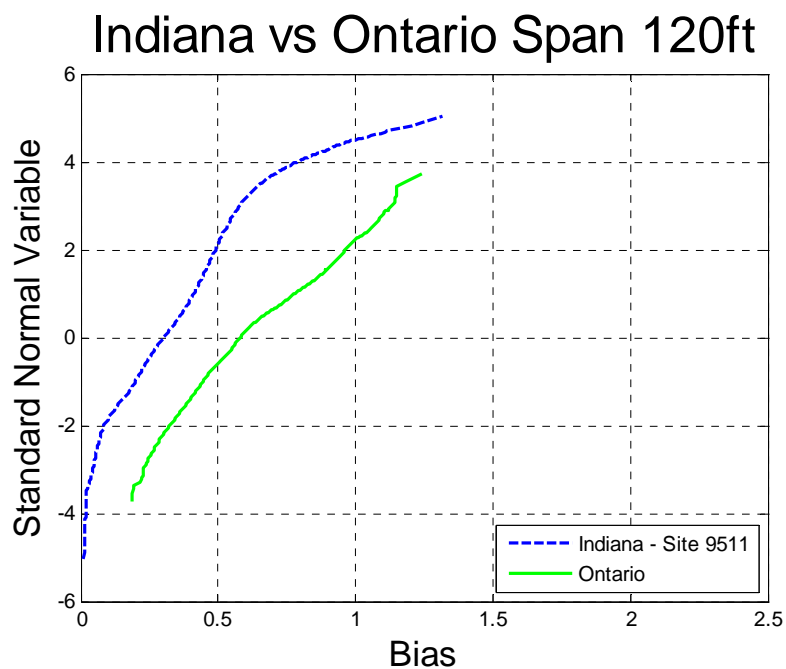


Figure 0-143 Comparison of Shear – Indiana Site 9511 vs. Ontario – Span 120ft

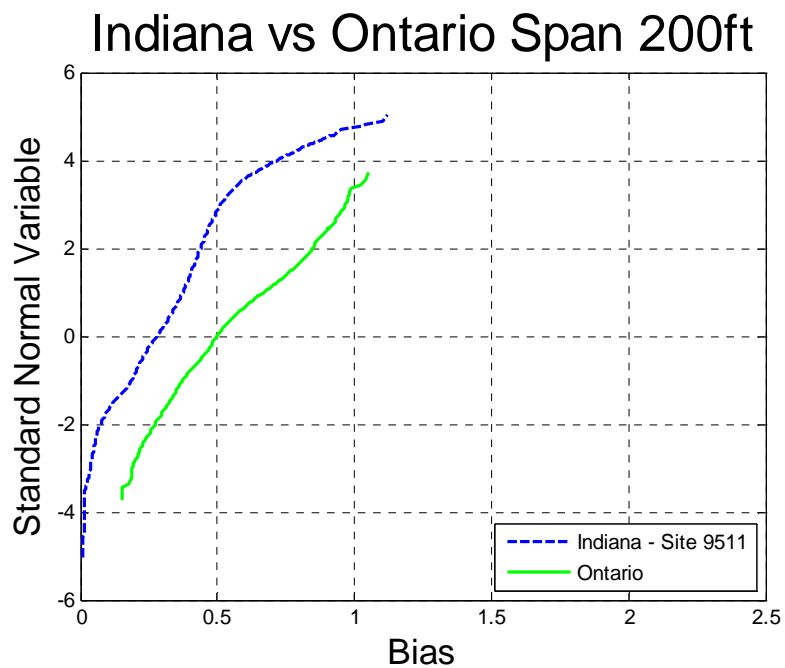


Figure 0-144 Comparison of Shear – Indiana Site 9511 vs. Ontario – Span 200ft

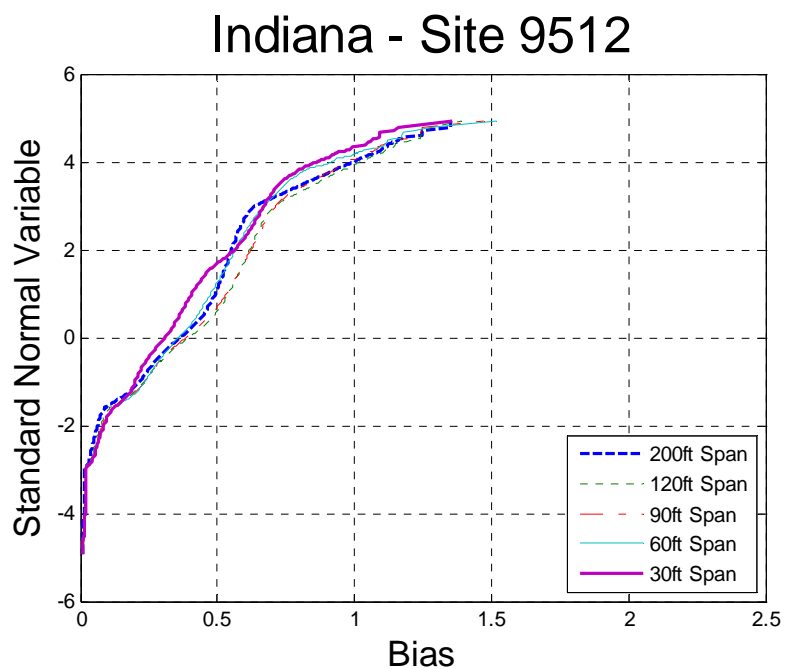


Figure 0-145 Cumulative Distribution Functions of Shear – Indiana Site 9512

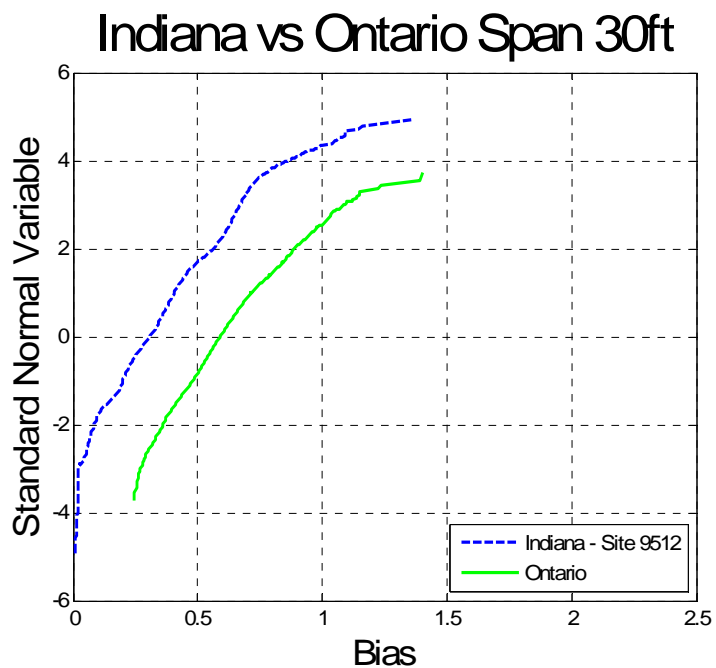


Figure 0-146 Comparison of Shear – Indiana Site 9512 vs. Ontario – Span 30ft

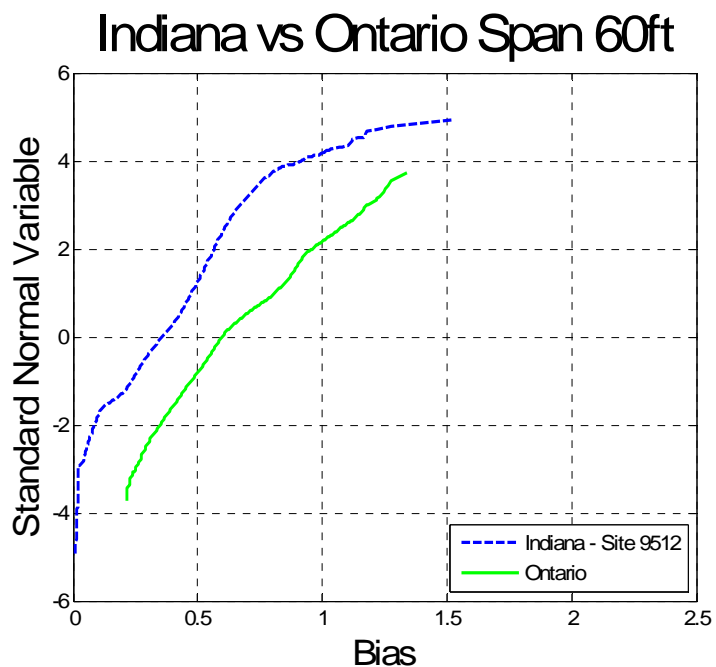


Figure 0-147 Comparison of Shear – Indiana Site 9512 vs. Ontario – Span 60ft

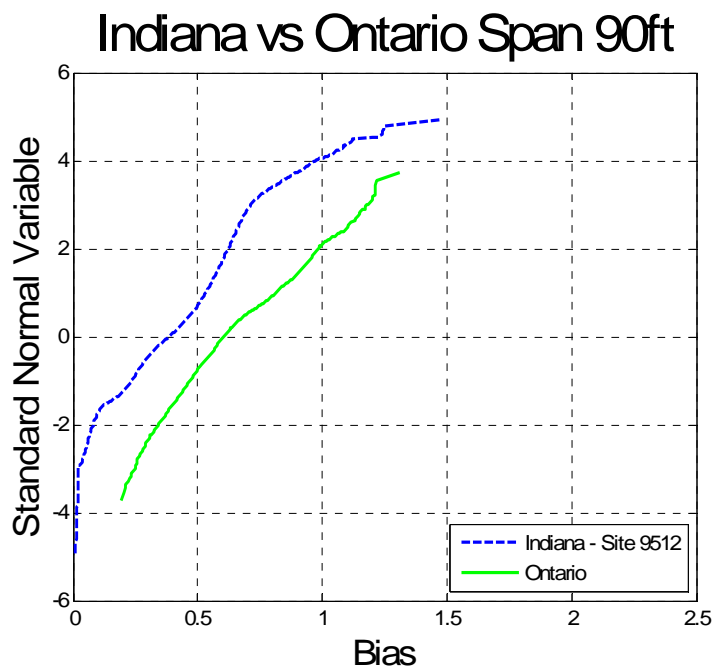


Figure 0-148 Comparison of Shear – Indiana Site 9512 vs. Ontario – Span 90ft

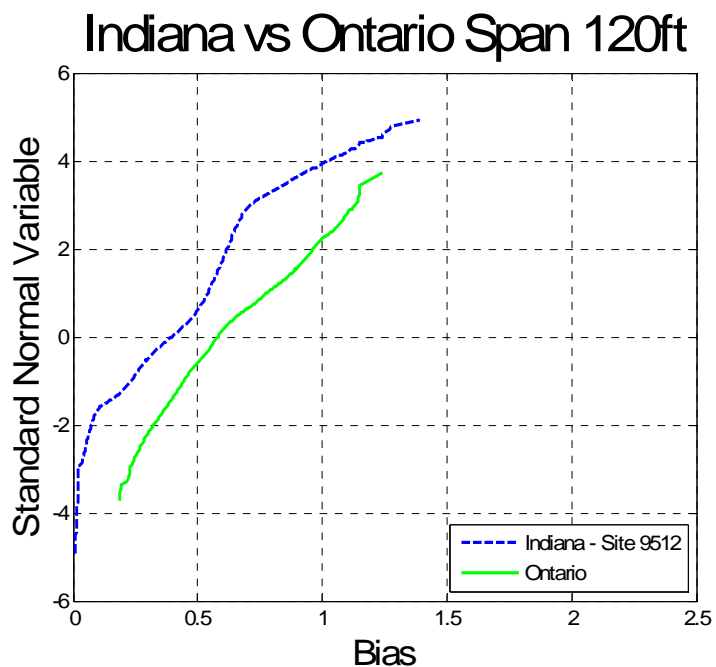


Figure 0-149 Comparison of Shear – Indiana Site 9512 vs. Ontario – Span 120ft

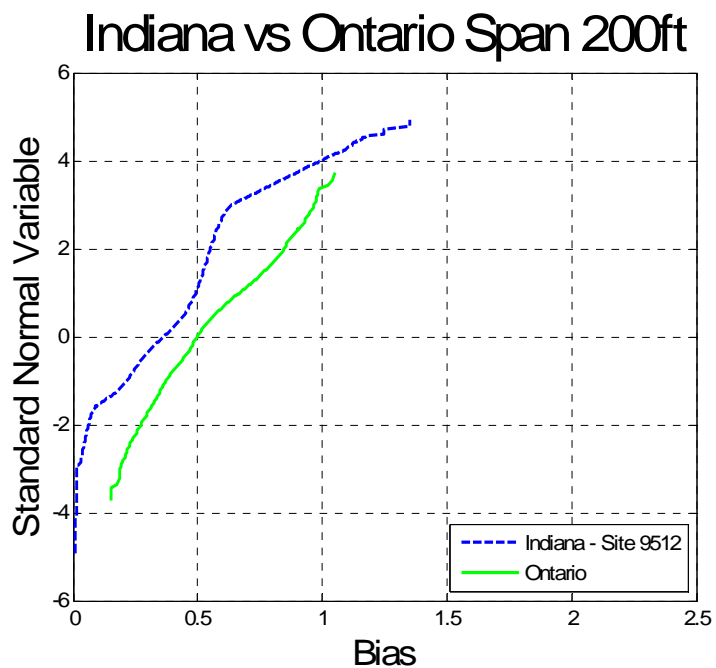


Figure 0-150 Comparison of Shear – Indiana Site 9512 vs. Ontario – Span 200ft

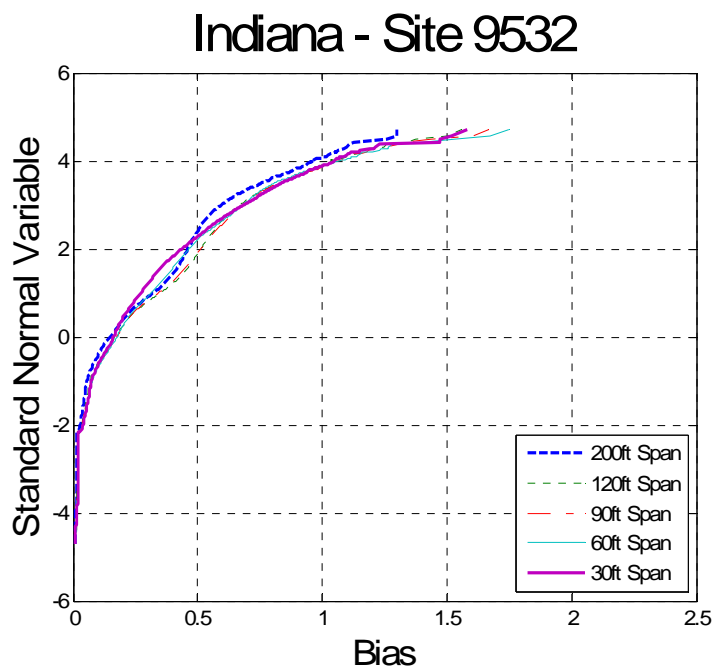


Figure 0-151 Cumulative Distribution Functions of Shear – Indiana Site 9532

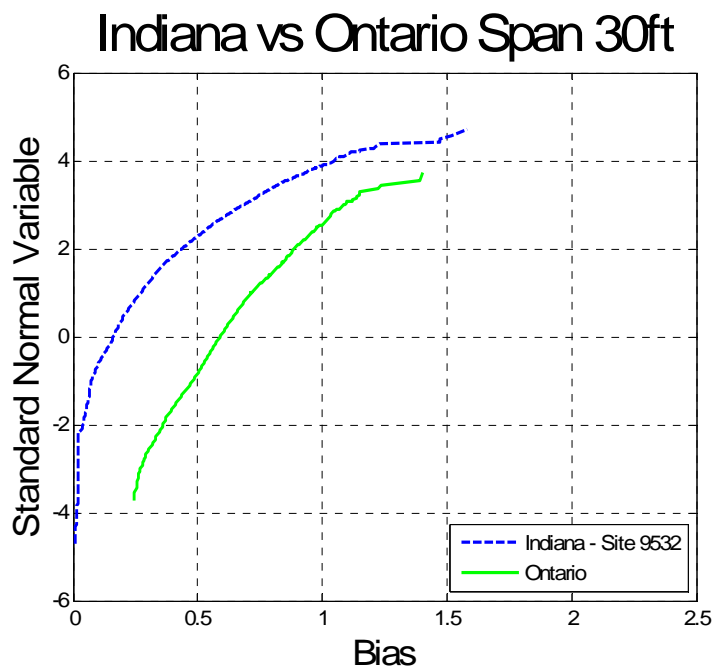


Figure 0-152 Comparison of Shear – Indiana Site 9532 vs. Ontario – Span 30ft

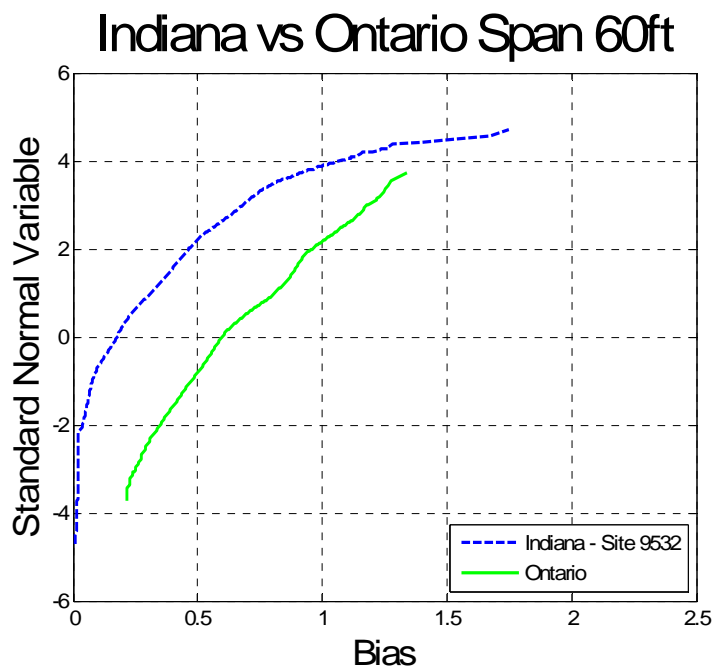


Figure 0-153 Comparison of Shear – Indiana Site 9532 vs. Ontario – Span 60ft

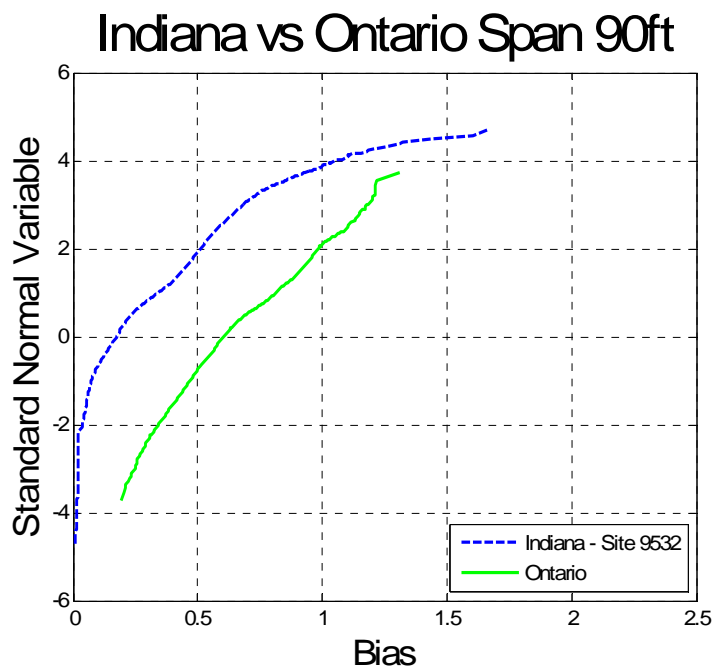


Figure 0-154 Comparison of Shear – Indiana Site 9532 vs. Ontario – Span 90ft

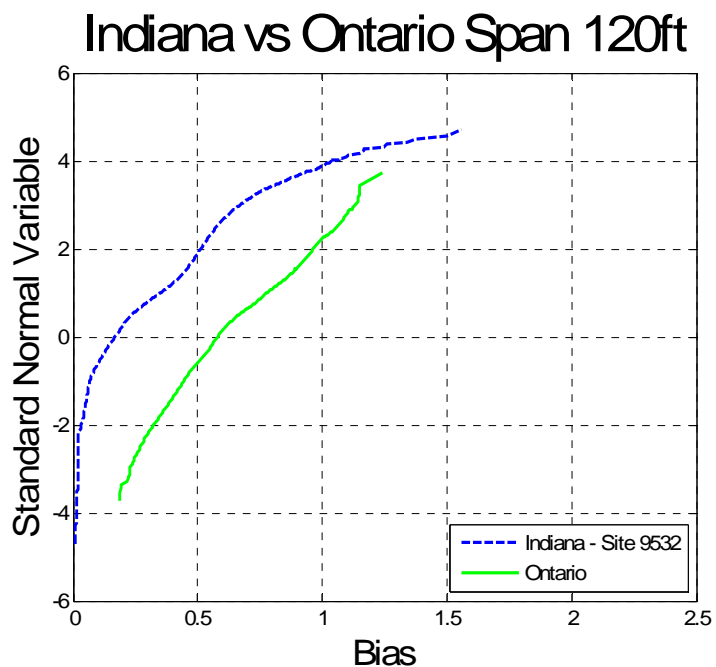


Figure 0-155 Comparison of Shear – Indiana Site 9532 vs. Ontario – Span 120ft

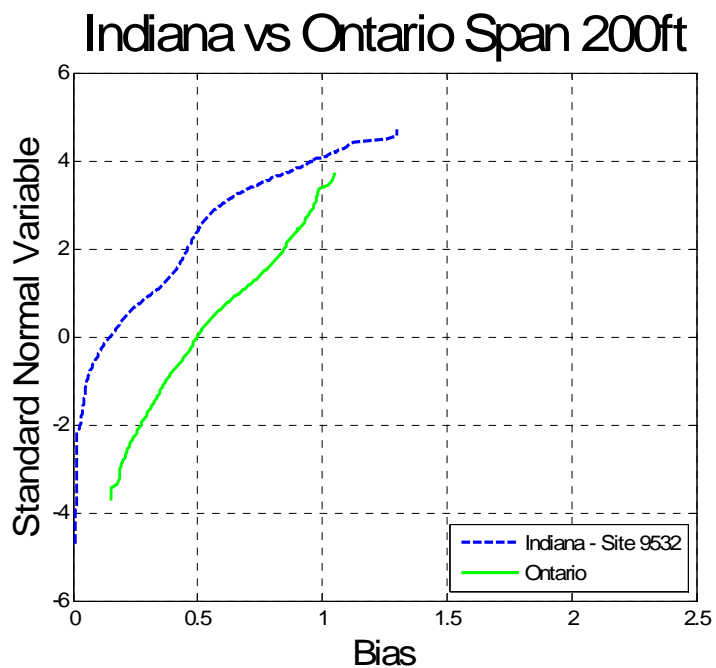


Figure 0-156 Comparison of Shear – Indiana Site 9532 vs. Ontario – Span 200ft

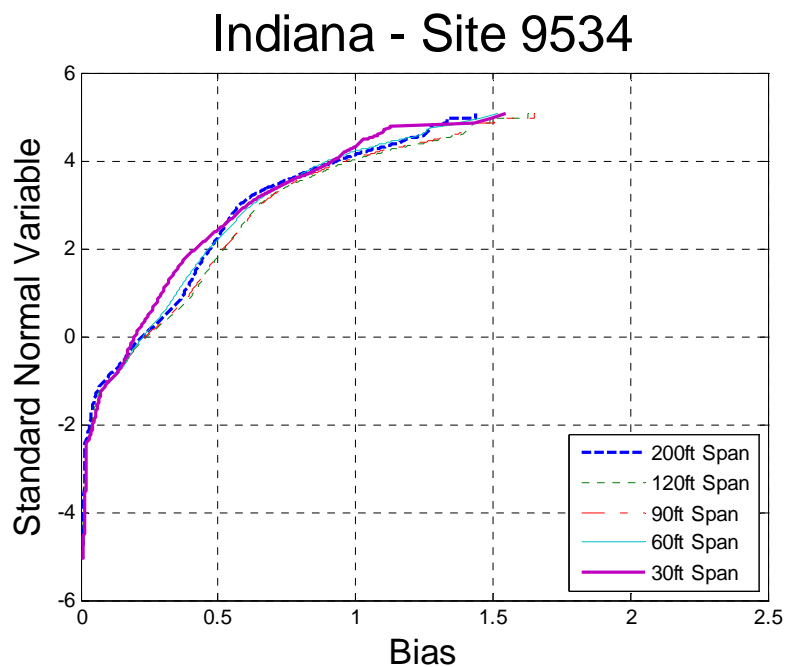


Figure 0-157 Cumulative Distribution Functions of Shear – Indiana Site 9534

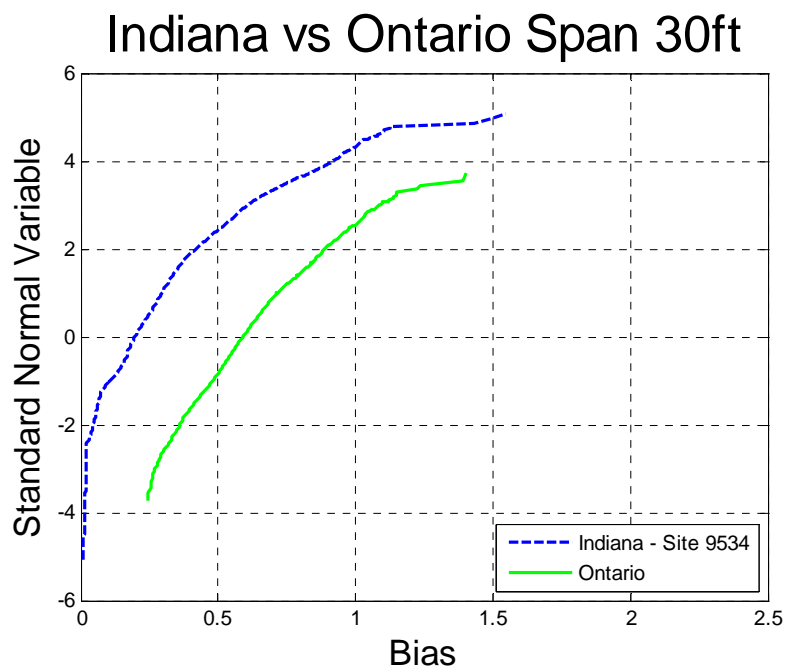


Figure 0-158 Comparison of Shear – Indiana Site 9534 vs. Ontario – Span 30ft

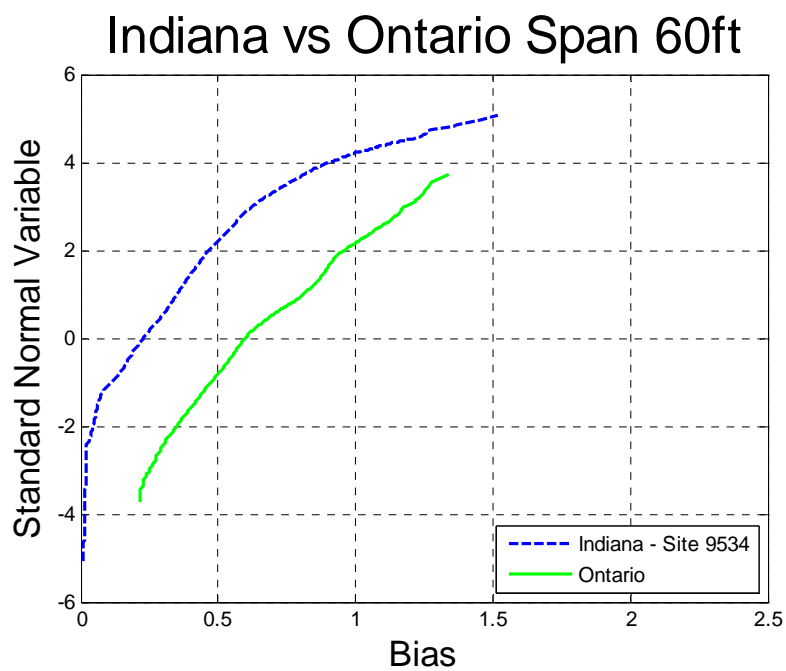


Figure 0-159 Comparison of Shear – Indiana Site 9534 vs. Ontario – Span 60ft

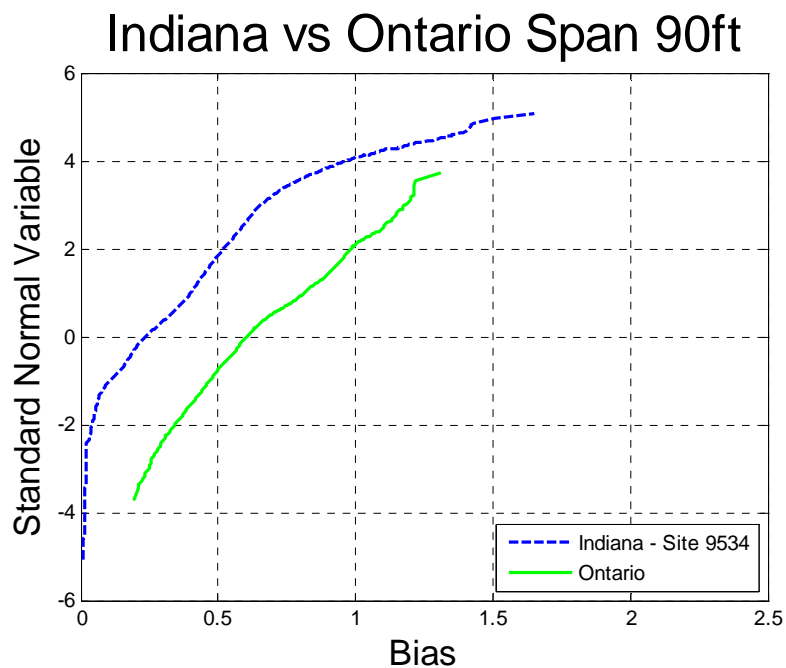


Figure 0-160 Comparison of Shear – Indiana Site 9534 vs. Ontario – Span 90ft

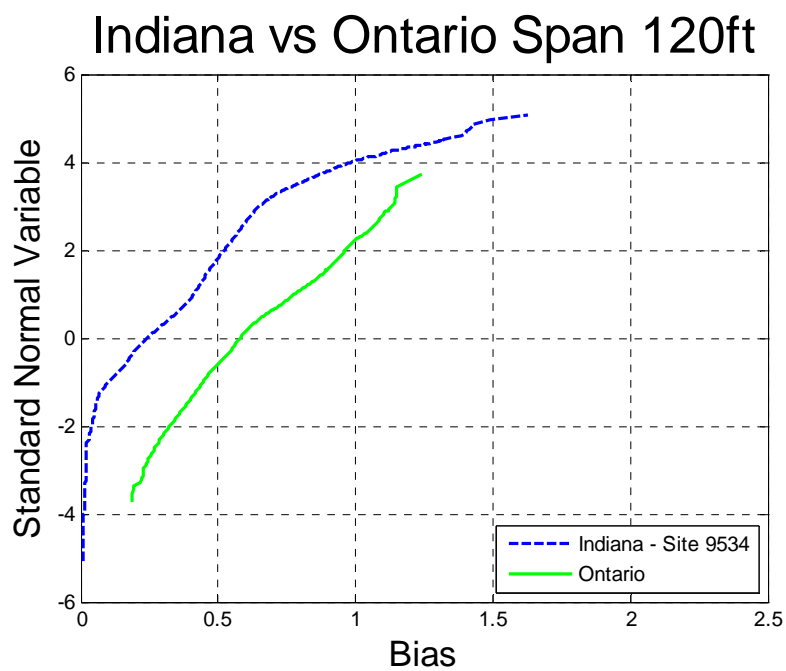


Figure 0-161 Comparison of Shear – Indiana Site 9534 vs. Ontario – Span 120ft

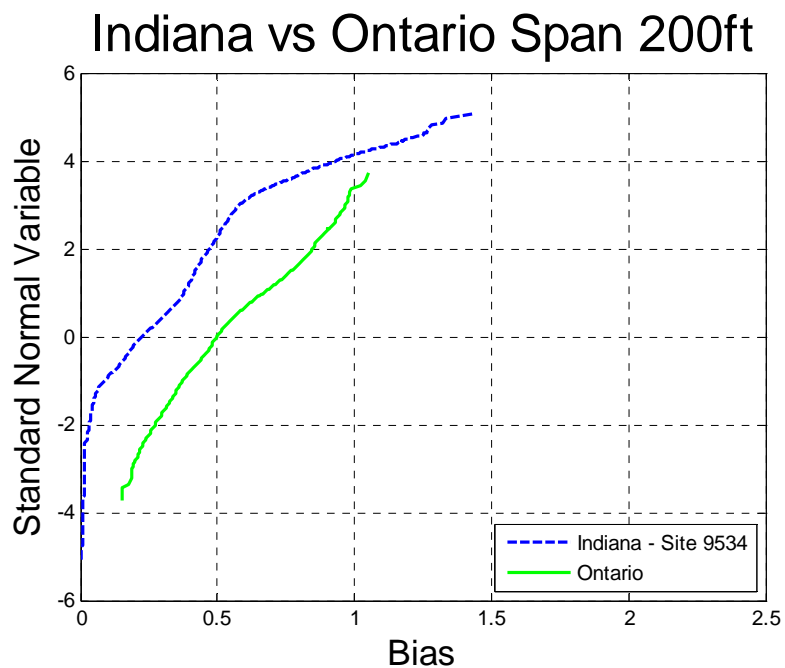


Figure 0-162 Comparison of Shear – Indiana Site 9534 vs. Ontario – Span 200ft

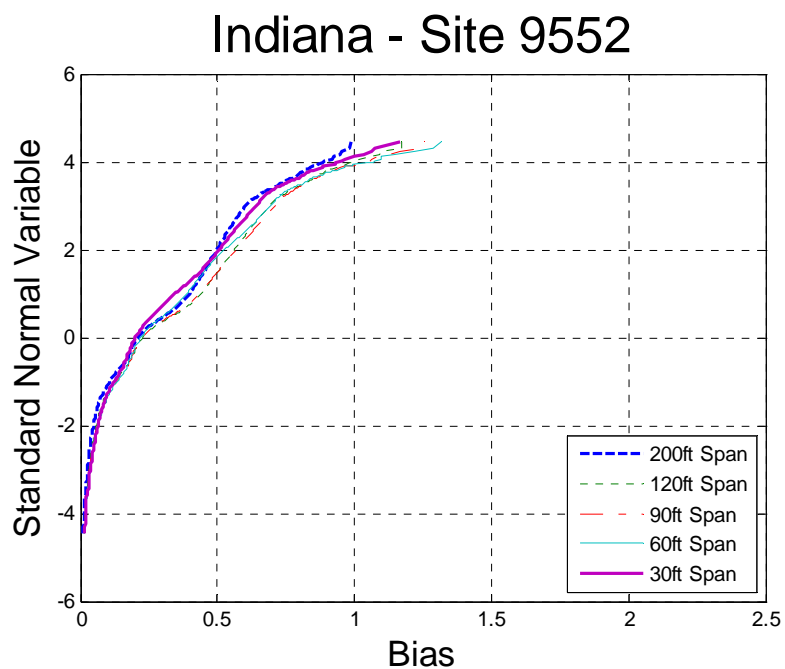


Figure 0-163 Cumulative Distribution Functions of Shear – Indiana Site 9552

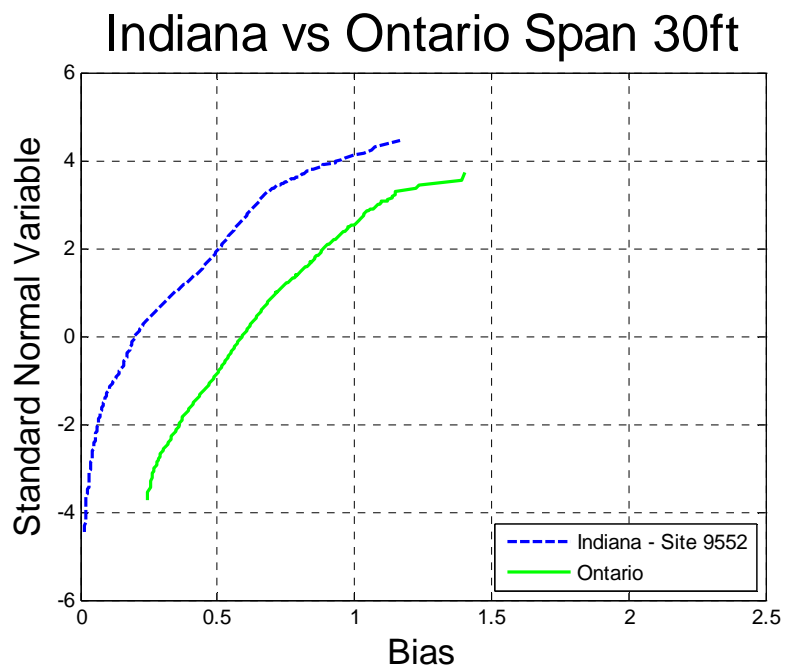


Figure 0-164 Comparison of Shear – Indiana Site 9552 vs. Ontario – Span 30ft

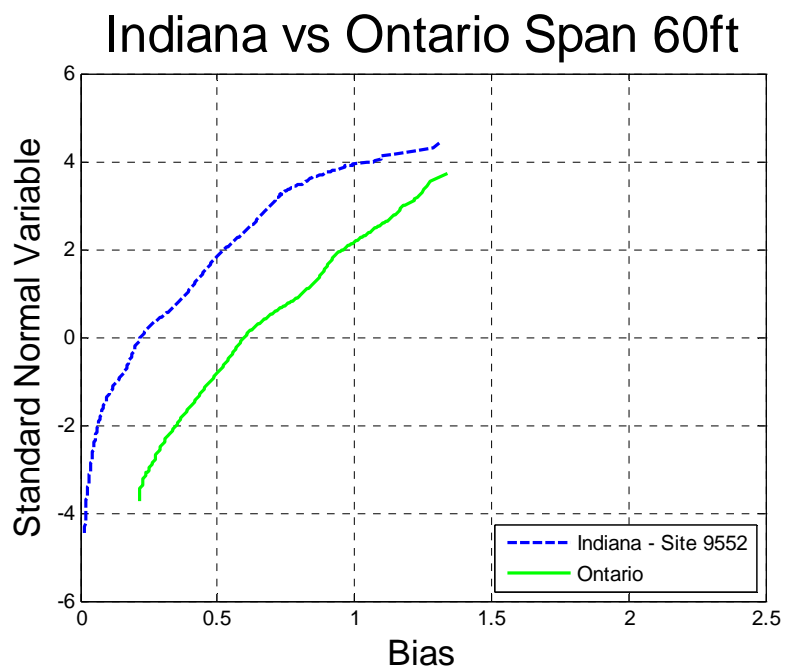


Figure 0-165 Comparison of Shear – Indiana Site 9552 vs. Ontario – Span 60ft

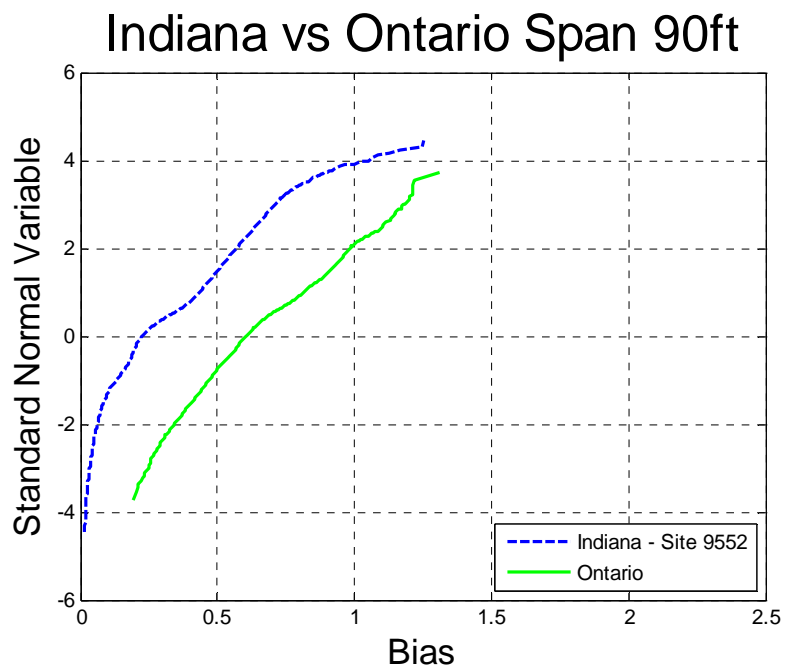


Figure 0-166 Comparison of Shear – Indiana Site 9552 vs. Ontario – Span 90ft

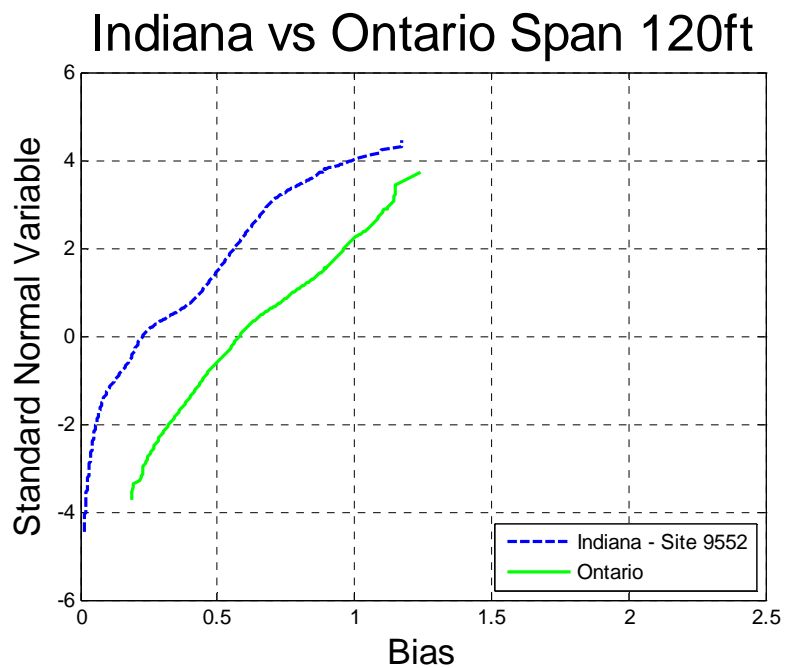


Figure 0-167 Comparison of Shear – Indiana Site 9552 vs. Ontario – Span 120ft

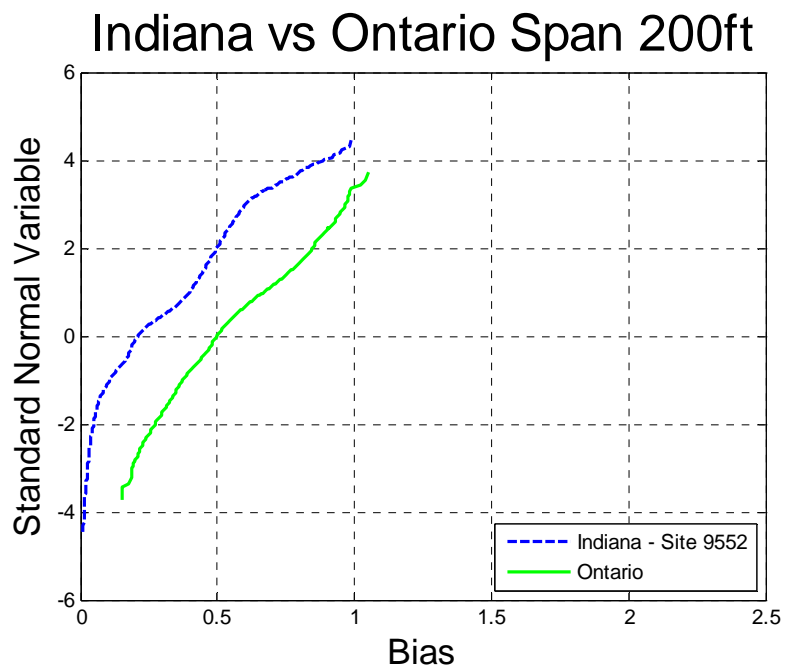


Figure 0-168 Comparison of Shear – Indiana Site 9552 vs. Ontario – Span 200ft

Mississippi – Live Load Effect

WIM data for Mississippi

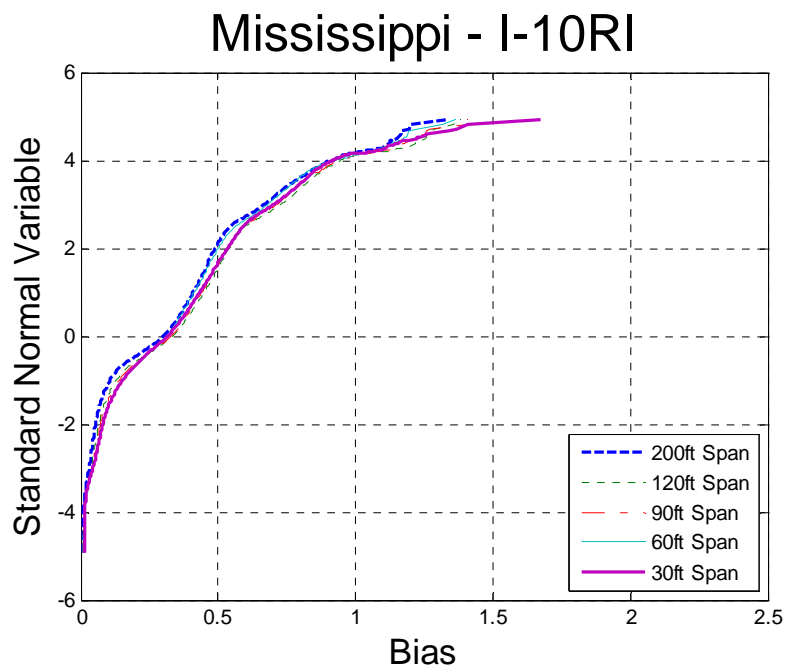
The truck survey includes weigh-in-motion (WIM) truck measurements obtained from NCHRP project. The data includes 12 months of traffic recorded at different locations. The total number of records is shown in Table 61. The data includes number of axles, gross vehicle weight (GVW), weight per axle and spacing between axles.

Table 61

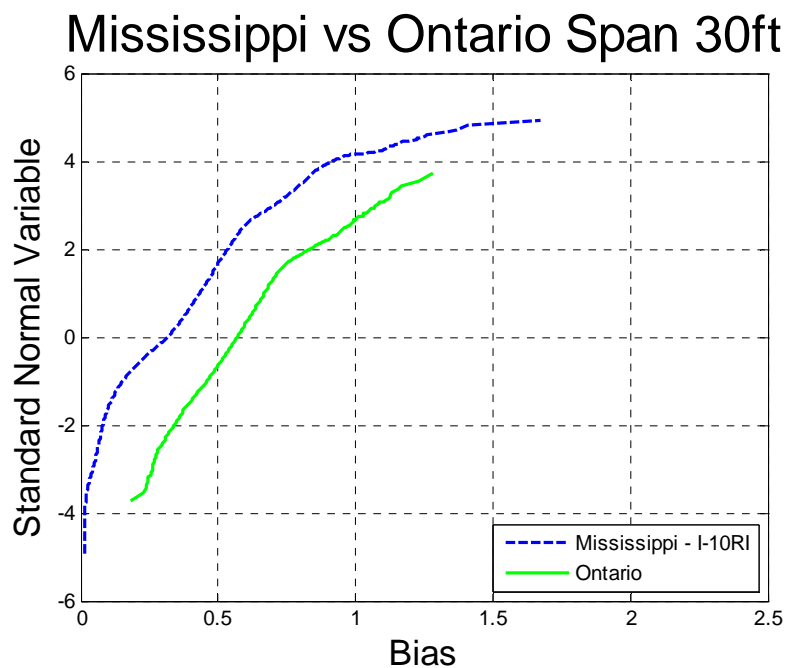
Site	Number of Trucks
I-10RI	2,548,678
I-55RI	1,453,909
I-55UI	1,328,555
US49PA	1,172,254
US61PA	206,467
TOTAL	6,709,863

Maximum Simple Span Moments

The maximum moment was calculated for each truck from the data. Analysis included simple spans with the span varying from 30 to 200 ft. The maximum moment was also calculated for the HL93 load and Tandem. Ratio between data truck moment and code load moment was plotted on the probability paper.

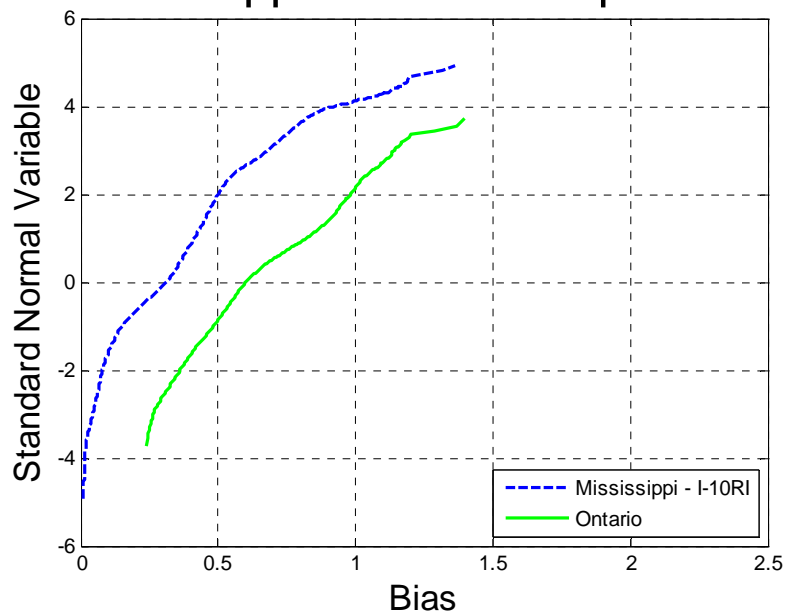


0-169 Cumulative Distribution Functions of Simple Span Moment – Mississippi – I-10RI



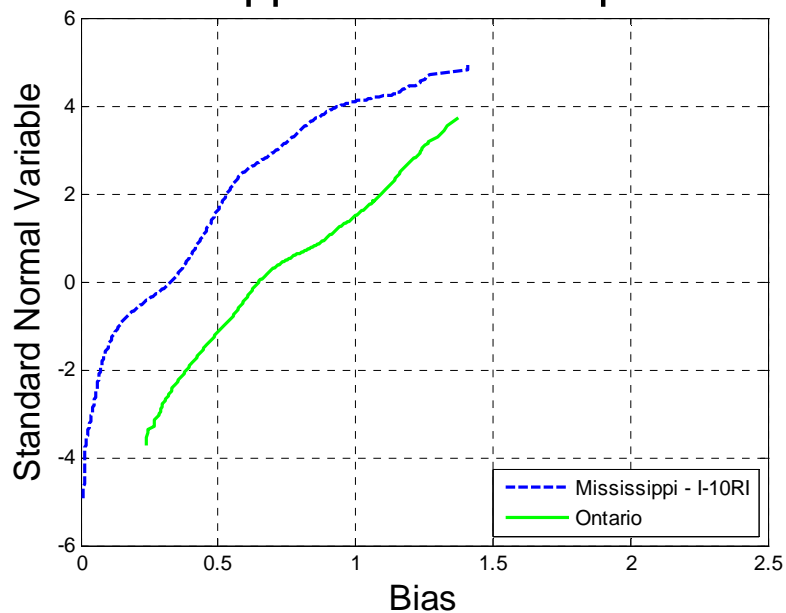
0-170 Comparison of Simple Span Moment – Mississippi – I-10RI vs. Ontario – Span 30ft

Mississippi vs Ontario Span 60ft



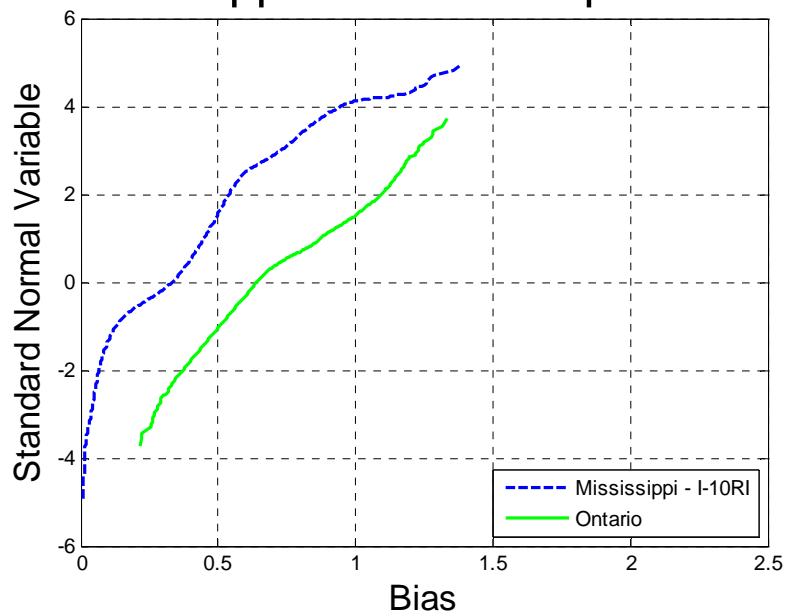
0-171 Comparison of Simple Span Moment – Mississippi – I-10RI vs. Ontario – Span 60ft

Mississippi vs Ontario Span 90ft



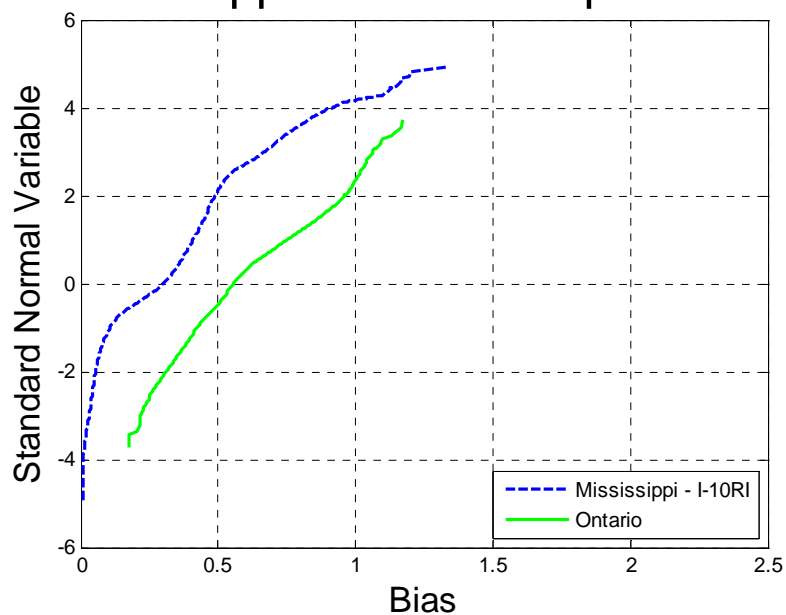
0-172 Comparison of Simple Span Moment – Mississippi – I-10RI vs. Ontario – Span 90ft

Mississippi vs Ontario Span 120ft

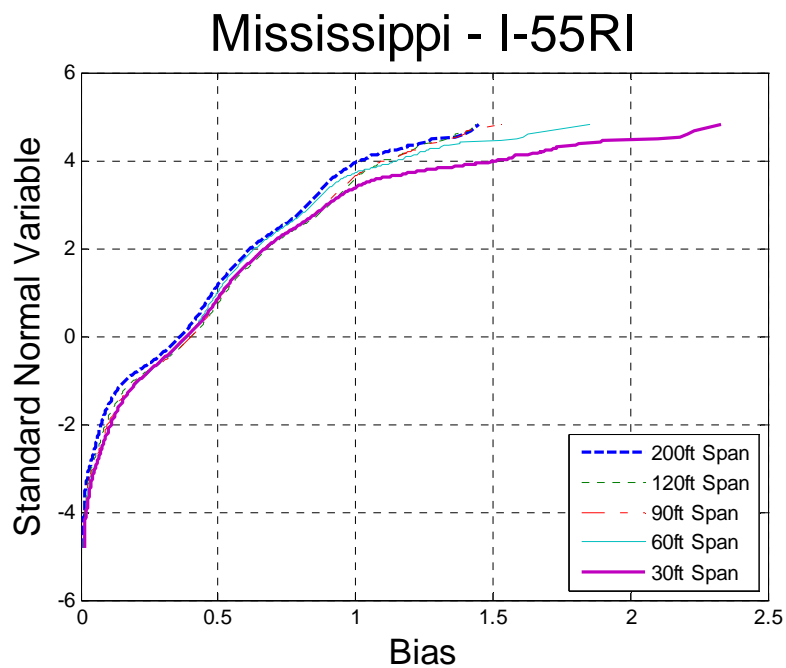


0-173 Comparison of Simple Span Moment – Mississippi – I-10RI vs. Ontario – Span 120ft

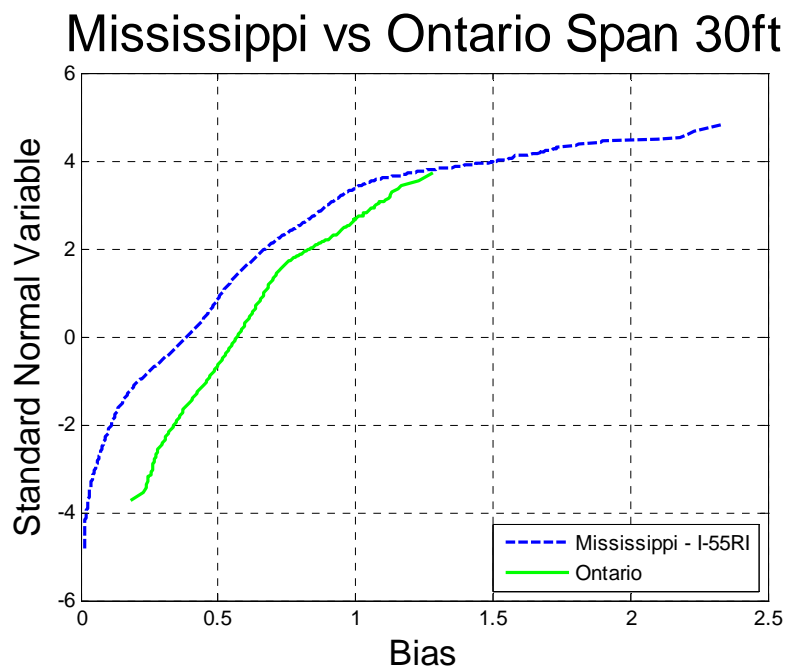
Mississippi vs Ontario Span 200ft



0-174 Comparison of Simple Span Moment – Mississippi – I-10RI vs. Ontario – Span 200ft

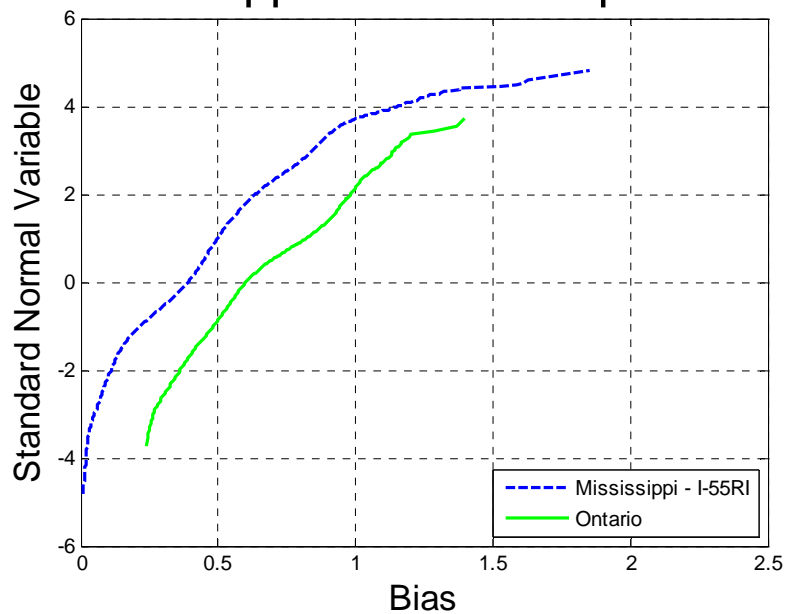


0-175 Cumulative Distribution Functions of Simple Span Moment – Mississippi – I-55RI



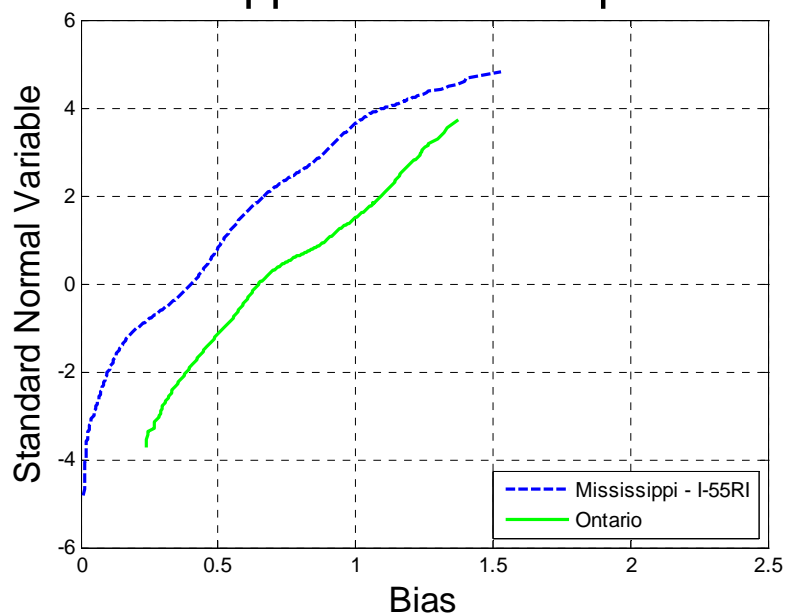
0-176 Comparison of Simple Span Moment – Mississippi – I-55RI vs. Ontario – Span 30ft

Mississippi vs Ontario Span 60ft



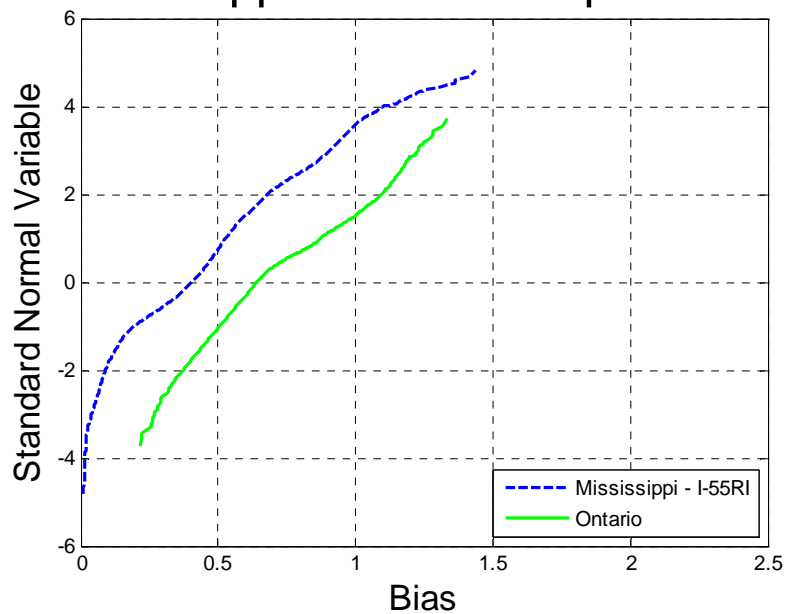
0-177 Comparison of Simple Span Moment – Mississippi – I-55RI vs. Ontario – Span 60ft

Mississippi vs Ontario Span 90ft



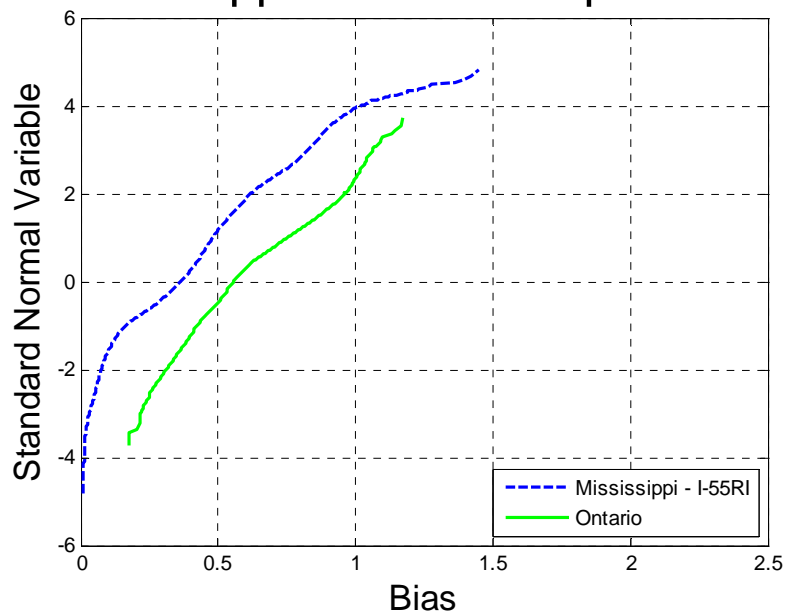
0-178 Comparison of Simple Span Moment – Mississippi – I-55RI vs. Ontario – Span 90ft

Mississippi vs Ontario Span 120ft

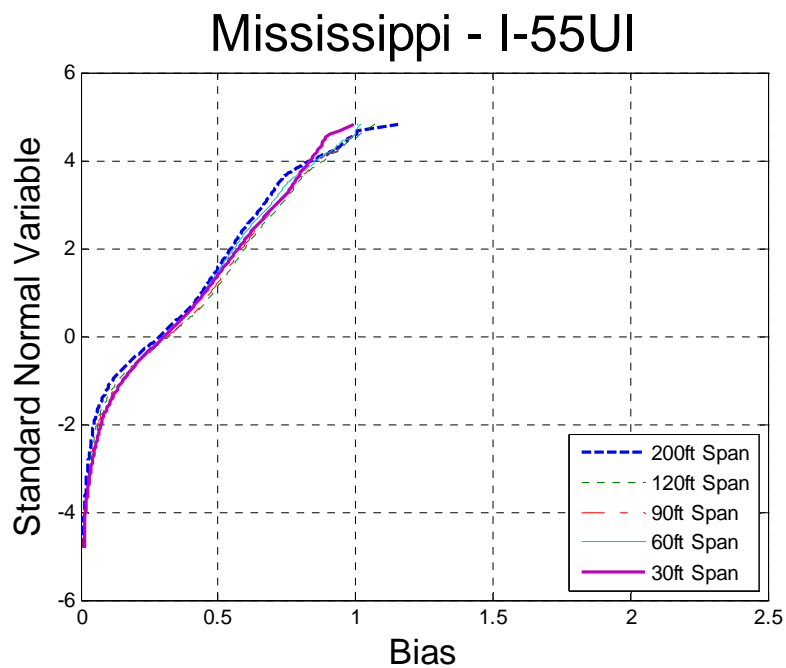


0-179 Comparison of Simple Span Moment – Mississippi – I-55RI vs. Ontario – Span 120ft

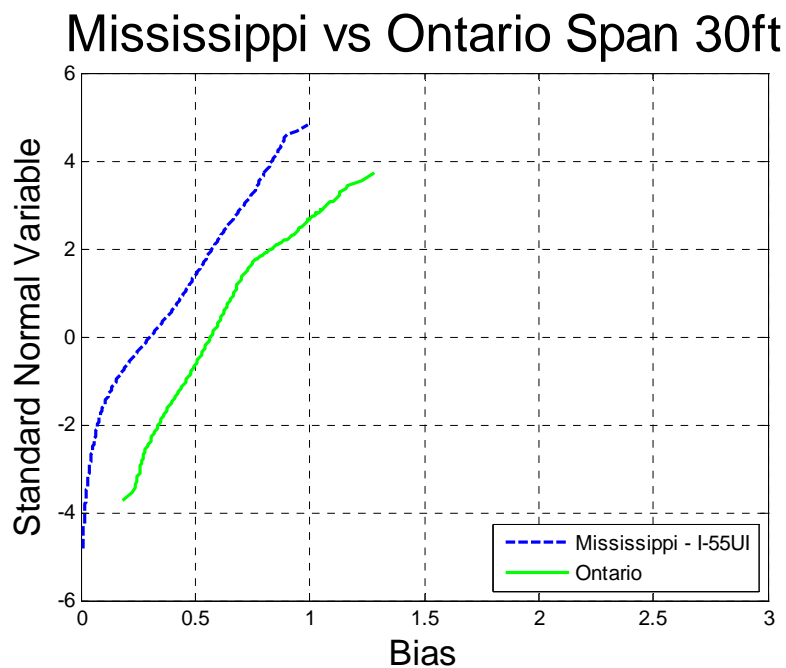
Mississippi vs Ontario Span 200ft



0-180 Comparison of Simple Span Moment – Mississippi – I-55RI vs. Ontario – Span 200ft

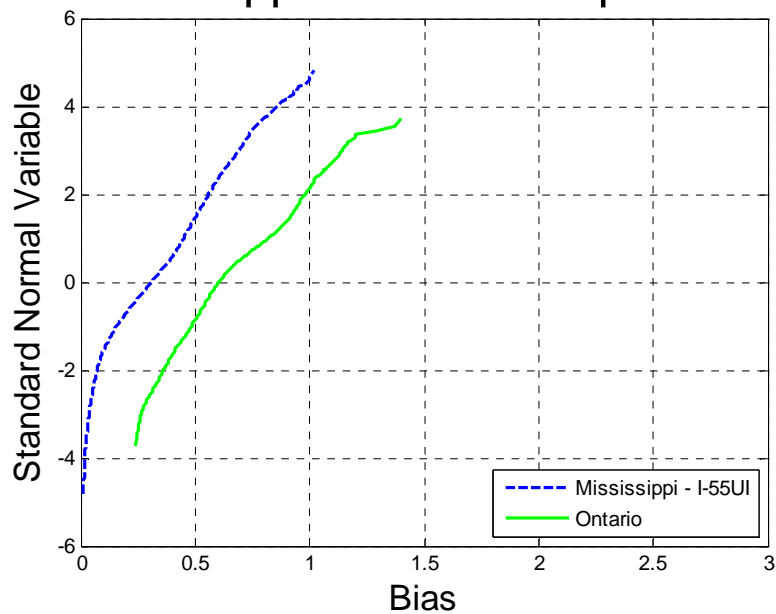


0-181 Cumulative Distribution Functions of Simple Span Moment – Mississippi – I-55UI



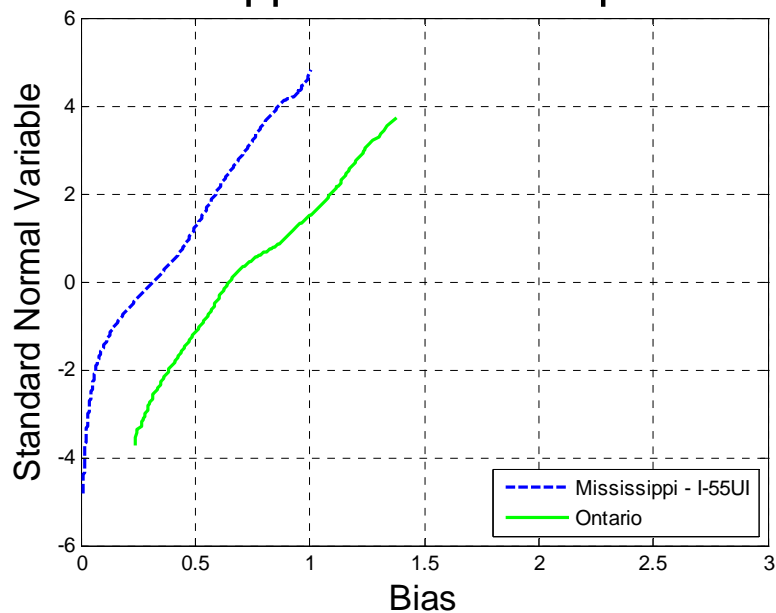
0-182 Comparison of Simple Span Moment – Mississippi – I-55UI vs. Ontario – Span 30ft

Mississippi vs Ontario Span 60ft



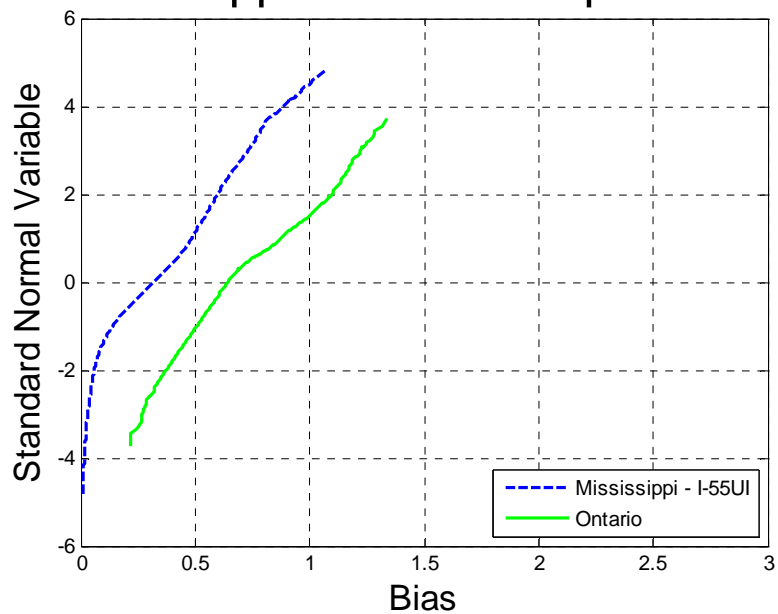
0-183 Comparison of Simple Span Moment – Mississippi – I-55UI vs. Ontario – Span 60ft

Mississippi vs Ontario Span 90ft



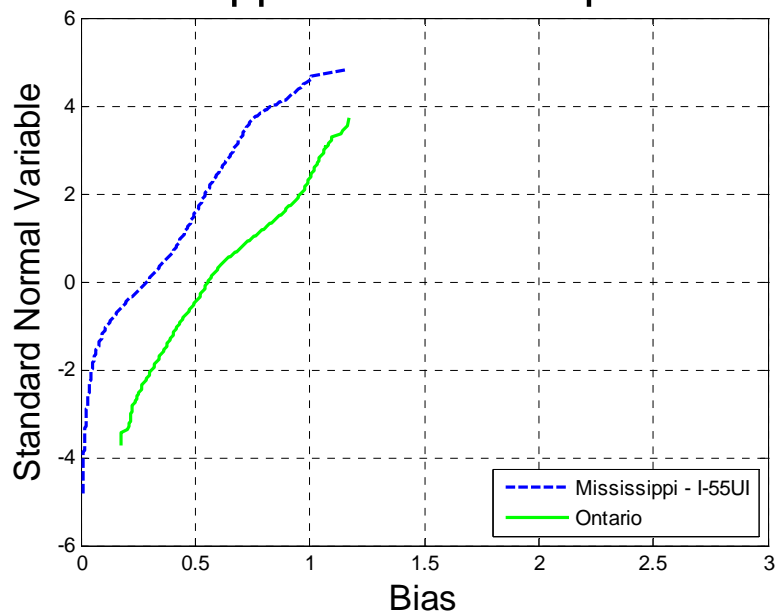
0-184 Comparison of Simple Span Moment – Mississippi – I-55UI vs. Ontario – Span 90ft

Mississippi vs Ontario Span 120ft

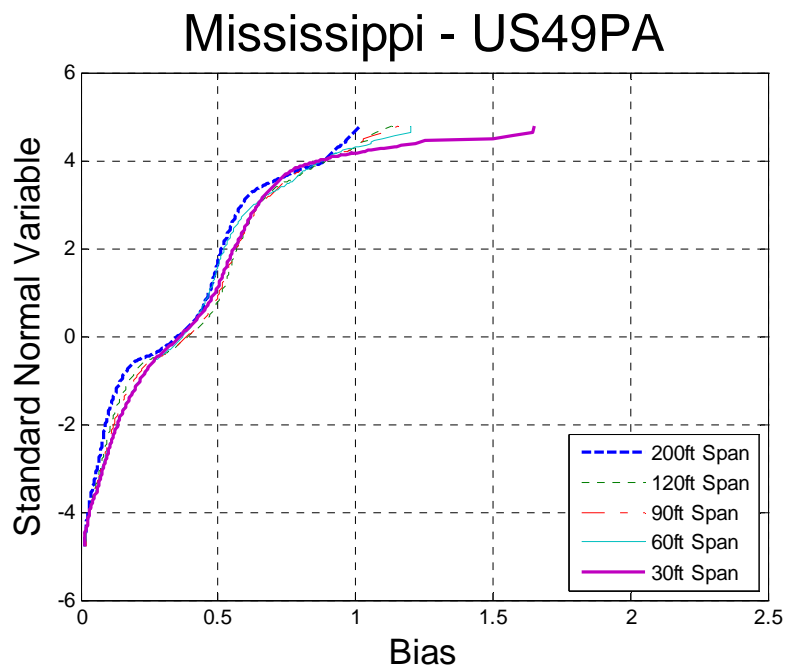


0-185 Comparison of Simple Span Moment – Mississippi – I-55UI vs. Ontario – Span 120ft

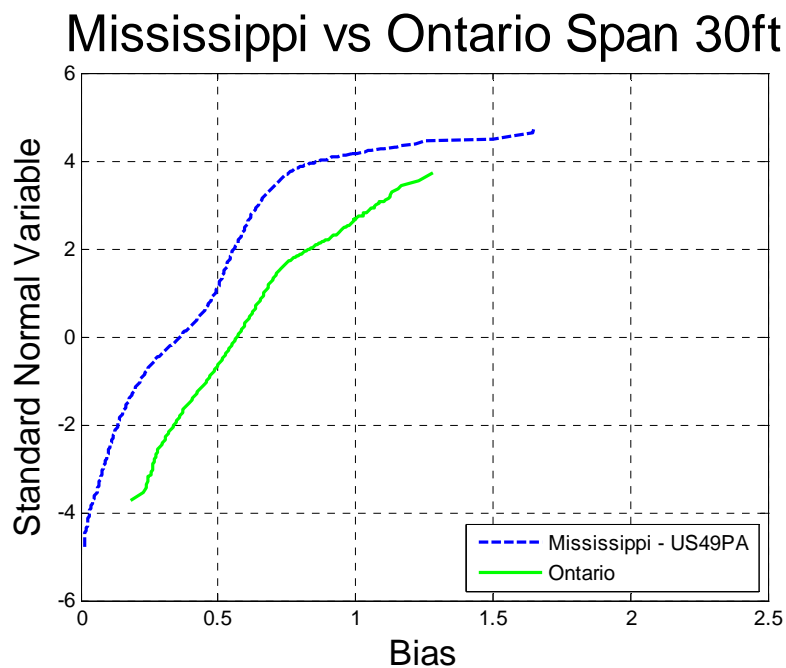
Mississippi vs Ontario Span 200ft



0-186 Comparison of Simple Span Moment – Mississippi – I-55UI vs. Ontario – Span 200ft

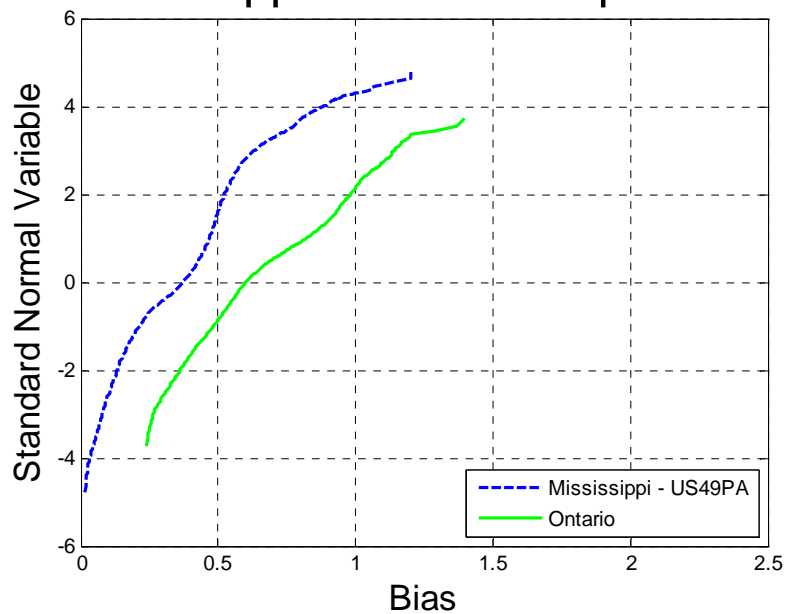


0-187 Cumulative Distribution Functions of Simple Span Moment – Mississippi – I-55UI



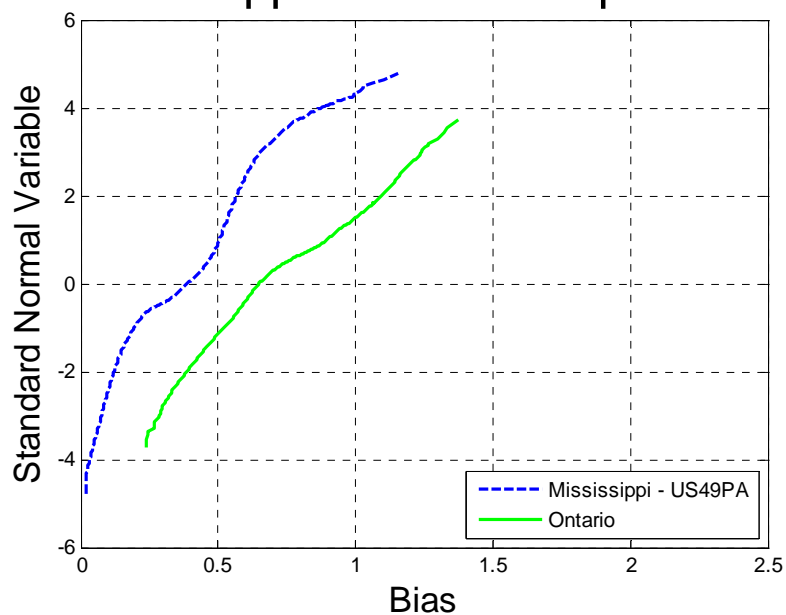
0-188 Comparison of Simple Span Moment – Mississippi – US49PA vs. Ontario – Span 30ft

Mississippi vs Ontario Span 60ft



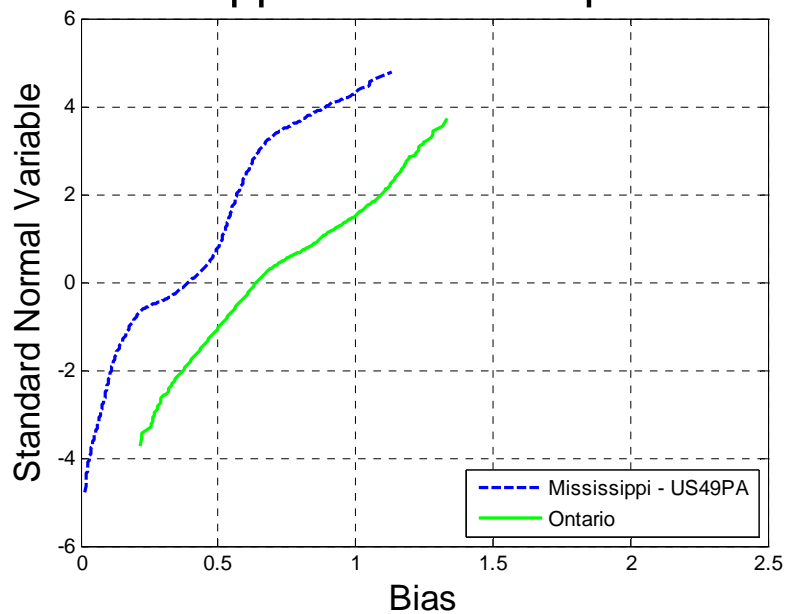
0-189 Comparison of Simple Span Moment – Mississippi – US49PA vs. Ontario – Span 60ft

Mississippi vs Ontario Span 90ft



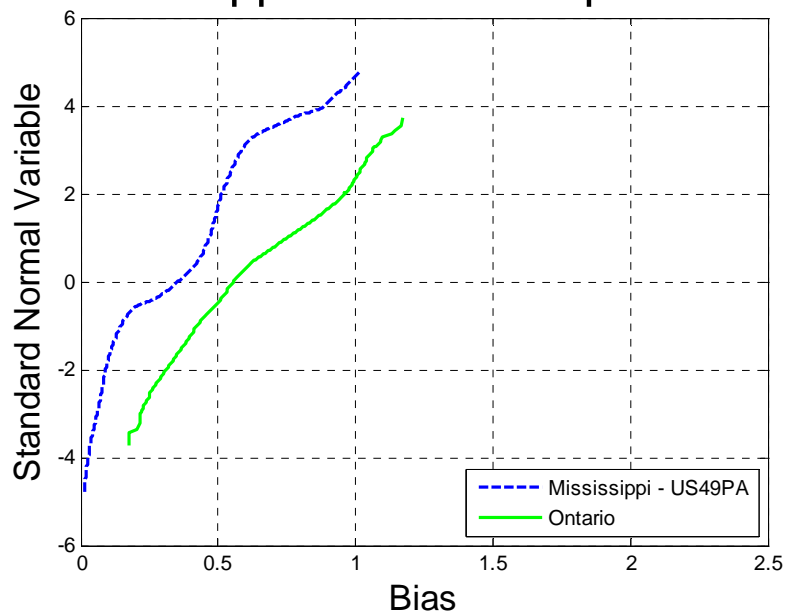
0-190 Comparison of Simple Span Moment – Mississippi – US49PA vs. Ontario – Span 90ft

Mississippi vs Ontario Span 120ft

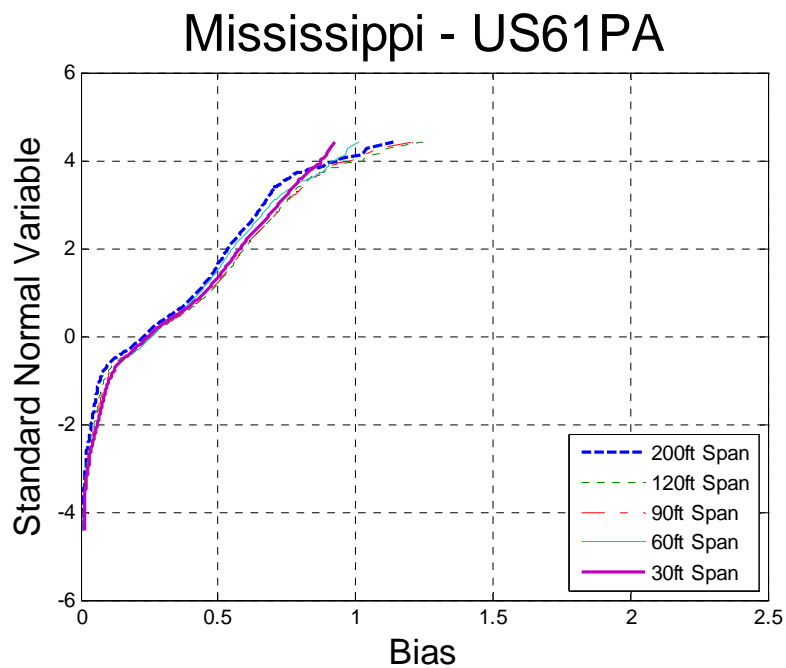


0-191 Comparison of Simple Span Moment – Mississippi – US49PA vs. Ontario – Span 120ft

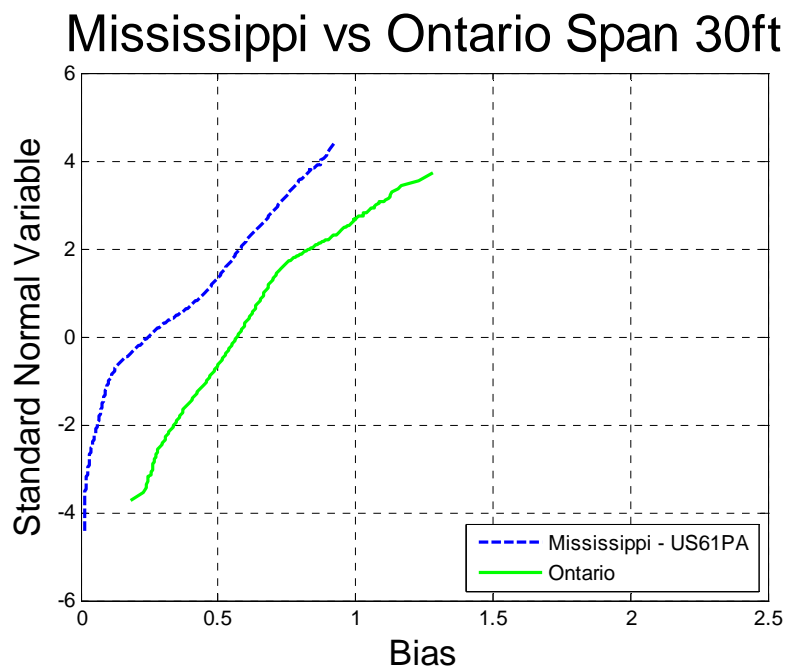
Mississippi vs Ontario Span 200ft



0-192 Comparison of Simple Span Moment – Mississippi – US49PA vs. Ontario – Span 200ft

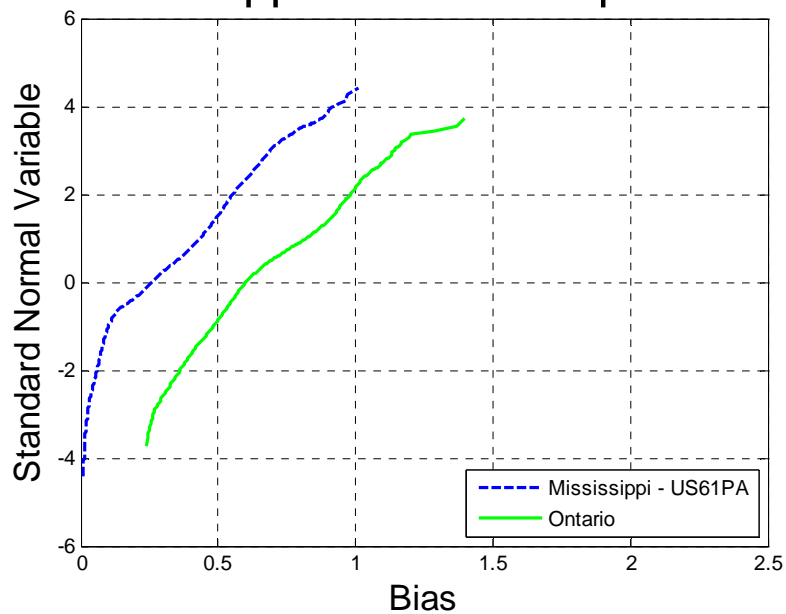


0-193 Cumulative Distribution Functions of Simple Span Moment – Mississippi – I-55UI



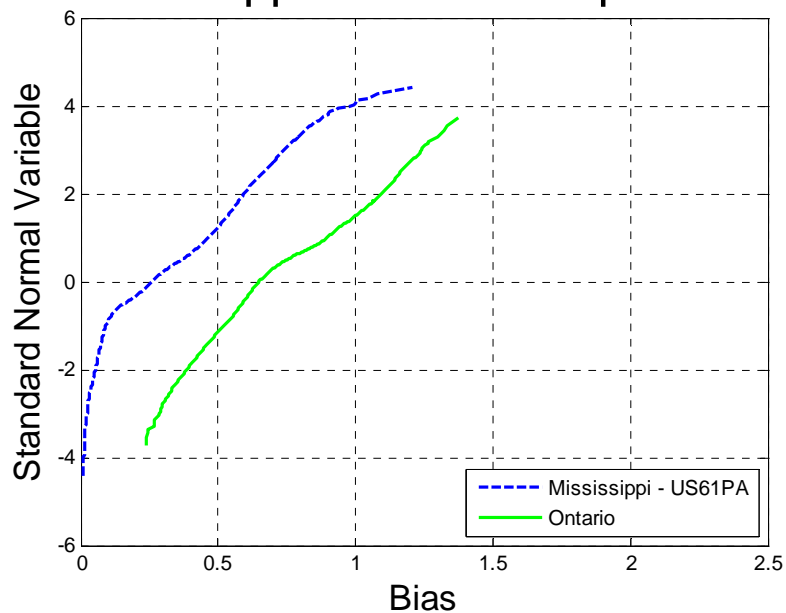
0-194 Comparison of Simple Span Moment – Mississippi – US61PA vs. Ontario – Span 30ft

Mississippi vs Ontario Span 60ft



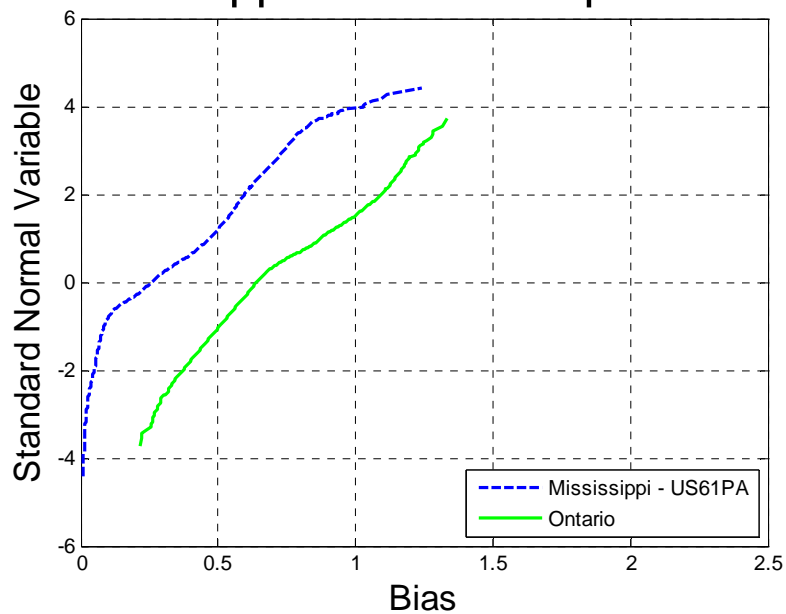
0-195 Comparison of Simple Span Moment – Mississippi – US61PA vs. Ontario – Span 60ft

Mississippi vs Ontario Span 90ft



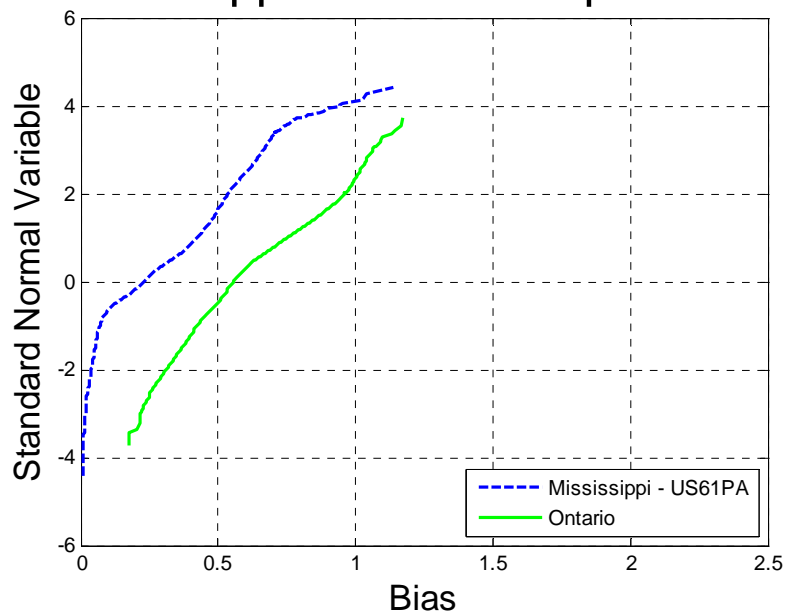
0-196 Comparison of Simple Span Moment – Mississippi – US61PA vs. Ontario – Span 90ft

Mississippi vs Ontario Span 120ft



0-197 Comparison of Simple Span Moment – Mississippi – US61PA vs. Ontario – Span 120ft

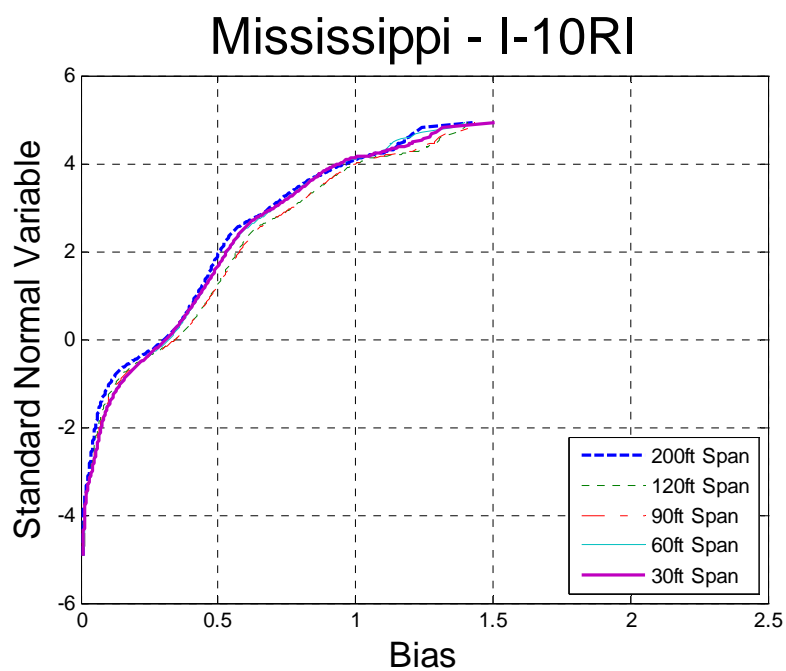
Mississippi vs Ontario Span 200ft



0-198 Comparison of Simple Span Moment – Mississippi – US61PA vs. Ontario – Span 200f

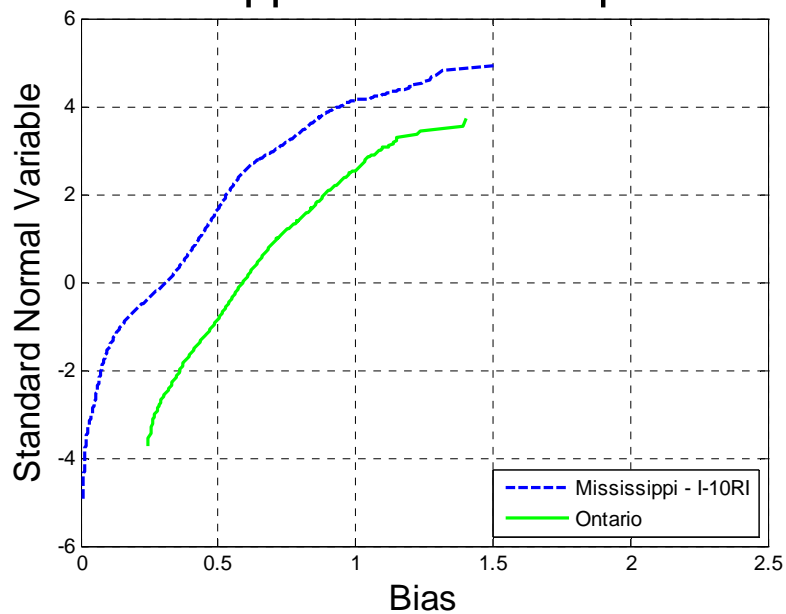
Maximum Shear

The maximum shear was calculated for each truck from the data. Analysis included simple spans with the span varying from 30 to 200 ft. The ratio of shear obtained from the data truck and the HL-93 load was plotted on the probability paper.



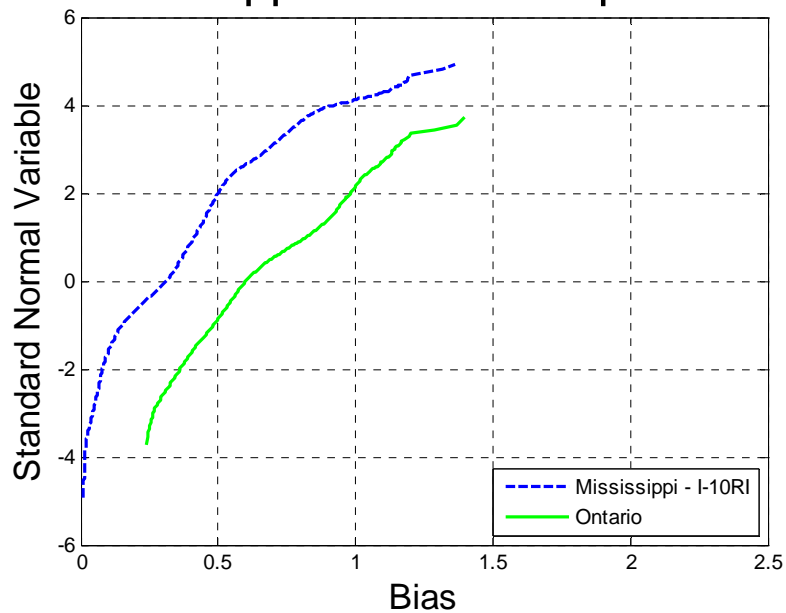
0-199 Cumulative Distribution Functions of Shear – Mississippi – I-10RI

Mississippi vs Ontario Span 30ft

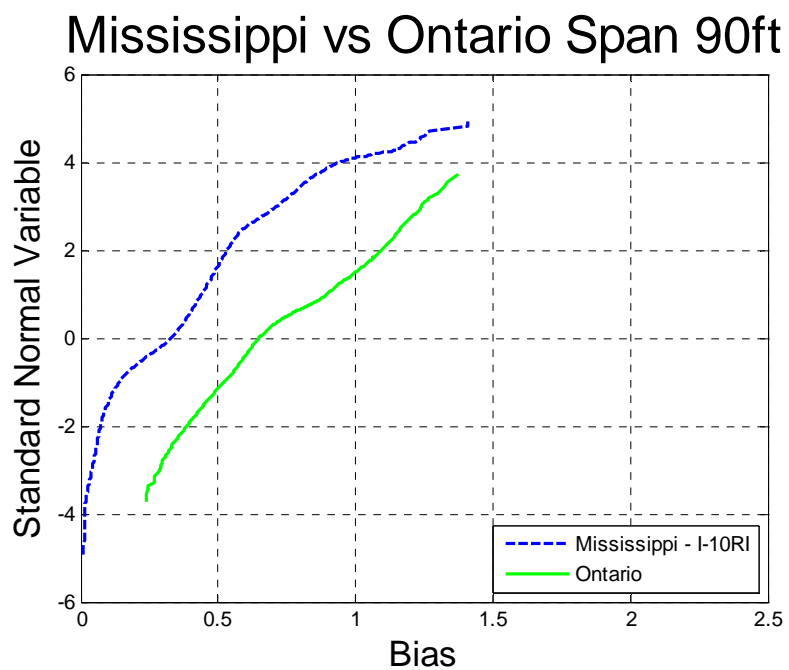


0-200 Comparison of Shear – Mississippi – I-10RI vs. Ontario – Span 30ft

Mississippi vs Ontario Span 60ft

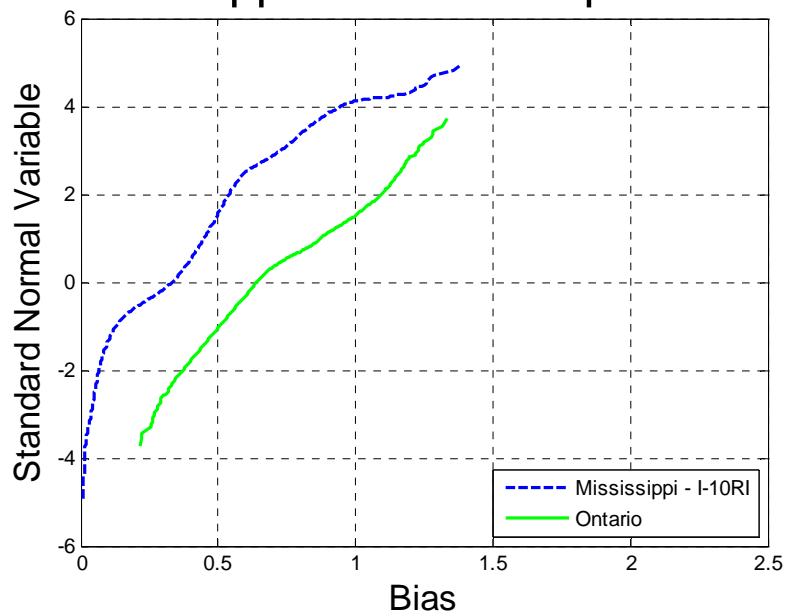


0-201 Comparison of Shear – Mississippi – I-10RI vs. Ontario – Span 60ft



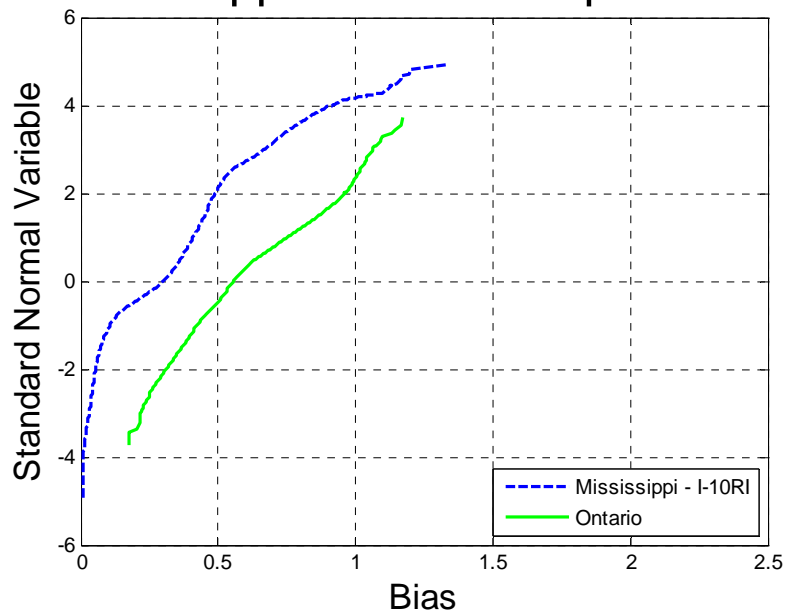
0-202 Comparison of Shear – Mississippi – I-10RI vs. Ontario – Span 90ft

Mississippi vs Ontario Span 120ft

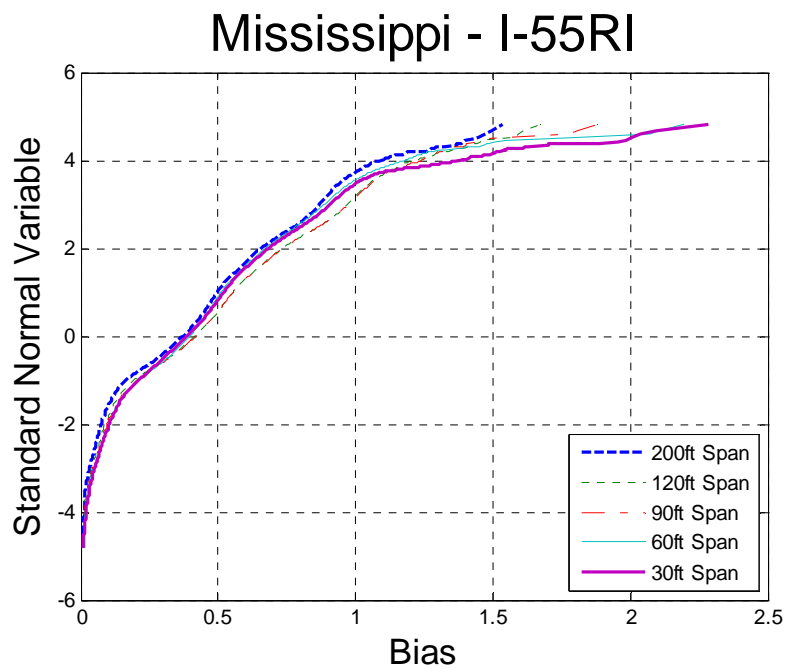


0-203 Comparison of Shear – Mississippi – I-10RI vs. Ontario – Span 120ft

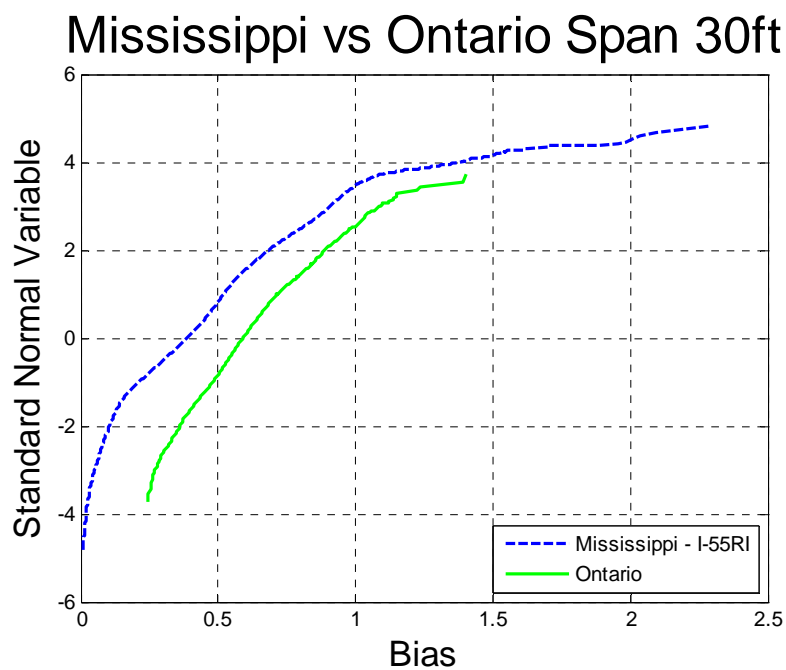
Mississippi vs Ontario Span 200ft



0-204 Comparison of Shear – Mississippi – I-10RI vs. Ontario – Span 200ft

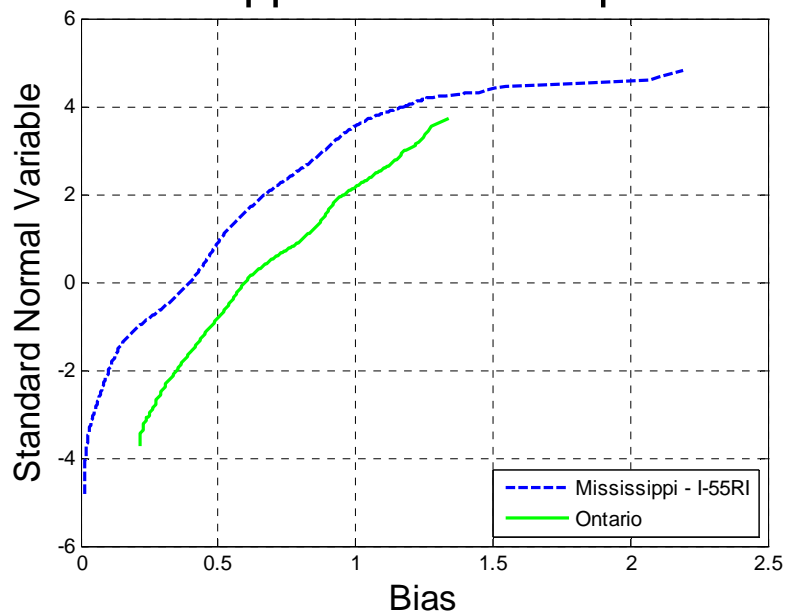


0-205 Cumulative Distribution Functions of Shear – Mississippi – I-55RI



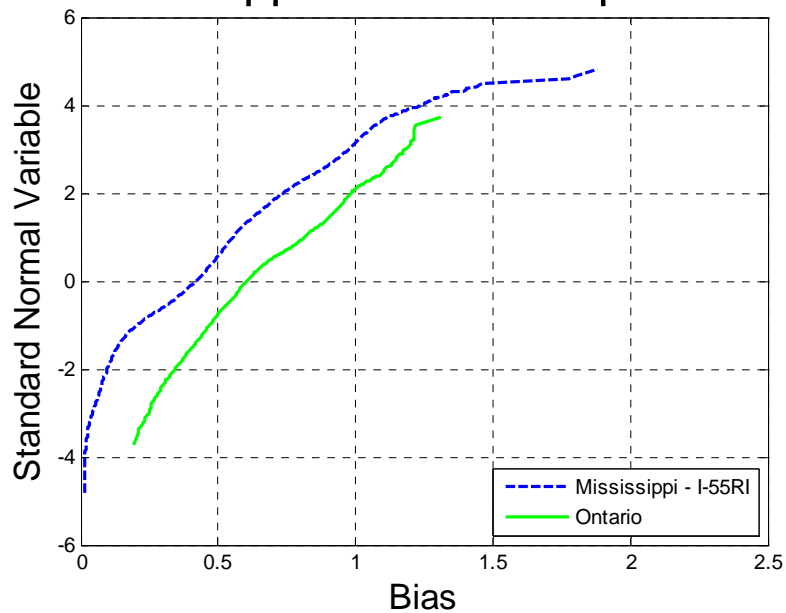
0-206 Comparison of Shear – Mississippi – I-55RI vs. Ontario – Span 30ft

Mississippi vs Ontario Span 60ft



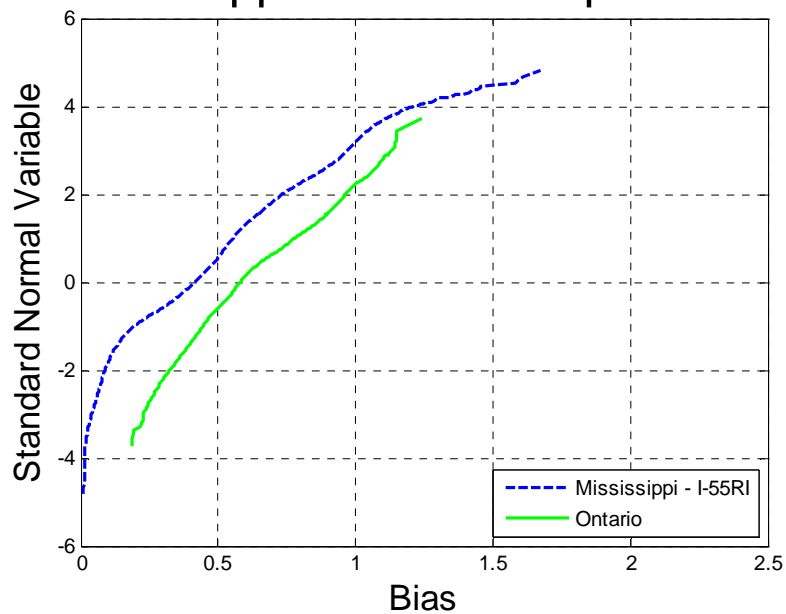
0-207 Comparison of Shear – Mississippi – I-55RI vs. Ontario – Span 60ft

Mississippi vs Ontario Span 90ft



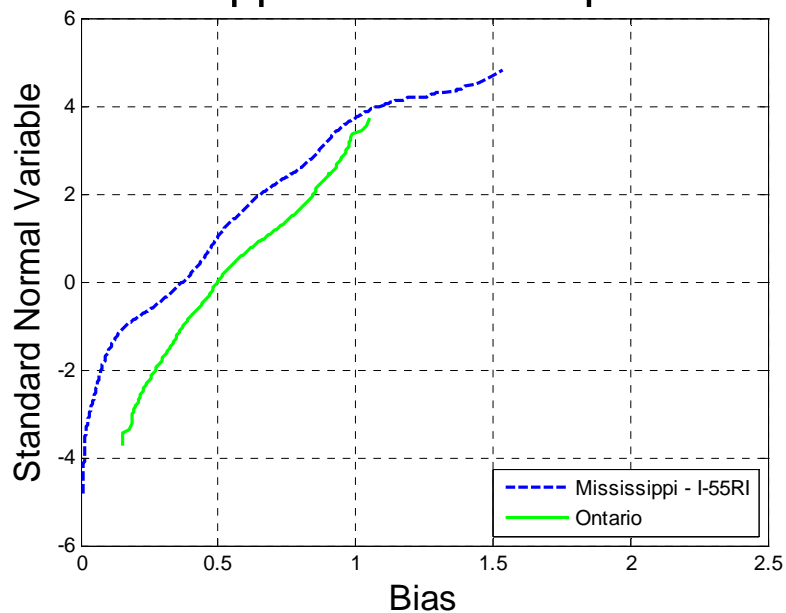
0-208 Comparison of Shear – Mississippi – I-55RI vs. Ontario – Span 90ft

Mississippi vs Ontario Span 120ft

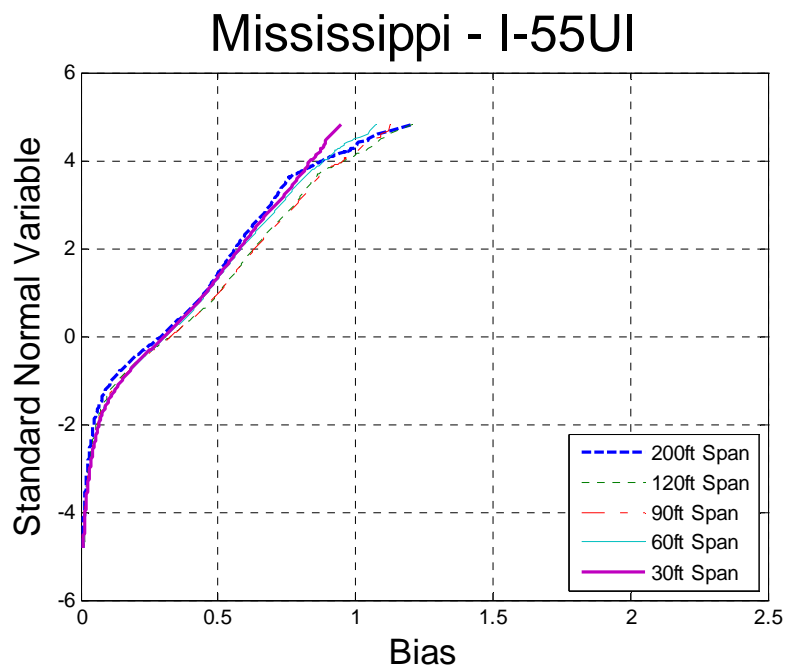


0-209 Comparison of Shear – Mississippi – I-55RI vs. Ontario – Span 120ft

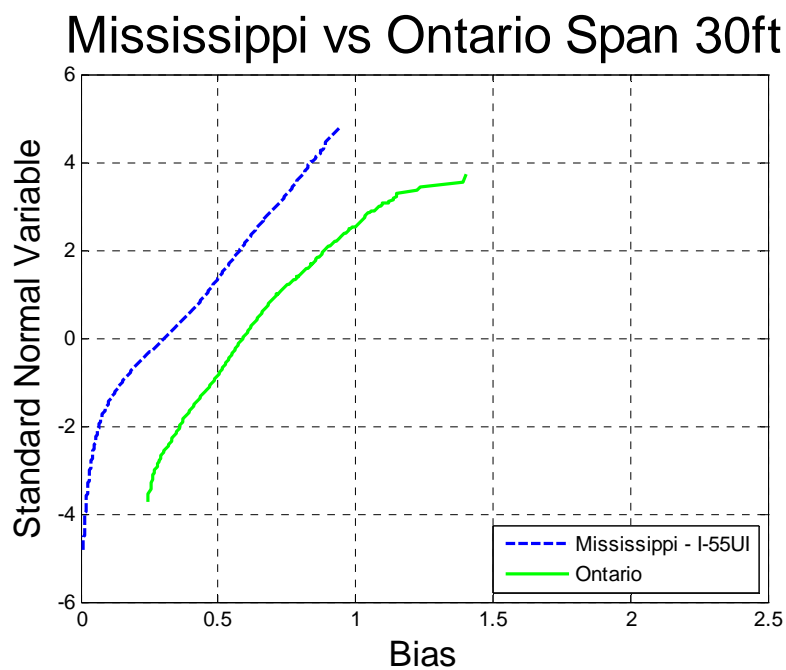
Mississippi vs Ontario Span 200ft



0-210 Comparison of Shear – Mississippi – I-55RI vs. Ontario – Span 200ft

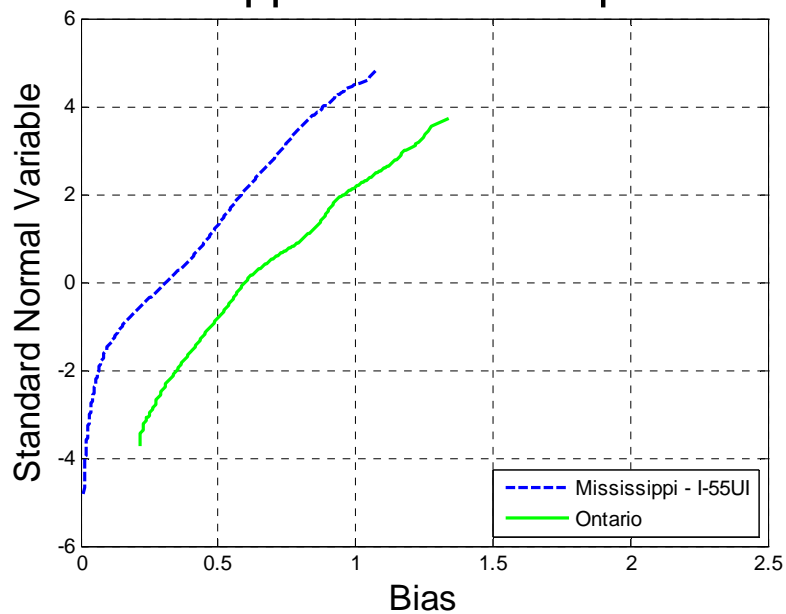


0-211 Cumulative Distribution Functions of Shear – Mississippi – I-55UI



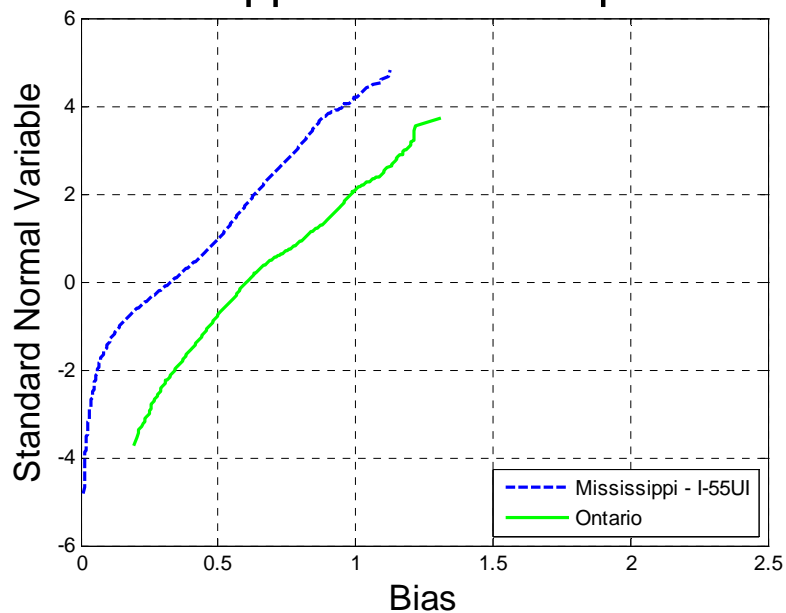
0-212 Comparison of Shear – Mississippi – I-55UI vs. Ontario – Span 30ft

Mississippi vs Ontario Span 60ft



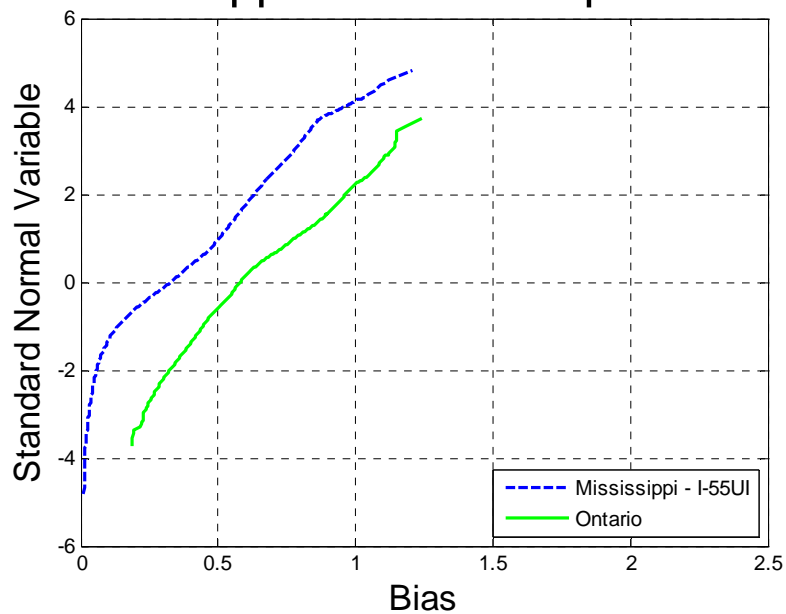
0-213 Comparison of Shear – Mississippi – I-55UI vs. Ontario – Span 60ft

Mississippi vs Ontario Span 90ft



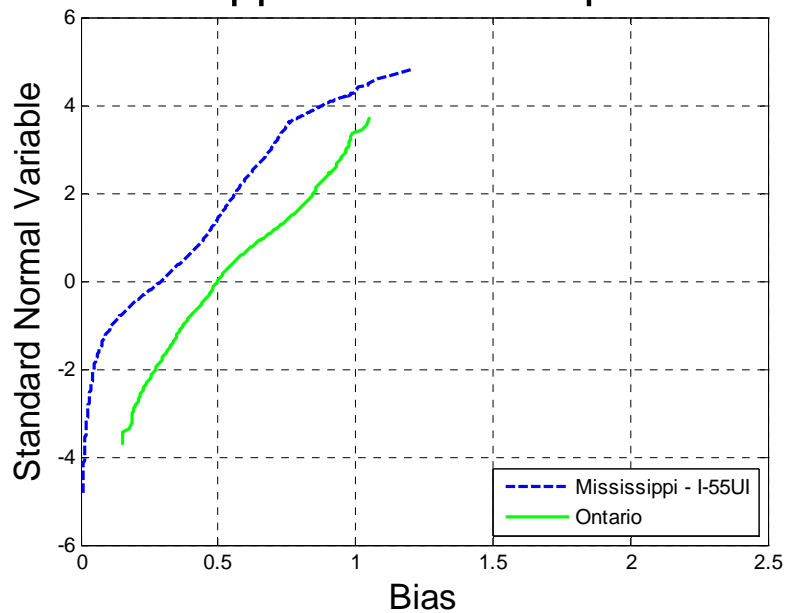
0-214 Comparison of Shear – Mississippi – I-55UI vs. Ontario – Span 90ft

Mississippi vs Ontario Span 120ft

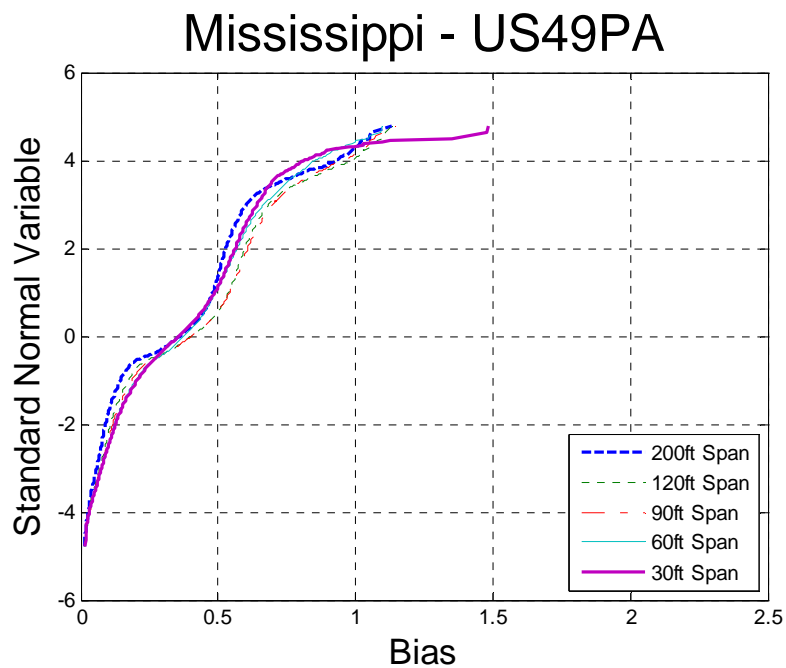


0-215 Comparison of Shear – Mississippi – I-55UI vs. Ontario – Span 120ft

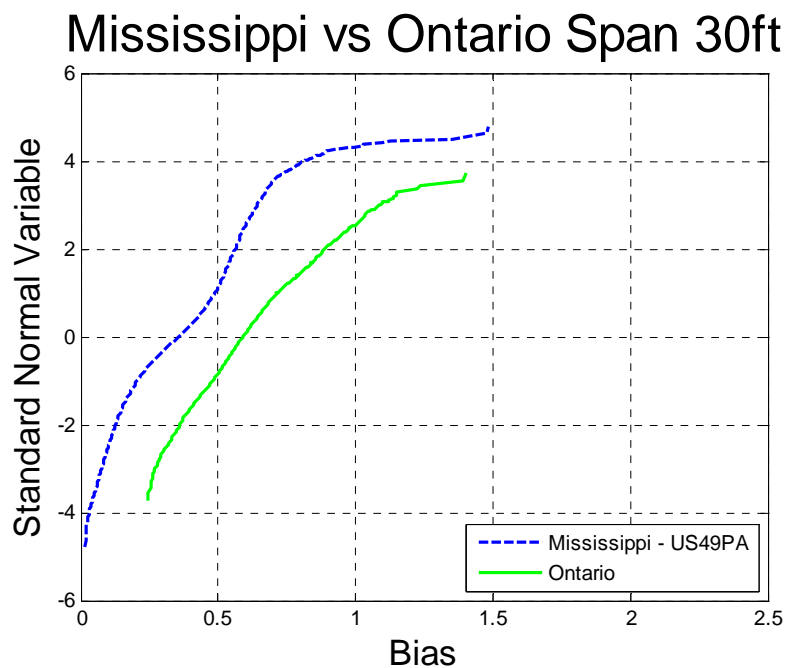
Mississippi vs Ontario Span 200ft



0-216 Comparison of Shear – Mississippi – I-55UI vs. Ontario – Span 200ft

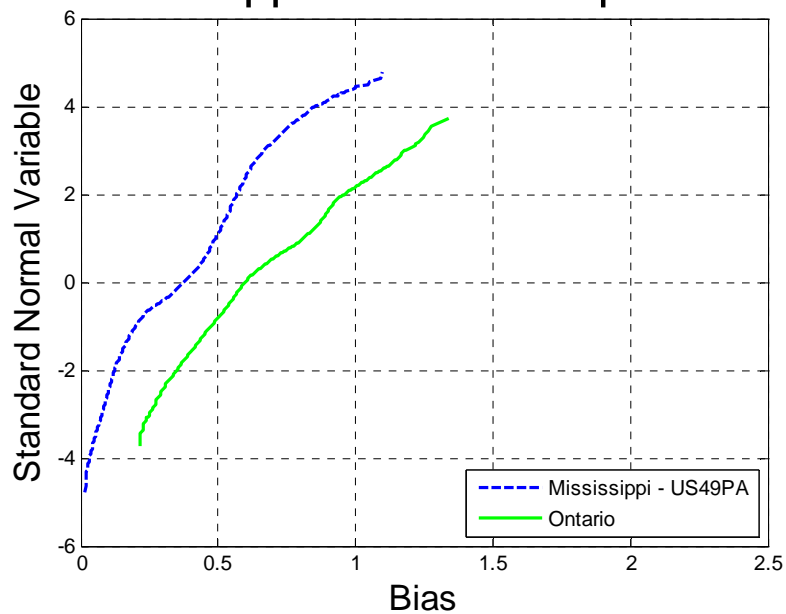


0-217 Cumulative Distribution Functions of Shear – Mississippi – US49PA



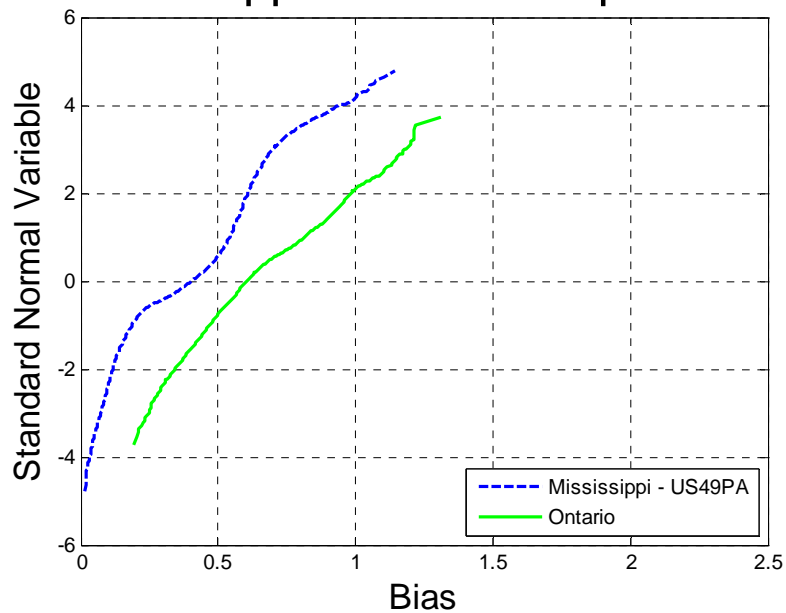
0-218 Comparison of Shear – Mississippi – US49PA vs. Ontario – Span 30ft

Mississippi vs Ontario Span 60ft



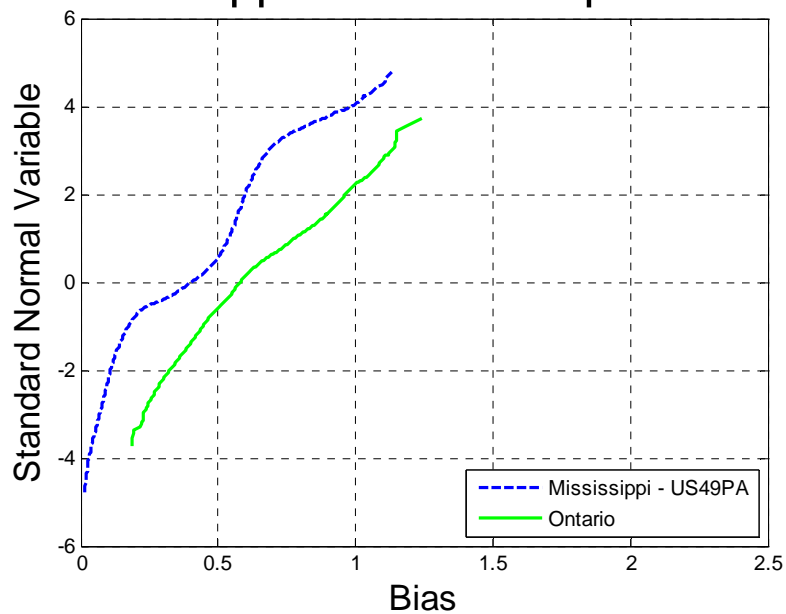
0-219 Comparison of Shear – Mississippi – US49PA vs. Ontario – Span 60ft

Mississippi vs Ontario Span 90ft



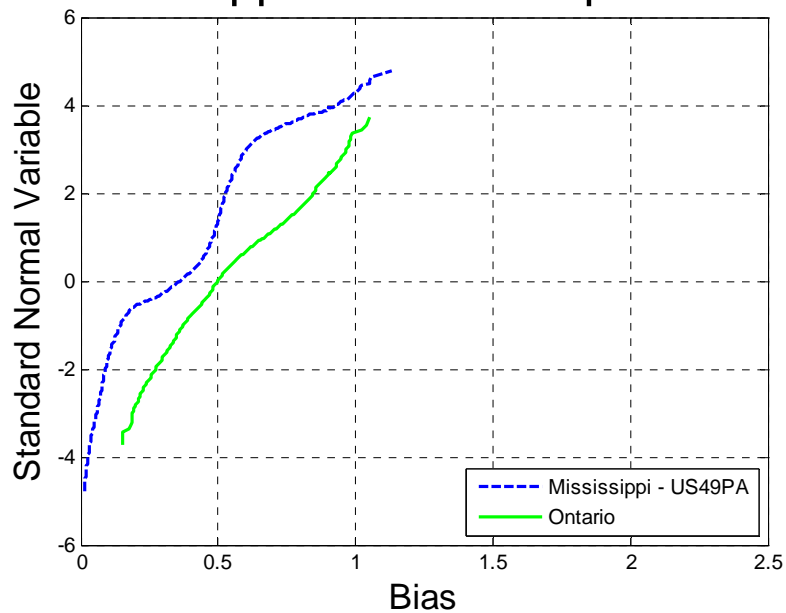
0-220 Comparison of Shear – Mississippi – US49PA vs. Ontario – Span 90ft

Mississippi vs Ontario Span 120ft

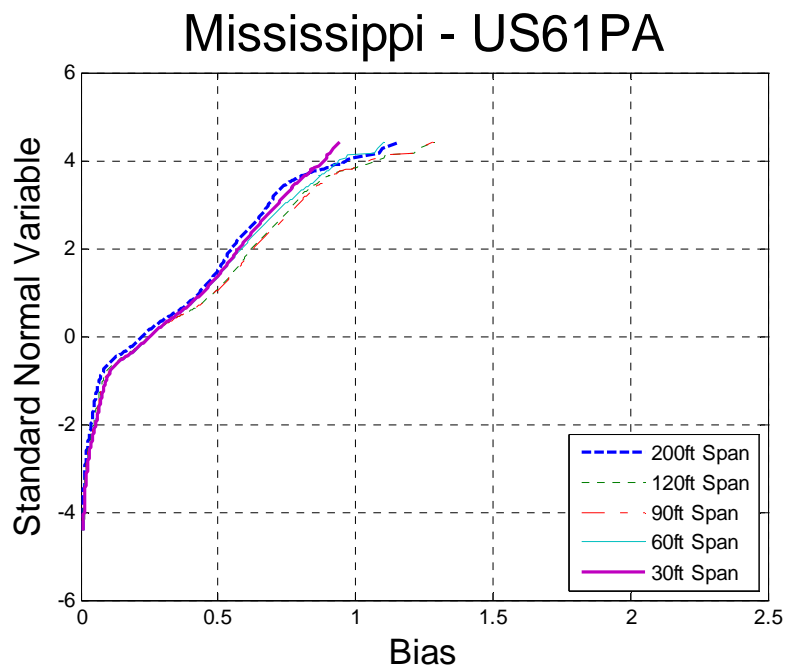


0-221 Comparison of Shear – Mississippi – US49PA vs. Ontario – Span 120ft

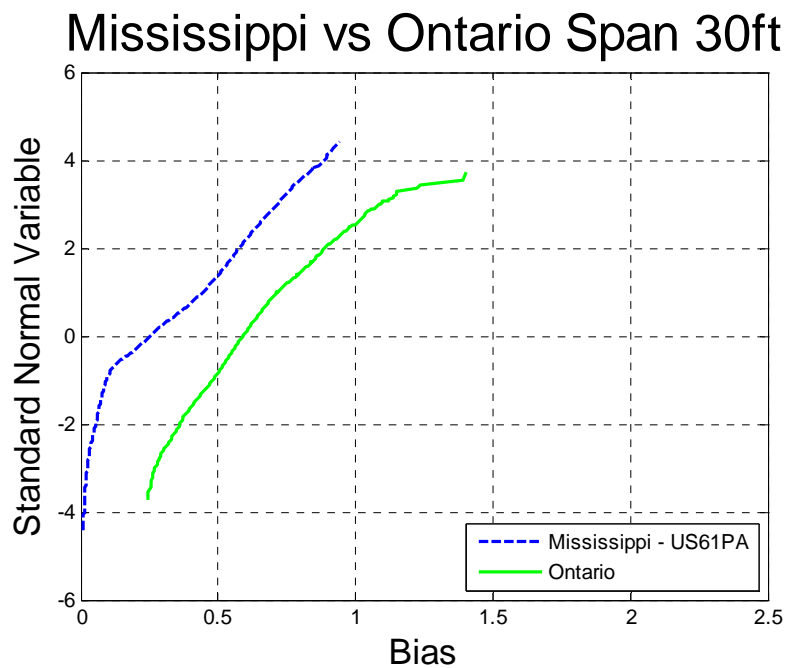
Mississippi vs Ontario Span 200ft



0-222 Comparison of Shear – Mississippi – US49PA vs. Ontario – Span 200ft

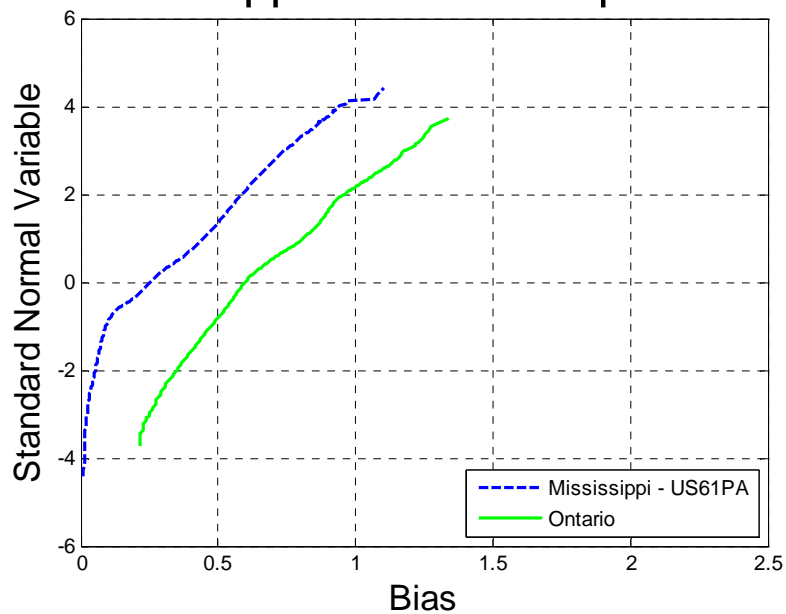


0-223 Cumulative Distribution Functions of Shear – Mississippi – US61PA



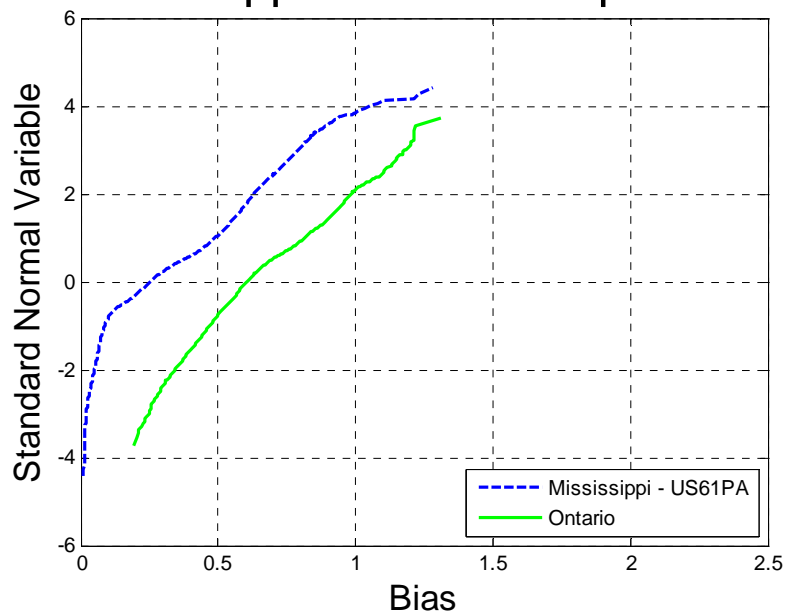
0-224 Comparison of Shear – Mississippi – US61PA vs. Ontario – Span 30ft

Mississippi vs Ontario Span 60ft



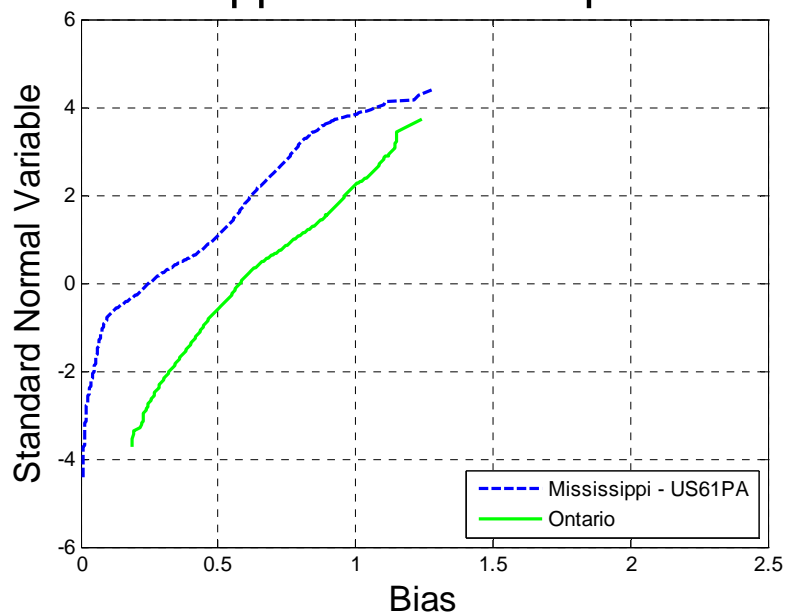
0-225 Comparison of Shear – Mississippi – US61PA vs. Ontario – Span 60ft

Mississippi vs Ontario Span 90ft



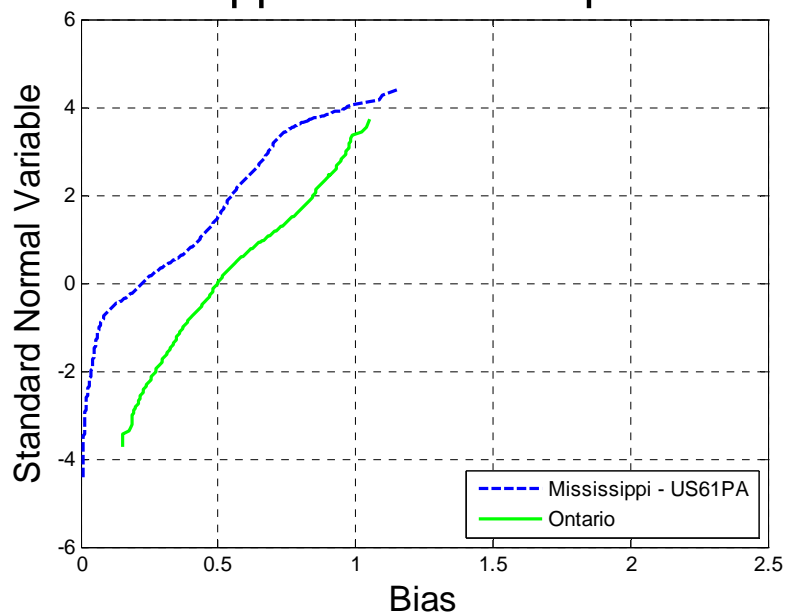
0-226 Comparison of Shear – Mississippi – US61PA vs. Ontario – Span 90ft

Mississippi vs Ontario Span 120ft



0-227 Comparison of Shear – Mississippi – US61PA vs. Ontario – Span 120ft

Mississippi vs Ontario Span 200ft



0-228 Comparison of Shear – Mississippi – US61PA vs. Ontario – Span 200ft

California – Live Load Effect

WIM data for California

The truck survey includes weigh-in-motion (WIM) truck measurements obtained from NCHRP project. The data includes 12 months of traffic recorded at different locations. The total number of records is shown in Table 62. The data includes number of axles, gross vehicle weight (GVW), weight per axle and spacing between axles.

Table 62

Site	Number of Trucks
Antelope EB 003	693,339
Antelope WB 004	766,188
Bowman 072	486,084
LA710 NB 060	2,987,141
LA710 SB 059	3,343,151
Lodi 001	2,556,978
TOTAL	10,832,881

Maximum Simple Span Moments

The maximum moment was calculated for each truck from the data. Analysis included simple spans with the span varying from 30 to 200 ft. The maximum moment was also calculated for the HL93 load and Tandem. Ratio between data truck moment and code load moment was plotted on the probability paper.

California - Antelope EB

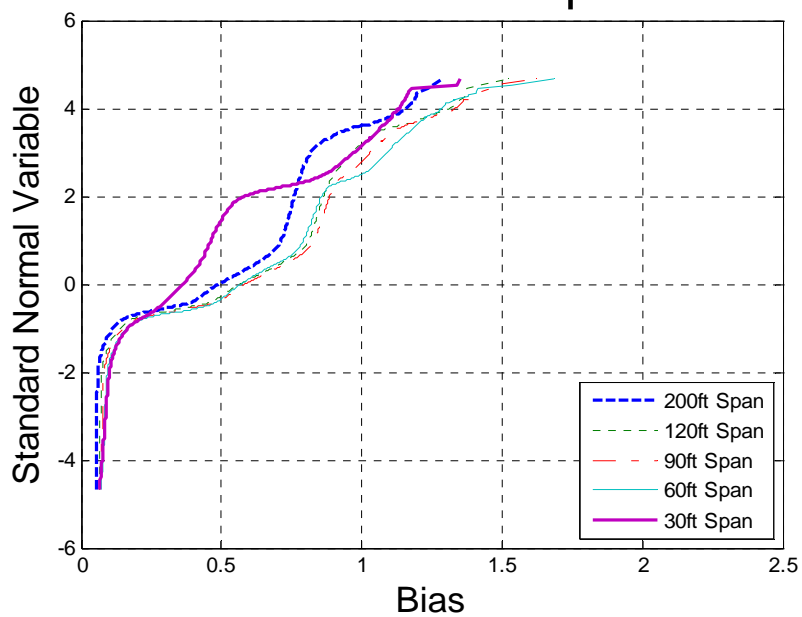


Figure 0-229 Cumulative Distribution Functions of Simple Span Moment – California – Antelope EB

California vs Ontario Span 30ft

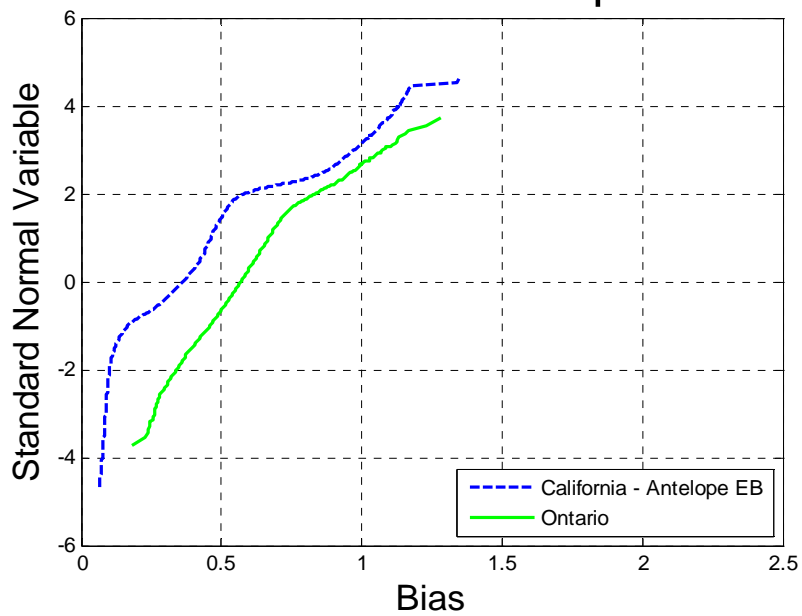


Figure 0-230 Comparison of Simple Span Moment – California – Antelope EB vs.
Ontario – Span 30ft

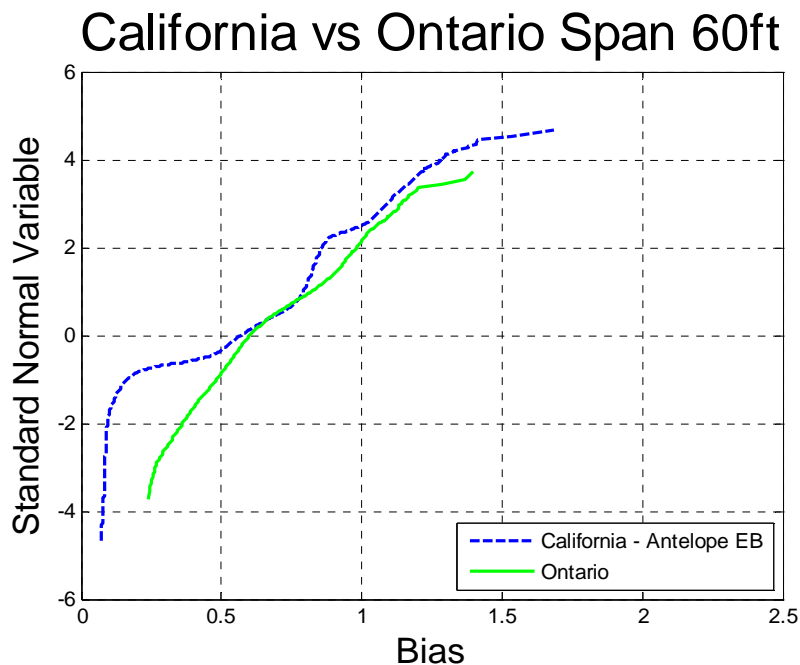


Figure 0-231 Comparison of Simple Span Moment – California – Antelope EB vs.
Ontario – Span 60ft

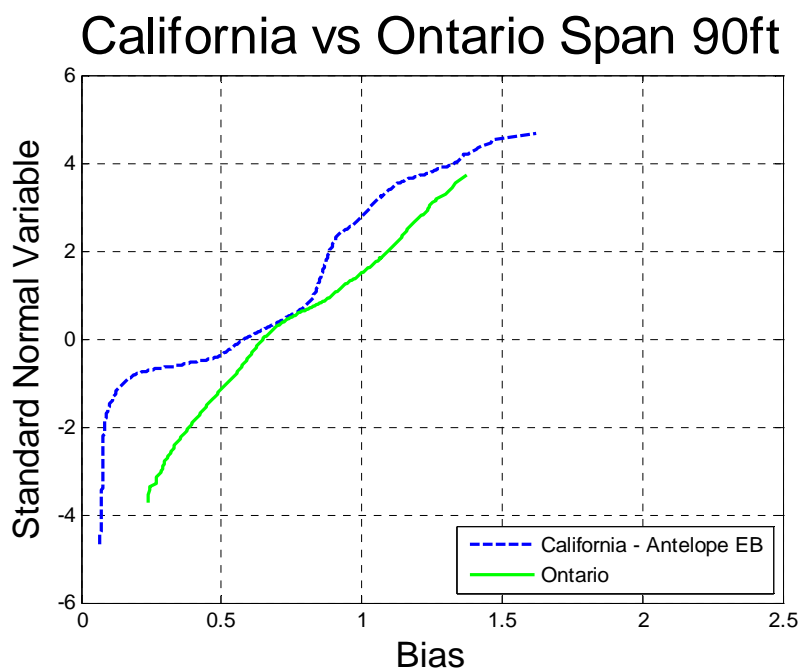


Figure 0-232 Comparison of Simple Span Moment – California – Antelope EB vs.
Ontario – Span 90ft

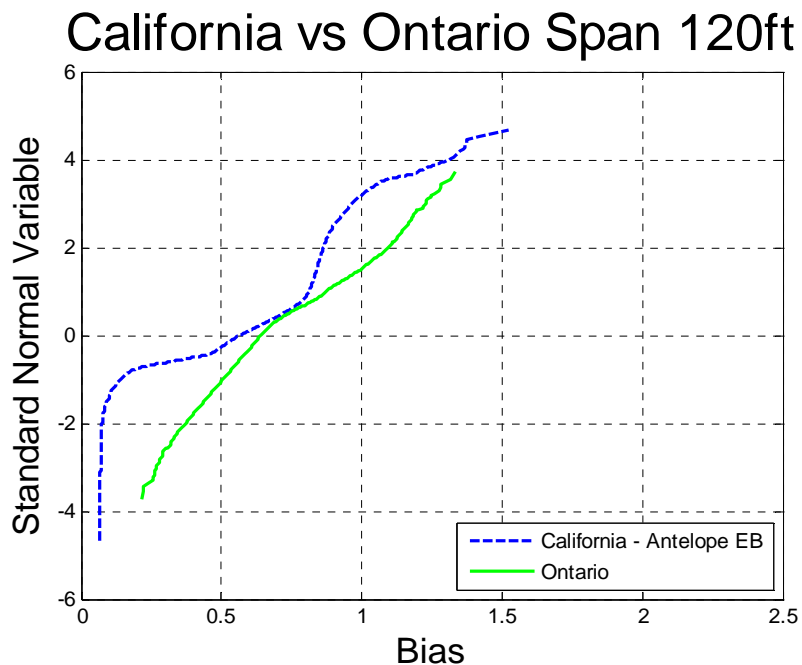


Figure 0-233 Comparison of Simple Span Moment – California – Antelope EB vs.
Ontario – Span 120ft

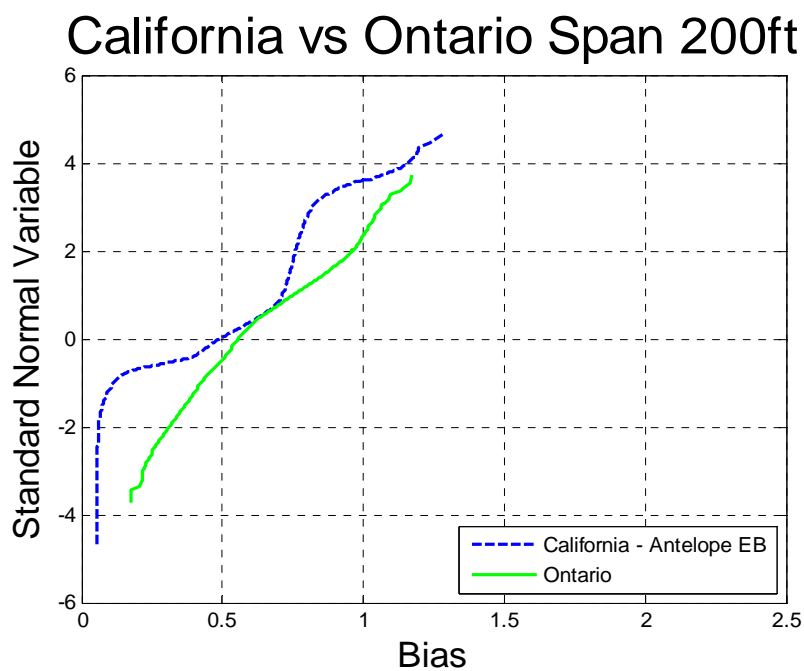


Figure 0-234 Comparison of Simple Span Moment – California – Antelope EB vs. Ontario – Span 200ft

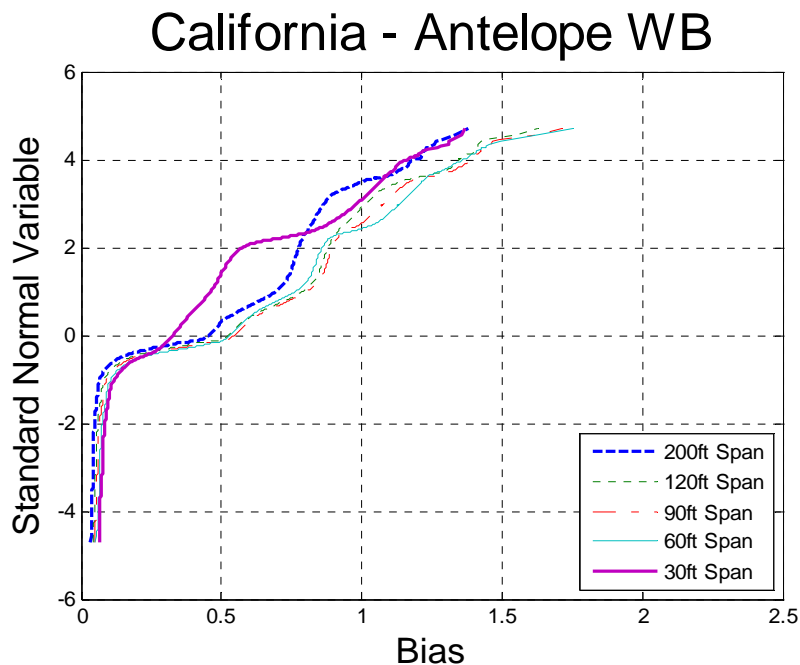


Figure 0-235 Cumulative Distribution Functions of Simple Span Moment – California – Antelope WB

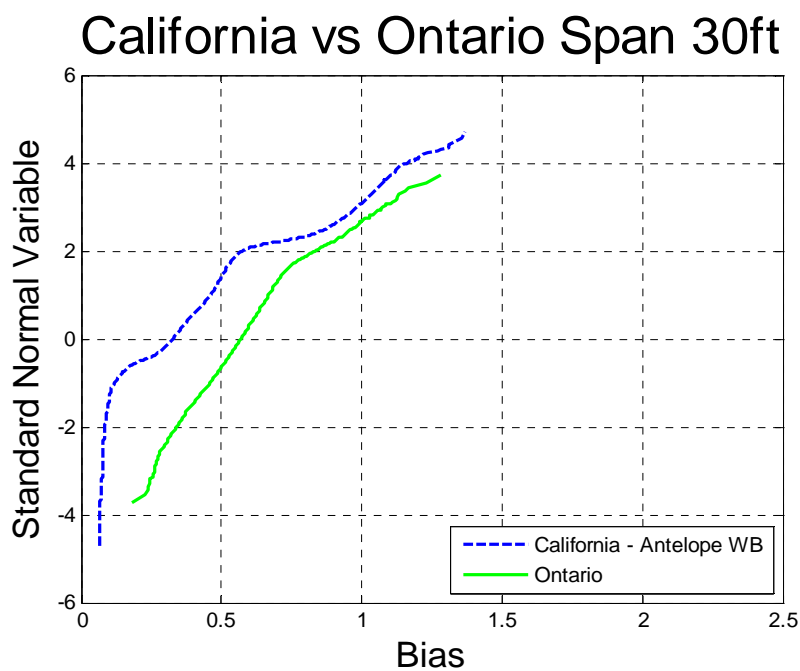


Figure 0-236 Comparison of Simple Span Moment – California – Antelope WB vs.
Ontario – Span 30ft

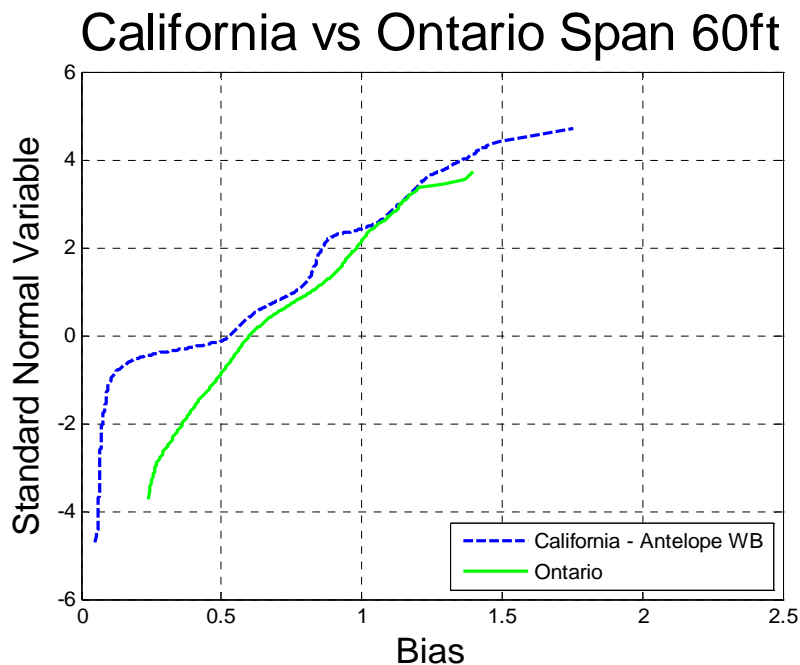


Figure 0-237 Comparison of Simple Span Moment – California – Antelope WB vs.
Ontario – Span 60ft

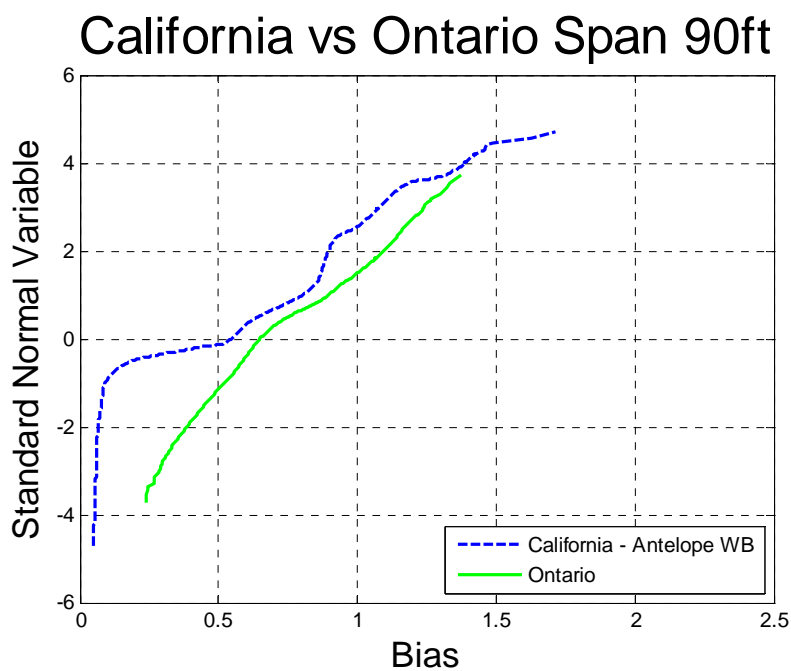


Figure 0-238 Comparison of Simple Span Moment – California – Antelope WB vs.
Ontario – Span 90ft

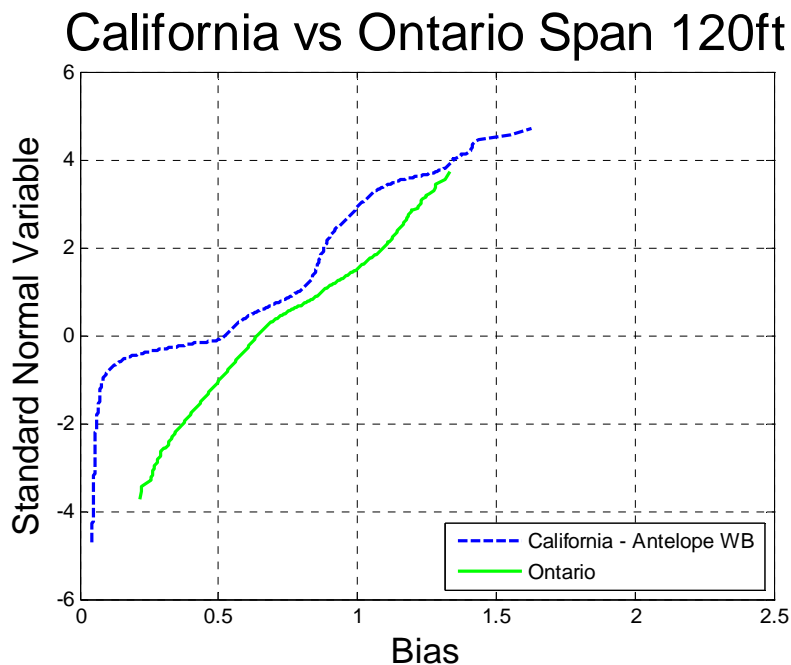


Figure 0-239 Comparison of Simple Span Moment – California – Antelope WB vs.
Ontario – Span 120ft

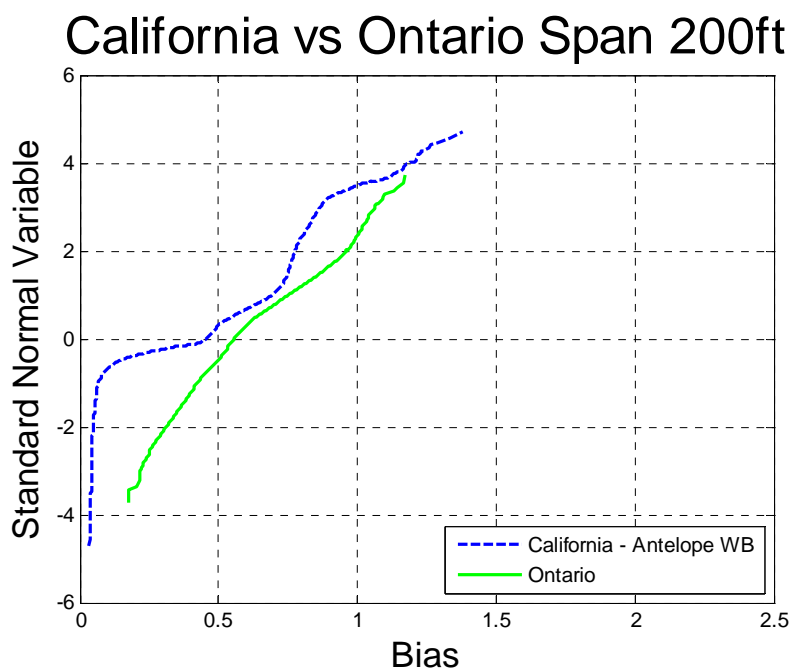


Figure 0-240 Comparison of Simple Span Moment – California – Antelope WB vs. Ontario – Span 200ft

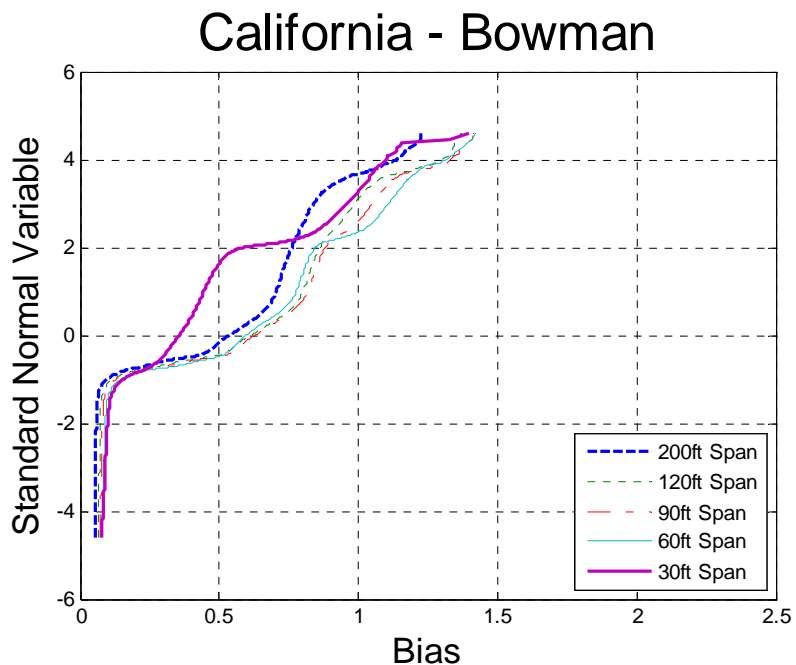


Figure 0-241 Cumulative Distribution Functions of Simple Span Moment – California – Bowman

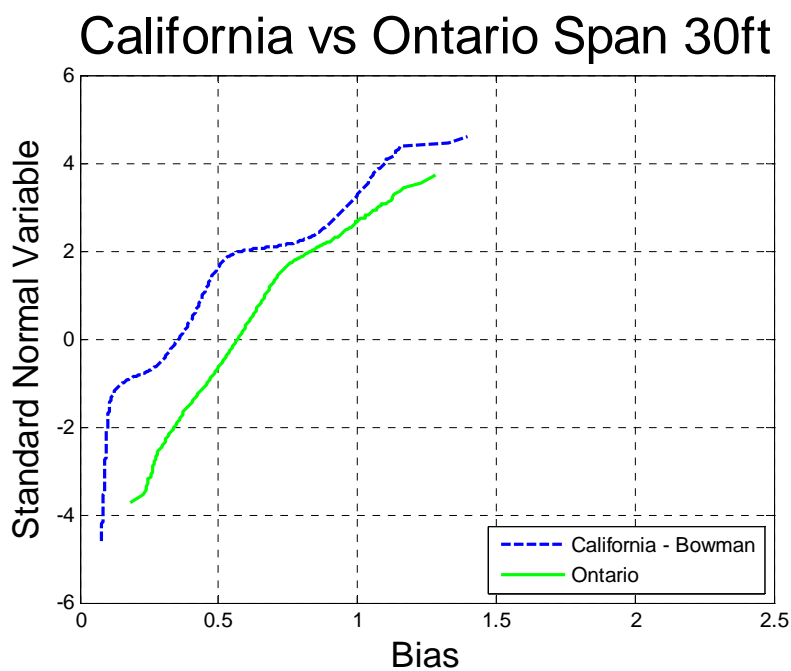


Figure 0-242 Comparison of Simple Span Moment – California – Bowman vs. Ontario –
Span 30ft

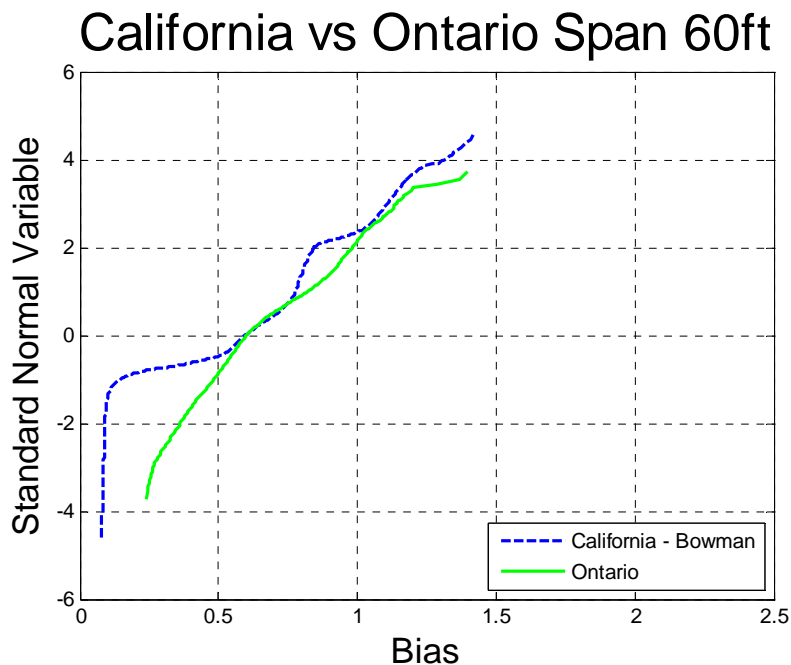


Figure 0-243 Comparison of Simple Span Moment – California – Bowman vs. Ontario –
Span 60ft

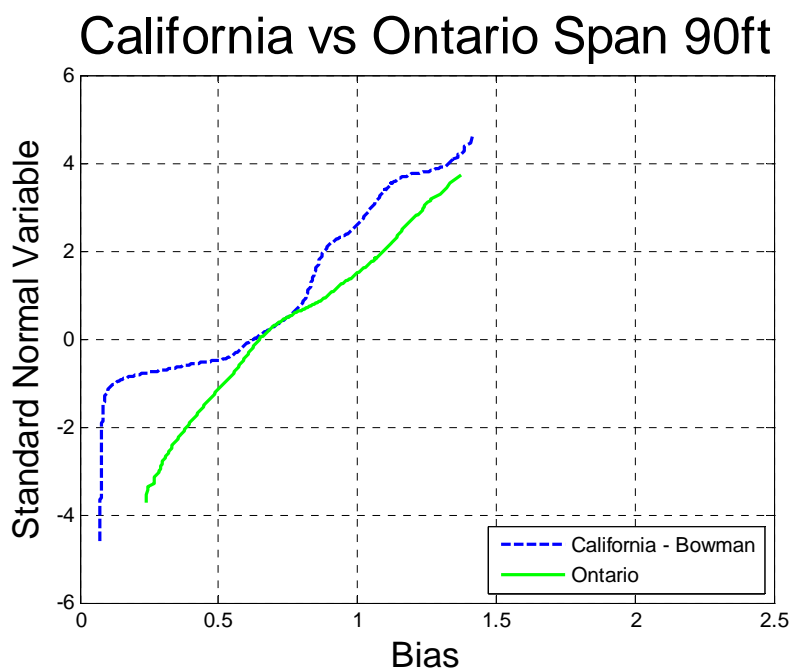


Figure 0-244 Comparison of Simple Span Moment – California – Bowman vs. Ontario –
Span 90ft

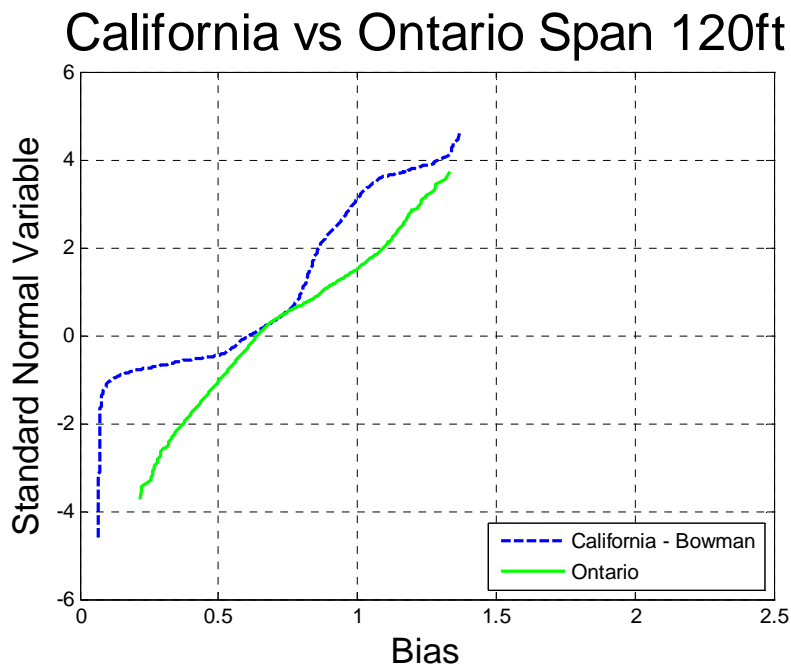


Figure 0-245 Comparison of Simple Span Moment – California – Bowman vs. Ontario –
Span 120ft

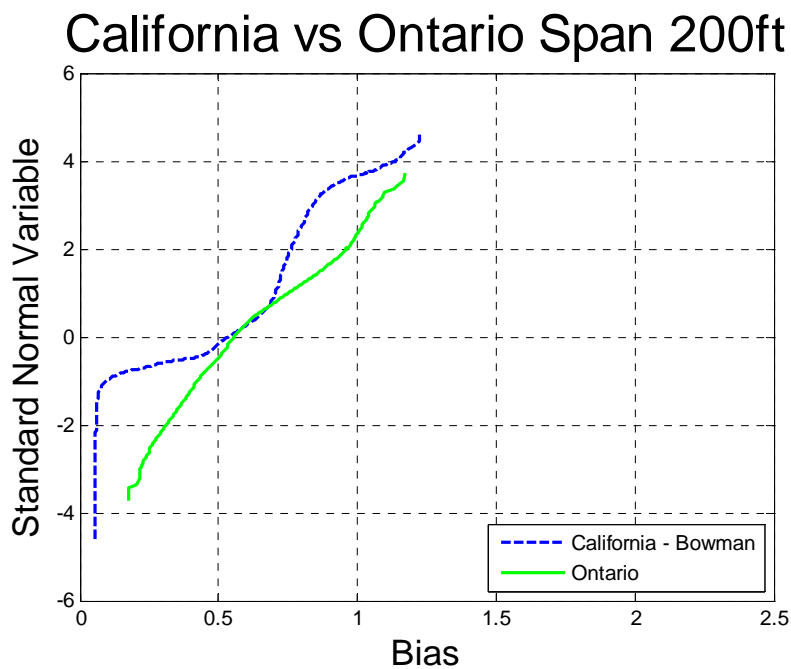


Figure 0-246 Comparison of Simple Span Moment – California – Bowman vs. Ontario –
Span 200ft

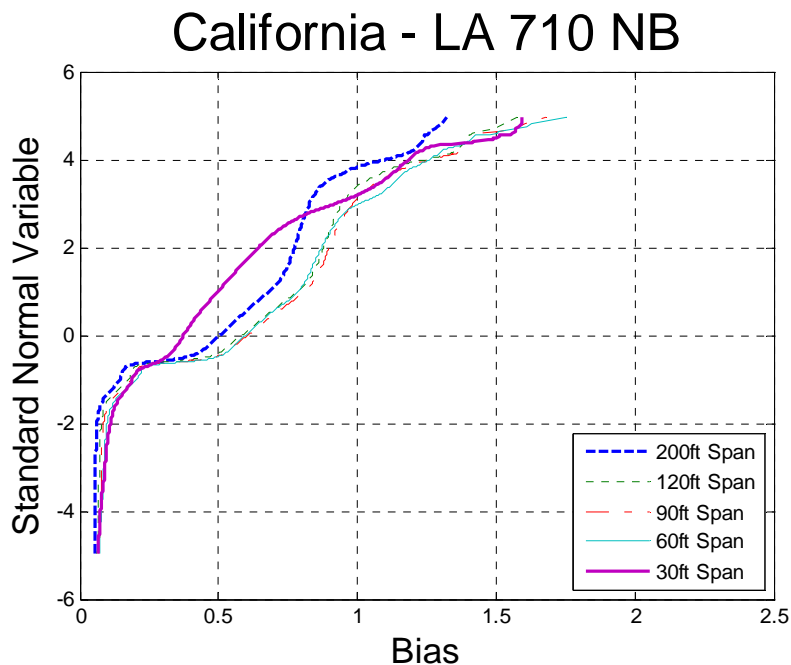


Figure 0-247 Cumulative Distribution Functions of Simple Span Moment – California –
LA710 NB

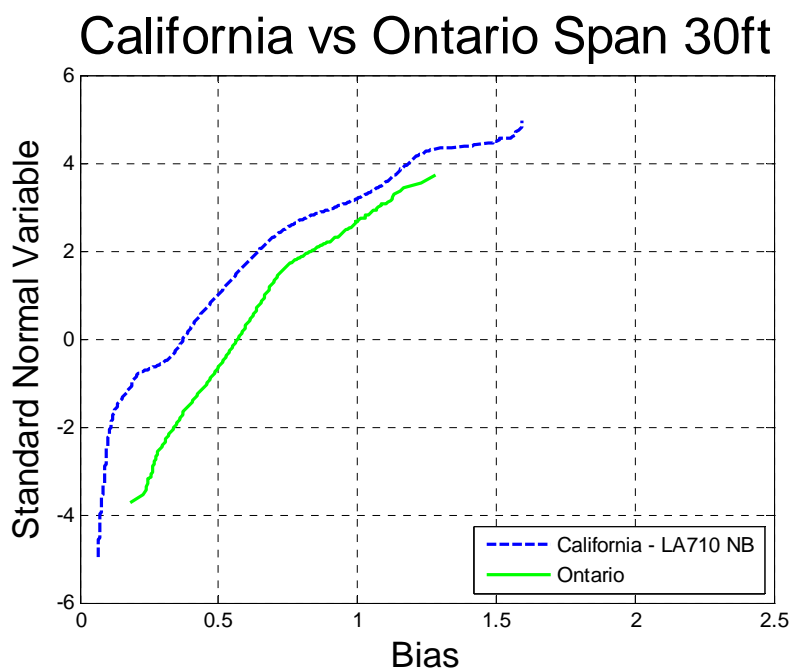


Figure 0-248 Comparison of Simple Span Moment – California – LA710 NB vs. Ontario
– Span 30ft

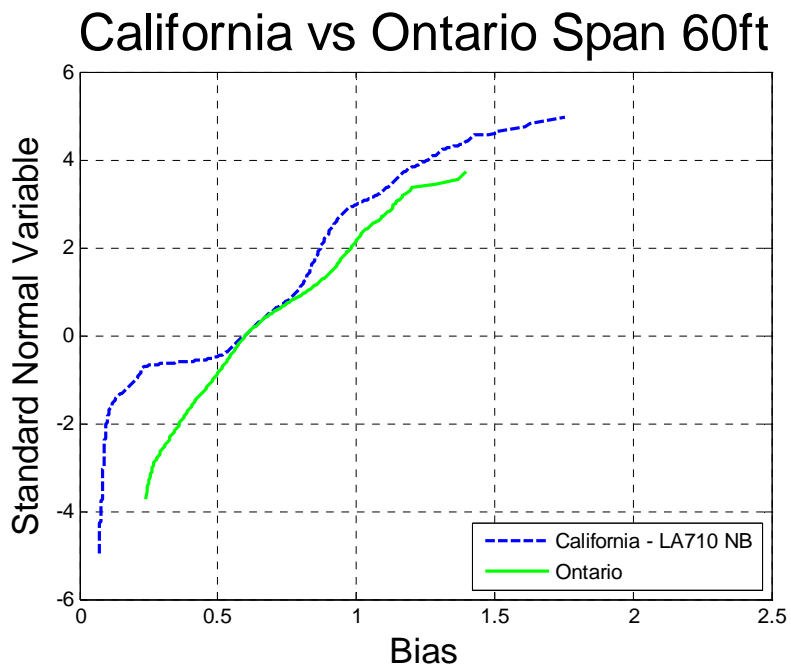


Figure 0-249 Comparison of Simple Span Moment – California – LA710 NB vs. Ontario
– Span 60ft

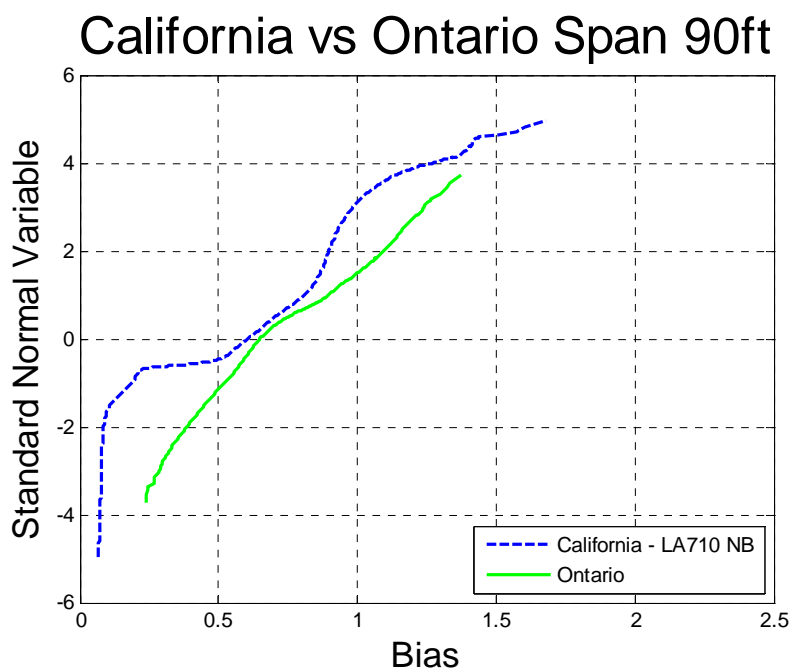


Figure 0-250 Comparison of Simple Span Moment – California – LA710 NB vs. Ontario
– Span 90ft

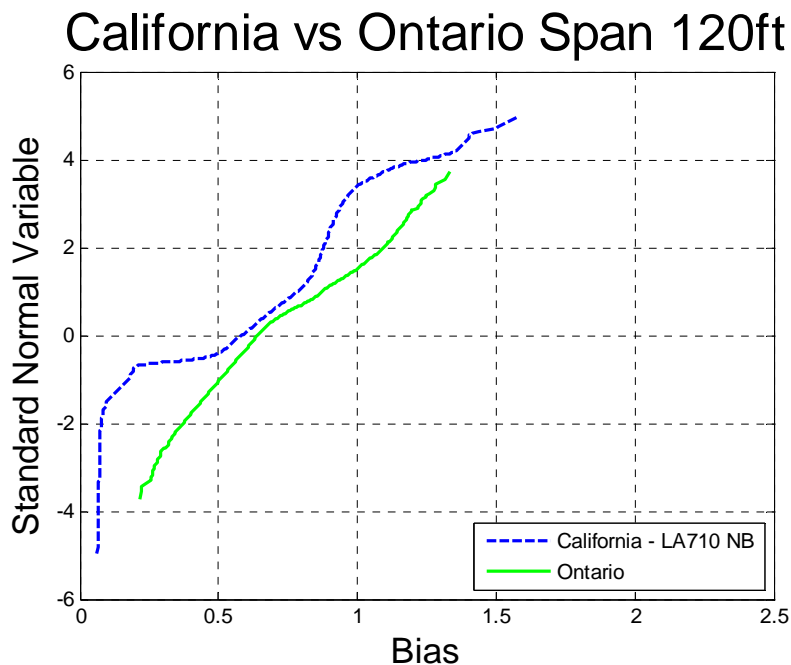


Figure 0-251 Comparison of Simple Span Moment – California – LA710 NB vs. Ontario
– Span 200ft

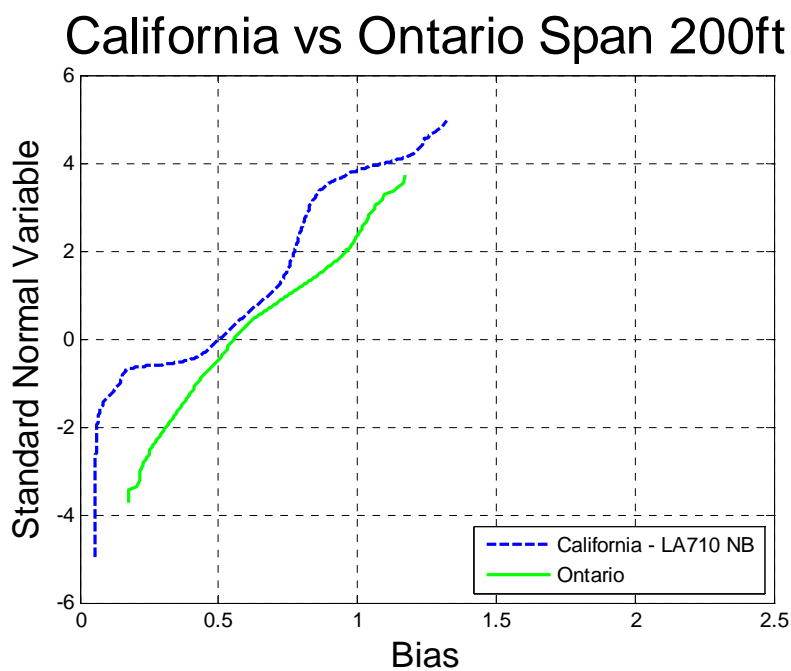


Figure 0-252 Comparison of Simple Span Moment – California – LA710 NB vs. Ontario
– Span 200ft

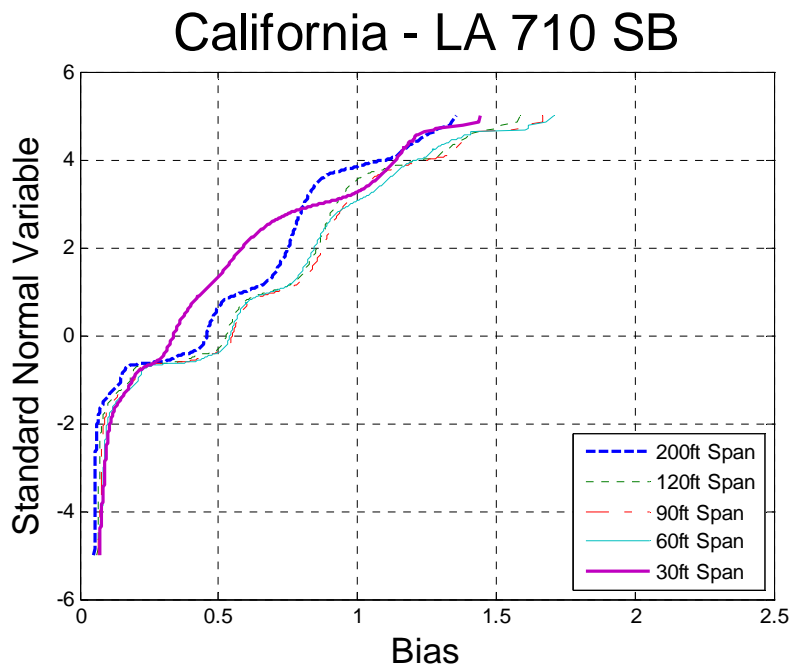


Figure 0-253 Cumulative Distribution Functions of Simple Span Moment – California –
LA710 SB

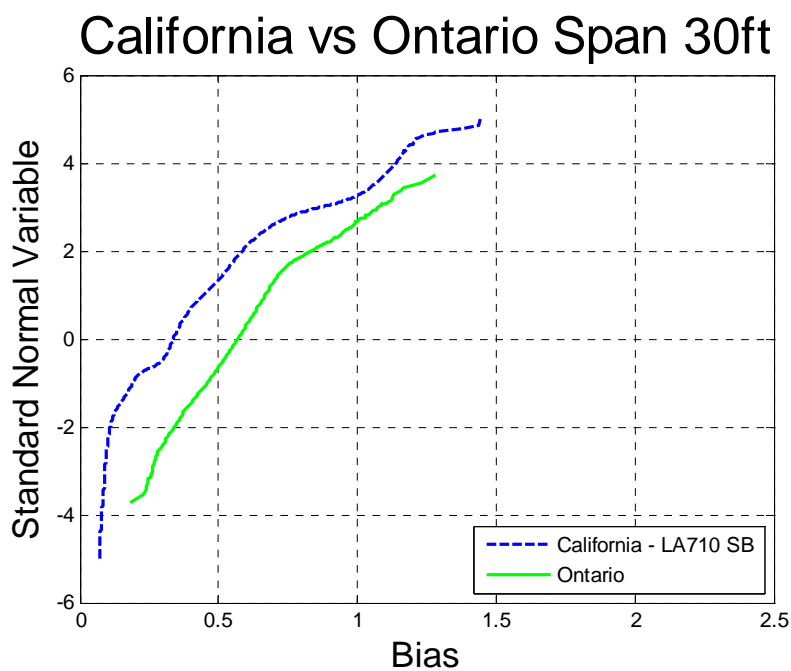


Figure 0-254 Comparison of Simple Span Moment – California – LA710 SB vs. Ontario
– Span 30ft

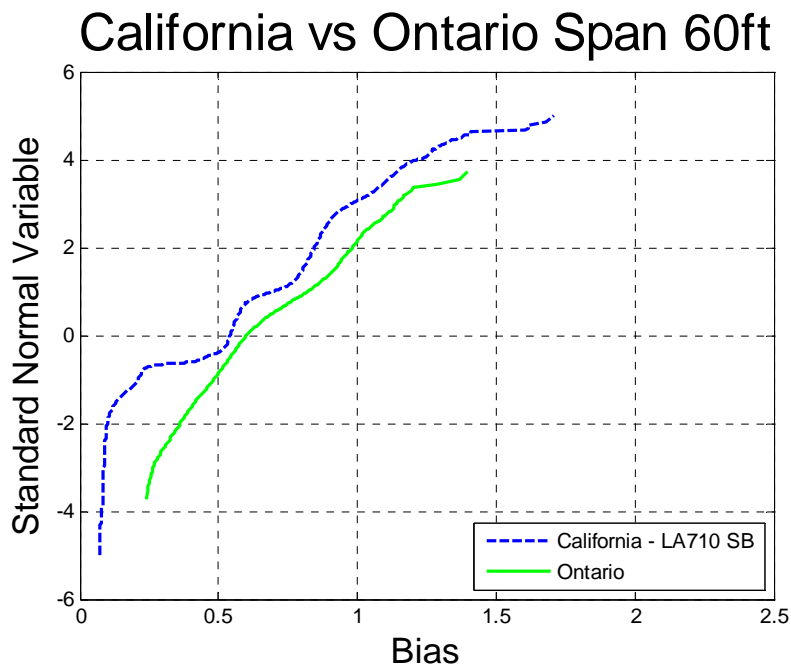


Figure 0-255 Comparison of Simple Span Moment – California – LA710 SB vs. Ontario
– Span 60ft

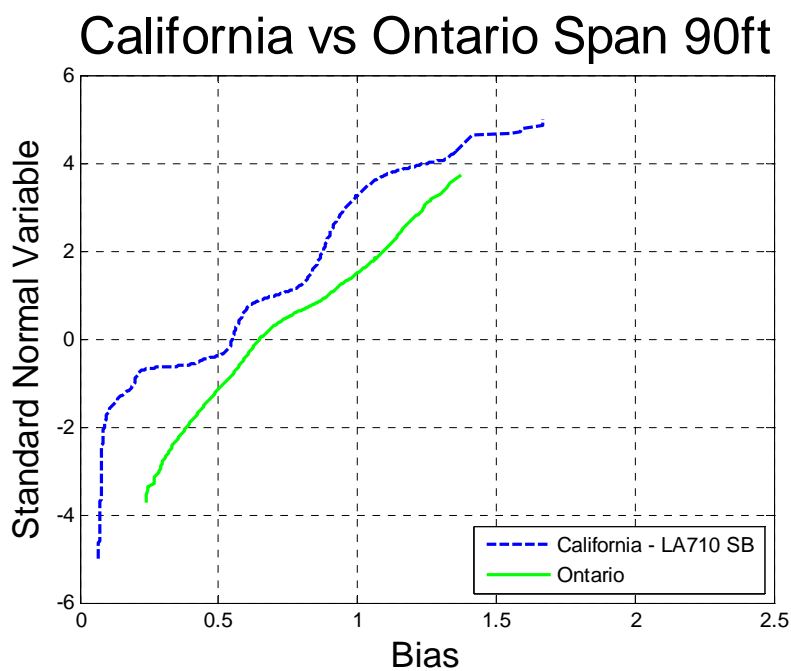


Figure 0-256 Comparison of Simple Span Moment – California – LA710 SB vs. Ontario
– Span 90ft

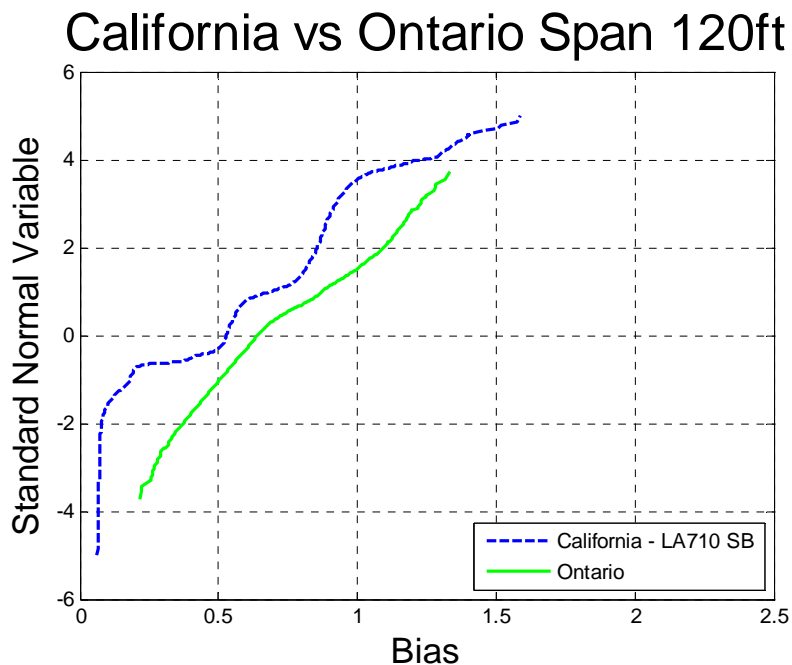


Figure 0-257 Comparison of Simple Span Moment – California – LA710 SB vs. Ontario
– Span 120ft

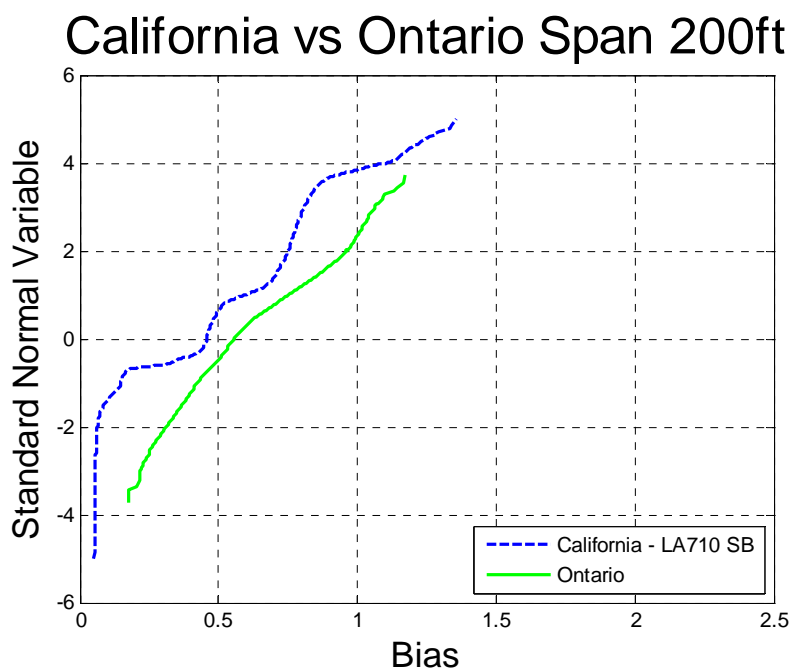


Figure 0-258 Comparison of Simple Span Moment – California – LA710 SB vs. Ontario
– Span 200ft

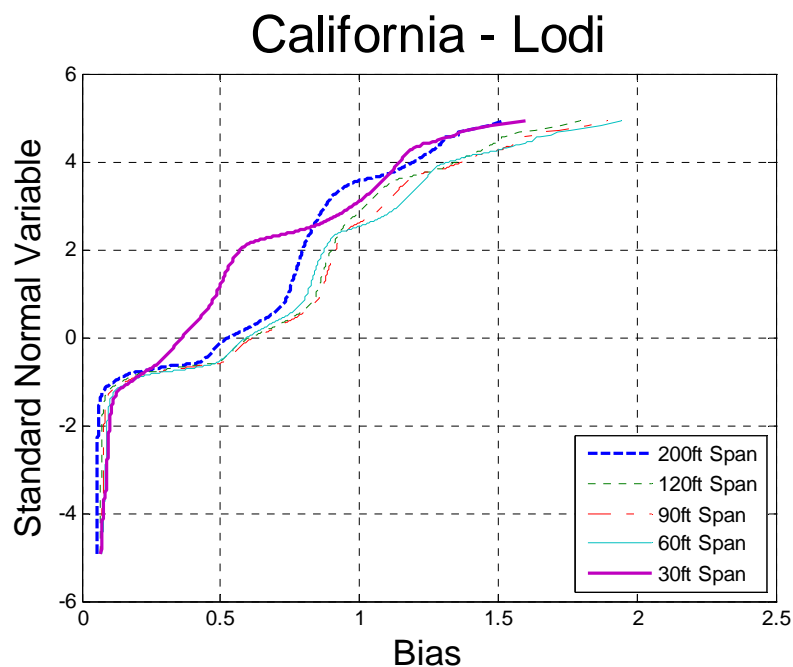


Figure 0-259 Cumulative Distribution Functions of Simple Span Moment – California –
Lodi

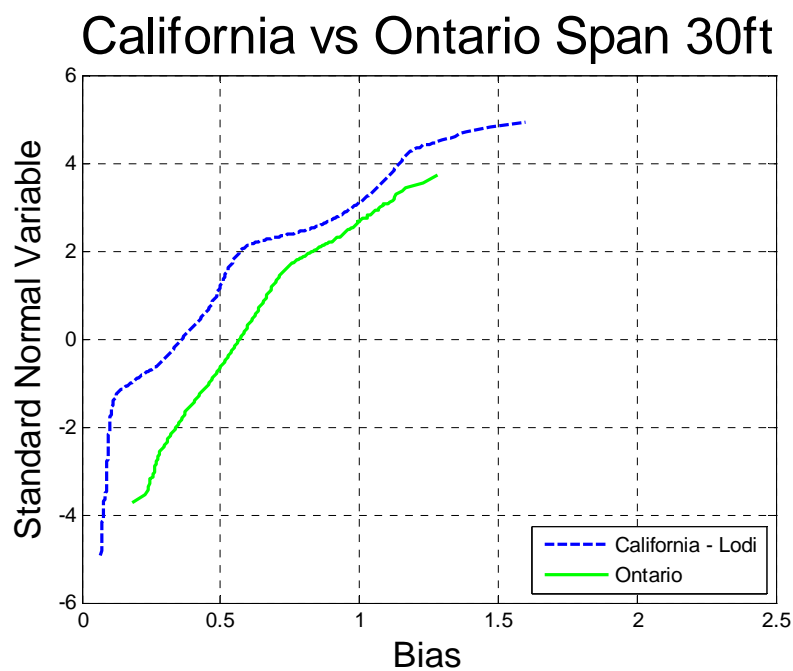


Figure 0-260 Comparison of Simple Span Moment – California – Lodi vs. Ontario –
Span 30ft

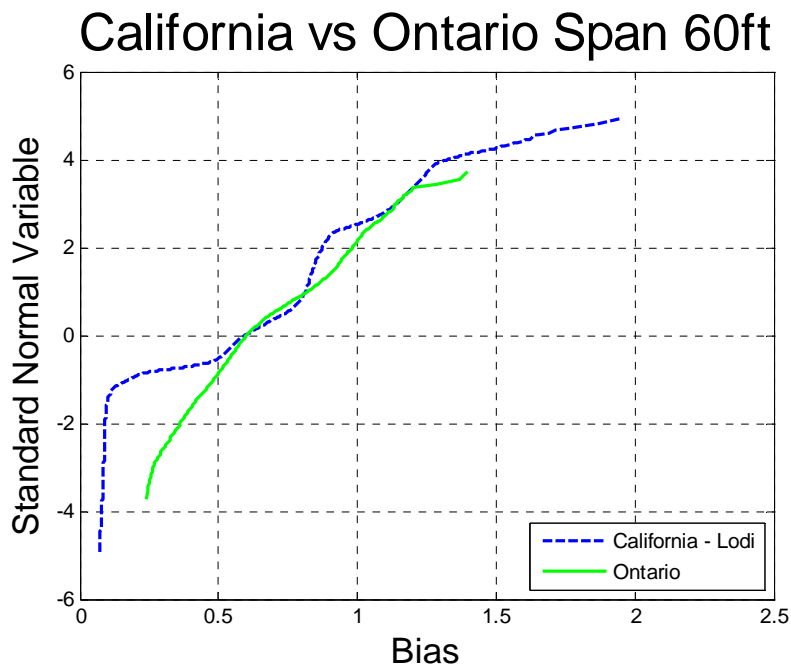


Figure 0-261 Comparison of Simple Span Moment – California – Lodi vs. Ontario –
Span 60ft

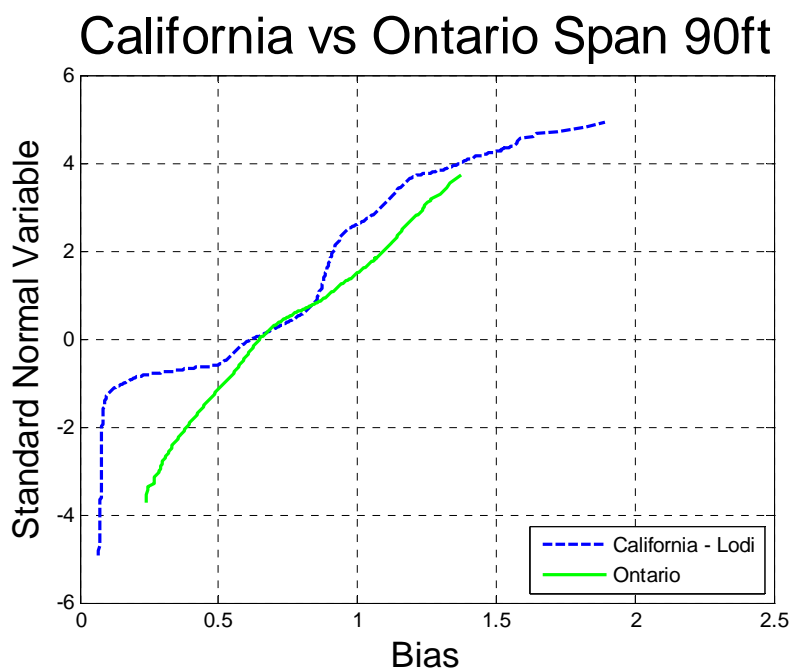


Figure 0-262 Comparison of Simple Span Moment – California – Lodi vs. Ontario –
Span 90ft

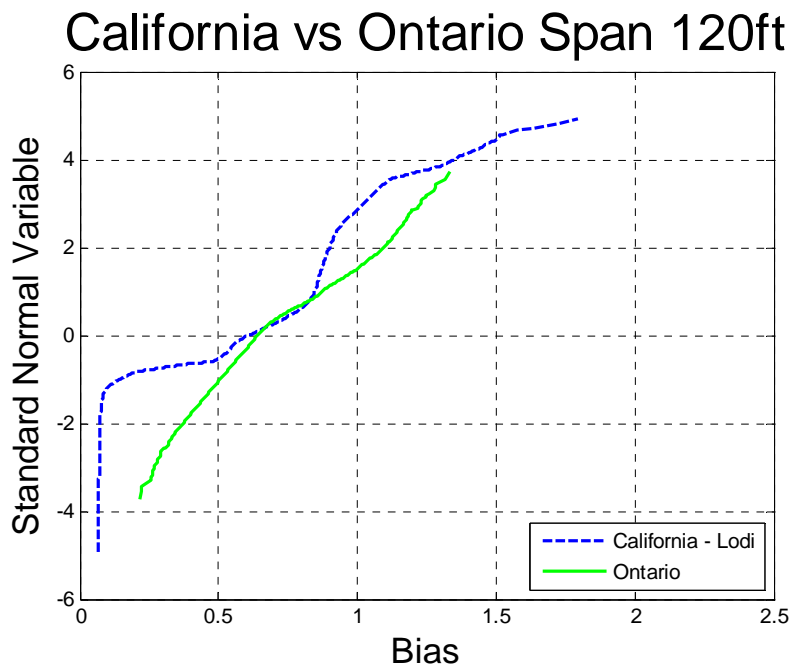


Figure 0-263 Comparison of Simple Span Moment – California – Lodi vs. Ontario –
Span 120ft

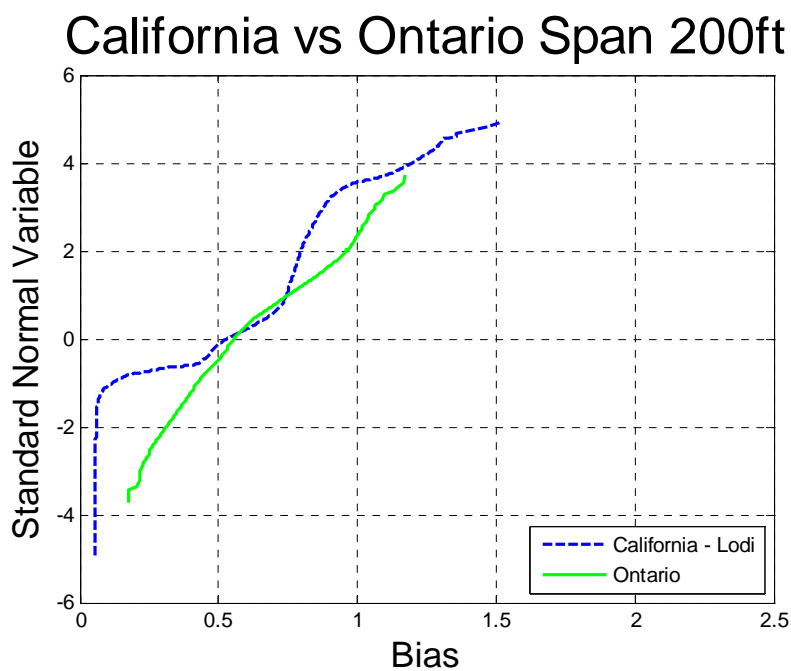


Figure 0-264 Comparison of Simple Span Moment – California – Lodi vs. Ontario – Span 200f

Maximum Shear

The maximum shear was calculated for each truck from the data. Analysis included simple spans with the span varying from 30 to 200 ft. The ratio of shear obtained from the data truck and the HL-93 load was plotted on the probability paper.

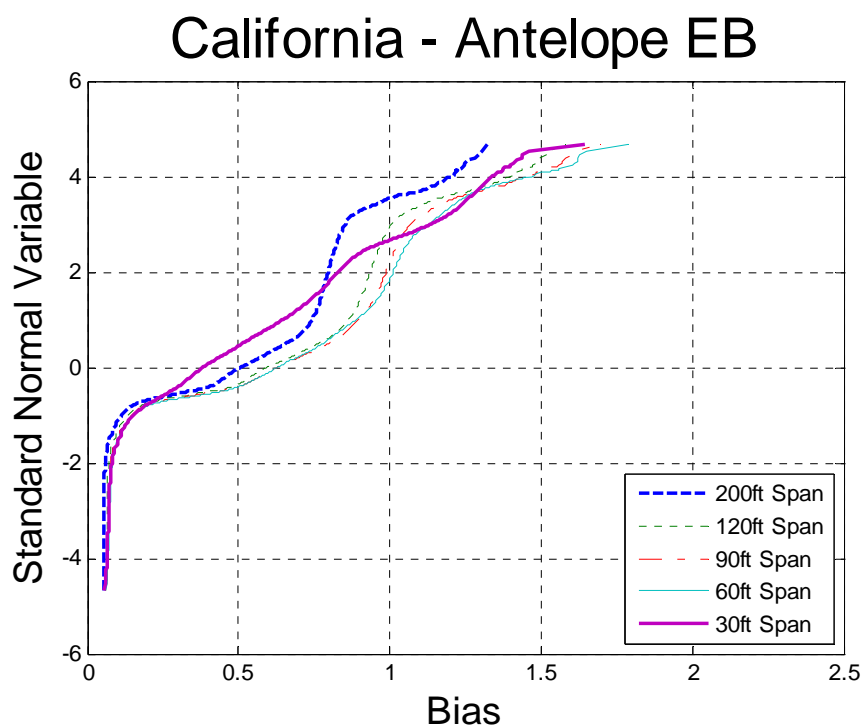


Figure 0-265 Cumulative Distribution Functions of Shear – California – Antelope EB

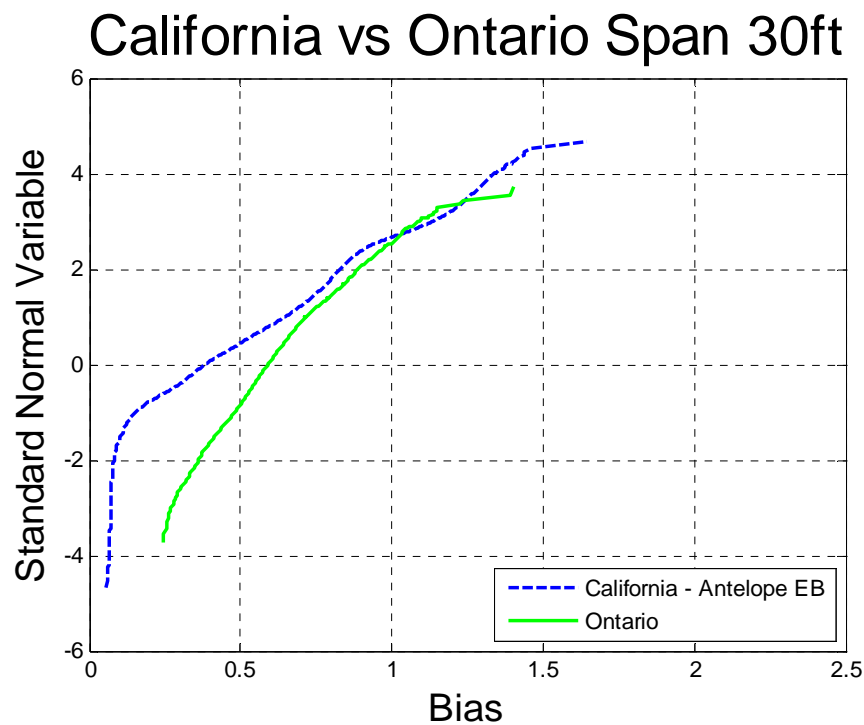


Figure 0-266 Comparison of Shear – California – Antelope EB vs. Ontario – Span 30ft

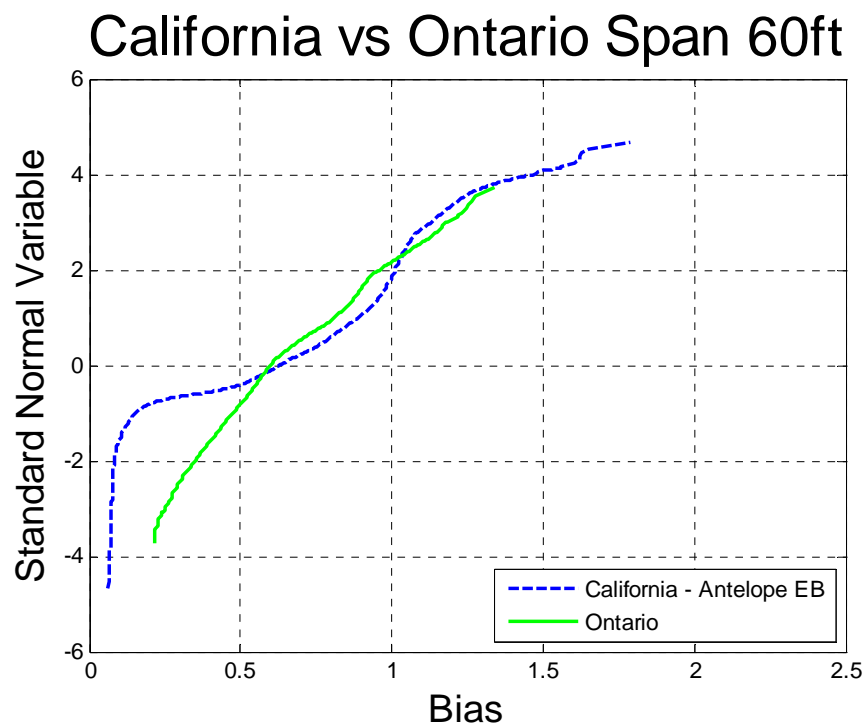


Figure 0-267 Comparison of Shear – California – Antelope EB vs. Ontario – Span 60ft

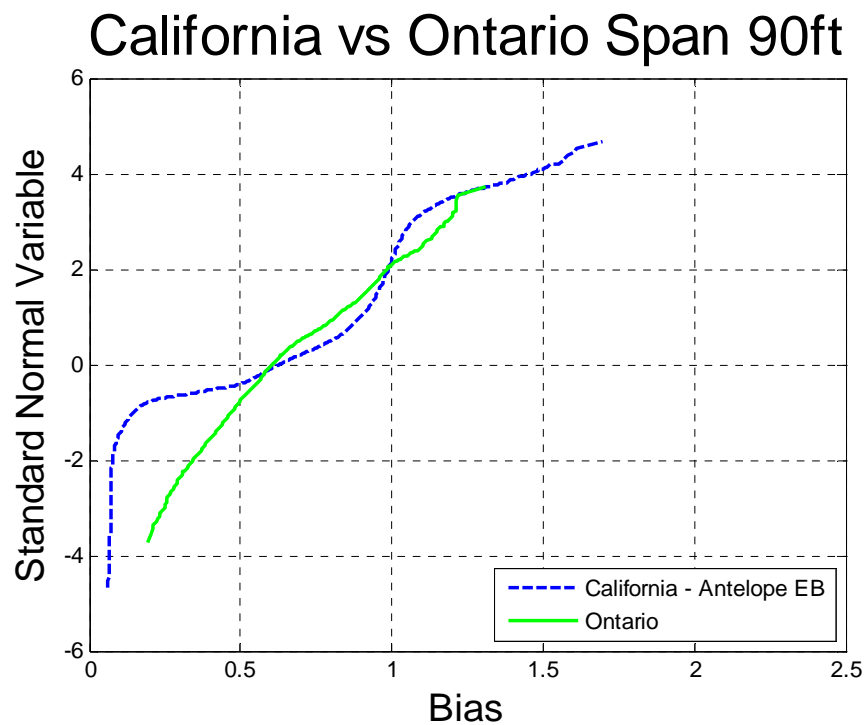


Figure 0-268 Comparison of Shear – California – Antelope EB vs. Ontario – Span 90ft

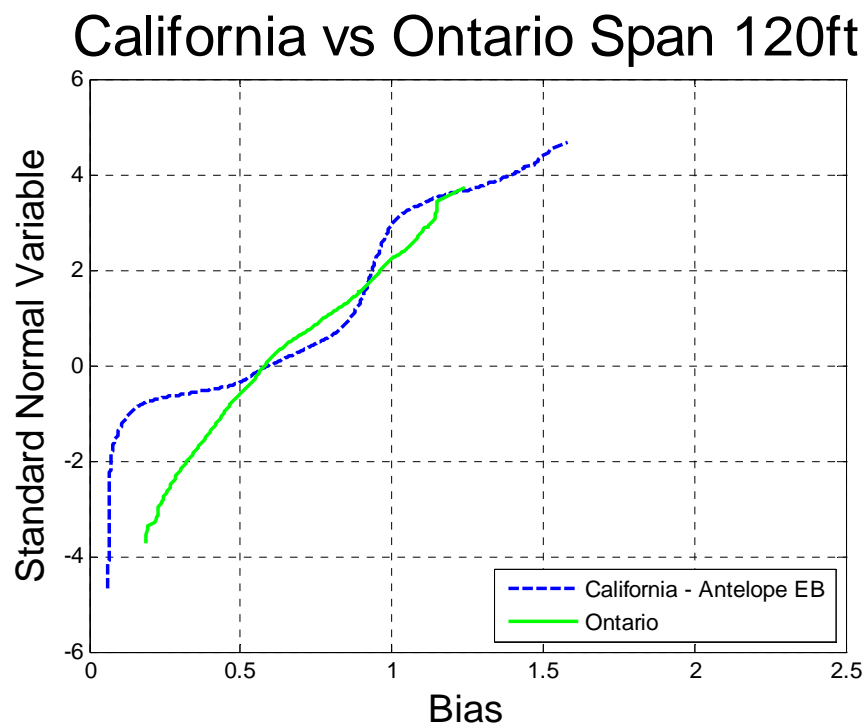


Figure 0-269 Comparison of Shear – California – Antelope EB vs. Ontario – Span 120ft

California vs Ontario Span 200ft

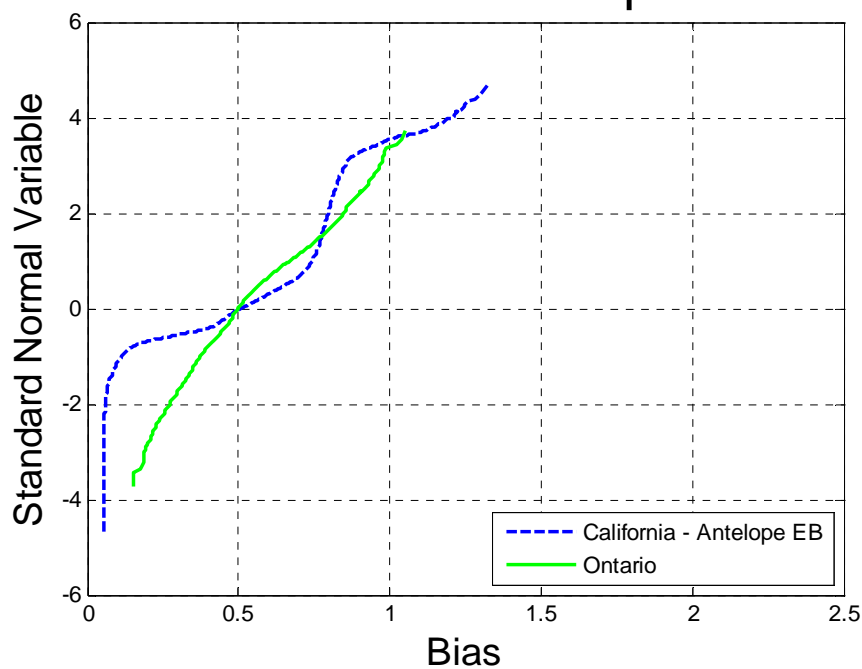


Figure 0-270 Comparison of Shear – California – Antelope EB vs. Ontario – Span 200ft

California - Antelope WB

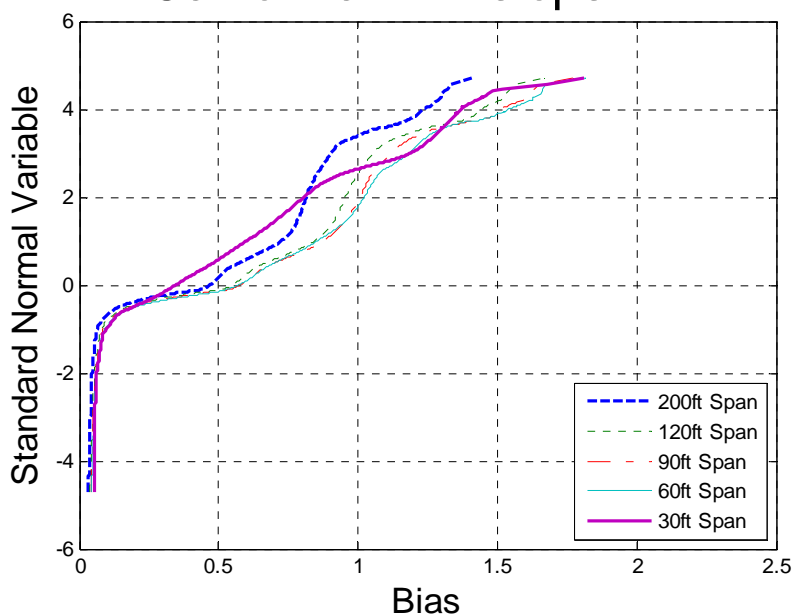


Figure 0-271 Cumulative Distribution Functions of Shear – California – Antelope WB

California vs Ontario Span 30ft

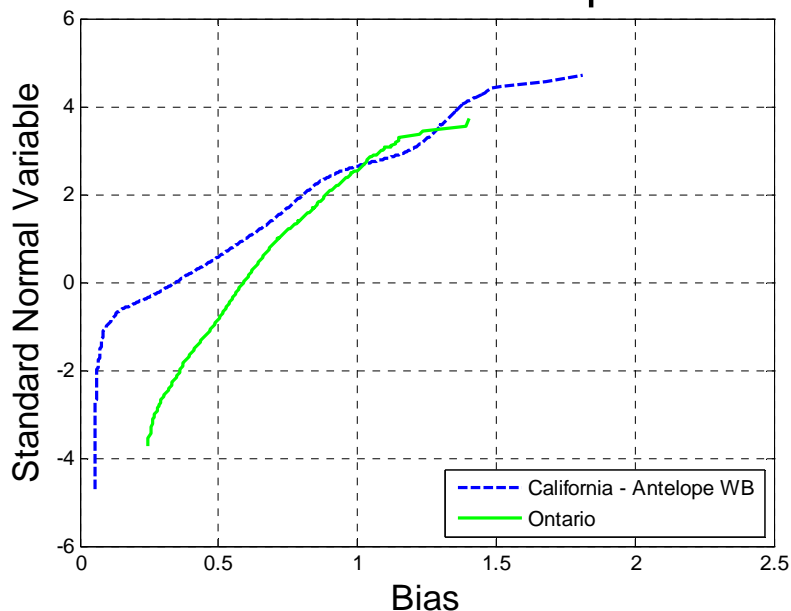


Figure 0-272 Comparison of Shear – California – Antelope WB vs. Ontario – Span 30ft

California vs Ontario Span 60ft

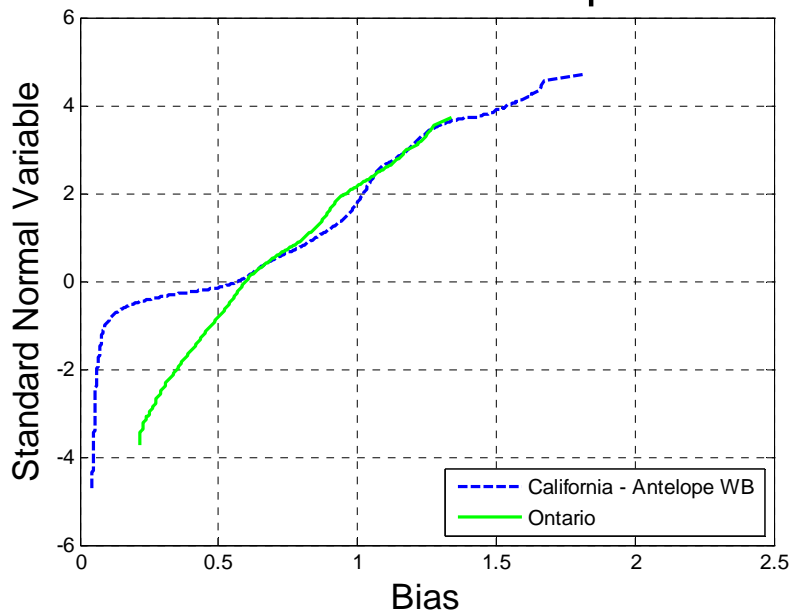


Figure 0-273 Comparison of Shear – California – Antelope WB vs. Ontario – Span 60ft

California vs Ontario Span 90ft

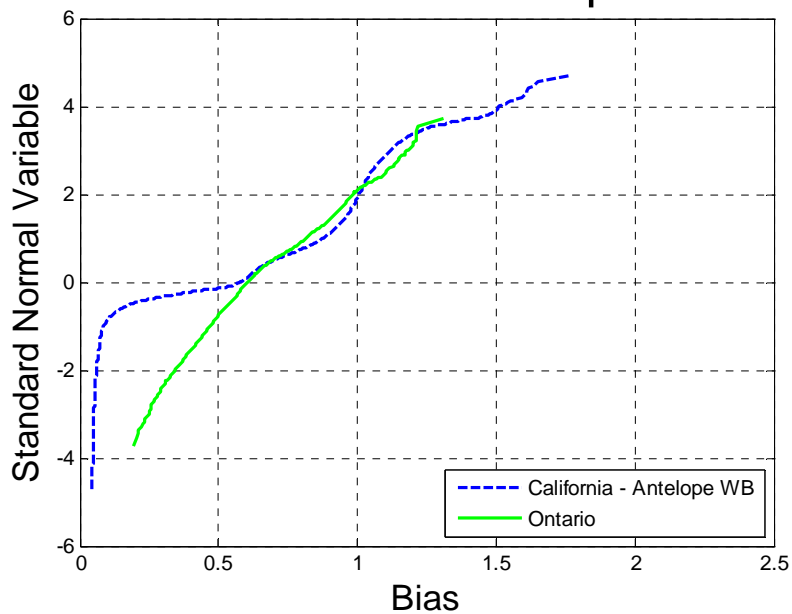


Figure 0-274 Comparison of Shear – California – Antelope WB vs. Ontario – Span 90ft

California vs Ontario Span 120ft

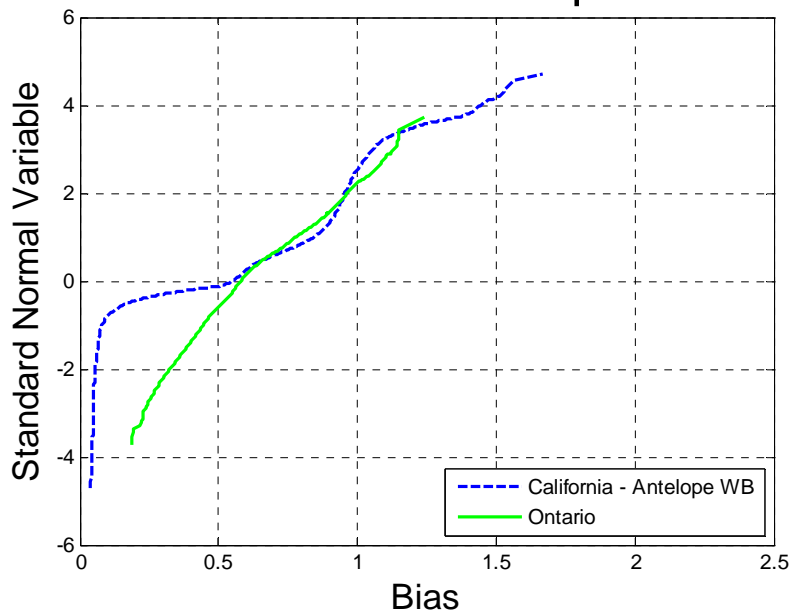


Figure 0-275 Comparison of Shear – California – Antelope WB vs. Ontario – Span 120ft

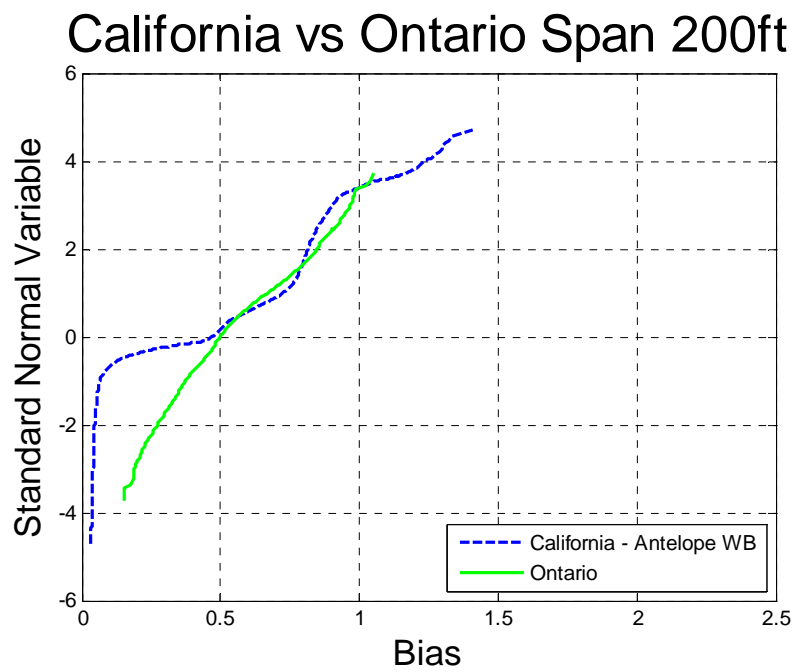


Figure 0-276 Comparison of Shear – California – Antelope WB vs. Ontario – Span 200ft

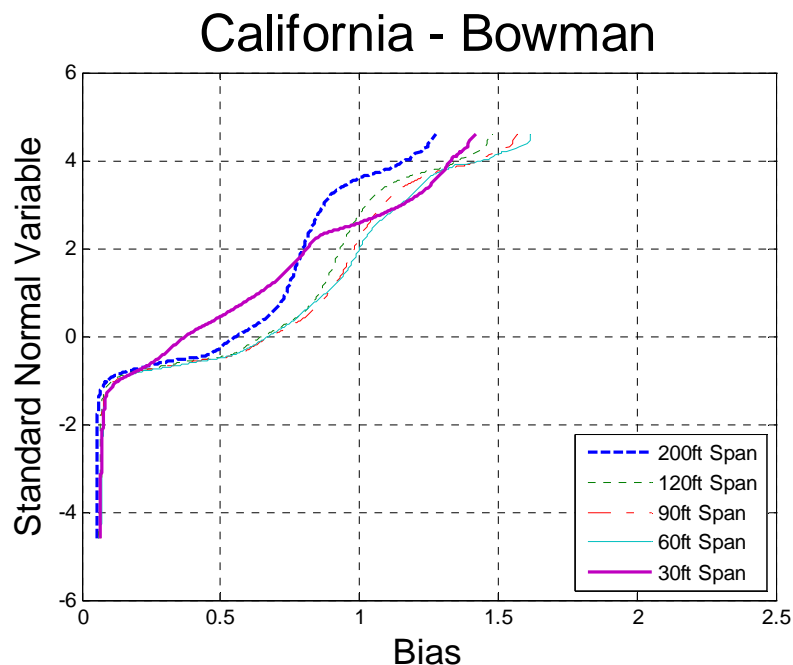


Figure 0-277 Cumulative Distribution Functions of Shear – California – Bowman

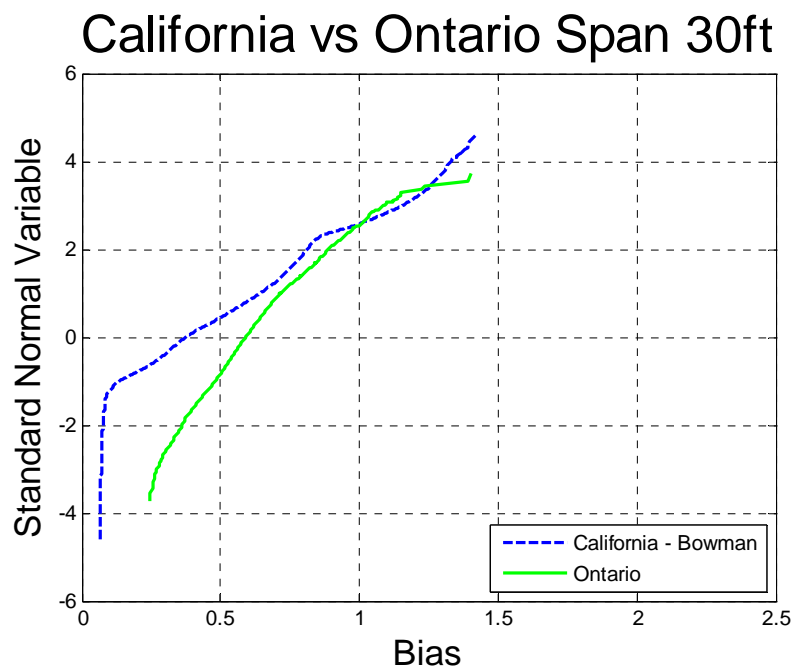


Figure 0-278 Comparison of Shear – California – Bowman vs. Ontario – Span 30ft

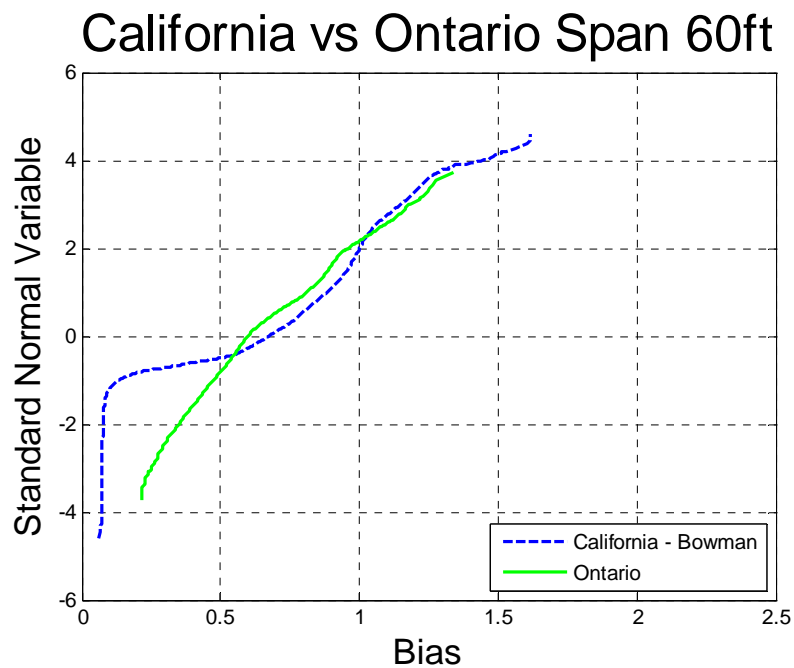


Figure 0-279 Comparison of Shear – California – Bowman vs. Ontario – Span 60ft

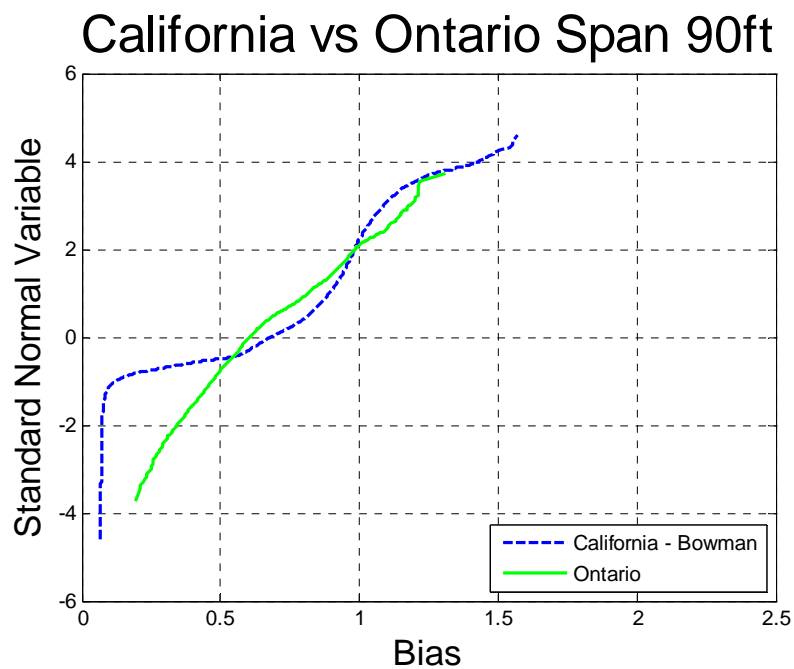


Figure 0-280 Comparison of Shear – California – Bowman vs. Ontario – Span 90ft

California vs Ontario Span 120ft

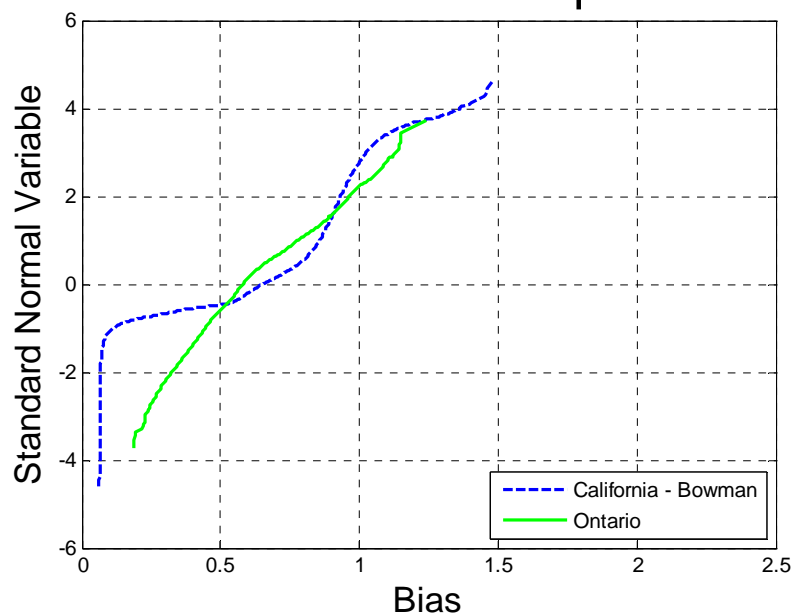


Figure 0-281 Comparison of Shear – California – Bowman vs. Ontario – Span 120ft

California vs Ontario Span 200ft

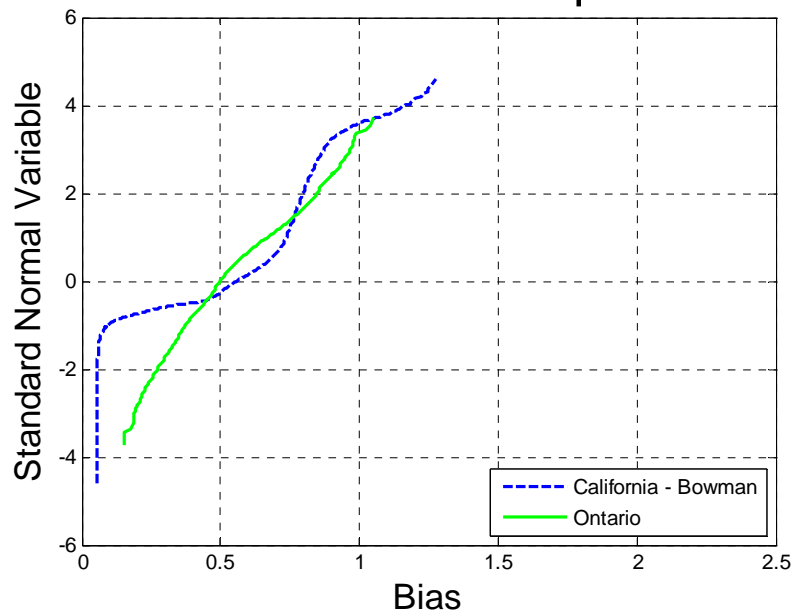


Figure 0-282 Comparison of Shear – California – Bowman vs. Ontario – Span 200ft

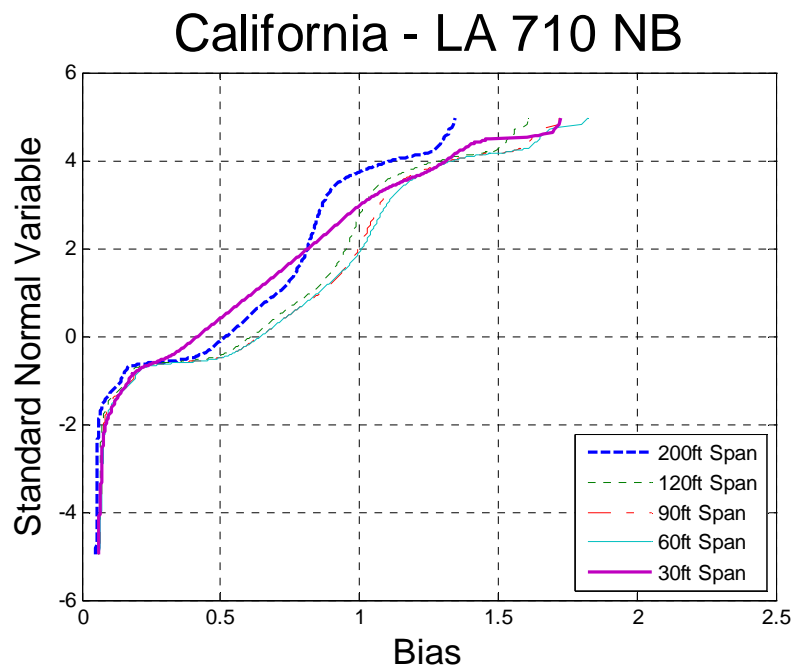


Figure 0-283 Cumulative Distribution Functions of Shear – California – LA710 NB

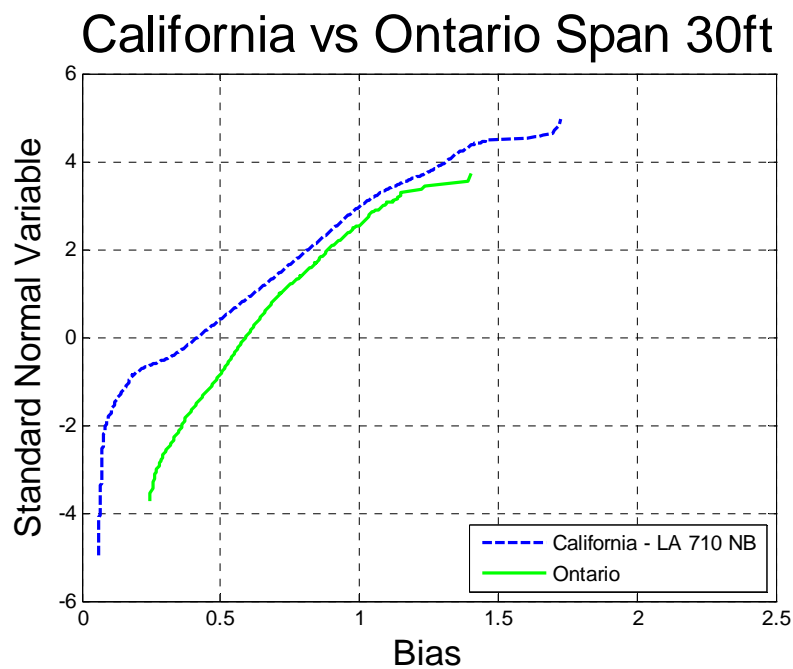


Figure 0-284 Comparison of Shear – California – LA710 NB vs. Ontario – Span 30ft

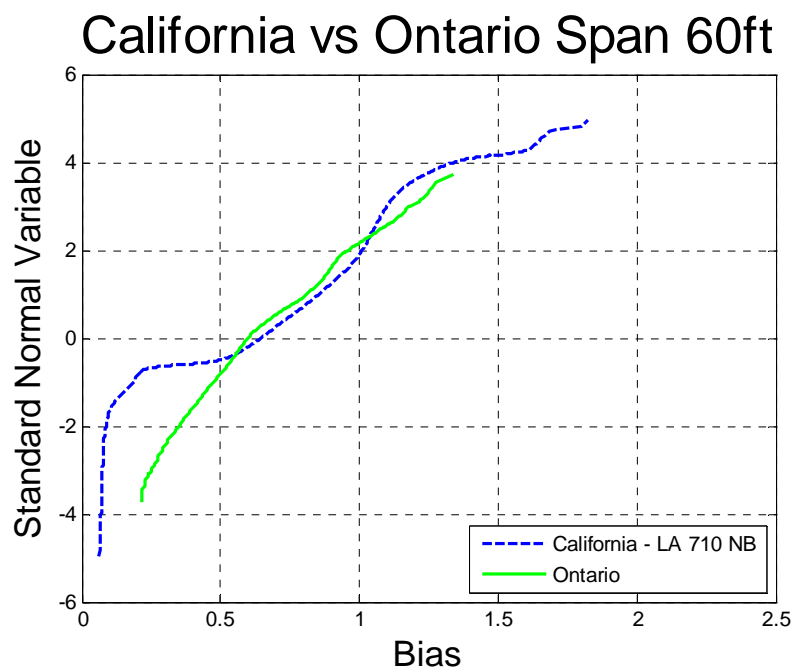


Figure 0-285 Comparison of Shear – California – LA710 NB vs. Ontario – Span 60ft

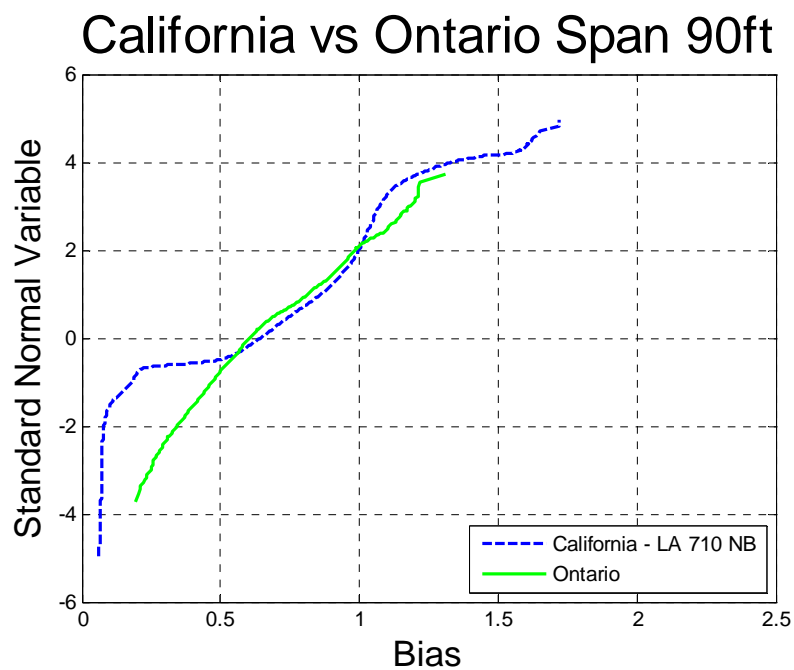


Figure 0-286 Comparison of Shear – California – LA710 NB vs. Ontario – Span 90ft

California vs Ontario Span 120ft

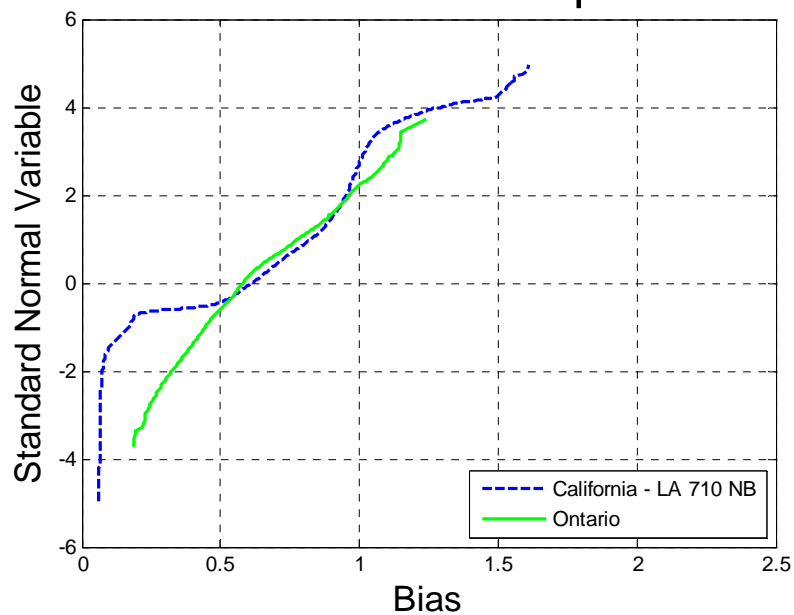


Figure 0-287 Comparison of Shear – California – LA710 NB vs. Ontario – Span 120ft

California vs Ontario Span 200ft

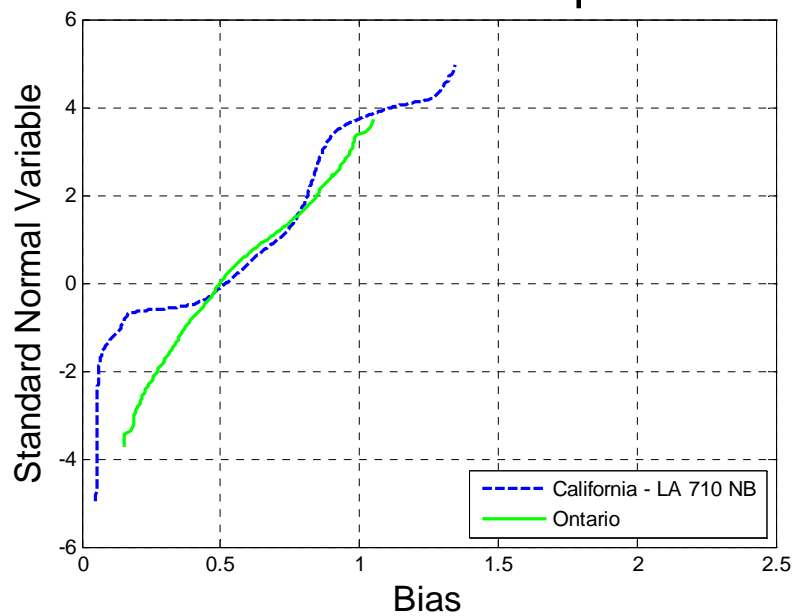


Figure 0-288 Comparison of Shear – California – LA710 NB vs. Ontario – Span 200ft

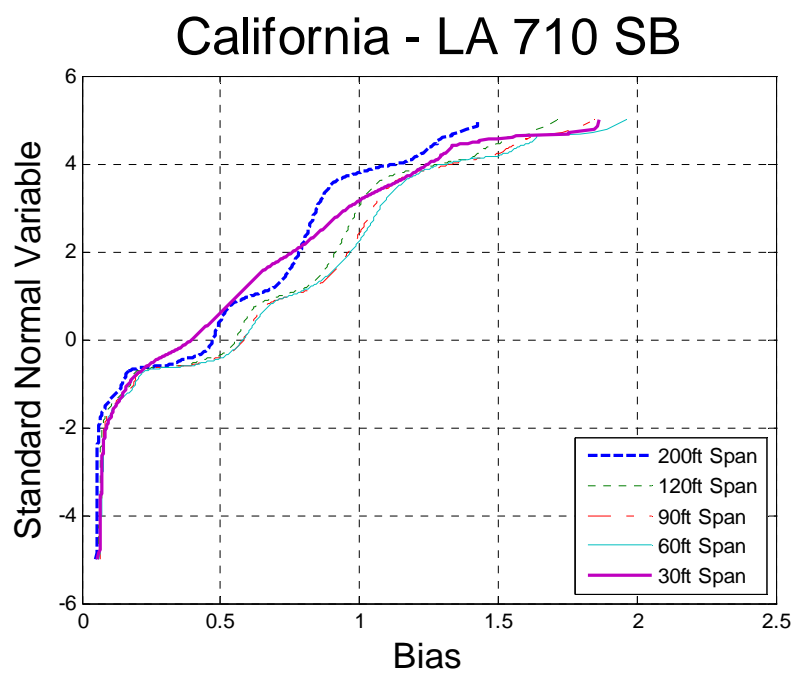


Figure 0-289 Cumulative Distribution Functions of Shear – California – LA710 SB

California vs Ontario Span 30ft

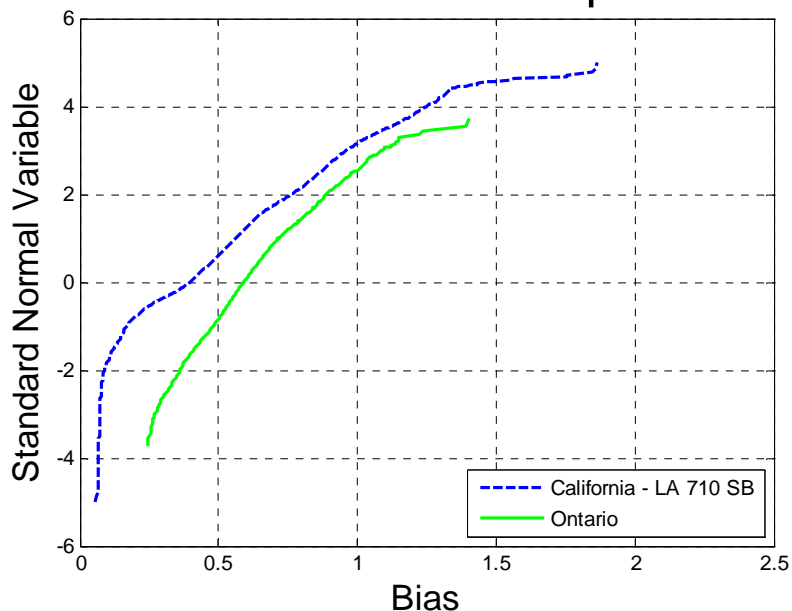
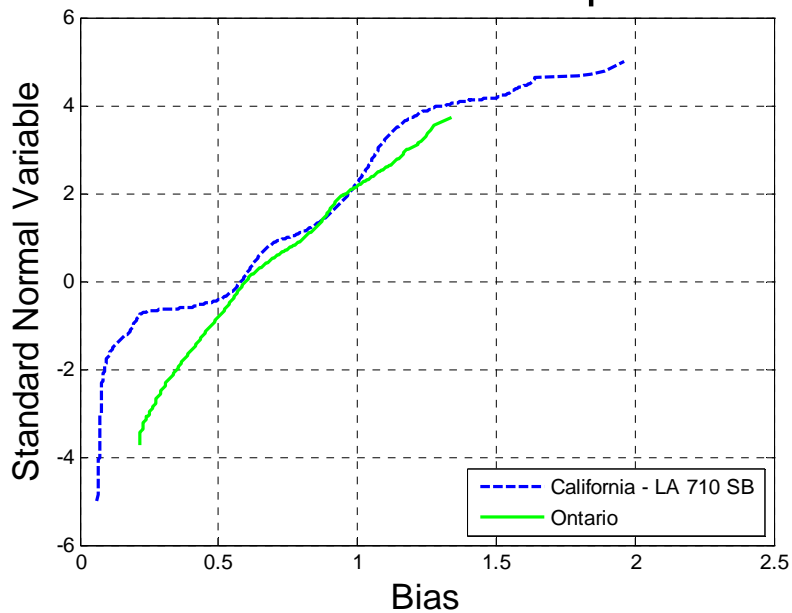


Figure 0-290 Comparison of Shear – California – LA710 SB vs. Ontario – Span 30ft

California vs Ontario Span 60ft



Comparison of Shear – California – LA710 SB vs. Ontario – Span 60ft

California vs Ontario Span 90ft

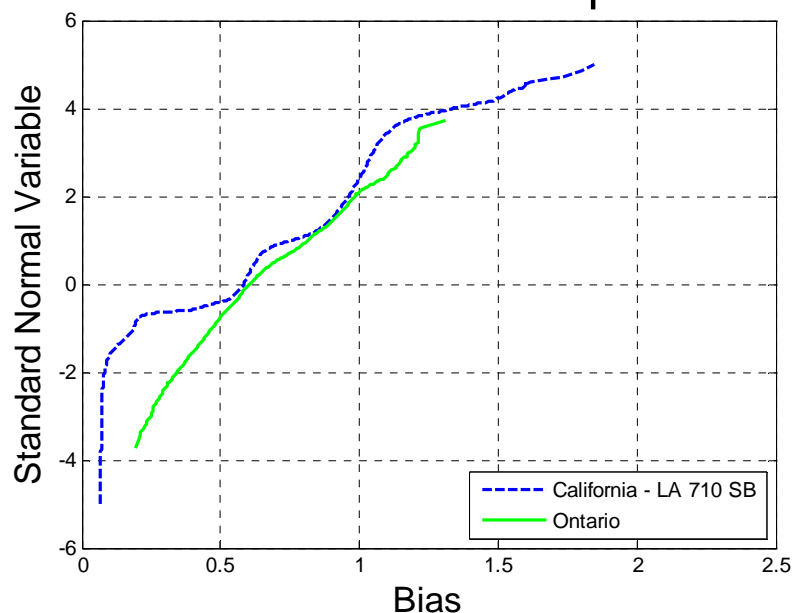


Figure 0-291 Comparison of Shear – California – LA710 SB vs. Ontario – Span 90ft

California vs Ontario Span 120ft

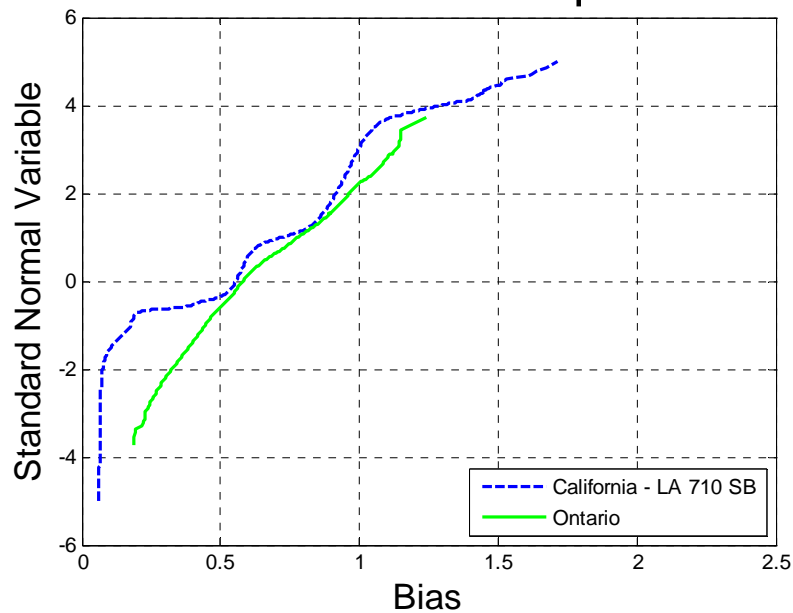


Figure 0-292 Comparison of Shear – California – LA710 SB vs. Ontario – Span 120ft

California vs Ontario Span 200ft

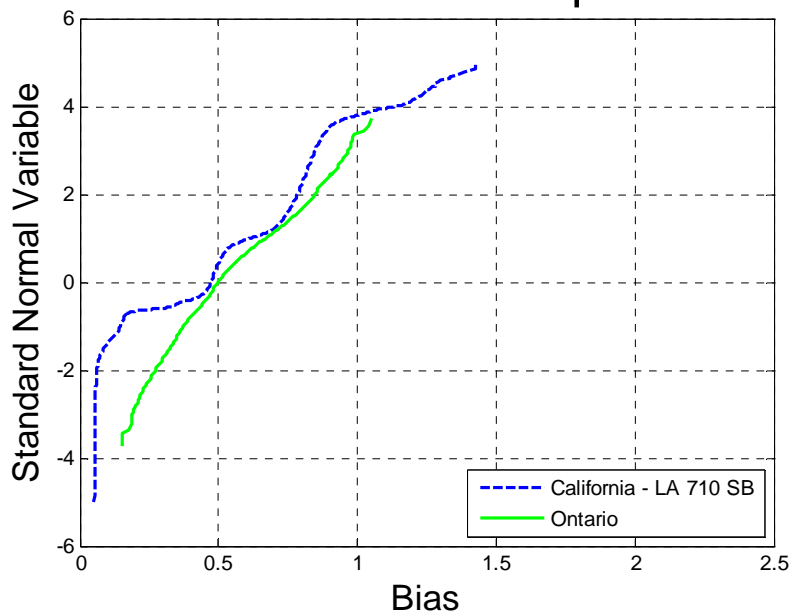


Figure 0-293 Comparison of Shear – California – LA710 SB vs. Ontario – Span 200ft

California - Lodi

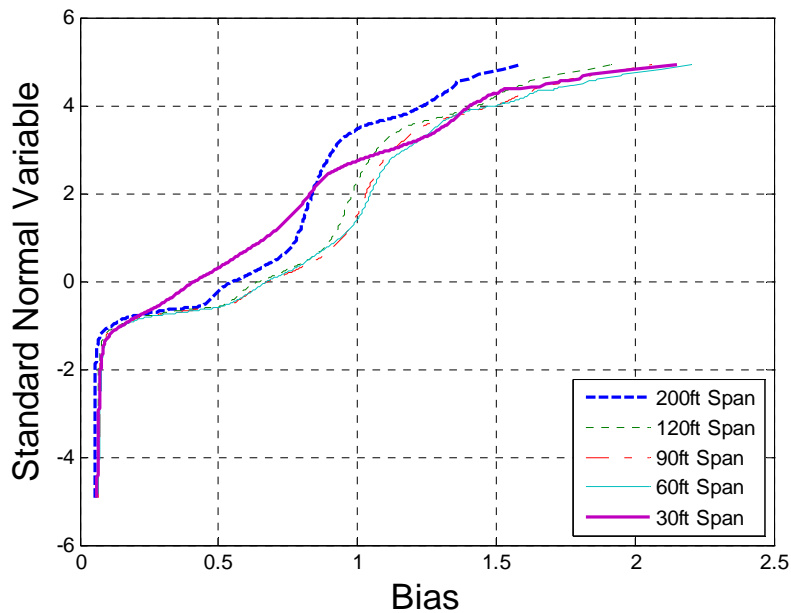


Figure 0-294 Cumulative Distribution Functions of Shear – California – Lodi

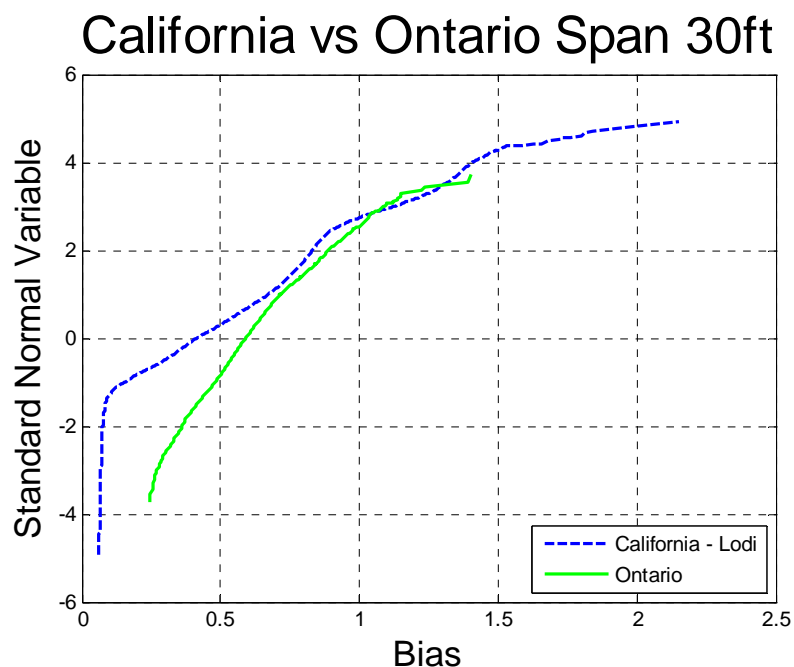


Figure 0-295 Comparison of Shear – California – Lodi vs. Ontario – Span 30ft

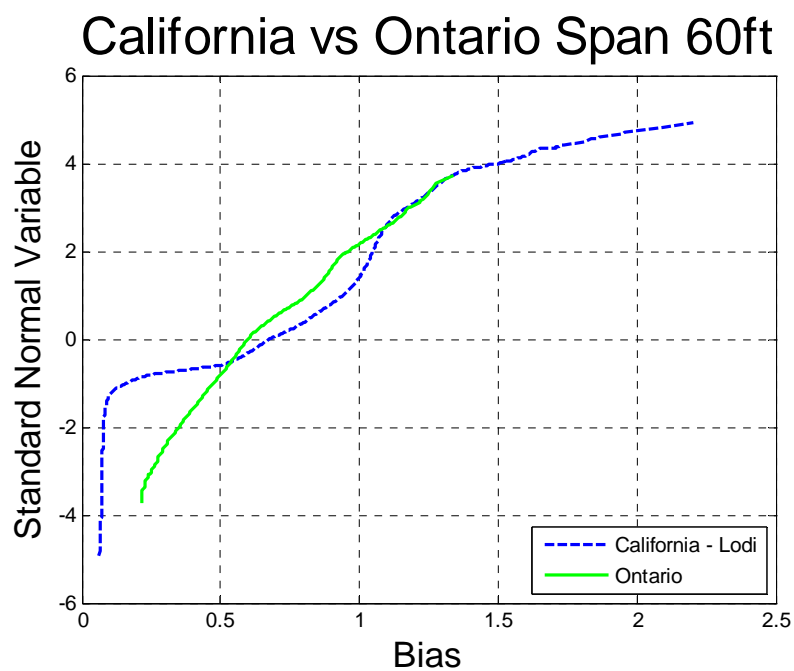


Figure 0-296 Comparison of Shear – California – Lodi vs. Ontario – Span 60ft

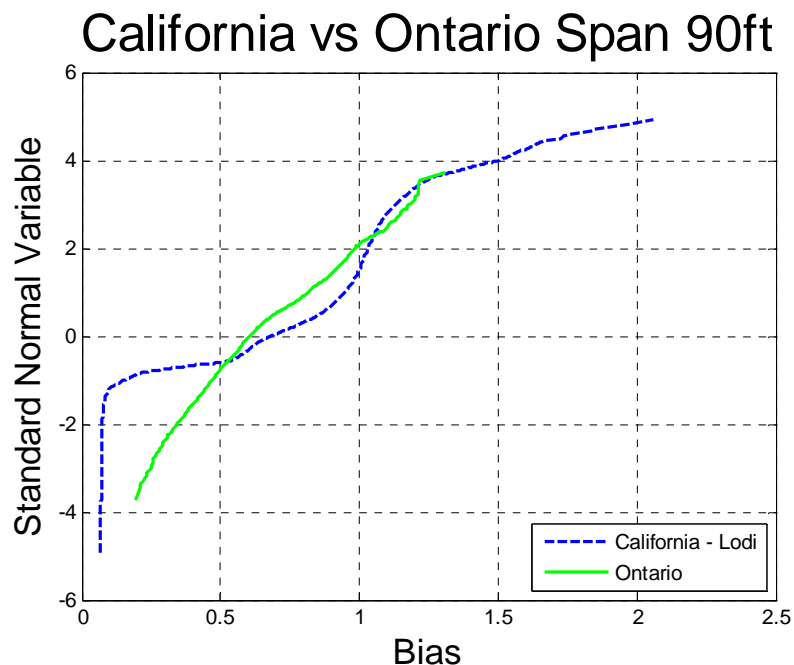


Figure 0-297 Comparison of Shear – California – Lodi vs. Ontario – Span 90ft

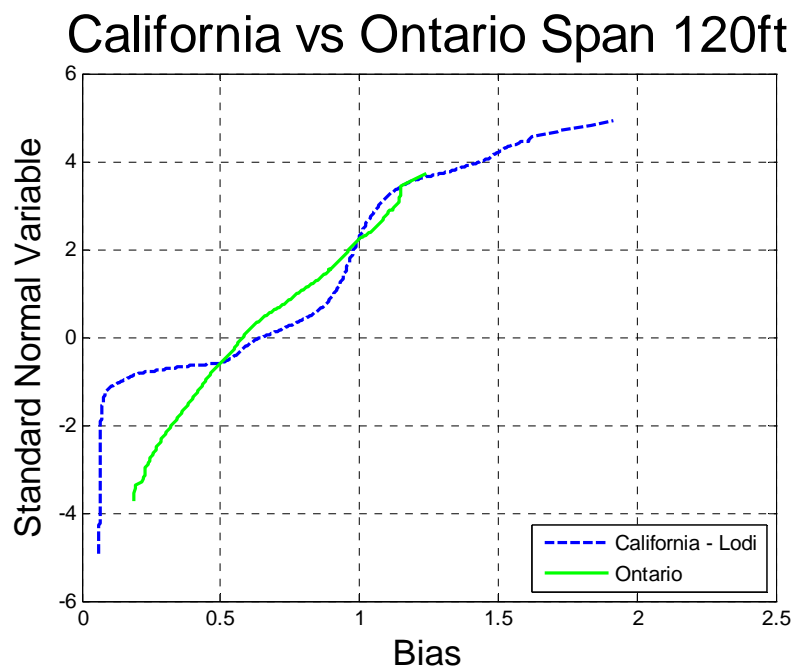


Figure 0-298 Comparison of Shear – California – Lodi vs. Ontario – Span 120ft

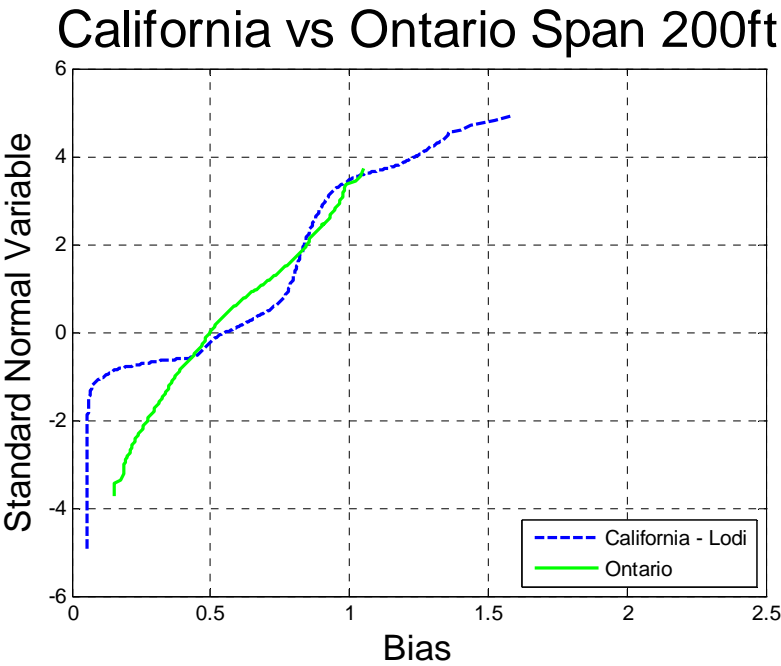


Figure 0-299 Comparison of Shear – California – Lodi vs. Ontario – Span 200ft

New York – Live Load Effect

WIM data for New York

The truck survey includes weigh-in-motion (WIM) truck measurements obtained from Oregon DOT. The data includes 12 months of traffic recorded at different locations. The total number of records is shown in Table 63. The data includes number of axles, gross vehicle weight (GVW), weight per axle and spacing between axles.

Table 63

Site	Number of Trucks
------	------------------

Site 0580	2,874,124
Site 2680	100,488
Site 8280	1,828,020
Site 8382	1,594,674
Site 9121	1,289,295
Site 9631	105,035
TOTAL	7,791,636

Maximum Simple Span Moments

The maximum moment was calculated for each truck from the data. Analysis included simple spans with the span varying from 30 to 200 ft. The maximum moment was also calculated for the HL93 load and Tandem. Ratio between data truck moment and code load moment was plotted on the probability paper.

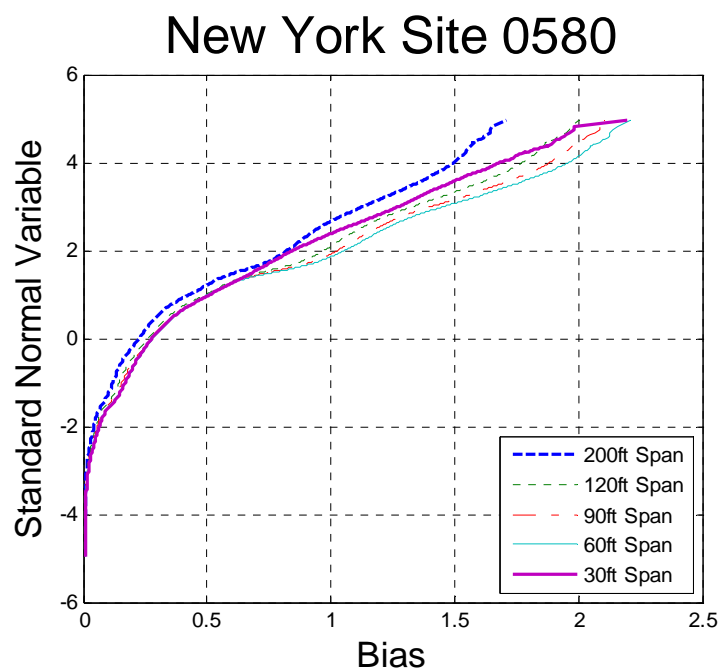


Figure 0-300 Cumulative Distribution Functions of Simple Span Moment– New York - Site 0580

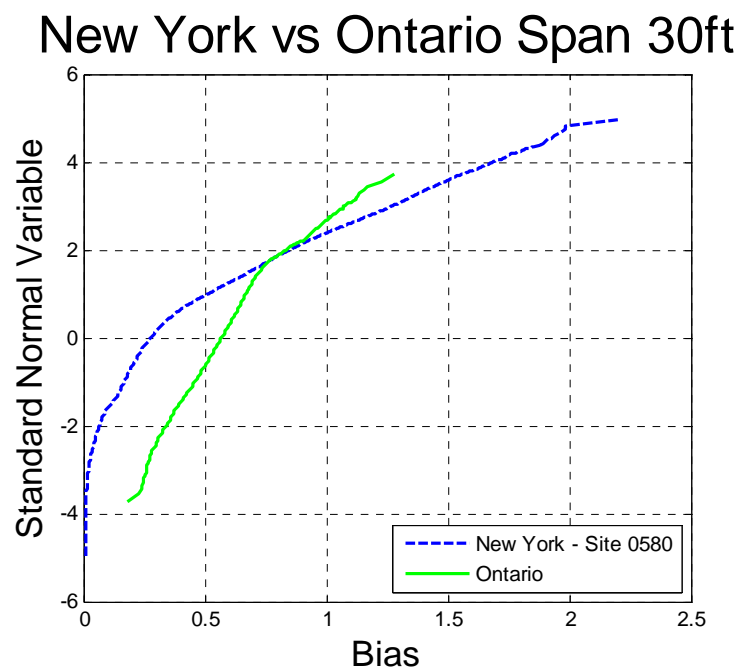


Figure 0-301 Comparison of Simple Span Moment – New York - Site 0580 vs. Ontario – Span 30ft

New York vs Ontario Span 60ft

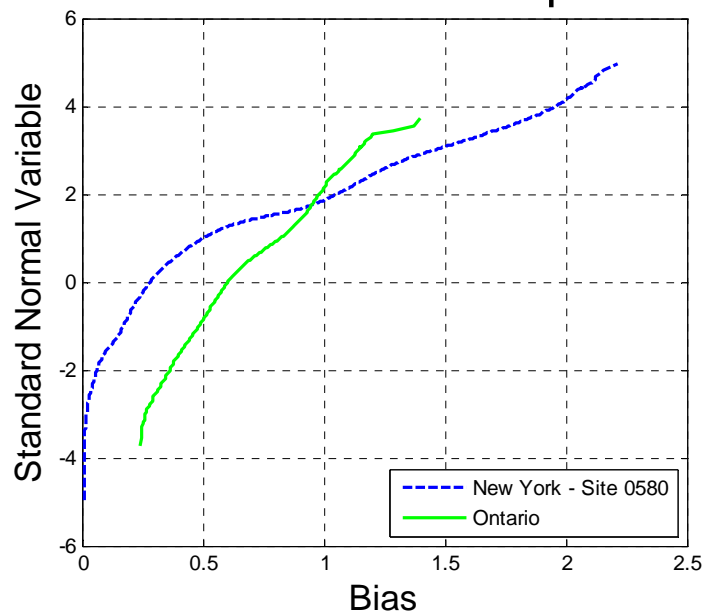


Figure 0-302 Comparison of Simple Span Moment – New York - Site 0580 vs. Ontario –
Span 60ft

New York vs Ontario Span 90ft

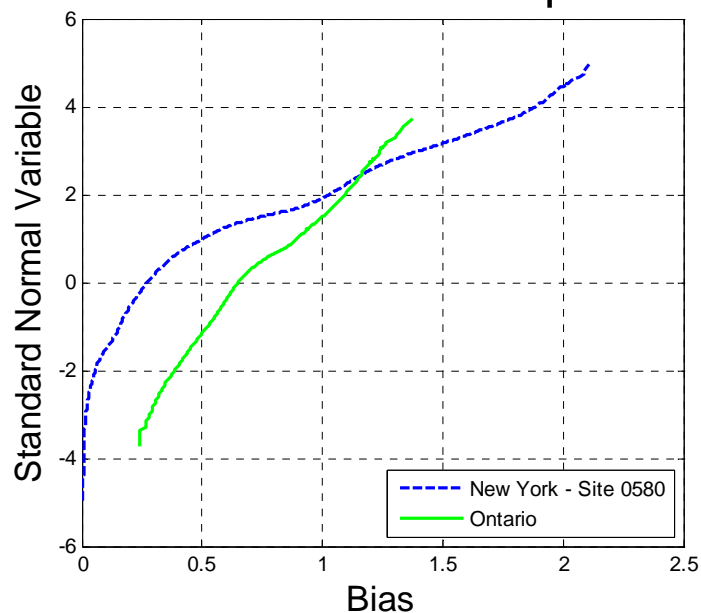


Figure 0-303 Comparison of Simple Span Moment – New York - Site 0580 vs. Ontario –
Span 90ft

New York vs Ontario Span 120ft

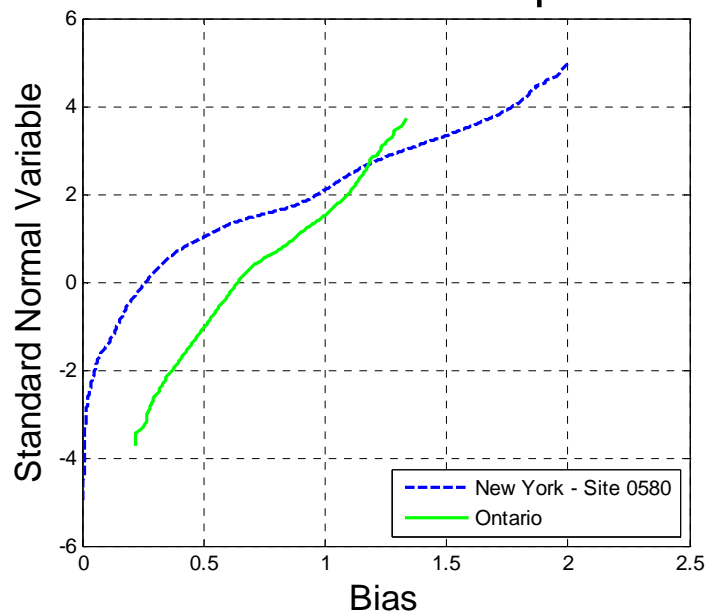


Figure 0-304 Comparison of Simple Span Moment – New York - Site 0580 vs. Ontario –
Span 120ft

New York vs Ontario Span 200ft

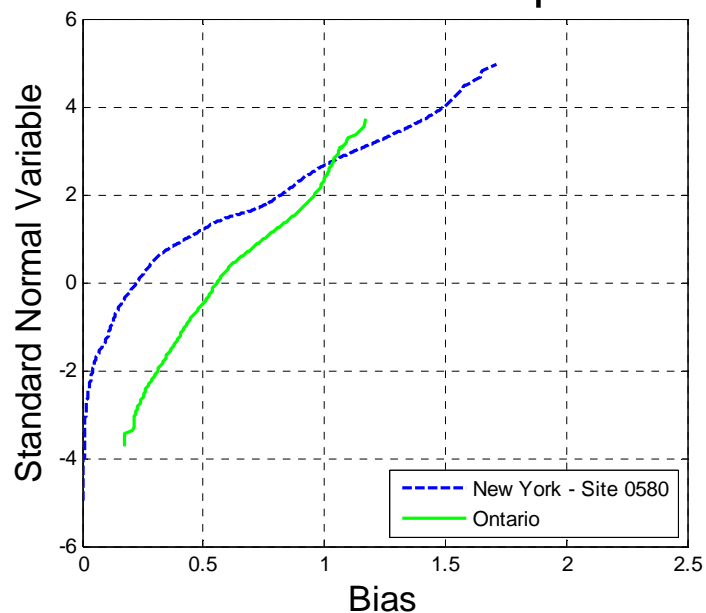


Figure 0-305 Comparison of Simple Span Moment – New York - Site 0580 vs. Ontario –
Span 200ft

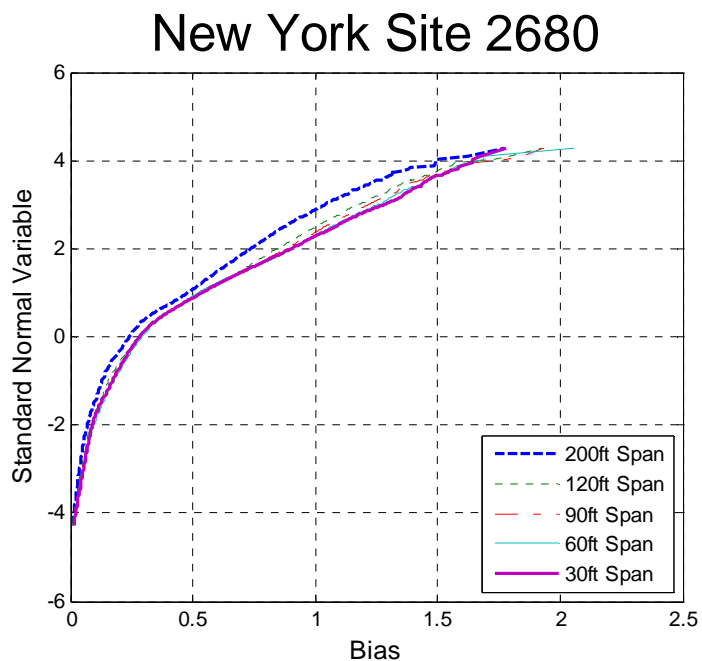


Figure 0-306 Cumulative Distribution Functions of Simple Span Moment– New York - Site 2680

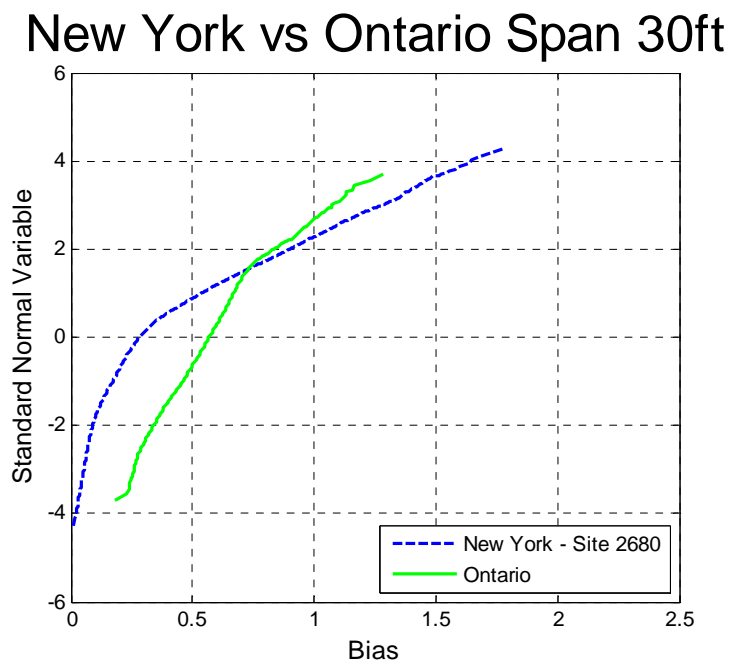


Figure 0-307 Comparison of Simple Span Moment – New York - Site 2680 vs. Ontario – Span 30ft

New York vs Ontario Span 60ft

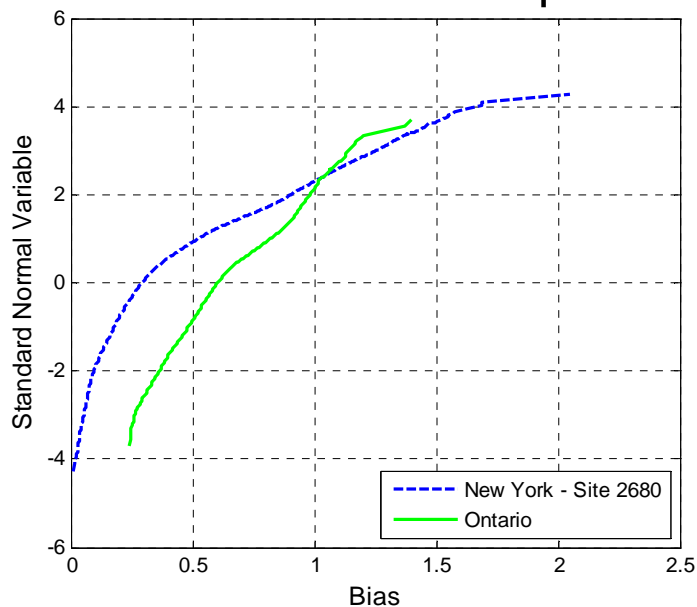


Figure 0-308 Comparison of Simple Span Moment – New York - Site 2680 vs. Ontario –
Span 60ft

New York vs Ontario Span 90ft

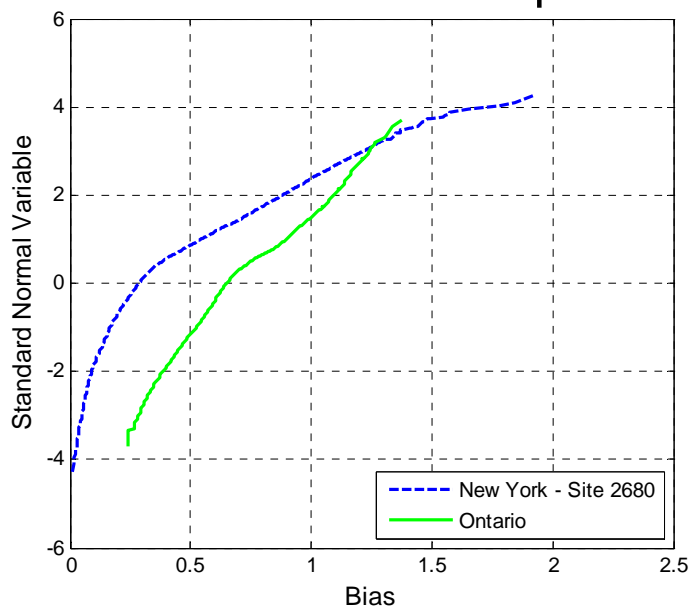


Figure 0-309 Comparison of Simple Span Moment – New York - Site 2680 vs. Ontario –
Span 90ft

New York vs Ontario Span 120ft

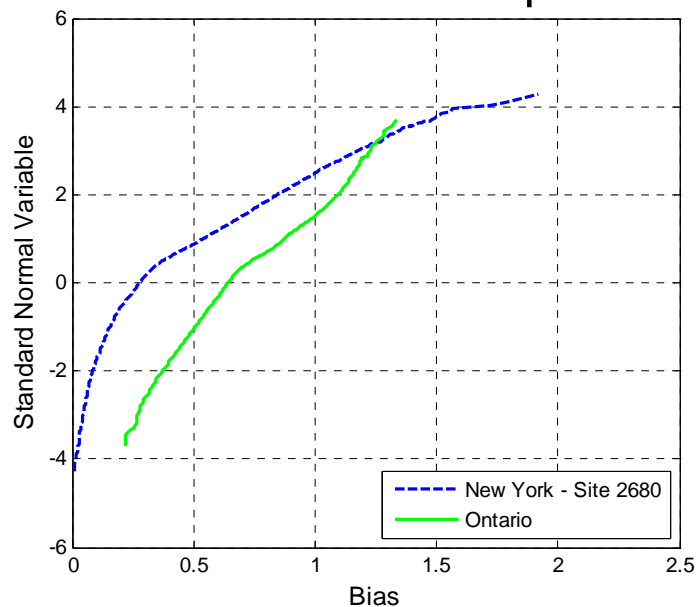


Figure 0-310 Comparison of Simple Span Moment – New York - Site 2680 vs. Ontario – Span 120ft

New York vs Ontario Span 200ft

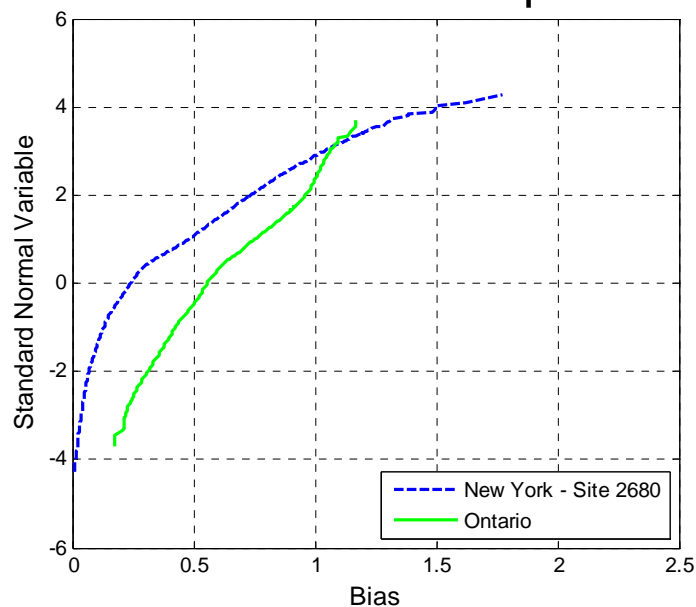


Figure 0-311 Comparison of Simple Span Moment – New York - Site 2680 vs. Ontario – Span 200ft

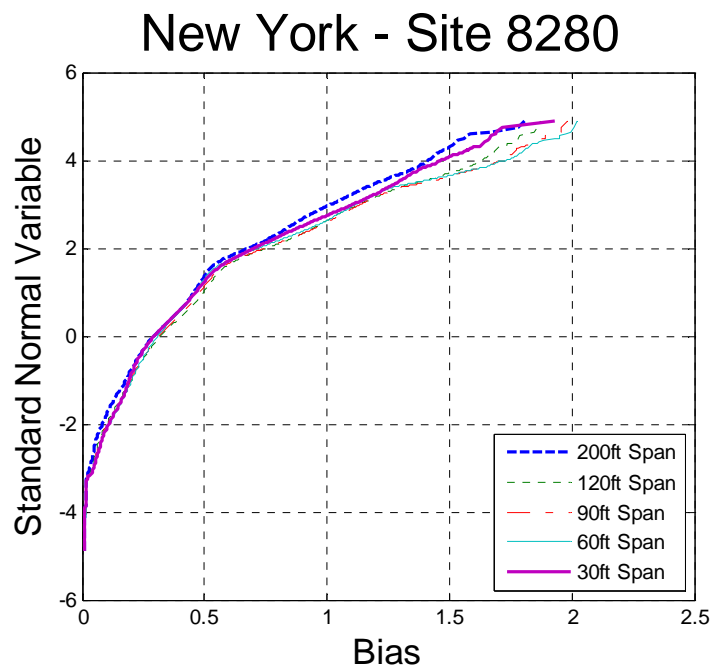


Figure 0-312 Cumulative Distribution Functions of Simple Span Moment– New York - Site 8280

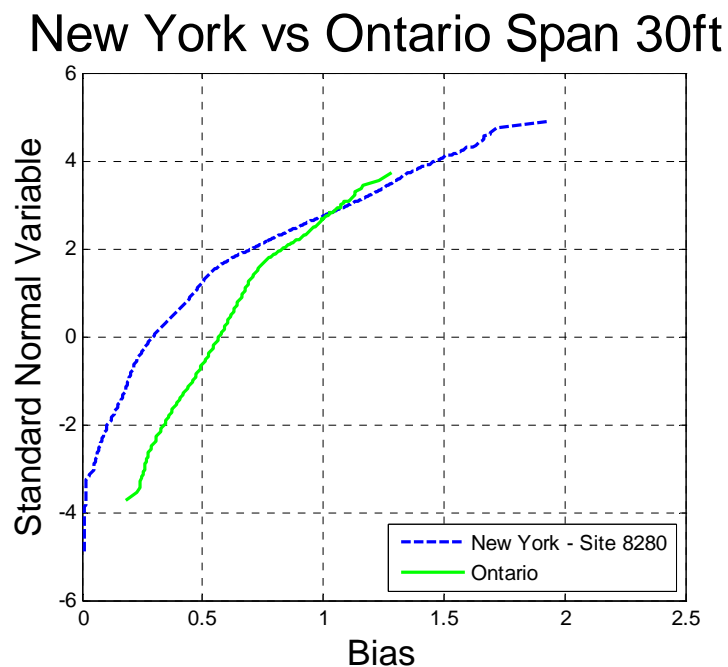


Figure 0-313 Comparison of Simple Span Moment – New York - Site 8280 vs. Ontario – Span 30ft

New York vs Ontario Span 60ft

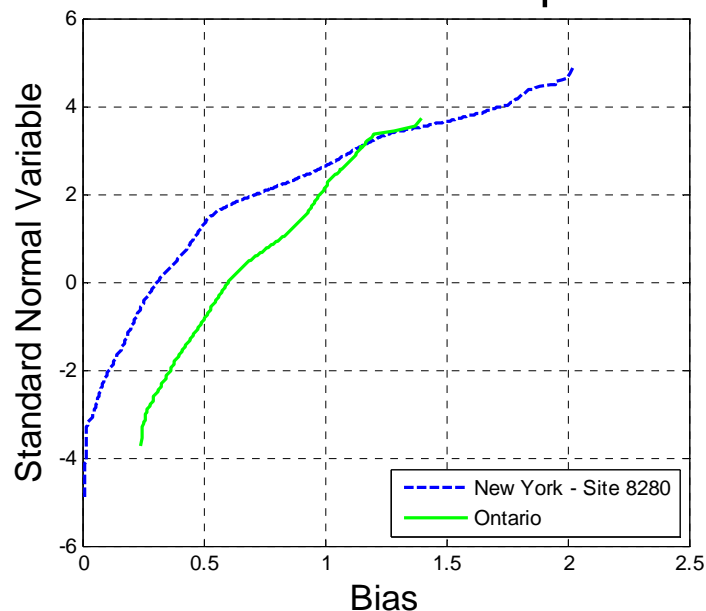


Figure 0-314 Comparison of Simple Span Moment – New York - Site 8280 vs. Ontario –
Span 60ft

New York vs Ontario Span 90ft

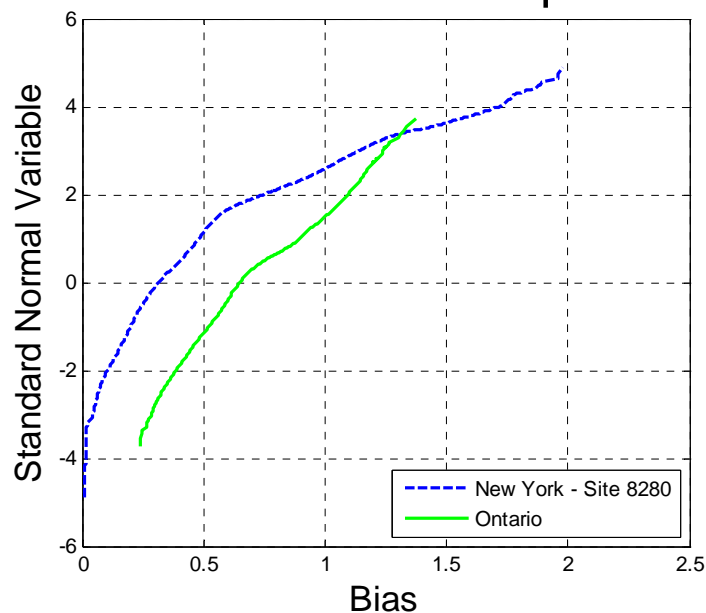


Figure 0-315 Comparison of Simple Span Moment – New York - Site 8280 vs. Ontario –
Span 90ft

New York vs Ontario Span 120ft

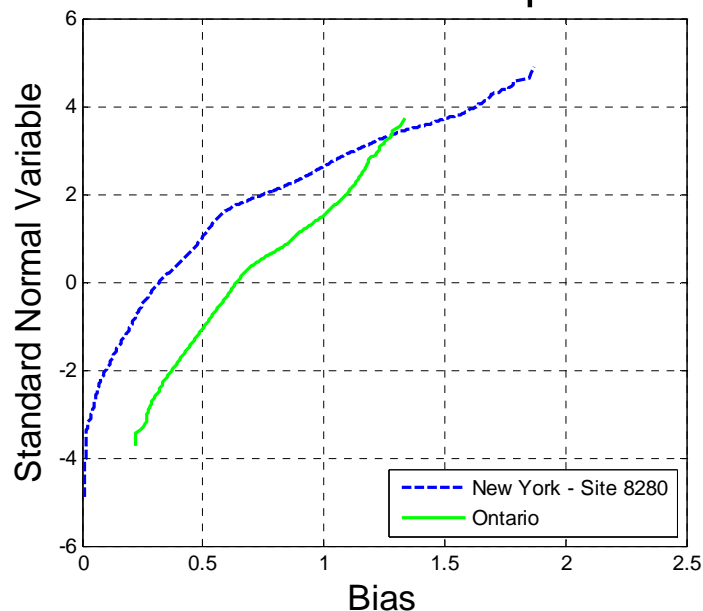


Figure 0-316 Comparison of Simple Span Moment – New York - Site 8280 vs. Ontario –
Span 120ft

New York vs Ontario Span 200ft

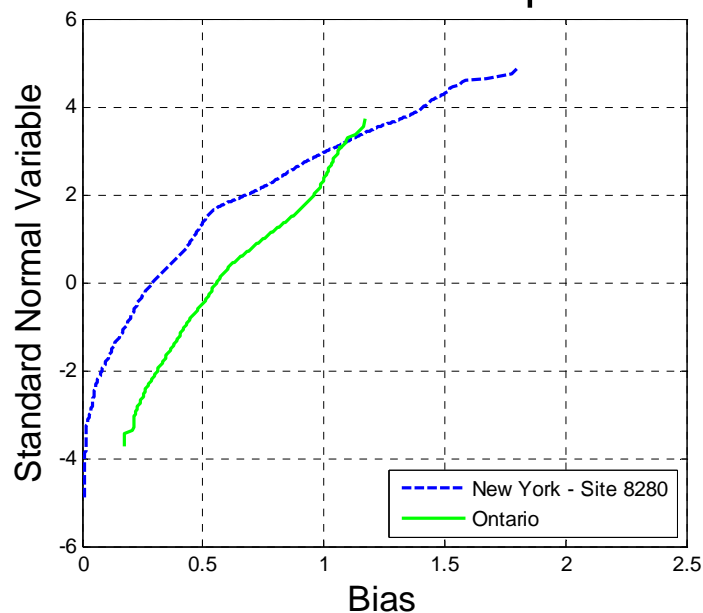


Figure 0-317 Comparison of Simple Span Moment – New York - Site 8280 vs. Ontario –
Span 200ft

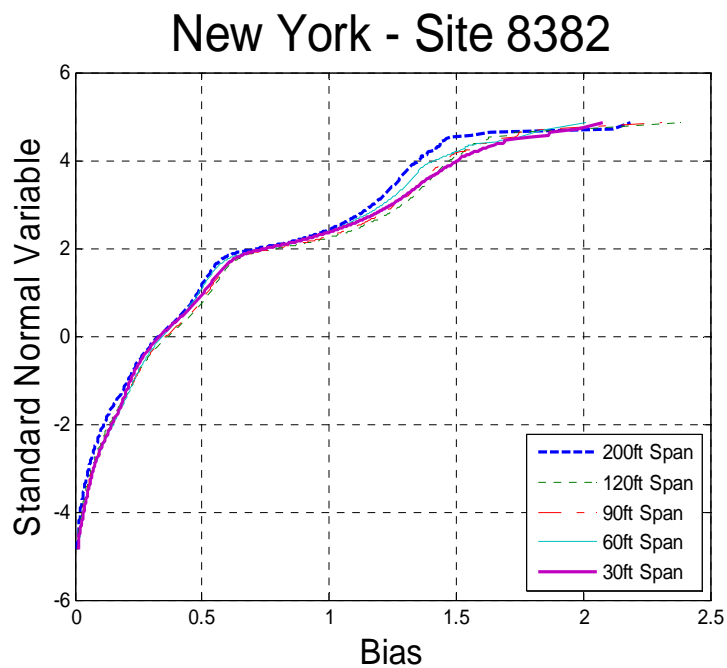


Figure 0-318 Cumulative Distribution Functions of Simple Span Moment– New York - Site 8382

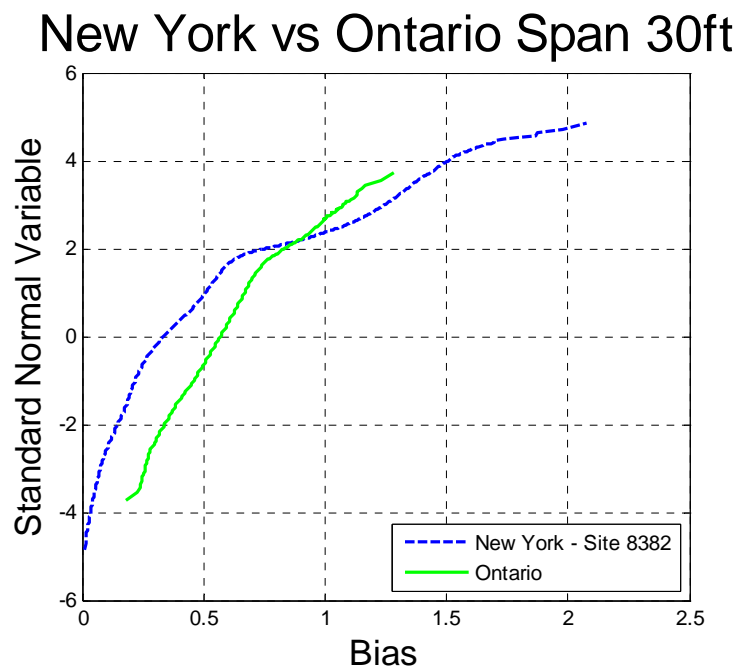


Figure 0-319 Comparison of Simple Span Moment – New York - Site 8382 vs. Ontario – Span 30ft

New York vs Ontario Span 60ft

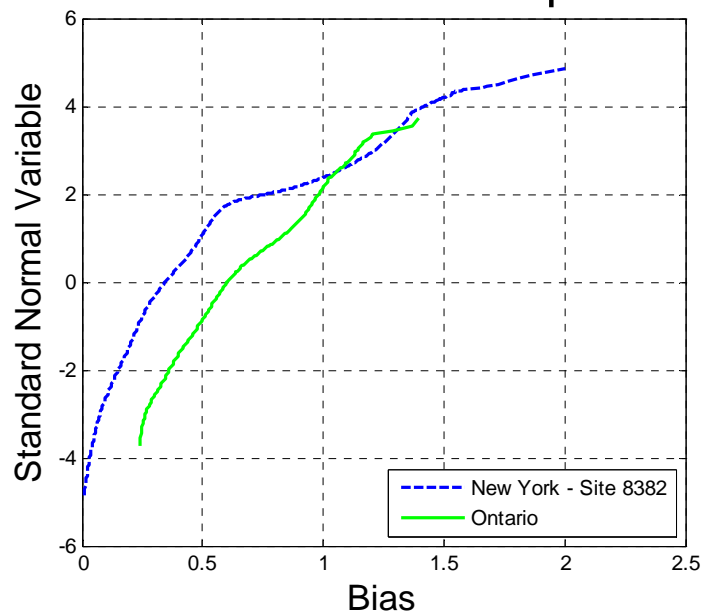


Figure 0-320 Comparison of Simple Span Moment – New York - Site 8382 vs. Ontario –
Span 60ft

New York vs Ontario Span 90ft

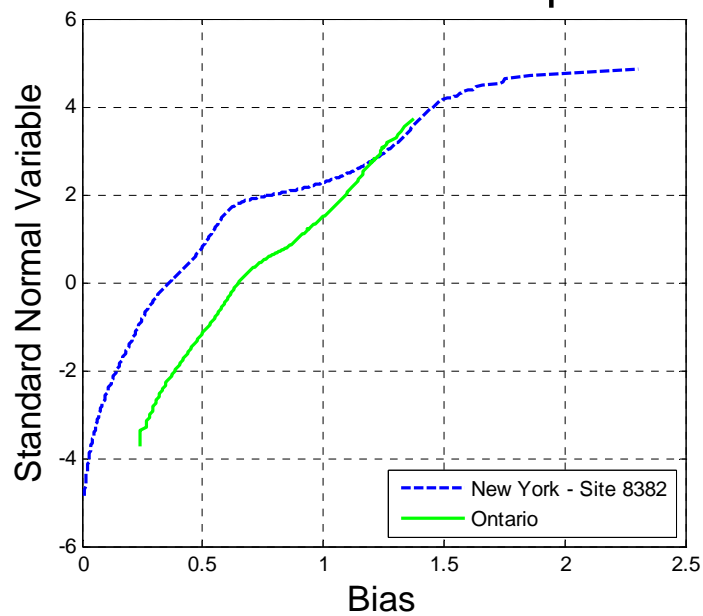


Figure 0-321 Comparison of Simple Span Moment – New York - Site 8382 vs. Ontario –
Span 90ft

New York vs Ontario Span 120ft

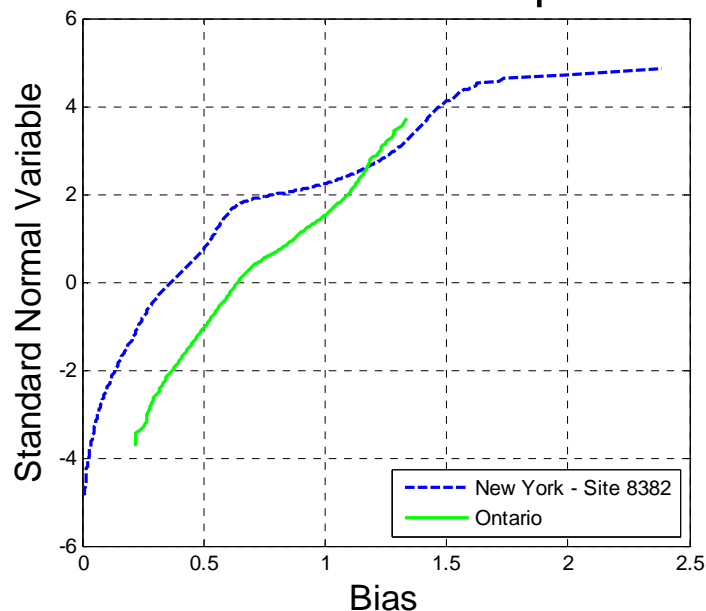


Figure 0-322 Comparison of Simple Span Moment – New York - Site 8382 vs. Ontario –
Span 120ft

New York vs Ontario Span 200ft

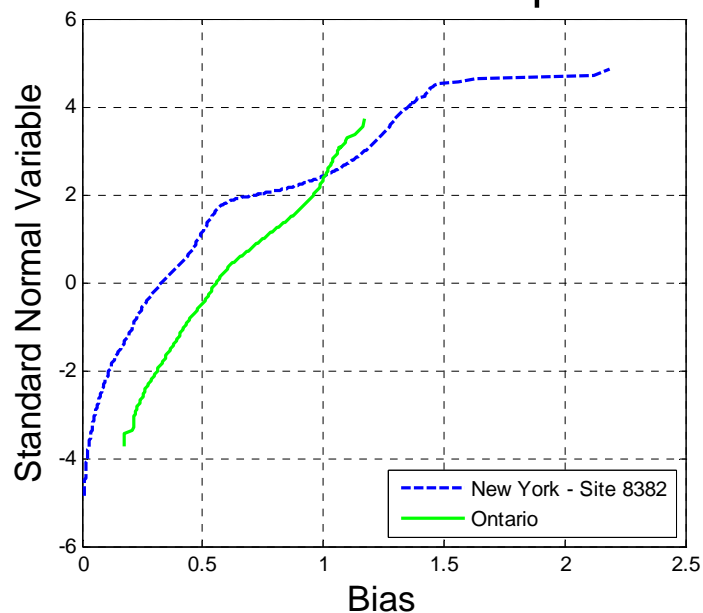


Figure 0-323 Comparison of Simple Span Moment – New York - Site 8382 vs. Ontario –
Span 200ft

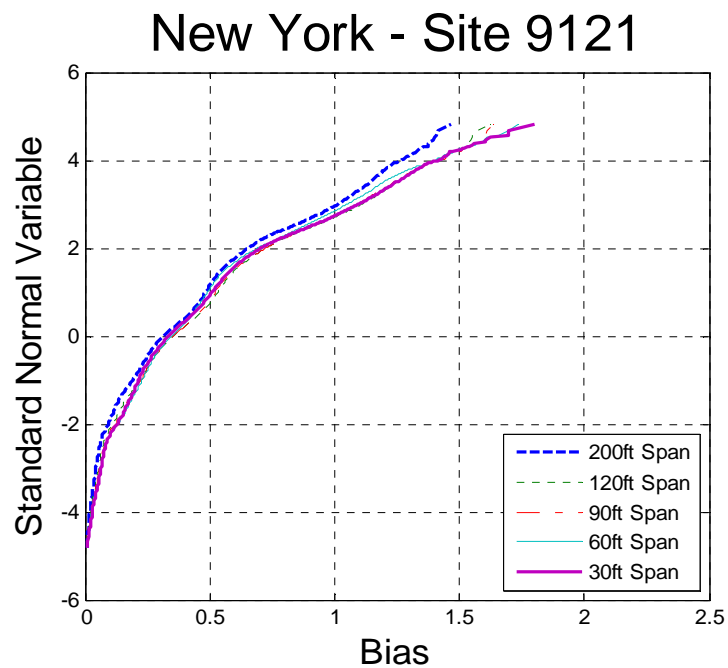


Figure 0-324 Cumulative Distribution Functions of Simple Span Moment– New York - Site 9121

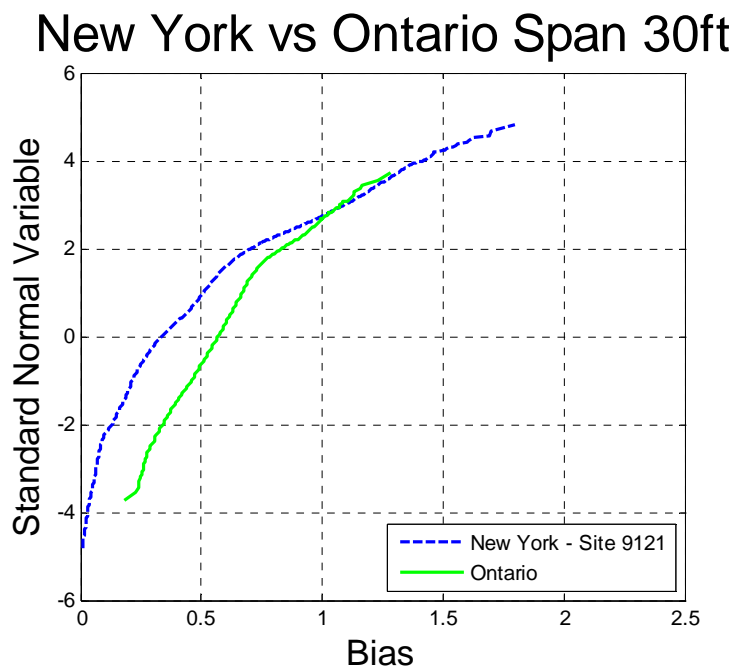


Figure 0-325 Comparison of Simple Span Moment – New York - Site 9121 vs. Ontario – Span 30ft

New York vs Ontario Span 60ft

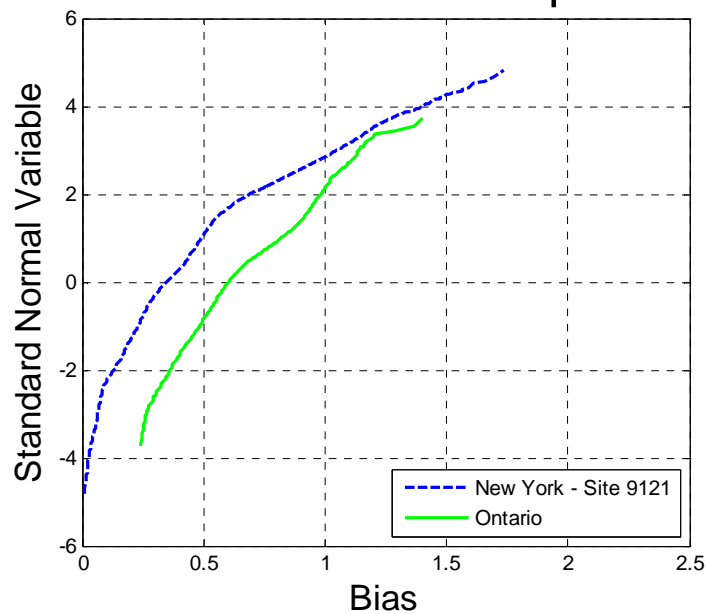


Figure 0-326 Comparison of Simple Span Moment – New York - Site 9121 vs. Ontario –
Span 60ft

New York vs Ontario Span 90ft

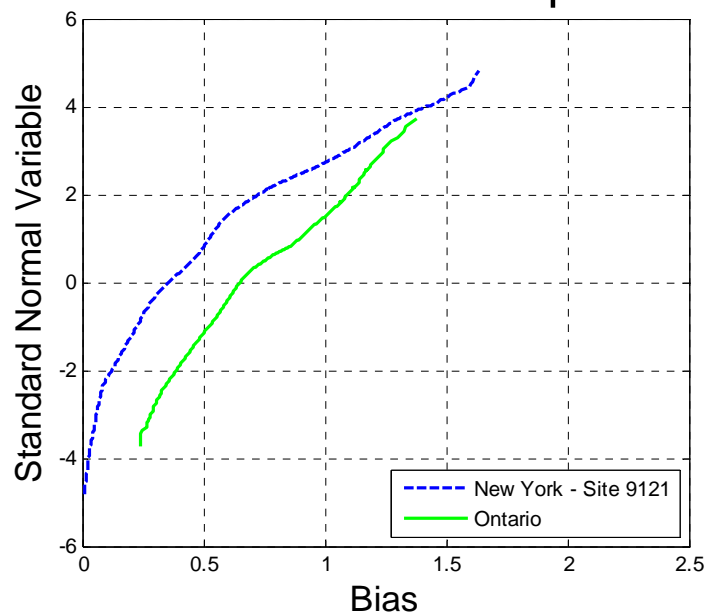


Figure 0-327 Comparison of Simple Span Moment – New York - Site 9121 vs. Ontario –
Span 90ft

New York vs Ontario Span 120ft

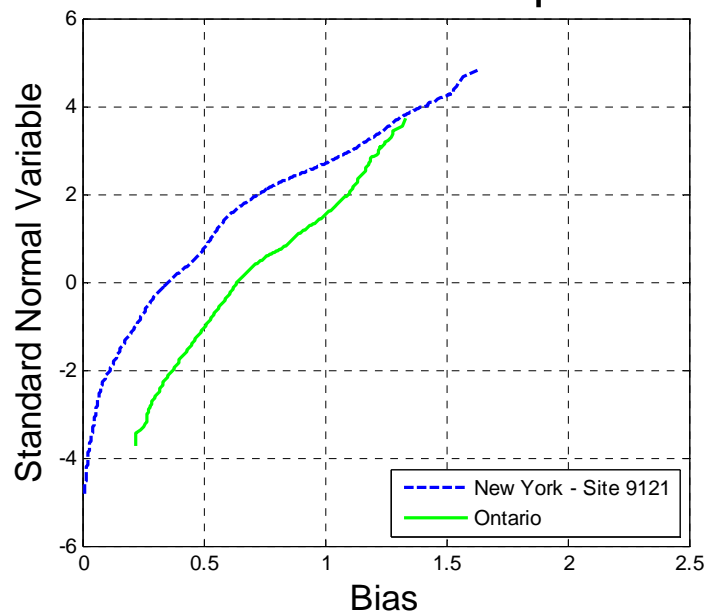


Figure 0-328 Comparison of Simple Span Moment – New York - Site 9121 vs. Ontario – Span 120ft

New York vs Ontario Span 200ft

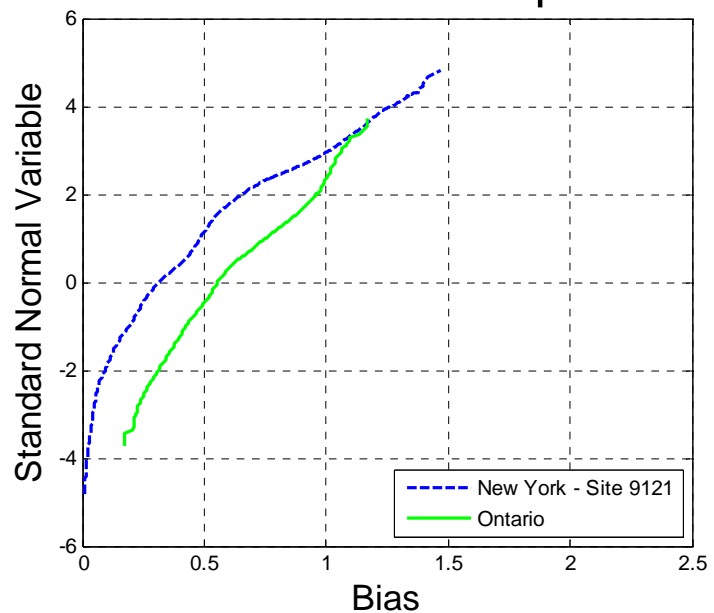


Figure 0-329 Comparison of Simple Span Moment – New York - Site 9121 vs. Ontario – Span 200ft

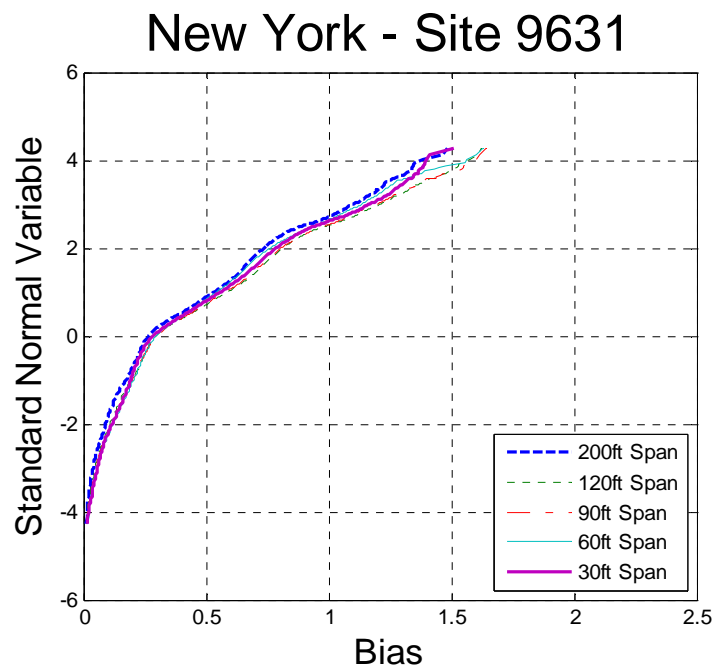


Figure 0-330 Cumulative Distribution Functions of Simple Span Moment– New York - Site 9631

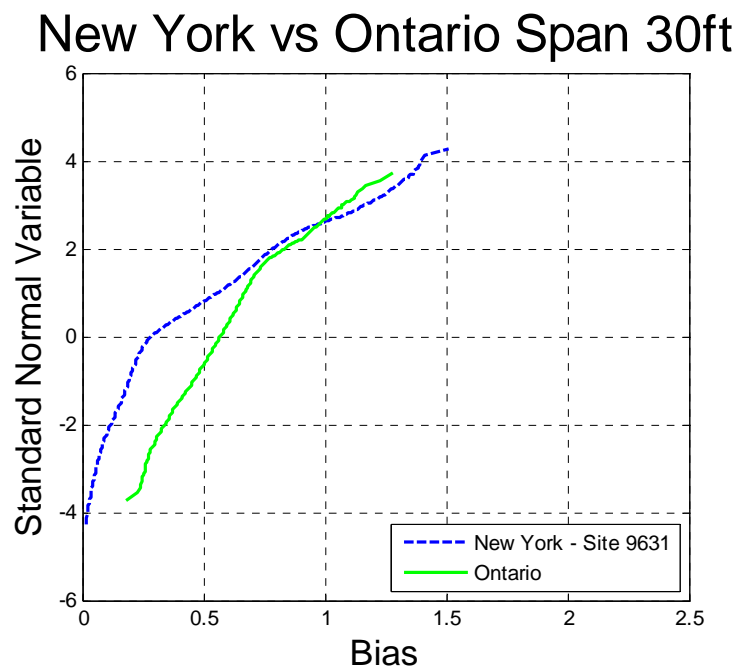


Figure 0-331 Comparison of Simple Span Moment – New York - Site 9631 vs. Ontario – Span 30ft

New York vs Ontario Span 60ft

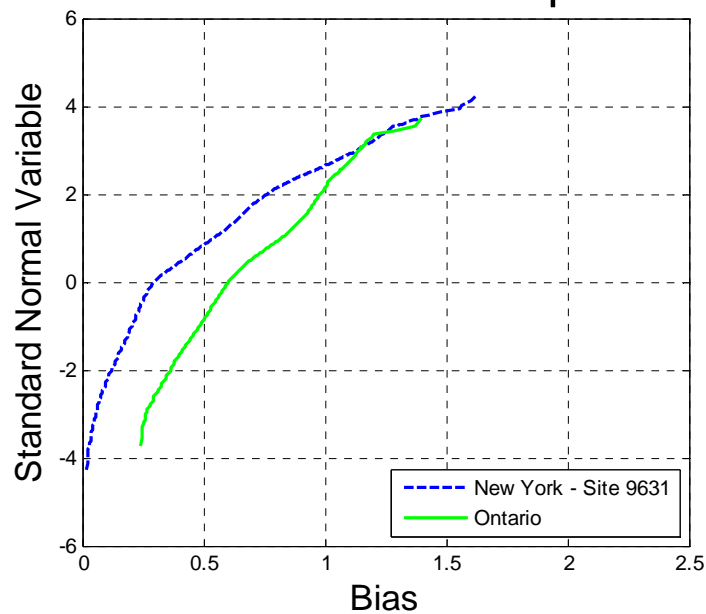


Figure 0-332 Comparison of Simple Span Moment – New York - Site 9631 vs. Ontario –
Span 60ft

New York vs Ontario Span 90ft

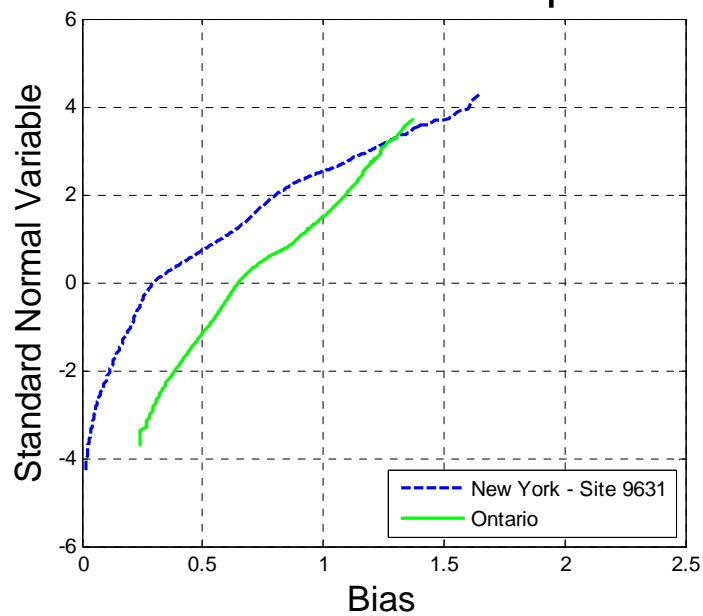


Figure 0-333 Comparison of Simple Span Moment – New York - Site 9631 vs. Ontario –
Span 90ft

New York vs Ontario Span 120ft

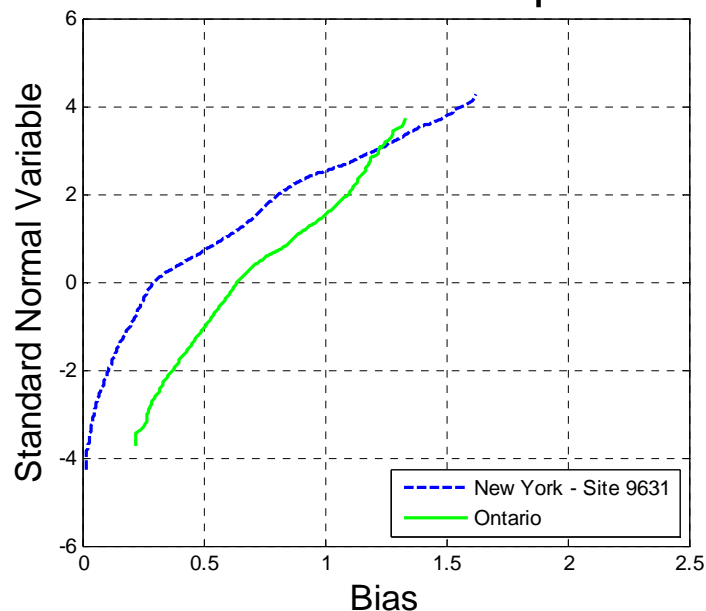


Figure 0-334 Comparison of Simple Span Moment – New York - Site 9631 vs. Ontario –
Span 120ft

New York vs Ontario Span 200ft

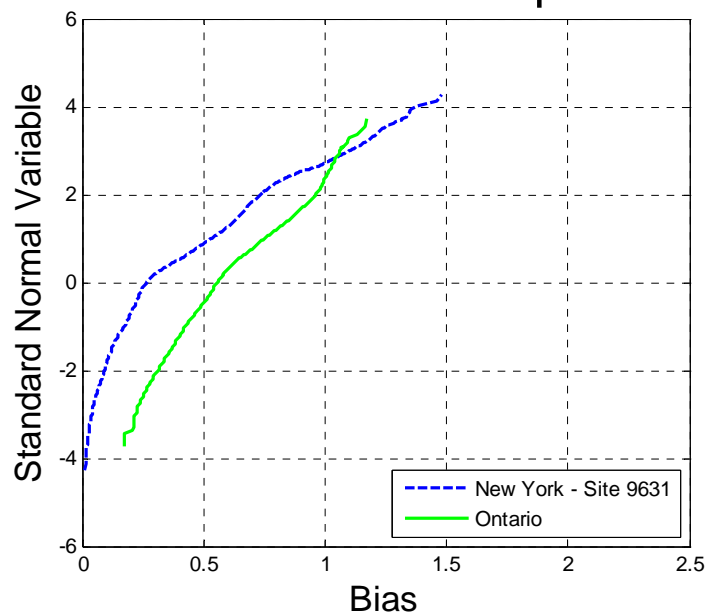


Figure 0-335 Comparison of Simple Span Moment – New York - Site 9631 vs. Ontario –
Span 200ft

Maximum Shear

The maximum shear was calculated for each truck from the data. Analysis included simple spans with the span varying from 30 to 200 ft. The ratio of shear obtained from the data truck and the HL-93 load was plotted on the probability paper.

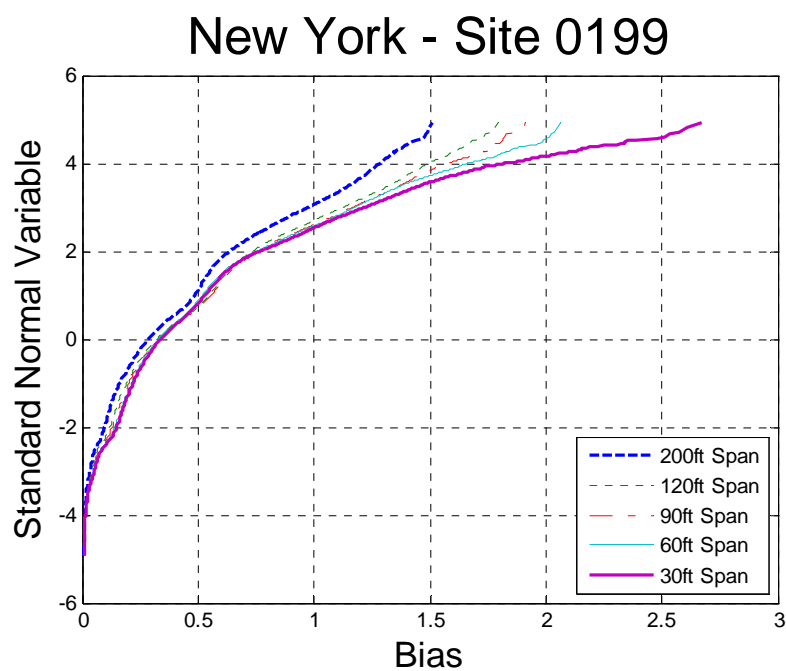


Figure 0-336 Cumulative Distribution Functions of Shear – New York Site 0199

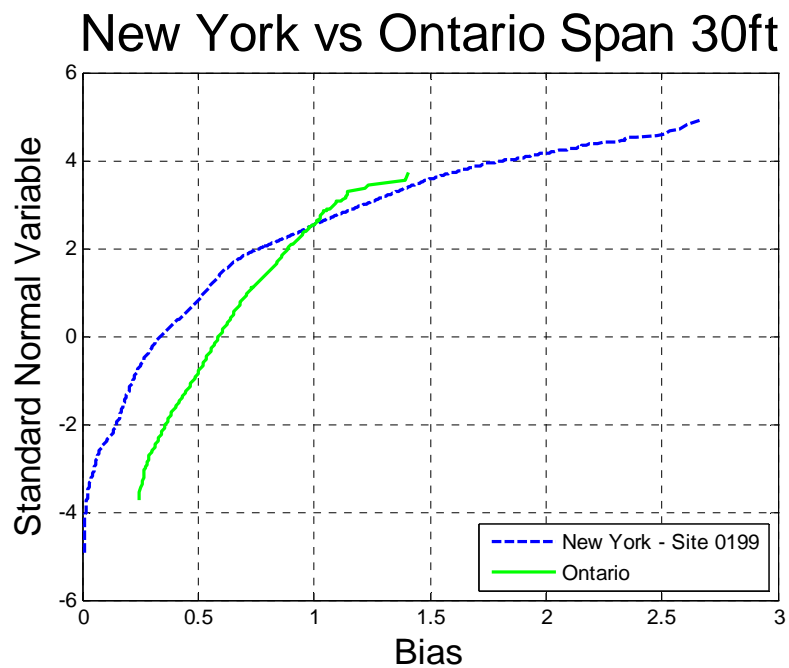


Figure 0-337 Comparison of Shear – New York Site 0199 vs. Ontario – Span 30ft

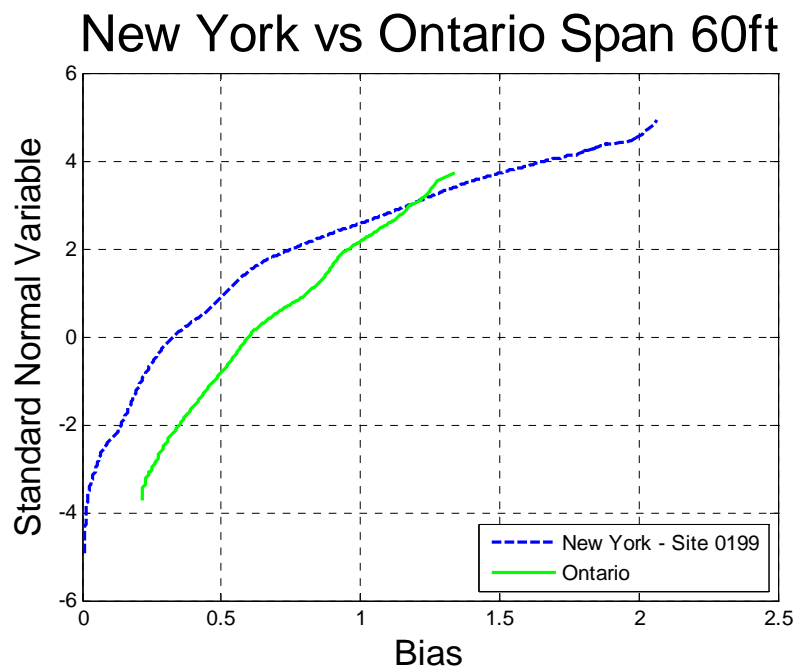


Figure 0-338 Comparison of Shear – New York Site 0199 vs. Ontario – Span 60ft

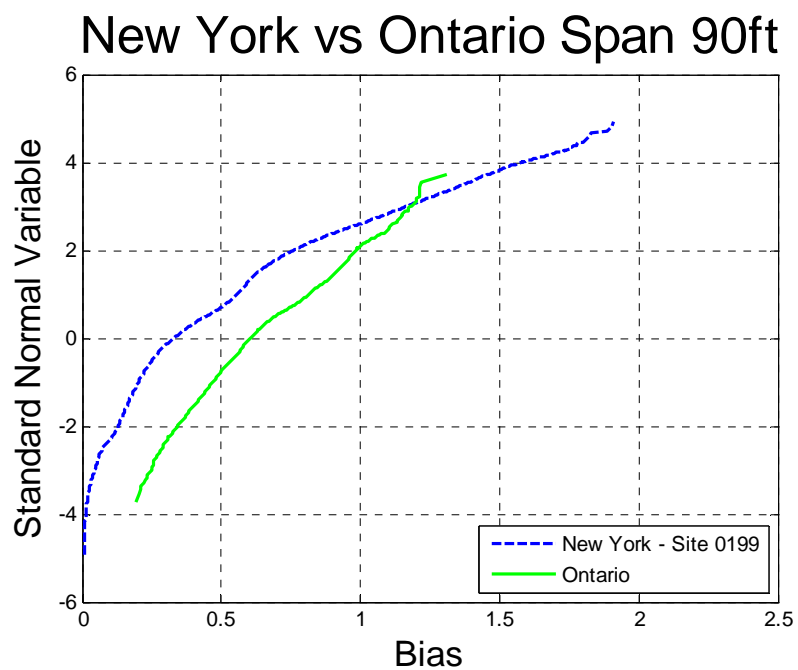


Figure 0-339 Comparison of Shear – New York Site 0199 vs. Ontario – Span 90ft

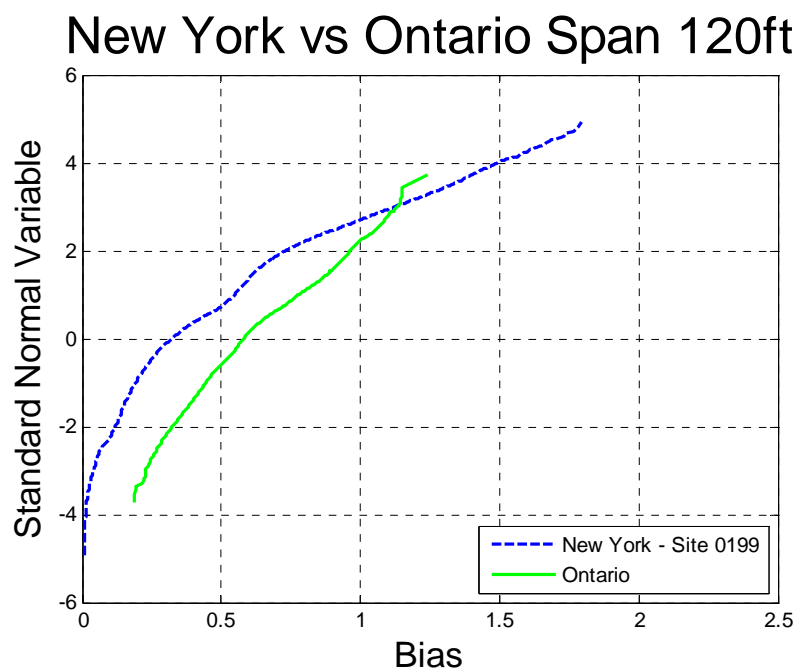


Figure 0-340 Comparison of Shear – New York Site 0199 vs. Ontario – Span 120ft

New York vs Ontario Span 200ft

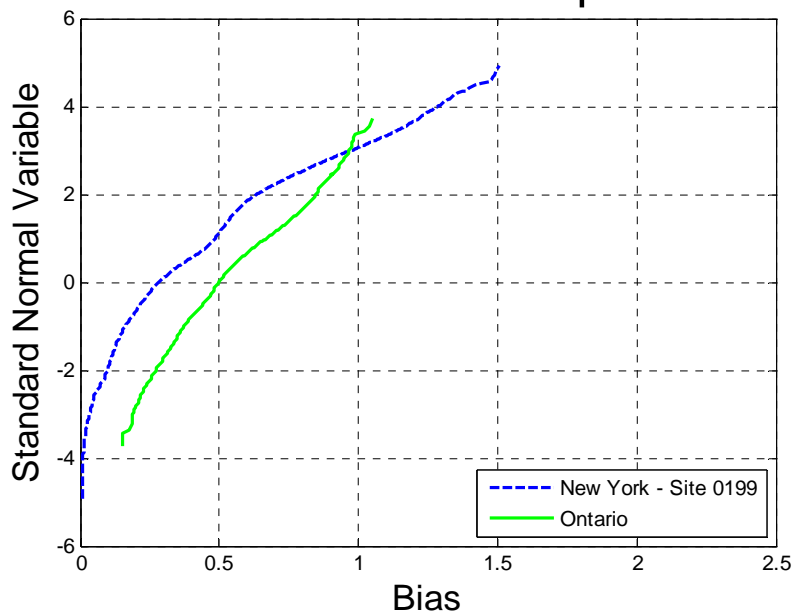


Figure 0-341 Comparison of Shear – New York Site 0199 vs. Ontario – Span 200ft

New York - Site 0580

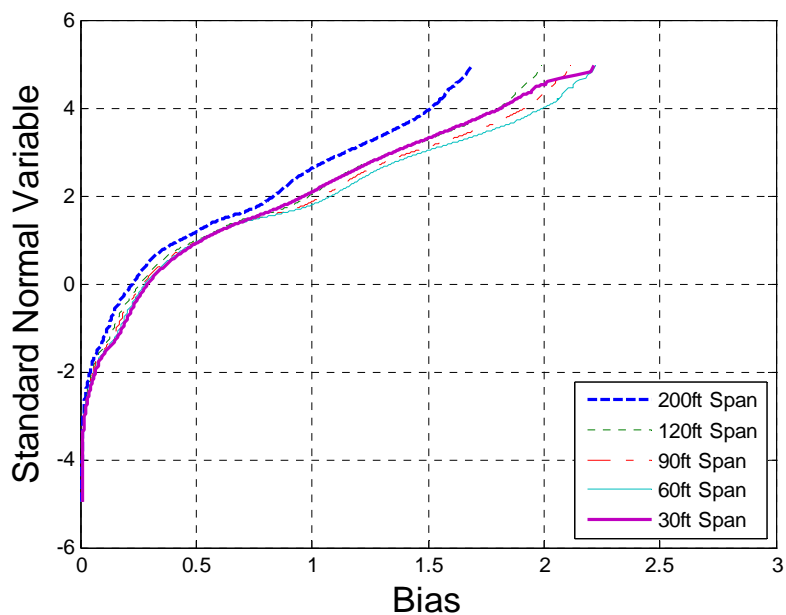


Figure 0-342 Cumulative Distribution Functions of Shear – New York Site 0199

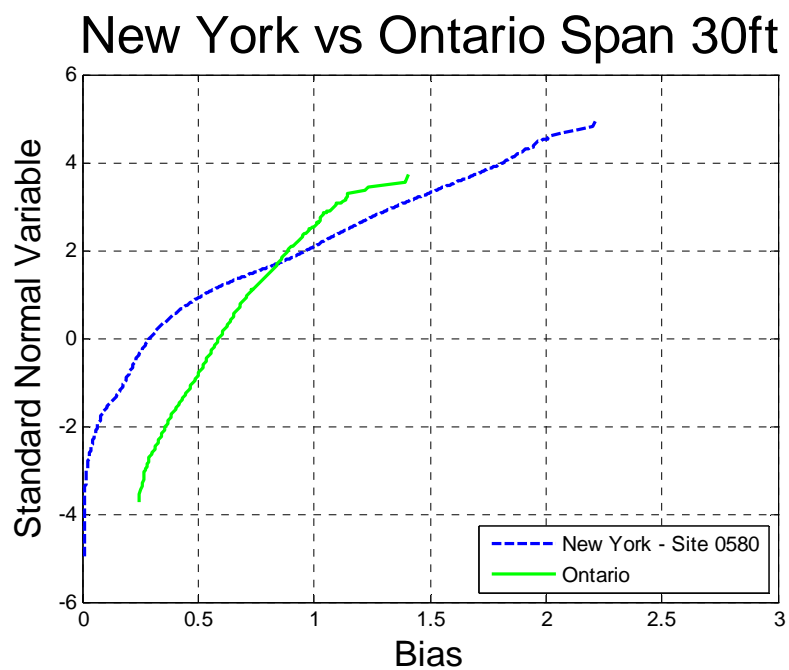


Figure 0-343 Comparison of Shear – New York Site 0580 vs. Ontario – Span 30ft

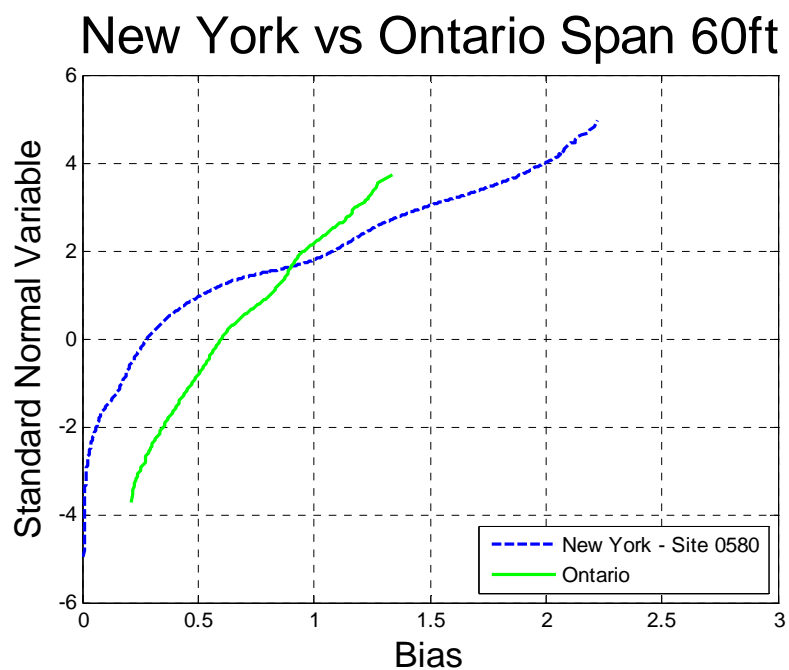


Figure 0-344 Comparison of Shear – New York Site 0580 vs. Ontario – Span 60ft

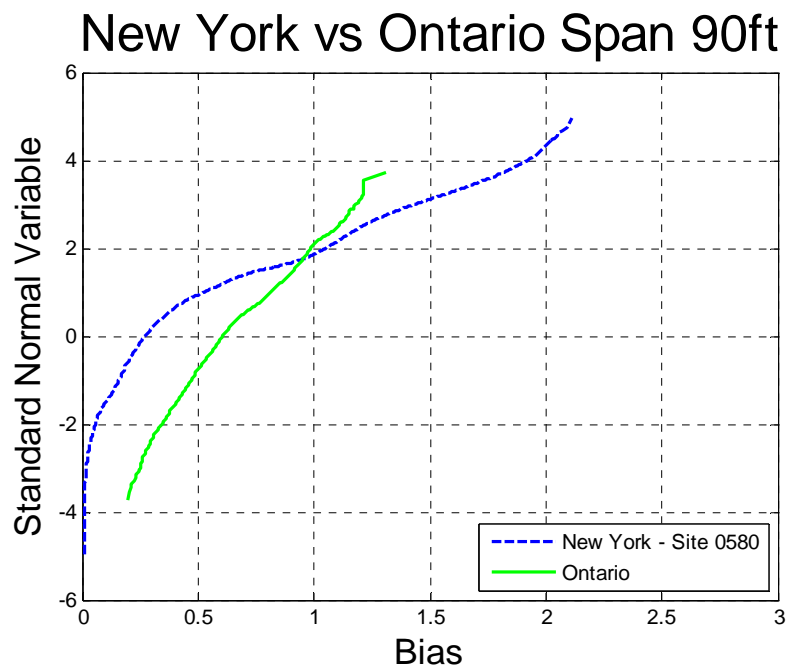


Figure 0-345 Comparison of Shear – New York Site 0580 vs. Ontario – Span 90ft

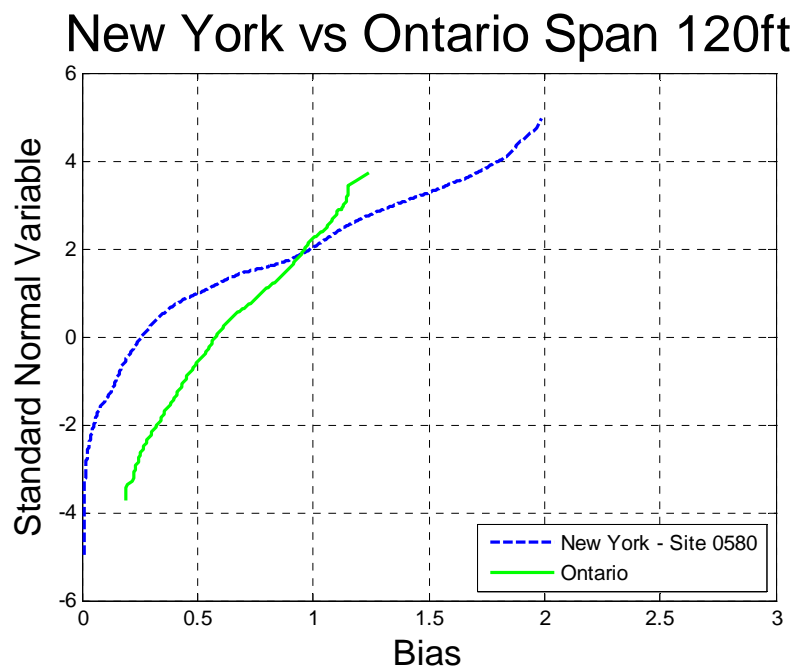


Figure 0-346 Comparison of Shear – New York Site 0580 vs. Ontario – Span 120ft

New York vs Ontario Span 200ft

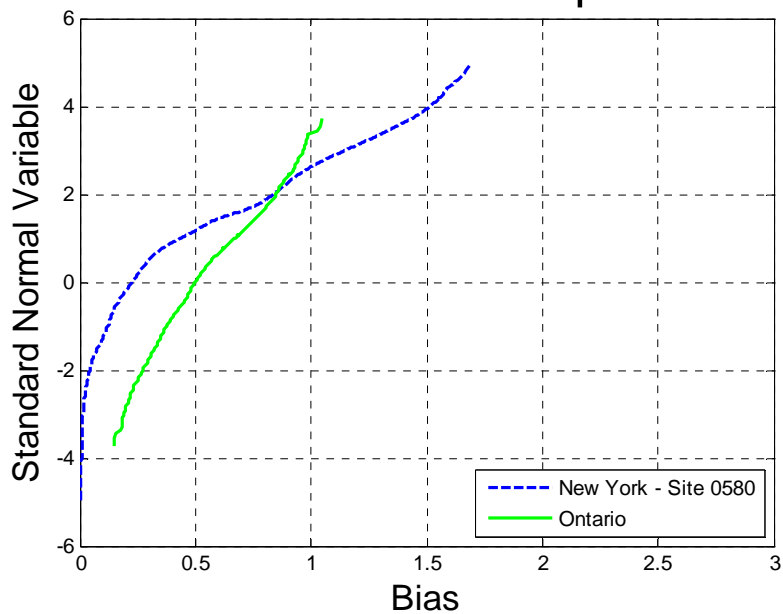


Figure 0-347 Comparison of Shear – New York Site 0580 vs. Ontario – Span 200ft

New York - Site 2680

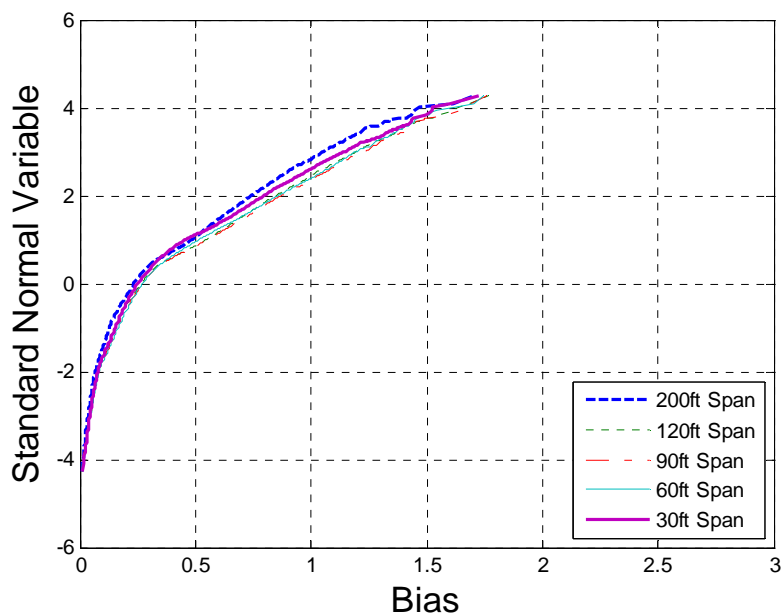


Figure 0-348 Cumulative Distribution Functions of Shear – New York Site 2680

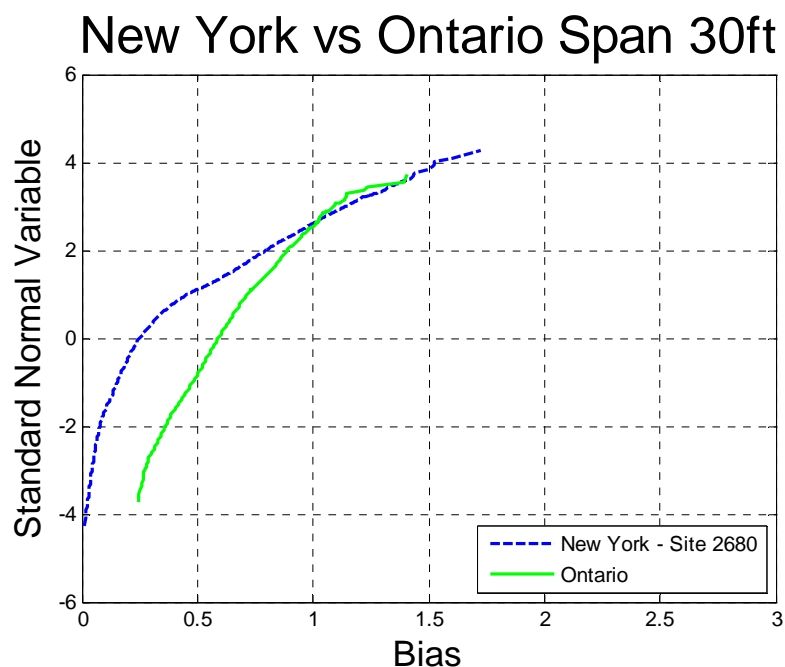


Figure 0-349 Comparison of Shear – New York Site 2680 vs. Ontario – Span 30ft

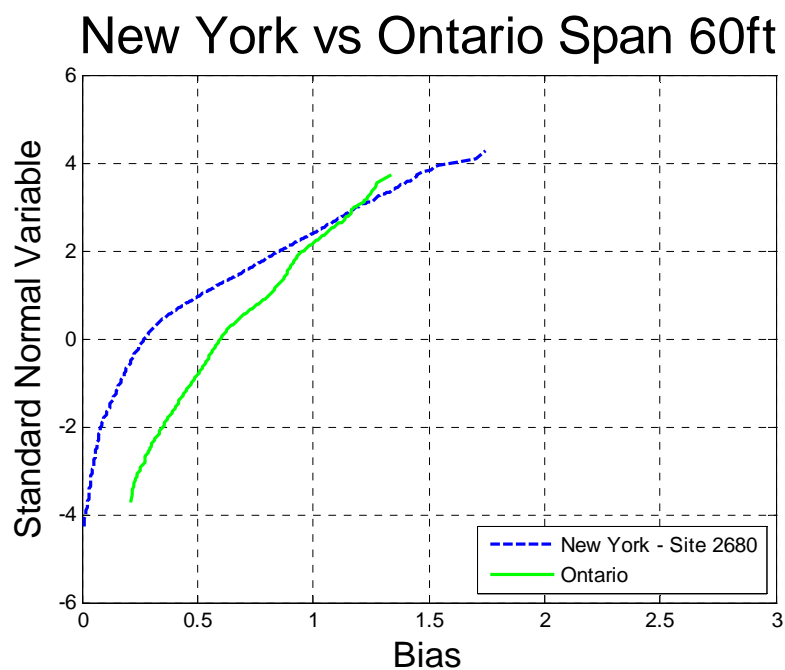


Figure 0-350 Comparison of Shear – New York Site 2680 vs. Ontario – Span 60ft

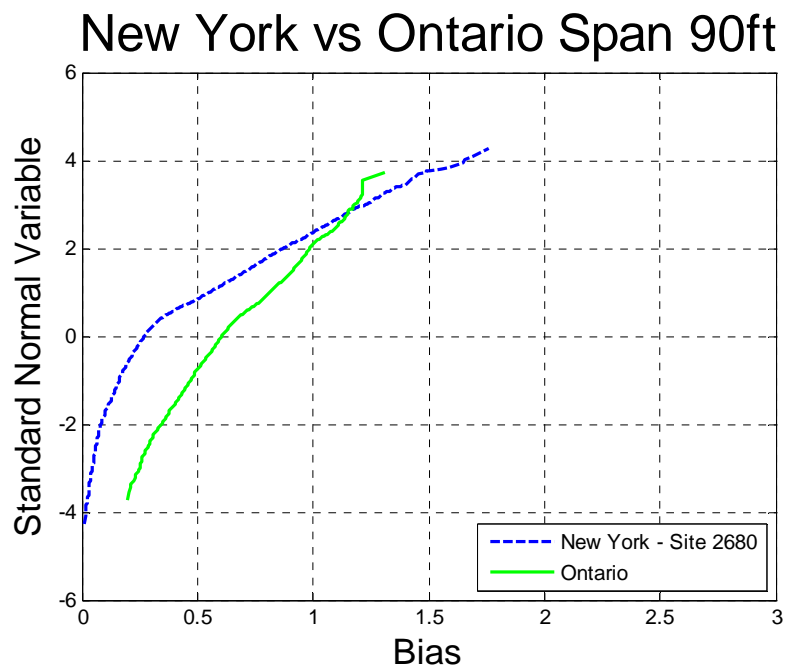


Figure 0-351 Comparison of Shear – New York Site 2680 vs. Ontario – Span 90ft

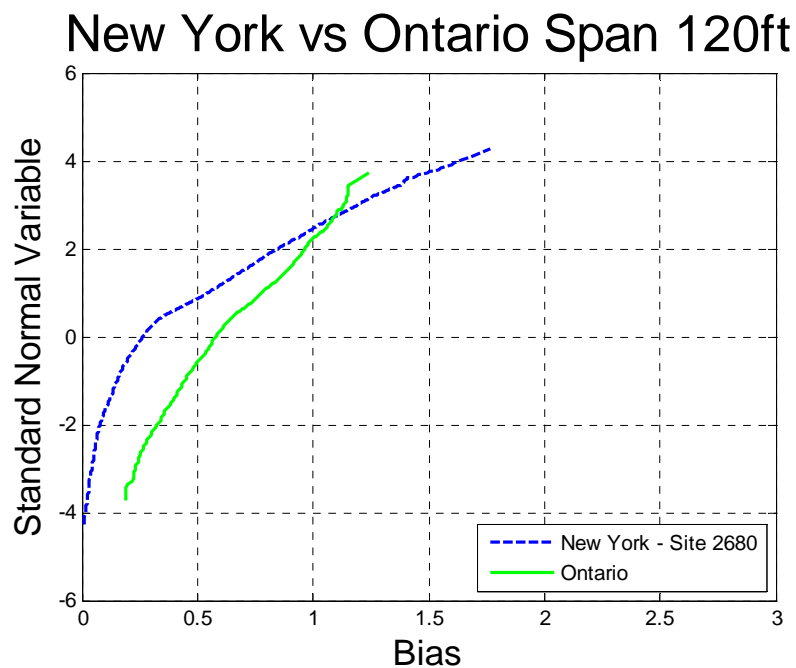


Figure 0-352 Comparison of Shear – New York Site 2680 vs. Ontario – Span 120ft

New York vs Ontario Span 200ft

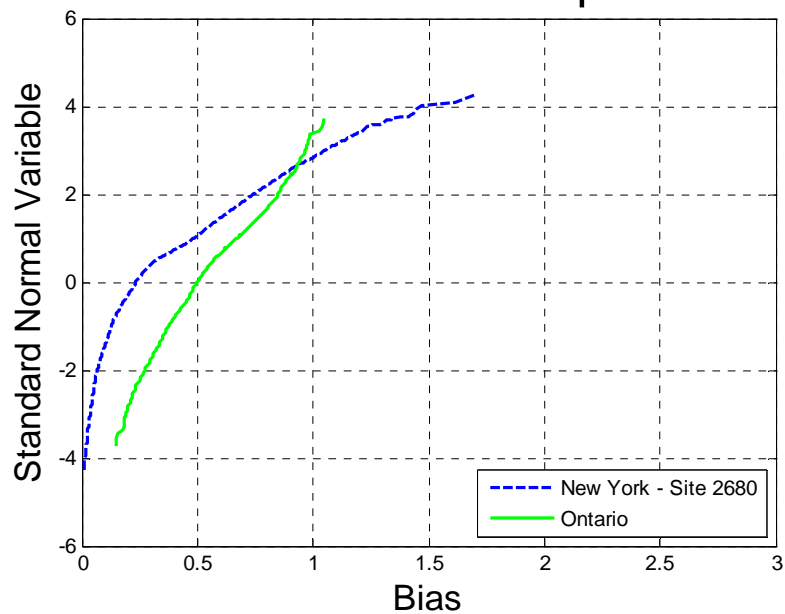


Figure 0-353 Comparison of Shear – New York Site 2680 vs. Ontario – Span 200ft

New York - Site 8280

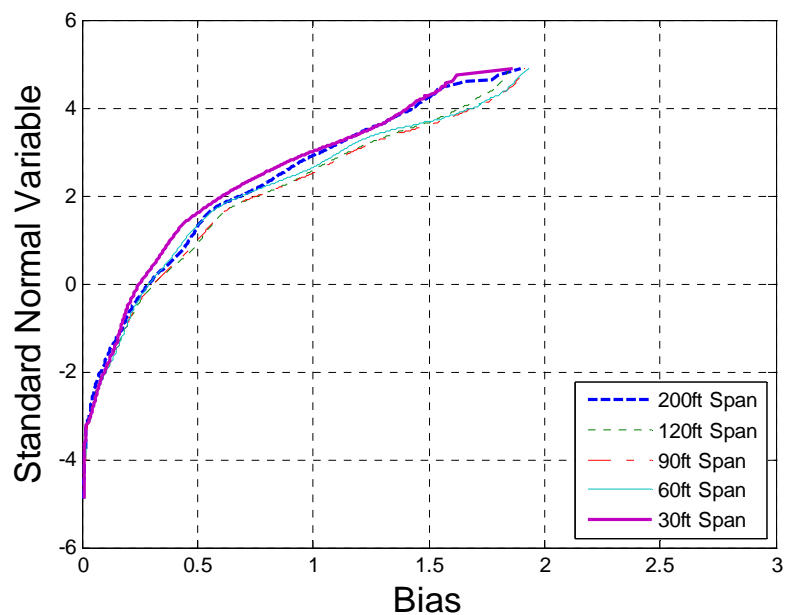


Figure 0-354 Cumulative Distribution Functions of Shear – New York Site 8280

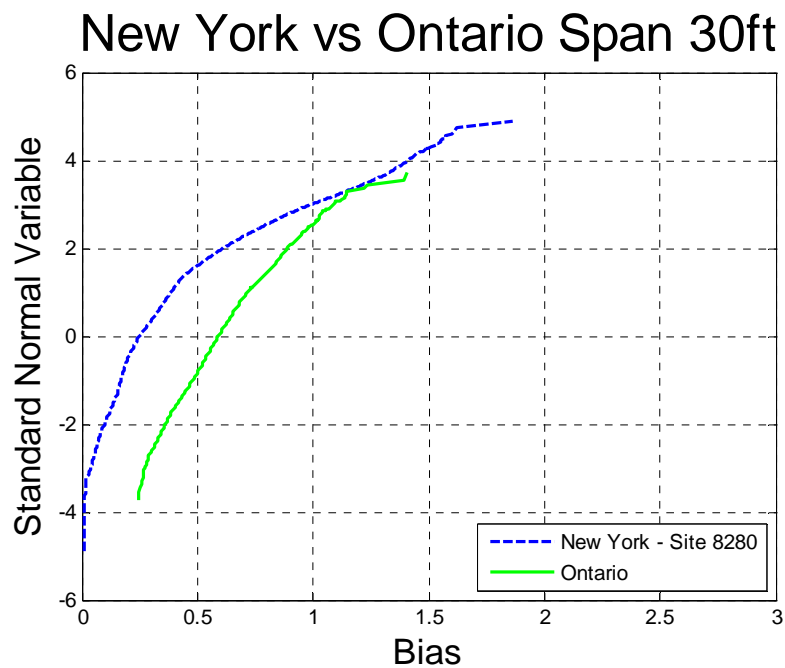


Figure 0-355 Comparison of Shear – New York Site 8280 vs. Ontario – Span 30ft

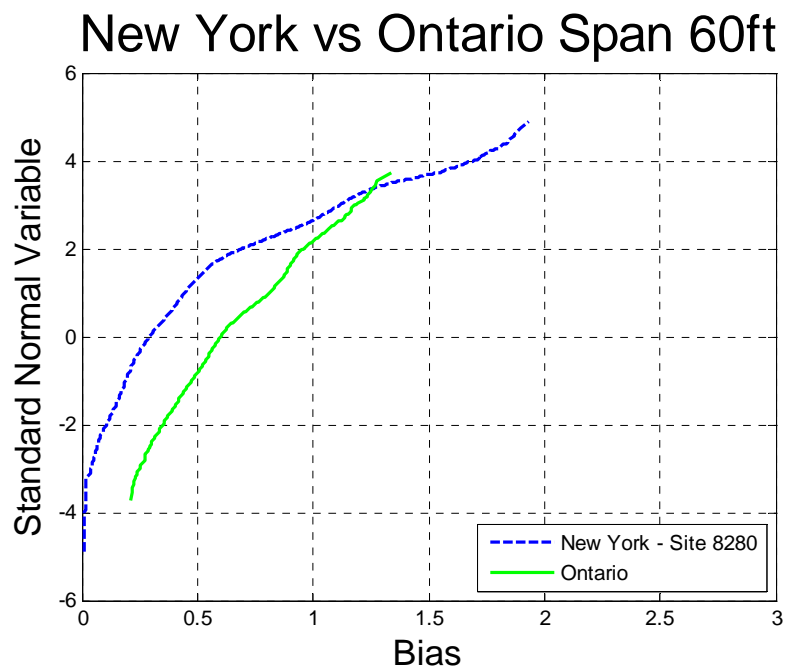


Figure 0-356 Comparison of Shear – New York Site 8280 vs. Ontario – Span 60ft

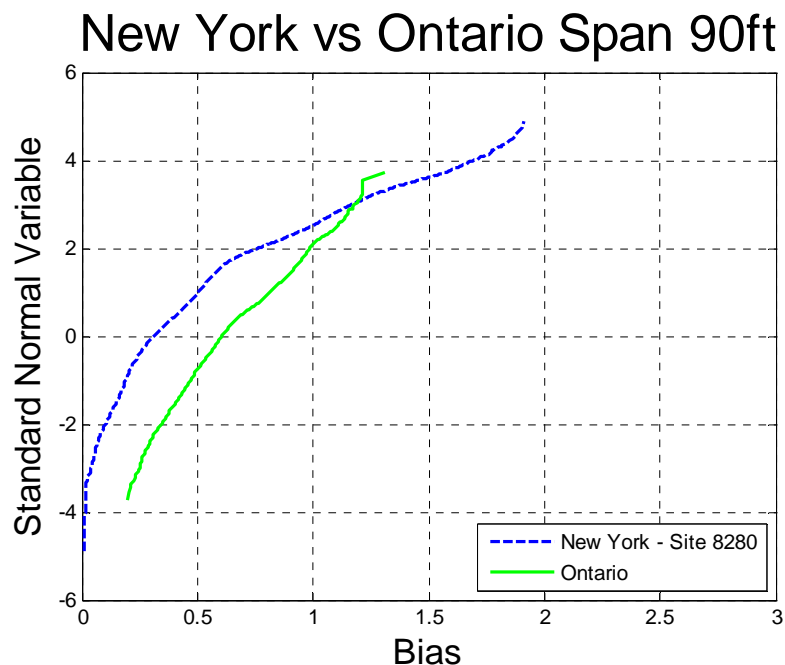


Figure 0-357 Comparison of Shear – New York Site 8280 vs. Ontario – Span 90ft

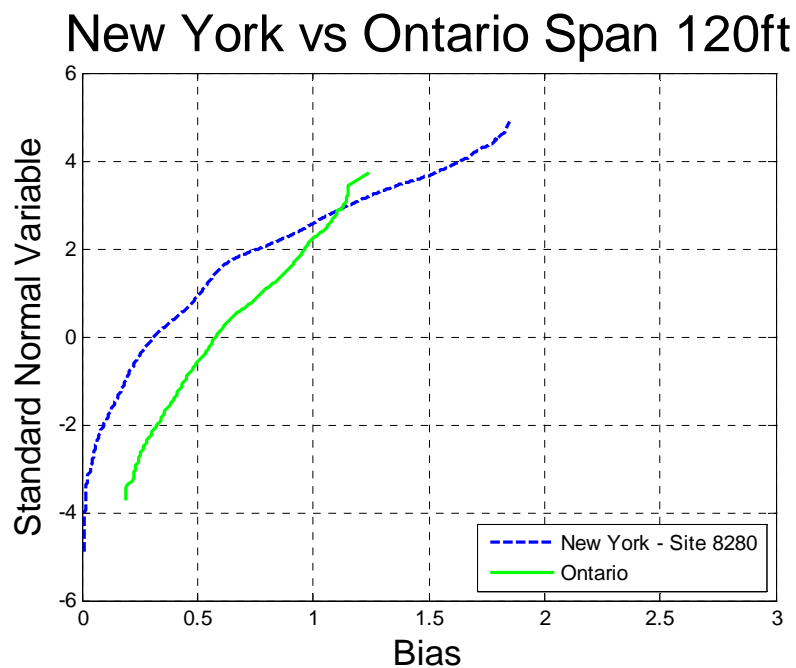


Figure 0-358 Comparison of Shear – New York Site 8280 vs. Ontario – Span 120ft

New York vs Ontario Span 200ft

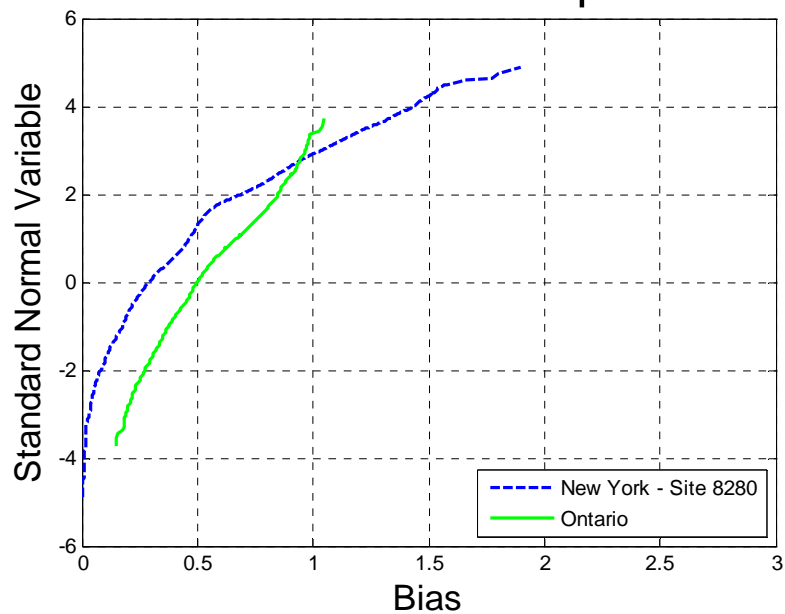


Figure 0-359 Comparison of Shear – New York Site 8280 vs. Ontario – Span 200ft

New York - Site 8382

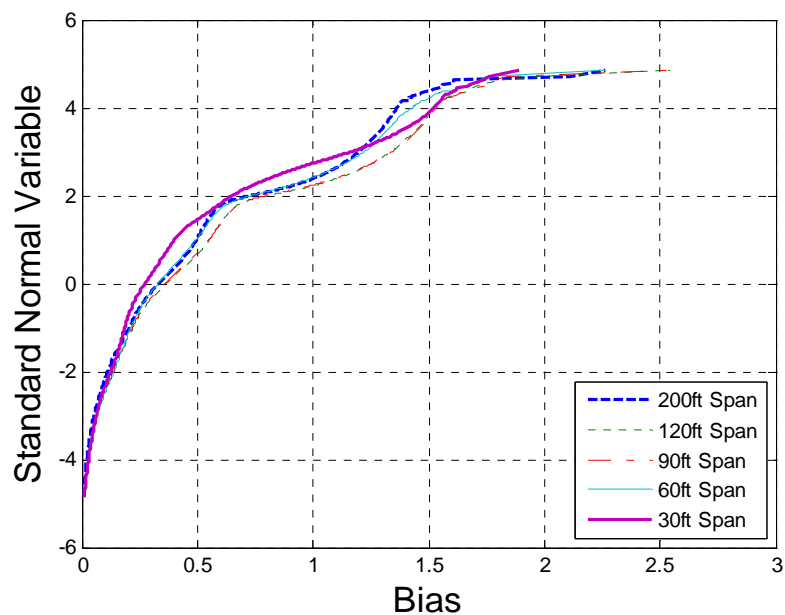


Figure 0-360 Cumulative Distribution Functions of Shear – New York Site 8382

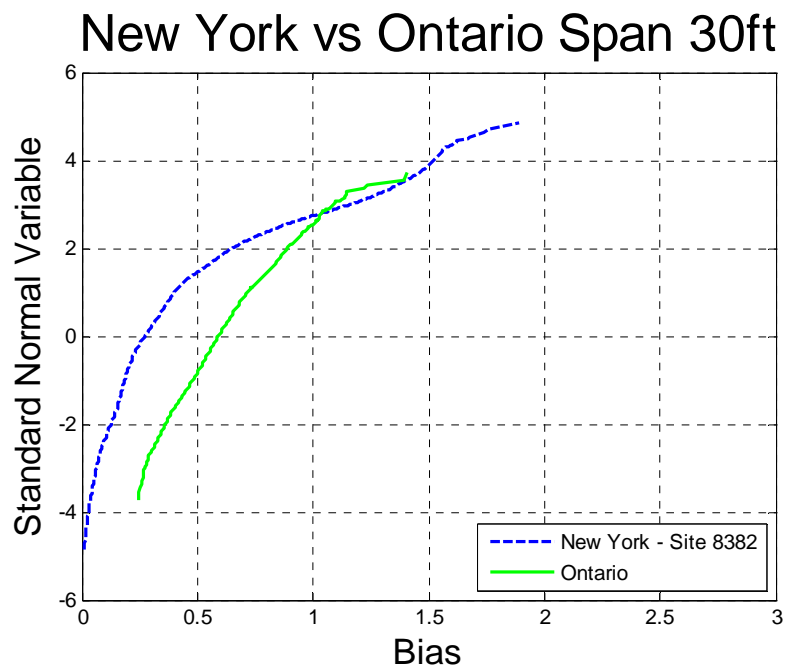


Figure 0-361 Comparison of Shear – New York Site 8382 vs. Ontario – Span 30ft

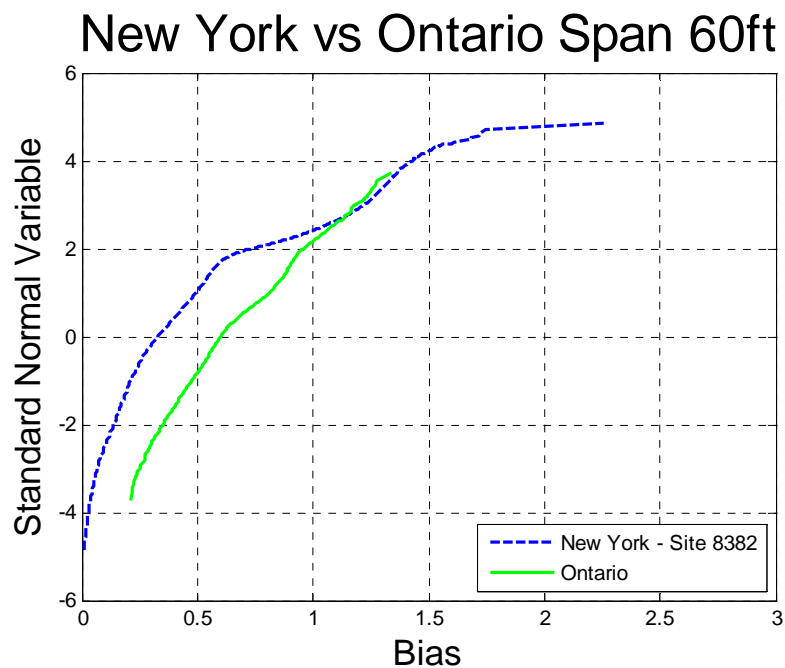


Figure 0-362 Comparison of Shear – New York Site 8382 vs. Ontario – Span 60ft

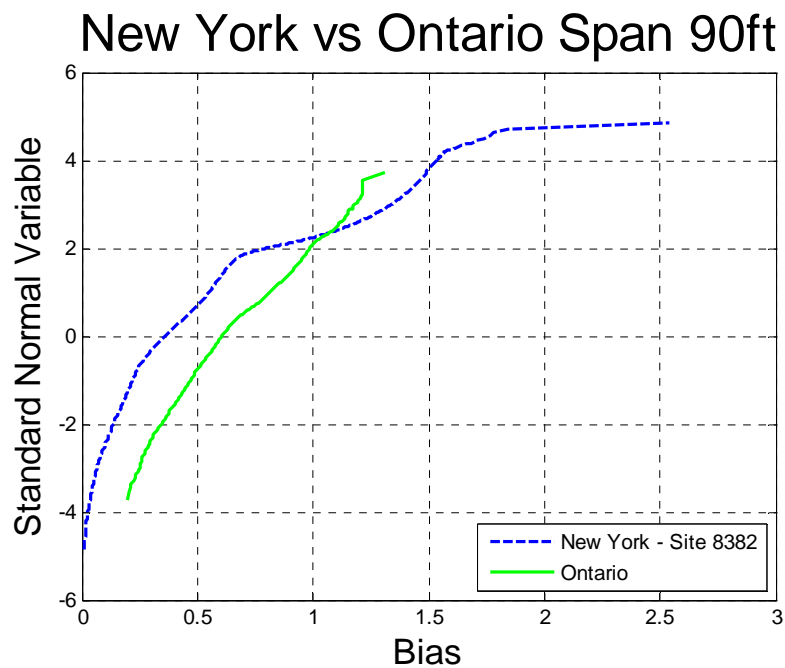


Figure 0-363 Comparison of Shear – New York Site 8382 vs. Ontario – Span 90ft

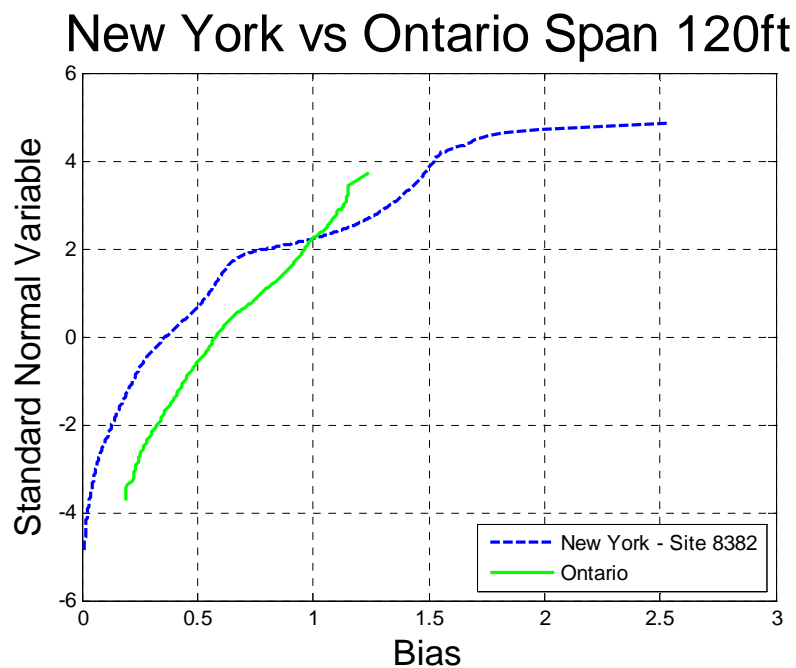


Figure 0-364 Comparison of Shear – New York Site 8382 vs. Ontario – Span 120ft

New York vs Ontario Span 200ft

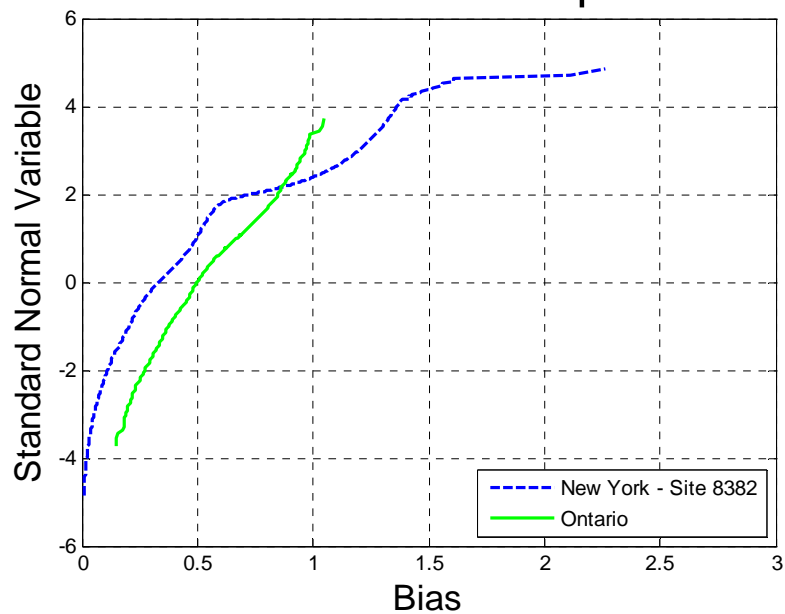


Figure 0-365 Comparison of Shear – New York Site 8382 vs. Ontario – Span 200ft

New York - Site 9121

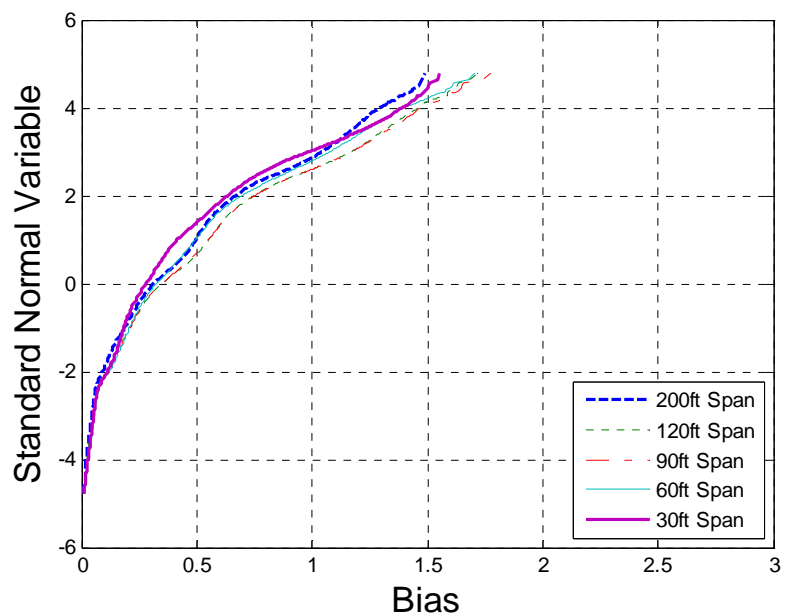


Figure 0-366 Cumulative Distribution Functions of Shear – New York Site 9121

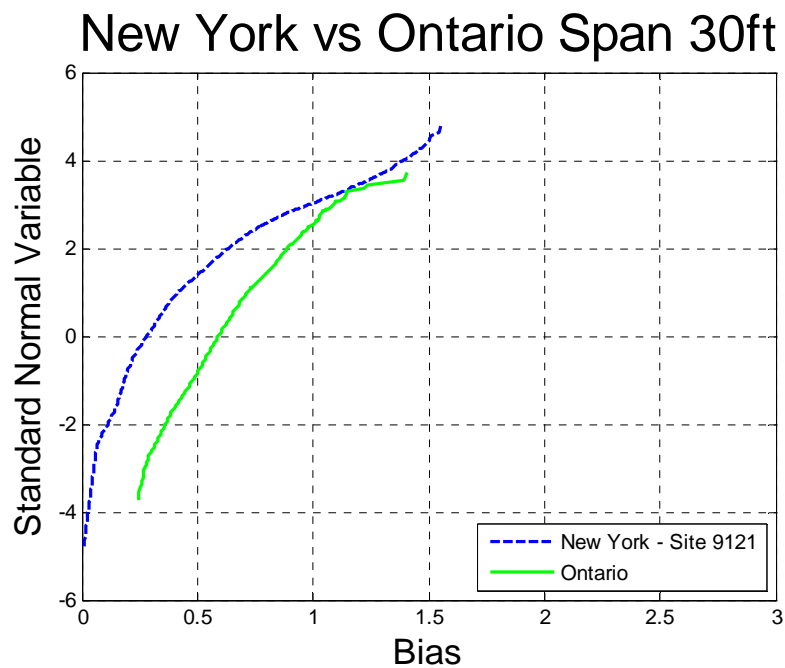


Figure 0-367 Comparison of Shear – New York Site 9121 vs. Ontario – Span 30ft

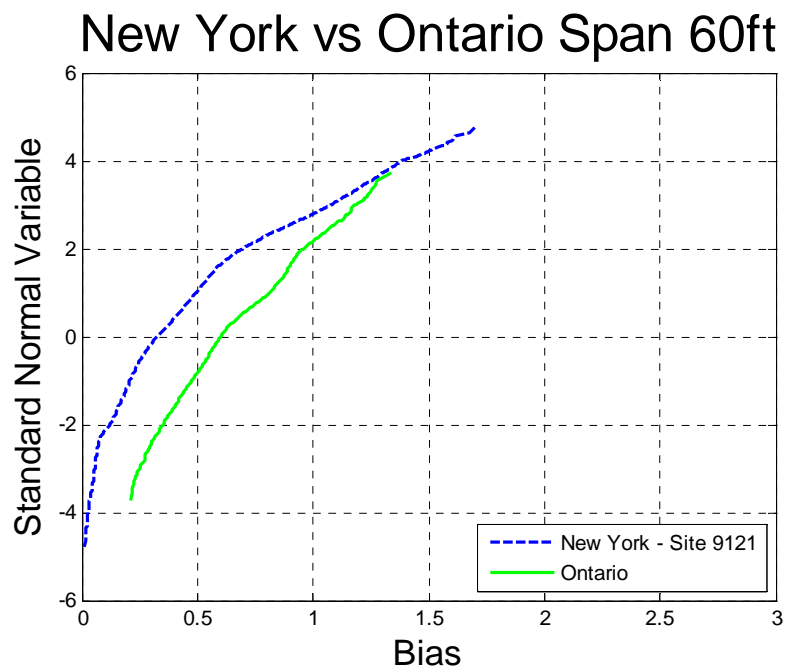


Figure 0-368 Comparison of Shear – New York Site 9121 vs. Ontario – Span 60ft

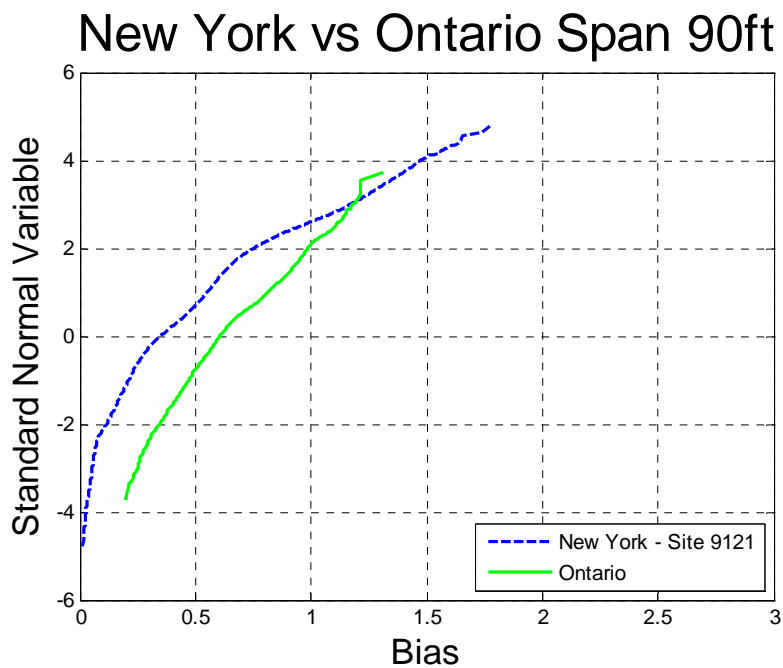


Figure 0-369 Comparison of Shear – New York Site 9121 vs. Ontario – Span 90ft

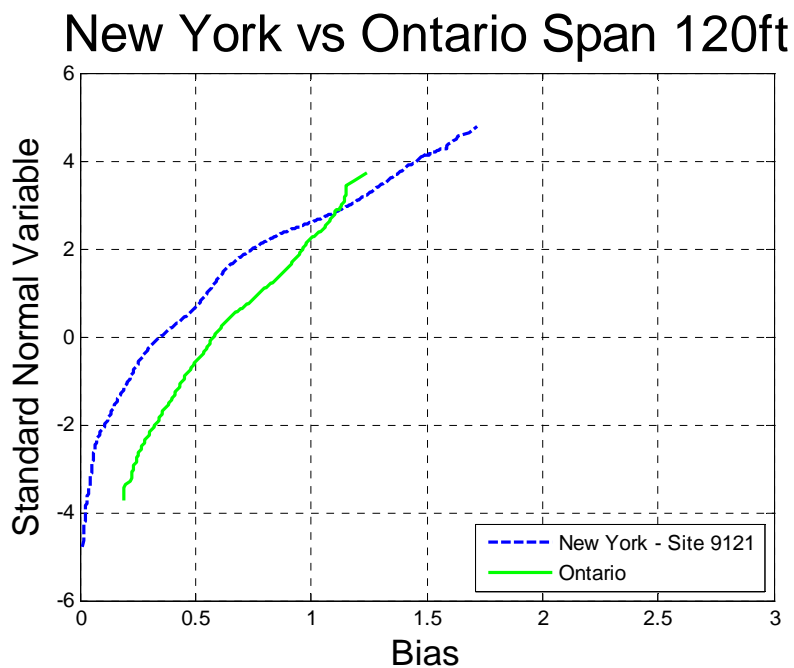


Figure 0-370 Comparison of Shear – New York Site 9121 vs. Ontario – Span 120ft

New York vs Ontario Span 200ft

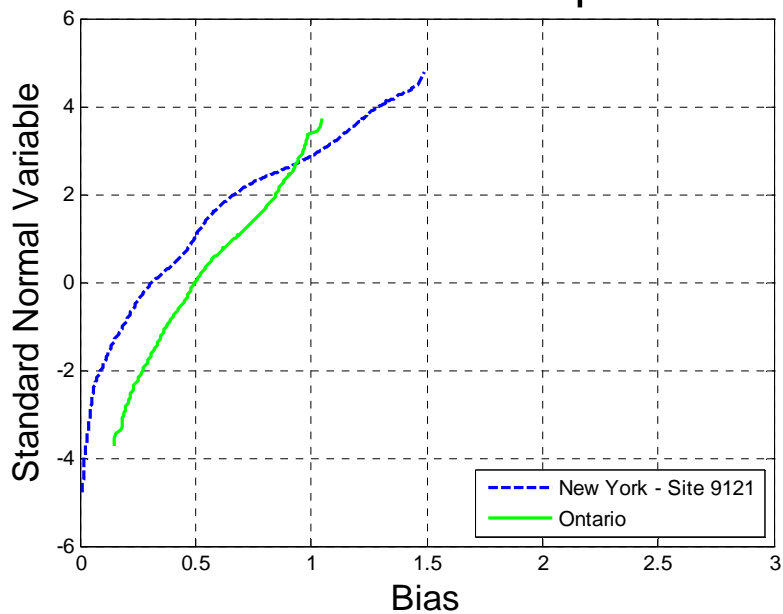


Figure 0-371 Comparison of Shear – New York Site 9121 vs. Ontario – Span 200ft

New York - Site 9631

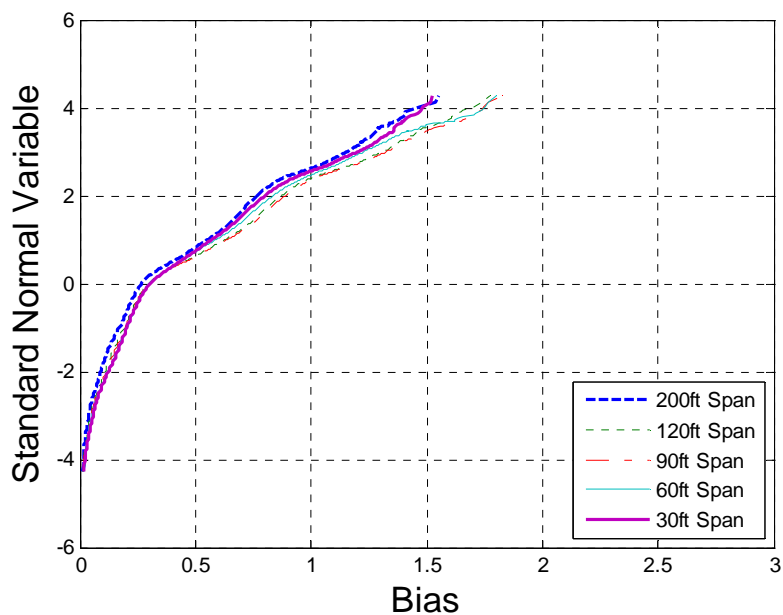


Figure 0-372 Cumulative Distribution Functions of Shear – New York Site 9631

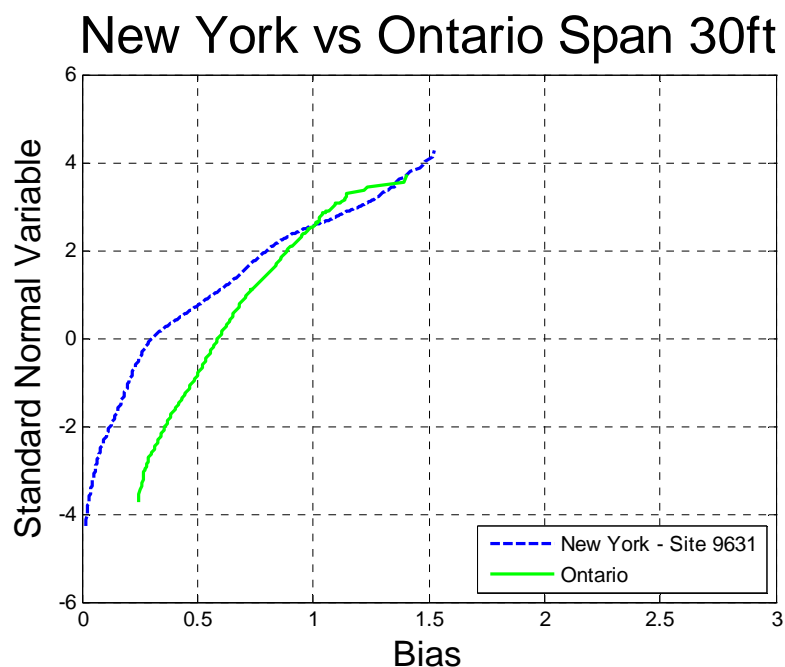


Figure 0-373 Comparison of Shear – New York Site 9631 vs. Ontario – Span 30ft

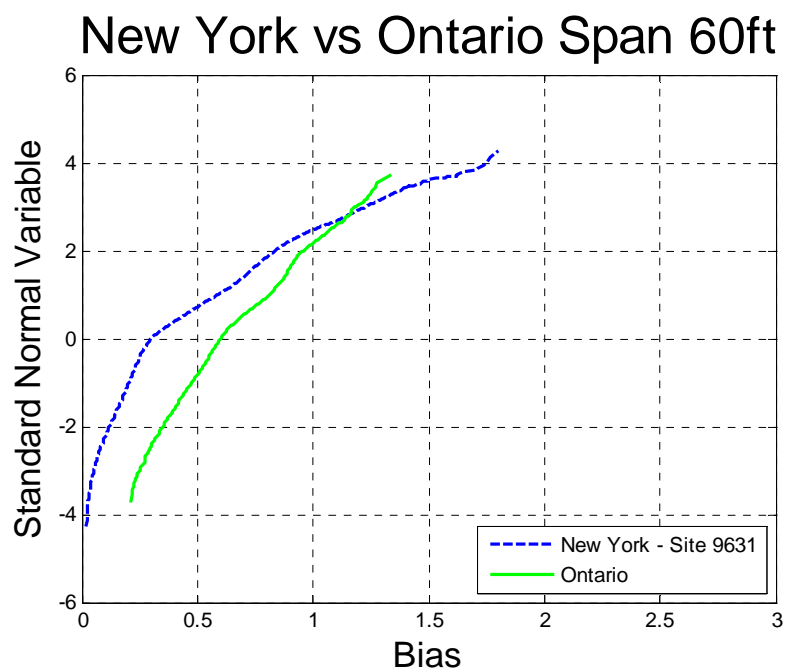


Figure 0-374 Comparison of Shear – New York Site 9631 vs. Ontario – Span 60ft

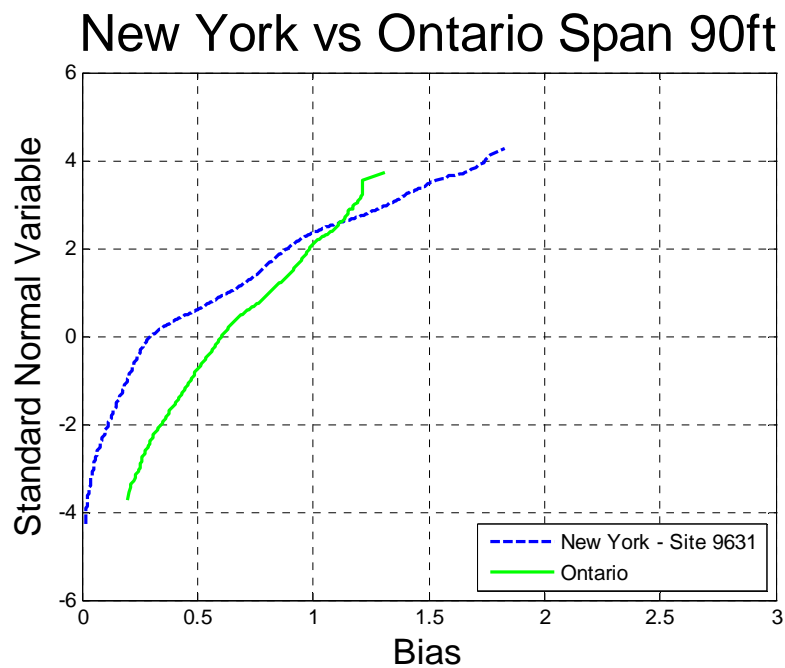


Figure 0-375 Comparison of Shear – New York Site 9631 vs. Ontario – Span 90ft

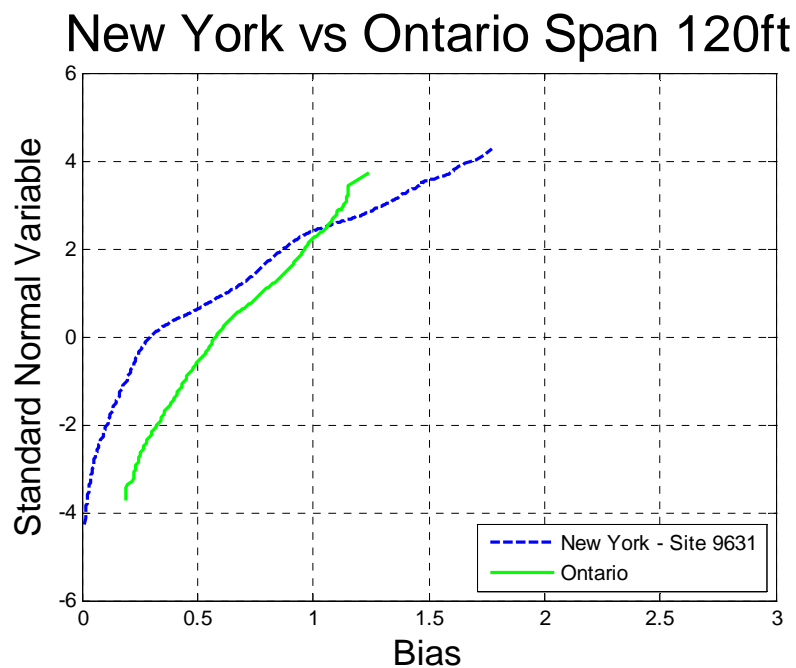


Figure 0-376 Comparison of Shear – New York Site 9631 vs. Ontario – Span 120ft

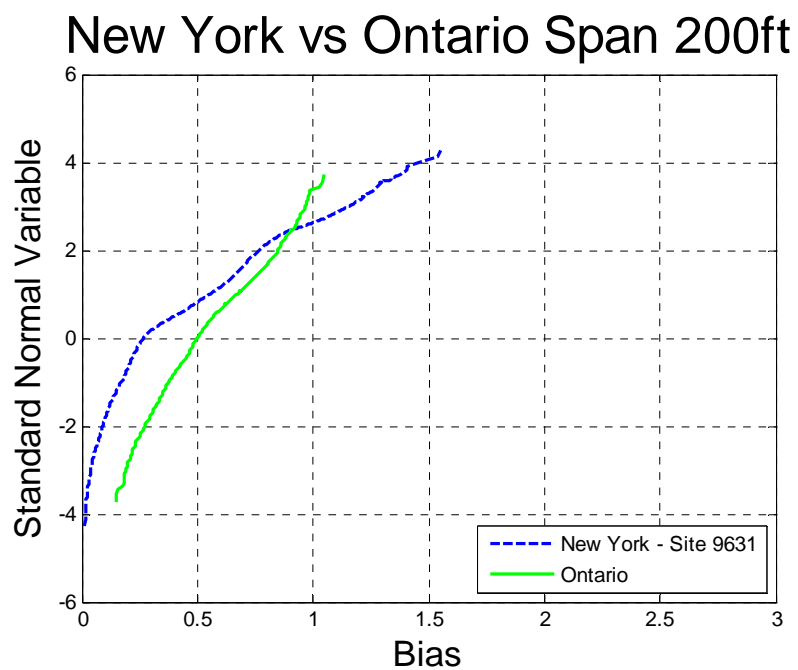


Figure 0-377 Comparison of Shear – New York Site 9631 vs. Ontario – Span 200ft